

This item was submitted to Loughborough University as a PhD thesis by the author and is made available in the Institutional Repository (<https://dspace.lboro.ac.uk/>) under the following Creative Commons Licence conditions.



For the full text of this licence, please go to:
<http://creativecommons.org/licenses/by-nc-nd/2.5/>

LOUGHBOROUGH
UNIVERSITY OF TECHNOLOGY
LIBRARY

AUTHOR/FILING TITLE

NAEEM, T

ACCESSION/COPY NO.

008462/01

VOL. NO.

CLASS MARK

LOAN COPY JUL 1994

26 JUN 1998

25 JUN 1999

27 JUN 2000

14 JAN 2000

95

7

26 JUN 1998

000 8462 01



This book was bound by

Badminton Press

18 Half Croft, Syston, Leicester, LE7 8LD

Telephone: Leicester (0533) 602918.

LOUGHBOROUGH
UNIVERSITY OF TECHNOLOGY
LIBRARY

AUTHOR/FILING TITLE

NAEEM, T

ACCESSION/COPY NO.

008462/01

VOL. NO.

CLASS MARK

LOAN COPY III

-9 JUN 1988
LOAN 1 MTH + 2
UNLESS RECALLED

30 JUN 1989

-5 JUL 1991

-3 JUL 1992

17 MAR 1994

30 JUN 1995

30 JUN 1995

27 JUN 1997

27 JUN 1997

26 JUN 1998

000 8462 01



This book was bound by

Badminton Press

18 Half Croft, Syston, Leicester, LE7 8LD

Telephone: Leicester (0533) 602918

THE RESISTANCE OF GLASS REINFORCED THERMOSETTING
POLYMERS TO THERMOHUMID CONDITIONS

by

MOHAMMED NAEEM

A Doctoral Thesis submitted in partial fulfilment
of the requirements for the award of
Doctor of Philosophy of the
Loughborough University of Technology

1985

Supervisor: John F Harper BSc(Eng), MSc
Department of Materials Engineering and Design

Loughborough University of Technology library	
Date	Mar 86
Class	
Acc. No.	008462/01

CERTIFICATE OF ORIGINALITY

This is to certify that I am responsible for the work submitted in this thesis, that the original work is my own except as specified in acknowledgements or in footnotes, and that neither the thesis nor the original work contained therein has been submitted to this or any other institution for a higher degree.

TO MY FAMILY

SYNOPSIS

Advanced composite materials based mainly on epoxy resins are being used in increasing numbers of components in the aerospace industry. Such components have to survive in a range of moisture and temperature environments in different parts of the world at varying altitudes. It is important therefore to have sufficient information about the behaviour of composite components to predict what effect these environments will have on their properties. The aim of the work reported in this thesis was to provide such information not only for epoxy based systems but to make comparisons with polyester and vinyl ester based materials.

Five glass fibre reinforced resin systems were used. Two vinyl esters, one polyester, one straight epoxy and one epoxy prepreg mixture. The effect of immersion in distilled water and exposure to humid air at 60% and 95% relative humidity was investigated at temperatures ranging from 25°C to 70°C, for periods of sixteen and forty days. During these periods moisture uptake for both unidirectional and bidirectional materials was recorded on a daily basis, and variations in glass transition temperature were determined. At the end of each period the ultimate tensile stress, tensile modulus, tensile strain to failure, interlaminar shear strength and interplanar shear strength of each material was determined.

The water absorption results for the vinyl ester resins, polyester and straight epoxy resin initially showed Fickian diffusion characteristics. In the epoxy prepreg material a two stage diffusion process was observed. No equilibrium water absorption plateau was obtained over forty days at 60% relative humidity for any of the materials, at any temperature. All the mechanical properties dropped under these conditions and this was shown to be as a result of degradation at the glass-resin interface. At 95% relative humidity the fall in mechanical properties was greater and not recoverable. Under these conditions plasticization of the matrix had occurred. All the material samples which were subject to hot water under-

went pronounced degradation. The degradation process was shown to be due to penetration of water at the glass-resin interface, followed by attack on the coupling agent and glass fibre surface. This degradation process was confirmed by micro-observations of the fracture surfaces.

ACKNOWLEDGEMENTS

I would like to express my thanks to Professor I A Menzies, the Head of Department and Director of Research, for the use of the Department's laboratory facilities.

My sincere thanks and gratitude to Mr J F Harper, my Supervisor, for his invaluable help, advice and guidance throughout the course of my research.

I would also like to thank all the technical staff for their assistance during this piece of research, and to Mrs Janet Smith, who transformed a very untidy draft into most attractive typescript.

Last, but not least, I would like to thank fellow postgraduates, especially Mr C P S Johal and Mr T Heumann for helpful discussions.

CONTENTS

	<u>Page No</u>
1.0 INTRODUCTION	1
2.0 LITERATURE SURVEY	7
2.1 The Chemistry of the Resins	7
2.1.1 General Resin Chemistry	7
2.1.2 Polyester Resins	8
2.1.3 Epoxy Resins	9
2.1.4 Vinyl Ester Resins	12
2.1.5 913 PrePreg	16
2.2 Environmental Effects on Fibre Reinforced Composites	18
2.2.1 The Effect of Moisture on Glass Fibres	19
2.2.2 The Effect of Moisture on the Interface	21
2.2.3 The Effect of Moisture on the Matrix	25
2.2.3.1 The Effect of Moisture on Epoxy Resins	26
2.2.3.2 The Effect of Moisture on Polyester Resins	28
2.2.3.3 The Effect of Moisture on Vinyl Ester Resins	32
2.2.4 The Effect of Moisture on Composite Properties	33
2.2.5 The Effect of Moisture on Glass-Transition-Temperature (T _g) of Resin	36
2.2.6 Measurement of T _g	37
2.2.6.1 Thermal Analysis	37
2.2.6.2 Dimensional Changes	39
2.2.6.3 Dynamic Thermomechanical Analysis	41
2.3 Diffusion	42
2.3.1 Theory of Diffusion	42
2.3.2 Determination of Diffusion Coefficient and the Maximum Moisture Content	48
2.3.3 Non-Fickian Diffusion	51

					<u>Page No.</u>
3.0	EXPERIMENTAL PROCEDURE	54
3.1	Materials Used	54
3.1.1	Fibre Reinforcement	54
3.1.2	Resin Matrix	54
3.1.2.1	Derakane Vinyl Ester Resins				54
3.1.2.2	Polyester Resin		55
3.1.2.3	Epoxy Resin		55
3.1.3	PrePreg Material	56
3.2	Equipment	56
3.3	Manufacturing Techniques	58
3.3.1	Laminate Lay-up Procedure		58
3.3.1.1	Vinylester 411, 470 and Polyester 272	58
3.3.1.2	Epoxy MY750		59
3.3.1.3	913 PrePreg		59
3.4	Curing Procedure	60
3.5	Test Specimen Preparation	60
3.6	Volume Fraction	61
3.7	Environmental Conditioning	62
3.7.1	Thermal Spiking	63
3.8	Mechanical Testing	64
3.8.1	Tensile Testing	64
3.8.2	Interlaminar Shear Testing	64
3.9	Glass-Transition Temperature		65
3.10	Microscopy	66
4.0	RESULTS	67
4.1	Weight Increase	67
4.2	Diffusion Data	68
4.2.1	Maximum Moisture Content		68
4.2.2	Diffusion Coefficient		68
4.2.3	Activation Energy	71
4.3	Glass Transition Temperature		72

	<u>Page No.</u>
4.4 Tensile Test	72
4.4.1 Ultimate Tensile Strength	73
4.4.2 Strain to Failure	74
4.4.3 Tensile Modulus	75
4.5 Interlaminar Shear Strength	75
4.6 In-Plane Shear Strength	76
5.0 DISCUSSION	77
5.1 Experimental Techniques	77
5.1.1 Volume Fraction of Fibres	77
5.1.2 Distribution of Fibres	78
5.1.3 Thickness of the Laminates	80
5.1.4 Voids Content	81
5.1.5 End Tabs	82
5.2 Water Absorption	83
5.2.1 Appearance Changes	85
5.2.2 Weight Increase	88
5.2.2.1 60 percent Relative Humidity	89
5.2.2.2 95 percent Relative Humidity	92
5.2.2.3 Water Bath	95
5.2.2.4 Thermal Spiking	100
5.3 Glass-Transition Temperature (T _g)	101
5.4 Mechanical Properties	102
5.4.1 Ultimate Tensile Strength	103
5.4.4.1 Tensile Failure Mode	105
5.4.2 Percent Elongation	109
5.4.3 Tensile Modulus	112
5.4.4 Interlaminar Shear Strength	115
5.4.5 In-Plane Shear Strength	119
5.5 The Effect of Thermal Spiking on the Mechanical Properties	121
5.5.1 Ultimate Tensile Strength	122
5.5.2 Percent Elongation	122
5.5.3 Tensile Modulus	122

						<u>Page No.</u>
5.5.4	Interlaminar Shear Strength	123
5.5.5	In-Plane Shear Strength	123
6.0	CONCLUSIONS AND RECOMMENDATIONS	124
REFERENCES	128
APPENDICES:	Appendix A	Diffusion Data	137
	Appendix B	Ultimate Tensile Strength	149
	Appendix C	Percent Elongation Data	159
	Appendix D	Tensile Modulus Data	169
	Appendix E	Interlaminar Shear Strength Data	179
	Appendix F	In-plane Shear Strength Data	189
TABLES	199
FIGURES	226

CHAPTER 1

INTRODUCTION

The addition of a fibrous material to another material (the matrix) in order to strengthen this matrix is not a novel idea, indeed it dates back to the ancient Egyptian's practice of reinforcing mud bricks with straw. The modern day equivalent of this process is the reinforcement of concrete by fine steel wires. Present day fibrous composite materials, composed of high strength fibre in a polymeric or metallic matrix are an important advance in material technology. Several reinforcing fibres besides glass and asbestos are now available, notably carbon, graphite, boron, aramid, aliphatic polyamide, etc. Glass can have a variety of different compositions. E-glass (E for electrical) is the most commonly used glass because it has good strength, stiffness, electrical and weathering properties. C-glass (C for corrosion) has a higher resistance to chemical corrosion than E glass but is more expensive and has lower strength properties. S glass is more expensive than E glass but has a higher strength and is more temperature resistant. It is used in special applications such as the aircraft industry where the higher modulus may justify the extra cost. The physical form of the fibres is also important; it may consist of monofilament, chopped strand, woven fabric or mat. The number of filaments per bundle influences both the mechanical and environmental properties.

Glass reinforced plastics (GRP) are perhaps the most widely used and the most familiar composite material, replacing wood, itself a naturally occurring fibre reinforced material, in many applications. GRP have advantages as structural materials over both unreinforced plastics and glass fibres used alone. Unreinforced plastics have low density and are easily processed. They have good weathering properties and require no surface protection. Disadvantages, which limit their use in structural applications, are low stiffness, low strength and creep under load.

Glass fibres are stiff and strong but so brittle that the high stiffness and strength cannot be fully utilised. By fabricating a composite material of glass fibres embedded in a plastic matrix, it is possible to combine many of the desirable properties of both constituents. Thus glass reinforced plastics are light, strong, constructional materials with weather resistant surfaces which are easily fabricated into complex shapes. The glass fibres enhance the poor stiffness, strength and creep resistance of the plastic matrix, whose purpose is to transmit the load into the stiff fibres and to protect them from damage.

A range of different GRP materials is now available depending on the choice of the matrix and the method of different reinforcement. There are two principal types of plastics, thermoplastics and thermosetting materials, but thermosets are the main plastics used as matrix. Thermoplastics such as polypropylene and polystyrene are solids which soften and flow on heating and return to the solid state on cooling. Thermosetting materials such as epoxides and polyesters are usually supplied as viscous syrups which set to a hard solid when activated by a catalyst, but remain solid on further heating. A unique feature of GRP materials is that they are usually formed during fabrication of a component. Traditionally this fabrication is by hand lay up in which glass fibre reinforcement is placed on a mould and impregnated with catalysed resin. The required thickness is built up in layers, the resin left to cure and the finished article removed from the mould. To facilitate this process glass fibres are supplied in sheet form, of which there are four main types: chopped strand mat, which consists of chopped glass fibres held randomly orientated in a mat by a chemical binder; woven roving which are coarse woven fabrics; unidirectionally aligned long fibres held together by a thin weft or by chemical binder and pre-preg material which is a tape or sheet of fibres impregnated with resin. As GRP finds further applications other fabrication techniques have been developed, such as spraying of chopped fibres and catalysed resin onto a mould, hot press moulding method, filament winding, pultrusion, resin injection etc.

The introduction of GRP coincided with both the development of radar and the outbreak of World War II. These two factors led to the early introduction of GRP into many applications, particularly in the field of radar antenna covers. The USA space programme and the advent of many new fibres and new matrix types gave an additional impetus to composite research and development in the early 1960s. The rapid increase in usage of GRP over the last forty years is shown in Figure 1. Today GRP is a common and widely accepted structural material. Composite bodies have the basic advantages that they can be fabricated from a wide choice of reinforcement and matrix materials; their properties may therefore vary over a very considerable range. In general, composite materials can possess a number of advantages relative to conventional bulk materials including metals. These are summarised below:

- i) increased strength and stiffness
- ii) lower densities
- iii) high fatigue resistance
- iv) relative ease of fabrication
- v) good corrosion resistance
- vi) good electrical and thermal resistance.

GRPs are by no means "wonder materials", the advantages must be balanced against the disadvantages when considering the use of GRP; they are relatively expensive materials, the properties are strongly directional dependent, properties are subject to large degree of scatter, they are non-weldable and require complicated joint structures, the long term properties are not fully understood.

The increasing use of fibre composite materials in industry has resulted in extensive research to determine their behaviour under different environmental conditions. The aerospace industry in particular is interested in fibre composites due to the advantages these materials offer over the more traditional metals. They offer, potential savings

in weight, the ability to tailor the material more closely to the design requirements and manufacturing advantages in being able to mould complex shapes and hence reduce the numbers of parts and the numbers of joining operations. For helicopters some applications require more compliance (hub) or more damage tolerance (blades) which glass fibres can provide. For some rotor blades, however, where more efficient complex shapes require increased stiffness, carbon fibres are being incorporated into hybrid carbon fibre/glass fibre designs. Most of these applications use the fibres in an epoxy resin.

These components have to survive in a range of different environments of moisture, temperature and loading in different parts of the world, at different altitudes. Air moisture content can vary between 0 and 100% relative humidity, and temperatures are typically in the range -40°C to 70°C in flight and up to 90°C on the runway. In supersonic aircraft the temperature can reach as high as 130°C . Further problems such as thermal spiking, can be created by rapid changes in the environmental conditions. Often the composites are under load when exposed to such environments. Consequently the effect of the environment on composites employed in various applications needs to be investigated. Many aircraft and military establishments have sponsored work to determine the effect of water absorption on the properties of fibre composite materials.

The current generation of epoxy resins used in high performance fibre composites absorb water from the atmosphere with the surface layer reaching equilibrium with the surrounding environment very quickly followed by diffusion of water into all of the material. The water absorbed is not usually in the liquid form but consists of molecules or groups of molecules linked by hydrogen bonds to the polymer. In addition liquid water can be absorbed by capillary action along any cracks which may be present or along the fibre matrix interface. Epoxy resins can absorb a maximum of between 1% and 10% by weight of moisture (depending on chemical

composition). In composites with 60% by volume of fibres the moisture uptake is between 0.3% and 3% by weight. The immediate effect of absorbed moisture is a swelling of the resin which counteracts to some extent the shrinkage during the curing process and it can result in significantly reduced residual thermal strains in laminates¹. Water absorption by the epoxy resins also leads to a reduction in the glass transition temperature and to a softening of the resin with a loss of resin stiffness and strength, particularly at elevated temperatures². In longer term the resin may be permanently damaged and a further degradation in properties may result³. These degraded resin properties manifest themselves in the fibre composites as loss of performance in the resin dominated properties, such as reductions in strength and stiffness under shear loading, compressive loading and loading perpendicular to the fibres². In some composites, such as those with glass fibres, the fibre properties may also be degraded by moisture absorption. As the properties of any composite depend on the behaviour of the matrix fibres and the interface it seems essential to know the rate of water absorption in glass epoxy composites in order to predict their long term behaviour. In many cases water absorption obeys Fick's law and diffusion is driven by the water concentration gradient between the environment and the material producing continuous absorption until saturation is reached⁴. In other cases however this model is seen not to be applicable, due to breakdown under certain conditions of humidity and temperature or during cycles of exposure to water vapour followed by drying which can initiate other mechanisms such as cracking or chemical breakdown^{5,6}.

Moisture and temperature may affect the performance of composite materials⁴, i.e. tensile strength, shear strength, elastic moduli and swelling (dimensional changes) etc. The quantity of water absorbed by a laminate is thus of considerable importance, in particular to the designer when setting design limits for structures operating in moist environments.

The objective of this research was to determine the moisture content as a function of time of composite materials when the material is either exposed to humid air at different temperatures or fully submerged in water at various temperatures. A second objective was to determine the effect of the moisture content on the mechanical properties. Tests were performed at temperatures of 25°, 40°, 50°, 60° and 70°C with the materials exposed to humid air at 60 and 95 percent relative humidities, and to distilled water. Changes in weight, ultimate tensile strength, tensile modulus, percent elongation, interlaminar shear strength and in-plane shear strength were measured over a 40 days period, and the effects of the environment on these parameters were assessed. The mechanical testing was carried out at the end of 16 and 40 day test periods. Five resin systems were tested under the same conditions so that comparisons could be made. Two of the resins were Vinylester 411-45 and 470-36 both manufactured by the Dow Chemical Company. These resins are relatively recent additions to the thermosetting family. They have some features in common with unsaturated polyesters and have structural features similar to those of epoxides. Vinylester resins are notable for their high elongation and their convenient processing characteristics. It is claimed that these resins possess good corrosion resistance because of fewer ester groups per unit of molecular weight than corrosion resistant polyesters. Furthermore, the ester linkages are formed only at the ends of the molecule. This is in contrast to polyesters where ester linkages form part of the repeating unit. These resins were compared with epoxy MY750, 913 Pre-Preg both manufactured by Ciba Geigy and Crystic 272 (isophthalic polyester) manufactured by the Scott-Bader Company. The 913 PrePreg was supplied as a part-cured epoxy resin preimpregnated glass. Its usefulness is that it allows the moulding of high volume fraction ($VF=0.60$) good quality laminates with excellent environmental and mechanical properties.

CHAPTER 2

LITERATURE REVIEW

2.1 THE CHEMISTRY OF THE RESINS

A description is given of the polymers which have been used as resin matrices in this work. This consists of a brief outline of the chemistry of the resins, a mention of any fabrication problems and a statement of the relative advantages and disadvantages of the different types.

2.1.1 General Resin Chemistry

Polymer resins may be divided into two types, thermoplastic and thermosetting. The former consists of linear or branched chain molecules and are fusible and normally soluble in conventional organic solvents. In contrast, the thermosets in their final form have a three dimensional network structure and are infusible and insoluble. Their thermal and chemical resistance is therefore generally superior to that of the thermoplastics. The majority of the resins used in reinforced plastics are of the thermosetting type. These are of relatively low molecular weight and in the curing process chain lengthening, chain branching and finally chain crosslinking occur. This is evidenced by a change from liquid state through gelation state to a solid state. Curing may require the addition of curing (crosslinking) agent and catalysts besides the application of heat. The crosslinking can occur either through an addition or a condensation reaction. An addition reaction is a chemical reaction in which simple molecules (monomers) are added to each other to form long-chain molecules (polymers) and no by-products are formed, whereas condensation reaction is a chemical reaction in which two or more molecules combine with the separation of water or some other simple substance. By the variation of the structure of the prepolymer and of the curing agent and of their relative proportions, the number and length of the crosslinks may be varied and hence the properties of the final polymer (see Table 2.1)¹.

2.1.2 Polyester Resins

Polyester resins form a very important sector of the thermosetting resin industry. In fact it has been said that they are the foundation of the glass reinforced plastics (GRP) industry⁸. The basic materials which make up a polyester resin are a dibasic organic acid or anhydride reacted with dihydric alcohol (glycol)⁹. An unsaturated polyester resin may be prepared by reacting unsaturated dibasic acid such as maleic anhydride with a glycol. The acid rapidly melts in the glycol with mould heating¹⁰. To obtain a polymer chain which can be crosslinked into a thermosetting resin a proportion of the dibasic acid used must contain an unsaturated group or double bond¹¹. The commonest components which are used in the preparation of simple polyester resin are shown in Figure 2. By varying the ratio of the two anhydrides the reactivity of the polyester can be varied from low to high. A high reactivity resin contains a high proportion of unsaturation. The other major component of a polyester resin is a reactive monomer, generally styrene. The proportion of styrene to resin is approximately one to two. This serves as solvent for the polymer chain and viscosity reducer. Other diluents are vinyl^{acetate}, toluene, methyl methacrylate, and diallyl phthalate¹². Good colour and weather resistance, necessary for GRP, can be obtained by replacing part of the styrene by another monomer, methyl methacrylate. By varying the glycols and dibasic acids used, a whole family of polyester resins can be made. For example, a resin based on isophthalic acid in place of orthophthalic acid will have reduced water absorption. Similarly changing the glycol to neo-pentyl glycol (NPG) or bisphenol A gives resins with improved chemical resistance. Hence the wide range of resins commercially available today. The polyester resin used in this work was Cryslic 272. It is an isophthalic polyester resin (Figure 4). It is claimed that it has high mechanical strength and excellent strength retention in wet environments at medium temperatures up to 80°C¹³. The reason styrene is used as the reactive monomer is because of its general ease of use and relatively low price.

The low molecular weight polyester syrup is crosslinked in the presence of a peroxide by copolymerisation with the styrene, or another vinyl monomer to form an insoluble crosslinked structure. Crosslinking occurs via a free radical polymerisation reaction which is initiated by the decomposition of the organic peroxide (Figure 5). Accelerators are often added to help the decomposition of the catalyst to form free radicals. Two types are commonly used. The first decomposes by the application of heat (e.g. benzoyl peroxide). The second when mixed with an accelerator, a metal salt such as cobalt naphthenate will decompose at room temperature e.g. methyl ketoneperoxide, (MEKP). Crosslinking of a simple polyester resin with styrene is shown in Figure 6. A post-cure may however be necessary for the development of optimum physical and mechanical properties. Because room temperature cures may be used and because no volatiles are evolved in the reaction and hence pressure need not be applied, it is possible to construct large structures from reinforced polyester resins.

Typical cast resin properties of various classes of polyester resin are shown in Table 2.2¹¹.

2.1.3 Epoxy Resins

Epoxy resins^{14,15} are like polyester resins in having no volatile reaction (cure) products, although there may be a volatile solvent present. They have superior mechanical and electrical properties, but are more expensive than polyester, and present fabrication problems at least in the field of large glass laminate products. Epoxy resins are among the best matrix materials for many fibre composites. There are several reasons for this:

- i) Epoxy resins adhere well to a wide variety of fillers, reinforcing agent and substrates;
- ii) The wide variety of available epoxy resins and the curing agent can be formulated to give a broad range of properties after cure;

- iii) The chemical reaction between epoxy resins and a curing agent does not release any volatiles or water. Hence the shrinkage after cure is usually lower than in vinyl ester ~~or polyester~~ resins;
- iv) Cured epoxy resins are not only resistant to chemicals, but they also provide good electrical insulation.

Table 2.3¹⁶ shows that epoxy resins have superior strength and elastic properties with a lower shrinkage on curing and a lower coefficient of thermal expansion. The strength of the interface bond between resin and fibre is also higher for epoxy resins. However they have the disadvantage of a higher viscosity before curing and they are more expensive.

By definition, an epoxy resin can be identified by the presence of two or more epoxides in the molecule. Figure 7 shows an epoxide group. Chemically, this is a very reactive group since it is under strain and readily opens¹⁷. These resins were first developed in the 1940s. The most common epoxy is made from bisphenol A; other types are epoxy novolac and cycloaliphatics. Depending upon the choice of curing agent, these versatile resins can be made to cure or harden either slowly (several hours) or very quickly (less than 1 minute) at room temperature or at elevated temperatures¹⁸. Versatility is also achieved in performance. Epoxy resins can be formulated to yield a variety of properties ranging from soft, flexible materials, to hard, tough, chemical resistant products. They can be modified into low viscosity liquids for easy pouring or converted to solid compositions for laminating and moulding applications.

The chemical structure of an epoxy is often complex. The structure depends on the specific cure conditions because more than one reaction can occur during cure and the kinetics of these reactions exhibit different temperature dependencies. The major portion of these resins are derived from bisphenol, acetone and epichlorohydrin, as shown in Figures 8 and 9. Figure 10 shows the structure of a bisphenol A epichlorohydrin.

This type of epoxy is useful for casting, laminating, adhesives and coatings. As stated before the most outstanding property is their excellent adhesion which is due in part to the secondary hydroxyl group located along the molecular chain. A more common formula for the epoxy resin product of bisphenol A and epichlorohydrin commonly referred to as a diglycidyl ether of bisphenol A (DGEBA resin) is shown in Figure 11. The value of n , the number of repeating units, is dependent on the quantities of epichlorohydrin and bisphenol A reacted together. If a large excess of epichlorohydrin is used the probability of producing a resin where $n = 0$ is increased. As the excess of epichlorohydrin is decreased so the value of " n " is increased. As n increases the molecular weight of the resin increases as does the viscosity. DGEBA resins vary in form from being moderately viscous (ca. 50 poises) to low melting solids (MP: 70°C).

The epoxy resin has to be cured (crosslinked) into a three dimensional network to be useful. This is done via a curing agent. The crosslinking of the resin can then occur through epoxide on hydroxyl groups, by direct linking of resin molecules, with the aid of a catalyst and linking via a reactive intermediate. Most reactions used to cure epoxy resins occur through the epoxide ring. It is the capability of this ring to react in a variety of ways with several different reactants that gives epoxy resins their versatility.

The resins as described cannot be crosslinked at a rapid enough rate by the application of heat alone and a curing agent must be added. The epoxy system is a very versatile one in that many different curing agents may be used and the properties of the final network structure therefore tailored to a certain extent to meet specific requirements.

The curing agents most widely used are those containing several active hydrogen atoms and can be written in the form RXH e.g. polyamines, polyphenols etc. The reaction is shown in Figure 12. The resin and curing agent usually have more than one reaction site per molecule thus accounting

for the three-dimensional network. The curing agent used for this work was a polyamine (HY 951 ex Ciba-Geigy - triethylenetetramine) - see Figure 13.

2.1.4 Vinyl Ester Resins

Vinyl ester resins are a relatively recent addition to the thermosetting family of resins suitable as matrices for fibre reinforcement. They were commercially introduced during the 1960s^{19,20}. Vinylesters are related to both polyester and epoxy resins and in fact show the more favourable properties of both of these. Because they contain unsaturated vinyl groups in the chain, they can be cured with vinyl monomers, such as styrene, in the same way as polyester, therefore making fabrication by hand lay-up techniques practicable. The backbone of a vinyl ester resin molecule however is identical with that of an epoxy and therefore the good mechanical properties exhibited in epoxides are also reflected in vinylesters. The definition of a vinylester resin is simply "a polymerizable resin in which the terminal positions of the resin are vinyl ester groups and in which the main polymeric chain between the terminal positions comprises the residue of a polyepoxide resin"²¹. A simple polyepoxide resin is synthesised by reacting epichlorohydrin with bisphenol A as shown in Figure 14. Advantages²² claimed for this system are as follows:

- i) The initial resin can have a precise chemical structure and is of relatively low molecular weight
- ii) The epoxy resin backbone conveys high resilience
- iii) The presence of hydroxyl groups promotes setting of and adhesion to reinforcing fibres such as glass and carbon
- iv) The terminal location of the reactive sites ensures a more uniform polymer structure, which may result in lower internal stresses

- v) The lower number of ester groups combined with a polyester resin means that the vinylesters have lower water absorption and improved chemical resistance.

Vinylesters are most commonly manufactured by terminating an epoxy resin with a vinyl group through the addition reaction of an epoxy resin with an acrylic monomer, such as acrylic acid (Figure 15). The reaction of an acid addition to the epoxide ring (esterification) is exothermic and produces a hydroxyl group without the formation of by-products (e.g. as in polyesterifications where water is produced). Epoxide resins that have been used to produce vinylester resins include the bisphenol A types (general-purpose adherent resistant vinyl esters), the phenolic-novolac types (heat resistant vinyl esters) and the tetrabromo bisphenol A types (fire-retardant vinyl esters). After production the vinyl ester is then diluted with a reactive monomer such as styrene.

The molecular weight of the epoxy resin portion can be controlled by reacting the diglycidyl ether of bisphenol A with specific amounts of bisphenol A²³. Physical properties such as tensile strength, tensile elongation and heat distortion temperature are relatable to the molecular weight of the epoxy resin portion of the vinyl ester resin. Thus vinyl ester resins can be tailor made to meet the requirements of specific applications. A direct comparison of the molecular structure of two chemical resistant resins, are a bisphenol A, fumaric acid polyester and the other a vinyl ester, will help to demonstrate the improved chemical resistance of the vinyl ester resins. The vinyl ester resin differs in two important aspects. Firstly it does not contain any ester groups within the main polymer chain. Secondly, the reactive vinyl sites, unlike the polyester, are situated at the ends of the vinyl ester chain. Since the ester groups are subject to hydrolytic acid, this makes the polyester much more vulnerable, and once attacked the chain is split up leaving it open to further chemical attack^{24,25}. In the vinyl ester, however, not only are there fewer ester groups, but also, even if they are attacked the main body of the molecule remains unaffected. The attack

mechanism is more complex for some types of chemical and optimum resistance to chlorinated solvents (like ethylene dichloride and monochlorobenzene) and the strongest bleaching agents (like chloride dioxide and sodium hypochlorite) has been achieved with vinyl esters having a higher crosslink density. These resins also have a higher glass transition temperature and may be used at higher operating temperatures. Figure 15 shows a comparison of the two molecular structures.

The epoxy resin products from the backbone of vinyl ester resin and DGEBA is in fact the backbone of the Derakane 411 series of resins. In studying the 411 series there are two forms of this resin marketed by Dow, mainly 411 and 411-C. Although of similar structure they differ in that 411 is of higher viscosity than 411-C. It is likely that they differ in the molecular weight backbone ($n = 1.3$) than 411-C ($n = 0.2$). The DGEBA backbone will provide vinyl ester resins, and in particular Derakane 411-45, with excellent mechanical properties and good thermal properties. Figure 17 shows the structure of Derakane 411-45. It is a general purpose vinyl ester resin, containing 45 weight percent styrene.

A further epoxy type used as a backbone for vinyl ester resins is the resin group of epoxy novolacs. These resins are produced by reacting epichlorohydrin with a novolac resin¹⁸ while novolac resins are a product of phenol and formaldehyde as shown in Figure 18. Further reaction can take place and a novolac of the general structure shown in Figure 19.

These novolac resins can then be reacted with epichlorohydrin to produce the epoxy novolac resin structure as shown in Figure 19. The important point to note is that unlike the DGEBA resins where there are only two epoxide groups, epoxy novolacs are multifunctional and the number of remnant epoxide groups are dependent on the value of n (number of epoxy groups is equal to $n+2$). It is worth mentioning that because of their multifunctionality these resins produce on cure a tightly crosslinked system with better elevated temperature performance, chemical resistance and adhesion than DGEBA resins. The epoxy novolac structure provides

the backbone for the Derakane 470 group of vinyl ester resins. Because of the properties of the backbone 470 resins have extended the useful operating temperature of vinyl ester resins while retaining excellent corrosion resistance.

The reaction between 470 type backbone and methacrylic acid is complicated by the fact that (unlike 411 type backbone where ester linkage is only present at the two ends of the backbone), ester linkages are formed similarly at both ends of the 470 type backbone and in addition at the site of each epoxide group within the repeating unit. Figure 21 shows the reaction of methacrylic acid with the 470 type epoxy unit. In the 470 series of resin, vinyl unsaturation is present at the terminal groups and within each repeating unit of epoxy novolac backbone. The result of this is that 470 series of resin is more highly crosslinked than the 411 types.

In the case of all the vinyl ester resins used in this work the cross-linkable monomer is styrene. The resins are cured by a free radical copolymerisation and it has been stated¹⁴ that this reaction can be promoted by heat which breaks down the peroxide catalyst into free radicals. However to enable the reaction to take place at room temperature initiators are used to promote the cure. The initiation (e.g. cobalt octoate, cobalt naphthenate, dimethyl aniline) act by breaking down the peroxide catalyst (e.g. methyl ethyl ketone peroxide) to give two free radicals. Each free radical is able to react with the vinyl monomer and in doing so forms a new free radical. See Figure 5. A rapid chain reaction is initiated and a crosslinked structure is built up by reaction of the free radical with the vinyl unsaturated groups within the vinyl ester resin. As the crosslinking proceeds the vinyl ester changes from a liquid to a waxy solid and finally to a hard solid. Although the cure takes place at room temperature the vinyl ester experiences an exotherm of the order of 200°C on cooling the vinyl ester is not totally cross-linked (or cured). This is due to 'gel effect' which partially inhibits the cure²⁶. The inhibition is caused by loss of mobility of the styrene

as the solid phase is formed during cure. To remobilise the styrene and effect full cure the vinyl ester is post cured at 80-100°C for two to three hours. Of the resins used the 470 series are far more reactive than 411. The catalyst/accelerator proportions used for these resins is based on a formulation found²⁷ to give complete cure with 411-45. These proportions were as follows

Catalyst "M"	(50% MEKP)	2 ml
Accelerator "R"	(6% cobalt octoate)	0.3 ml
Accelerator "D"	(10% DMA)	0.05 ml
Per 100g of resin.		

In addition to hardening the resin, the cure also shrinks the resin. The amount of shrinkage is dependent upon the crosslink density of the resin and so 470-36 will exhibit more shrinkage than 411-45.

Table 24 shows typical physical properties of the vinyl ester resin. The mechanical properties of a vinyl ester resin are generally superior to those of conventional polyester resins and comparable with those of established epoxy resins^{28,29}. During the curing of vinyl ester resins the carbon to carbon double bonds ($-C=C-$, vinyl groups) at the ends of the chain virtually all react leaving very few $-C=C-$ bonds to be susceptible to oxidation and other types of chemical attack. The few ester groups in vinyl ester resins contribute towards the superior chemical resistance of vinyl ester resins³⁰.

2.1.5 913 PrePreg

913 PrePreg is manufactured by Ciba Geigy Ltd, and for this work was supplied as a part cured epoxy resin preimpregnated glass. Its usefulness is that it allows the moulding of high volume fraction ($VF = 0.60$) good quality laminates with excellent environmental and mechanical properties.

The resin system of the 913 system is known to contain two epoxy resin types and a further additive with dicyandiamide hardener²¹. The two epoxy resins are MY 750 and MY 720, and the MY 750 portion is in excess of the MY 720 portion. MY 750 is a general purpose resin produced by Ciba Geigy and is a diglycidylether of bisphenol-A (DGEBA) resin. The structure is shown in Figure 11.

This structure can be compared to the epoxy backbone of Derakane 411-45. It can be seen that 411-45 is the vinyl ester equivalent of the epoxy resin MY 750. MY 750 imparts excellent strength and toughness to a glass or carbon fibre laminate. However it does not have the high temperature properties that MY ⁷²⁰~~270~~ has. This epoxy resin has a much more complex molecular structure as shown in Figure 22.

The name or chemical nature of the third additive has not been made available to Loughborough University of Technology but information gained from Ciba Geigy stated that it improved the impact properties of the cured PrePreg as well as acting as a processing additive. It is likely that the unknown additive is thermoplastic in nature and a considered guess is that it is a member of the polysulphone group of plastics.

MY 750 and MY 720 can be cured by adding an amine hardener. For example the reaction between a primary amine and the epoxy resin would progress as shown in Figure 23.

The secondary amine can react with further epoxy groups or other polymer chains and in this manner crosslinks are formed (Figure 24). However, these simple curing agents are not suitable for PrePreg as they would not allow the PrePreg to have any shelf-life (913 has a shelf-life of one month at 25°C and 18 months at -18°C) and the quality of the cured article would not be of the order required. For this reason 913 PrePreg contains a more complex amine hardener, dicyandiamide (DICY), see Figure 25.

DICY is often referred to as a latent curing-agent and it is this property that makes it so attractive for PrePreg. There is little or no reaction with the PrePreg at room temperature but full cure is rapidly reached at elevated temperatures. The 913 PrePreg is supplied B-staged (or part-cured) and the part-cure takes place during manufacture after the glass or carbon has become impregnated by the resin. This part-cure imparts handleability to the PrePreg. At a later stage when fully cured at higher temperatures (up to 150°C), the following reactions take place:

- i) epoxy-epoxy reaction are catalysed by the tertiary amine, and
- ii) reaction between -OH groups on epoxy with hardener cyanide groups.

2.2 ENVIRONMENTAL EFFECTS ON FIBRE REINFORCED COMPOSITES

Fibre reinforced plastics are being used increasingly in the aerospace industry because of their strength and stiffness, combined with their low density and the low cost of the finished components. In a service environment, fibre composite structures will be exposed to ultra-violet radiation, lightening strikes and atmospheric moisture and consideration must be given to their effect on mechanical properties.

Most aerospace applications use fibres in polymeric matrices, usually epoxy resin. The polymeric matrix^{31,32} will absorb moisture directly from the atmosphere. Reinforcing the resin with fibres does not prevent such moisture absorption from occurring. The effect of this moisture uptake is to plasticise the resin and to lower the glass transition temperature (T_g), and thus to influence directly the load carrying properties of the material. The strength properties that are dependent upon matrix properties such as compressive strength, interlaminar shear strength etc. will suffer most degradation. As moisture content increases so will the degree of degradation.

A gaseous or liquid environment may produce profound changes in properties of composite materials. These can best be understood in terms of the effect of these environments on the individual constituents, i.e. fibre, matrix and interface. These regions are shown in Figure 26. It is generally recognised that the glass/matrix interface is the determining factor of the reinforcement mechanism, especially wet strength retention³³. A summary of the main changes which can occur is given in Table 2.5^{34,35} and also described in the following sections.

2.2.1 The Effect of Moisture on Glass Fibres

The E glass fibres commonly used in fibre composites consist of 55 per cent SiO_2 as the main component and oxides of other metals such as Al, Mg, Ca as the remainder³³. The fibres are coated with a coupling agent which protects the glass and assists its binding to the matrix.

Glass fibres are brittle and their strength is very sensitive to imperfections such as voids, cracks, surface scratches etc. The classical brittle fracture theory postulated by Griffith³⁶ assigns the following approximate expression to the brittle strength:

$$\sigma_u = \sqrt{\frac{VE}{\pi c}}$$

where V = specific surface energy

E = Young's modulus

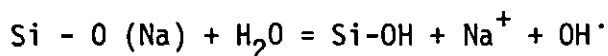
c = crack length

The environmental factors (especially humidity) tend to reduce specific surface energy (V) and with it the tensile strength. In fact the "virgin" strength of glass measured in a liquid nitrogen (-196°C) environment³⁷ is about 10^6 psi as against $200\text{--}500 \times 10^3$ psi under ambient conditions. The energy required for glass to absorb water molecules (interface energy)

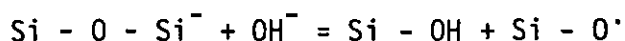
while submerged in water is lower than the energy required for glass to adsorb water molecules in the air. Hence a lower critical stress is required for the spontaneous propagation of existing cracks in a water environment⁶.

The presence of liquid water on the untreated glass surface can lead to stress corrosion³⁸. This is caused by the water leaching alkali salts out of the glass. The presence of a protective coating on the fibres does not totally prevent attack. Evidence of attack on the coated fibre/resin interfaces has included leaching of sodium salts from the glass³⁹. The degradation of glass fibres by moisture attack occurs in three stages:

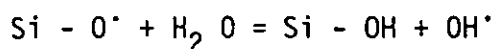
The first stage of attack consists of the following chemical reactions, with the sodium ions migrating outward:



During the second stage the OH^- ions disrupt the strong siloxane bond (the main structural backbone of glass), producing a $\text{Si}-\text{O}^-$ molecule:



which in turn decomposes another water molecule (the third stage, a repetition of the first):



Consequently an alkaline medium is created, the OH^- concentration being equivalent to that of the released Na^+ . This in turn gradually raises the pH level.

Islinger et al⁴⁰ have suggested that moisture can attack glass surfaces forming alkali hydroxide and silica hydrosol gel solutions. The presence of the alkali hydroxide could further enhance the corrosive action of the moisture, changing an initially reversible absorption process into an irreversible one.

The environment also affects the strength properties of the fibres. Glass fibres are susceptible to water leaching of the soluble oxides such as K_2O and Na_2O . After prolonged exposure, leaching results in surface pits and reduction of properties. The presence of dissolved salts in the water around the fibre can lead to the generation of osmotic pressure which may eventually produce debonding at the interface even in the absence of an applied stress. Therefore, surface degradation of the glass (with resulting reduction in composite strength) is unavoidable unless the surface is protected by a strongly-bonded polymeric coating³⁵.

2.2.2 The Effect of Moisture on the Interface

A composite material must contain an interface region that transfers stress between the matrix and fibres⁴¹. The boundary between resin and reinforcement is sometimes regarded as a third phase or 'interphase' region. Some kind of adhesive bond either physical, mechanical or chemical, is essential between the matrix and fibres. Such a bond enables the matrix to transfer loads between the fibres. The matrix also protects the fibre against mechanical damage or chemical attack. The fibres are usually coated with a coupling agent and the primary function of the coupling agent is to provide a strong chemical link between the oxides groups on the fibre surface and the polymer molecules of the resin. The basic principles are illustrated in Figure 27. The general chemical formula for silane coupling agent is $R-SiX_3$ ³⁵. This is a multifunctional molecule which reacts at one end with the surface of the glass and at the other end with the polymer phase. A mass of indirect evidence already cited^{42,51} suggests that properties of composites particularly mechanical properties, are often limited by failure at the interface, and this is supported by direct evidence of separation of the interface by visual

observations and electron micrography. It has been suggested that the weakest portion of the fibre reinforced plastic system is the glass/coupling agent interface^{52,53}. This interface is especially weak when water is present. Bernett and Zisman⁵⁶ observed that a clean glass surface exposed to ordinary atmospheric conditions immediately picks up a molecular layer of water. Water can only reach a bonded interface by diffusion both through the matrix and along the interfacial layer. The path length for diffusion may be stunted when ingress into a composite is assisted by capillary flow along channels, for example voids or stress cracks^{57,59}. The word 'wicking' has been correctly used to describe this process, but it has also been used rather loosely to denote the accumulation of water in the channels formed around filaments that are debonding. The appearance of wicking is indicated by the spread of debonding from exposed fibre ends in some systems. This occurs either because there is only a physical bond that can be rapidly displaced by water, or because diffusion along the interfacial layer is much faster than diffusion through the matrix⁵⁹. Wicking in these senses, however, is by no means general and diffusion of water through the matrix can equally well cause debonding^{42,44,60}.

Optical retardation is an experimental method used to detect fibre debonding in a matrix⁶¹. Measurements using this technique have been used to detect the bonding of coated and uncoated fibres in a polyester composite. The samples were immersed in distilled water at 20°C and at 100°C with fibres embedded to a depth of less than 10 µm. With the coated fibres no debonding was determined during periods of immersion at 20°C for up to 10 months. In hot water debonding was only detected after relatively long immersion times. During the initial period of resin swelling, the chemical bonding introduced by the coupling agent is able to withstand the tensile interfacial stresses produced. Debonding is eventually initiated by the growth of discontinuous bubble-like regions at the fibre interfaces. In boiling water these appeared after 4 hours and eventually joined to produce complete debonding (after about 60 hours). It must be stressed, however, that these observations are for polyester resins and may not apply in other resin systems. The resins used in determining

the above results were films approximately 200 μm thick. Consequently the results may only be used to compare the different environments and the effect of coating the fibres. With the uncoated fibres an increase in the resin retardation after 20 minutes indicated the initiation of debonding. Complete debonding occurred after about 2 hours. In boiling water debonding occurred after only a few minutes.

* In the usual GRP materials two types of chemical bond are susceptible to hydrolysis, siloxane and ester linkages. The former occurs in the glass between the glass and coupling agent, and within the coupling agent⁶²⁻⁶⁵. The presence of water, which may diffuse through the resin to the interface, the covalent H-O bond hydrolyses as shown in Figure 28. Since this process is reversible the covalent bond can reform when the water is away. Thus, in the presence of a simple shear stress parallel to the interface (Figure 28b) the surfaces can slide past each other without permanent bond failure. Direct experimental evidence for this reversible bond process has been obtained by Fourier transform infra-red spectroscopy⁶⁶. The ester linkages occur in polyester resins, in anhydride-hardened epoxides and in some coupling agents. The hydrolytic degradation of polyester and epoxy resins is well established^{42,44,67,68,69}. It is accompanied by the extraction of low molecular weight materials and the formation of characteristic circular cracks. The rates of hydrolysis can be appreciable in the context of the life desired for GRP structures, although it is difficult to measure for the separate materials when they are combined in a composite.

Vaughan et al⁷⁰ studied the influence of moisture on the glass-coupling agent and the resin-coupling agent interfaces and the ultimate effects on the resulting reinforced epoxy commercial laminates. It was found that the presence of water affected the physical properties of the laminate after prolonged immersion. During short immersion periods no significant indication of moisture attack on silane finished glass fabric was detected.

According to Eakins⁴¹ the degree of order of successive molecular layers decreases with increasing distance from an interface and their response to external stress decreases similarly. He suggested that the effect of water penetration on the resin is twofold:

- i) remote layers undergo swelling, whereas those close to the interface are stiffened and their capacity for energy absorption is reduced;
- ii) the water forms very thin layers at the interface, counteracting the matrix-fibre bond and creating an alkaline medium at high temperatures which intensifies the debonding process and may eventually lead to failure at relatively low load levels.

Pressure pockets generated at the fibre matrix interface during immersions cause further disruption of the glass resin bond⁷¹. There are at least three mechanisms by which diffused water can lead to the generation of internal pockets of pressure⁷².

i) *Gas release:*

This can occur by the reaction of dissolved hydrolysible chlorine in the unreacted resins with, for example, calcium carbonate inclusions from the atmosphere. The gas evolved is carbon dioxide. This can only occur if hydrolysible chlorine is present in the resin, epoxy resins are the main example.

ii) *Hydration:*

Impurities such as Al_2O_3 or clay may be introduced into the resin or fibres during handling, or from the atmosphere. Pressure from the hydration of such inorganic salts can lead to crack propagation.

iii) *Osmosis:*

When a solute is dissolved in a solvent, the chemical potential of the solvent diminishes. Chemical equilibrium can only be obtained if the solvent and the solution have different pressures. In practice the

exchange of solvent without equalisation of pressure can be realised with the aid of semi-permeable membranes*. Whether the resin can sustain such pressures will be determined by the degree of crosslinking. The observed higher incidence of fractures in composites exposed to fresh water than in composites exposed to salt water indicates that ions as well as alkali metal ions are less readily able to permeate hot, wet resins.

Debonding is often a spontaneous process, and so must be favoured by a consequent decrease in the energy of the system⁷³. In the absence of an external load, there are three main sources of energy change. Strain energy in the resin and glass due to their differential volume change, the chemical energy change of network (e.g. hydrolysis), and surface energy changes on debonded interfaces separate.

2.2.3 The Effect of Moisture on the Matrix

In a composite the role of the polymeric matrix is two-fold: protection against environmental attack; and a load transmitting medium.

When left in a humid environment resins absorb water molecules by a diffusion process³⁸. The molecules become attached by hydrogen bonding to polar groups such as hydroxyl and amine groups which exist in the resin structure. The molecular network then expands, to an extent governed by the crosslink density, and the resin swells. In some cases this can produce voids in the resin. Water penetration of the matrix takes place by the following mechanisms⁷⁴: (a) through fibre-matrix interfaces (capillary); (b) through the resin (diffusional), and (c) through cracks and voids in the composites. The capillary mechanism is much more prominent than its diffusional counterpart. As for the third mechanism, its contribution depends mainly on the size and distribution of the cracks and voids.

* A porous material capable of sustaining a pressure differential and which allows free passage to the solvent, but not to the solute.

The water will cause plasticisation of the resin and will reduce the value of the transition temperature T_g between the glassy state and rubbery state. The water also reduces the stiffness of the resin and causes it to swell.

2.2.3.1 The Effect of Moisture on Epoxy Resins

Epoxy resins absorb atmospheric moisture, apparently by instantaneous surface adsorption and subsequent diffusion through the interior. The absorbed water is not liquid, but exists rather in the form of hydrogen bonded molecules or clusters within the polymer. The rate at which water diffuses into the epoxy resin is much lower than that for polyesters. On the other hand the total quantity of water absorbed by epoxy castings after prolonged periods is surprisingly high - often 4-7% w/w^{74,75}.

Water absorption by epoxy polymers depends on their chemical structure, in general the more 'polar' the polymer the larger the amount of water absorbed. Cured epoxy resins when immersed in the liquid water absorb several weight percent, the amount being a function of the structure of the resin and the type of hardener used to effect cure^{76,77}. The results presented by Rashid⁷⁶ establish clearly that the amount of water absorbed by the epoxy resins depends on the type of hardener used and the chemical structure of the crosslinks determines the water sorption behaviour. The polyamide cured resin absorbs nearly four times as much water as the anhydride-cured resin. It was also noted that for the resins cured with the polyamide or phthalic anhydride the water absorption was not reversible even at modest temperatures. Water absorption by the diamine-cured resins was reversible.

The importance of absorbed water is due to its effect on the properties of the resin. The resin's glass transition temperature is lowered^{78,79}, and elastic moduli and compressive strength are reduced. Over recent years there have been a number of reports on water absorption in cured

epoxy resins⁸⁰, their composites⁸¹ and the effect of thermal cycling⁷⁵.

One of the more extreme environmental conditions experienced by an epoxy composite matrix occurs during a supersonic dash of a fighter aircraft. The aircraft dives from high altitudes (where outer surface temperature is -20 to -55°C) into a supersonic, low-altitude run during which aerodynamic heating raises the surface temperature to 100 - 150°C , in a matter of minutes. On reduction of speed the outer surface temperature drops extremely rapidly at rates up to about $500^{\circ}\text{C}/\text{min}$, thus exposing the epoxy composite to a thermal spike. Simulation of such thermal spikes has been shown to increase the amount of moisture absorbed by the epoxy or epoxy composite⁸²⁻⁸⁶. However, after a certain number of consecutive thermal spikes, the amount of moisture absorbed ceases to increase. Browning⁸¹⁻⁸³ suggested that such increases result from micro-cracks caused by the moisture and temperature gradients present during the thermal spike. The damage does not occur unless the thermal spike maximum temperature exceeds the T_g of the moist epoxy.

Work on unfilled epoxy resins⁶ has shown that the weight increase of samples exposed to hot water was greater than the weight increase of the samples exposed to cold water. Dimensional changes also tend to follow the same pattern. Specimens exposed to hot water undergo pronounced degradation, which sets in shortly after exposure and is associated with a significant irrecoverable weight loss. Degraded specimens are characterised by higher void content and lower strength compared with their cold water counterparts. The degradation process is attributed to penetration of water into the matrix-fibre interfaces and is followed by an attack, at high temperatures, on the glass-fibre surface and coupling agent. The observed weight loss has been attributed to leaching. As no such behaviour was detected in the unfilled samples, the leached material must have originated mainly in the glass-fibres, or in the coupling agent phase (which helps to bind the fibres to the matrix). Samples exposed to a hot water environment were then placed in a cold water environment together with some fresh samples. The samples previously exposed to hot water gained significantly more weight than their cold water

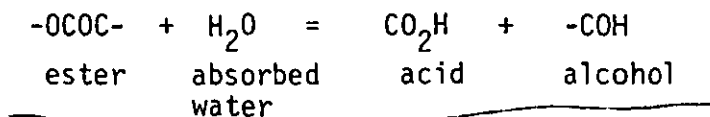
counterparts. This confirms the assumption whereby leaching by hot water resulted in higher void content within composite interfaces, which was in turn reflected by subsequent higher water absorption.

The work reported in references 75-86 indicates that at room temperature properties are not significantly altered by water absorption. There is also general agreement that the presence of absorbed moisture does result in a diminution of mechanical properties at elevated temperature. Figures typically range from a 15-60% loss of interlaminar shear strength and a 0-60% loss of flexural strength of moisture content levels which would be expected to occur in service. The slight permanent loss of properties which occurs in some cases is most probably due to swelling of the matrix and the production of voids. It is known that the ILSS of a composite decreases by about 7% for every 1% void content⁸⁷.

Water absorption by fibre-reinforced epoxy resin can significantly alter its conducting and dielectric properties⁸⁸, but these changes are usually found to be reversible on drying. In the case of carbon-fibre composites the effect of the absorbed water is to decrease its conductivity in a direction normal to fibre alignment. This is due to a decrease in fibre-to-fibre contact. In addition, the swelling which occurs acts like an externally applied strain and also increases resistivity. Conductivity is greatly increased in glass-fibre reinforced epoxy resin which has absorbed more than a certain amount of water.

2.2.3.2 The Effect of Moisture on Polyester Resins

Polyesters are known to be susceptible to hydrolysis i.e. to chemical attack by water. Their molecular mass is reduced by the reaction and consequently their physical properties. Polyester contain ester groups in the main chain. Hydrolysis of the ester groups may be expressed by:



In work by Steel⁸⁹, styrenated unsaturated polyesters were found to be incompletely cured in air due to inhibition of the curing reaction in the presence of oxygen. The system resulting from such a cure had low heat stability, low resistance to hydrolysis, and showed greater swelling in solvents than those cured in the absence of air. Postcuring in water or an inert medium led to a further reaction of the residual styrene-monomer and anhydrides with radicals fixed in the network⁹⁰. Increases in the glass transition temperature (T_g) however, were also observed for polyesters that had been postcured in water when the residual monomer had been completely exhausted⁹⁰.

✓ Steel⁹¹ observed that unstressed castings of polyester resins showed gross disc cracking when exposed to hot water for long periods of time. He studied the kinetics of crack formation and suggested that plots of crack initiation time against temperature followed the Arrhenius relationship, being linear down to 40°C for at least one resin, with an activation energy of about 100 kJ mol⁻¹. These plots are reproduced in Figure 29. Steel observed that for a given resin, cracking always occurred at the same water absorption level, and deduced that (at least in some cases) cracking would never occur at ambient temperatures, since the critical water uptake level would exceed the equilibrium absorption value. Another conclusion emerging from this study was that the crack initiation time increased slightly with post-cure time. The explanation offered by Steel concentrated on the rupture of polyester chains either by swelling forces or by the hydrolytic scission of ester groups.

About the same time as Steel was reporting these findings, another study by Ashbee et al⁵¹ was directed to the same disc cracking phenomenon. The cracks, in unsaturated polyester resins, were studied by optical and electron microscopy. The size, number and orientation of the cracks were different in different polyester resins. Sometimes the orientation was random, but in other cases most of the cracks were roughly parallel to the specimen surfaces. These authors proposed that the cause was osmosis arising from water-soluble inclusions.

Pritchard et al⁹² reported the time taken to produce disc cracks in polyester glass laminates exposed to hot water on one side only, as in a tank or pipe. Most of the cracks were confined to the region just below the surface exposed to water. The surface regions also underwent a different kind of cracking, probably as a result of shrinkage through further cure.

Work on glass reinforced polyester⁹³ has produced a plausible explanation for the weight variation of samples submerged at high temperatures in a water bath. Initially the water uptake followed a pattern predicted by the Fickian diffusion model (see Section 2.3). Deviation from the calculated values occurred after the development of microcracks on the surface and inside the sample. These cracks were formed owing to the moist, high temperature environment. After a few hours material loss was observed. As long as the moisture gain was greater than the material loss the weight of the sample increased. Once the weight of the lost material exceeded the weight of the absorbed moisture, the weight of the sample decreased. Of course when the material was lost the measured weight change no longer corresponded to the moisture content of the material.

Numerical values for the percentage weight loss of polyester resin and glass reinforced polyester exposed to water at different temperatures have been determined⁹⁴. Although the polymeric composites behave like the resin kinetically, the equilibrium water uptakes and weight losses are influenced by the presence of the fibre. The composites take up more water than the pure resin, especially at higher temperatures, at which debonding of the fibres from the matrix is more evident and induces localized water entrapment is more evident. Apicella et al⁹⁴ found that weight losses after a fixed time are also strongly influenced by the test temperature. The higher weight losses observed for the composite, especially at 90°C, may indicate that segregation or incomplete curing of some prepolymer components may occur around inclusions. Unreacted components or partially bonded groups may be desorbed easily and preferentially to the debonded and water-coated fibres.

Apicella et al⁹⁴ concluded that the exposure of the resin and composites to water at different temperatures induced modifications in the mechanical properties. The chemical attack on the ester linkage may be responsible for the low heat resistance in the presence of absorbed water. Embrittlement of the matrix results in the loss of segments which plasticize the unaged resin. The degradation mechanism may be associated with both the low chemical resistance and the possible migration of some of the components initially present in the thermoset.

In further work Apicella et al⁹⁵ also noted the low hydrolytic stability for the isophthalic resins, which underwent significant weight losses and embrittlement after conditioning in water. Moreover, both isophthalic and bisphenol B resins showed the formation of randomly distributed disc shaped fractures of sizes ranging from 0.1 to 1.0 mm, probably due to hydrolysis, which further depressed the mechanical strength. Crack formation was observed in the system B to a much lower extent than in the isophthalic resin and only after four times longer exposure periods.

Glass-polyester laminates used for the construction of boat hulls sometimes develop small blisters in localized regions below the waterline. These blisters are developed slowly as a result of immersion in water. It is commonly found that small, lightweight craft, such as canoes, are free from blisters, because they are lifted from the water after use, whereas boats of 10 metres in length remain in the water for months at a time. The extent of the problem is almost as much a matter for controversy as the cause; some reports indicate that only a few percent of all polyester boats suffer from noticeable blisters⁹⁶, while others suggest that the defect is more common⁹⁷. Blisters have also been observed in swimming pool liners and in chemical process equipment. Once a laminate has been seen, then any blisters which form will do so more rapidly at high temperatures than at low ones. Klunder and Wilson reported⁹⁸ that the time to blister in distilled water, for a 4 mm thick chopped strand mat orthophthalic laminate with an isophthalic

gelcoat, was two years at 20°C, 720h at 40°C, 480h at 60°C, 120h at 80°C and 48h in boiling water. Naturally the higher temperatures have relevance only for laboratory test panels and for special applications such as water tanks and pipes.

2.2.3.3 The Effect of Moisture on Vinyl Ester Resins

Vinyl esters are a relatively recent development in the field of synthetic resins. Consequently there is very little information available on their behaviour. The main body of the literature refers to epoxide and polyester resins.

By far the largest use of vinyl esters is in making corrosion resistant equipment. There are numerous reports and data concerning the chemical resistance of resins and composites. These include published papers on the corrosion behaviour and mechanisms due to immersion in different liquids i.e. sodium hydroxide, acids, oil, etc⁹⁹⁻¹⁰⁵. Little information is available on the effect of water on the vinyl ester resin or composite.

Like the polyester resins, the vinyl ester resins are known to be susceptible to hydrolysis¹⁰³, that is the water degrades bonds in the backbone of the resin. The bond most susceptible to hydrolysis is the ester linkage. Hydrolysis of ester linkages may occur in hot water where it is a reaction of some concern for the general purpose polyesters. The reaction is accelerated by acid or base. The presence of styrene as a co-reactant in the resin blends is beneficial in reducing the extent of the reaction. In addition, vinyl esters have a methyl group deriving from methacrylic acid which shields the vulnerable ester linkage. Further, most of the vinyl esters have but two ester linkages per molecule which should make them less susceptible to attack than the true polyester resins.

The relative hydrolytic stability of the resins can be related firstly to their tendency to undergo disc-cracking. Loader¹⁰⁶ studied the water

absorption of unsaturated polyester resins and compared them with vinylester resins. The experimental method he used was to expose specimens of cured polyester and vinylester resins to deionised water at 20°C, 50°C and 80°C, and to monitor appearance and weight. The results obtained showed that disc-cracking did not occur in any of the vinylester resins, at 20°C, 50°C and 80°C, whereas disc-cracking was observed for the polyester resins.

Apicella et al⁹⁵ also observed from their work, that the vinylester resin showed the highest stability on ageing, which was slightly higher than that of the bisphenol A polyester. Although these systems were also embrittled by the long term conditioning in water, the effect was less evident.

2.2.4 The Effect of Moisture on Composite Properties

Moisture and temperature may affect the performance of composite materials, i.e. tensile strength, shear strength, elastic moduli, fatigue behaviour, creep, swelling (dimensional changes) and electrical resistance. The absorption of moisture from humid environments at room temperature is in general a reversible process and with most advanced composites there is no degradation in room temperature mechanical properties¹⁰⁷. Because moist resins soften at elevated temperatures, resin dominated strengths and stiffnesses are significantly less at these temperatures, than those for dry composites. Certain combinations of temperature and moisture (and stress) can produce microcracking in the resin or at the fibre/matrix interface which will degrade the mechanical properties even at room temperature. For instance 15% to 60% less inter-laminar shear strength can be expected at temperatures and moisture contents expected in service³⁸. In compression, the fibres rely on the matrix to provide the support necessary to prevent fibre buckling; under hot/wet conditions the resin softens and the compression strength is reduced (Figure 30). Since the compressive strength is reduced under hot/wet conditions, the flexural strength shows a similar trend⁸⁶ (Figure 31) and exhibits compression face failures. Tests on chopped strand mat

(CSM) polyester laminates reported by Scott Baden¹⁰⁸, give stiffness retention data after 300 days immersion in distilled water at 20°C. For laminates with unsealed and sealed edges, it was found that 89% and 97% of the initial flexural modulus was retained. When immersed in water at high temperatures, strength properties depend on the temperature resistance of the resin. Modulus retention data for several CSM reinforced polyester resins immersed in distilled water at 100°C for 50 days are reported by Pritchard¹⁰⁹. Table 2.6 gives flexural modulus retention data taken from this paper. It is seen that modulus retention varies from 58% for orthophthalic resin to 97% for bisphenol types. Strength retention data for various CSM reinforced polyester resins immersed in distilled water at 100°C for 50 days are given by Pritchard¹⁰⁹. Table 2.7 shows flexural strength retention data. There is a significant reduction in tensile strength, although modulus values, shown in Table 2.7, were less affected. As expected the vinylester and bisphenol laminates have the superior properties.

The effect of moisture and temperature on resin properties and resin dominated composites properties have been generalised¹¹⁰ into a simple algebraic expression for incorporation into available composite micro-mechanics equations:

$$\frac{\text{Wet resin mechanical property at test temperature}}{\text{Dry resin mechanical property at room temperature}} \approx \left| \frac{T_s - T}{T_s - T_0} \right|^{\frac{1}{2}}$$

where T_s is the glass transition temperature of the wet resin, T is the test temperature and T_0 is 273°K. This kind of relationship is shown in Figure 32 for unidirectional flexural strength, in-plane shear strength, in-plane shear modulus, transverse modulus and matrix tensile strength.

The following relationship has been proposed which relates the effect of absorbed moisture to the mechanical properties of composite materials (under prolonged exposure i.e. 35,000 hours)⁶:

$$\sigma_u = \alpha + \beta \log W$$

where σ_u is the ultimate tensile stress, W is the amount of absorbed water and α and β are empirical constants.

Experimental work on glass-reinforced polyester has indicated a significant difference in the tensile and flexural strengths of dry and wet samples⁶. The samples were exposed to water at 25-75°C for periods of up to a year. The high scatter of results made them difficult to evaluate, however two distinct processes, one reversible and one irreversible, related to strength degradation, were indicated. Detachment and plasticising of the resin which is reversible and the disruption of chemical bonds, which are irreversible were observed. The work by Ishali⁶ indicated that there are three main effects when GRP samples are exposed to water.

Initially water penetrates into the relatively large spaces in the matrix phase, such as pores, cracks, unbonded parts of the interface etc.

Secondly water penetrates to the fibre-matrix interfaces. In hot water exposure this has three effects: (a) degradation or rupturing of the interfacial bonds provided by the coupling agent, (b) exposure of the glass fibres which in turn lead to water molecules being absorbed onto the surface. This results in a significant reduction in their surface energy and subsequent tensile strength, (c) chemical degradation within the composite.

Finally the effect of leaching causes irrecoverable weight loss with time in both longitudinal and transverse composite samples under hot water exposure. Unfilled samples showing an absence of weight loss indicated the degradation mainly occurs at the glass surface or at fibre-matrix interfaces.

2.2.5 The Effects of Moisture on the Glass Transition Temperature (T_g) of Resin

The glass transition temperature, T_g, of a polymer is defined as the temperature above which it is soft and below which it is hard. The hard polymer is a glass like material, while the soft polymer varies from a rubbery material to an oil¹¹¹.

From a practical standpoint it is more appropriate to discuss a glass transition temperature region rather than a single T_g, as the change for a hard polymeric material to a soft material takes place over a temperature range. This range, as illustrated in Figure 33, for a typical crosslinked amorphous polymer, is characterised by a decreasing modulus with increasing temperature. A very rapid decrease in modulus occurs with increasing temperatures above T_g.

It is well recognised¹¹¹ that the T_g of a polymer can be lowered by mixing with miscible liquid (diluent) that has a lower glass transition temperature than the polymer. This process is referred to as plasticisation. Many polymers, such as epoxy resins, polyester resins etc. absorb moisture from high humidity environments. Moisture is a plasticizer for such systems, producing a lower value of T_g. Similar effects are observed in composites⁸⁶. The reduction in T_g is approximately linear with moisture uptake (Figure 34)¹⁰⁷ and for epoxy resins there is a 100°C decrease in T_g for about 5% moisture uptake. This reduction in T_g can be modelled by a free volume theory of mixtures of two components^{111,112}. For a diluent such as water in a polymer this gives¹¹¹:

$$T_g = [\alpha_p V_p T_{gp} + \alpha_d (1-V_p) T_{gd}] / [\alpha_p V + \alpha_d (1-V)]$$

where α is the thermal coefficient of volume expansion, V_p is the volume fraction of polymer, the suffix p stands for polymer and the suffix d stands for diluent. A value for the T_g for water has to be used and this is usually taken as about 273K.

2.2.6 Measurement of T_g

2.2.6.1 Thermal Analysis

i) Differential Thermal Analysis (DTA)

Differential thermal analysis or thermal spectrometry, measures the heat-energy change occurring in a substance as a function of temperature. Experimentally, the sample is heated side by side with an inert reference material at a uniform rate, and the temperature difference between them is measured as a function of temperature, as shown in Figure 35. The resulting curve is called a thermogram or a thermal spectrum, from which information on the temperature, heat, and rate of transformation can be derived. As DTA directly measures the heat-energy change occurring in a substance, it is theoretically possible to detect and measure any physical transition and chemical reaction that is accompanied by heat-energy change. This implies an extremely broad scope for the DTA technique, as most changes in state and chemical reactions are accompanied by heat-energy changes. Physical transitions that can be studied or have been studied by DTA are: glass transition, crystallization from the melt, crystalline disorientation, and melting. Among the chemical reactions that can be studied by DTA are polymerisations and various other chemical reactions of interest in the polymer area. Chemical reactions may involve either a polymer reacting with another polymer or with some chemicals, or a transformation caused by some form of energy such as radiation or heat. Chemical reactions may include oxidation, vulcanization, crosslinking, curing etc.

ii) Differential Scanning Calorimetry (DSC)

Most studies by DSC on polymers focus on T_g measurements and specific heat changes in glass transition regions where there is an abrupt change. The sample and reference are heated separately by individually controlled heater elements (Figure 36). The power to these heaters is adjusted continuously in response to any thermal effects in the sample. In this way sample and reference are at identical temperatures. The differential power required to achieve this condition is recorded as the ordinate on the recorder, with the programmed temperature of the system as the abscissa. Schematic DTA or DSC curves are plotted as a function of time or temperature at a constant rate of heating. The ordinate represents ΔT the difference between the sample and reference temperatures for DTA measurements or $d\Delta Q/dt$ the power difference between the sample and reference cells for DSC measurements. Schematic DTA or DSC curves illustrating many typical phenomena are shown in Figure 37. The peak area between the curve and a baseline is proportional to the enthalpy change in the sample. A shift in the baseline results from change in the mass of the sample.

Generally first-order transitions should give narrow peaks. Physical transitions in polymers are often from structures of varied size and configuration, and yield spectra much broader than similar transitions in low molecular weight compounds.

Second-order transitions or glass transitions cause abrupt changes in curve shape. The sample absorbs more heat because of its higher heat capacity.

Chemical reactions such as polymerization, curing (which may be either endothermic or exothermic), oxidation, or crosslinking (which are always endothermic) give broad peaks.

The curves for cooling scans are inverse to those for heating to the extent that the transitions and processes are reversible. Cooling

transition often either occurs at lower temperatures due to supercooling or tends to be spread out over a wider temperature interval.

DSC instruments can analyse solid and liquid samples - solid samples can be in foil, powder, crystal or granular form. Materials such as polymer films can be conveniently sampled by cutting out sections of the film with a standard paper punch or centre borer. Solid polymers can be sliced into thin sections with a razor blade or knife. A sample is placed in an aluminium pan which is sealed using a sample pan crimper. The proper weight of the sample depends upon the problem and may vary between 0.5 mg and 10 mg. Small samples permit higher scan speeds, yield maximum resolution and thus better qualitative results; yield most regular peak shapes; permit better sample contact with controlled atmosphere and better removal of decomposition products; and are recommended where the transition energy to be measured is very high. Whereas large samples permit observation of small transitions; yield more precise quantitative measurements; and produce large quantities of volatile products for detection by the effluent analysis system.

2.2.6.2 Dimensional Changes

i) Dilatometry

Thermodilatometric analysis is the continuous monitoring of the length, area or volume of a specimen as a function of temperature or time isothermally. The technique is a classical physical one and has been used widely in polymer science to study many processes e.g. polymerisation kinetics, glass transition temperature, melting and crystallisation kinetics. Many of these original studies were made on the simplest of apparatus on polymer samples stored over mercury in glass dilatometers, and heated externally with a thermostatted liquid bath whose temperature could be held accurately at a fixed temperature or heated slowly at a constant rate. Most modern thermodilatometers monitor the linear expansion of a solid or glass sample through a mechanical push rod which lightly rests on the free end of a sample. The sample is heated externally with

an oven. The push rod's weight is compensated by a support system which balances the weight and only a nominal pressure of less than 1 gram is exerted on the sample. For most accurate and absolute measurements a differential system is adopted in which the expansion of the sample is compared to that of a standard.

In most commercial dilatometers the measuring device is a linear variable differential transformer which responds to the end of the push rod. Other systems have used deflection methods e.g. strain gauges, and mechanical levers. These have been reported elsewhere¹¹³. These instruments are particularly sensitive to linear dimensional changes and so are useful in detecting small changes associated with the onset of transitions within the polymer. Specimens of 3-6 mm can conveniently be handled on the Stanton-Redcroft TMA691.

ii) Thermomechanical Analysis (TMA)

If an increased load is applied to a polymer sample, in tension, or under compression at constant temperature, it will deform elastically (initially) and then yield when permanent deformation occurs. The load-deformation curve is an important parameter of all materials since it defines Young's modulus, yield stress, uniform drawing or necking, brittle, weak or ductile behaviour. These properties are temperature dependent, and brittle materials become more or less ductile as the glass transition is approached, and using an environmental chamber it is possible to determine stress-strain curves as a function of temperature. TMA attempts to determine the effect of temperature on mechanical properties by continuously varying the temperature and to do this the sample is subjected to a constant strain. It is an attempt to measure single point mechanical properties as a function of temperature. However, as with dilatometry, TMA is used to evaluate coefficients of expansion, and these are sensitive to transitions within the polymers, α , β and γ transitions and also melting points. This has been used by Halden et al¹¹⁴ to detect transitions in glassy polymers. The softening temperature, heat distortion temperature, or sample deflection temperature are readily measured.

Studies can be made on thin strips of polymer film or on fibres by clamping the two ends - one to a firm support and the other to the push rod. The use of point bending tests can also be made on rigid samples held on knife edges and bent centrally between the edges, by the push rod.

2.2.6.3 Dynamic Thermomechanical Analyses

Dynamic thermomechanical analysis (DTMA) techniques measure mechanical properties on samples under an oscillatory load and are extremely useful technically in considering the overall performance of polymers, since the mechanical properties are measured as a function of temperature and frequency. These properties are also very sensitive to molecular structure, and changes with temperature have been useful in determining glass-transition regions, the presence of crystallinity, phase separation and crosslinking.

There are many types of instruments available commercial and research, which differ in the type of measurement made and the frequency of the loads applied. Some measure Young's modulus, others shear and even the bulk modulus. Each technique has its own limitations and restrictions in use, and also range of applications. In general, polymers are viscoelastic and as such, in deforming, energy is stored elastically, as potential energy, and some is dissipated as heat. The energy lost as heat manifests itself as mechanical damping. For each test, an elastic modulus and mechanical damping are measured as a function of temperature and oscillatory load frequency. To exploit the full potential of the techniques, measurements should be made over a wide range of temperatures and frequencies as possible. Within the limitations of the technique, however, it is generally better to choose low frequencies e.g. 1 Hz rather than high frequencies, $10^4 - 10^6$ Hz. Secondary transitions are more readily detected at low frequencies.

2.3 DIFFUSION

In order to account for moisture effects in the design of composite structures, it is necessary to be able to predict both the total moisture content and profile as a function of the service environment. A knowledge of the diffusion characteristics of composite materials is also necessary for the purpose of performing accelerated environmental conditioning prior to mechanical testing. It is well recognised that absorbed moisture can have undesirable effects upon the elevated temperature, resin-dependent material properties of composites currently in use⁵. The predominate mechanism for the transfer of this absorbed moisture in glass reinforced plastics has been shown to be a diffusion-controlled process. Detailed knowledge of the nature of this diffusion process is essential in determining the amount of absorbed moisture and its distribution inside a laminate over the service life of a composite structure.

When a dry composite material is placed in wet environments it is considered that the surfaces immediately come into equilibrium and are saturated. Water then penetrates into the composite so that a water profile exists across the specimen thickness, as shown in Figure 38⁵. If saturation is achieved, a uniform distribution of water exists through the thickness of the material.

The rate at which water is absorbed by a composite depends on the nature of the fibres and the matrix, the orientation of fibres with respect to the direction of water penetration, the temperature, the difference in water concentration between the composite and the environment, applied stress and if the absorbed water interacts with or damages the composite. The time necessary for water to penetrate to the centre of the composite depends on the rate of water absorption and the material thickness.

2.3.1 Theory of Diffusion

The transmission of a penetrant through a homogeneous polymer normally occurs by an activated diffusion process. The penetrant dissolves in the

surface layer, migrates through the bulk material under a concentration gradient and evaporates from the surface. Provided a constant concentration difference is maintained across the material, a steady state of flow is attained, with a constant transmission rate, after a relatively short transient-state build up.

Most of the evidence in the literature^{2,4} suggests that moisture is absorbed by a bulk diffusion mechanism in the resin and that for sheet laminates the rate of absorption can be described by Fick's law of diffusion. The basic equations relating to diffusion behaviour are well established, being defined by analogy to the heat transfer process as follows:

The rate of permeation F is defined as the amount of penetrant passing, during unit time, through a surface of unit area normal to the direction of flow,

$$\text{i.e.} \quad F = \frac{Q}{A_t} \quad (1)$$

where Q is the total amount of penetrant which has passed through area A in time t .

In the steady state of flow F is constant and the rate of permeation is directly proportional to the concentration gradient, i.e.

$$F = -D \frac{dc}{dx} \quad (2)$$

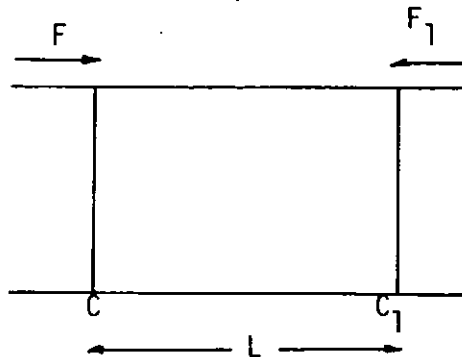
where D is the diffusion coefficient

c is the concentration of diffusing matter

x is the distance normal to the plane.

The units of F are Mass, Length⁻², Time⁻¹, and those of D are Length² and Time⁻¹. The inclusion of the minus sign means that matter flows down a concentration gradient. This is called Fick's first law of diffusion¹¹⁵.

The first law is mainly useful under steady state conditions. Another equation must be set up in order to deal with non-stationary state of flow where concentration is a function of time as well as distance. Consider a volume element enclosed by two planes spaced a distance L apart and associated with concentrations of diffusing matter C and C_1 respectively and rates of permeation F and F_1 respectively.



If the concentration gradient may be considered uniform between the two planes then the concentrations may be related by

$$C_1 = C + L \frac{dc}{dx} \quad (3)$$

The rate of permeation across the first plane is given by

$$F = -D \frac{dc}{dx}$$

and the rate of permeation across the second plane is then

$$\begin{aligned}
 F_1 &= -D \frac{d}{dx} \left(C + L \frac{dc}{dx} \right) \\
 &= -D \frac{dc}{dx} - L \frac{d}{dx} \left(D \frac{dc}{dx} \right)
 \end{aligned} \tag{4}$$

The rate of accumulation of diffusion matter in the volume element is

$$-L \frac{dc}{dt} \tag{5}$$

and this must be equal to the differences of the rates of the permeations across the two respective planes i.e.

$$-L \frac{dc}{dt} = F_1 - F = -L \frac{d}{dt} \left(\frac{dc}{dx} \right) \tag{6}$$

and thus we obtain Fick's Second Law:

$$\frac{dc}{dt} = \frac{d}{dx} \left(D \frac{dc}{dx} \right) \tag{7}$$

If D is constant with respect to distance and concentration then

$$\frac{dc}{dt} = D \frac{d^2c}{dx^2} \tag{8}$$

The distribution of water in a large flat sheet during absorption or desorption is governed by one dimensional (i.e. through the thickness) case of Fick's Second Law (equation 8).

Equation 8 can be solved analytically, given a concentration independent diffusion coefficient and the appropriate boundary conditions. In the case where the initial concentrations of penetrant are uniform throughout the sheet, the boundary conditions are

$$C = C_0 \text{ at } t = 0 \text{ and all } x \quad (9)$$

where C_0 is the initial concentration. If the sheet is suspended in an atmosphere containing a different amount of penetrant than the one in which it was initially conditioned, and assuming that both surfaces of the specimens attain equilibrium as soon as the absorption and desorption begins, then the boundary conditions would be

$$C = C_m \text{ at } x = 0 \text{ and } x = h \text{ at } t > 0 \quad (10)$$

where h is the thickness of the sheet and C_m is the equilibrium concentration. After some length of time, the sheet would absorb the penetrant and the boundary conditions would become

$$C = C_m \text{ at } t = \infty \text{ and all } x \quad (11)$$

With the boundary conditions given in equations 9, 10 and 11, one solution that can be obtained for equation 8 is^{116,117}

$$\frac{C_t - C_0}{C_m - C_0} = 1 - \frac{4}{\pi} \sum_{n=0}^{\infty} (2n+1)^{-1} \sin \left| \frac{(2n+1)\pi x}{h} \right| \exp \left| \frac{-D(2n+1)^2 \pi^2 t}{h^2} \right| \quad (12)$$

The total amount of moisture in the material is obtained by integrating equation 12 through the thickness of the sheet

$$M = \int_0^h C(x,t)dx \quad (13)$$

The result of this integration is (119)

$$G \equiv \frac{m-m_i}{m_m-m_i} = 1 - \frac{8}{\pi^2} \sum_{n=0}^{\infty} (2n+1)^{-2} \exp \left| \frac{-D(2n+1)^2 \pi^2 t}{h^2} \right| \quad (14)$$

m_i is the initial weight of the moisture in the material (i.e. the weight prior to exposure to the moist environment) and m_m is the weight of moisture in the material when the material is fully saturated in equilibrium with its environment.

A parameter of practical interest is the percent weight gain, defined as

$$M = \frac{\text{weight of moist material} - \text{weight of dry material}}{\text{weight of dry material}} \times 100$$

$$M = \frac{W - W_d}{W_d} \times 100 = \frac{m - m_d}{m_d} \times 100 \quad (15)$$

The total weight of the material is equal to the sum of the dry weight W_d and the weight of the absorbed moisture

$$W = W_d + (m/g) \quad (16)$$

The subscripts i and m refer to the uniform initial and fully saturated conditions, respectively. Equations (14)-(16) give

$$M = G(m_m - m_i) + m_i \quad (17)$$

Another solution to equation 9, given the boundary conditions - equations 9, 10 and 11 is (118)

$$G = \frac{m - m_i}{m_m - m_i} = 4 \left(\frac{Dt}{h^2} \right)^{\frac{1}{2}} \left(\frac{1}{\pi^2} + 2 \sum_{n=0}^{\infty} (-1)^n \operatorname{erf} C \frac{nh}{2(Dt)^{\frac{1}{2}}} \right) \quad (18)$$

Equation 18 is most suitable for small times, while equation 14 is best used for moderate and large times. The value of D can be deduced from the initial gradient of a graph as a function of $(t^{\frac{1}{2}}/h)$, that is

$$D = \left(\frac{\pi}{16} \right) \left(\frac{F}{t^{\frac{1}{2}}/h} \right)^2 \quad (19)$$

F is the initial gradient of a graph.

2.3.2 Determination of Diffusion Coefficient (D) and the Maximum Moisture Content (m_m)

If a material (either homogeneous or composite) is exposed to a moist environment, depending upon the environmental conditions and the condition of the materials, the material either absorbs or loses moisture as manifested by weight gain or weight loss. The objective is to determine the percent moisture content (m) of the material as a function of time (t) (see equation 15). The moisture content (percent weight gain) is plotted

versus $(t)^{\frac{1}{2}}$ as shown in Figure 30⁴. Initially when $(t < t_L)$ all curves are straight lines, the slope being proportional to the diffusivity of the material. After a long period of time the curve approaches asymptotically the maximum moisture content (M_m). The value of M_m is a constant when the material is fully submerged in a liquid, it varies with the relative humidity when the material is exposed to moist air¹¹⁸. In the latter case this may be expressed as

$$M_m = a (\phi/100)^b \quad (20)$$

where a and b are experimentally determined constants for each material (a is the saturation moisture content in percent of the material in a 100% RH environment). For many materials b in equation 20 can be set approximately to unity¹¹⁹. This approximation usually provides an adequate description of moisture content as a function of relative humidity, although deviations frequently occur in very wet environments⁷⁴.

The diffusivity D is obtained from the initial slope $(t < t_L)$ of the M_m versus $(t)^{\frac{1}{2}}$ curve, Figure 39

$$D = \pi \left(\frac{h}{4M_m} \right)^2 \left(\frac{M_2 - M_1}{(t_L)^{\frac{1}{2}} - (t)^{\frac{1}{2}}} \right)^2 \quad (21)$$

where D = mass diffusivity ($\text{mm}^2 \text{ s}^{-1}$)
 h = thickness of the sample (mm)
 M = percent moisture
 t = time (seconds)
 M_m = maximum moisture content

Since most moisture diffusion experiments include moisture diffusion through six surfaces, the value for D in equation 21 is in error. For

the true one-dimensional diffusion coefficient $D = 0$, a correction factor given by Shen and Springer¹¹⁸ can be used giving

$$D_{\infty} = D \left(1 + \frac{h}{w} + \frac{h}{l} \right)^{-2} \quad (22)$$

where w and l are the laminate width and length respectively.

The initial rate of moisture uptake depends on the temperature¹²¹ because the diffusion coefficient is temperature dependent according to an Arrhenius relationship^{2,4}

$$D = D_0 \exp (-E/RT) \quad (23)$$

where D is the diffusion coefficient ($\text{mm}^2 \text{s}^{-1}$)

D_0 is a constant for the resin system ($\text{mm}^2 \text{s}^{-1}$)

E is the activation energy of diffusion (kJ mol^{-1})

R is the gas constant $\text{kJ/gm } ^\circ\text{C}$

and T is the absolute temperature ($^\circ\text{C}$)

Taking the natural log of equation 23 yields

$$\ln D = \ln D_0 - \left(\frac{E}{R} \right) \frac{1}{T} \quad (24)$$

Thus a plot of $\ln D$ versus $1/T$ should yield a straight line (Figure 41). A value of E can then be determined from the slope of the line.

The moisture uptake described by equation 21 indicates that the initial rate of uptake depends on the thickness of the laminate. Typical curves for moisture uptake for laminates with different thickness are shown in

Figure 42³⁸. Since the diffusion of moisture is usually only through the resin the diffusion coefficient will clearly depend on the volume fraction V_f of the fibres in the composites. For diffusion parallel to the fibres, the resin cross-section is $(1 - V_f)$ and the diffusion coefficient is given by¹¹⁸

$$D_{11} = D_r (1 - V_f) \quad (25)$$

where D_r is the diffusion coefficient for resin alone. For diffusion perpendicular to the fibre, the diffusion coefficient is

$$D_{22} = (1 - V_f/\pi) D_r^{1/2} \quad (26)$$

For other angles α to the fibres¹²⁸

$$D_\alpha = D_{11} \cos^2 \alpha + D_{22} \sin^2 \alpha \quad (27)$$

2.3.3 Non-Fickian Diffusion

The fundamental characteristics of Fickian and non-Fickian behaviour were described by Crank¹²⁰. Essentially, in Fickian diffusion, the absorption (weight gain) and desorption (weight loss) curves when plotted against $(\text{time})^{1/2}$ are always concave towards the $(\text{time})^{1/2}$ axis and asymptotically reach the final equilibrium value. Calculations performed on the basis of Fick's law fail if:

- a) cracks develop in the material or delamination occurs, essentially altering the structure of the materials'

- b) moisture propagates along the fibre-matrix interfaces;
- c) there are voids in the matrix, and
- d) the matrix itself (even without cracks) exhibits non-Fickian behaviour.

The first three of these conditions involves some form of discontinuity inside the material. Frequently, such discontinuities can be minimised by appropriate manufacturing procedures. Non-Fickian behaviour is a material characteristic. Bonniau and Bunsell⁷⁷ found that the hardener used to cure the epoxy resin had an effect on diffusion kinetics for cured glass fibre reinforced laminates: a diamine hardener resulted in classical diffusion, a dicyandiamide hardener gave Langmuir two-phase diffusion behaviour, and an anhydride hardener resulted in such damage above 40°C that it was not possible to describe the diffusion.

Experimental evidence indicates⁴ that for many materials (especially for epoxy based composites) Fickian diffusion is a reasonable approximation. However, moisture absorption and desorption in some polymers proceeds by non-Fickian processes. Non-Fickian absorption-desorption processes exhibit a maximum saturation level. However the moisture content may not remain constant at this 'apparent' maximum level, but may decrease or increase as time progresses. A more general theory of diffusion, known as the Langmuir model, introduces the concept that water molecules can become trapped by the composite, so that at any given moment, only a fraction of water molecules can diffuse freely^{122,123}. Two parameters are introduced, which are (i) the probability, α , of a trapped molecule being freed and (ii) the probability, β , of a free molecule being trapped. With this two phase diffusion model the weight gain M% as a function of time t is written in terms of four parameters, the diffusivity D , weight gain at saturation $M_m\%$, the probability α of a molecule of water passing from a combined state to the free phase and the probability β of a molecule of water passing from the free to the combined phase. The general form of the absorption curve for this type of diffusion is given by¹²².

$$\text{For } \alpha < \frac{D\pi^2}{h^2} \quad \text{and} \quad \beta < \frac{D\pi^2}{h^2} \quad (28)$$

we can write

$$M\% = M_m \left[1 - \frac{\beta}{\alpha+\beta} \exp[-\alpha.t] - \frac{\alpha}{\alpha+\beta} \frac{8}{\pi^2} \sum_{n=0}^{\infty} \frac{1}{(2n+1)^2} \exp\left[-\frac{Dt}{h^2} \pi^2 (2n+1)^2\right] \right] \quad (29)$$

For $\frac{Dt}{h^2} > 0.05$ this reduces to

$$M\% = M_m \left[1 - \frac{\beta}{\alpha+\beta} \exp[-\alpha.t] - \frac{\alpha}{\alpha+\beta} \frac{8}{\pi^2} \exp\left[-\frac{Dt}{h^2} \pi^2\right] \right] \quad (30)$$

For $\frac{Dt}{h^2} < 0.05$

$$M\% = M_m \frac{\alpha}{\alpha+\beta} \cdot \frac{4}{\pi} \sqrt{\frac{Dt}{h^2}} \quad (31)$$

It can be seen that the two phase model reduces to the single phase case when $\alpha = 1$, $\beta = 0$. The two phase model leads to the type of absorption curve shown in Figure 43³⁸.

Whether or not moisture transport through a composite is by Fickian diffusion depends not only on the material but also upon environmental conditions. Equations based on Fick's law are more apt to describe the moisture transport at low temperatures and for materials exposed to humid air. Deviations from Fick's law solutions become more pronounced at elevated temperatures and for materials immersed in liquids. Salts, water, solvents and hydrocarbons are especially detrimental to the material.

CHAPTER 3

EXPERIMENTAL PROCEDURE

3.1 MATERIALS USED

3.1.1 Fibre Reinforcement

The glass fibre used in this work was Equerove 23/24 (CRC Fibreglass Ltd). It is a 600 tex fibre (600g/kilometre) of nominally 13 micron filament. The size and coupling agent are formulated for use with epoxy resins. It was purchased on 10 kg cheeses and wound onto the laminate frames as required. Properties of the roving used are given in Table 3.1^{124,125}. This type of fibre was chosen because of its similarities to 913 PrePreg.

3.1.2 Resin Matrix

3.1.2.1 Derakane*Vinyl Ester Resins

The Derakane Vinyl Ester resins 411-45 and 470-36 were used in this work, the molecular structures and related properties of which are described in earlier sections. 411-45 is manufactured by reacting a bisphenol-A epoxy resin backbone with methacrylic acid and diluting it with 45 per cent styrene. 470-36 is derived from an epoxy novolac resin reacted with methacrylic acid and diluted with 36 per cent styrene. Even with higher styrene content, 411-45 is more viscous than 470-36, making it a little more difficult in hand lay-ups, however since it has a longer gel time this effect is balanced out. Both resins have extremely good "wet-out" properties. With both vinyl esters Methyl Ethyl Ketone Peroxide (MEKP) was used as a catalyst for room temperature curing. Cobalt Octoate (Cob-Oct) and Dimethyl Aniline (DMA) accelerators were used to initiate the cure. The proportions of catalyst and accelerators used for both these resins listed in Table 3.2. These proportions were found to give a gel time of approximately 45 minutes at room temperature, a convenient

* Derakane is the trade mark of Dow Chemical Company.

period enabling the fibres to be completely wetted out. When mixing these with the resin, care had to be taken so that accelerator and catalysts did not come into contact with each other, since they are explosive if mixed in certain proportions. The accelerators were first mixed into the resin. The catalyst was then added immediately before use. When the catalyst was added it caused a chemical reaction resulting in the mixture "boiling" consequently the resin was left for approximately five minutes after the MEKP had been added to the reaction to take place and the bubbles caused by the boiling to disappear.

3.1.2.2 Polyester Resin

Crystic 272 (ex-Scott Bader), an isophthalic polyester resin was used in this work. It was chosen because it has similar mechanical properties to those of vinyl ester resins and also has good processing characteristics. Methyl Ethyl Ketone Peroxide (MEKP) was used as a catalyst for room temperature curing. Only cobalt octoate accelerator was used to initiate the cure. The proportions of catalyst and accelerator used with the resin are shown in Table 32. These proportions were found to give a gel time of approximately 35-40 minutes. When mixing the resin with MEKP and cobalt octoate the same precautions were taken as with the vinyl ester resins.

3.1.2.3 Epoxy Resins

MY 750 (ex-Ciba Geigy) was used. It is based on the glycidation of bisphenol A with epichlorohydrin.

When the laminates were made using MY 750 as the matrix material, some difficulties were encountered with wet out and solids because it is a highly viscous resin. It was decided that a solvent should be added to lower the viscosity of the resin. Dichloromethane was used as the solvent. This facilitated "wet-out" and when a vacuum was applied to these laminates both dichloromethane and voids were removed. (N.B. Ciba-Geigy also add

dichloromethane to their "resin mix" when manufacturing 913 and 914 PrePregs). To crosslink this structure a triethylenetetramine was used as curing agent, no accelerator was required. The proportions of solvent and hardener added are shown in Table 3.3.

3.1.3 PrePreg Material

913 PrePreg (ex Ciba-Geigy) was used in this work. It comprises of a modified epoxy resin preimpregnated into unidirectional E glass. 913 contains a latent curing agent so that curing will only take place at elevated temperatures so that materials can be stored for long periods at -18°C . The fibres contained in the PrePreg material used in this work were the Equerove E glass as described in Section 3.1.1 so comparisons can be made between these epoxy resin prepreg materials and the other composite materials without differences in fibre characteristics obscuring the comparisons. Curing was carried out under pressure with applied heat in a simple compression moulding process. It was cured for 20 minutes at 140°C . It is claimed that cured 913 PrePreg laminates have outstanding environmental resistance¹²⁶.

3.2 EQUIPMENT

The unidirectional composites slabs were manufactured within a basic metal frame. The approximate internal dimensions of the frame were 230 mm x 300 mm, and thickness was approximately 2 mm. A special filament winding rig modified at the University, was used to wind the glass fibre roving around the metal frame. The rig simultaneously rotated the frame along its longitudinal axis while moving a feeder arm in the lateral direction. The roving was fed through a ring on the feeder arm and attached to one end of the frame. On winding the roving was wound onto the frame while moving along its length. Thus the density of glass fibre on each pass was controlled by the lateral movement of the arm and the rotational speed of the frame. Eight passes at a constant speed were required for each frame to obtain the necessary fibre thickness. Square frames with internal

dimensions of 230 mm x 260 mm were used for the $\pm 45^\circ$ samples. After two passes along one axis each frame was removed from the rig and replaced so that roving could be wound on at 90° to the initial winding. Four passes were applied in this direction, and to complete, two further passes were wound on in the initial direction. Figure 44 shows the filament winder.

Drying of the specimens was done in an ordinary air circulation oven and an environmental cabinet was used for conditioning them in which the selected conditions of temperature and humidity could be maintained. A Grant's water bath was used for water immersion tests.

Tensile tests on the samples were carried out on a 100 kN Dartec servo-hydraulic testing machine at a constant rate of extension and results were recorded in the form of stress-strain curves on a chart plotter. An extensometer was used for strain measurement while load was taken via the load cell in the test machine. The interlaminar shear testing of the samples was done using an Instron testing machine.

The Polymer Laboratories' Dynamic Mechanical Thermal Analyser was used to determine the glass-transition temperature of the samples. In normal operation a bar sample is clamped rigidly at both ends and its central point vibrated sinusoidally by the drive clamp. The stress experienced by the sample, via the ceramic drive shaft is proportional to the current supplied to the vibrator. The strain in the sample is proportional to the sample displacement and is monitored by non-loading eddy current transducers and the metal target on the drive shaft. The drive shaft is supported on light metal diaphragms which allow longitudinal but not lateral motion.

3.3 MANUFACTURING TECHNIQUES

3.3.1 Laminate Lay-Up Procedure

3.3.1.1 Derakane Vinyl Ester 411, 470 and Polyester 272

Glass fibre was wound onto the metal frame as previously described. 150 gms of the appropriate resin was weighed out and thoroughly mixed with appropriate catalyst and accelerators. The resin was then placed in a refrigerator for 2 to 3 minutes, both to allow escape of gas produced by the reaction with the catalyst and to cool the resin in order to increase gelling time.

In order to impregnate the fibres, approximately one-third of the resin was initially poured on to a horizontal sheet of glass, which was just large enough to fit inside the frame. Then the fibre-wound frame was pressed onto the glass plate, allowing resin to soak the fibres from below. The remainder of the resin was then added to the top surface of the fibres and allowed to thoroughly soak the glass fibre, the wetting out being encouraged by manual working of the fibres surface using a ribbed roller. The gelling time of both vinyl esters and polyester resins, 40-50 minutes, allowed sufficient time for the resin to be thoroughly soaked, and for complete wet out of the fibres to occur. Greater care was needed in applying the resin to the cross-ply laminates. It was necessary to work the resin in both fibre directions.

When visual examination of the system showed complete wet-out i.e. no dry fibres were evident through the resin, excess resin and air bubbles in the system were forced off the side of the frame with a straight metal edge strip. A second piece of glass of the same size as the first was pressed on top of the fibres. The method of removing voids proved very efficient, with no voids being evident to the naked eye in the test specimens. Finally, weights totalling 45kg were placed on top of the glass plate as shown in Figure 45.

It should be noted that clear plastic sheets (Melinex sheets) impregnated with a release agent were placed between the glass sheets and the metal frame to prevent adhesion of the resin to the glass.

3.3.1.2 Epoxy MY-750

Prior to wetting of the fibres, 150 grams of resin was weighed out and thoroughly mixed with dichloromethane; hardener was then added. The proportions are shown in Table 3.3. The procedure to wet out the fibres with the resin was the same as described in the previous section.

When the system showed complete wet out i.e. no dry fibres, the laminate was placed in the vacuum chamber and a vacuum was applied for about 20 minutes to remove the dichloromethane and the voids. This method of removing the dichloromethane and the voids proved very efficient. The laminate was then removed from the vacuum chamber, and excess resin and any remaining air bubbles in the system were forced off the side of the frame with a straight metal edge strip. Finally weights totalling 45 kg were placed on the top of the glass plate. Melinex sheets were again placed between glass plates and the metal frame to prevent adhesion of the resin to the glass.

3.3.1.3 Epoxy 913 PrePreg

The epoxy PrePreg laminates were made from Ciba-Geigy Fibredux 913 material. It is supplied as a continuous roll of resin coated fibres in sheet form. The laminates were manufactured using the compression moulding technique recommended by Ciba-Geigy. The lay-up sequence in the compression mould was as follows: 1 layer Tygaflor, 1 layer of woven glass mat, 1 layer of absorbing fabric, 1 layer of Tygavac, 16 layers of 913 PrePreg 230 mm x 150 mm, 1 layer of Tygavac, 1 layer of absorbing fabric, 1 layer of woven glass mat and finally 1 layer of Tygaflor. Tygavac is the bleeder cloth, which absorbs the excessive resin and Tygaflor is the release film.

The laminate sandwich was held between two mild steel compression moulding plates and moulded in an electric or steam heated press. The pressure on the plates was raised to 2000 kN/m² and then the temperature increased from ambient to 150°C at maximum of 15°C/min etc. The heating

softened the resin and allowed the surplus resin in the PrePreg to be squeezed out of the laminate thus consolidating the material and eliminating voids. The laminate was left under full pressure at 150°C for 20 minutes after which it was ejected from the press, and cooled down to room temperature.

3.4 CURING PROCEDURE

The vinyl esters, polyester and epoxy were cured at room temperature for a period of 24 hours. This was followed by a post-cure at 80°C for 2 hours for vinylesters and epoxy. The polyester was post-cured at 80°C for 3 hours. The laminates were post-cured to ensure that crosslinking was complete. 913 PrePreg laminates were not post-cured.

3.5 TEST SPECIMEN PREPARATION

From the unidirectional slabs, specimens were cut for tensile and interlaminar shear tests and from the cross-ply slabs specimens were cut at 45° angle for in-plane shear tests. Tensile test and in-plane shear specimens were made in accordance with BS 2782 specification¹²⁷, method 320E, and as shown in Figure 46. Preparation of test pieces initially involved cutting the laminate slab out of the steel frame using a diamond tipped circular saw. Up to five tensile specimens and two strips 12 mm wide, for interlaminar specimens could be obtained from each slab. Only three in-plane shear specimens were obtained from each of the cross-ply laminates. Care was taken not to obtain specimens from the edges of the slab due to distortions of fibre alignment and the presence of excess resin in these areas. Having cut out the specimens, their edges were smoothed on a linisher and aluminium alloy HS30 end tabs were bonded to them using Araldite MY750 epoxy resin with HY 951 hardener. A curing period of 24 hours was allowed at room temperature.

The specimens for the interlaminar shear tests were prepared according to BS 2782 Part 3, method 341A¹²⁸. The minimum thickness of each specimen

was $2 \text{ mm} \pm 2\%$, the overall length was 6 times the mean thickness and the width $10.0 \pm 2 \text{ mm}$. The interlaminar shear strength specimens were prepared as follows.

Strips approximately 12 mm wide were cut lengthwise for each composite slab on a circular diamond cutting wheel. The cut edges were polished down to 1200 grade silicon carbide paper and a width of $10 \pm 0.5 \text{ mm}$, great care being taken to keep the edges parallel. The strips were cut into lengths 6 times the thickness and, keeping the corners square, were polished down to 1200 silicon carbide paper and a length of 6 times the mean thickness.

3.6 VOLUME FRACTION ANALYSIS

Small samples were cut from the centre of each slab in order to analyse the percent fibre content. These small samples, 1-2 grams, were placed in a crucible and heated to 600°C for 2 hours. This ensured that all the resin was burnt off. The remaining glass fibres could then be weighed, and volume fraction could then be determined, from the following measurements and calculations:

Measurements before heating:

- i) Weight of crucible - A;
- ii) Weight of crucible + sample - B;

therefore the weight of the sample $W_s = B - A$

Measurements after heating:

- iii) Weight of crucible and fibres - C;

therefore the weight of fibres $W_f = C - A$,

and the weight of the resin $W_r = W_s - W_f$.

The following densities, obtained from the manufacturers, were used in the final calculations:

E glass	=	2.54 g/cc
Vinylester 411	=	1.12 g/cc
Vinylester 470	=	1.18 g/cc
Epoxy MY 750	=	1.19 g/cc
Polyester 272	=	1.20 g/cc
PrePreg 913	=	1.23 g/cc

The volume fraction of fibres was calculated from the following equation:

$$V_f = \frac{W_f \rho_f}{W_r \rho_r + W_f \rho_f} \times 100$$

where ρ_f is the density of the glass fibre
and ρ_r is the density of the resin.

3.7 ENVIRONMENTAL CONDITIONING

Before placing the test specimens into moist environments (humid air and liquid) they were dried in an air oven at 35°C, until their weight became stabilised and no more weight loss was observed. The specimens were weighed regularly on a Stanton Analytical Balance. On average it took 48 hours for the weight to become stabilised. The specimens thus dried were placed in the appropriate environmental conditions and their weights were taken by weighing them periodically. Three sets of conditioning were used, (i) 60 percent relative humidity, (ii) 95 percent relative humidity, and (iii) water immersion at 25°C, 40°C, 50°C, 60°C and 70°C. Three sets of samples were placed in the moist environment: (i) unidirectional tensile specimens and $\pm 45^\circ$ tensile specimens without the aluminium tabs for weights measurements, (ii) specimens as in (i) but with tabs for mechanical testing, and (iii) interlaminar shear specimens.

The specimens were left in the moist environment for a total of 40 days. The mechanical testing was carried out after 16 and 40 days respectively. The tensile specimens were placed on a special holder so that the environment surrounded the specimens as shown in Figure 47. The interlaminar shear specimens were placed in small trays standing upright so that the moisture could enter from both sides.

The environmental conditions were produced in a microprocessor controlled environmental cabinet (Figure 48) in which humidification was by the injection of atomised distilled water on the heaters in a separate chamber. The temperatures of the environmental chamber were controlled by heaters and were kept within $\pm 1^{\circ}\text{C}$. A Grant's water bath was used for water immersion tests. The bath was filled with distilled water. The set temperature of the bath was maintained at $\pm 0.5^{\circ}\text{C}$. To protect the adhesive from water attack during immersion the aluminium tabs were coated in silicon grease.

3.7.1 Thermal Spiking

Sudden, large temperature changes, referred to as "thermal spikes" are encountered, for example by aircraft flying supersonic speeds. Thermal spikes may alter the moisture absorption as well as the mechanical properties of the composite materials. To investigate this, unidirectional and $\pm 45^{\circ}$ specimens manufactured from each resin matrix were placed in the environmental cabinet for 40 days and spiked daily. The humidity inside the cabinet was kept constant at 95%, but the temperature was varied between 25° and 70°C . Spiking was performed in the following sequence.

- i) The specimens were oven dried at 35°C for 48 hours
- ii) The specimens were placed inside the environmental cabinet at 95% RH, 25°C .
- iii) The specimens were kept at 95% RH; 25°C for 18 hours.

- iv) The temperature was raised to 70°C in 1 hour
- v) The specimens were kept at 95% RH, 70°C for 4 hours
- vi) The specimens were removed from the cabinet for weighing after 4 hours at 95% RH, 70°C.
- vii) The door of the cabinet was left open to bring the temperature down to 25°C in one hour
- viii) The specimens were replaced in the cabinet again at 95% RH, 25°C after weighing.

The whole sequence was repeated daily for 40 days.

3.8 MECHANICAL TESTING

3.8.1 Tensile Testing

A servohydraulic test machine was used to test the specimens to failure on which a constant rate of grip separation of 5 mm/min was used for all tensile specimens in accordance with BS 2782¹²⁷. Strain was measured with an extensometer which fed via an amplifier into the chart recorder. In order to eliminate any effect of slippage of the extensometer knife edges, strips of double sided tape were used on the specimens under the grips. Load was measured directly through the load cell of the test machine and fed into the chart recorder. Results obtained were the graphical plot of load vs strain from the duration of the test. With the cross-ply samples the maximum load was read from the digital display on the console of the machine. Figures 49 to 52 show the experimental set up, i.e. testing machine, control panel of the testing machine, grips and the extensometer.

3.8.2 Interlaminar Shear Testing

The specimens were tested on the three-point bending rig as shown in Figure 53. Such rigs are used to determine the cross-breaking strength of rigid materials. However with composite materials of appropriate size the rig can be used to determine the apparent interlaminar shear strength

of the material. The Instron machine was fitted with a 500 kg load cell and geared to give a cross-head speed of 0.1 cm/min and chart speed of 10 cm/min. The dimensions of the specimen to be tested were measured and the rig was set up as shown in Figure 54. A force was uniformly applied across the width of the test piece under member B by moving the supports A and C upwards as shown in Figure 55, until the maximum force that the test piece could withstand had been reached. In all cases the failure mode was by shear.

3.9 GLASS-TRANSITION TEMPERATURE

The glass-transition temperature (T_g) was measured by using a Dynamic Mechanical Thermal Analyser (DMTA) developed by Polymer Laboratories (PL) hence the name "PL-DMTA". Figure 56 shows the PL-DMTA, and Figures 57 to 60 show schematic views of the mechanical load, clamping arrangement, drive shaft components and clamping frame support. The mechanical head houses the sample in a temperature enclosure where it is subjected to small amplitude sinusoidal oscillation.

A bar sample (38 mm long, 12 mm wide and 2-3 mm thick) was clamped rigidly at both ends as shown in Figures 61 and 62 and its central point vibrated sinusoidally by the drive shaft. The sample was then heated inside the mechanical head at a rate of $4^{\circ}\text{C}/\text{min}$. The temperature programmer controls the balanced heat oven to produce uniform heating. The temperature range for Vinylester 411, 470, Polyester 272, and Epoxy 750 was set from 25°C to 150°C , whereas for 913 PrePreg the range was from 25°C to 200°C because of its high T_g . The temperature was controlled to within 0.2°C by a platinum resistance thermometer situated immediately behind the sample. For high temperature argon gas was introduced from pipes in the rear bulkhead. As temperature is raised DMTA senses any change in molecular mobility in the samples. When samples pass through a glass transition temperature they soften. This can be seen because a downward displacement is recorded. Apart from measuring T_g it also measured damping factor ($\tan \delta$) and modulus E (N/m^2).

3.10 MICROSCOPY

Sections were taken from unidirectional and cross-ply samples to see the fibre distribution in the composites. The surface was polished and subjected to optical and scanning electron microscope examination in unetched conditions. The polishing of the surface consisted of wet grinding on consecutively finer silicon carbide paper up to a longitudinal finish on 600 grit. The fine scratches from silicon carbide papers were removed by using alumina powder (i.e. 5 micron) on Selvyt cloth, with water as lubricant.

The fracture surface of the specimens was subjected to scanning electron microscopy. The scanning electron microscope used was a Cambridge Instruments microscope. The fracture surface was cleaned ultrasonically and gold coated before examination.

CHAPTER 4

RESULTS

This chapter presents the results of the experimental work. Three sets of environmental conditions were used i.e. 60% RH, 95% RH and water immersion at the following temperatures 25^o, 40^o, 50^o, 60^o and 70^oC. For each environmental condition the following parameters were measured:

- a) Weight increase (%)
- b) Maximum moisture content (%)
- c) Diffusion coefficient (mm² s⁻¹)
- d) Glass transition temperature (°C)
- e) Ultimate tensile strength after 16 and 40 days (MPa)
- f) Strain at tensile failure after 16 and 40 days (%)
- g) Tensile modulus (0.25% strain modulus) after 16 and 40 days (GPa)
- h) Interlaminar shear strength after 16 and 40 days (MPa)
- i) In-plane shear strength after 16 and 40 days (MPa).
- j) Volume fraction (%).

4.1 WEIGHT INCREASE

The weight increase of unidirectional tensile specimens and ±45^o specimens were measured. The nominal dimensions of the specimens were in accordance with BS 2782 as stated in Section 3.5. All the specimens were without the aluminium tabs.

The specimens were dried in the air oven, and their dried weight " W_d " was measured. The specimens were then placed in a constant temperature, constant moist environment and their weight ' W ' was recorded as a function of time. The weight of the samples was recorded each day. From these values the moisture content (per cent weight gain) was calculated as follows:

$$\frac{W - W_d}{W_d} \times 100$$

where W_d is the dried weight of the samples and W is the moist weight of the sample.

The average percent moisture content was plotted graphically against time $(\text{time})^{\frac{1}{2}}$ in $(\text{days})^{\frac{1}{2}}$, as illustrated in Figures 63-132. Each point on the graph represents the average result of five samples. All five data points were within ± 10 percent for both 0° and $\pm 45^\circ$ samples.

4.2 DIFFUSION DATA

4.2.1 Maximum Moisture Content

The initial percent weight increased linearly with the square root of time and then attained a plateau value after some time, as shown in Figures 63-132. The plateau value is defined as the apparent maximum moisture content (%). For 60% RH this plateau value was not clearly defined, i.e. the weight of the specimens was still increasing after 40 days. So the maximum moisture content in this case was taken as the value at the 40th day, for the calculation of diffusion coefficient. The values for the maximum moisture content of both 0° and $\pm 45^\circ$ specimens at different environmental conditions are given in Appendix A.

4.2.2 Diffusion Coefficient

The diffusion coefficient was calculated from the following expression. A full description of the expression was given in Section 2.3:

$$D = \left(\frac{\pi h}{4M_m} \right) \left(\frac{M_2 - M_1}{t_2 - t_1} \right)$$

where D = diffusion coefficient ($\text{mm}^2 \text{ s}^{-1}$)

h = thickness of the specimen (mm)

M_m = maximum moisture content (%)

M_1 and M_2 are the percentage uptake of water by weight after times t_1 and t_2 respectively and are taken from the linear portion of the percent average moisture against square root of time plots, see Figures 63-132. Since most moisture diffusion experiments include moisture diffusion through six surfaces, the value of D in the above equation is in error. For the true one-dimensional diffusion coefficient D_x , the following correction factor given by Shen and Springer⁴ can be used

$$D_x = D(1 + h/w + h/l)^{-2}$$

where w , h and l are the laminate width, thickness and length respectively.

Therefore the equation for one dimensional diffusion coefficient is:

$$D_x = \pi(h/4M_m)^2 \left(\frac{M_2 - M_1}{t_2 - t_1} \right)^2 (1 + h/w + h/l)^{-2}$$

where D_x = diffusion coefficient ($\text{mm}^2 \text{ s}^{-1}$)

M_m = maximum moisture content (%)

$\frac{M_2 - M_1}{t_2 - t_1}$ = initial slope of the % average moisture content against square root of time curve

h = thickness of the laminate (mm)

w = width of the laminate (mm)

l = length of the laminate (mm)

A basic computer program was written to fit the best straight line (least squares) through the first 20 data points, i.e. % average moisture and square root of time points. The program also calculated the following parameters:

- i) initial slope of the curve $\left(\frac{M_2 - M_1}{t_2 - t_1} \right)$

- ii) intercept on Y axis
- iii) Pearson's correlation coefficient
- iv) standard deviation

The following formulae were used in the program. For n points on a graph $(X_1, Y_1), (X_2, Y_2), \dots (X_n, Y_n)$ the 'best' straight line fit has the equation

$$Y = mx + C$$

For given values X_i the corresponding Y values on the 'best' straight line are $mx_i + C$

$$\therefore \text{Slope } m = \frac{n \sum X_i Y_i - \sum X_i \sum Y_i}{n \sum X_i^2 - (\sum X_i)^2}$$

and

$$\text{Intercept } C = \frac{\sum X_i^2 \cdot \sum Y_i - \sum X_i \sum X_i Y_i}{n \sum X_i^2 - (\sum X_i)^2}$$

Pearson's correlation coefficient r

$$r = \frac{\sum (X_i - \bar{X})(Y_i - \bar{Y})}{\sqrt{[\sum (X_i - \bar{X})^2 \sum (Y_i - \bar{Y})^2]}}$$

where \bar{X} and \bar{Y} are the mean values of X and Y and n is the number of (X, Y) points. \sum indicates summation.

$$\text{Standard deviation} = \sqrt{\frac{n \sum X^2 - (\sum X)^2}{n(n-1)}}$$

If the Pearson's correlation coefficient (r) value is close to ± 1 , it indicates that the line through the data points is a straight line. However if the r value is zero or close to zero, it is not straight through the data points. A low standard deviation value also indicates a good straight line through the data points. A high value is caused by a poor fit and may be due to a bad scatter of points.

In all cases a reasonable straight line through the initial part of percent moisture content against square root of time curve was found. The r values were in the range of 0.96 to 0.99, standard deviation values were in the range of 3.03×10^{-3} to 3.52×10^{-2} and the C values were close to zero indicating the curve passed through the origin. The small scatter of points indicated by the standard deviation values shows the benefit of the computer program in consistently calculating the initial slope of the curve.

4.2.3 Activation Energy (kJ mol^{-1})

The initial rate of moisture uptake depends on the temperature because the diffusion coefficient is temperature dependent according to an Arrhenius relationship^{8,4}.

$$D = D_0 \exp (-E/RT)$$

where D = diffusion coefficient ($\text{mm}^2 \text{ s}^{-1}$)

D_0 = permeability index ($\text{mm}^2 \text{ s}^{-1}$)

E = activation energy for diffusion (kJ mol^{-1})

R = universal gas constant $8.315 \text{ J/mol}^{-1} \text{ } ^\circ\text{K}$

T = exposure temperature $^\circ\text{K}$

Taking the natural log of the above equation yields

$$\ln D = \ln D_0 - \left(\frac{E}{R}\right) \frac{1}{T}$$

Thus a plot of $\ln D$ versus $1/T$ yielded a straight line, as shown in Figures 133-163. A value of activation energy (E) was then determined from the slope of the line, as described in Section 2.3.

4.3 GLASS TRANSITION TEMPERATURE (T_g °C)

Polymer Laboratories - Dynamic Mechanical Thermal Analyser (PL-DMTA), was used to evaluate the glass transition temperature on the composite samples. As the percent moisture content increased the glass transition temperature of the samples decreased. The results are shown graphically in Figures 164 -169 in which percent moisture was plotted against the glass transition temperature. Appendix A shows the detailed experimental results of the T_g °C for different resin matrices for various percent moisture levels. Figure 170 shows the general form of graph obtained from the PL-DMTA, from which the T_g °C of the sample was read off directly.

Attempts were also made to evaluate the T_g °C of the specimens by Differential Scanning Calorimetry (DSC), but it was unsuccessful due to reproducibility of the results. The full description of the apparatus is given in Section 2.2.6.1.

4.4 TENSILE TEST

All the specimens were tested on a 100 kN Dartec servohydraulic test machine. The specimens were positioned in self-tightening wedge shaped grips and pulled to complete failure. The strain was measured with an extensometer. Tests were always performed as soon as possible after removing the specimens from the environmental cabinet or from the water bath. The tests were carried out after 16 and 40 days conditioning

respectively. Prior to testing the thickness and width of each test piece was measured at three points along its length and the mean value recorded. Two types of load/strain curves were obtained for the longitudinal tensile specimens as shown in Figures 171a and 171b. In some cases the load/strain curve had a 'jump' as shown in Figure 171b, this was due to the longitudinal cracks running along the length of the specimen near to their edges. The jump does not affect the measurement of the tensile modulus, as this was obtained by measuring the load at 0.25% strain. At these low levels of stress and strain "jumps" were not observed. However when measuring stress and strain difficulties were encountered. When there was a "jump", there appeared to be two points that could be considered as candidate values for load at failure and strain at failure. Point C was the point at which the "jump" occurred. There was no tensile failure of the fibres however and therefore no justifications in using either the value for load or strain as true values of tensile stress or strain. At point A, there was tensile failure of the specimens and this point is a far more worthwhile candidate for values of stress and strain. So it was decided to take point A as load at failure. The strain to tensile failure was at point B (Figure 171a). The load-strain curve which showed a "jump", the strain was calculated at points D and E respectively. The difference in strain values δx (Figure 171b) was subtracted from the strain value at point B.

4.4.1 Ultimate Tensile Strength (UTS)

From the load/strain graphs the maximum load applied to each sample was obtained by reading the highest point reached by the curve. The UTS was calculated from:

$$\sigma' = \frac{A}{Wt} \text{ kN/mm}^2 \text{ or MPa}$$

where σ = UTS (MPa)

A = maximum load (kN)

W = average width (mm)

t = average thickness (mm)

The results calculated for each composite were normalised to 45% volume fraction of glass fibre. The value of 45% was chosen because it represented the volume fraction usually obtained with hand lay-up samples. Five tensile specimens were tested for each environmental condition. Each point on the graph represents the average result of these five specimens. Figures 172-181 show the plots of percent moisture content against UTS for each resin matrix and for every environmental condition. Appendix B shows detailed experimental results for each environmental condition for unidirectional specimens. The mean, standard deviation (S.D) and the coefficient of variation (CV) are reported. The following formulae were used to calculate the mean, S.D. and C.V.

$$\bar{X} = \frac{\sum X}{n}$$

$$S.D. = \sqrt{\frac{n\sum X^2 - (\sum X)^2}{n(n-1)}}$$

$$C.V. = \frac{S.D}{\bar{X}} \times 100$$

where X = the value of an observation
and n = the number of observation(s)

4.4.2 Strain to Tensile Failure

The percent elongation at failure of the unidirectional specimens was obtained from the linear portion of load-strain graph as shown in Figures 171a and 171b, and discussed in Section 4.4. The detailed experimental results are summarised in Appendix C. The mean value, S.D. and C.V. were calculated for each set of results. Figures 182-191 show the graphical plots of percent elongation against percent moisture content, for each resin matrix.

4.4.3 Tensile Modulus (E)

The tensile modulus was obtained by measuring load at 0.25% strain as shown in Figure 171. The initial point of the load/strain curve was not linear and the curve was extrapolated back to determine the origin as shown in Figure 171. The E was calculated from

$$E = \frac{\text{Stress}}{\text{Strain}} \text{ (GPa)}$$

where $\text{Stress} = \frac{A'}{Wt}$ (From Figure 171a)

A' = load (kN)

W = width of the specimen (mm)

t = thickness of the specimen (mm)

Strain = Point B' on the graph (From Figure 171a).

The results calculated from each composite were normalised to 45% volume fraction of glass fibre. Detailed results are presented in Appendix D. Figures 192-201 are the plots of tensile modulus against percent moisture content for the different materials.

4.5 INTERLAMINAR SHEAR STRENGTH (ILSS)

From the ILSS test a graph of load against extension was obtained for each specimen tested. The general form of this graph is shown in Figure 202. For each specimen the ILSS was calculated using the following equation

$$S = \frac{0.75F}{Wt} \text{ (MPa)}$$

where S = ILSS (MPa)

F = maximum force (N)

W = width of the test piece (mm)

t = thickness of the test piece

When the samples were removed from the environmental cabinet or from the water bath, they were weighed before being tested. Five samples were tested for each environmental condition. The results are given in Appendix E. Figures 203-212 show the plots of the percent moisture against ILSS for the five materials. In all the cases samples failed in the case of the shear mode as shown in Figure 213.

4.6 IN-PLANE SHEAR STRENGTH (IPSS)

This test was for $\pm 45^\circ$ samples. The samples were tested on a 100 kN Dartec servohydraulic test machine. The specimens were positioned in self-tightening wedge shaped grips and pulled to complete failure. The load-extension graph was not plotted on the chart recorder, because the strain to failure was very high and the extensometer was not calibrated to read high strain values. Therefore only load was recorded by reading directly from the digital display on the console of the machine. Five specimens were tested for each environmental condition. The IPSS was calculated by using the following expression

$$\tau_U = 0.5 P_U / Wt$$

where τ_U = IPSS (MPa)

P_U = load at failure (kN)

W = width of the specimen (mm)

t = thickness of the specimen (mm)

Appendix F shows the detailed experimental results for the five materials. Figures 214-223 show the plots of percent moisture content against IPSS for each of the resin matrices.

CHAPTER 5

DISCUSSION

5.1 EXPERIMENTAL TECHNIQUES

The filament winding method has several advantages. Firstly there is a plane of symmetry about the plane of the metal frame itself. This makes several $0^\circ/90^\circ$ configurations possible, while the similarity to the 8 layer symmetrical (16 strips) prepreg configuration allows easy comparison with 913 PrePreg. Attempts were made to keep the volume fraction of fibres and the thickness of the laminates constant throughout the work, but this was not possible due to the difficulties encountered during the manufacturing of the specimens.

5.1.1 Volume Fraction of Fibres

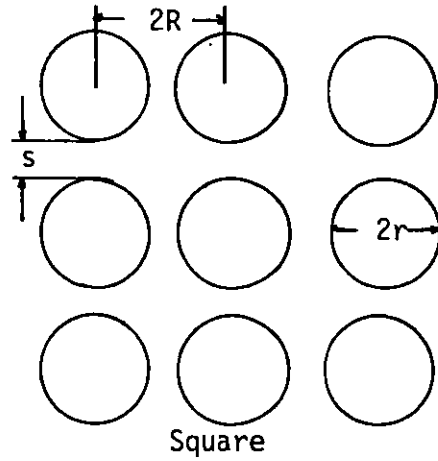
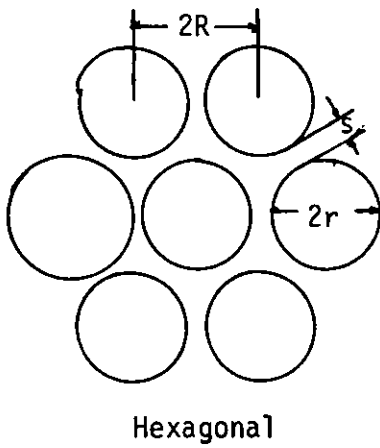
The volume fraction results showed a maximum variation of 26 percent between the lowest value (0.37), and highest value (0.50), for both vinyl ester resins and polyester resin. The low volume fractions obtained resulted from problems during the fabrication of the composite slabs. A long working time was needed to ensure that all the fibres had been wetted with resin. Consequently the viscosity increased due to the air curing and the task of removing excess resin was made extremely difficult. Oxygen in air will also inhibit the complete cure of an exposed vinyl ester or polyester resin surface²⁰. This inhibited surface may vary in depth, and may result in reduced weatherability, poor chemical resistance and/or premature failure. This problem can be overcome by preventing or reducing contact of the curing surface with air. However, with epoxy resin the scatter was small, between 5 and 10%, and the volume fractions figures were slightly higher, between 0.48 and 0.55. The reason for this was the addition of dichloromethane to the resin which lowered the viscosity of the resin and also increased the gelation time from 1 hour to 3 hours. Consequently there was more time for complete wet out of the fibres and more time to remove excess resin from the laminate.

The results also showed that there was a considerable difference between the volume fraction of glass fibres in epoxy prepreg and the wet hand laid up samples. The 913 PrePreg purchased had an initial resin content of 39%. After pressing and moulding the volume fractions of fibres obtained was between 0.55 and 0.60.

Despite these different volume fractions of glass between laminates, within laminates the volume of glass fibre was constant. The effect of this scatter on final ultimate tensile strength and modulus was cancelled by normalising the results to a constant value for volume fraction of 0.45 as explained in the results section. This involved extrapolation of results, which cannot be regarded as an ideal procedure. However it is not possible to normalise the weight increases that occur in the laminates during environmental conditionings. Therefore directly comparing the moisture absorption behaviour of the different composites is unfair. Rao et al¹²⁹ have investigated the effect of fibre volume fraction on equilibrium moisture contents, and have shown that for glass-epoxy composites, the equilibrium moisture level decreases with increased fibre fraction. It can be seen from Figure 224, that the maximum absorption occurs for an all resin specimen (fibre volume fraction = 0) and the minimum for that with highest fibre fraction (fibre volume fraction = 1).

5.1.2 Distribution of Fibres

In a unidirectional laminate, all the fibres are aligned parallel to each other. In an ideal situation, and for the purposes of theoretical analysis, the fibres can be considered to be arranged on a square or hexagonal lattice, as shown below, with each fibre having a circular cross-section and the same diameter. In practice glass and organic fibres closely approximate to a circular cross-section with a smooth surface finish.



$2R$ is the centre to centre spacing of the fibres, S is separation of the fibres, r is the radius of the fibres. For the ideal arrangements the volume fraction of fibres V_F is related to the fibre radius by:

$$V_F = \frac{\pi}{2\sqrt{3}} \left(\frac{r}{R}\right)^2 \quad (\text{hexagonal})$$

$$V_F = \frac{\pi}{4} \left(\frac{r}{R}\right)^2 \quad (\text{square})$$

The maximum value of V_F will occur when fibres are touching, i.e. $r = R$. For a hexagonal array $V_F = 0.907$ and for a square array $V_F = 0.785$.

Experimental studies of the distribution of fibres in unidirectional laminate show that these ideal distributions do not occur in practice except in small localised regions³⁵. For the work under discussion, Figures 226-227 show a low volume fraction laminate and a high volume fraction laminate. In some regions the packing closely approximates to a hexagonal array, but resin rich regions with irregular packing occur throughout the laminate. In the low volume fraction laminate the packing was often very irregular, some fibre bunching and large

resin rich regions occurring as shown in Figure 226. Misalignment of the fibres was also more pronounced in low volume fraction laminates. The irregular dispersion of the fibres will have a significant effect on some properties, notably the transverse strength and modulus. One of the main consequences of non-regular packing is the difficulty of achieving volume fractions greater than 0.70 and this value must be regarded as the practical limit for commercial materials. Another aspect of the fibre packing and spacing which is important in many processing operations, particularly where the resin is introduced into a closed mould containing dry fibres, is the wetting out of the fibre by flow of the resin through the packed fibres. At high volume fraction and with small diameter fibres the spacing between the fibres is very small and long times and high pressures are required for complete infiltration.

✓ 5.1.3 Thickness of the Laminates

The samples with a low volume fraction were usually thicker than the samples with high volume fraction. The thickness of both vinyl ester and polyester samples varied from 2 mm to 2.50 mm, whereas the thickness for 913 PrePreg and epoxy MY750 ranged from 2 to 2.10 mm respectively. Thickness is an important quantity when considering the moisture uptake of a composite. Work on polyester resin has shown that there is an exponential relationship between sample thickness and water transmission rate.⁹⁶ As the thickness increases the water transmission rate falls (Figure 225). The thickness of the specimens for water absorption work was in the range of 2.00 to 2.10 mm.

An alternative technique for producing high fibre volume fraction and constant thickness specimens is 'leaky moulds'. In this technique, the fibres are impregnated with the resin in a leaky mould. Resin is poured onto the base of the mould, the fibres placed on top, and more resin is poured onto the fibre. A laminating roller is used to speed up the wetting out procedure and ensure complete impregnation of the fibres by

the resin. Once this process is complete, the lid is placed on the mould and clamps applied to each corner to produce the compression force. Spacers, which determine the thickness of the laminate are inserted in the gaps around the edge of the mould and the excess resin is squeezed out of the ends, taking with it any air which may still be present in the fibres. The void content of the resulting laminate is extremely low. Using this method, and by keeping both the amount of the fibres on each metal frame and the laminate thickness constant, it is possible to produce good quality laminates. However at present this technique is not suitable for producing $0/90^\circ$ laminates, due to excessive voids. Hence this fabrication technique was not used during this research.

5.1.4 Voids Content

The main advantage of the fabrication technique used in this work was that specimens were produced with no voids. The specimens with any visible air bubbles were discarded. Two main methods were used to determine void content in the 0° and $\pm 45^\circ$ laminates. Firstly, voids were readily detected in polished specimens, i.e. the cut samples were polished and examined under optical microscopes. This method was quick and reliable. Secondly, the density method was used. This is the most widely used method, which assumes that $V_v = 1 - (V_f + V_r)$, where $V_f = W_f \cdot \rho_c / \rho_f$ and $V_r = (\rho_c / \rho_r)(1 - W_f)$ where W and ρ are weight fraction and density, respectively. The subscripts c, f and r refer to composite, fibre and resin, respectively. The void content of all the specimens was less than 1 percent. The method was difficult to perform and sometimes gave negative answers. This may be due to the following:

1. Very accurate determination of ρ_c , ρ_f , ρ_r and W_f was required
2. Only small samples were used, not necessarily representative
3. There may be a polymeric coating on the fibres, of different density from that of the resin.

Another method which may be used in determining void content is an ultrasonic scanning technique (C-scan). This method is the non-destructive examination of void distribution and delamination faults in composite materials. The test sample is scanned by an ultrasonic pulse and the attenuation in the material is measured. The information is processed to produce a two-dimensional image of the sample.

Voids can arise from two main causes. Firstly incomplete wetting out of the fibres by the resin. This results in entrapment of air and is more likely in systems where the dry fibres are closely spaced and the viscosity of the resin high. Secondly, the presence of volatiles produced during the curing cycle. The void content and distribution can therefore be seen to depend on fibre volume fraction and distribution, resin properties and processing conditions such as temperature, pressure and time. It has been shown that regardless of resin type, fibre type and fibre surface treatment, the interlaminar shear strength of composite materials decreases by about 7 percent for each 1 percent of voids up to a total void content of 4 percent⁸⁷. According to Judd and Wright⁸⁷, voids also reduce the magnitude of the following mechanical properties:

1. Interlaminar shear strength
2. Longitudinal and transverse flexural strength and modulus
3. Longitudinal and transverse tensile strength and modulus.

5.1.5 End Tabs

Aluminium end tabs were stuck onto the ends of the unidirectional and $\pm 45^\circ$ samples for tensile and in plane shear tests. The tabs were stuck using epoxy resin MY 750 and HY951 hardener. The tabs were attached prior to any environmental conditioning. To protect the adhesive from moisture attack during water immersion silicon grease was smeared around the tabs. Such a procedure was only partially effective, however, as moisture diffuses from inside the composite to the outer surfaces and will eventually penetrate the bondline. As well as attacking the composite the environ-

mental conditions severely attack the adhesive used for the end tabs, which in some cases led to their detachment. In such cases it was possible to fit temporary tabs to the samples as they were placed in the test rig.

5.2 WATER ABSORPTION

As stated previously under service conditions a component may take many years to reach its equilibrium moisture content. To test composite materials in a moist state they have to be conditioned at an elevated temperature in order to reduce the time. Boiling water has been used as a quick method to condition specimens, but is not satisfactory because it tends to leach soluble components from the resin and fibre/resin interface. Conditioning is better done in warm humid air. It was therefore decided to use the following conditions:

- i) 60% RH at 25⁰, 40⁰, 50⁰, 60⁰ and 70⁰C for 40 days
- ii) 95% RH at 25⁰, 40⁰, 50⁰, 60⁰ and 70⁰C for 40 days
- iii) Water immersion at 25⁰, 40⁰, 50⁰, 60⁰ and 70⁰C for 40 days.

In order to generate more informative data for the five resin matrices, it was decided to condition the samples for 40 days, rather than longer periods of time. Unidirectional and $\pm 45^0$ samples were used for moisture uptake results for two reasons. Firstly the geometry of the diffusion path is dependent on the fibre arrangement and volume fraction. Secondly, the interface has different diffusion characteristics and a wicking or capillary action can occur along the interface causing rapid diffusion.

In the discussion which follows degradation mechanism will be introduced which relates to both vinyl ester resin and polyester resin. The degradation mechanisms discussed are also applicable to epoxy based resins, but the particulars are different.

Degradation of plastics may be brought about by two means i.e. physical and chemical. The physical degradation is the deterioration of resin properties without breaking chemical bonds. It is associated with solvents and water. As opposed to chemical deterioration, physical degradation may be reversible. Water can chemically attack both resin and glass. These processes are extremely slow, and the primary corrosion mechanism is physical, caused by water diffusion into the matrix. Water adsorbs strongly at the glass-resin interface, and water attack is usually recognisable by the cloudiness or opaqueness of glass-resin laminates. This was noticeable with both vinyl ester resins and polyester resins for water immersion at 60° and 70°C respectively. The chemical degradation is deterioration of a resin or composite in which chemical bonds are broken. This may include an attack of the reinforcing material as well as the resin. It is well known that laminates are not as resistant to attack as are resin castings^{130,131}. As pointed out above some of the damage is physical, caused by diffusion of water or solvent into the laminate, where it can collect at the resin-glass interface. The major chemical degradation mechanisms for vinylester resins and polyester resin applicable in this situation was found to be hydrolysis. Hot water attacked the glass reinforced plastics by hydrolysis of the resin, fibres and interfacial bond. Hydrolysis of ester linkages may occur in hot water, where it is a reaction of some concern for the polyester resin. The reaction is accelerated by acid or base. The presence of the styrene as a co-reactant in the resin blends is beneficial in reducing the extent of the reaction. In addition, vinylester resins have a methyl group derived from methacrylic acid which shields the vulnerable ester linkage. Further, most of the vinyl ester resins have only two ester linkages per molecule which makes them less susceptible to attack than the polyester resins.

Epoxy base resins do not contain hydrolysable ester groups and so the water has less scope for producing fresh osmotic solutes by hydrolysis. The accommodation of water in crosslinked epoxides is a complex matter. It appears probable that much of the water is bound to hydroxyl and other polar groups, rather than in the free state.

5.2.1 Appearance Changes

None of the samples tested in 60% RH and 95% RH showed any appearance changes after 40 days at 25^o, 40^o, 50^o, 60^o and 70^oC. During water immersion, there were no significant changes in appearance in any of the samples at 25^o and 40^oC after 40 days. However as the temperature increased several specimens suffered external damage. At 50^oC, surface cracks were visible on epoxy MY 750 samples after 40 days, other samples were unaffected. At 60^oC for the same material, the cracks were observed after 16 days and at 70^oC the cracks were observed only after 7 days. Figure 228 shows the surface appearance of epoxy MY 750 specimens, exposed to water at 70^oC after 40 days. The micrograph shows that hot water has leached away resin from the surface of the specimens, making the fibres visible to the naked eye. Although this photograph was taken after 40 days this damage was apparent after 7 days, i.e. the fibres were visible to the naked eye. The epoxy MY 750 samples appear to have more surface cracks and cracks were also much deeper than other materials tested (Figure 228b). At 60^oC in the water bath, the fibres on the epoxy samples became visible after 16 days. At this stage the surface was examined under the scanning electron microscope. The resultant micrographs were similar to those shown in Figure 228.

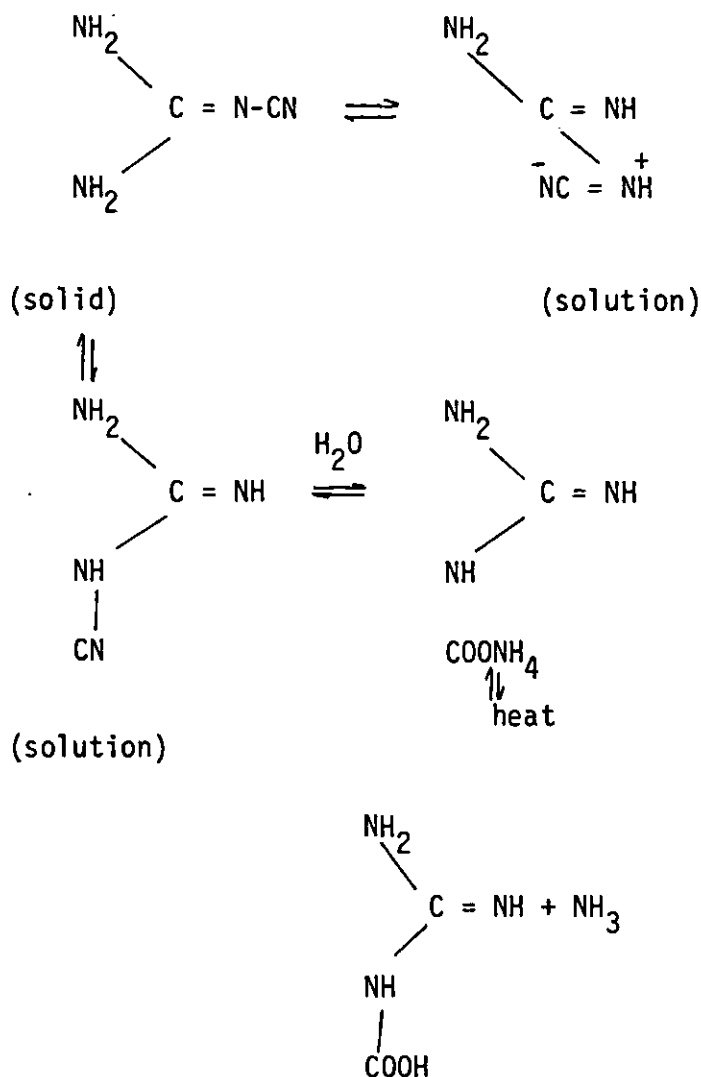
There were no surface cracks observed in the polyester 272 at 50^oC and 60^oC respectively. At 70^oC, the cracks were noticed after 35 days. Figure 229 shows the surface appearance of polyester 272 after 40 days in the water bath at 70^oC. It can be seen from the photograph, that hot water has 'washed' away some of the resin from the surface. The surface was also examined under the scanning electron microscope (Figure 229c). The random fibre distribution shown in Figures 228-229 was due to the action of the laminating roller during manufacture of the specimens.

Neither of the vinyl ester resin composites exhibited any surface cracking within the time period of the experiments. It is believed that this can be attributed to the relatively few ester groups available for hydrolysis. Moreover vinylesters are formulated so that the few ester linkages present

are located at the ends of molecules rather than randomly. The number of accessible hydrolysable ester groups in polyester affects the extent of hydrolysis leaching in hot water and therefore affects the formation of surface cracks.

Figure 230 shows the surface appearance of 913 PrePreg after 40 days at 70°C. The photograph shows a series of white patches on the surface of the specimen. These patches started to appear after 20 days at the centre of the samples. After 35 days, the whole sample surface developed white patches. Apart from the white patches, the sample's surface also showed small rectangular bubbles (blisters). It is believed that white patches are due to leaching out of the resin from the surface and the formation of blisters are due to osmotic pressure. The water diffuses through the resin and separates out at voids. In the process it dissolves any soluble materials in the surrounding glass and resin. The resin acts as a semi-permeable membrane and the osmotic pressure develops inside the hole because the water continues to diffuse to the regions with the largest concentration of soluble material. The pressures are eventually sufficient to cause rupture and blister formation. There was no sign of any blistering at 25°, 40°, 50° and 60°C for 913 PrePreg.

The curing agent used in 913 PrePreg is a complex amine hardener, dicyandiamide (DICY). This is often referred to as a latent curing-agent and it is this property that makes it so attractive for PrePreg. There is little or no reaction with the PrePreg at room temperatures. DICY has very low solubility in water at ambient temperatures, but becomes much more soluble at high temperatures e.g. 70°C and above. When DICY dissolves in water it undergoes reactions such as those illustrated below¹³⁰, which produces free ammonia:



An accumulation of free ammonia might be expected within the confined space of the water bath and some diffusion within the laminates could also occur. The presence of ammonia accelerates the hydrolysis of glass fibres¹³¹ and ammonia with the laminate interior would also be expected to increase the rate of water absorption, by acting as a source of osmotic pressure.

Another possible manifestation of osmotic pressure in composite material is the initiation of fibre-resin debonding by the development of pressure pockets at the surface of fibres, following the diffusion of water to

the fibre-resin interface and leaching of water-soluble substances from the fibre surfaces. Figure 230(b) shows the appearance of debonding which occurred in the system. The location of debonding was confined to the uppermost layer of glass (nearest to the exposed surface). Sectioning through the white patches previously mentioned, showed substantial debonding had occurred in specimens exposed at 70°C (Figure 230(b)). Debonding of the fibres from the matrix was also observed in other systems. Both vinylester resins showed debonding at 60°C and 70°C after 40 days. Debonding was also observed with Polyester 272 at the same temperatures after 40 days. The debonding was more severe in the 913 PrePreg and epoxy MY750. The resultant micrographs are similar to those shown in Figure 231.

None of the samples tested in humid air showed any colour changes after 40 days at 25°, 40°, 50°, 60° and 70°C. During water immersion, the colour of each resin tended to fade. The significant changes occurred at higher temperatures i.e. at 60° and 70°C respectively. Polyester 272 changed its colour from white to cloudiness, and both the vinylester resins (470-36 and 411-45) showed colour changes. The 913 PrePreg changed its colour from dark red to light red. The changes in colour indicate a change in properties of the matrix material. This is a physical degradation, i.e. deterioration of the resin properties without breaking chemical bonds. At lower temperatures i.e. at 25°, 40° and 50°C, the colour changes are reversible. At these temperatures when the samples were dried in a vacuum oven at 35°C for a week, the original colour was restored. At high temperatures it was not possible, indicating permanent damage to the composite and especially to the matrix. The specimens most affected were Polyester 272 and both epoxy base resins i.e. MY750 and 913 PrePreg.

5.2.2 Weight Increase

The plots of weight percent water absorption versus the square root of time for the five materials at 25°, 40°, 50°, 60° and 70°C for 60% RH, 95% RH and water bath are shown in Figures 63-132. It is clear from

these graphs that the initial rate of weight increase and the final weight after 40 days depends on:

- a) the material
- b) the temperature
- c) the environment (% RH).

5.2.2.1 60 Percent Relative Humidity

Figures 63-72 show the plots of weight changes from the five materials exposed at 25^o, 40^o, 50^o, 60^o and 70^oC as functions of time for both 0^o and $\pm 45^{\circ}$ fibre orientation. A number of observations can be made concerning the water absorption behaviour shown in Figures 63-72. Firstly, the vinyl ester resins tend to pick up less moisture than other materials. This is because the vinylester resins have relatively few ester groups available for hydrolysis, and also the methyl group which shields the ester linkage increases resistance to hydrolysis. Vinylester 470-36 tended to absorb more moisture than Vinylester 411-45, because of its higher crosslink density and more ester groups for hydrolysis.

The second observation, which can be made, is that the absorption behaviour at 25^o, 40^o, 50^o, 60^o and 70^oC appears to conform 'approximately' to Fickian behaviour for both 0^o and $\pm 45^{\circ}$ fibre orientation for both vinyl ester resins, polyester resin and epoxy MY750. The definition of the Fickian behaviour is that the initial percent weight increases linearly with the square root of time and is followed by a levelling of the weight (saturation). For both vinylester resins, polyester resin and epoxy MY750 the initial percent weight increased linearly with square root of time but there was no sign of the weight being levelled off. This was due to the exposure time, which was not long enough for the materials to reach an equilibrium point. The absorption behaviour for 913 PrePreg compared to the other materials tested was different i.e. the initial percent weight increased linearly with the square root of time, then there was a slight relaxation in increase in percent weight followed by

further rapid increase in percent weight rather than reaching an equilibrium point. This is known as two phase diffusion behaviour. The 913 PrePreg is known to contain two epoxy resin types and a further additive with dicyandiamide hardener (see Section 2.1.5). So therefore it is possible that each resin has different diffusion characteristics. Other workers⁷⁷ have also found that the hardener used to cure the epoxy resin had an effect on the diffusion kinetics for cured glass fibre reinforced laminates, a diamine hardener resulted in classical diffusion behaviour (Fickian), whereas a dicyandiamide hardener gave a two phase diffusion behaviour and an anhydride hardener resulted in such damage above 40°C that it was not possible to describe the diffusion behaviour.

The third observation, which can be made, is that the rate of moisture absorption increased with temperature as did the apparent equilibrium moisture content (Figures 73-82).

The apparent diffusivities were calculated showing that water absorption initially followed Fick's law.

Figures 134 and 135 show the graphical plots of log of the diffusion coefficient versus the inverse of the absolute temperature for the five composite materials tested, yielding an activation energy of diffusion. The values for activation energy of diffusion were similar for the five materials tested. The values ranged from 12.891 kJ mol⁻¹ for 913 PrePreg to 19.052 kJ mol⁻¹ for 470-36 Vinylester. All the materials tested showed a strong empirical linear relationship between diffusion coefficient and the temperature, indicating that the diffusion coefficient depends on the temperature, as given by the Arrhenius equation:

$$D = D_0 \exp (-E/RT)$$

The full results for diffusion data for both 0° and $\pm 45^\circ$ samples respectively are given in Appendix A.

The diffusion plots for 0° and $\pm 45^\circ$ specimens show that the initial rate of water absorption for Epoxy MY750 and 913 PrePreg is much slower than both vinylester resins and polyester resin, although the total quantity of water absorbed by both resins after 40 days was higher, so it seems that the low initial permeability simply delays any effects associated with water uptake. The accommodation of water in crosslinked epoxides is a complex matter, it appears probable that much of the water is bound to hydroxyl and other polar groups, rather than in the free state. Epoxides do not contain hydrolysible ester groups and so the water has less scope for producing fresh osmotic solutes by hydrolysis, it appears probable that much of the water is bound to hydroxyl and other polar groups, rather than in the free state, whereas both vinylester and polyester resin contain hydrolysable ester groups. Direct comparison between 0° and $\pm 45^\circ$ data shows that the initial water absorption for $\pm 45^\circ$ specimens is much faster (i.e. higher diffusion coefficient values) under the same exposure conditions. This was due to the rapid diffusion along the fibre-resin interface for the $\pm 45^\circ$ samples. The fibre-resin interface has different diffusion characteristics and a wicking or capillary action can occur along the interface causing rapid diffusion. Figures 149, 152, 155, 158 and 161 show the diffusion plots for 0° and $\pm 45^\circ$ specimens. It can be seen from the plots that the lines of the graph for the 0° and $\pm 45^\circ$ composites are almost parallel, but the activation energies for diffusion for both laminates are not the same. Additional data are necessary to ascertain whether this apparent difference in activation energies between the unidirectional and $\pm 45^\circ$ laminates is real or due to a limited data base.

Other workers¹³² found that activation energies for graphite/epoxy unidirectional and bidirectional (0/90) composites were different under identical exposure conditions. They also found that good correlation between the data and Fick's law was obtained for both the neat resin

and the unidirectional composites, while the correlation for the bi-directional laminate was rather poor. The activation energy values for neat resin, unidirectional and bidirectional were 13.4 kJ mol^{-1} , 9.47 kJ mol^{-1} and 6.98 kJ mol^{-1} respectively.

5.2.2.2 95 Percent Relative Humidity

Figures 83-102 show the plots of weight change of specimens exposed to 95% RH at 25° , 40° , 50° , 60° and 70°C as functions of time for both 0° and $\pm 45^{\circ}$ fibre orientation. The rate of moisture absorption increased with temperature as did the "apparent" equilibrium moisture content, as compared to 60% RH. Epoxy MY750 and 913 PrePreg absorbed the most moisture at 40° , 50° , 60° and 70°C , while Vinylester 411-45 absorbed the least. As will be seen later, absorbing a smaller amount of moisture does not necessarily mean a smaller degradation in mechanical properties. Both Vinylester 470-36 and Polyester 272 absorbed more moisture than Vinylester 411-45. At 25°C , the amount of moisture absorbed by all the specimens was similar with the exception of epoxy MY750 which absorbed slightly more.

The water absorption behaviour of both vinylester resins and polyester resin (at all temperatures tested) appears to conform to Fickian behaviour. The initial percent weight increased linearly with square root of time and was followed by a slow increase in percent weight. As the temperature increased, the time taken by the specimens to reach equilibrium moisture content decreased. The equilibrium moisture content did not always remain constant after it reached a level value, but kept either increasing or decreasing. This was particularly true at higher temperatures. This may be due to thermal spiking effects i.e. removing samples from higher temperature/humidity to room temperature/low humidity, for weighing.

The water absorption behaviour of Epoxy MY750 resin at 25° , 40° , 50° and 60°C appears to conform to Fickian behaviour. At 70°C the initial

moisture absorption was linear with $(\text{time})^{\frac{1}{2}}$, but instead of reaching a final equilibrium value, the rate of moisture uptake started to increase rapidly. The weight was still increasing after 40 days. The same picture was observed with $\pm 45^{\circ}$ specimens. This suggests that there may be a change in the chemical structure. Another possible explanation for this behaviour is that, the working temperature (70°C) is approaching the glass transition temperature of the resin (90°C).

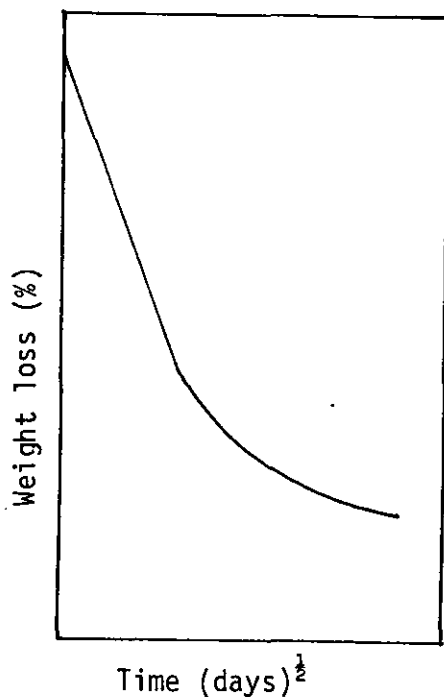
The water absorption behaviour of 913 PrePreg at all the temperatures tested, exhibited non-Fickian behaviour. The initial percent weight increased linearly with $(\text{time})^{\frac{1}{2}}$, then there was slight relaxation in increase in weight followed by a further rapid increase in percent weight rather than an equilibrium point. The weight was still increasing after 40 days for both 0° and $\pm 45^{\circ}$ specimens.

The apparent diffusivities were calculated, assuming that the initial water absorption followed Fick's law. The values for diffusion coefficient, for all the materials tested are presented in Appendix A. Figures 135 and 136 show the plots of log of diffusion coefficient against the inverse of the absolute temperatures for the five composite materials, yielding an activation energy of diffusion. Both vinyl ester resins and polyester resins showed strong empirical linear relationship between the temperature and diffusion coefficient. For epoxy MY750, this empirical linear relationship was not obtained, because at 70°C , the calculated diffusion coefficient was slightly lower than that at 60°C . This cannot be possible, because the diffusion process is strongly temperature dependent. This indicates that the absorption curve at 70°C did not exhibit Fickian behaviour. Although for 913 PrePreg, the overall water absorption behaviour was non-Fickian at all the temperatures, the relationship between temperature and diffusion coefficient is reasonably linear. The values for activation energy were lower than that for 60% RH for both 0° and $\pm 45^{\circ}$ composites. This is because there is less energy required at higher environmental conditioning (95% RH) for the water molecules to diffuse into the matrix than at lower environmental conditioning (60% RH). The values are given in Appendix A.

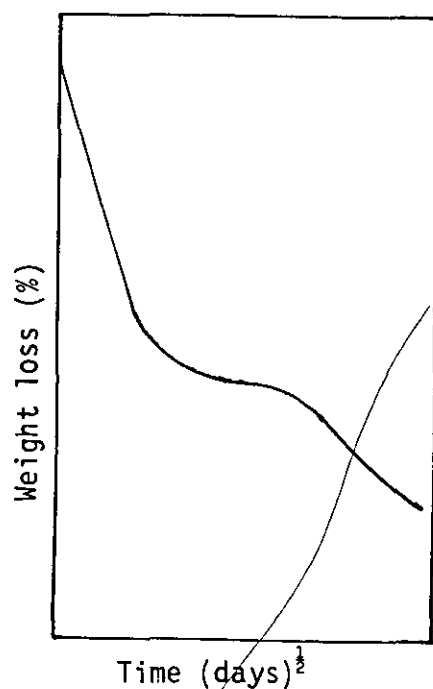
The direct comparison between unidirectional and $\pm 45^\circ$ data shows a much faster initial moisture pick-up for the $\pm 45^\circ$ laminates under the same exposure conditions. Figures 150, 153, 156, 159 and 162 show the Arrhenius plots for 411-45, 470-36, 272, 750 and 913 respectively. The maximum moisture content for $\pm 45^\circ$ was also higher than 0° specimens due to the rapid diffusion along the fibre-resin interface.

The whole process was reversible i.e. sample weight returned to its original value when dried at 35°C . The 913 PrePreg samples took a long time for the weight to reach its original value. This was due to the fact that it absorbed the most moisture. It was also interesting to observe the shape of the desorption (weight loss) when plotted against $(\text{time})^{\frac{1}{2}}$. For both vinylester resins, polyester resin and epoxy resin, the weight decreased linearly with square root of time and eventually reached an equilibrium point as shown below, whereas with 913 PrePreg the desorption process was a two stage process similar to the absorption (weight gain) process.

Desorption curve for 411, 470,
272 and 750



Desorption curve for 913



Therefore it is possible from these desorption curves to predict whether the absorption mechanism is Fickian or non-Fickian. Essentially, in Fickian diffusion, the absorption (weight gain) and desorption (weight loss) curves when plotted against $(\text{time})^{\frac{1}{2}}$ are always concave towards the $(\text{time})^{\frac{1}{2}}$ axis and asymptotically reach the final equilibrium value. The desorption curves for $\pm 45^{\circ}$ specimens were similar to those for 0° specimens.

5.2.2.3 Water Bath

The plots of weight percent water absorption versus the square root of time for the five materials at 25° , 40° , 50° , 60° and 70° are shown in Figures 103-120. The initial rate of moisture absorption increased, as did the apparent equilibrium moisture. In some cases the maximum moisture content was lower than that obtained for 95% RH. It is difficult to make direct comparison of water absorption behaviour of the specimens which have been exposed to water bath and to 95% RH. This is due to leaching out of water soluble constituent parts from the composite, when the specimens are immersed in the water bath. The leaching out of the water soluble constituent can even happen at lower temperatures, although it becomes more apparent as the temperature increases. This was demonstrated by drying the samples at 35°C in an air oven, after removing them from the water bath, after 40 days. All the samples tested at 25° , 40° , and 50°C showed small weight losses except 913 PrePreg which did not show any weight losses. The weight losses may be attributed to lost resin. Attempts were made to analyse extracted materials using infra-red spectroscopy to see what organic materials were leached out, but this was unsuccessful because there was insufficient extracted material. Loader¹⁰⁶ pointed out the extraction losses in vinylester and polyester may be attributed to the loss of water-soluble volatile materials such as methyl ethyl ketone. As the test temperature increased, the weight losses also increased (Table 5.1). However this weight loss did not show on the water absorption curves (Figures 103-107) because as long as the moisture gain was greater than the material loss, the weight of the specimen increased. Once the weight of the lost material exceeded

the weight of the absorbed moisture, the weight of the specimen decreased (Figures 109-112). The shape of the desorption curve was similar to that described in Section 5.2.2.2. The 913 PrePreg again took a long time for the weight to reach its original value.

From the absorption (weight gain) and desorption (weight loss) curves, it was possible to see the water absorption of 913 PrePreg was different to other materials tested. The absorption mechanism of 411, 470, 272 and 750 for both 0° and $\pm 45^{\circ}$ appears to conform, at least approximately to Fickian behaviour. After an initial linear increase with square root of time, the weight nearly levelled off. The rate at which the weight was increasing was very slow. With 913 PrePreg, the initial weight increased linearly with square root of time, followed by a slight relaxation in weight increase, and after 9 days, a further rapid increase in the percent. After 40 days, the weight was still increasing at much faster rates than others. At 25°C Polyester 272 absorbed the most moisture and Vinylester 411-45 absorbed the least. As the temperature increased, both 913 PrePreg and Epoxy MY750 absorbed moisture, while Vinylester 411-45 absorbed the least.

When specimens were tested in a water bath at 60°C , mechanisms other than simple water absorption began to affect the weight gain. The initial linear increase of percent weight for both vinylester resins and polyester resin was followed by an equilibrium point. The percent weight levelled off after 4 days. With 913 PrePreg, after the initial linear increase with $(\text{time})^{\frac{1}{2}}$, there was slight relaxation in weight increase, followed by rapid increase in weight. There was no equilibrium point, the weight was still increasing after 40 days. This non-Fickian behaviour was also observed with $\pm 45^{\circ}$ laminates. With Epoxy MY750 the initial linear percent weight increase was followed by saturation. After saturation, irregular changes in specimen weight were observed, but after 16 days, the weight of the specimens started to decrease rapidly (Figure 109). This sharp drop in weight was followed by a more steady fall. This was due to permanent microdamage (Figure 232), with the accompanying loss of

resin and the fibre material. This sharp drop in weight was also observed by other workers^{4,130}. The initiation mechanism of these microcracks depends on osmotic pressure generation, or alternatively on debonding cracks. The osmotic centres accelerate water absorption and eventually generate microcracks; the cracking process is assisted to an unknown extent by debonding (Figure 233). Water also penetrates to the fibre-matrix interface and fibre-coupling agent interface, the consequences of which are believed to be as follows:

- a) Interfacial bonds provided by the coupling agent are ruptured or degraded;
- b) Glass fibres are exposed and water molecules are absorbed on to their surfaces, with a significant reduction of their surface energy and subsequent tensile strength; and
- c) The degradation of glass fibre, also loss of interfacial bonding through degradation or the coupling agent.

Direct evidence of the nature and location of the degradation caused by hot water absorption is provided by photomicrographs in Figures 234-236. The differences in the series are clear; the fibre contours of the specimens previously exposed to hot water are distorted and roughened. Some indication of the leaching action on the glass fibres was also provided by atomic-absorption spectrometry analysis of the extracted materials. The analysis of the water solution showed distinct traces of silica, sodium and potassium compounds. Attempts were also made to analyse extracted materials using infra-red spectroscopy to see what organic materials were leached out, but this was unsuccessful because there was insufficient extracted material. The same trend was observed with $\pm 45^\circ$ specimens (Figure 110). Both vinyl ester and polyester resins showed Fickian behaviour, whereas with Epoxy MY750, there was a weight decrease again after 16 days. Microcracking and debonding was observed with Epoxy MY750 specimens. The 913 system did not show Fickian behaviour and the weight was still increasing after 40 days.

The absorption behaviour of the five materials at 70°C is shown in Figures 111 and 112. Epoxy MY750 showed the same behaviour as with 60°C, but this time the weight started to decrease after only 7 days and continued to drop sharply with square root of time. The examination of the specimens again showed microcracking of the matrix similar to that shown in Figure 232, massive debonding of the fibres from the matrix similar to that shown in Figure 233, degradation of the glass fibres and massive surface cracks. The analysis of the water by atomic absorption spectrometry showed distinct traces of silica, sodium and potassium compounds, indicating the leaching of the soluble oxides from the glass fibres. Both the vinylester resins showed a small decrease in percent weight after 12 days for 411-45 and 30 days for 470-36 (Figures 113, 114, 115 and 116). At this stage it was decided to place unfilled specimens of 411-45, 470-36 and 750 in the water bath to observe the water absorption behaviour. The results obtained were interesting, especially with both vinylester resins. The absorption curves for both vinylesters did not show any weight loss, whereas the absorption curve for Epoxy MY750 did show weight loss. The absence of such weight loss in the unfilled specimens of both vinylester resins indicates that the degradation process takes place mainly at the glass surfaces or at the fibre-matrix interfaces. Other workers¹³⁵ have also indicated that deterioration of the glass-resin interface has been the major cause of degradation in glass reinforced vinylester. A further question arises as to whether this deterioration occurs at glass-coupling agent interface or the resin-coupling agent interface. The glass-coupling agent interface is the weakest in the glass reinforced plastic materials, and when water reaches this interface the siloxane bonds between the silica coupling agent and the glass surface are easily hydrolysed. The reformation of some of these bonds upon drying has been demonstrated¹³⁶, implying that degradation of this interface is reversible.

The analysis of the water medium used for immersion of both vinylester resin specimens showed slight traces of silica, sodium and potassium compounds similar to those obtained for Epoxy MY750 specimens. Attempts were also made to analyse the material extracted from the water solutions

by infrared to see if there were any traces of resin, or coupling agent, but it was not successful because there was insufficient extracted material. There was no sign of any microcracking with both vinylester specimens, as observed with Epoxy MY750, but both showed debonding between glass fibres and the matrix.

There was no sign of any weight loss with Polyester 272 and 913 PrePreg. With Polyester 272, the initial linear increase in percent weight was followed by a saturation point, but after 16 days the weight started to increase rapidly (Figure 117). The higher weight uptake for the samples was due to the debonding of some of the fibres which traps additional water, and also the formation of the surface cracks which increase the water uptake. The surface cracks were observed after 14 days which coincided with the onset of increase in the weight of the specimens. There was no equilibrium point obtained for 913 PrePreg, the weight was still increasing after 40 days, but at a very slow rate.

Although the initial absorption behaviour of all specimens tested at 60°C and 70°C showed Fickian behaviour, the overall process is non-Fickian. The fundamental characteristics of non-Fickian behaviour are that if cracks develop in the material or debonding occurs^{and} essentially^{they} alter the chemical structure of the material. Figures 137 and 138 show plots of log of the diffusion coefficient versus inverse of the absolute temperature for the five materials. For all the materials tested, 913 PrePreg, Polyester 272, Vinylester 411-45 and Vinylester 470-36 showed a strong empirical linear relationship between diffusion coefficient and temperature. For Epoxy MY750, there was no such linear relationship because of extensive damage done to the samples at 60°C and 70°C during immersion. The same was observed with $\pm 45^\circ$ specimens (Figure 138). The $\pm 45^\circ$ specimens again showed the initial rate of absorption of water was much greater than 0° specimens for all the samples (Figures 151, 154, 157, 160, 163). The activation energy values for both 0° and $\pm 45^\circ$ specimens were much lower than for 60% RH, which was as expected, because at higher environmental conditions, there was less force required for

the water molecules to diffuse into the resin matrix, but values compared to 95% RH were almost the same or slightly lower. The activation energy values are listed in Appendix A. Figures 139 to 148 show the Arrhenius plots for the five materials separately. The plots show the comparison between the three different environmental conditions i.e. 60% RH, 95% RH and water immersion. It can be seen that as the conditions get more severe, the rate of water uptake increases rapidly (higher diffusion coefficient) at any temperature. The graphs also show that the slopes of the lines are almost parallel to each other, indicating similarities in the activation energy values. The same was observed with $\pm 45^\circ$ specimens.

Redrying of the specimens after being removed from water bath after 40 days at 60° and 70°C showed weight losses (Table 5.1). The weight of 913 PrePreg specimens did not return to its original value. The samples were left for 60 days at 35°C in a vacuum oven. The weight levelled off at 0.300%, after 45 days. The weight may have returned to its original value, if the specimens were left for a long time, but this was impracticable.

5.2.2.4 Thermal Spiking

The specimens were held at 95% RH, 25°C for 18 hours and spiked daily for 4 hours at 95%, 70°C . This procedure was repeated daily for 40 days. The data obtained for 0° and $\pm 45^\circ$ specimens are presented in Figures 123, 132. The results show that thermal spiking did not change significantly the moisture absorption characteristics of the material as represented by the moisture content as a function of time, the maximum moisture content and the diffusion coefficient. The initial rate of moisture uptake and the final moisture content was higher than 95%, 25°C but lower than 95% RH, 70°C . The absorption behaviour for 411-45, 470-36, 272 and 750 for 0° and $\pm 45^\circ$ laminates appears to conform approximately to Fickian behaviour. The initial linear relationship between percent weight gain and square root of time was observed followed by levelling out of the

weight. The moisture behaviour for 913 PrePreg was non-Fickian type. From these results it is not possible to assess the effect of thermal spiking on the absorption behaviour of the materials.

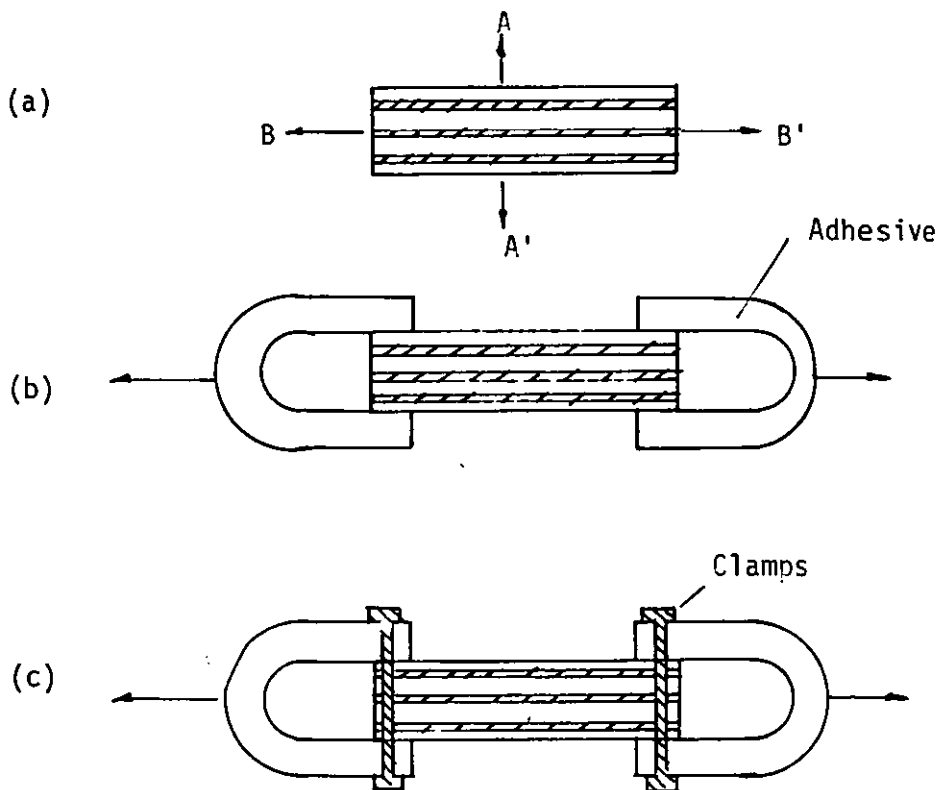
The relationship between thermal spikes and material behaviour are not fully understood yet. In fact some of the evidence is contradictory. Significant changes have been observed in some materials subjected to thermal spikes^{79,138}, while only minor changes were found in some other materials under presumably similar spike conditions^{81,139}. Other workers^{136,137} found that increases in both the initial rate of moisture uptake and final moisture content were due to the formation of microcracks in the resin.

5.3 GLASS-TRANSITION TEMPERATURE (T_g)

The T_g is an important parameter with moisture transfer process. In practice, the transition occurs over a temperature range. However, the T_g is a convenient parameter for molecular structure of the material. The moisture acts as a plasticiser, thus lowering the value of T_g of the resin. The lowering of T_g with increasing moisture content is illustrated in Figures 164-169. The results show that 913 and 750 suffered the largest decrease in T_g, 18° and 80°C respectively, because both absorbed the most amount of moisture. The initial drop in T_g was small for all the materials. The T_g decreased by 8°, 12° and 70°C, respectively for 411-45, 470-36 and 272. The amount of moisture absorbed by 411-45, 470-36 and 272 was 0.62%, 0.82% and 0.9% respectively. It is very difficult to compare the reduction in T_g for the material tested because all absorbed different amounts of moisture (Figure 169).

5.4 MECHANICAL PROPERTIES

It is well known in the fibre composite technology that the fibre-matrix interface gives fibre composites their structural integrity. In particular, the large differences between the elastic properties of the matrix and fibres have to be communicated through the interface or, in other words, the stress acting on the matrix is transmitted to the fibres across the interface. The interface in a fibre-matrix composite is a surface which is common to both fibre and matrix and the immediate region about this surface. It has physical and mechanical properties which are neither those of the fibre nor those of the matrix. An example of the role of the fibre-matrix interface is illustrated below:



Schematic diagram of a layer composite material to illustrate the importance of the interface bond strength

The composite material is represented by alternate sheets of material with different elastic properties (Figure a). In the absence of a chemical, physical or mechanical bond between the layers the composite has no tensile strength direction AA' normal to the layer planes. The strength and modulus in direction BB', parallel to the layers, depends on the way the sample is gripped. If no bond exists and a simple adhesive grip is made to the outer layers and no normal force is exerted, (Figure b) the strength is limited to the strength of the outer layers since the applied load is taken up entirely by these layers. On the other hand, if the layers are all clamped together in the grips (Figure c), all the layers take the load and the composite will be much stronger and stiffer. It follows from this example that in order to use the high strength and stiffness of the fibres, they have to be strongly bonded to the matrix. However this interface bond strength is easily affected even without stresses produced by external loads, i.e. water at the interface and microresidual stress effects on interface. Shrinkage stresses during cure and thermal stresses due to differences between the thermal expansion coefficients of the matrix and fibre also affect the microstress at the interface in a composite material and are additional to the stresses produced by external loads. The stresses due to curing arise from a combination of resin shrinkage during the curing process and differential thermal contraction after post-curing at an elevated temperature.

5.4.1 Ultimate Tensile Strength (UTS)

The UTS of all the materials conditioned at 60% RH and tested after 16 and 40 days, respectively decreased with moisture content as shown in Figures 172-181. The UTS for 411-45, 470-36 and 272 decreased slightly as the test temperature was increased, generally less than 6% at all temperatures for 411-45, and less than 8% for 470-36 and 272 at all temperatures except at 70°C when the decrease was 12% for both materials. The decrease for 913 and 750 at 250°C was 8% and 5% respectively. As the conditioning temperature was increased, both suffered large drops in UTS than the other materials. The UTS decreased by 20% and 15%,

respectively for 913 and 750 tested at 70°C. Both 913 and 750 absorbed more moisture than the other materials at all temperatures, and this was reflected in the drop of UTS. The high drop in UTS at high temperatures, especially for 913 and 750 tends to indicate that the tensile properties of the glass fibre were also affected by moisture. The absorbed moisture proceeds along the glass-resin interface faster than through the resin. The interfacial bond between the fibres and the resin was also affected as indicated by the ILSS (Section 5.4.4). At low moisture levels, the UTS drop was due to degradation of the matrix, since the UTS of the composites is less sensitive to moisture than that of the matrix due to strong influence of the fibres on the strength of the samples. The UTS degradation was reversible for all the materials at all temperatures, when the specimens were redried and tested (Table 5.2). Hence no fibre damage or permanent interface damage.

The UTS of all the materials conditioned at 95% RH decreased rapidly as the test temperature was increased (Figures 172-181), due to more moisture being absorbed by all the materials. The UTS decreased by 11%, 12%, 7%, 20% and 15%, respectively for 411-45, 470-36, 272, 913 and 750 tested at 25°C after 40 days. As the test temperature increased, the amount of moisture absorbed by all the specimens also increased, with 913 and 750 absorbing the most moisture at 70°C and 411-45 absorbing the least. However, the fact that 411-45 absorbed low moisture did not mean smaller degradation in UTS. The amount of moisture absorbed by 411-45 at 70°C after 16 and 40 days was 0.559% and 0.602%, respectively, and for 913 at the same conditions it was 1.44% and 1.84%, respectively. The UTS decreased by 34% and 42% for 411-45 after 16 and 40 days at 70°C, whereas the decrease for 913 was 30% and 40% respectively. Both 272 and 470-36 showed similar trends to 411-45. These results show that both 913 and 750 exhibit strong relationships between percentage moisture content and percentage decrease in UTS. Both materials show that the drop in UTS was gradual, as the percentage moisture increased, whereas for 411-45, 470-36 and 272, after the small drop in UTS at low moisture levels, there was sudden large decrease in UTS when the amount of moisture absorbed by the three materials increased slightly.

decreased drastically after 40 days. The test conditions in this study were rather severe and may not represent environments in which these materials would be routinely exposed. As mentioned earlier, other mechanisms than simple water absorption affected the samples, i.e. leaching of resin, leaching of the interface and fibres. Hot water attacks Vinylester and Polyester laminates by hydrolysis of the resin, fibres and interfacial bond. The debonding was observed with all the materials, with consequential decline in UTS. When hot water penetrates the fibre-matrix interface, it is believed the consequences are as follows:

- (a) interfacial bonds provided by the coupling agent are degraded;
- (b) glass fibres are exposed and water molecules are absorbed on their surfaces, with significant reduction of their surface energy and subsequent tensile strength. The UTS decreased by 58% and 56% respectively for 411-45 and 750 tested at 70°C after 40 days. This decrease was higher than other materials tested at the same temperature, i.e. 51%, 45% and 48% for 470-36, 272 and 913. This makes sense, because both 411-45 and 750 showed excessive leaching of the resin, and interface hence the fibres were exposed to hot water attack. No recovery of the strength was seen for any materials tested at all temperatures (Table 5.4).

5.4.4.1 Tensile Failure Mode

Two types of tensile failure modes were observed when the specimens were tested. The specimens conditioned at 60% RH at various temperatures, and tested after 16 and 40 days, respectively, showed a typical 'brush' like failure with obvious fibre pull-out (Figure 237a). This type of failure was also observed in specimens tested after drying. When the composite is loaded the stress on the fibres is related to the stress on the laminate by:

$$\sigma_{11} = \sigma_f V_f + \sigma_m (1 - V_f)$$

where σ_{11} = stress parallel to fibres

So, therefore the results suggest that there is some sort of threshold level of water at which 411-45, 470-36 and 272 are strongly affected. Similar trends were observed with ILSS results.

The degradation of UTS was due to the deterioration of the fibre-resin interface. A further question arises as to whether this is a result of deterioration of the glass/coupling agent interface on the resin/coupling agent interface. It is believed that the glass/coupling agent interface is the weakest in glass reinforced plastic materials. Once the water reaches this interface, the siloxane bonds between the silane coupling agent and the glass surface are easily hydrolysed. Glass fibres are moisture sensitive, so it would appear that interface degradation in all the samples is perhaps easily attained. Once the water attacks the fibres, the strength of the fibres is drastically reduced, which in turn reduces the composite strength, as indicated by the UTS results. The degradation of UTS was irreversible (Table 5.3) indicating permanent damage done to the samples. The reversible portion of this degradation may be due to reformation of some siloxane bonds at the glass/coupling agent interface. It appears that more than one process is responsible for the strength degradation of fibre-reinforced resin systems. These are resin property changes, interface and fibre degradation.

The UTS of all the materials decreased drastically after being conditioned in water at all temperatures. At low temperatures (25, 40°C), both 411-45 and 470-36 showed smaller decreases than the other materials. The degradation mechanism was similar to that described for 95% RH, and it was irreversible damage. As the test temperature was increased, the amount of moisture absorbed by some materials also increased. Other materials showed excessive leaching out of the resin, interface and fibre. The degradation was due to a strong attack of water on the fibre-resin interface and also on fibres. This results in loss of strength of the fibres due to 'corrosion' which contributes to strength loss of the laminates. At high temperature (60-70°C) the strength of all the materials

V_f = volume fraction of fibres

σ_f = stress on fibre

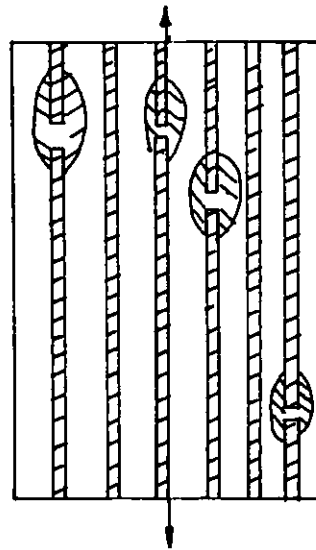
σ_m = stress on matrix

As the force was applied longitudinal cracks caused by shear stress at the interface appeared in the bulk of the specimens and propagated rapidly along the fibre-resin interface to occupy the complete length of the test piece. This debonding was followed by pronounced audible signals of cracking as fibres pull-out, usually starting at the specimen edge and propagating across the entire width. This caused total destruction of the laminate and the force dropped immediately to zero.

The tensile failure mode of the 411-45, 470-36, 272 and 750 specimens changed, after being conditioned at 95% and water bath. The outer layer of these specimens showed a distinctly "clamped" failure with large islands of fibres^{still} intact with their reinforcing fibres. The internal part of the specimens still showed the more typical "brush" type of failure (Figure 237b). The 913 PrePreg specimens only showed small "clumps" of resin and fibres intact while the main failure was "brush" type (Figure 237c).

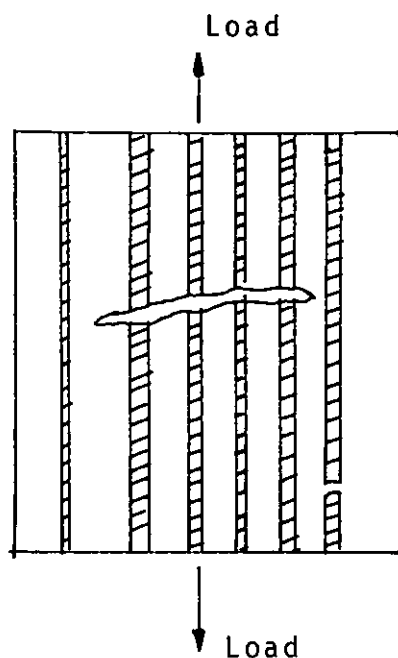
The above discussion neglects some significant features of the strength of fibres such as the variation of strength from fibre to fibre and the distribution of flaw sizes along each fibre. The composite consists of a set of parallel fibres assumed to be strong and stiff with respect to the matrix material in which they are mbedded. The fibres treated are high strength brittle fibres whose strength is dependent upon the degree of surface imperfections. It is assumed that flaws in the fibres are distributed randomly and that the statistical information for the strength of single fibres applies¹⁴⁵. When a composite is loaded, and as the load increases a fibre fracture will occur at one of the serious flaw or imperfections. When such a fibre breaks, the stress in the vicinity of the broken fibre is disturbed substantially so that the axial

stress in the fibre vanishes at the fibre break and gradually builds up to its undisturbed stress value due to shear stresses being transferred across the fibre-matrix interface. The basis of the cumulative weakening model is shown schematically below. The cracking of fibres and matrix can occur before complete separation of the fracture surface, hence "brush" type of fracture.



Region of stress
relaxation near break
in fibre

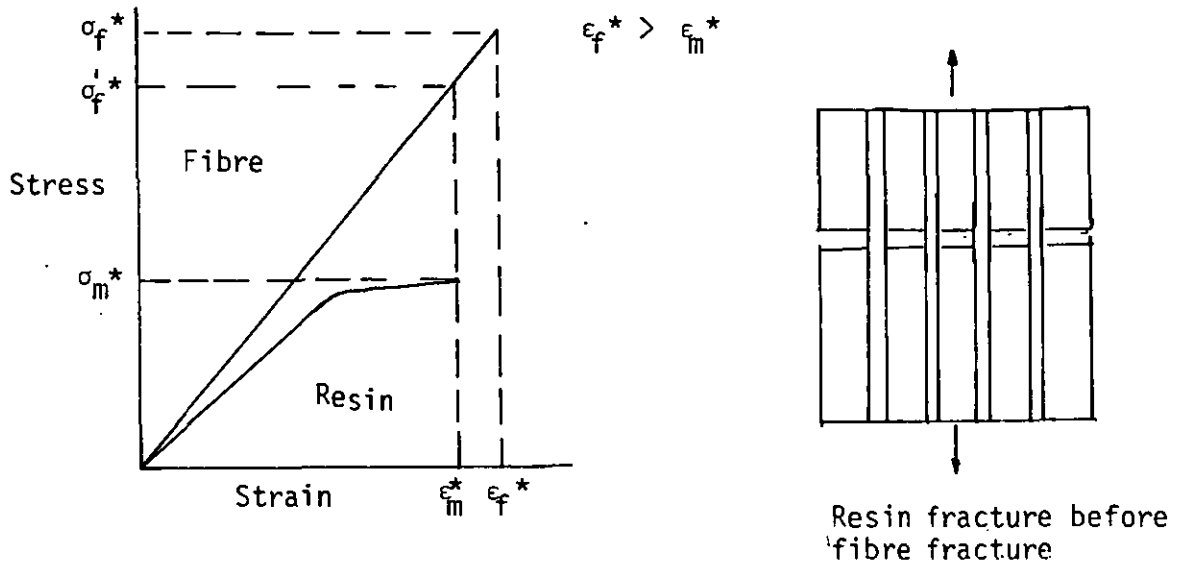
As mentioned in the previous section, the mechanical properties of the glass fibre are reduced by moisture. The presence of moisture will also affect the fibre fracture. The initial stages of the fracture follows those described above for the cumulative weakening model. As each fibre breaks, the redistribution of stress leads to additional stresses on the neighbouring fibres, i.e. there is a stress magnification effect. Thus there is an increased probability that fracture will occur in the immediately adjacent fibres: This increases as load increases and eventually sequential fibre fracture occurs. When fibre fracture occurs, the load transferred to the matrix is large and cannot be supported, so that the matrix fractures when the fibres fracture, hence "clamped" failure. The strength obtained from this type of fracture is low as indicated by UTS results. The model is illustrated schematically below.



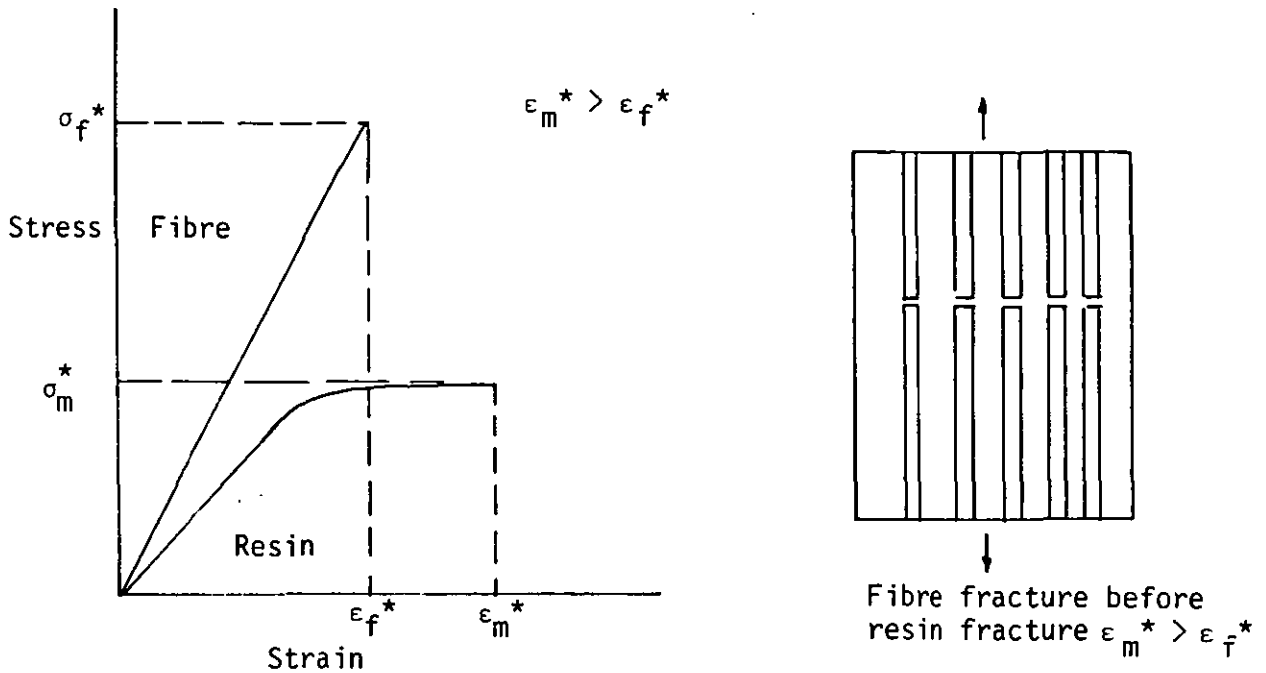
5.4.2 Percent Elongation (E1)

For unidirectional composites tested in tension parallel to the fibres $\epsilon_c = \epsilon_m = \epsilon_f$, provided that there is a strong fibre-matrix bond, where ϵ = strain and subscripts c, m, f apply to the composite, matrix and fibre respectively. When the interfacial bond is affected by moisture, the response of the composite will depend on the relative strains to failure of the matrix and fibres and two possible situations can occur. Firstly $\epsilon_f^* > \epsilon_m^*$ and secondly $\epsilon_m^* > \epsilon_f^*$, where ϵ_f^* and ϵ_m^* are failure strains in uniaxial tension of the fibres and the matrix respectively. Mild conditioning (60% RH) at 25^o, 40^o and 50^oC appears to have little effect on the percentage elongation. However as the temperature increased, all the materials showed significant drop in percentage elongation. The percentage elongation decreased by 10%, 10%, 11%, 16% and 12% respectively for 411-45, 470-36, 272, 913 and 750 at 70^oC after 40 days. As mentioned in Section 5.4.1, the deterioration of mechanical properties was due to water at the fibre-resin interface. The deterioration of the percentage elongation was reversible, i.e. it returned to its original value as the moisture diffused out (Table 5.5). The same trends were observed with UTS and E. Since the degradation of the

interfacial bond was small, the resin will fracture before fibres as illustrated below when tensile load is applied.



The matrix takes only a small proportion of the load because $\epsilon_f > \epsilon_m$ so that when the matrix fractures the transfer of load to the fibres is insufficient to cause fracture. At high environmental conditioning (95% RH and water bath), the amount of moisture absorbed by the specimens also increases. The high moisture content reduces the mechanical properties of the composite drastically due to strong attack of water at the interface and on the fibres. Moisture has the effect of flexibilising the matrix ($\epsilon_m^* > \epsilon_f^*$) or in other words, reducing the elastic moduli, the mechanical properties of fibres are significantly reduced. When the load is applied fibres fracture before the matrix as illustrated below. The load transferred to the matrix when fibre fracture occurs is very large, and cannot be supported, so that the matrix fractures when fibres fracture.



The drop in percentage elongation for all the materials at all temperatures was more obvious, often being conditioned at 95% (Figures 182-191). The percentage elongation decreased by 9%, 12%, 12%, 16% and 11% respectively at 40°C after 40 days. As the test temperature increased, all the materials continued to absorb more moisture. This was reflected on the drop of percentage elongation which increased as the percentage moisture increased. At 70°C 411-45 and 470-36 were worst affected, although both absorbed least amount of moisture. The percentage elongation decreased by 30%, 32%, 27%, 26% and 17% respectively for 411-45, 470-36, 272, 913 and 750 at 70°C after 40 days. Similar trends were observed with UTS and E results. The attack of water at fibre-resin interface and on the fibres was permanent even at low temperatures. No recovery was seen with the dried samples (Table 5.6).

At 25°C and 40°C in water, all the specimens showed similar decrease in percentage elongation, although all absorbed different amounts of moisture with 913 and 750 absorbing the most. As the temperature was increased the drop in percentage elongation also increased with the

411-45 and 470-36 showing the largest drop, although both absorbed the least amount of moisture. Large reductions of percentage elongation for all materials was due to leaching or resin and leaching at the interface which resulted in excessive debonding. There was also strong attack of water on the fibres. No recovery was seen at all temperatures (Table 5.7). The full results are listed in Appendix C.

5.4.3 Tensile Modulus (ϵ)

When a tensile load is applied parallel to the fibres in a unidirectional laminate, the strain (ϵ_1) in the matrix will be the same as the strain in the fibre if the bond between the fibre and the matrix is perfect. If both fibres and matrix behave elastically then the corresponding stresses are given by:

$$\sigma_f = E_f \epsilon_1, \quad \sigma_m = E_m \epsilon_1$$

where σ_f = stress of fibres
 σ_m = stress of matrix
 ϵ_1 = strain
 E_f = Young's modulus of fibre
 E_m = Young's modulus of matrix

It follows that $E_f > E_m$ the stress in the fibres is greater than in the matrix. This is, of course, the underlying basis of fibre reinforcement since the fibres bear the major part of the applied load. It is undoubted that degradation in the resin matrix properties would behave in a parallel degradation in composite properties. For unidirectional laminates, the simple rule of mixtures, can be used to calculate the composite modulus from given fibre and resin matrix moduli:

$$E_c = V_f E_f + V_m E_m$$

where the subscripts c, f and m refer to the composite, fibre and matrix respectively. V is the volume fraction, and E is elastic modulus. It is obvious that if E_m decreases E_c decreases accordingly, as moisture may reduce the interfacial bonding strength of the composite and cause a loss of efficiency of stress transfer between fibres. Moisture has the effect of flexibilising the resin, or in other words reducing the modulus, hence reduction in the composite's stiffness. Full results for the five materials are listed in Appendix D.

The tensile modulus decreased slightly after 16 and 40 days, respectively for 272, 913 and 750, after being conditioned at 60% RH. 411-45 showed slight increase at 40°, 50° and 70°C and 470-36 showed slight increase at all temperatures. The small increase in tensile modulus is consistent with that found by the other workers^{94,95,141}. This increase is attributed to moisture relieving the internal stress generated by different coefficient of expansion of the fibre and resin as the matrix cools from curing temperatures. The small decrease suffered by some materials was due to deterioration of the matrix, which reduces its stiffness as moisture increases. This process was reversible, in that tensile modulus returned to its original value when the environmental conditions changed and the water diffused out (Table 5.8).

When the specimens were conditioned at 95% RH, the tensile modulus drop for all the materials was more obvious. The drop for 411-45 and 470-36 was small at 25°, 40° and 50°C, compared to the other materials. The tensile modulus decreased by 7%, 11%, 14%, 16% and 15% respectively at for 411-45, 470-36, 272, 913 and 750 at 25°C after 40 days. The amount of moisture absorbed by all materials at 25°C was similar. Full results are represented in Appendix D. As the temperature increased, the amount of moisture absorbed by all the materials increased, with 913 and 750 absorbing the most amount and 411-45 absorbing the least amount. The

tensile modulus decreased by 22%, 16%, 18%, 27% and 27% respectively for 411-45, 470-36, 272, 913 and 750 at 60°C after 40 days. The results showed that both 913 and 750 exhibit strong relationships between percentage moisture content and percentage decrease in tensile modulus, similar to that observed with UTS results. Both materials show the drop in modulus was gradual, as the percentage moisture increased, whereas for 411-45, 470-36 and to some extent 272, after the small drop in modulus at low moisture levels, there was a large and sudden decrease in modulus although absorbed moisture was still small. The tensile modulus decreased by 28%, 31%, 25%, 28% and 32% respectively for 411-45, 470-36, 272, 913 and 750 at 70°C after 40 days. 913 and 750 absorbed the most moisture at 70°C after 40 days, while the 411-45 absorbed the least.

The mechanism of degradation was similar to that observed with UTS. Deterioration of the glass-resin interface has been shown to be a major cause of degradation in glass reinforced composites. When this glass-resin interface is affected by water, the strength and modulus are also affected, since large differences between the elastic properties of the matrix and fibres have to be communicated through the interface. The results show that even at low temperatures (25°C, 40°C), the fibre-resin bond was affected by water. Once the water reaches the interface, it also affects the fibres reducing the strength and stiffness of the fibres. The fact that all the materials showed fairly high drop in the modulus at all the temperatures, also supports this contention. If the matrix was only attacked by the water, the drop in the modulus would have been small (i.e. $E_f > E_r$). The degradation was reversible for 411-45 and 470-36 at 25°C and 40°C but no recovery was seen for 272, 913 and 750. This suggests that the interface bond for 411-45 and 470-36 was less affected than other materials. As the test temperature was increased, none of the materials showed complete recovery, with 913 and 750 worst affected (Table 5.9).

When the specimens were conditioned in water at 25° and 40°C, the drop in tensile modulus for 411-45 and 470-36 was small compared to other materials. The tensile modulus decreased by 10%, 16%, 26%, 27% and 27% for 411-45, 470-36, 272, 913 and 750, at 40°C after 40 days. As the temperature was increased, both 913 and 750 were worst affected at all temperatures, but for different reasons. The drop for 913 was due to absorbed moisture, whereas the drop for 750 was due to excessive leaching out of water. Both 411-470 and 470-36 also showed leaching at higher temperatures. Excessive debonding was observed with all the materials. When hot water penetrates the fibre-resin interface the interfacial bonds provided by the coupling agent are degraded and the glass fibres are exposed. Glass fibre is susceptible to water leaching of the soluble oxides such as K_2O and Na_2O . After prolonged exposure leaching results in surface pits (Figure 236b) and reduction of properties. The presence of dissolved salts in the water around the fibre can lead to the generation of osmotic pressures which eventually produces debonding at the interface even in the absence of an applied stress. No recovery was seen for any material at all temperatures (Table 5.10) indicating permanent damage done to the samples even at low temperature.

5.4.4 Interlaminar Shear Strength (ILSS)

It has long been recognised that the glass-resin interface in composite exerts a strong influence on the shear properties of the composite materials. It also affects the ability of matrix materials to transfer stress among the glass fibres. It has been proved that the bonding strength between resin and fibres could be decreased by moisture¹⁴²⁻¹⁴³. Sometimes it may cause an irreversible effect on the composite materials. An ILSS test was used to observe the moisture effect on the composite interfacial regions. Full results for the five materials tested are presented in Appendix E.

The specimens which were conditioned at 60% RH, at 25^o, 40^o, 50^o, 60^o and 70^oC and tested after 16 and 40 days, did not show any direct relationship between percentage absorbed moisture and percentage drop in ILSS. The ILSS did not always decrease but sometimes showed a slight increase as the percentage moisture increased (Figures 203-212). This was due to the scatter of the experimental results rather than any significant effect of moisture. Every time the specimens were conditioned at different temperatures and tested, they were from different slabs. Therefore it may be possible, that the interfacial bond between the fibre and the matrix varies from slab to slab, hence the scatter of the results. Only at high temperatures (60-70^oC), after 40 days, did some of the specimens show any significant decrease in ILSS. The ILSS decreased by 6%, 10%, 6% and 2% respectively for 411-45, 272, 913 and 750 at 70^oC after 40 days. At the same temperature 470-36 showed increase of 4%, but at 60^oC the same material showed a decrease of 4%. The specimens which did show slight decrease in ILSS were mainly due to the attack of water at the fibre-resin interface. It is believed that water proceeds along the glass-resin interface much faster than through the resin. Therefore it seems that the bonding that exists at the interface in the glass-resin composites, is easily affected by even a small amount of absorbed moisture. At high temperatures (60-70^oC) the resin properties also change, which would cause a reduction of ILSS. The resin simply becomes weaker to the high temperature exposure. A lower resin strength will have an adverse effect on composites property in which the matrix is required to carry a large portion of the applied load, e.g. ILSS, if a shear failure mode occurs. An edge view of an interlaminar shear crack is shown in Figure 239. The micrograph shows that failure has occurred by shear failure of the resin and fracture close to or at the fibre matrix interface. Shear zones have grown ahead of the crack and some local interface debonding has occurred. The decrease in ILSS of the samples due to uptake of water was reversible in that the ILSS returned to its original value when the environmental conditions changed and the moisture diffused out (Table 5.11). Examinations of the specimens revealed relatively good fibre-resin adhesion (Figure 239a), the examination of the fracture surface showed less fibre pull-out has occurred indicating good bond between fibre and matrix (Figure 240a).

When the specimens were conditioned at 95% RH, the ILSS drop for all the materials was more obvious. The drop for 411-45 and 470-36 at 25°C and 40°C was small compared to the other materials although the amount of moisture absorbed by all the specimens was similar. The ILSS decreased by 4% and 7% respectively for 411-45 and 470-36 at 40°C. At the same temperature, the decrease for 272, 913 and 750 was 16%, 23% and 15%. These results show that the moisture has degrading effects on the interface bond, especially for 913. The high volume fraction of glass fibres in 913 PrePreg may in part be responsible for the high drop in ILSS of this composite. Water penetration into composites is due to through fibre-resin interfaces (capillary) and through the resin (diffusional). The amount of water penetrating the composite by a capillary action will depend on the volume fraction of the sample. In 913 penetration by the capillary action would have been more substantial than in any of the other composites, due to the material's high volume fraction. Increasing fibre content tends to impede the penetration of the resin and strong interfacial bonds cannot be formed if the resin does not wet the fibres. In such a case the ILSS would be expected to decrease with increasing fibre content. As the test temperature increased, the drop in ILSS for all the materials increased, with 913 and 750 being worst affected. The ILSS decreased by 23%, 22%, 27%, 38% and 32% respectively for 411-45, 470-36, 272, 913 and 750 tested after 40 days at 70°C. 913 and 750 absorbed the most moisture at 70°C after 40 days, i.e. 161% and 195% respectively, while 411-45, 470-36 and 272 absorbed the least, i.e. 0.55%, 0.80% and 0.80% respectively. The results show that 913 and 750 were worst affected at all temperatures, but the decrease was gradual as percentage moisture increased, suggesting that some sort of correlation existed between percentage moisture content and percentage decrease. 411-45, 470-36, both showed that the decrease at 25°, 40° and 50°C was small, but as the temperature increased both suffered a sharp drop. The results indicate that the deterioration of the glass-resin interface for 411-45 and 470-36 was only slightly affected up to 0.50% moisture, whereas for 913 and 750 the deterioration was greater even at low moisture level. The fact that most of the ILSS loss was irreversible at 25° and 40°C for 913 and 750 also supports the contention (Table 5.12).

At high temperatures (50⁰, 60⁰ and 70⁰C) all the materials showed that the ILSS loss was irreversible, with 913 and 750 both worst affected. The reversible portion of this degradation was due to drying off the water at the interface. The reversible changes which are likely to occur at the interface are: (i) chemical breakdown by hydrolysis; (ii) chemical break down by UV radiation; (iii) chemical break down by thermal activation, and (iv) chemical break down by stress induced effects associated with swelling. Debonding was also observed at high temperatures (60⁰ and 70⁰C) with all the specimens (Figure 238b).

When the specimens were conditioned in water at 25⁰ and 40⁰C, the drop in ILSS for 411-45 and 470-36 was small compared to other materials. The ILSS decreased by 6% and 7%, respectively, for 411-45 and 470-36 at 40⁰C. At the same temperature, the ILSS decreased by 18%, 18% and 23%, respectively, for 272, 913 and 750. The loss of ILSS was irreversible for all the materials (Table 5.13). The irreversible loss was due to chemical breakdown of interface by hydrolysis and chemical breakdown by thermal activation. Debonding was observed with 272, 913 and 750 specimens at 40⁰C. Leaching of the interface will lead to the debonding between fibres and resin (Figure 238c). These effects became more pronounced as the temperature was increased. At 60⁰ and 70⁰C all the specimens except 913, showed excessive leaching of the resin and microcracking was also observed with 750. More leaching out of the water soluble elements was observed with ILSS samples compared to tensile specimens, because the ILSS specimens are very small (2 mm x 12 mm x 18 mm) so that diffusion of water into the specimens was much faster. Attempts were made to analyse the extracted material, but it was unsuccessful due to the small amount. The ILSS decreased by 33%, 24%, 38%, 43% and 36%, respectively, for 411-45, 470-36, 272, 913 and 750. The loss of ILSS was irreversible (Table 5.13). Examination of the fractured surface showed holes left in the plastic matrix, indicating poor bond between the fibres and the matrix. There were corresponding changes in the appearance at the matrix fracture indicating that a degree of adhesion affected the overall fracture process (Figure 240b).

5.4.5 In-Plane Shear Strength (IPSS)

It is known that the strength of $\pm 45^\circ$ composite specimens is less dominated by fibres but depends on the shear properties of resin and interface. The strength is dominated by matrix properties because crack propagation can occur entirely by shear of the matrix without disturbing or fracturing the fibres. Thus loss of stiffness of matrix material and bonding strength of the interface may cause a reduction in strength of $\pm 45^\circ$ specimens.

The specimens which were conditioned at 60% RH at 25° , 40° , 50° , 60° and 70°C , and tested after 16 and 40 days showed a slight decrease in IPSS (Figures 214-223). Full results are listed in Appendix F. Some specimens showed slight increase rather than decrease as the percentage moisture increased. This may be due to the scatter of the experimental results, rather than effect of absorbed moisture. Only at 70°C , after 40 days did the specimens show any significant decrease in IPSS. The IPSS decreased by 7%, 12%, 14%, 12% and 5%, respectively, for 411-45, 470-36, 272, 913 and 750. The deterioration of IPSS was due to changes in the matrix properties and preface of water at the interface. Moisture has the effect of flexibilising the resin or in other words, reducing the elastic moduli. As mentioned previously changes in matrix moduli have little effect on longitudinal tensile strength and modulus because the matrix plays only a minor role. However, the effect on in-plane shear strength may be substantial because the resin contribution is large. The decrease in IPSS of the samples due to uptake of water was reversible in that the IPSS returned to its original value when the environmental conditions change and the moisture diffuses out (Table 5.14). The results show that overall behaviour was similar to that observed with ILSS specimens. This is not unexpected, since both IPSS and ILSS depend on the direction of shear displacements. For a given resin matrix, the shear strength depends on the stress concentration effects associated with the presence of fibres and on the strength of the interfacial bond. At low V_F the stress concentration factor is relatively insensitive to V_F , but it rises rapidly when V_F is greater

than 0.60. For composites with brittle resins (750, 913) the stress concentration effect will lead to values of IPSS lower than the shear strength of the pure resin. The strength of the laminates with more flexible resins is approximately the same as the pure resin because any stress concentrations are relaxed by local deformation processes. The same arguments apply to the effect of weakly bonded interfaces.

The initial drop for 411-45 and 470-36 was small compared to other materials, when the specimens were conditioned at 95% RH at 25°C and 40°C. The IPSS decreased by 9%, 9%, 21%, 24% and 14% respectively for 411-45, 470-36, 272, 913 and 750. The amount of moisture absorbed by all the samples was similar. The same trend was observed at 40°, 50° and 60°C. As the temperature was increased, both 913 and 750 absorbed most moisture, while 411-45 absorbed the least. The 913 specimen suffered a drop in IPSS at all temperatures, but the drop was gradual as the percentage moisture increased. The same trend was observed with 750 specimens. The initial drop in IPSS for 411-45 and 470-36 was small, but as the temperature increased a sudden drop occurred, although the amount of moisture absorbed by the specimens was small. The degradation was reversible for 411-45 and 470-36 at 25° and 40°C. None of the other materials showed complete recovery (Table 5.15). At 50°, 60° and 70°C, none of the samples showed recovery, indicating the specimens suffered permanent damage. The changes in matrix properties were due to the diffusion of the environment through the polymer. The irreversible changes suffered by the matrix were due to chemical break down by thermal activation and chemical break down by stress induced effects associated with swelling. These became more significant after prolonged exposure at high temperatures. The same changes as those in the matrix occur at the interface. The presence of moisture results in swelling of the resin which is partly constrained by the presence of the fibres. The degree of constraint depends on the fibre geometry and volume fraction. Under non-equilibrium conditions the water content is not uniform and the concentration gradients lead to stress and strain gradients in the material. Similarly even when the moisture content is uniform, the

different swelling characteristics of adjacent laminae in a laminate leads to a build-up of internal stresses.

The specimens conditioned in water at 25^o, 40^o and 50^oC and tested after 16 and 40 days respectively showed that loss of IPSS was higher than 95% RH. The increase in loss was due to two reasons, firstly, the amount of moisture being absorbed by the specimens, and secondly, the leaching of resin and interface. As mentioned in previous sections leaching of the resin was taking place, even at low temperatures (25^o, 40^o and 50^o). The leaching of the resin will change the chemical composition of the resin, and reduce the shear properties of the resin. These changes were irreversible for all the materials (Table 5.16). The IPSS decreased by 10%, 10%, 20%, 23% and 25% respectively for 411-45, 470-36, 272, 913 and 750 at 40^oC after 40 days. At high temperatures (60^o, 70^oC) both 411-45 and 750 showed excessive leaching of the resin, interface and fibres. Microcracking of the matrix was also observed with 750 specimens at 60^o and 70^oC. Leaching was also observed in the 272 and 470-36 specimens. Both 913 and 750 showed a big drop in IPSS at 70^oC after 40 days, but for different reasons, with 913 the drop was due to the strong attack of water of the matrix and the interface, whereas with 750, the large drop was due to excessive leaching of resin, microcracking of the resin and leaching of the interface. The IPSS decreased by 30%, 38%, 38%, 46% and 46% respectively for 411-45, 470-36, 272, 913 and 750. No recovery was seen for any of the materials. Figure 241a shows the failed specimens under load. It is obvious that a large crazing area due to debonding of the interface can be observed with high moisture contents. Figure 240b shows the fracture surface of $\pm 45^{\circ}$ specimens. This kind of fracture was observed with all the specimens i.e. dry, low moisture and high moisture content.

5.5 THE EFFECT OF THERMAL SPIKING ON THE MECHANICAL PROPERTIES

As mentioned before, thermal spiking did not change significantly the moisture absorption characteristic of the material as represented by the moisture content as a function of time. The specimens were conditioned

at 95% RH, 25°C for 18 hours, and spiked daily at 95% RH, 70°C for 4 hours for 40 days. The amount of moisture absorbed by the specimens after 16 and 40 days was slightly lower than the specimens conditioned at 95% RH, 70°C. This was also reflected on the drop of the mechanical properties as discussed below.

5.5.1 Ultimate Tensile Strength (UTS)

The UTS results for all the materials tested after 16 and 40 days, respectively are presented in Appendix B. Both 913 and 750 absorbed the most moisture after 40 days, while 411-45, 470-36 and 272 absorbed the least. However absorbing a smaller amount of moisture did not mean a smaller degradation in UTS. The UTS decreased by 38%, 30%, 36%, 33% and 34% respectively for 411-45, 470-36, 272, 913 and 750 tested after 40 days. The decrease IN UTS was mainly a result of deterioration of glass fibre-resin interfacial bond and attack of water on the fibre surface. The fact that most of the strength loss was irreversible also supports this contention (Table 5.17). The drop in UTS was small compared to specimens which were conditioned at 95% RH, 70°C.

5.5.2 Percentage Elongation

The percentage elongation results for all the materials tested after 16 and 40 days, respectively, are listed in Appendix C. The percentage elongation decreased by 22%, 31%, 21%, 20% and 13% for 411-45, 470-36, 272, 913 and 750. The loss was irreversible, indicating that the damage was permanent (Table 5.17). The mechanism of degradation was the same as described above.

5.5.3 Tensile Modulus

The tensile modulus results for all the materials tested after 16 and 40 days are listed in Appendix D. The decrease was similar to that obtained for specimens when conditioned at 95% RH, 70°C. The tensile modulus decreased

by 25%, 23%, 18%, 23% and 31% for 411-45, 470-36, 272, 913 and 750 after 40 days. The mechanism of degradation was the same as described in Section 5.5.1. No recovery was seen for any of the materials (Table 5.17).

5.5.4 Interlaminar Shear Strength (ILSS)

The ILSS results were similar to those obtained with the specimens conditioned at 95% RH, 70°C and also the degradation mechanism was the same. The full results are listed in Appendix E. The ILSS decreased by 20%, 12%, 23%, 26% and 19%, respectively, for 411-45, 470-36, 272, 913 and 750. The fact that most of the ILSS loss was irreversible, suggests that there was strong attack of water at the glass-resin interface bond (Table 5.17).

5.5.5 In-Plane Shear Strength (IPSS)

As stated previously the strength of $\pm 45^\circ$ laminates is less dominated by fibres but depends on the shear properties of resin and interface. Both 913 and 750 absorbed the most moisture after 40 days, this was also reflected on the decrease in IPSS. The IPSS decreased by 39% and 35% respectively for 913 and 750 after 40 days. The decrease for 411-45, 470-36, 272 was 32%, 24% and 27%. These results were similar to that obtained with 95%, 70°C. The attack of moisture on the matrix and interfacial bond was irreversible because no recovery was seen for redried specimens (Table 5.17).

CHAPTER 7

CONCLUSIONS AND RECOMMENDATIONS

The experimental results, and analysis previously discussed lead to the following conclusions:

1. The hand lay-up technique used produces good quality laminates with very low void content ($< 1.0\%$). More work is needed to produce laminates with constant thickness and volume fraction.
2. Moisture absorption characteristics
 - a) The Vinylester resin absorbed less moisture than polyester and epoxy resins because of the relatively few ester groups available for hydrolysis and also because of the methyl group which shields the ester linkage increasing the resistance to hydrolysis. 470-36 resin absorbs more than 411-45 resin, because of its high cross-link density and because it contains more ester groups for hydrolysis.
 - b) The initial rate of water absorption and the final amount of water absorbed depends on the material, the temperature and the percentage relative humidity.
 - c) The initial rate of moisture absorption for 913 and 750 is slow (low diffusion coefficient values) for 0° and $\pm 45^{\circ}$ laminates, although both absorb the most moisture over a 40 day period.
 - d) Direct comparison between 0° and $\pm 45^{\circ}$ data show that the initial water absorption for $\pm 45^{\circ}$ laminates is much faster (high diffusion coefficient values) under the same exposure conditions.

- e) The results show that the diffusion coefficient depends on the temperature, as given by the Arrhenius equation

$$D = D_0 \exp (-E/RT)$$

for all composites tested.

- f) The absorption behaviour for 411-45, 470-36, 272 and 750 composites immersed in distilled water and humid air (60% and 95% RH) confirm Fickian behaviour for 0° and $\pm 45^\circ$ fibre orientation. The absorption behaviour for 913, initially follows Fick's law, but overall behaviour is non-Fickian. No classical equilibrium absorption plateau was obtained at any temperature due to the short exposure times. These observations suggest that further work should be continued on longer exposure times.
- g) Epoxy MY-750 specimens exposed to water at 60° and 70°C undergo pronounced degradation, which occurs shortly after exposure and is associated with a significant irrecoverable weight loss. The degradation process is attributed to penetration of water into the fibre-matrix interfaces and is followed by an attack on the glass fibre surfaces and coupling agent. As a result, glass constituents are leached out and removed from the system by diffusion. Analysis of hot water showed distinct traces of silica compounds. Similar behaviour was observed with 411-45 and 470-36 laminates at 70°C only.
- h) Visual observations and scanning electron micrographs show surface cracks, microcracks and debonding as a result of prolonged exposure to hot, wet atmospheres. Microcracks are only observed with 750 samples. No surface cracks are observed with 411-45 and 470-36 samples.

- i) The activation energy for diffusion is similar for all the unidirectional materials tested indicating that the mechanism of diffusion is not grossly different. The activation energy for diffusion of 0° and $\pm 45^{\circ}$ laminates is not the same. This suggests that the diffusion of water through 0° and $\pm 45^{\circ}$ fibre orientation is different.

3. Mechanical Properties (UTS, % EI, E, ILSS, IPSS)

- a) For 0° and $\pm 45^{\circ}$ laminates there is little change in mechanical properties at 25° , 40° , 50° and 60°C after conditioning at 60% RH. At 70°C the longitudinal tensile strength of all the materials shows a significant drop, with 913 and 750 worst affected. At this temperature, there was penetration of water at the fibre-resin interface and attack at the fibre surfaces. This reduced the strength dominant properties of the fibre. However the degradation is reversible when water diffuses out.
- b) The drop in mechanical properties for 411-45, 470-36 and 272 is small after being conditioned at 95% RH at 25° , 40° and 50°C as compared with 913 and 750. However as the temperature increases the drop is similar or in some cases more than 913 and 750, although the amount of moisture absorbed by 411-45, 470-36 and 272 is low. The degradation process is attributed to penetration of water into the fibre-matrix interfaces and is followed by an attack on the glass fibre surfaces. All the specimens show significantly lower UTS, % EI, E, ILSS and IPSS compared with 60% RH. The reason for this decrease was found to be the degradation effect in the fibrous phase in the case of a drop in UTS, EI and E; and in ILSS and IPSS in the case of matrix and interfacial phase. No recovery of the mechanical properties is seen at any temperature for the dried specimens.
- c) The specimens under water exposure at 25° , 40° and 50°C are characterised by higher moisture content than their counterparts exposed at 95% RH, this reflects in turn in a higher drop in mechanical

properties, with 913 and 750 worst affected. The specimens exposed at 60° and 70°C show significantly lower mechanical properties. This is attributed to the temperature controlled attack on the glass fibre surface and interfacial coupling agent phase by the water, with consequent leaching and removal of glass constituent molecules. Microscopic examination shows roughened and distorted contours, as well as other consequences of the degradation process. On the other hand, cold water exposed specimens show smooth circular contours like their reference counterparts exposed to 60% RH and 95% RH. No recovery of mechanical properties is seen with redried specimens.

- d) The tensile failure of the specimens tested resulted in two distinct failure modes. When tested after dry conditioning and conditioning at 60% RH at all temperatures, the specimens show a typical "brush" like failure with obvious fibre pull-out. When tested after conditioning at 95% RH and in water a different failure mode is observed. The outer layer of these specimens shows a distinctly "clumped" failure with large islands of resin intact along with their reinforcing fibres. The internal part of these specimens still showed the more typical brush type failure.
4. Thermal spiking does not change significantly the moisture absorption characteristics of the material. The initial and final water uptake is higher than 95%, 25°C but lower than 95%, 70°C. The drop in mechanical properties is similar to that obtained with 95%, 70°C. these results suggest that more work is needed with a wide range of temperatures and humidity.
5. All the specimens show a decrease in T_g as percentage moisture increases, with 913 and 750 worst affected.

REFERENCES

1. CURTIS P T: RAE Technical Report 80045 (1980).
2. BROWNING C E, HUSMAN G E and WHITNEY J M: ASTM STP 617 (1977).
3. LEVY R L: AFML-TR-77-41 (1977).
4. SPRINGER G S and SHEN C H: Journal of Composite Materials, Vol 10, (1976), p2.
5. SHIRRELL C D: ASTM-STP 658 (1978), p21.
6. ISHAI O: Polymer Engineering and Science, Vol 15 [7] (1975), p486.
7. JUDD N C W and WRIGHT W R: Reinforced Plastics, Vol 22, [2], (1978), p39.
8. PARYN N: Composites, Vol 3 (1972), p21.
9. DRIVER W E: *"Plastic Chemistry and Technology"*, Pub. by Van Nostrand Reinhold Company (1979).
10. LUBIN G (Ed): *"Handbook of Fibre Glass and Advanced Plastics Composites"*, Pub. by Van Nostrand Reinhold Company (1969).
11. WEATHERHEAD R G: Reinforced Plastics, Vol 23, [5], (1979), pp148-156.
12. LUBIN G (Ed): *"Handbook of Composites"*, Pub. by Van Nostrand Reinhold Company (1982).
13. SCOTT BADER CO (UK): *"Information Bulletin"*, Crystic 272 (1982).
14. PRITCHARD G (Ed): *"Developments in Reinforced Plastics - 1"*, Pub. by Applied Science Publishers (1980).
15. POTTER W G: *"Epoxide Resins"*, Pub. by Iliffe (1970).
16. JOHNSON A F: *"Engineering Design Properties of GRP"*, Pub. by British Plastics Federation (1979).
17. PARKER D B V: *"Polymer Chemistry"*, Pub. by Applied Science (1974).
18. BRUINS P E: *"Epoxy Resin Technology"*, Pub. by Interscience (1968).
19. MAY C A and NEWAY H A: 20th SPI Reinforced Plastics/Composites Conf. (1965) Section 6.D.

20. LINOW W H, BEARDEN C R and NEUDNDORF W R: 21st SPI Reinforced Plastics/Composites Conf. (1966) Section 1-D.
21. VETTERS C M: 28th SPI Reinforced Plastics/Composites Conf. (1970), Section 4-B.
22. ANDERSON F T and MESSICK B V: *"Developments in Reinforced Plastics - 1"*, (Ed) Pritchard G. Pub. by Applied Science (1980), p29.
23. NIESSE J and FENNER O: Nat. Association of Corrosion Engineers, Corrosion 78 (1978), Paper 105.
24. Vinylester Resins, Reinforced Plastics (1973), p106.
25. STAVINOHA R F and MACRAE J D: 27th SPI Reinforced Plastics/Composites (1972), Section 2.E.
26. RHOADES G.V: First Year Progress Report, MOD Agreement 2170/092, Loughborough University, (1984).
27. RICHMOND K M: PhD Thesis, Loughborough University (1983).
28. PHILLIPS L N and MURPHY D J: RAE Tech. Memo. Mat. 201 (1974).
29. ROLSTON J A: Chemical Engineering (Jan 1980), pp 96-110.
30. VARCO P and SEAMARK M J: RPG Conf. *"New and Improved Resin Systems"*, (1973), Paper 3.
31. SHEN C and SPRINGER G S: Journal of Composite Materials, Vol 11, (1977), pp 2-6.
32. TRABOCCO R E and STANDER M: ASTM-STP 602 (1976) p 67.
33. ISHIDA H and KOENIG J L: Polymer Engineering and Science, Vol 18, [2], (1978), p 128.
34. HOGG P J and HULL D: Journal of Composite Materials, (1980), p441.
35. HULL D: *"An Introduction to Composite Materials"*, Pub. by Cambridge University Press (1980).
36. GRIFFITHS A A: Phil. Trans. Roy Soc., Vol A221 (1920), p 163.

37. HOLLINGER D L and PLANT H T: 21st SPI Reinforced Plastics/Composites Conf. (1966), Section 13-B.
38. DOREY G: AGARD Conf. Proceedings No LS-124 (1980), Paper 10.
39. CHARLES R J: Journal of Applied Physics, Vol. 29 (1958) p 1549.
40. ISLINGER J S: WADC Tech. Report 59,600, [3], (1961).
41. EAKINS W J: ASTM-STP 452, (1969), p 137.
42. JAMES D I, NORMAN R H and STONE M E: Plastics Polymer, Vol 36, (1968) p 21.
43. LAIRD J A and NELSON F W: 19th SPI Reinforced Plastics/Composites Conf. (1964), Section 11-C.
44. HANDS D, JAMES D I, NORMAN R M and STONE M E: 5th BPF Reinforced Plastics Conf. (1966), Paper 16.
45. WAKE W R and NORMAN R H: 4th BPF Reinforced Plastics Conf. (1964), Paper 1.
46. KENYON A S and DUFFEY H J: Polymer Engineering and Science, Vol 7, [3], (1967), p 189.
47. THROCKMORTON P E, HICKMAN H M and BROWNE M F: 18th SPI Reinforced Plastics/Composites Conf. (1963), Section 14-A.
48. BROUTMAN L J: 19th SPI Reinforced Plastics/Composites Conf. (1964), Section 9-C.
49. MCGARRY F J and WILLNER A M: 23rd SPI Reinforced Plastics/Composites Conf. (1968), Section 14-B.
50. OWEN M J, DUKES R and SMITH T R: 23rd SPI Reinforced Plastics/Composites Conf. (1968), Section 14-A.
51. SMITH T R and OWEN M J: 6th BPF Reinforced Plastics Conf. (1968), Paper 27.
52. VANDERBILT B M and SIMKO J P: 15th SPI Reinforced Plastics/Composites Conf. (1960), Section 10-D.

53. VANDERBILT B M: Modern Plastics, Vol 37 (1959), p 125.
54. EAKINS W J: SPI Trans. Vol. 1 (1961), p 199.
55. McNEIL W D, BENNETT B and LEININGER R I: 19th SPI Reinforced Plastics/Composites Conf. (1964), Section 11-B.
56. BENNETT M K and ZISMAN W A: AD 671 180 NRL 6705 (1968).
57. FRIED N, KAMINETSKY J and SILVERGLEIT M: 21st SPI Reinforced Plastics/Composites Conf. (1966), Section 14-A.
58. DESAI M B and McGARRY F J: 14th SPI Reinforced Plastics/Composites (1959), Section 16-E.
59. LAIRD J A and NELSON F W: SPE Trans. Vol. 4 (1967), p 120.
60. NORMAN R J, JAMES D L and GALE G H: Chemical Eng. Lond., Vol. 182, (1964), p 243.
61. ASHBEE K H G and WYATT R C: Proc Roy Soc., Vol 312 (1969), p 553.
62. PLUEDDEMANN E P (Ed): *"Composite Materials"*, Pub. by Academic Press, Vol. 6 (1974).
63. PLUEDDEMANN E P: 25th SPI Reinforced Plastics/Composites Conf. (1970), Section 13-D.
64. PLUEDDEMANN E P: Modern Plastics, Vol. 47 (1970), p 92.
65. PLUEDDEMANN E P: Nat Sample Tech Conf. (1968), p 453.
66. ISAIDA H and KOENIG J L: 35th SPI Reinforced Plastics/Composites Conf. (1980), Section 23-A.
67. ASHBEE K H G, FRANK F C and WYATT R C, Proc. Roy Soc. Vol. 300A, (1967), p 415.
68. HOLTMANN R: 21st SPI Reinforced Plastics/Composites Conf. (1966), Section 13-C.
69. STEEL D J: Trans. J. Plastic Inst., Vol. 35, (1967), p 429.

70. VAUGHAN D J et al: Composites, Vol. 4 (1973), p 131.
71. ISHAI O and MAZOR A: Journal of Composite Materials, Vol. 9, (1975), p 370.
72. FARRAR N R and ASHBEE K H G: Journal of Applied Physics, Vol. 11, (1971), p 1009.
73. PARKYN B (Ed): *"Glass Reinforced Plastics"*, Pub. by Iliffe Books, (1970).
74. DELASI R and WHITESIDE J B: ASTM-STP 658, 1958, p 2.
75. APICELLA A, NICOLASIS L, ASTARITA G and DRIOLI E: Polymer, Vol. 20 (1979), p 1143.
76. RASHID H U: PhD Thesis, University of Sheffield (Oct 1978).
77. BONNIAU P and BUNSELL A R: Journal of Composite Materials, Vol 15, (1981), p 272.
78. BANKS L and EILLIS B: Polymer Bulletin, Vol. 1 (1979), p 377.
79. McKAGUE E L, REYNOLDS D J and HALKIES J E: Journal of Polymer Science, Vol. 22 (1978), p 1643.
80. BREWIS D M, COMYN J, SHALASH R J A and TEGG J L: Polymer, Vol. 21, (1980), p 357.
81. LOOSE A C and SPRINGER G S: Journal of Composite Materials, Vol. 13 (1979), p 17.
82. VERETTE R M: AIAA Paper No 75-101, American Institute of Aeronautics and Astronautics Aircraft Systems and Technology Meeting, Los Angeles (Aug 1975).
83. VERETTE R M: Journal of Aircraft, Vol. 14, [1], (1977), p 90.
84. BROWNING C E: Polymer Engineering and Science, Vol. 18, [1], (1978), p 16.
85. BROWNING C E: ASTM-STP 546 (1974), p 284.

86. BROWNING C E, HUSMAN C E and WHITNEY J M: AFML-TR-77-17 (1977).
87. JUDD N C W and WRIGHT W W: SAMPE J., Vol. 14 (1978), p 10.
88. BUNSELL A R: *"Developments in Reinforced Plastics - 2"*, (Ed), by Pritchard G. Pub. by Applied Science Publishers (1984), p 1.
89. ALT B: Kunststoffe, Vol. 59 (1969), p 986.
90. CHEN S A and TSAI P K: Polymer Engineering and Science, Vol. 17, (1977) p 775.
91. STEEL D J: Trans. J. Plastics Inst., Vol. 35 (1967), p 429.
92. PRITCHARD G, SWAMPILLAI, G J and TANESA N: Trans. I. Chem. E. Vol. 56 (1978), p 96.
93. SANDERS B A and TUNG R W: Journal of Composite Materials, Vol. 14, (1980), p 213.
94. APICELLA A, MIGLIARESI C, NICODEMO L, NICOLAIS L, IACCARINO L and ROCCOTELLI S: Composites Vol. 13 (1982), p 406.
95. APICELLA A, MIGLIARESI C, NICOLAIS L, IACCARINO L and ROCCOTELLI S: Composites, Vol. 14 [4], (1983), p 387.
96. SCOTT BADER CO LTD: Tech. Note No. 9 (1973).
97. OLFORD A C: Osmosis: Cause and Effect. Yacht Brokers, Designers and Surveyors Association Report (1978).
98. KLUNDER J and WILSON A W: Reinforced Plastics Group Meeting, Plastics and Rubber Institute, Birmingham, 26th Oct (1977).
99. HOJO H and TSUDA K: 34th SPI Reinforced Plastics/Composites Conf. (1979), Section 13-B.
100. SAMS L L, PIEGSA I G and ANDERSON T F: 28th SPI Reinforced Plastics/Composites Conf. (1973), Section 13-A.
101. BURRELL P P and O'HEARN T P: 37th SPI Reinforced Plastics/Composites Conf. (1982), Section

102. CANEY J E and LAUNIKITIS M B: 28th SPI Reinforced Plastics/Composites Conf. (1973), Section 8-A.
103. STAVINOHA R F and MacRAE J D: 27th SPI Reinforced Plastics/Composites Conf. (1972), Section 2-E.
104. JASPERS H and WYNES T: 35th SPI Reinforced Plastics/Composites Conf. (1980), Section 10-F.
105. ALLEN R C: 33rd SPI Reinforced Plastics/Composites Conf. (1978), Section 6-D.
106. LOADER T R: 16th BPF Reinforced Plastics Conf. (1984), p 161.
107. WRIGHT W R: Composites, Vol. 12 (1981), p 201.
108. SCOTT BADER CO LTD: *"Polyester Handbook"*, Crystic Monograph, No 2 (1972).
109. PRITCHARD G and TANEJA N: 29th SPI Reinforced Plastics/Composites Conf. (1974), Section 2-C.
110. CHAMIS C C, LANK R F and SINCLAIR J H: ASTM-STP 658, (1978), p 160.
111. BUECHE F: *"Physical Properties of Polymers"*, Pub. by Interscience (1962).
112. WILLIAMS M L, LANDEL R F and FERRY J D: Journal of Am. Chem. Soc. Vol. 77, (1955), p 3701.
113. DANIELS T: *"Thermal Analysis"*, Pub. by Kogan Press, (1973).
114. HALDON R A and SIMHA R: Bull. Amer. Physic. Soc. Vol. 12, (1967), p 368.
115. FICK A: Ann. Phys. LPZ, Vol. 170 (1855).
116. CRANK J: *"The Mathematics of Diffusion"*, Pub. by Oxford University Press (1956).
117. JOST W: *"Diffusion in Solids, Liquids, Gases"*, Pub. by Academic Press, (1960).

118. SPRINGER G S: *"Developments in Reinforced Plastics - 2"*, (Ed), Pritchard G. Pub. by Applied Science Publishers (1984), p 43.
119. CURTIS P T: RAE TM Mat 375, (1981).
120. CRANK J: *"The Mathematics of Diffusion"*, 2nd Ed. Pub. by Clarendon Press, (1975).
121. AUGL J M and BERGER A C: NSW/WOL TR 77-13, AD A0 46294, (1977).
122. CANTER H G and KIBLER K G: *Journal of Composites Materials*, Vol. 12 (1978), p 265.
123. DEWIMILLE B and BUNSELL A R: *Journal of Phys. D*. Vol. 15, (1982), p.2079.
124. Fibreglass Product Sheet FPL 420, Weaving, Winding, Pultrusion, Rovings, (1983).
125. HANCOX N L (Ed): *"Fibre Composite Hybrid Materials"*, Pub. by Applied Science Ltd. (1981).
126. CIBA-GEIGY: Information Sheet, FTA 46d: Fibredux 913 (1983).
127. BS 2782: Part 3; Method 320E (1976).
128. BS 2782: Part 3; Method 341A (1976).
129. RAO R M V G K, BALASUBRAMANIAN N and MANAS CHANDA: *Journal of Reinforced Plastics and Composites*, Vol. 3 (July 1984), p 232.
130. KASTURIARAEHCHI K A and PRITCHARD G: *Composites Vol 14*, [3], (1983), p 244.
131. HSU A C T, JEMIAN W A and WILCOX R C: *Journal of Material Science*, Vol. 11, (1976), p 2099.
132. WHITNEY J M and BROWNING C E: ASTM-STP 658 (1978), p 43.
133. DOREY G: Royal Aircraft Establishment, Personal communication (1984).
134. EDWARDS D B and SRIDHARAN N S: *Polymer Composites*, Vol. 3, [1], (Jan 1982), p 1.

135. SCOLA D A: 31st SPI Reinforced Plastics/Composites Conf. (1976), Section.
136. LUNDEMO C Y and THOR J E: Journal of Composite Materials, Vol. 11 (1977), p 276.
137. CAMAHART J L, RENNHACK E H and COONS W C: ASTM-STP 602, (1976), p 37.
138. MEKAUGE Jr E L, HALKIAS J E, and REYNOLDS J P: Journal of Composite Materials, Vol. 9 (1975), p 2.
139. BOHLMANN R E and DERBY E A: AIAA Tech Paper, Vol. A (A77-2572610-39), (1977), p 219.
140. ROYLANCE D and ROYLANCE M: ASTM-STP 602 (1976), p 85.
141. STERMAN S and MARSELEN J G: *"Fundamental Aspects of Fibre Reinforced Plastics Composites"*, Pub. by John Wiley, New York (1968).
142. FIELD S Y and ASHBEE K H G: Polymer Engineering and Science, Vol. 12, [1], (1972), p 30.
143. ISHAI O and LAVENGOOD R E: Polymer Engineering and Science, Vol. 11, [3], (1971), p 226.
144. JONES B H: Plastic and Polymers (1968).
145. ROSEN B W: *"Fibre Composite Materials"*, ASM, Metals Park Ohio (1965), p 37, Chapter 3.

APPENDIX A
DIFFUSION DATA

<u>Table</u>	<u>Title</u>
A 1	60% RH: 0°
A 2	60% RH: ±45°
A 3	95% RH: 0°
A 4	95% RH: ±45°
A 5	Water Immersion: 0°
A 6	Water Immersion: ±45°
A 7	Thermal spike: 0°
A 8	Thermal spike: ±45°
A 9	Summary of constants: 0°
A 10	Summary of contents: ±45°
A 11	Glass transition temperature

TABLE A1:

Test Conditions = 60% RH
 Laminate Lay-up Orientation = 0°

Temp. °C	411-45		470-36		272		913		750	
	D mm ² s ⁻¹	M _m %	D mm ² s ⁻¹	M _m %	D mm ² s ⁻¹	M _m %	D mm ² s ⁻¹	M _m %	D mm ² s ⁻¹	M _m %
25	3.601x10 ⁻⁷	0.151	2.768x10 ⁻⁷	0.119	3.278x10 ⁻⁷	0.158	1.532x10 ⁻⁷	0.136	2.412x10 ⁻⁷	0.148
40	4.767x10 ⁻⁷	0.173	4.224x10 ⁻⁷	0.203	4.226x10 ⁻⁷	0.198	1.806x10 ⁻⁷	0.278	2.998x10 ⁻⁷	0.263
50	5.446x10 ⁻⁷	0.212	5.096x10 ⁻⁷	0.262	5.612x10 ⁻⁷	0.238	1.936x10 ⁻⁷	0.344	4.263x10 ⁻⁷	0.287
60	6.448x10 ⁻⁷	0.248	6.564x10 ⁻⁷	0.309	6.835x10 ⁻⁷	0.278	2.399x10 ⁻⁷	0.515	5.966x10 ⁻⁷	0.399
70	7.433x10 ⁻⁷	0.289	7.663x10 ⁻⁷	0.361	8.103x10 ⁻⁷	0.323	2.755x10 ⁻⁷	0.646	6.393x10 ⁻⁷	0.457

D = Diffusion Coefficient

M_m = Maximum Moisture Content

TABLE A2:

Test Conditions = 60% RH
 Laminate Lay-Up Orientation = $\pm 45^\circ$

Temp. °C	411-45		470-36		272		913		750	
	D mm ² s ⁻¹	M _m %	D mm ² s ⁻¹	M _m %	D mm ² s ⁻¹	M _m %	D mm ² s ⁻¹	M _m %	D mm ² s ⁻¹	M _m %
25	3.196x10 ⁻⁷	0.119	3.273x10 ⁻⁷	0.126	3.107x10 ⁻⁷	0.145	1.426x10 ⁻⁷	0.137	2.969x10 ⁻⁷	0.153
40	4.577x10 ⁻⁷	0.158	4.557x10 ⁻⁷	0.202	4.197x10 ⁻⁷	0.194	1.889x10 ⁻⁷	0.272	4.134x10 ⁻⁷	0.261
50	5.381x10 ⁻⁷	0.191	5.463x10 ⁻⁷	0.241	4.354x10 ⁻⁷	0.233	8.066x10 ⁻⁷	0.352	5.241x10 ⁻⁷	0.294
60	6.880x10 ⁻⁷	0.204	6.706x10 ⁻⁷	0.263	5.392x10 ⁻⁷	0.283	3.045x10 ⁻⁷	0.468	6.315x10 ⁻⁷	0.360
70	9.088x10 ⁻⁷	0.241	7.767x10 ⁻⁷	0.320	7.125x10 ⁻⁷	0.296	3.623x10 ⁻⁷	0.627	7.639x10 ⁻⁷	0.446

D = Diffusion Coefficient

M_m = Maximum Moisture Content

TABLE A3:

Test Conditions = 95% RH
 Laminate Lay-up Orientation 0°

Temp. °C	411-45		470-36		272		913		750	
	D mm ² s ⁻¹	M _m %	D mm ² s ⁻¹	M _m %	D mm ² s ⁻¹	M _m %	D mm ² s ⁻¹	M _m %	D mm ² s ⁻¹	M _m %
25	5.292x10 ⁻⁷	0.262	3.981x10 ⁻⁷	0.327	6.281x10 ⁻⁷	0.359	1.802x10 ⁻⁷	0.293	3.229x10 ⁻⁷	0.447
40	6.374x10 ⁻⁷	0.351	5.406x10 ⁻⁷	0.366	7.319x10 ⁻⁷	0.370	2.122x10 ⁻⁷	0.742	4.294x10 ⁻⁷	0.524
50	7.311x10 ⁻⁷	0.386	6.833x10 ⁻⁷	0.519	8.427x10 ⁻⁷	0.494	2.758x10 ⁻⁷	0.976	5.419x10 ⁻⁷	0.747
60	7.854x10 ⁻⁷	0.447	9.044x10 ⁻⁷	0.644	9.258x10 ⁻⁷	0.570	3.004x10 ⁻⁷	1.55	6.693x10 ⁻⁷	0.889
70	9.0213x10 ⁻⁷	0.602	9.611x10 ⁻⁷	0.805	9.625x10 ⁻⁷	0.701	3.915x10 ⁻⁷	1.84	6.422x10 ⁻⁷	1.55

D = Diffusion Coefficient

M_m = Maximum Moisture Content

TABLE A4:

Test Conditions = 95% RH
 Laminate Lay-Up Orientation = $\pm 45^\circ$

Temp. °C	411-45		470-36		272		913		750	
	D mm ² s ⁻¹	M _m %	D mm ² s ⁻¹	M _m %	D mm ² s ⁻¹	M _m %	D mm ² s ⁻¹	M _m %	D mm ² s ⁻¹	M _m %
25	6.522x10 ⁻⁷	0.280	3.685x10 ⁻⁷	0.309	7.267x10 ⁻⁷	0.326	2.760x10 ⁻⁷	0.282	4.848x10 ⁻⁷	0.430
40	9.657x10 ⁻⁷	0.326	5.653x10 ⁻⁷	0.379	8.712x10 ⁻⁷	0.359	2.922x10 ⁻⁷	0.710	6.549x10 ⁻⁷	0.518
50	1.002x10 ⁻⁶	0.386	7.217x10 ⁻⁷	0.511	1.017x10 ⁻⁶	0.425	3.454x10 ⁻⁷	1.030	5.622x10 ⁻⁷	0.853
60	1.283x10 ⁻⁶	0.461	8.669x10 ⁻⁷	0.594	1.152x10 ⁻⁶	0.473	4.119x10 ⁻⁷	1.580	7.847x10 ⁻⁷	1.080
70	1.396x10 ⁻⁶	0.549	9.690x10 ⁻⁷	0.784	1.277x10 ⁻⁶	0.605	4.237x10 ⁻⁷	1.970	6.498x10 ⁻⁷	1.940

D = Diffusion Coefficient

M_m = Maximum Moisture Content

TABLE A5:

Test Conditions = Water Immersion
Laminate Lay-Up Orientation = 0°

Temp. °C	411-45		470-36		272		913		750	
	D mm ² s ⁻¹	M _m %	D mm ² s ⁻¹	M _m %	D mm ² s ⁻¹	M _m %	D mm ² s ⁻¹	M _m %	D mm ² s ⁻¹	M _m %
25	6.710x10 ⁻⁷	0.279	4.001x10 ⁻⁷	0.366	6.749x10 ⁻⁷	0.417	1.927x10 ⁻⁷	0.366	4.143x10 ⁻⁷	0.351
40	8.313x10 ⁻⁷	0.366	5.877x10 ⁻⁷	0.397	8.009x10 ⁻⁷	0.481	2.368x10 ⁻⁷	0.710	4.906x10 ⁻⁷	0.881
50	9.605x10 ⁻⁷	0.378	7.201x10 ⁻⁷	0.463	8.861x10 ⁻⁷	0.602	2.470x10 ⁻⁷	1.320	6.625x10 ⁻⁷	1.18
60	1.145x10 ⁻⁶	0.433	9.258x10 ⁻⁷	0.563	9.993x10 ⁻⁷	0.644	3.311x10 ⁻⁷	2.28	8.101x10 ⁻⁷	0.682
70	1.288x10 ⁻⁶	0.378	1.039x10 ⁻⁶	0.598	1.0437x10 ⁻⁶	0.677	4.124x10 ⁻⁷	2.88	1.328x10 ⁻⁶	0.671

D = Diffusion Coefficient

M_m = Maximum Moisture Content

TABLE A6:

Test Conditions = Water Temperature
Laminate Lay-Up Orientation = $\pm 45^\circ$

Temp. °C	411-45		470-36		272		913		750	
	D $\text{mm}^2 \text{ s}^{-1}$	M _m %	D $\text{mm}^2 \text{ s}^{-1}$	M _m %	D $\text{mm}^2 \text{ s}^{-1}$	M _m %	D $\text{mm}^2 \text{ s}^{-1}$	M _m %	D $\text{mm}^2 \text{ s}^{-1}$	M _m %
25	7.658×10^{-7}	0.287	6.093×10^{-7}	0.300	9.226×10^{-7}	0.302	2.771×10^{-7}	0.316	4.387×10^{-7}	0.336
40	1.219×10^{-6}	0.338	7.581×10^{-7}	0.408	1.158×10^{-6}	0.351	3.496×10^{-7}	0.850	7.604×10^{-7}	0.704
50	1.499×10^{-6}	0.347	9.024×10^{-7}	0.440	1.490×10^{-6}	0.472	3.612×10^{-7}	1.180	9.908×10^{-7}	0.855
60	1.897×10^{-6}	0.365	1.160×10^{-6}	0.521	1.526×10^{-6}	0.553	4.194×10^{-7}	2.21	1.109×10^{-6}	0.723
70	2.292×10^{-6}	0.379	1.429×10^{-6}	0.503	1.815×10^{-6}	0.752	4.683×10^{-7}	3.46	1.591×10^{-6}	0.821

D = Diffusion Coefficient

M_m = Maximum Moisture Content

TABLE A7:

Test Conditions = Thermal spike
Laminate Lay-up orientation = 0°

Resin Matrix	Diffusion Coefficient (mm ² s ⁻¹)	Maximum Moisture Content (%)
411-45	8.037 x 10 ⁻⁷	0.397
470-36	8.373 x 10 ⁻⁷	0.515
272	8.865 x 10 ⁻⁷	0.685
913	2.956 x 10 ⁻⁷	1.660
750	5.903 x 10 ⁻⁷	1.050

TABLE A8:

Test Conditions = Thermal spike
Laminate Lay-up orientation = $\pm 45^\circ$

Resin Matrix	Diffusion Coefficient ($\text{mm}^2 \text{s}^{-1}$)	Maximum Moisture Content (%)
411-45	8.129×10^{-7}	0.311
470-36	7.373×10^{-7}	0.521
272	1.003×10^{-6}	0.493
913	3.283×10^{-7}	1.710
750	5.096×10^{-6}	1.080

TABLE A9: Summary of the Constants D_0 and E ($D = D_0 \exp (-E/RT)$)

Laminate Lay-Up Orientation = 0°

Environment	411-45		470-36		272		913		750	
	D_0	E	D_0	E	D_0	E	D_0	E	D_0	E
60% RH	7.599×10^{-7}	13.649	7.989×10^{-7}	19.052	8.315×10^{-7}	17.175	2.824×10^{-7}	12.891	6.541×10^{-7}	18.470
95% RH	9.189×10^{-7}	10.104	9.955×10^{-7}	17.210	9.661×10^{-7}	8.097	3.812×10^{-7}	13.062	7.524×10^{-7}	13.511
Water Immersion	1.320×10^{-6}	12.618	1.102×10^{-6}	17.160	1.078×10^{-6}	8.266	3.967×10^{-7}	14.426	9.955×10^{-7}	15.854

$D_0 = \text{mm}^2 \text{ s}^{-1}$

$E = \text{kJ mol}^{-1}$

TABLE A10: Summary of the Constants D_0 and E ($D = D_0 \exp(-E/RT)$)Laminate Lay-Up Orientation = $\pm 45^\circ$

Environment	411-45		470-36		272		913		750	
	D_0	E	D_0	E	D_0	E	D_0	E	D_0	E
60% RH	9.375×10^{-7}	19.741	7.989×10^{-7}	16.738	7.229×10^{-7}	15.734	3.736×10^{-7}	17.629	7.831×10^{-7}	17.919
95% RH	1.485×10^{-6}	14.361	1.078×10^{-6}	18.253	1.317×10^{-6}	10.692	4.341×10^{-7}	6.411	9.098×10^{-7}	10.582
Water Immersion	2.424×10^{-6}	20.741	1.330×10^{-6}	16.117	1.851×10^{-6}	12.833	4.894×10^{-7}	9.788	1.317×10^{-6}	14.738

 $D_0 = \text{mm}^2 \text{ s}^{-1}$ $E = \text{kJ mol}^{-1}$

TABLE A11: Summary of Experimental Data on the Effects of Moisture on the Glass-Transition Temperature of the Composites (°C)

411-45		470-36		272		913		750	
Moisture %	Tg °C	Moisture %	Tg °C	Moisture %	Tg °C	Moisture %	Tg °C	Moisture %	Tg °C
Dried	105	Dried	128	Dried	97	Dried	175	Dried	90
0.233	105	0.244	127	0.299	96	0.530	174	0.236	89
0.306	102	0.398	126	0.409	96	0.680	174	0.516	87
0.335	102	0.428	125	0.519	95	0.768	172	0.652	86
0.378	102	0.529	123	0.638	93	0.820	169	0.737	83
0.411	101	0.536	123	0.654	92	0.921	160	0.809	81
0.458	99	0.593	122	0.718	91	0.963	156	0.922	81
0.523	98	0.633	120	0.820	90	1.10	146	1.03	80
0.610	97	0.750	119	0.880	88	1.50	120	1.15	75
0.624	97	0.820	116	0.893	88	1.80	108	1.30	75
0.633	97	0.950	116	0.902	88	2.18	100	1.46	72
-	-	-	-	-	-	2.28	98	-	-
-	-	-	-	-	-	3.17	96	-	-
-	-	-	-	-	-	3.27	95	-	-

APPENDIX BSUMMARY OF EXPERIMENTAL DATA ON THE EFFECTS OF
MOISTURE AND TEMPERATURE ON THE ULTIMATE TENSILE STRENGTH OF
COMPOSITE MATERIALS (MPa)

<u>Table</u>	<u>Title</u>
B1	Dried
B2	60% RH: 16 days
B3	60% RH: 40 days
B4	95% RH: 16 days
B5	95% RH: 40 days
B6	Water Immersion: 16 days
B7	Water Immersion: 40 days
B8	Thermal spike: 16 days
B9	Thermal spike 40 days

TABLE B1:

Test Conditions = Dried
Laminate Lay-Up Orientation = 0°

Resin Matrix	Mean Value	Standard Deviation (SD)	Coefficient of Deviation (CV)
411-45	835.98	50.232	6.009
470-36	940.37	24.785	2.636
272	896.04	76.222	8.506
913	997.97	50.399	5.051
750	898.26	33.337	3.711

TABLE B2:

Test conditions: 60% RH, After 16 days
Laminate lay-up orientation = 0°

Temperature °C	411-45				470-36				272				913				750			
	Mean Value	SD	CV (%)	Retention %	Mean Value	SD	CV (%)	Retention %	Mean Value	SD	CV (%)	Retention %	Mean Value	SD	CV (%)	Retention %	Mean Value	SD	CV (%)	Retention %
25	823.95	73.327	8.899	98.56	949.76	35.299	3.715	101.67	853.83	16.360	1.910	97.33	944.43	33.798	9.578	94.59	870.00	15.127	1.509	96.88
40	825.89	20.228	2.449	98.79	937.36	20.379	2.174	99.68	883.35	50.609	5.731	98.53	926.73	100.138	10.811	92.86	852.92	53.667	6.297	94.88
50	839.52	75.266	8.965	100.40	921.21	2.645	0.287	97.96	853.43	9.712	1.139	94.74	924.36	26.501	2.867	92.59	824.25	37.072	4.500	91.87
60	830.73	24.785	2.983	99.37	913.02	17.677	1.936	97.18	825.92	26.987	3.269	92.08	822.37	26.807	3.261	82.36	820.03	19.720	2.405	91.37
70	812.07	34.984	4.308	97.14	902.39	53.853	5.965	96.06	822.87	9.032	1.097	91.85	818.17	52.538	6.424	81.96	786.57	29.086	3.700	87.64

TABLE B3:

Test Conditions: 60% RH: 40 days
Laminate lay-up orientation 0°

Temp °C	411-45				470-36				272				913				750			
	Mean Value	SD	CV (%)	Retention %	Mean Value	SD	CV (%)	Retention %	Mean Value	SD	CV (%)	Retention %	Mean Value	SD	CV (%)	Retention %	Mean Value	SD	CV (%)	Retention %
25	822.710	25.454	3.093	98.41	935.22	50.802	5.432	99.45	853.83	16.360	1.910	95.21	916.76	55.506	6.049	91.78	857.21	93.43	22.485	95.43
40	815.31	30.007	3.680	97.53	903.71	32.785	3.627	96.11	860.71	28.418	3.303	96.09	879.31	29.055	3.251	88.076	826.38	91.98	29.280	91.99
50	858.53	25.055	2.918	102.70	901.71	26.537	3.026	95.89	827.01	36.207	4.379	92.42	874.41	15.565	1.782	81.36	803.51	89.42	24.878	89.45
60	801.55	21.528	2.658	95.88	858.42	51.496	6.044	90.75	836.44	32.994	3.946	93.30	812.88	11.064	1.427	81.36	774.28	86.19	50.411	86.198
70	792.79	52.531	6.626	94.84	822.06	66.805	8.129	87.46	791.53	37.372	4.724	88.28	793.32	33.83	4.266	79.26	772.73	86.08	22.847	86.015

TABLE B4:

Test Conditions: 95% RH: 16 days
 Laminate lay-up orientation 0°

Temperature°C	411-45				470-36				272				913				750			
	Mean Value	SD	CV (%)	Retention %	Mean Value	SD	CV (%)	Retention %	Mean Value	SD	CV (%)	Retention %	Mean Value	SD	CV (%)	Retention %	Mean Value	SD	CV (%)	Retention %
25	751.82	17.875	2.378	89.93	836.91	33.645	4.010	89.04	831.52	26.950	3.711	92.75	858.91	4.041	0.378	85.97	774.77	19.619	2.741	86.19
40	724.75	17.875	3.662	86.69	819.40	11.239	1.371	87.23	781.30	30.038	3.848	87.50	806.73	42.523	4.477	80.76	701.43	32.323	5.111	78.06
50	730.53	42.570	5.827	87.39	810.51	27.883	3.436	86.17	759.50	69.669	9.175	84.71	701.79	22.045	3.140	70.24	650.33	32.170	5.577	72.33
60	669.95	17.875	2.668	77.99	740.93	41.546	5.546	78.73	719.97	46.024	6.443	79.69	709.83	9.201	1.296	71.04	648.66	28.988	4.463	72.16
70	543.82	34.984	4.308	65.65	539.44	25.600	4.993	57.39	640.19	7.937	1.240	71.43	717.62	18.567	2.177	71.84	634.44	29.086	3.700	70.60

TABLE B5:

Test Conditions: 95% RH: 40 days
Laminate lay-up orientation 0°

Temperature °C	411-45				470-36				272				913				750			
	Mean Value	SD	CV (%)	Retention %	Mean Value	SD	CV (%)	Retention %	Mean Value	SD	CV (%)	Retention %	Mean Value	SD	CV (%)	Retention %	Mean Value	SD	CV (%)	Retention %
25	745.45	3.035	0.448	87.17	826.59	24.076	2.731	87.98	831.50	20.639	3.204	92.75	791.10	5.859	0.604	72.96	740.50	56.676	6.969	82.41
40	701.33	10.110	1.441	83.89	737.07	16.093	2.183	78.40	717.05	24.676	3.442	80.03	702.85	30.817	3.654	70.44	638.71	25.024	3.094	71.05
50	619.23	30.927	6.082	74.07	647.59	20.902	3.079	68.83	680.83	7.416	1.089	75.89	647.85	54.609	8.427	64.83	612.83	22.338	3.808	68.65
60	508.50	18.774	3.032	60.83	586.05	18.946	3.232	62.34	658.57	29.177	4.434	78.44	608.91	22.691	3.727	60.92	601.32	46.754	6.783	66.93
70	487.76	20.775	5.082	57.99	555.52	25.591	4.942	59.04	557.53	15.959	8.864	62.28	598.26	38.976	6.515	69.92	582.90	48.487	8.612	64.82

TABLE B6:

Test Conditions: Water bath - 16 days
Laminate lay-up orientation = 0°

Temperature °C	411-45				470-36				272				913				750			
	Mean Value	SD	CV (%)	Retention %	Mean Value	SD	CV (%)	Retention %	Mean Value	SD	CV (%)	Retention %	Mean Value	SD	CV (%)	Retention %	Mean Value	SD	CV (%)	Retention %
25	789.88	38.856	5.690	94.49	852.39	9.848	1.165	90.75	735.35	23.402	3.769	82.03	749.23	10.099	1.348	75.05	624.84	15.726	2.209	69.49
40	712.61	6.183	0.870	85.24	750.87	13.916	1.854	79.89	692.32	8.366	1.209	77.23	698.31	4.031	0.577	69.94	610.04	33.906	5.530	67.93
50	674.75	22.563	3.343	77.48	698.46	36.215	5.692	74.26	663.53	27.610	4.455	73.99	656.91	22.489	2.682	65.73	616.02	28.124	4.643	68.59
60	641.76	29.761	4.641	76.74	654.28	22.883	3.501	69.61	643.59	34.06	5.295	71.46	619.03	5.439	0.879	62.06	610.71	26.487	4.340	67.93
70	518.87	31.536	6.782	62.07	506.28	15.596	2.768	53.83	589.17	20.205	3.767	65.76	614.09	3.535	0.471	61.53	605.60	13.453	1.822	67.37

TABLE B7:

Test Conditions: Water bath - 40 days
Laminate lay-up orientation = 0°

Temperature °C	411-45				470.36				272				913				750			
	Mean Value	SD	CV (%)	Retention %	Mean Value	SD	CV (%)	Retention %	Mean Value	SD	CV (%)	Retention %	Mean Value	SD	CV (%)	Retention %	Mean Value	SD	CV (%)	Retention %
25	738.49	40.645	6.350	88.34	849.83	9.343	1.124	90.32	674.18	28.661	5.037	75.22	772.15	30.052	4.161	72.35	595.17	12.096	1.614	66.26
40	682.68	20.760	3.047	81.66	689.18	44.440	6.447	73.29	601.34	14.399	2.395	67.08	650.38	16.103	2.477	71.14	575.97	23.115	4.557	64.03
50	470.69	33.102	6.879	56.31	479.41	28.856	6.021	50.96	557.14	84.316	5.447	62.17	547.27	14.099	1.872	54.81	500.27	26.158	4.547	55.67
60	435.03	32.345	7.444	52.04	457.18	35.449	7.757	48.62	542.89	5.377	0.991	60.49	519.27	19.922	3.836	52.00	471.59	14.023	2.977	52.46
70	353.47	12.649	4.130	42.28	459.77	35.501	7.728	48.94	493.65	23.383	5.612	55.02	518.53	16.048	3.092	51.90	389.07	26.376	6.074	43.32

TABLE B8:

Test Conditions: Thermal spike: 16 days
Laminate lay-up orientation = 0°

Resin Matrix	Mean Value	SD	CV (%)	Retention (%)
411-45	664.94	10.020	1.504	79.54
470-36	777.59	15.381	1.978	82.69
272	776.54	30.298	3.902	86.66
913	769.48	55.013	7.149	77.10
750	654.66	31.620	4.831	72.88

TABLE B9:

Test Conditions: Thermal spike; 40 days
Laminate lay-up orientation = 0°

Resin Matrix	Mean Value	SD	CV (%)	Retention (%)
411-45	519.79	14.539	2.797	62.17
470-36	659.19	21.127	3.205	70.10
272	573.03	25.637	4.474	63.95
913	665.54	24.718	3.714	66.68
750	597.59	15.978	2.674	66.52

APPENDIX C

SUMMARY OF EXPERIMENTAL DATA ON THE
EFFECTS OF MOISTURE AND TEMPERATURE ON THE
PERCENTAGE ELONGATION OF THE COMPOSITE MATERIALS

<u>Table</u>	<u>Title</u>
C1	Dried
C2	60% RH; 16 days
C3	60% RH; 40 days
C4	95% RH; 16 days
C5	95% RH; 40 days
C6	Water Immersion: 16 days
C7	Water Immersion: 40 days
C8	Thermal Spike: 16 days
C9	Thermal Spike: 40 days

TABLE C1:

Test conditions: dried
Laminate lay-up orientation = 0°

Resin Matrix	Mean Value	Standard Deviation (SD)	Coefficient of Variation (CV) (%)
411-45	2.512	0.016	0.637
470-36	2.620	0.081	3.092
272	2.512	0.050	1.990
913	2.300	0.047	2.044
750	2.124	0.019	0.895

TABLE C2:

Test Conditions: 60% RH: 16 days
Laminate lay-up orientation = 0°

Temperature °C	411-45				470-36				272				913				750			
	Mean Value	SD	CV (%)	Retention %	Mean Value	SD	CV (%)	Retention %	Mean Value	SD	CV (%)	Retention %	Mean Value	SD	CV (%)	Retention %	Mean Value	SD	CV (%)	Retention %
25	2.490	0.016	0.658	98.73	2.498	0.038	1.546	95.34	2.470	0.052	2.142	98.33	2.215	0.029	1.354	96.30	2.110	0.011	0.547	99.34
40	2.460	0.047	1.944	97.93	2.575	0.049	1.941	99.04	2.475	0.049	2.020	98.53	2.180	0.083	3.837	94.78	2.125	0.050	2.352	100.00
50	2.447	0.050	2.057	97.41	2.490	0.100	4.042	95.77	2.373	0.046	1.946	94.47	2.167	0.115	5.329	94.22	2.023	0.064	3.172	95.24
60	2.500	0.081	3.265	99.52	2.400	0.081	3.402	92.31	2.425	0.095	3.948	94.54	2.150	0.057	2.685	93.48	2.000	0.082	4.082	94.16
70	2.500	0.081	3.265	99.52	2.375	0.125	5.298	91.35	2.300	0.081	3.549	91.56	2.025	0.095	4.723	98.04	1.913	0.062	3.289	90.07

TABLE C3:

Test Conditions: 60% RH: 40 days
Laminate lay-up orientation = 0°

Temperature °C	411-45				470-36				272				913				750			
	Mean Value	SD	CV (%)	Retention %	Mean Value	SD	CV (%)	Retention %	Mean Value	SD	CV (%)	Retention %	Mean Value	SD	CV (%)	Retention %	Mean Value	SD	CV (%)	Retention %
25	2.475	0.025	5.084	98.53	2.538	0.094	3.729	97.62	2.445	0.052	2.150	97.33	2.175	0.049	2.253	94.56	2.150	0.040	3.888	101.20
40	2.400	0	0	95.54	2.500	0.081	3.265	96.15	2.425	0.049	2.061	96.50	2.160	0.054	2.535	93.91	2.080	0.054	2.658	97.93
50	2.445	0.052	2.151	97.33	2.500	0.115	4.618	96.15	2.395	0.010	0.417	85.34	2.225	0.049	2.247	96.74	2.076	0.095	4.614	97.69
60	2.470	0.047	1.927	98.33	8.355	0.064	2.718	90.58	2.427	0.046	1.903	96.62	2.060	0.043	2.097	89.55	2.000	0.099	4.999	94.16
70	2.260	0.054	2.423	89.97	2.325	0.050	2.150	87.42	2.225	0.049	2.247	88.57	1.925	0.050	2.597	83.69	1.867	0.057	3.092	87.91

TABLE C4:

Test Conditions: 95% RH: 16 days
Laminate lay-up orientation = 0°

Temperature °C	411-45				470-36				272				913				750			
	Mean Value	SD	CV (%)	Retention %	Mean Value	SD	CV (%)	Retention %	Mean Value	SD	CV (%)	Retention %	Mean Value	SD	CV (%)	Retention %	Mean Value	SD	CV (%)	Retention %
25	2.412	0.081	3.265	96.02	2.524	0.100	4.347	97.08	2.413	0.023	0.956	96.06	2.263	0.034	1.532	98.39	1.980	0.092	4.498	93.22
40	2.400	0.028	1.178	95.54	2.507	0.030	1.218	96.42	2.340	0.089	3.822	93.15	1.960	0.048	2.499	85.22	1.920	0.076	3.966	90.40
50	2.355	0.081	3.711	99.95	2.456	0.019	0.799	94.46	2.300	0.081	3.549	91.56	2.035	0.041	2.026	88.45	1.870	0.047	2.533	88.04
60	2.100	0.064	2.718	87.58	2.175	0.095	4.401	83.65	2.263	0.047	2.115	90.08	1.970	0.047	2.416	86.65	1.900	0.016	0.859	89.46
70	2.255	0.028	1.179	89.77	2.070	0.058	2.830	79.62	2.200	0	0	87.56	1.967	0.115	5.871	85.52	1.840	0.038	2.073	86.63

TABLE C5:

Test Conditions: 95% RH: 40 days
Laminate lay-up orientation = 0°

Temperature °C	411-45				470-36				272				913				750			
	Mean Value	SD	CV (%)	Retention %	Mean Value	SD	CV (%)	Retention %	Mean Value	SD	CV (%)	Retention %	Mean Value	SD	CV (%)	Retention %	Mean Value	SD	CV (%)	Retention %
25	2.340	0.095	4.069	92.65	2.340	0.026	1.049	90.00	2.235	0.047	2.114	88.97	2.247	0.050	2.240	97.69	1.880	0.170	5.695	88.52
40	2.305	0.071	3.118	91.76	2.293	0.050	2.194	88.19	2.215	0.059	2.696	88.18	1.944	0.043	2.230	84.52	1.885	0.086	4.614	88.75
50	2.020	0.019	1.015	80.41	2.185	0.057	2.816	84.04	2.225	0.049	8.247	88.57	1.940	0.115	5.928	84.35	1.825	0.050	2.666	85.92
60	1.885	0.054	8.681	75.04	1.940	0.048	2.525	74.21	2.215	0.095	4.505	88.18	1.875	0.050	2.667	81.52	1.870	0.047	2.545	88.04
70	1.760	0.041	2.376	70.07	1.760	0.115	6.383	67.69	1.825	0.127	7.065	72.65	1.700	0.099	5.882	73.91	1.790	0.174	9.750	84.27

TABLE C6:

Test Conditions: Water bath: 16 days
Laminate lay-up Orientation = 0°

Temperature °C	411-45				470-36				272				913				750			
	Mean Value	SD	CV (%)	Retention %	Mean Value	SD	CV (%)	Retention %	Mean Value	SD	CV (%)	Retention %	Mean Value	SD	CV (%)	Retention %	Mean Value	SD	CV (%)	Retention %
25	2.6143	0.115	4.745	97.25	2.513	0.120	4.769	96.65	2.356	0.086	3.702	92.99	2.225	0.049	2.247	96.74	2.050	0.092	4.498	96.52
40	2.245	0.052	2.342	89.39	2.225	0.166	7.462	85.58	2.235	0.047	2.114	86.98	2.095	0.025	1.201	91.09	2.020	0.054	2.681	95.11
50	2.290	0.110	4.621	91.16	1.990	0.132	6.641	76.54	2.287	0.162	7.123	91.04	2.040	0.117	5.772	88.52	2.050	0.129	6.297	96.52
60	2.080	0.076	3.661	82.81	1.900	0.081	4.297	73.08	2.175	0.050	2.298	86.58	1.875	0.050	2.667	81.52	1.925	0.050	2.597	90.63
70	1.540	0.060	3.896	61.30	1.840	0.028	1.554	70.77	1.725	0.095	5.550	68.67	1.840	0.056	3.074	80.00	1.670	0.042	2.540	78.63

TABLE C7:

Test Conditions: Water bath: 40 days
 Laminate lay-up orientation = 0°

Temperature °C	411-45				470-36				272				913				750			
	Mean Value	SD	CV (%)	Retention %	Mean Value	SD	CV (%)	Retention %	Mean Value	SD	CV (%)	Retention %	Mean Value	SD	CV (%)	Retention %	Mean Value	SD	CV (%)	Retention %
25	2.395	0.047	1.973	95.34	2.395	0.032	1.059	92.12	2.188	0.160	7.329	87.11	2.208	0.0170	0.810	96.00	1.900	0.100	5.263	89.45
40	2.225	0.049	2.247	88.57	8.150	0.050	2.194	82.69	2.125	0.050	2.352	84.59	1.975	0.095	4.847	85.66	1.850	0.057	3.120	97.09
50	1.840	0.057	2.935	73.25	1.930	0.057	2.816	74.23	2.050	0.034	1.689	81.61	1.865	0.078	4.233	81.09	1.473	0.106	7.256	89.35
60	1.625	0.029	1.846	64.69	1.710	0.048	2.525	65.77	1.820	0.073	4.012	72.45	1.665	0.055	3.307	72.39	1.723	0.095	5.550	83.24
70	1.360	0.037	2.751	54.14	1.812	0.115	6.383	69.69	1.540	0.054	3.556	61.31	1.607	0.030	1.901	69.87	1.562	0.057	3.712	73.07

TABLE C8:

Test Conditions: Thermal spike; 16 days
Laminate lay-up Orientation = 0°

Resin Matrix	Mean Value	SD	CV (%)	Retention (%)
411-45	2.350	0.050	2.128	93.55
470-36	2.425	0.083	3.419	92.56
272	2.485	0.057	2.303	98.93
913	1.933	0.047	2.438	84.04
720	1.920	0.046	2.443	90.39

TABLE C9:

Test Conditions: Thermal spike: 40 days
Laminate lay-up Orientation = 0°

Resin Matrix	Mean Value	SD	CV (%)	Retention (%)
411-45	1.950	0.049	2.499	77.63
470-36	1.800	0.0707	3.928	68.70
272	1.975	0.0802	4.198	78.62
913	1.850	0.050	2.703	80.44
750	1.850	0.050	2.703	87.09

APPENDIX D

SUMMARY OF EXPERIMENTAL DATA ON THE
EFFECTS OF MOISTURE AND TEMPERATURE ON THE
TENSILE MODULUS OF COMPOSITE MATERIALS (GPa)

<u>Table</u>	<u>Title</u>
D1	Dried
D2	60% RH: 16 days
D3	60% RH: 40 days
D4	95% RH: 16 days
D5	95% RH: 40 days
D6	Water Immersion: 16 days
D7	Water Immersion: 40 days
D8	Thermal Spike: 16 days
D9	Thermal Spike: 40 days

TABLE D1:

Test Conditions: dried
Laminate lay-up Orientation = 0°

Resin Matrix	Mean Value	Standard Deviation (SD)	Coefficient of Variation (CV)(%)
411-45	35.327	3.162	8.951
470-36	36.748	1.527	4.155
272	38.566	1.535	3.981
913	46.366	1.730	3.732
750	46.060	2.704	4.785

TABLE D2:

Test Conditions: 60% RH: 16 days
Laminate lay-up Orientation = 0°

Temperature °C	411-45				470-36				272				913				750			
	Mean Value	SD	CV (%)	Retention %	Mean Value	SD	CV (%)	Retention %	Mean Value	SD	CV (%)	Retention %	Mean Value	SD	CV (%)	Retention %	Mean Value	SD	CV (%)	Retention %
25	35.059	1.730	4.934	99.24	39.983	1.535	3.829	108.81	36.424	1.500	4.137	94.46	44.980	2.001	4.449	97.01	43.650	1.632	3.797	94.89
40	34.379	1.291	3.756	97.32	36.232	2.768	7.522	98.59	36.689	1.685	4.603	95.08	43.680	4.393	10.122	94.12	41.41	3.162	7.712	90.02
50	34.653	8.704	7.803	98.09	36.383	0.577	1.589	99.07	34.950	0.577	1.589	90.420	45.750	1.154	2.528	98.67	39.87	0.481	2.544	86.956
60	33.022	0.787	2.385	93.47	40.608	1.881	4.634	110.31	35.115	0.861	2.456	90.97	39.944	0.922	2.310	86.14	42.67	1.527	3.608	92.76
70	33.779	0.582	1.725	95.62	39.215	0.957	2.470	106.72	36.895	1.517	4.114	95.59	41.522	4.690	11.440	89.55	42.329	0.957	2.293	92.02

TABLE D3:

Test Conditions: 60% RH: 40 days
 Laminate lay-up Orientation = 0°

Temperature °C	411-45				470-36				272				913				750			
	Mean Value	SD	CV (%)	Retention %	Mean Value	SD	CV (%)	Retention %	Mean Value	SD	CV (%)	Retention %	Mean Value	SD	CV (%)	Retention %	Mean Value	SD	CV (%)	Retention %
25	35.075	0.913	7.602	99.29	40.019	2.601	6.501	108.20	37.544	0.761	2.029	97.35	44.559	1.527	3.149	96.10	44.809	2.217	5.010	97.41
40	35.454	0.850	2.398	100.36	37.363	1.732	4.618	101.67	36.45	2.169	6.009	94.30	40.913	4.349	10.805	88.02	41.705	1.303	3.164	97.93
50	36.357	0.570	1.570	102.93	37.365	1.892	5.081	101.67	35.570	1.500	4.255	92.15	40.180	1.500	3.773	96.66	39.575	1.707	4.351	86.03
60	32.904	1.357	4.128	93.14	32.516	2.320	6.184	102.09	35.518	1.992	5.612	92.02	40.542	0.967	2.140	85.86	38.973	4.932	12.757	84.72
70	36.339	3.361	9.088	102.87	38.325	2.986	7.806	104.29	35.707	1.792	5.024	92.49	44.45	2.449	5.567	95.87	42.440	1.000	2.380	92.26

TABLE D4:

Test Conditions: 95% RH: 16 days
Laminate lay-up orientation = 0°

Temperature °C	411-45				470-36				272				913				750			
	Mean Value	SD	CV (%)	Retention %	Mean Value	SD	CV (%)	Retention %	Mean Value	SD	CV (%)	Retention %	Mean Value	SD	CV (%)	Retention %	Mean Value	SD	CV (%)	Retention %
25	33.766	0.787	2.385	95.58	33.766	0.577	1.589	91.88	34.591	0.331	0.957	89.61	40.199	0.929	2.312	86.69	40.005	1.707	4.296	86.96
40	30.666	0.575	1.812	86.81	33.636	0.923	2.754	91.53	33.446	3.356	10.650	86.44	42.855	2.645	6.225	92.43	37.398	2.387	6.417	81.30
50	32.011	1.179	3.783	90.61	32.242	1.054	2.942	87.740	34.479	1.682	4.883	89.32	36.884	1.768	4.793	79.55	35.875	1.707	5.378	77.95
60	31.525	1.593	4.977	89.24	34.625	0.878	2.536	94.22	32.883	3.295	10.100	85.19	38.950	2.254	5.787	84.01	36.261	5.766	2.061	78.83
70	23.755	0.570	1.913	67.280	26.793	2.768	7.522	72.91	29.649	0.519	1.755	76.82	35.308	2.411	6.829	76.15	30.220	1.631	5.129	65.69

TABLE D5:

Test Conditions: 95% RH: 40 days
Laminate lay-up Orientation = 0°

Temperature °C	411-45				470-36				272				913				750			
	Mean Value	SD	CV (%)	Retention %	Mean Value	SD	CV (%)	Retention %	Mean Value	SD	CV (%)	Retention %	Mean Value	SD	CV (%)	Retention %	Mean Value	SD	CV (%)	Retention %
25	32.732	0.803	2.954	92.692	32.732	1.927	5.783	89.08	32.215	1.215	3.677	86.05	39.002	0.645	1.685	84.12	39.365	4.242	10.347	85.65
40	31.003	1.498	4.833	87.76	32.558	0.908	2.489	88.59	33.295	0.743	2.255	86.26	39.193	1.000	2.597	84.53	34.676	1.892	5.526	75.40
50	31.143	1.286	4.679	88.15	30.651	1.069	3.144	83.41	31.774	0.666	2.098	82.31	36.643	1.154	3.149	79.03	33.838	0.457	3.113	73.56
60	27.501	1.436	4.612	77.85	31.018	1.772	5.714	84.41	31.567	1.066	3.402	81.78	33.768	0.980	2.903	72.81	33.798	1.707	5.136	73.46
70	25.359	1.298	5.121	71.83	25.359	2.302	7.830	69.01	28.913	2.345	6.514	74.90	33.856	2.370	7.004	73.02	31.285	3.674	11.481	68.01

TABLE D6:

Test Conditions: Water bath: 16 days
Laminate lay-up Orientation = 0°

Temperature °C	411-45				470-36				272				913				750			
	Mean Value	SD	CV (%)	Retention %	Mean Value	SD	CV (%)	Retention %	Mean Value	SD	CV (%)	Retention %	Mean Value	SD	CV (%)	Retention %	Mean Value	SD	CV (%)	Retention %
25	33.253	2.993	9.000	94.13	34.639	2.645	7.559	94.26	33.976	2.880	8.574	88.03	35.158	0.425	1.202	75.93	30.844	0.577	1.982	66.96
40	32.238	0.985	3.085	91.26	34.632	3.592	10.342	94.24	31.645	1.095	3.466	81.98	34.290	0.577	1.673	73.96	30.900	0.957	3.113	67.17
50	28.904	1.138	3.939	81.82	35.234	2.410	6.830	95.88	30.939	2.081	6.788	80.15	32.336	1.776	5.492	69.79	31.911	1.732	5.871	69.34
60	29.203	2.485	9.511	82.66	34.053	2.943	8.658	92.66	29.637	3.018	10.186	76.78	32.327	0.599	1.854	64.82	31.936	1.290	4.098	69.43
70	34.396	2.916	8.481	97.33	30.116	3.555	11.591	77.98	28.150	2.217	6.202	72.93	33.352	0.975	8.925	71.93	35.820	2.828	7.644	77.87

TABLE D7:

Test Conditions: Water Bath: 40 days
Laminate Lay-up Orientation = 0°

Temperature °C	411-45				470-36				272				913				750			
	Mean Value	SD	CV (%)	Retention %	Mean Value	SD	CV (%)	Retention %	Mean Value	SD	CV (%)	Retention %	Mean Value	SD	CV (%)	Retention %	Mean Value	SD	CV (%)	Retention %
25	30.422	2.203	7.242	86.12	30.422	2.509	7.746	82.79	32.231	3.286	10.399	83.49	31.940	1.047	3.279	68.89	32.333	0.957	3.389	69.56
40	31.787	0.833	2.621	89.99	32.649	2.380	7.324	88.85	28.618	1.223	4.280	74.14	33.907	1.892	5.608	73.12	33.432	1.414	4.419	72.67
50	24.730	1.953	7.788	70.00	29.533	2.607	8.869	80.37	28.319	0.577	2.083	73.37	32.307	4.072	12.605	69.68	28.207	2.535	9.088	61.46
60	26.730	1.287	4.816	75.66	26.886	1.290	4.871	73.16	30.922	0.951	3.122	74.14	31.834	2.045	6.424	68.66	28.236	1.414	5.050	61.46
70	25.116	1.551	6.177	71.09	26.806	3.781	14.33	72.95	30.932	3.209	10.220	80.14	30.873	3.583	11.61	66.59	26.889	4.219	15.860	58.45

TABLE D8: Test Conditions: Thermal Spike: 16 days
Laminate Lay-up Orientation = 0°

Resin Matrix	Mean Value	SD	CV (%)	Retention (%)
411-45	30.225	1.082	3.576	95.55
470-36	31.876	0.833	2.612	86.74
272	30.799	0.350	1.159	79.86
913	40.283	3.805	9.446	86.88
750	39.091	10.779	27.573	84.87

TABLE D9:

Test Conditions: Thermal Spike: 40 days
Laminate lay-up Orientation = 0°

Resin Matrix	Mean Value	SD	CV (%)	Retention (%)
411-45	26.411	1.009	3.827	74.76
470-36	36.033	1.337	3.711	98.05
272	29.606	2.515	8.493	76.77
913	35.926	2.124	5.913	77.84
750	31.989	1.269	3.969	69.25

APPENDIX E

SUMMARY OF EXPERIMENTAL DATA ON THE
EFFECTS OF MOISTURE AND TEMPERATURE ON THE
INTERLAMINAR SHEAR STRENGTH OF THE COMPOSITE MATERIALS (MPa)

<u>Table</u>	<u>Title</u>
E1	Dried
E2	60% RH: 16 days
E3	60% RH: 40 days
E4	95% RH: 16 days
E5	95% RH: 40 days
E6	Water Immersion: 16 days
E7	Water Immersion: 40 days
E8	Thermal Spike: 16 days
E9	Thermal Spike: 40 days

TABLE E1:

Test Conditions: dried
Laminate lay-up Orientation = 0°

Resin Matrix	Volume Fraction %	Mean Value	Standard Deviation (SD)	Coefficient of Variation (CV)%
411-45	39.00	58.110	2.344	4.034
470-36	38.00	65.620	2.700	4.115
272	38.00	67.460	2.933	4.348
913	58.220	90.781	3.334	3.673
750	38.00	53.770	4.022	7.480

TABLE E2:

Test Conditions = 60% RH: 16 days
 Laminate lay-up Orientation = 0°

Temperature °C	411-45					470-36					272					913					750				
	Mean Value	SD	CV (%)	Retn. %*	VF %	Mean Value	SD	CV (%)	Retn. %*	VF %	Mean Value	SD	CV (%)	Retn. %*	VF %	Mean Value	SD	CV (%)	Retn. %*	VF %	Mean Value	SD	CV (%)	Retn. %*	VF %
25	57.999	2.839	4.895	98.91	45.00	66.957	1.860	2.821	100.5	52.00	67.363	7.829	12.310	99.86	39.00	88.789	0.825	0.929	97.81	59.00	54.586	6.500	12.560	101.52	50.00
40	57.122	2.745	4.805	98.30	47.00	66.370	3.834	5.791	101.14	54.00	65.073	1.732	2.685	96.46	37.00	90.844	1.258	1.386	100.71	56.70	52.332	4.500	8.695	97.32	39.00
50	56.965	1.479	2.597	98.03	47.00	65.343	4.711	7.226	99.58	54.00	67.397	0.836	1.245	99.91	37.00	89.225	3.033	3.400	98.29	56.70	53.643	1.303	2.450	99.76	37.00
60	57.203	1.888	3.300	94.57	47.00	64.680	4.320	6.664	99.91	56.00	59.554	2.606	4.385	88.28	37.5	84.632	1.676	1.981	93.27	56.70	52.227	8.018	14.474	99.77	37.00
70	54.953	0.127	0.232	94.57	47.00	65.489	4.024	6.173	99.81	54.00	58.120	0.975	1.679	86.15	37.2	84.182	2.033	3.576	92.73	57.00	52.393	1.930	3.713	97.44	39.00

* = % Retention

TABLE E3:

Test Conditions = 60% RH, 40 days
Laminate lay-up Orientation = 0°

Temperature °C	411-45					470-36					272					913					750				
	Mean Value	SD	CV (%)	Retn. %*	VF %	Mean Value	SD	CV (%)	Retn. %*	VF %	Mean Value	SD	CV (%)	Retn. %*	VF %	Mean Value	SD	CV (%)	Retn. %*	VF %	Mean Value	SD	CV (%)	Retn. %*	VF %
25	58.772	2.450	4.169	101.14	42.00	66.333	1.694	2.554	101.09	52.00	66.843	4.031	6.225	99.09	40.00	89.150	3.244	3.639	98.20	56.70	53.302	1.000	1.886	99.92	40.00
40	57.301	3.135	5.472	98.61	47.00	68.343	1.224	1.801	104.15	54.00	64.759	2.983	4.608	95.99	37.00	90.055	1.516	1.673	99.201	56.70	52.290	2.645	4.949	97.25	38.00
50	57.065	2.550	4.469	98.21	47.00	66.679	4.764	7.197	101.16	54.00	69.173	2.362	3.416	102.50	37.00	85.954	3.114	3.629	94.683	57.00	52.375	2.645	5.087	97.41	37.00
60	57.519	3.559	6.188	98.98	45.00	62.571	5.128	8.198	95.35	56.00	60.786	4.242	7.190	90.11	37.50	85.861	3.874	4.512	94.851	57.00	53.964	4.324	7.891	100.36	39.00
70	54.892	0.691	1.283	94.46	47.00	68.844	5.069	7.657	101.87	54.00	60.462	3.385	5.652	89.63	37.22	85.074	4.764	5.618	93.712	56.00	52.757	3.033	5.810	98.12	41.50

* = % retention

TABLE E4:

Test Conditions = 95% RH: 16 days
Laminate lay-up Orientation = 0°

Temperature °C	411-45					470-36					272					913					750				
	Mean Value	SD	CV (%)	Retn. %*	VF %	Mean Value	SD	CV (%)	Retn. %*	VF %	Mean Value	SD	CV (%)	Retn. %*	VF %	Mean Value	SD	CV (%)	Retn. %*	VF %	Mean Value	SD	CV (%)	Retn. %*	VF %
25	56.831	3.033	5.388	97.85	39.00	63.490	6.188	9.933	96.75	38.00	65.344	4.393	6.800	96.92	38.00	78.053	1.785	2.286	85.98	62.73	51.770	1.290	2.556	96.28	39.00
40	56.685	3.615	6.378	97.55	37.80	62.117	1.732	2.793	94.66	48.30	57.929	2.387	4.173	85.87	39.00	73.699	2.509	3.419	81.18	62.00	48.609	2.607	5.501	90.40	46.20
50	54.181	0.513	0.977	93.24	47.00	59.380	2.146	3.493	90.46	39.50	55.186	2.667	4.856	81.806	39.00	71.060	4.009	5.642	78.28	60.00	47.556	2.828	5.772	88.44	42.00
60	52.523	1.767	3.262	90.57	47.00	58.489	2.803	4.792	89.13	55.00	54.408	2.217	4.087	80.65	42.00	69.554	2.346	3.374	76.62	56.00	45.516	4.582	10.183	84.64	42.00
70	46.140	5.281	11.014	79.41	38.00	54.110	2.081	3.952	82.46	38.00	50.870	0.577	1.147	75.41	38.00	57.620	2.879	4.996	63.47	58.22	42.608	0.607	1.555	79.24	46.00

* = % retention

TABLE E5:

Test Conditions = 95% RH: 40 days
Laminate lay-up Orientation = 0°

Temperature °C	411-45					470-36					272					913					750				
	Mean Value	SD	CV (%)	Retn. %*	VF %	Mean Value	SD	CV (%)	Retn. %*	VF %	Mean Value	SD	CV (%)	Retn. %*	VF %	Mean Value	SD	CV (%)	Retn. %*	VF %	Mean Value	SD	CV (%)	Retn. %*	VF %
25	55.991	3.479	6.214	96.35	44.00	61.649	6.058	9.898	93.95	48.00	63.505	4.438	7.067	94.86	38.00	74.820	2.827	3.849	82.418	62.73	47.535	0.707	1.501	88.40	46.20
40	55.723	1.208	2.167	95.89	37.80	60.967	3.130	5.165	92.76	48.30	56.796	4.037	7.158	84.76	39.00	69.893	2.437	3.485	77.00	62.73	45.543	2.683	5.807	84.70	40.20
50	54.812	1.857	3.389	94.33	47.00	58.186	2.912	4.837	88.67	41.50	55.982	4.037	7.287	82.99	39.00	62.320	3.128	5.019	68.65	55.80	43.452	2.701	5.925	80.81	47.00
60	48.836	4.298	8.801	84.04	47.00	53.419	8.158	15.272	81.41	55.00	51.292	5.305	10.801	76.03	39.00	61.355	3.678	5.994	67.587	56.00	42.953	4.725	11.119	79.86	48.00
70	45.020	3.827	8.349	77.47	44.00	51.511	3.346	6.536	73.135	48.30	49.740	6.363	13.540	73.74	38.00	56.576	2.065	2.651	62.321	58.00	36.876	1.341	3.665	68.59	46.00

* = % retention

TABLE E6:

Test Conditions = Water Bath: 16 days
Laminate lay-up Orientation = 0°

Temperature °C	411-45					470-36					272					913					750				
	Mean Value	SD	CV (%)	Retn. %*	VF %	Mean Value	SD	CV (%)	Retn. %*	VF %	Mean Value	SD	CV (%)	Retn. %*	VF %	Mean Value	SD	CV (%)	Retn. %*	VF %	Mean Value	SD	CV (%)	Retn. %*	VF %
25	56.645	3.184	5.621	97.48	44.00	60.817	3.646	6.018	92.68	48.30	59.370	1.923	3.271	88.01	38.00	78.050	2.390	3.061	85.98	63.00	43.540	1.284	2.848	80.97	40.00
40	55.763	0.830	1.488	95.96	47.00	62.183	2.387	3.834	94.73	54.00	56.261	2.489	4.462	83.40	37.00	78.205	1.095	1.408	80.15	56.70	45.485	2.509	5.397	86.45	37.00
50	54.187	2.430	4.486	93.25	45.00	59.778	1.140	1.887	91.09	48.3	50.243	2.588	5.197	74.48	38.00	63.238	2.720	4.302	69.66	67.73	42.330	2.190	5.024	78.72	54.00
60	48.614	2.203	4.433	83.66	47.00	60.447	5.458	9.008	92.12	57.00	48.897	2.687	5.506	72.83	37.5	62.907	0.905	1.438	56.70	56.70	46.847	3.577	7.71	87.12	39.00
70	49.253	8.812	19.135	84.76	44.00	53.104	0.577	1.075	80.93	49.00	48.21	1.000	2.083	71.48	38.00	50.210	2.866	5.708	55.31	58.22	36.730	2.886	7.945	68.31	40.00

* = % retention

TABLE E7:

Test Conditions = Water Bath: 40 days
 Laminate lay-up Orientation = 0°

Temperature °C	411-45					470-36					272					913					750				
	Mean Value	SD	CV (%)	Retn. %*	VF %	Mean Value	SD	CV (%)	Retn. %*	VF %	Mean Value	SD	CV (%)	Retn. %*	VF %	Mean Value	SD	CV (%)	Retn. %*	VF %	Mean Value	SD	CV (%)	Retn. %*	VF %
25	56.263	1.581	2.811	96.82	44.60	64.263	3.701	5.765	97.93	48.30	56.483	0.707	1.262	83.73	38.00	74.820	3.489	4.662	82.48	62.73	40.632	0.831	2.081	75.563	46.
40	54.825	2.483	4.529	94.35	47.00	61.450	2.190	3.556	93.65	54.00	55.103	3.209	5.831	81.68	37.00	74.630	4.449	5.980	82.55	56.70	41.323	2.714	6.757	76.851	37.
50	52.287	3.379	7.227	89.81	45.00	59.779	2.503	4.119	91.10	48.30	49.474	5.458	11.113	73.33	38.60	58.860	2.745	4.665	64.837	67.73	40.737	2.588	6.438	75.783	53.
60	41.916	1.904	4.542	72.16	47.00	56.204	4.827	8.528	85.65	54.30	48.818	2.190	4.526	73.37	37.5	58.711	4.506	8.454	58.711	52.70	41.141	1.303	3.195	76.153	39.
70	39.664	1.135	2.862	60.34	44.00	49.580	1.258	2.554	75.56	49.00	44.88	4.219	9.502	66.53	38.00	52.124	2.683	5.604	52.194	58.22	36.88	3.701	10.224	68.589	46.

* = % retention

TABLE E8:

Test Conditions: Thermal spike: 16 days
Laminate lay-up Orientation = 0°

Resin Matrix	Mean Value	SD	CV (%)	Retention (%)	VF (%)
411-45	52.639	2.829	5.376	90.59	47.20
470-36	61.399	2.744	4.471	93.57	52.00
272	57.132	1.506	2.636	84.69	40.00
913	73.372	5.059	6.895	80.82	57.00
750	47.414	1.419	2.978	88.17	42.00

TABLE E9:

Test Conditions: Thermal spike: 40 days
Laminate lay-up Orientation = 0°

Resin Matrix	Mean Value	SD	CV (%)	Retention (%)	VF (%)
411-45	46.316	1.835	3.963	79.70	47.20
470-36	58.334	0.925	1.585	88.89	52.00
272	51.812	2.550	4.921	76.81	40.00
913	67.380	2.202	3.268	74.22	57.00
750	43.563	0.985	2.261	81.02	42.00

APPENDIX F

SUMMARY OF EXPERIMENTAL DATA ON THE
EFFECTS OF MOISTURE AND TEMPERATURE ON THE
IN-PLANE SHEAR STRENGTH OF COMPOSITE MATERIALS (MPa)

<u>Table</u>	<u>Title</u>
F 1	Dried
F 2	60% RH: 16 days
F 3	60% RH: 40 days
F 4	95% RH: 16 days
F 5	95% RH: 40 days
F 6	Water Immersion: 16 days
F 7	Water Immersion: 40 days
F 8	Thermal Spike: 16 days
F 9	Thermal Spike: 40 days

TABLE F1:

Test Conditions: dried
Laminate lay-up Orientation = $\pm 45^\circ$

Resin Matrix	Volume Fraction (%)	Mean Value	Standard Deviation (SD)	Coefficient of Variation (CV)
411-45	45.00	69.910	1.200	1.716
470-36	45.00	64.780	1.923	2.969
272	48.00	65.240	1.616	2.478
913	55.00	98.615	2.333	2.366
750	45.00	65.370	2.754	4.213

TABLE F2:

Test Conditions = 60% RH: 16 days
Laminate lay-up Orientation = #45°

Temperature °C	411-45					470-36					272					913					750				
	Mean Value	SD	CV (%)	Retn. %*	VF %	Mean Value	SD	CV (%)	Retn. %*	VF %	Mean Value	SD	CV (%)	Retn. %*	VF %	Mean Value	SD	CV (%)	Retn. %*	VF %	Mean Value	SD	CV (%)	Retn. %*	VF %
25	68.88	0.692	1.288	98.52	49.00	63.38	5.385	8.54	97.88	48.00	64.66	1.154	1.785	99.12	42.00	98.31	1.573	1.608	99.68	65.00	64.05	2.081	3.3269	97.98	50.00
40	70.15	1.616	2.309	100.70	41.00	64.22	0.577	0.960	99.14	49.86	65.77	5.496	8.363	100.8	40.7	98.29	4.927	5.013	99.67	57.00	63.50	4.041	6.381	97.17	48.00
50	69.29	1.159	1.673	99.09	48.00	67.04	0.577	0.866	103.5	46.00	64.21	0.655	1.036	98.42	38.00	98.53	4.579	4.647	99.91	58.00	63.11	1.000	1.587	96.54	59.10
60	71.86	5.495	7.647	103.51	44.00	61.66	4.041	6.483	95.18	49.00	65.63	8.321	12.678	100.6	42.00	85.85	1.427	1.663	87.05	57.00	65.88	3.000	1.562	100.7	58.00
70	67.59	2.753	4.076	96.68	48.00	59.67	2.307	3.870	92.11	50.8	61.08	1.348	2.209	93.60	45.00	97.2	0.910	1.043	88.42	57.16	62.12	0.063	0.102	95.03	57.00

* = % retention

TABLE F3:

Test Conditions = 60% RH: 40 days
Laminate lay-up Orientation = ±45°

Temperature °C	411-45					470-36					272					913					750				
	Mean Value	SD	CV (%)	Retn. %*	VF %	Mean Value	SD	CV (%)	Retn. %*	VF %	Mean Value	SD	CV (%)	Retn. %*	VF %	Mean Value	SD	CV (%)	Retn. %*	VF %	Mean Value	SD	CV (%)	Retn. %*	VF %
25	68.68	8.705	15.726	98.24	48.00	64.58	8.506	10.113	99.69	50.00	66.20	0.816	1.237	101.47	48.80	97.2	1.918	1.943	98.56	65.3	64.65	2.886	4.475	97.80	48.00
40	64.09	0.125	0.196	91.67	45.00	63.45	1.258	1.992	97.95	50.00	62.2	0.888	1.428	95.34	37.00	101.76	9.665	9.498	103.18	56.00	64.34	1.000	1.562	98.42	58.44
50	68.75	2.441	3.550	99.06	48.00	68.22	2.000	2.941	105.2	54.00	64.15	2.799	4.363	99.33	39.00	95.30	0.821	0.862	96.63	59.00	61.71	8.18	13.355	94.40	59.10
60	69.25	7.209	10.409	99.05	45.00	62.78	1.527	2.490	96.91	49.00	56.70	0.179	0.316	86.91	43.00	87.26	2.860	3.278	88.48	62.00	83.98	2.088	3.170	97.88	50.00
70	65.16	1.531	2.340	93.21	48.00	57.28	4.358	7.649	88.43	51.20	55.90	1.310	2.344	85.69	45.00	86.59	1.439	1.661	87.81	58.20	64.92	7.406	11.346	97.90	53.2

* = % retention

TABLE F4:

Test Conditions = 95% RH: 16 days
Laminate lay-up Orientation = ±45°

Temperature °C	411-45					470-36					272					913					750				
	Mean Value	SD	CV (%)	Retn. %*	VF %	Mean Value	SD	CV (%)	Retn. %*	VF %	Mean Value	SD	CV (%)	Retn. %*	VF %	Mean Value	SD	CV (%)	Retn. %*	VF %	Mean Value	SD	CV (%)	Retn. %*	VF %
25	63.89	2.394	3.794	91.37	43.00	65.24	1.674	2.659	97.68	43.00	59.95	0.115	0.192	91.89	44.00	83.98	0.491	0.585	85.16	61.80	65.97	1.154	1.758	100.9	45.00
40	65.59	0.662	1.058	89.54	46.00	59.00	2.986	5.092	91.08	47.60	53.05	3.231	6.077	81.56	41.00	79.02	7.805	9.805	80.13	55.00	53.00	1.527	2.900	81.08	55.00
50	60.09	3.097	5.155	85.96	47.00	57.28	2.309	4.229	88.42	45.40	55.706	3.724	6.686	85.39	43.00	73.01	2.084	2.855	74.03	64.00	46.00	2.430	5.006	70.37	44.70
60	54.30	0.694	1.278	77.30	50.00	54.80	0.577	1.056	84.59	50.00	49.57	1.935	3.904	75.99	45.00	69.47	0.806	1.160	70.44	55.00	45.67	2.645	5.629	69.70	53.00
70	47.19	0.693	1.278	67.49	47.00	49.51	1.299	2.608	76.42	48.80	47.19	3.364	5.975	72.33	47.00	69.37	2.295	3.309	70.34	55.00	44.53	2.085	4.698	68.11	45.00

* = % retention

TABLE F5:

Test Conditions = 95% RH, 40 days
 Laminate lay-up Orientation = - 45°

Temperature °C	411-45					470-36					272					913					750				
	Mean Value	SD	CV (%)	Retn. %*	VF %	Mean Value	SD	CV (%)	Retn. %*	VF %	Mean Value	SD	CV (%)	Retn. %*	VF %	Mean Value	SD	CV (%)	Retn. %*	VF %	Mean Value	SD	CV (%)	Retn. %*	VF %
25	63.05	0.492	0.770	90.18	42.00	58.41	1.110	1.907	90.16	49.00	51.315	1.728	3.367	78.66	44.00	74.48	0.994	1.334	75.52	61.80	62.71	4.500	7.228	95.92	44.00
40	61.39	1.958	3.191	87.82	46.00	57.74	0.577	1.004	89.13	45.22	52.88	0.173	81.02	97.00	97.00	77.44	2.594	3.350	77.14	55.00	50.71	1.000	1.980	77.57	57.00
50	60.95	1.650	2.717	87.18	48.00	51.23	2.516	4.778	79.88	48.80	53.88	1.967	3.656	92.59	44.00	71.01	4.023	5.667	71.99	63.00	49.20	7.637	15.481	75.25	50.00
60	55.37	8.703	15.772	79.20	47.5	54.19	2.681	3.831	83.62	52.10	44.61	1.457	3.264	68.38	46.00	65.80	3.946	5.992	66.72	55.00	45.57	3.601	8.012	69.7	55.00
70	47.82	3.285	6.880	61.40	47.00	48.80	2.500	5.181	75.33	50.00	45.21	2.653	5.732	68.29	47.00	61.25	3.870	6.317	62.11	54.00	48.81	6.379	11.351	74.66	50.20

* = % retention

TABLE F6:

Test Conditions = Water bath, 16 days
Laminate lay-up Orientation = ±45°

Temp °C	411-45					470-36					272					913					750				
	Mean Value	SD	CV (%)	Retn %*	VF %	Mean Value	SD	CV (%)	Retn %*	VF %	Mean Value	SD	CV (%)	Retn %*	VF %	Mean Value	SD	CV (%)	Retn %*	VF %	Mean Value	SD	CV (%)	Retn %*	VF %
25	64.13	2.298	3.593	91.73	41.00	64.13	3.511	5.458	98.99	41.00	58.00	0.635	1.097	89.00	41.00	74.56	4.046	5.426	75.60	58.00	64.129	2.943	4.599	88.11	55.00
40	63.12	4.688	7.427	90.28	47.5	64.36	3.511	5.458	99.35	47.5	57.94	1.185	2.159	84.21	38.4	73.53	4.876	6.631	74.56	57.17	53.91	2.645	4.899	82.47	56.00
50	62.30	3.022	5.397	89.11	40.00	61.53	2.160	3.541	94.98	52.00	57.59	2.380	4.139	88.27	38.00	73.41	2.606	3.551	74.44	58.60	59.85	1.7880	2.991	91.56	59.10
60	53.77	1.966	3.658	76.91	45.00	60.88	6.658	10.975	93.98	51.00	58.36	0.953	1.630	89.45	37.00	72.73	6.027	8.287	73.74	53.09	59.26	1.527	2.524	91.86	57.00
70	46.91	0.640	1.365	67.09	42.00	59.87	0.167	0.279	92.42	56.00	50.64	0	0	77.62	45.00	61.13	0.325	0.533	61.98	55.00	59.11	1.414	2.396	90.42	54.00

* = % retention

TABLE F7:

Test Conditions = Water Bath: 40 days
 Laminate lay-up Orientation = $\pm 45^\circ$

Temperature °C	411-45					470-36					272					913					750				
	Mean Value	SD	CV (%)	Retn. %*	VF %	Mean Value	SD	CV (%)	Retn. %*	VF %	Mean Value	SD	CV (%)	Retn. %*	VF %	Mean Value	SD	CV (%)	Retn. %*	VF %	Mean Value	SD	CV (%)	Retn. %*	VF %
25	56.88	3.618	6.361	81.36	40.00	60.51	2.217	3.680	93.41	49.00	56.98	1.002	1.761	87.33	48.00	74.55	4.189	5.619	75.59	58.10	59.04	1.260	2.301	84.14	55.00
40	58.81	0.360	0.446	84.12	47.00	58.17	3.605	6.216	89.79	47.50	52.63	2.805	5.391	79.75	39.00	76.09	1.030	1.354	77.15	57.17	48.97	2.645	5.399	74.91	53.00
50	56.00	6.953	11.530	80.10	42.00	58.29	2.888	4.876	89.98	50.8	54.64	3.109	5.691	63.75	40.00	68.83	0.481	0.699	69.79	58.60	52.05	0.494	0.950	79.35	59.10
60	50.16	1.707	3.404	71.76	47.00	57.98	9.018	15.639	89.51	51.00	55.75	4.839	8.682	85.45	39.00	65.31	1.129	1.729	64.84	55.00	53.22	3.000	5.660	0.08	57.00
70	45.99	0.819	1.820	65.08	47.2	39.69	0.816	2.093	61.27	46.00	49.16	2.459	5.570	67.69	48.00	53.59	0.661	1.232	54.34	50.00	35.11	0.836	2.404	53.09	57.00

* = % retention

TABLE F8:

Test Conditions: Thermal spike: 16 days
Laminate lay-up Orientation = $\pm 45^\circ$

Resin Matrix	Mean Value	SD	CV (%)	Retention (%)	VF (%)
411-45	57.927	6.027	10.405	82.86	49.00
470-36	58.541	2.503	4.275	90.37	52.00
272	54.204	2.443	4.507	83.08	45.00
913	76.297	3.809	4.994	77.36	53.00
750	56.490	1.775	3.142	86.42	45.00

TABLE F9:

Test Conditions: Thermal spike: 40 days
Laminate Lay-up Orientation = $\pm 45^{\circ}$

Resin Matrix	Mean Value	SD	CV (%)	Retention (%)	VF (%)
411-45	47.730	2.658	5.569	68.27	49.00
470-36	49.388	1.453	2.942	76.24	52.80
272	42.624	1.677	3.523	72.99	45.00
913	60.635	1.905	3.153	61.48	53.00
750	42.625	2.489	5.839	65.20	45.00

T A B L E S

TABLE 2.1: The Effect of Increasing Crosslink Density on Certain Physical Properties (7)

Physical Properties	Effect
Modulus of Elasticity	Increase
Ultimate impact strength	Decrease
Elongation at break	Decrease
Temperature resistance	Increase
Surface hardness	Increase
Electrical resistance	Increase
Resistance to swelling	Increase
Resistance to creep	Increase
Moisture resistance	Increase
Acid resistance	Increase
Alkali resistance	Increase

TABLE 2.2: Typical Properties of Cured Polyester Resins⁽¹¹⁾

Resin Type	Cast Resin Properties				HDT °C	Glass %	Laminate Properties		
	Flexural Strength (MPa)	Tensile Strength (MPa)	Tensile Modulus (GPa)	Elongation %			Flexural Strength (MPa)	Tensile Strength (MPa)	Tensile Modulus (GPa)
Orthophthalic	100	65-75	3.2	20-40	55-110	30	150	90	7
Isophthalic	140	70-85	3.5	3.5	75-130	30	230	120	8
NPG orthophthalic	130	70	3.4	2.4	110	30	170	90	7
Isophthalic NPG	130	60	3.4	2.5	90-115	30	150	85	7
Bisphenol A	130	60-75	3.2	2.9	70	30	150	90	7

NPG = Neo-Pentyl Glycol

TABLE 2.3: Comparison of Typical Properties of Epoxy and Polyester Resins Used in Composite Materials⁽¹⁶⁾

Property	Epoxy Resins	Polyester Resins
Density (mg cm^{-3})	1.1-1.4	1.2-1.5
Young's Modulus (GN m^{-2})	3-6	2-45
Poisson's Ratio	0.38-0.40	0.37-0.39
Tensile Strength (MN m^{-2})	35-100	40-90
Compressive Strength (MN m^{-2})	100-200	90-250
Elongation to Break (%)	1-6	2.0
Coefficient of Thermal Expansion ($10^{-6} \text{ }^{\circ}\text{C}^{-1}$)	60	100-200
Heat Distortion ($^{\circ}\text{C}$)	50-300	50-110
Shrinkage on Curing (%)	1-2	4-8
Water Absorption 24h to 20°C (%)	0.1-0.4	0.1-0.3

TABLE 2.4: Typical Properties of the Vinyl Ester Resins

Clear Casting Property	411-45	470-36
Flexural strength (MPa)	124	130
Tensile strength (MPa)	82.7	75.8
Tensile modulus (GPa)	3.1	3.8
% Elongation	50	3.0
Heat distortion temperature ($^{\circ}\text{C}$)	102	138
Barcol hardness	35	40

TABLE 2.5: Aspects of Property Deterioration in the Polymer-based Composite Materials^(29,30)

Materials Feature	Reversible Changes	Irreversible Changes
Resin	<ul style="list-style-type: none"> i) Water swelling ii) Temperature flexibility iii) Physical ordering of local molecular regions 	<ul style="list-style-type: none"> i) Chemical breakdown by hydrolysis ii) Chemical breakdown by UV radiation iii) Chemical breakdown by thermal activation iv) Chemical breakdown by stress induced effects associated with swelling and applied stress v) Physical ordering of local molecular regions vi) Chemical composition changes by leaching vii) Precipitation and swelling phenomena to produce voids and cracks viii) Non-uniform de-swelling to produce surface cracks and crazes
Interface	Flexibilising interface	<ul style="list-style-type: none"> i) Chemical breakdown as above (i),(ii),(iii),(iv) ii) Debonding due to internally generated stress associated with shrinkage and swelling and the applied stress iii) Leaching of interface

/Continued

TABLE 2.5: continued

Materials Feature	Reversible Changes	Irreversible Changes
Fibre		<div><div>i)</div><div>ii)</div><div>iii)</div><div>Leaching of fibre</div><div>Loss of strength due to corrosion</div><div>Chemical breakdown by UV radiation</div></div>

TABLE 2.6: Flexural Modulus Retention Data for CSM/Polyester After 50 Days Immersion in Distilled Water at 100°C (109)

Polyester Resin Type	% Flexural Modulus Retention
Orthophthalic	58
Isophthalic	72
Bisphenol	97
Vinyl ester	77

TABLE 2.7: Flexural Strength Retention Data for CSM/Polyester After 50 Days Immersion in Distilled Water at 100°C (109)

Polyester Resin Rype	% Flexural Strength Retention
Orthophthalic	37
Isophthalic	41
Bisphenol	49
Vinyl ester	53

TABLE 3.1: Properties of Equerove 23/24

Roving	Equerove 23/24
Material	E-glass fibre
Tensile strength	2.4 (GPa)
Tensile modulus	71 (GPa)
Elongation	3.37 (%)
Density	2.54 (g cm ⁻³)
Mass/Unit length	600 (g/km)
Fibre diameter	13 (μm)

TABLE 3.2: Proportions of Catalyst and Acceleration Used with Vinyl ester and Polyester Resins

Resin (100g)	Methyl ethyl ketone peroxide (MEKP) 50% cm ³	Cobalt octoate 6% cm ³	Dimethyl aniline 10% cm ³
Vinyl ester 411-45	2.00	0.30	0.05
Vinyl ester 470-36	2.00	0.30	0.05
Crystic 272	1.500	0.15	-

TABLE 3.3: Proportions of Hardener and Solvent Used with Epoxy MY750 Resin

Resin (100g)	Hardener HY 951 Triethylenetetramine	Dichloromethane
Epoxy MY750	10-15g	15-20g

Resin Matrix	25°C	40°C	50°C	60°C	70°C
411-45	0.045 (%)	0.090 (%)	0.103 (%)	0.168 (%)	0.210 (%)
470-36	0.027 (%)	0.053 (%)	0.099 (%)	0.123 (%)	0.136 (%)
272	0.022	0.039	0.088	0.099	0.157
750	0.077	0.133	0.168	0.337	0.533
913	No weight losses were observed				

TABLE 5.1: Weight losses of the specimen, after being removed from the water bath and redried at 35°C

TABLE 5.2: The Effect of Temperature at 60% RH after 40 days and redrying on ultimate tensile strength

Temperature °C	411-45		470-36		272		913		750	
	UTS (MPa)	Redried (MPa)	UTS (MPa)	Redried (MPa)	UTS (MPa)	Redried (MPa)	UTS (MPa)	Redried (MPa)	UTS (MPa)	Redried (MPa)
25	822.710	836.20	935.22	940.15	853.83	898.12	916.76	998.33	857.21	896.33
40	815.31	835.80	903.71	938.33	860.71	897.34	879.31	998.33	826.38	898.33
50	858.53	836.10	901.71	940.00	827.01	898.20	874.41	997.14	803.51	899.33
60	801.55	830.33	858.42	938.33	836.44	898.10	812.30	990.33	774.28	891.07
70	892.79	829.40	822.06	930.40	791.53	891.60	793.32	988.33	772.53	883.24
Dried (UTS) (MPa)	835.98		940.37		896.04		997.97		898.26	

TABLE 5.3: The Effect of Temperature at 95% RH and redrying on ultimate tensile strength

Temperature °C	411-45		470-36		272		913		750	
	UTS (MPa)	Redried (MPa)	UTS (MPa)	Redried (MPa)	UTS (MPa)	Redried (MPa)	UTS (MPa)	Redried (MPa)	UTS (MPa)	Redried (MPa)
25	745.45	820.44	826.59	883.74	831.50	857.27	791.10	927.44	740.50	867.28
40	701.33	815.40	737.07	819.22	717.05	868.33	702.85	893.37	638.71	802.40
50	619.23	783.44	647.59	802.33	680.93	799.27	647.85	802.77	612.82	768.33
60	588.50	702.57	586.05	798.44	658.57	781.03	608.91	793.27	601.32	756.00
70	487.76	699.44	555.52	763.27	557.53	699.27	598.26	702.30	582.90	628.27
Dried	835.98		940.27		896.04		997.97		898.26	

TABLE 5.4: The Effect of Temperature in Water Bath after 40 days and redrying on ultimate tensile strength

Temperature °C	411-45		470-36		272		913		750	
	UTS (MPa)	Redried (MPa)	UTS (MPa)	Redried (MPa)	UTS (MPa)	Redried (MPa)	UTS (MPa)	Redried (MPa)	UTS (MPa)	Redried (MPa)
25	738.49	821.33	849.83	931.33	674.18	894.33	722.15	992.27	595.17	889.33
40	682.68	788.27	689.18	886.27	601.34	827.57	650.38	887.67	575.97	760.27
50	470.69	702.33	479.41	733.74	557.14	714.44	547.27	727.44	500.27	637.22
60	435.03	656.33	457.18	527.88	542.89	629.27	519.27	Not dried	471.59	487.22
70	353.47	427.22	459.97	513.67	493.15	506.27	518.53	Not dried	389.87	377.14
Dried UTS (MPa)	835.98		940.37		896.04		997.97		898.26	

TABLE 5.5: The Effect of Temperature at 60% RH after 40 days and redrying on Percentage Elongation

Temperature °C	411-45		470-36		272		913		750	
	% Elongation	Redried % El	% Elongation	Redried % El	% Elongation	Redried % El	% Elongation	Redried % El	% Elongation	Redried % El
25	2.475	2.500	2.538	2.612	2.445	2.530	2.175	2.189	2.150	2.130
40	2.400	2.493	2.500	2.630	2.425	2.520	2.160	2.300	2.080	2.100
50	2.445	2.521	2.500	2.600	2.395	2.521	2.225	2.290	2.075	2.110
60	2.470	2.530	2.355	2.583	2.427	2.500	2.060	2.270	2.000	2.300
70	2.260	2.210	2.325	2.596	2.225	2.510	1.925	2.230	1.867	2.100
Dried (% El)	2.512		2.620		2.512		2.300		2.124	

TABLE 5.6: The Effect of Temperature at 95% after 40 days and redrying on Percentage Elongation

Temperature °C	411-45		470-36		272		913		750	
	% Elongation	Redried % El	% Elongation	Redried % El	% Elongation	Redried % El	% Elongation	Redried % El	% Elongation	Redried % El
25	2.340	2.470	2.340	2.573	2.235	2.790	2.247	2.200	1.880	2.100
40	2.305	2.436	2.295	2.560	2.215	2.400	1.944	2.150	1.885	2.00
50	2.020	2.300	2.185	2.50	2.225	2.300	1.940	2.050	1.825	2.00
60	1.895	2.150	1.940	2.46	2.215	2.110	1.875	1.950	1.870	1.85
70	1.760	2.06	1.760	2.09	1.825	2.000	1.700	1.900	1.790	1.80
Dried (% El)	2.512		2.620		2.512		2.300		2.124	

TABLE 5.7: The Effect of Temperature in Water Bath after 40 days and redrying on Percentage Elongation

Temperature °C	411-45		470-36		272		913		750	
	% Elongation	Redried % El	% Elongation	Redried % El	% Elongation	Redried % El	% Elongation	Redried % El	% Elongation	Redried % El
25	2.395	2.400	2.395	2.380	2.188	2.330	2.208	2.200	1.900	2.000
40	2.225	1.990	2.150	2.000	2.125	2.330	1.975	1.900	1.850	1.880
50	1.840	1.800	1.930	1.800	2.050	2.000	1.865	1.700	1.473	1.500
60	1.625	1.600	1.710	1.720	1.820	1.900	1.665	-	1.723	1.500
70	1.360	1.440	1.812	1.633	1.540	1.433	1.610	-	1.552	1.400
Dried (%El)	2.512		2.620		2.512		2.300		2.124	

TABLE 5.8: The Effect of Temperature at 60% RH after 40 days and redrying on Tensile Modulus

Temperature °C	411-45		470-36		272		913		750	
	E (GPa)	Redried (GPa)	E (GPa)	Redried (GPa)	E (GPa)	Redried (GPa)	E (GPa)	Redried (GPa)	E (GPa)	Redried (GPa)
25	35.075	35.300	40.019	39.200	37.544	38.570	44.559	46.900	44.809	46.200
40	35.454	35.240	37.363	37.800	36.415	38.600	40.813	46.890	41.705	46.070
50	36.357	35.327	37.365	37.750	35.570	38.510	40.180	46.370	39.575	46.070
60	32.904	35.327	37.516	36.680	35.518	38.520	40.542	46.800	38.973	46.233
70	36.339	35.333	38.325	37.700	35.707	38.600	44.450	46.800	42.440	46.110
Dried (E GPa)	35.327		36.748		38.566		46.366		46.060	

TABLE 5.9: The Effect of Temperature at 95% RH after 40 days and redrying on Tensile Modulus

Temperature °C	411-45		470-36		272		913		750	
	E (GPa)	Redried (GPa)	E (GPa)	Redried (GPa)	E (GPa)	Redried (GPa)	E (GPa)	Redried (GPa)	E (GPa)	Redried (GPa)
25	32.735	35.002	32.732	36.003	33.215	36.274	39.002	45.257	39.365	44.277
40	31.003	34.576	32.558	35.470	33.295	36.184	39.193	43.460	34.676	43.185
50	31.143	33.277	30.651	34.274	31.774	35.270	36.643	42.884	33.835	40.277
60	27.501	32.447	31.018	33.378	31.567	34.280	33.768	40.284	33.798	38.277
70	25.359	30.388	25.359	31.274	28.913	33.370	33.856	36.277	31.285	36.270
Dried E (GPa)	35.327		36.748		38.566		46.366		46.060	

TABLE 5.10: The Effect of Temperature in Water Bath after 40 days and redrying on Tensile Modulus

Temperature °C	411-45		470-36		272		913		750	
	E (GPa)	Redried (GPa)	E (GPa)	Redried (GPa)	E (GPa)	Redried (GPa)	E (GPa)	Redried (GPa)	E (GPa)	Redried (GPa)
25	30.472	32.333	30.422	34.240	32.231	36.334	31.940	44.223	32.333	45.340
40	31.787	32.440	32.649	34.400	28.618	35.334	33.907	43.370	33.432	43.240
50	24.730	29.405	29.533	27.374	28.319	29.684	32.307	40.270	28.207	37.240
60	26.730	26.840	26.886	26.974	30.822	29.337	31.838	-	28.236	26.280
70	25.116	26.840	26.806	26.40	30.932	29.840	30.873	-	26.889	27.333
Dried E (GPa)	35.327		36.748		38.566		46.366		46.060	

TABLE 5.11: The Effect of Temperature at 60% RH after 40 days and redrying on the ILSS

Temperature °C	411-45		470-36		272		913		750	
	ILSS (MPa)	Redried (MPa)	ILSS (MPa)	Redried (MPa)	ILSS (MPa)	Redried (MPa)	ILSS (MPa)	Redried (MPa)	ILSS (MPa)	Redried (MPa)
25	58.772	59.200	66.333	66.890	66.843	67.500	89.150	91.880	53.302	53.800
40	57.301	58.800	68.343	66.620	64.759	68.600	90.055	91.700	52.290	53.780
50	57.065	58.400	66.679	66.000	69.173	68.370	85.954	89.988	52.375	54.200
60	57.519	58.230	62.571	65.900	60.786	67.700	85.861	90.334	53.964	53.900
70	54.892	56.700	68.844	65.880	60.462	66.890	85.074	89.999	52.757	53.900
Dried ILSS (MPa)	58.110		65.620		67.460		90-781		53.770	

TABLE 5.12: The Effect of Temperature at 95% RH after 40 days and redrying on the ILSS

Temperature °C	411-45		470-36		272		913		750	
	ILSS (MPa)	Redried (MPa)	ILSS (MPa)	Redried (MPa)	ILSS (MPa)	Redried (MPa)	ILSS (MPa)	Redried (MPa)	ILSS (MPa)	Redried (MPa)
25	55.991	57.230	61.649	64.374	63.505	65.887	74.820	85.337	47.535	50.200
40	55.723	57.031	60.867	64.370	56.796	65.020	69.893	83.277	45.543	50.337
50	54.812	55.337	58.186	62.933	55.982	63.237	62.320	82.277	43.452	50.020
60	48.836	53.704	53.419	60.244	51.292	60.277	61.355	80.193	42.953	47.277
70	45.020	53.270	51.511	60.488	49.740	54.284	56.576	79.204	36.876	46.280
Dried ILSS (MPa)	58.110		65.620		67.460		90.781		53.770	

TABLE 5.13: The Effect of Temperature in Water Bath after 40 days and redrying on the ILSS

Temperature °C	411-45		470-36		272		913		750	
	ILSS (MPa)	Redried (MPa)	ILSS (MPa)	Redried (MPa)	ILSS (MPa)	Redried (MPa)	ILSS (MPa)	Redried (MPa)	ILSS (MPa)	Redried (MPa)
25	56.265	56.377	64.263	64.148	56.483	62.778	74.820	84.277	40.632	49.337
40	54.825	55.384	61.450	62.248	55.103	61.244	74.630	83.780	41.323	49.220
50	52.287	53.200	59.779	61.402	49.474	58.334	58.860	82.220	40.737	41.220
60	41.916	46.880	*56.204	58.880	48.818	52.440	58.711	-	41.141	39.000
70	39.664	42.004	49.580	53.440	44.880	48.370	52.124	-	36.880	35.200
Dried ILSS (MPa)	58.110		65.620		67.460		90.781		53.770	

TABLE 5.14: The Effect of Temperature at 60% after 40 days and redrying on IPSS

Temperature °C	411-45		470-36		272		913		750	
	IPSS (MPa)	Redried (MPa)	IPSS (MPa)	Redried (MPa)	IPSS (MPa)	Redried (MPa)	IPSS (MPa)	Redried (MPa)	IPSS (MPa)	Redried (MPa)
25	68.68	69.880	64.58	65.00	66.20	65.990	97.2	98.00	64.65	65.800
40	64.09	69.980	63.45	64.920	62.2	66.200	101.76	99.998	64.34	65.740
50	68.75	69.780	68.22	64.800	64.15	65.940	95.30	99.220	64.23	65.380
60	69.25	69.883	62.78	65.100	56.70	65.330	87.26	100.20	63.98	65.970
70	65.16	69.770	57.28	64.980	55.90	65.402	86.598	98.675	61.92	65.700
Dried IPSS (MPa)	69.910		64.780		65.240		98.615		65.370	

TABLE 5.15: The Effect of Temperature at 95% RH after 40 days and redrying on IPSS

Temperature °C	411-45		470-36		272		913		750	
	IPSS (MPa)	Redried (MPa)	IPSS (MPa)	Redried (MPa)	IPSS (MPa)	Redried (MPa)	IPSS (MPa)	Redried (MPa)	IPSS (MPa)	Redried (MPa)
25	63.05	68.233	58.41	63.237	51.315	60.277	74.48	89.277	62.71	63.222
40	61.39	67.223	57.74	63.887	52.88	60.144	77.44	88.278	50.71	60.240
50	60.95	63.406	51.23	59.274	53.88	57.227	71.01	87.444	49.20	60.388
60	55.37	59.244	54.19	57.244	44.61	55.274	65.80	83.224	45.57	57.237
70	47.82	53.244	48.80	52.244	45.21	51.374	61.25	81.280	48.81	52.448
Dried IPSS (MPa)	69.91		64.78		65.24		98.615		65.37	

TABLE 5.16: The Effect of Temperature in Water Bath after 40 days and redrying on IPSS

Temperature °C	411-45		470-36		272		913		750	
	IPSS (MPa)	Redried (MPa)	IPSS (MPa)	Redried (MPa)	IPSS (MPa)	Redried (MPa)	IPSS (MPa)	Redried (MPa)	IPSS (MPa)	Redried (MPa)
25	56.88	59.74	60.51	63.378	56.88	63.37	74.55	90.848	55.04	57.240
40	58.81	58.24	58.17	60.244	52.63	61.294	76.09	87.333	48.97	49.338
50	56.00	47.44	58.29	59.183	54.64	60.274	68.83	80.274	52.05	49.444
60	50.16	53.34	57.98	58.280	55.75	58.288	65.31	-	53.22	52.080
70	45.99	49.248	39.69	44.274	44.16	50.248	53.59	-	35.11	36.240
Dried IPSS (MPa)	69.91		64.78		65.24		98.605		65.37	

TABLE 5.17: The Effect of Thermal Spikes after 40 days and redrying on the Mechanical Properties

Resin Matrix	UTS (MPa)		Elongation (%)		Tensile Modulus (GPa)		ILSS (MPa)		IPSS (MPa)	
	After 40 Days	Redried	After 40 Days	Redried	After 40 Days	Redried	After 40 Days	Redried	After 40 Days	Redried
411-45	519.79	799.33	1.950	1.885	26.411	33.223	42.316	56.440	47.730	64.332
470-36	659.19	895.33	1.800	1.920	30.033	33.884	58.334	59.220	49.388	63.240
272	573.03	820.27	1.975	1.820	29.606	35.241	51.812	60.220	47.624	60.100
913	665.54	850.40	1.850	1.890	35.926	39.244	67.380	83.180	60.635	89.201
750	597.59	799.06	1.850	1.734	31.989	39.400	43.563	48.240	42.625	53.240
411-45 (Dried)	835.98		2.512		35.327		58.110		69.910	
470-36 (Dried)	940.37		2.620		36.748		65.620		64.780	
272 (Dried)	896.04		2.512		38.566		67.460		65.240	
913 (Dried)	997.97		2.300		46.366		90.781		98.615	
750 (Dried)	898.26		2.124		46.060		53.770		65.370	

FIGURES

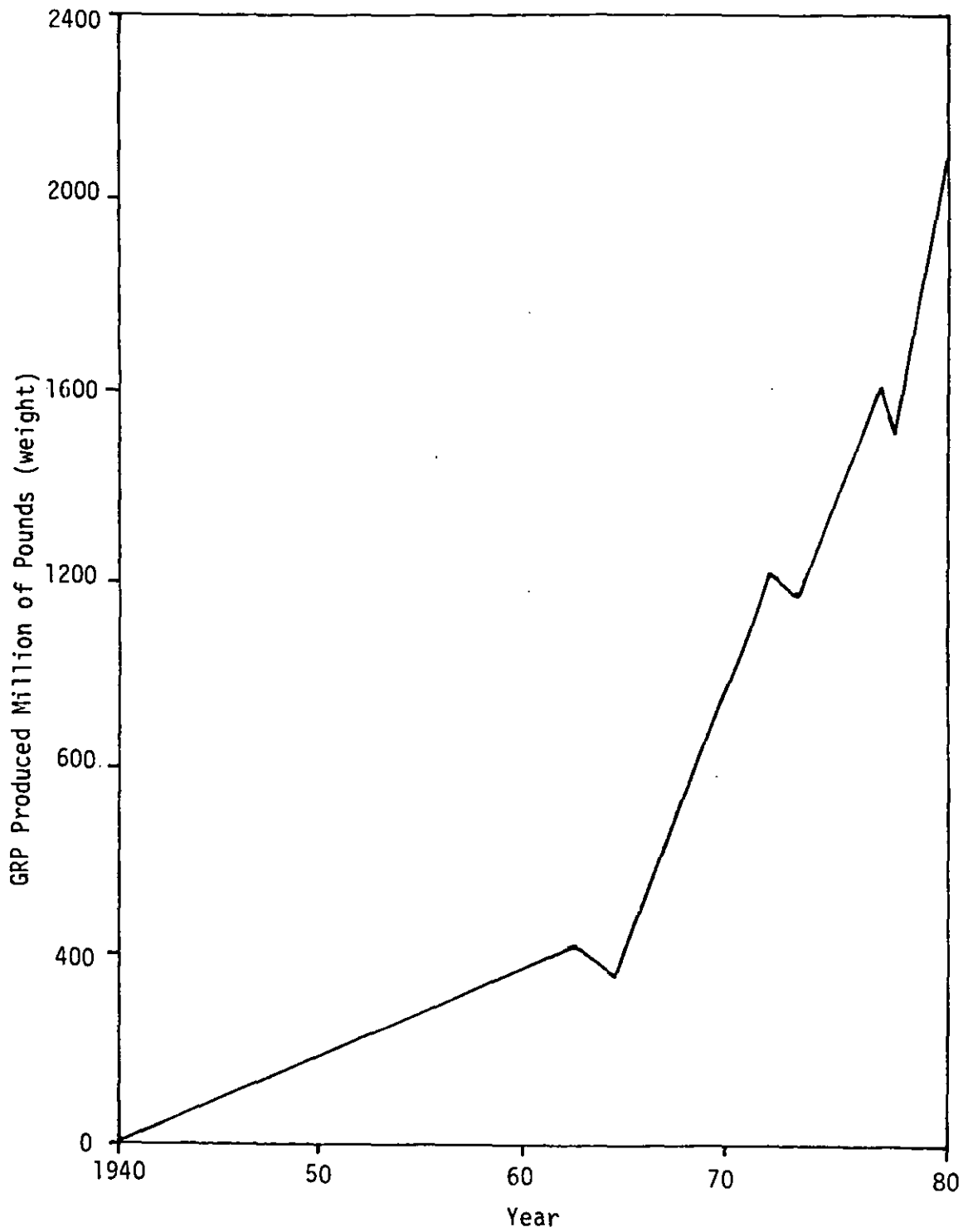
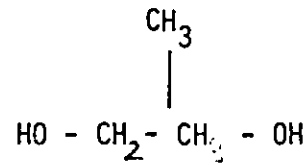
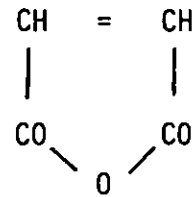


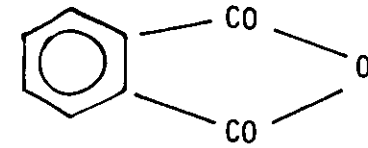
FIGURE 1: The Rapid Growth in the Production of GRP



Propylene glycol



Maleic anhydride



Phthalic anhydride

FIGURE 2: The Commonest Components which are used for Preparation of Simple Polyester Resin

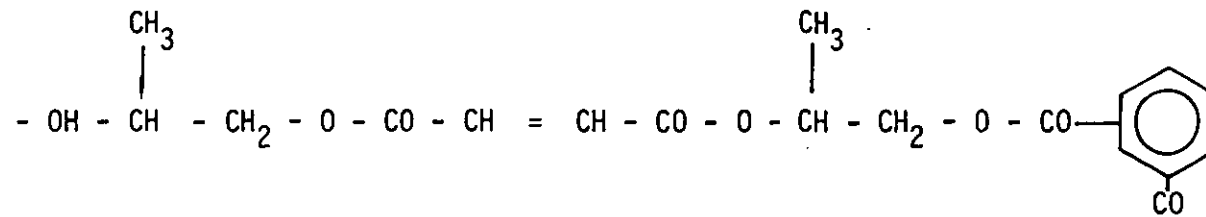


FIGURE 3: Simple Structure for Polyester Resin

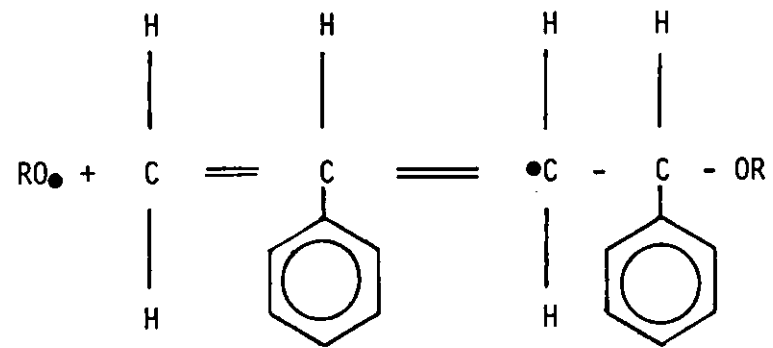
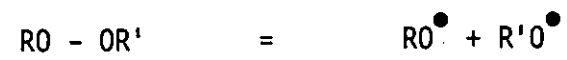


FIGURE 5: The Action of the Peroxide Free Radicals with the Styrene

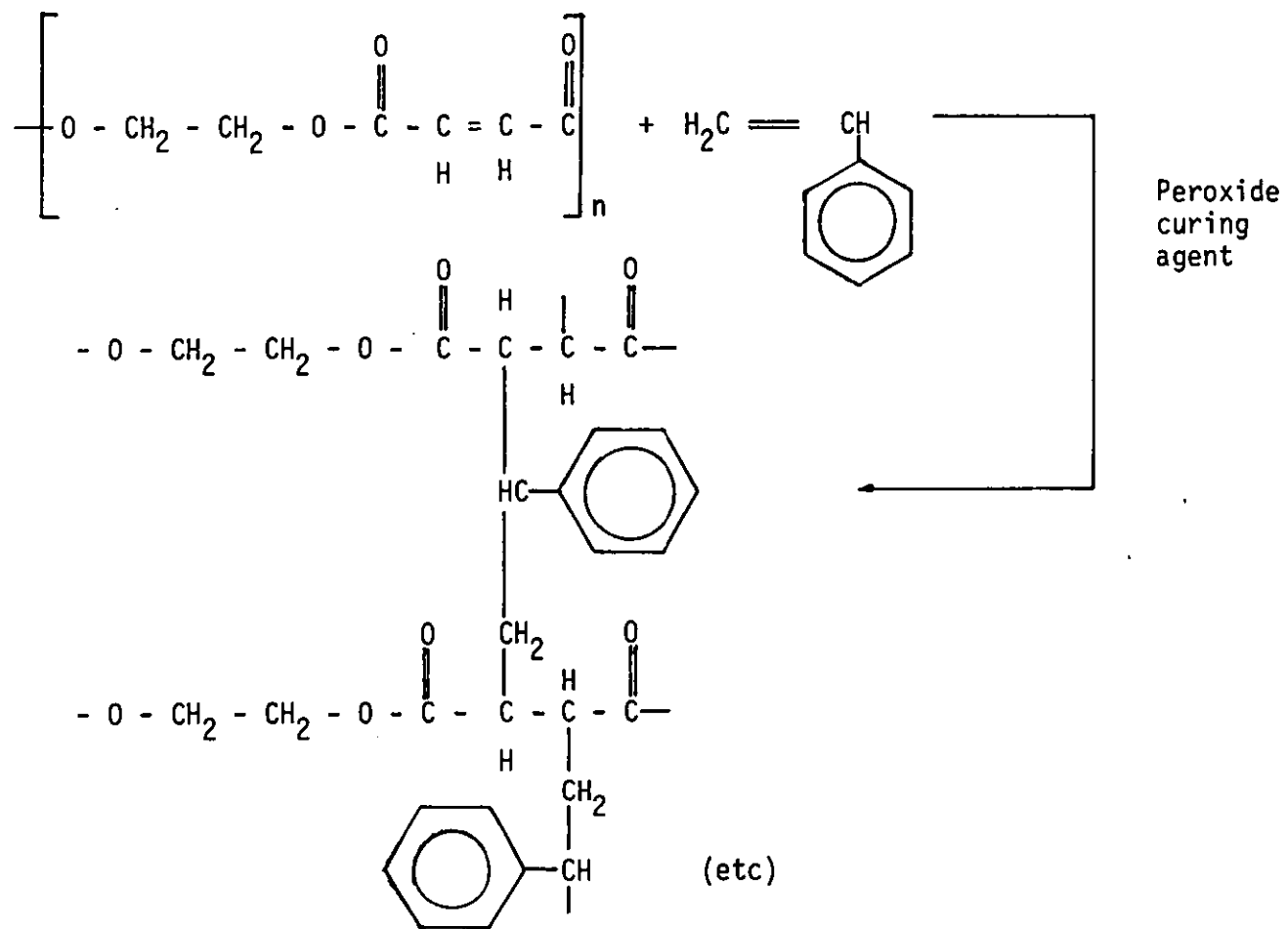


FIGURE 6: Crosslinking of a Simple Polyester Resin with Styrene

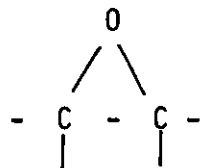


FIGURE 7: The Epoxide Group

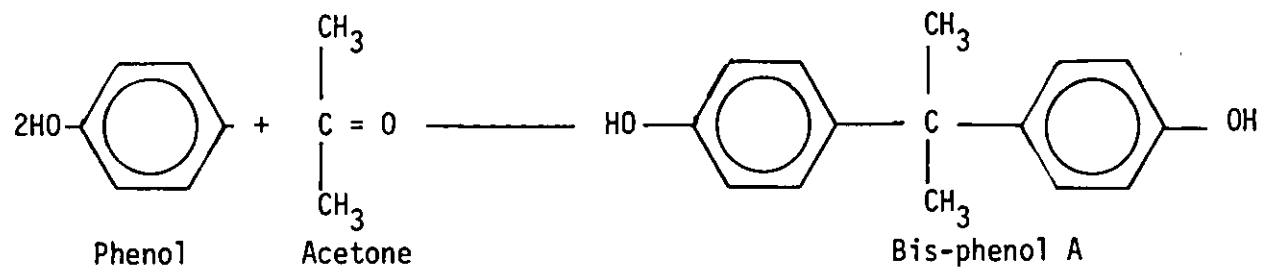


FIGURE 8: Bisphenol-A

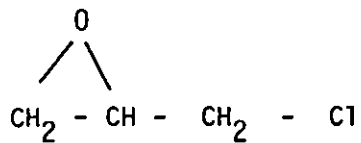
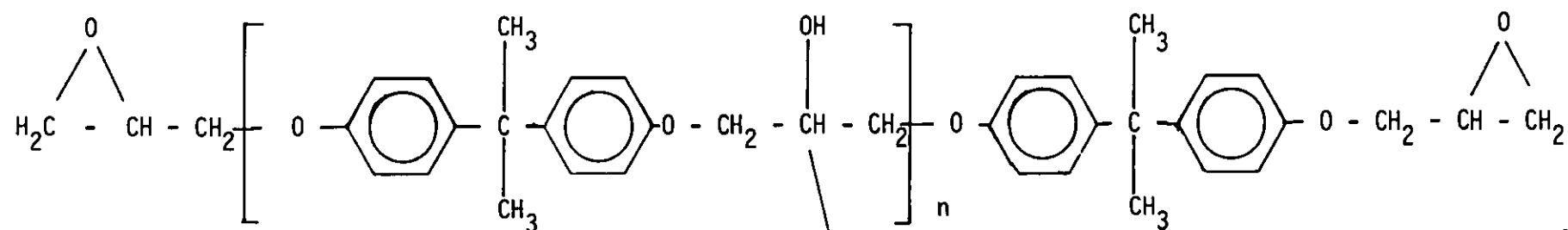


FIGURE 9: Epichlorohydrin



repeating unit

$n = 0 \text{ to } 3$

FIGURE 10: Bisphenol-A/Epichlorohydrin Epoxy

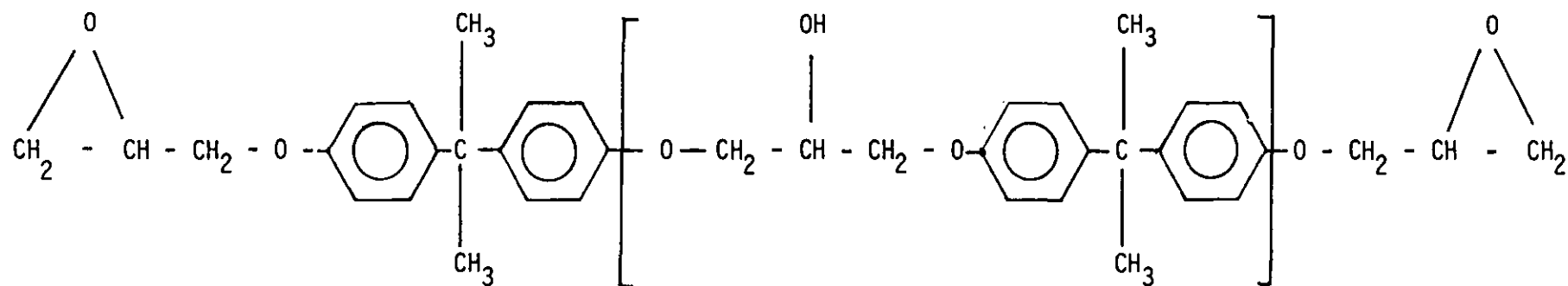


FIGURE 11: The Diglycidyl Ether of Bisphenol-A Resin (DGEBA)

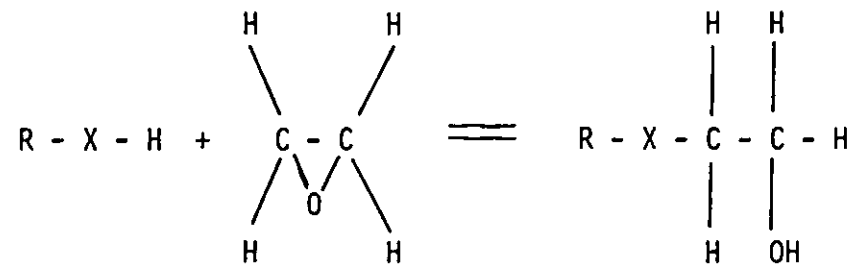


FIGURE 12: The Reaction of the Epoxy Ring with the Curing Agent

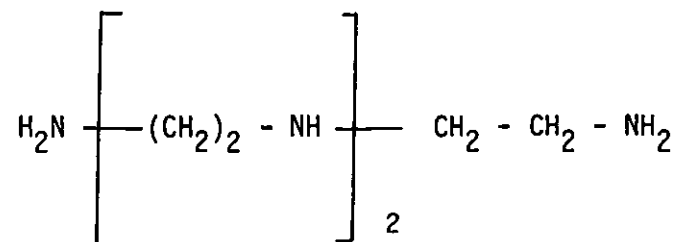


FIGURE 13: HY951 (ex. Ciba-Geigy) Triethylenetetramine

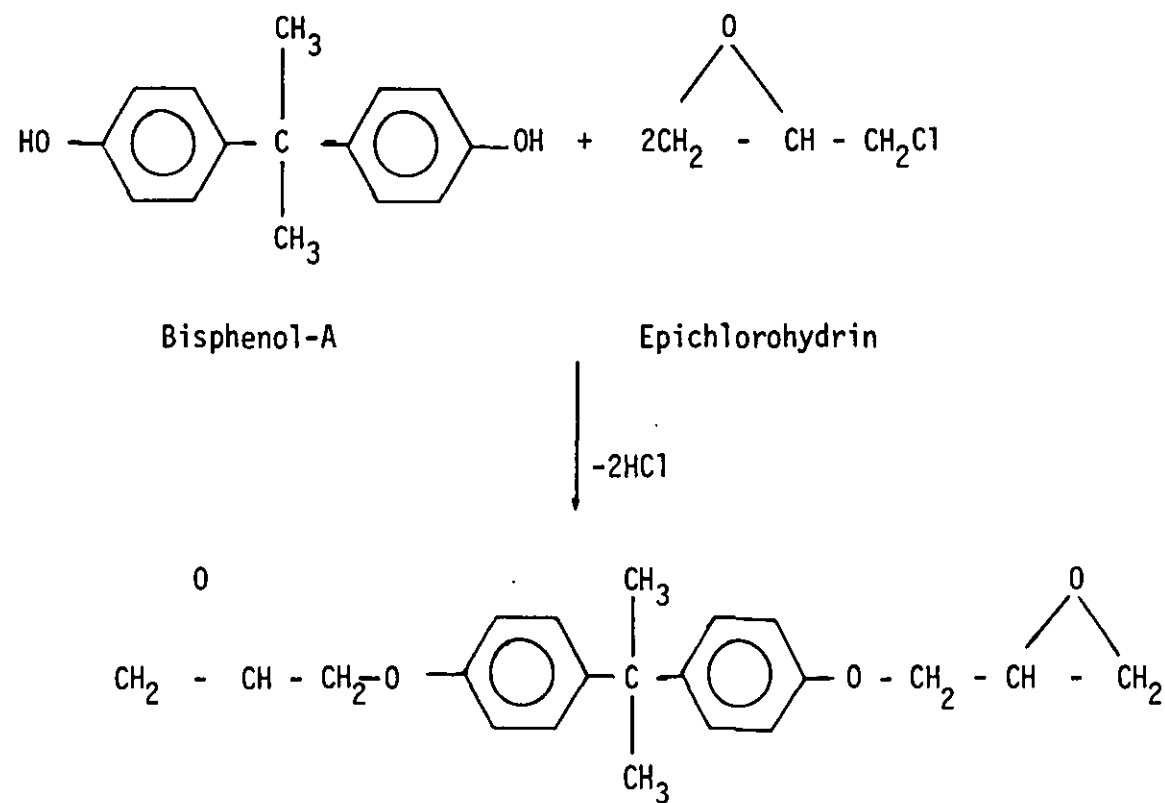


FIGURE 14: The Reaction of Epichlorohydrin with Bisphenol-A to Produce a Simple Polyepoxide Resin

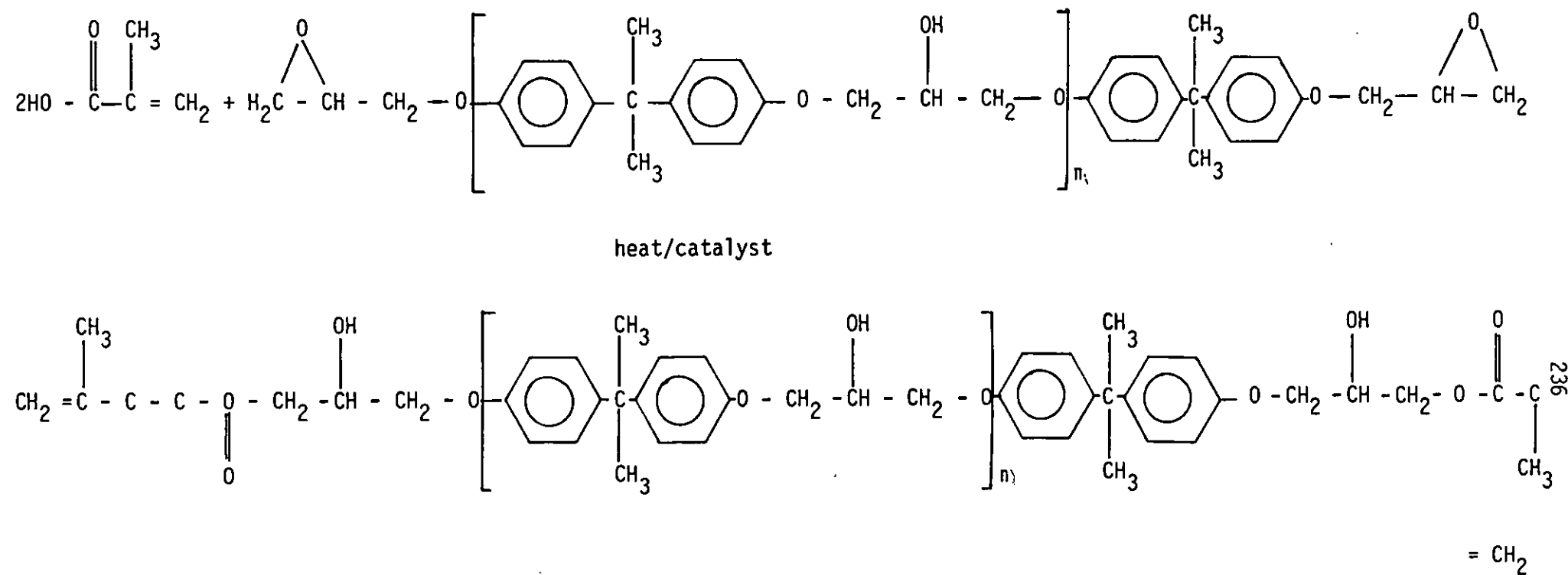
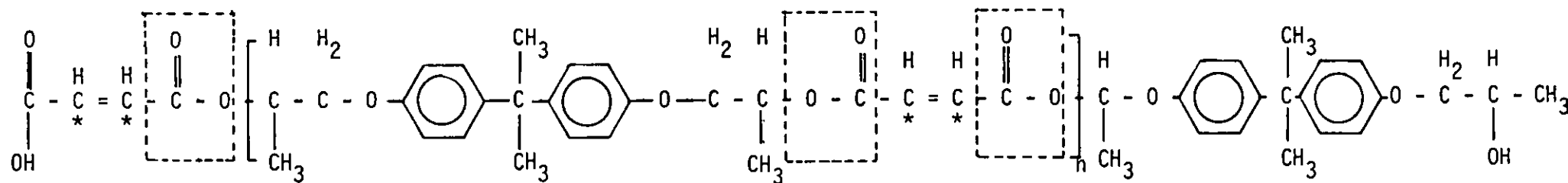
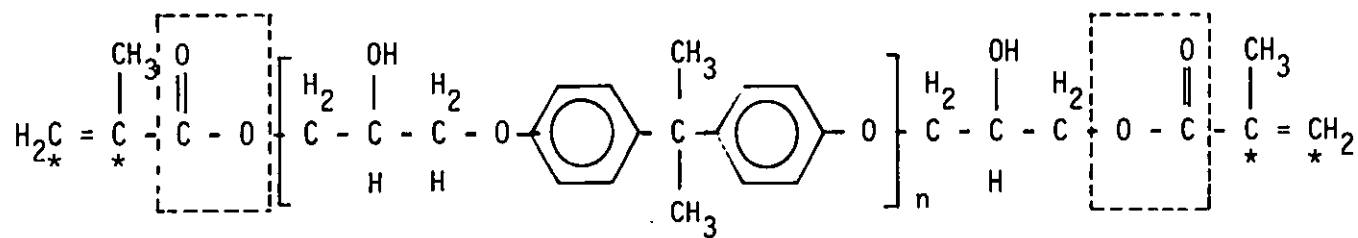


FIGURE 15: Reaction of Methacrylic Acid with DGEBA to Produce Vinyl Ester Resin

FIGURE 16: Comparison of the Structure of a Vinyl Ester with a Polyester



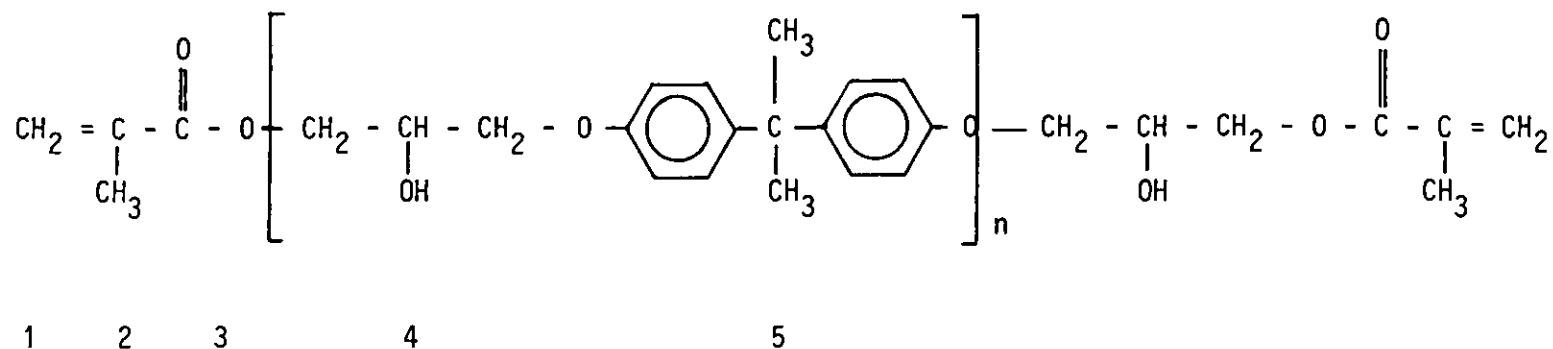
Bisphenol-A-Fumaric Acid Polyester



Derakane Vinyl Ester

* Reactive sites

[-] Ester groups



1. Thermal vinyl unsaturation - gives fast green strength, also gives high corrosion resistance.
2. Methyl group - shields the ester linkage increasing resistance to hydrolysis.
3. Ester group - gives resistance to hydrolysis by alkaline solutions.
4. Secondary hydroxyl - gives strong bond between fibres and resin.
5. Epoxy backbone - improves toughness, also provides superior acid resistance.

FIGURE 17: Derakane 411-45 Vinyl Ester Resin

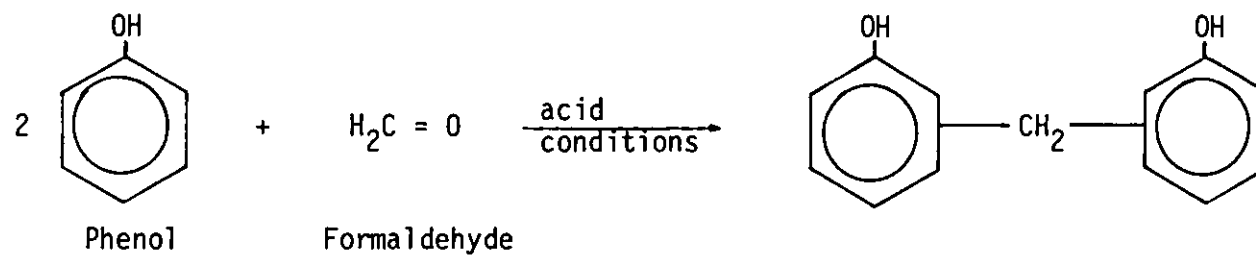


FIGURE 18: Reaction of Phenol with Formaldehyde to Produce a Novolac Resin Structure

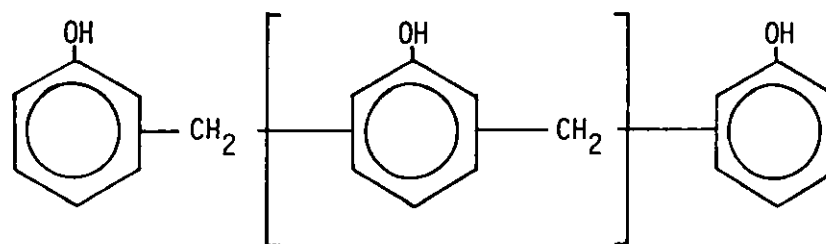


FIGURE 19: Novolac General Structure

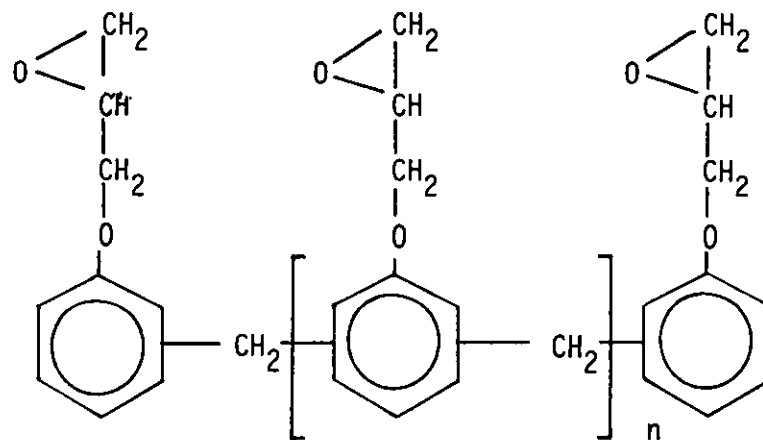
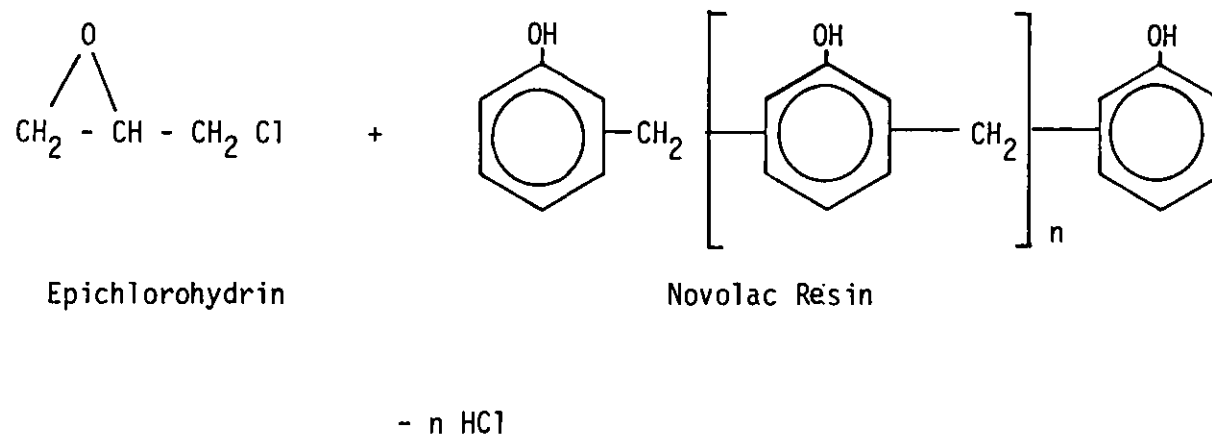


FIGURE 20: Reaction of a Novolac Resin with Epichlorohydrin to Produce an Epoxy

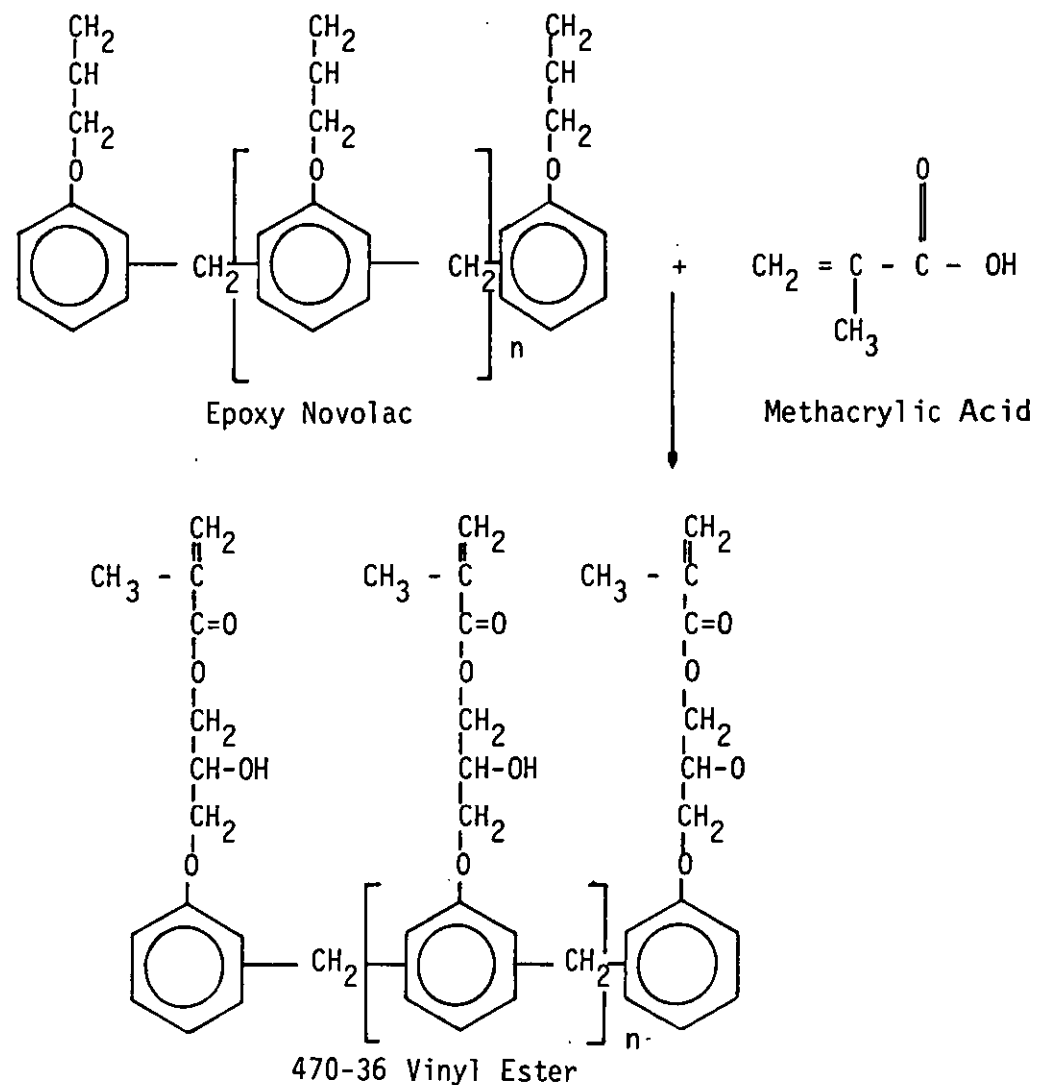


FIGURE 21: The Reaction of Methacrylic Acid with an Epoxy Novolac to Produce the 470 Vinyl Ester

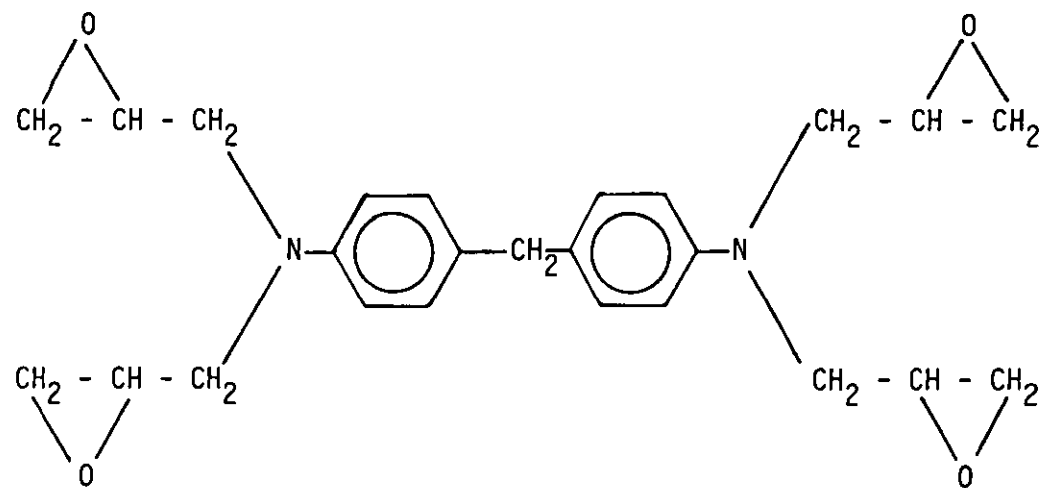
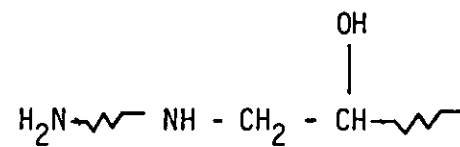
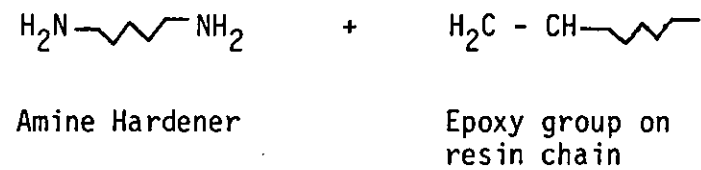


FIGURE 22: MY-720 Epoxy Resin



Epoxy resin with secondary amine group

FIGURE 23: The Reaction Between the Amine Hardener and the Epoxy Resin

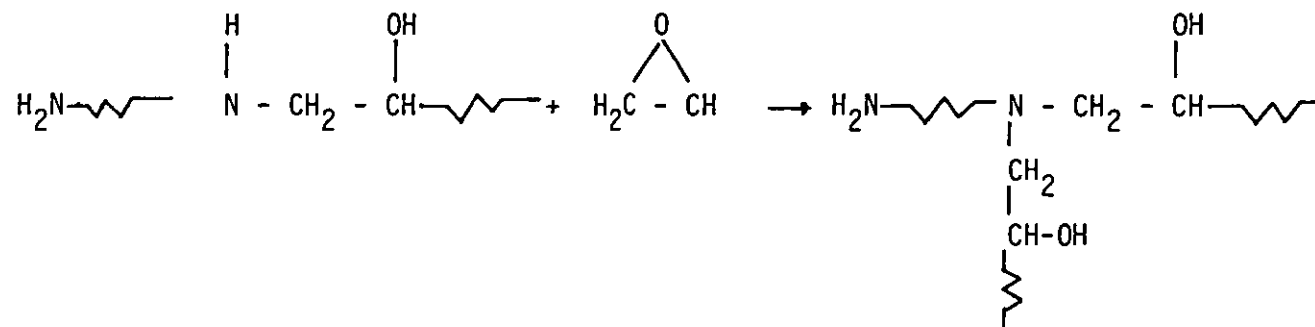


FIGURE 24: The Reaction of a Secondary Amine with an Epoxy Group to Form a Crosslink

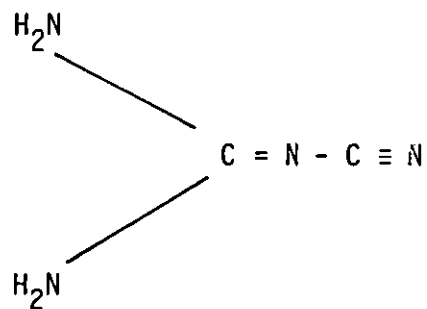
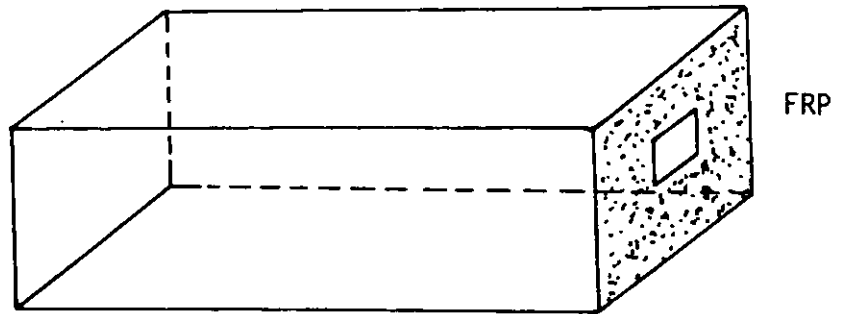


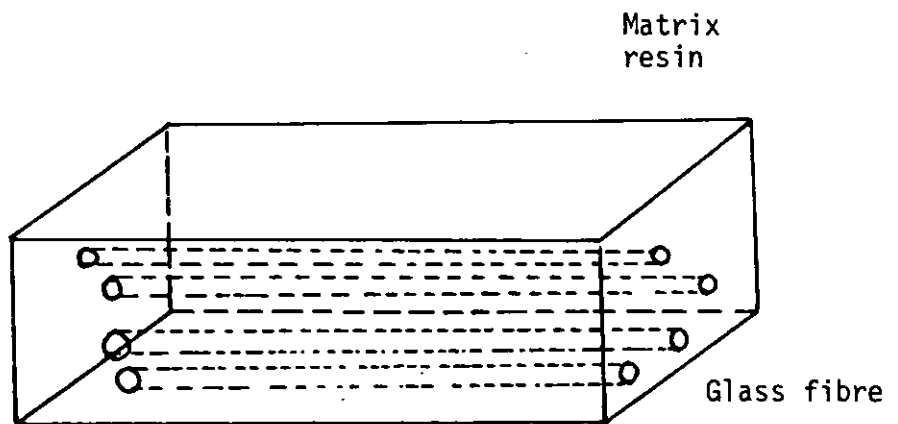
FIGURE 25: Dicyandiamide

FIGURE 26: Schematic Diagrams of Glass-fibre Reinforced Plastics Showing a Composite Structure

(A)



(B)



(C)

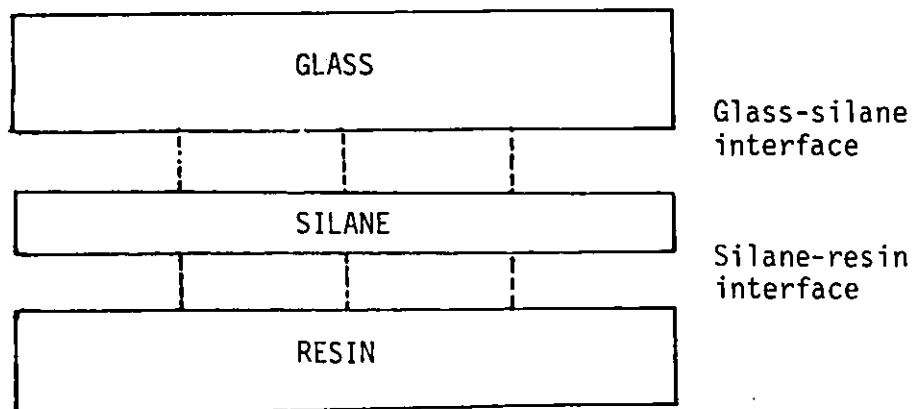
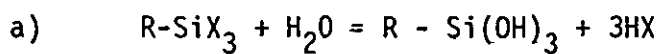
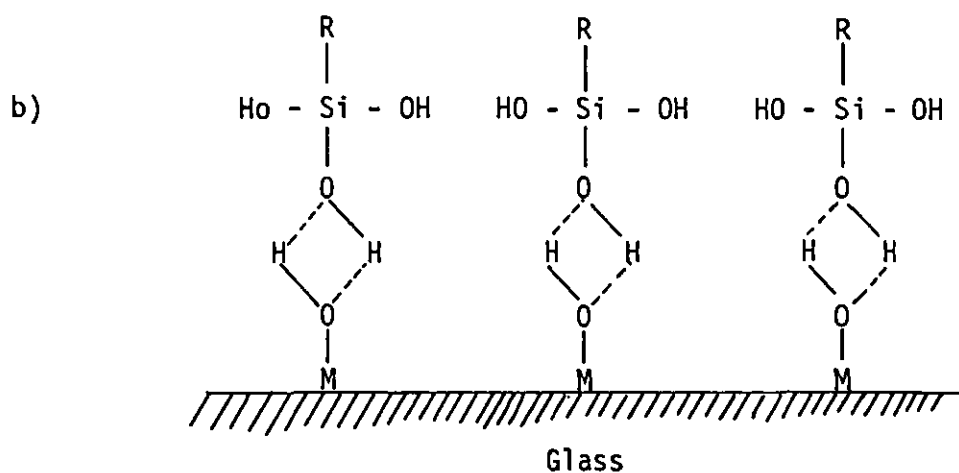


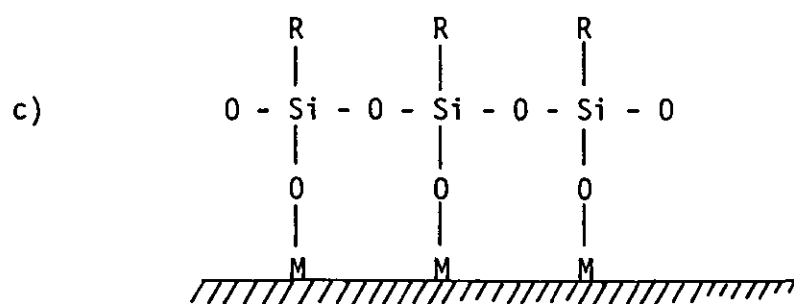
FIGURE 27: Function of Coupling Agent



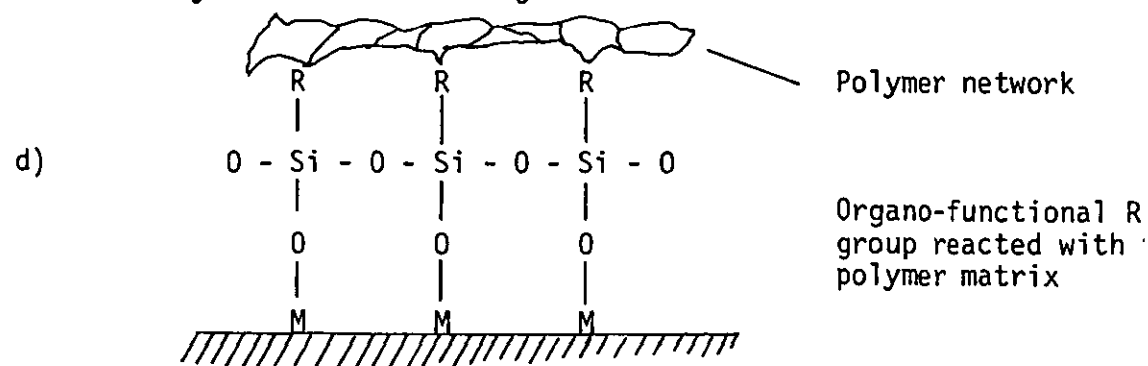
Hydrolysis of Organo-silane to corresponding silanol

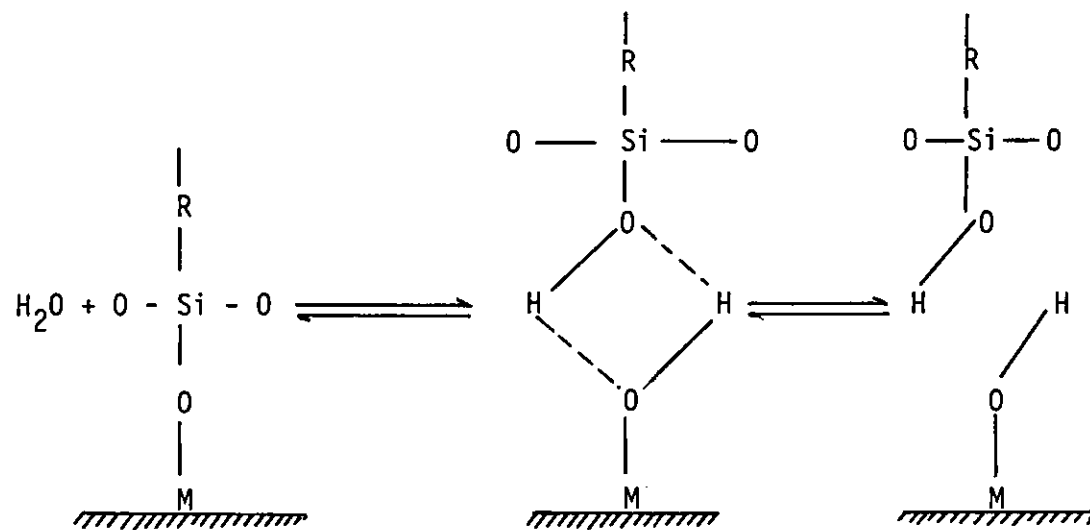


Hydrogen bonding between hydroxyl groups of silanol and glass surface.

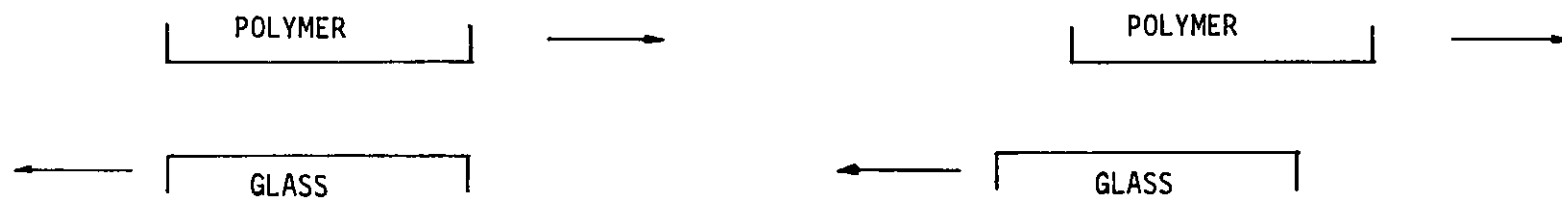


Polysiloxane bonded to glass surface





(a) Mechanisms of reversible bond formation associated with hydrolysis as proposed by Plueddemann³⁵



(b) Shear displacements without permanent damage of the interface bond

FIGURE 28

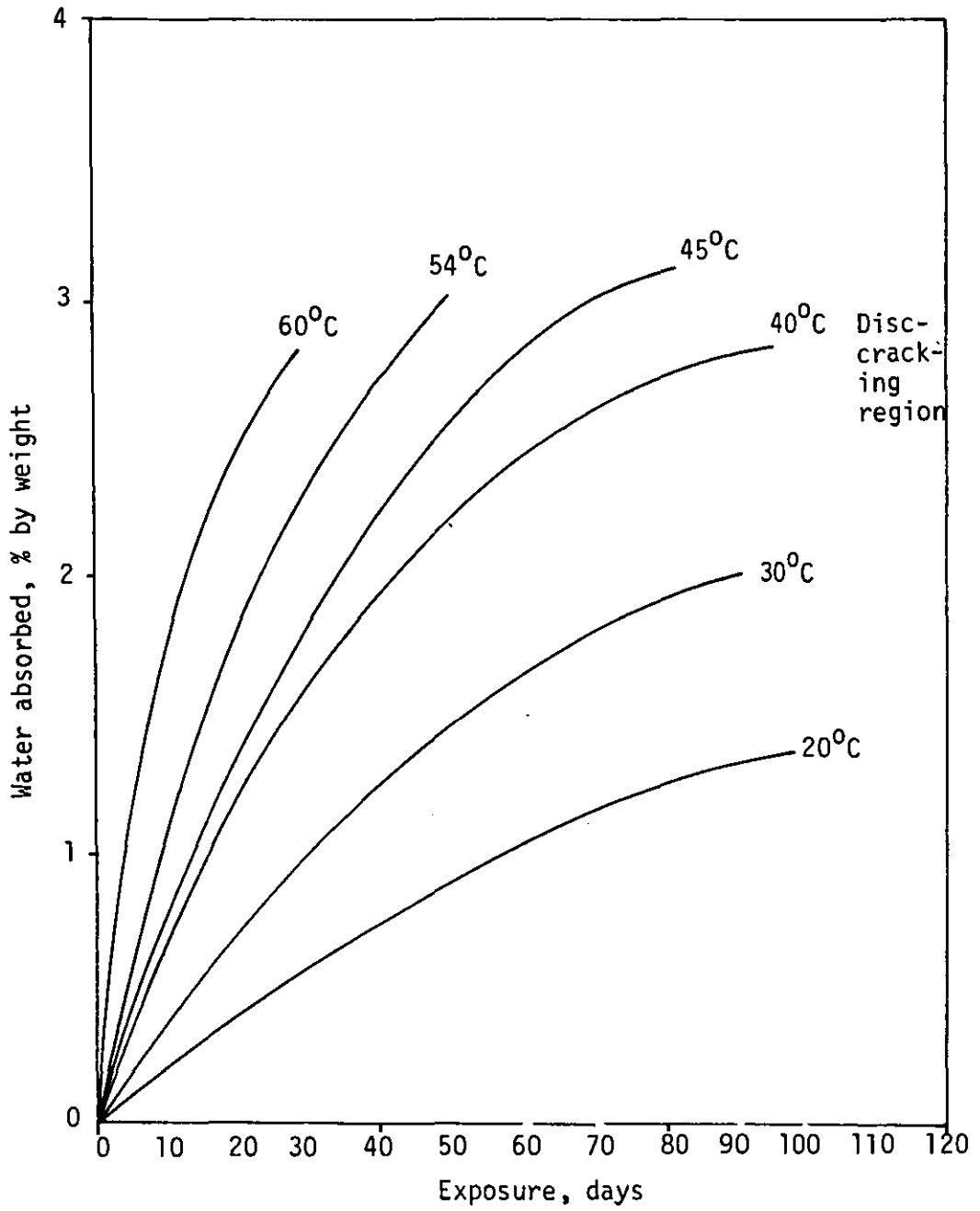


FIGURE 29: Rate of Disc Crack Initiation in Polyester Casting as Function of Water Temperature
(After Ref 91)

FIGURE 30: High Temperature Compression Strength at Dry and Wet 0° CFRP Laminates

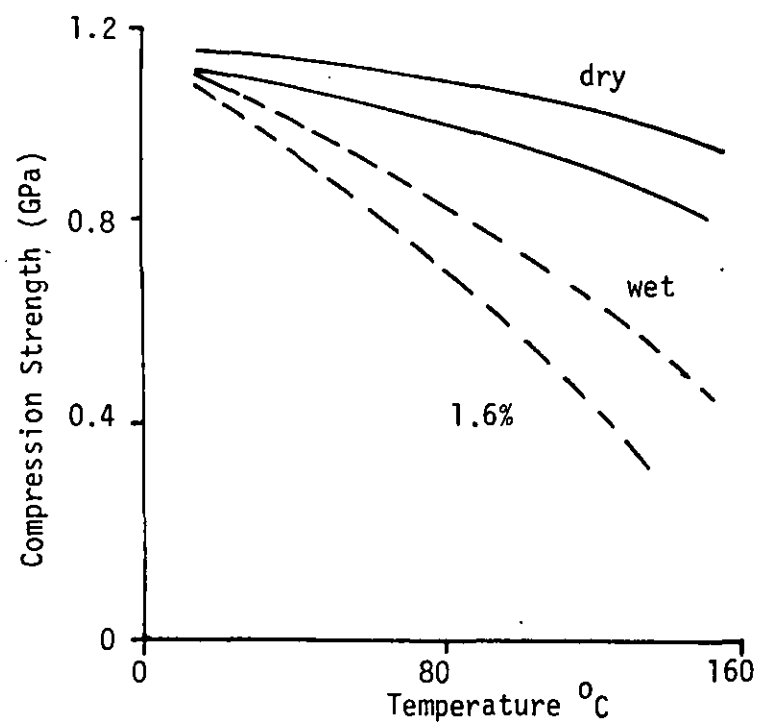
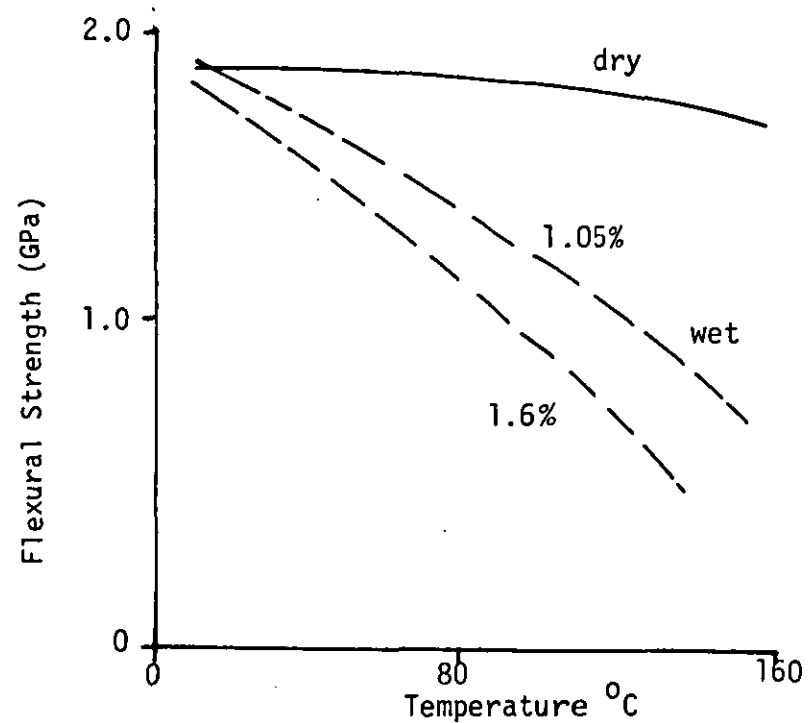


FIGURE 31: High Temperature Flexural Strength of Dry and Wet 0° CFRP Laminates



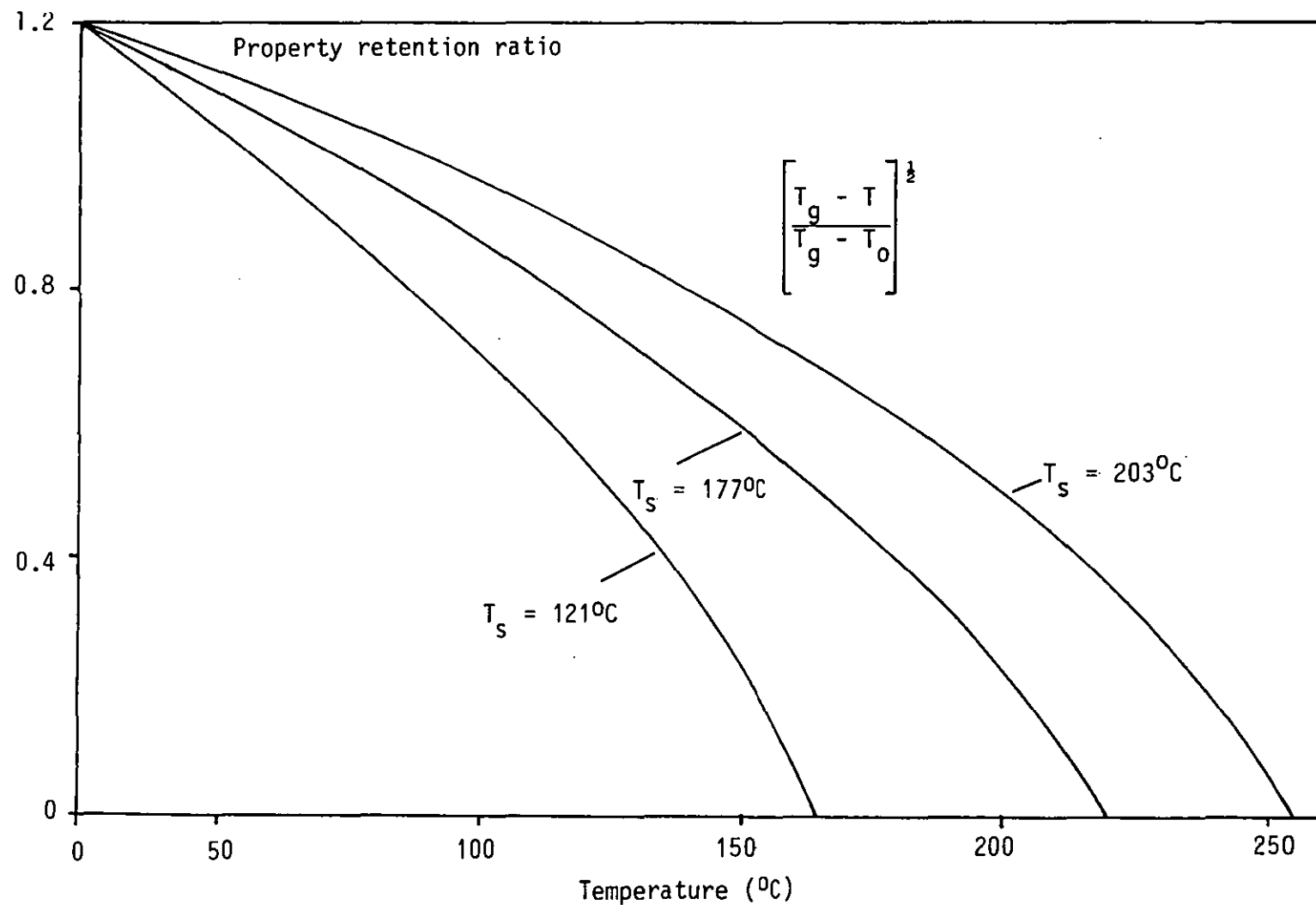


FIGURE 32: Generalised effect of temperature and T_g on matrix-dominated properties of composite (After chamis et al)¹¹⁰

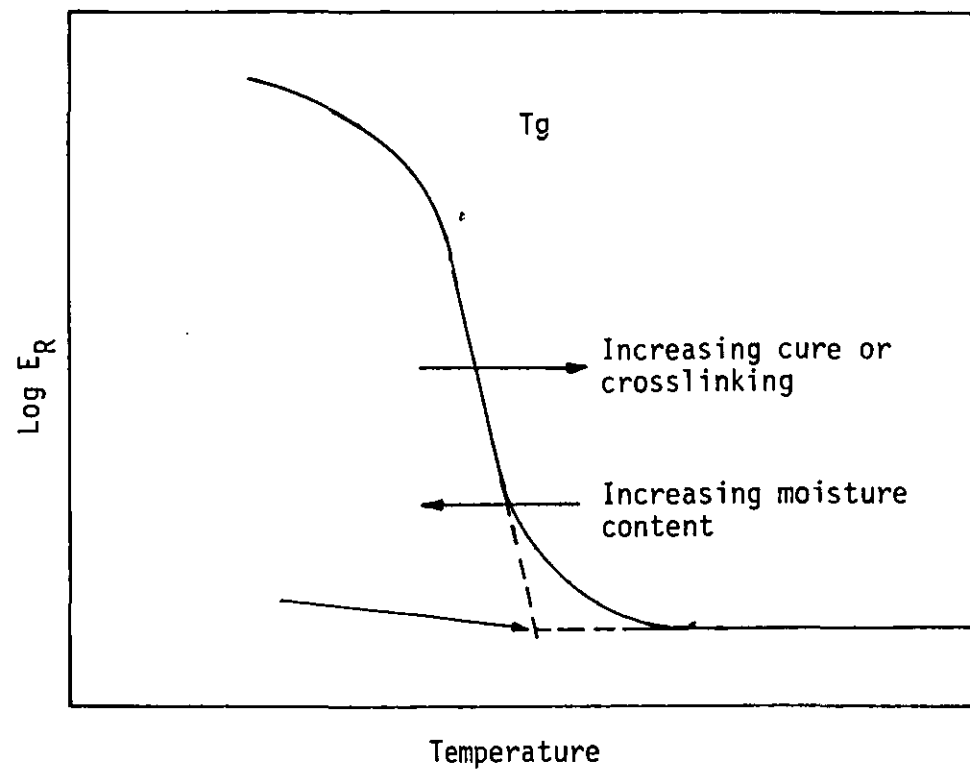


FIGURE 33: Modulus, E_R , Versus Temperature for Typical Epoxy Resin Illustrating Glass Transition Temperature⁸⁶

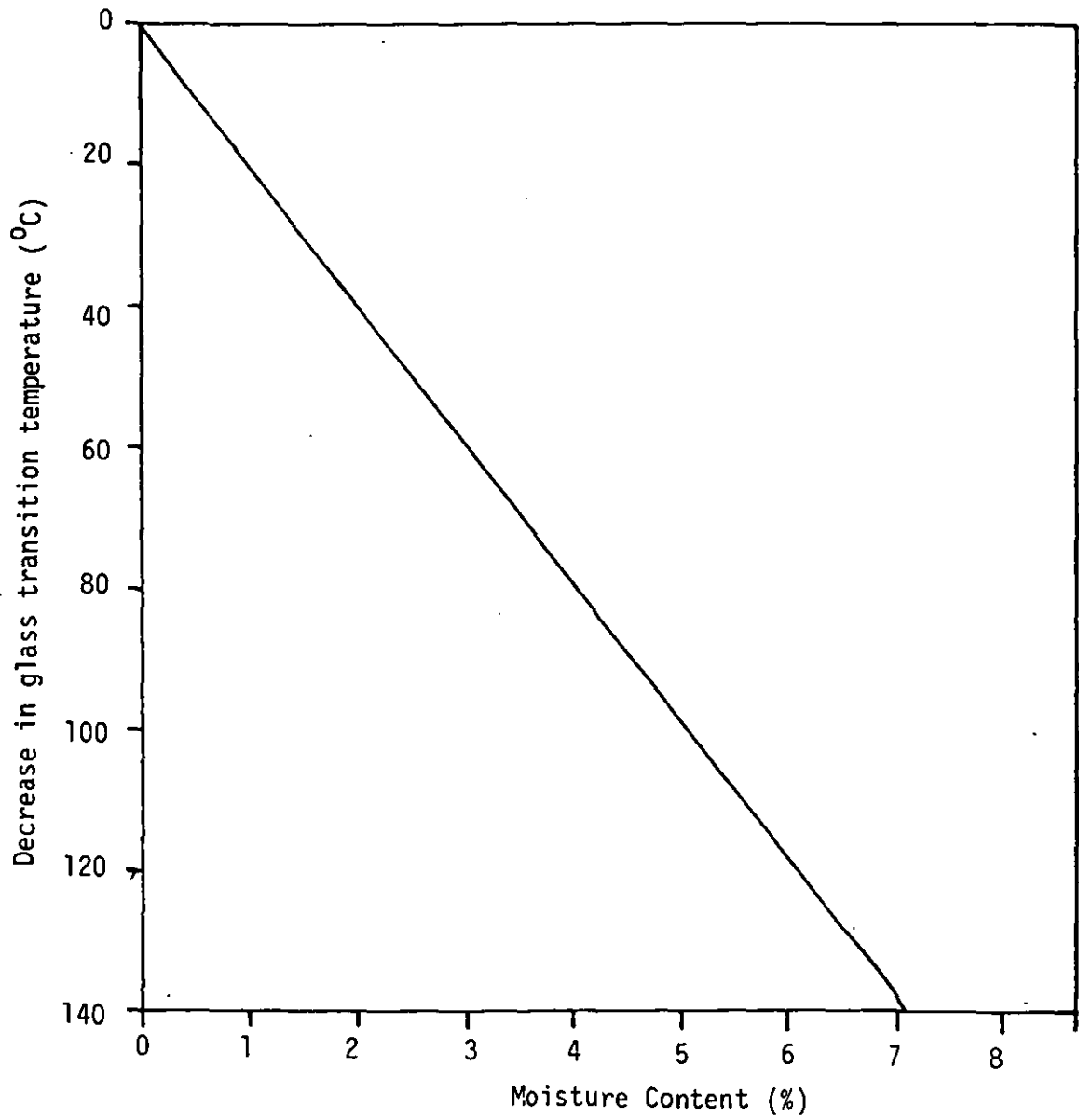


FIGURE 34: Decrease in T_g of Epoxy Resin with Moisture Absorption for Epoxy Resins

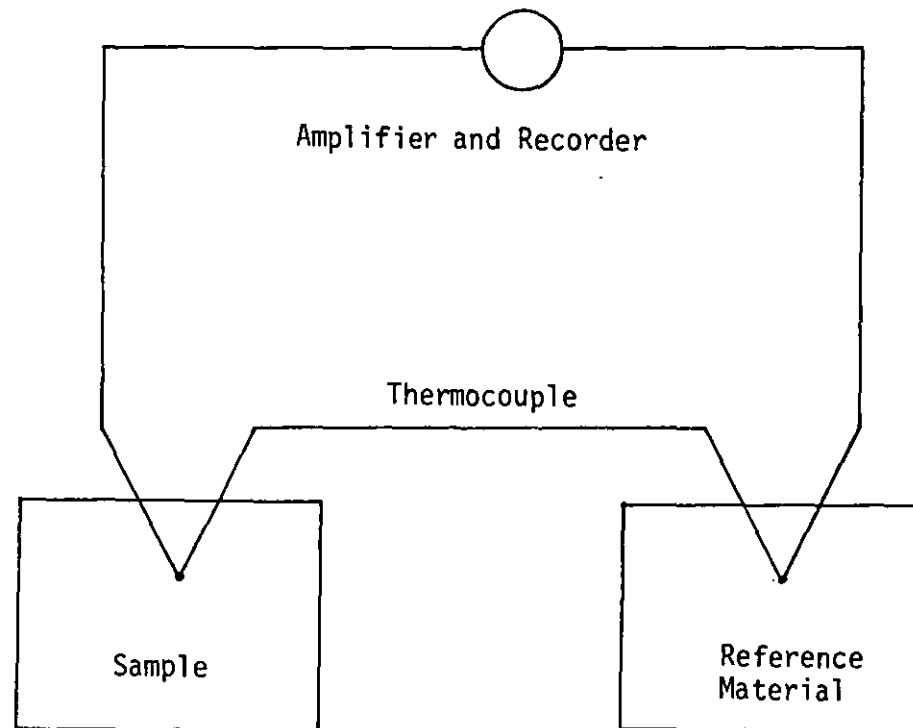


FIGURE 35: Basic DTA Circuit

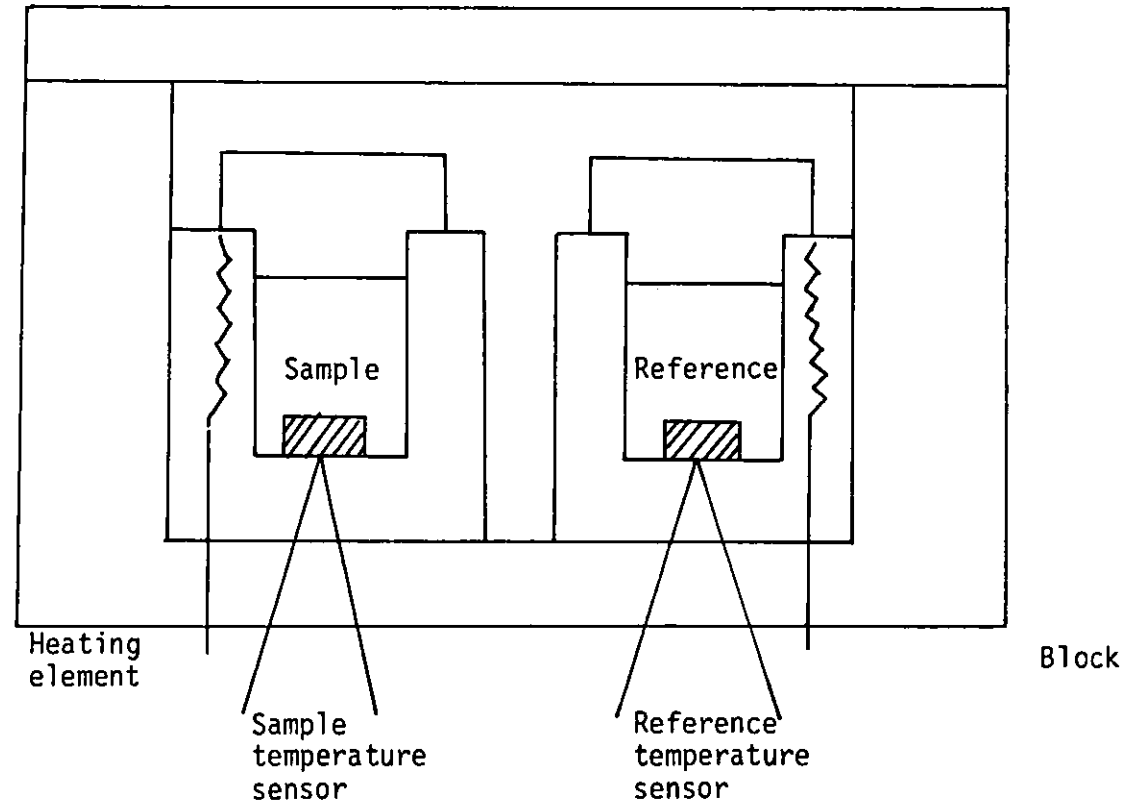


FIGURE 36: Essential Elements of DSC Cell

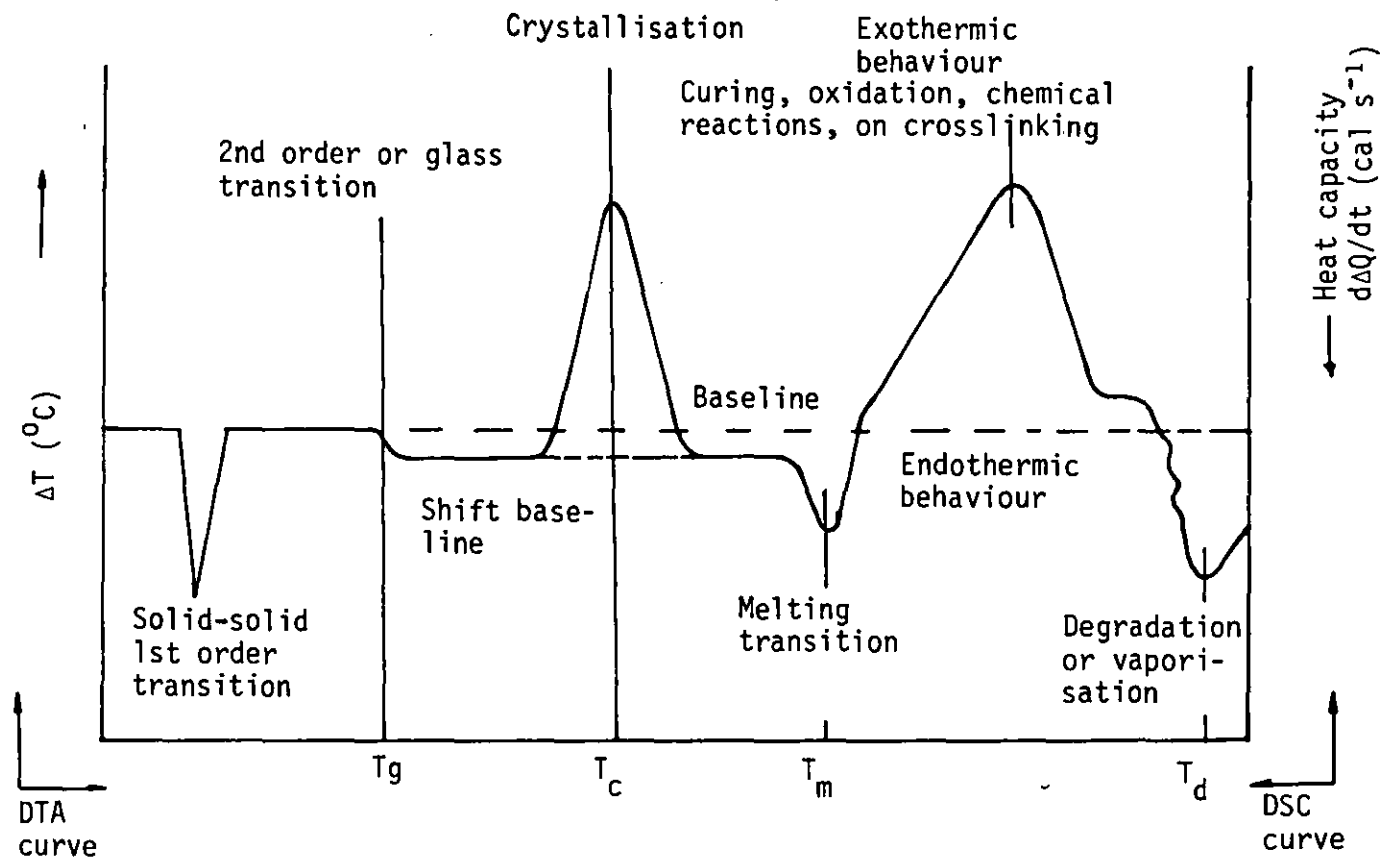


FIGURE 37: Schematic DTA or DSC Curve

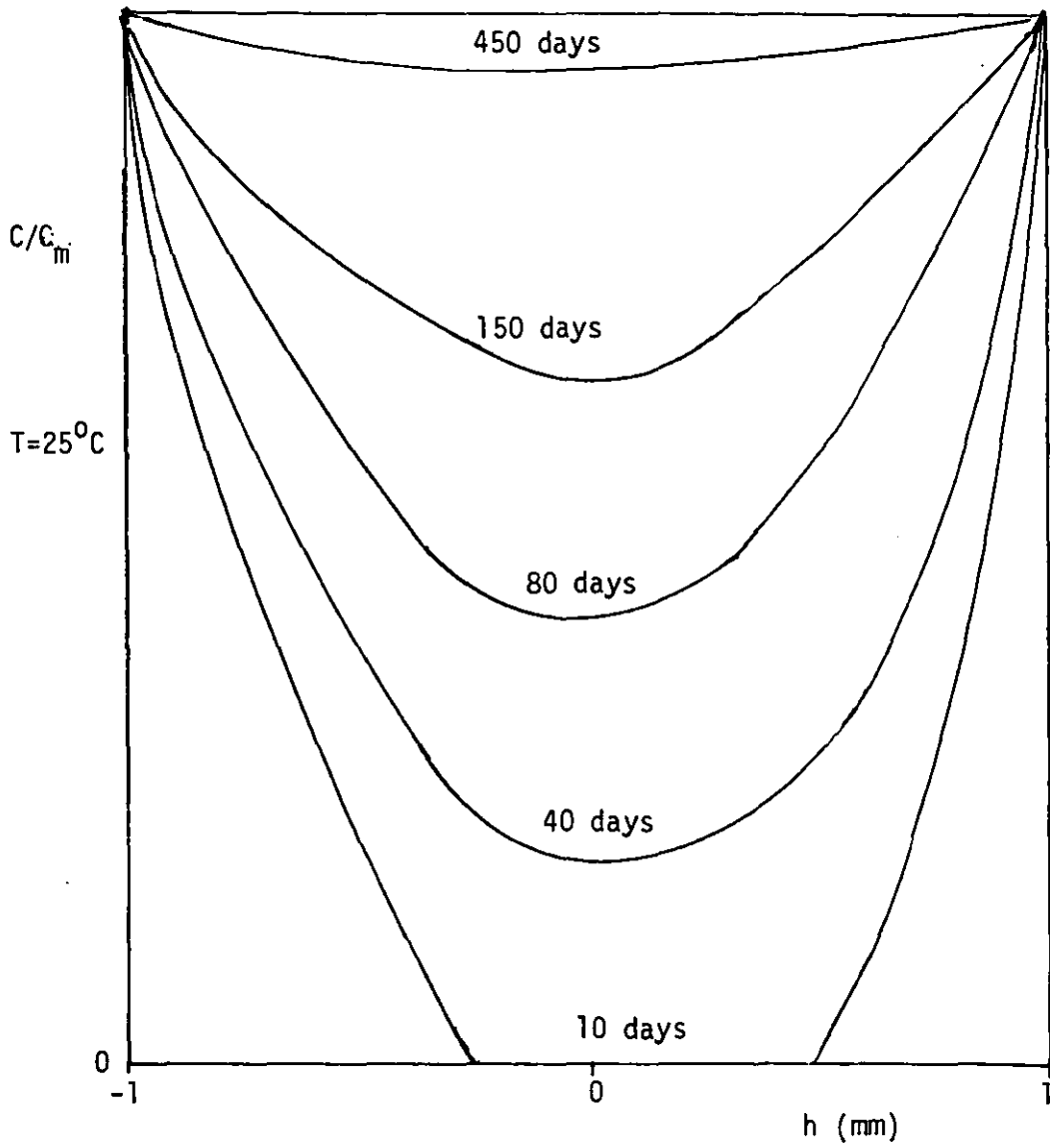


FIGURE 38: Absorbed Water Profiles Across the Thickness of a Composite Plate at Different Times After Exposure to Humid Conditions and Assuming Simple Diffusion. C and C_m are the Water Concentration and Maximum Concentration at Saturation in Composite; h = thickness⁵

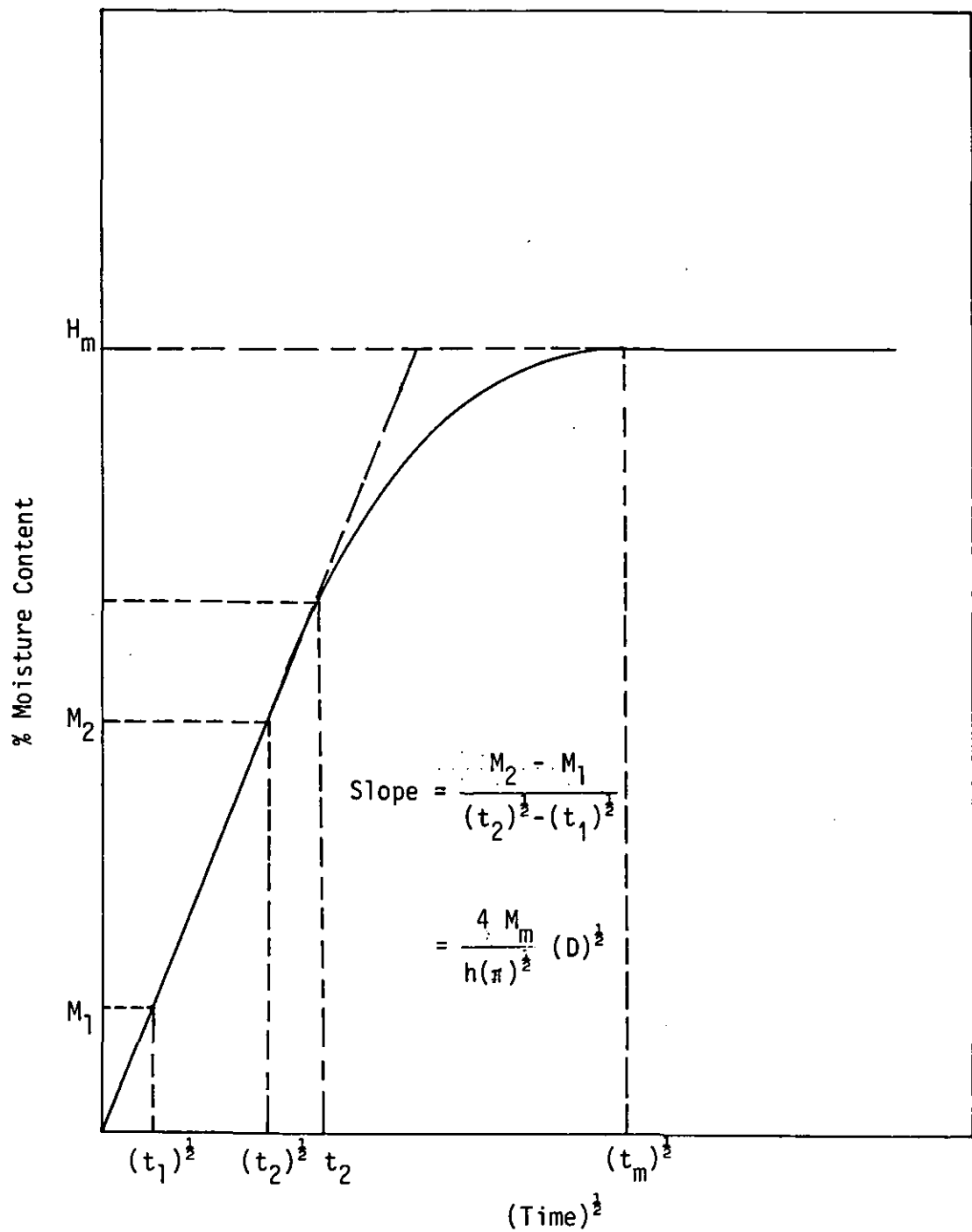


FIGURE 39: Illustration of the change of moisture content with the square root of time. For $t < t_2$ the slope is constant⁴

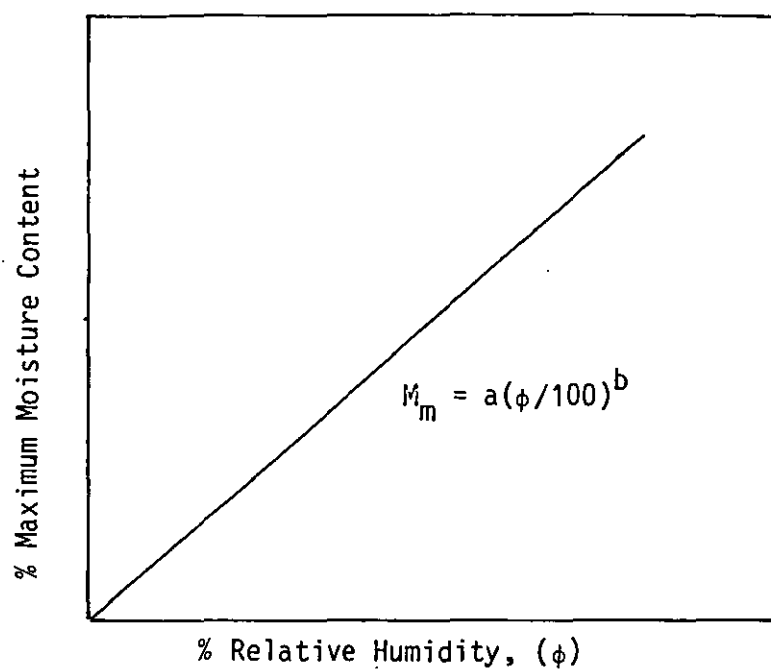


FIGURE 40: Maximum moisture content as a function of relative humidity⁴

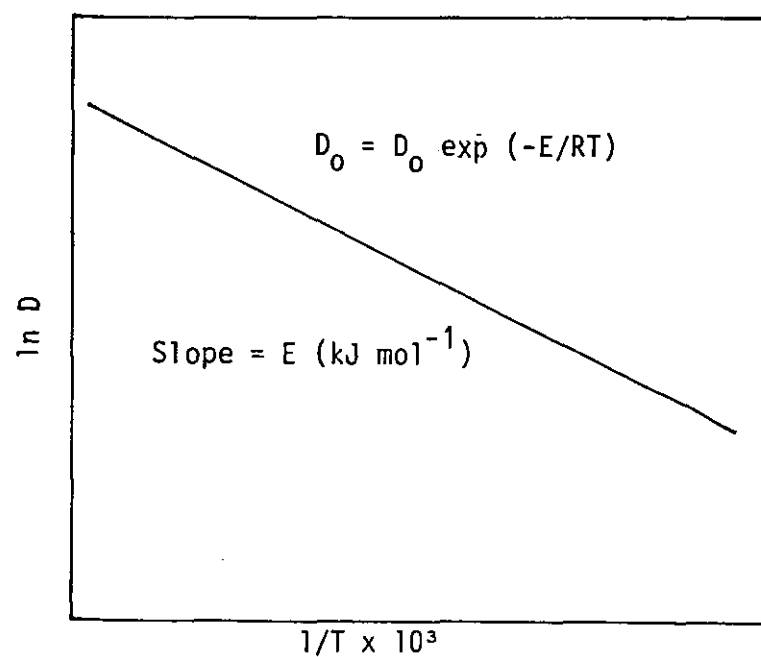


FIGURE 41: Relationship between diffusion coefficient and temperature

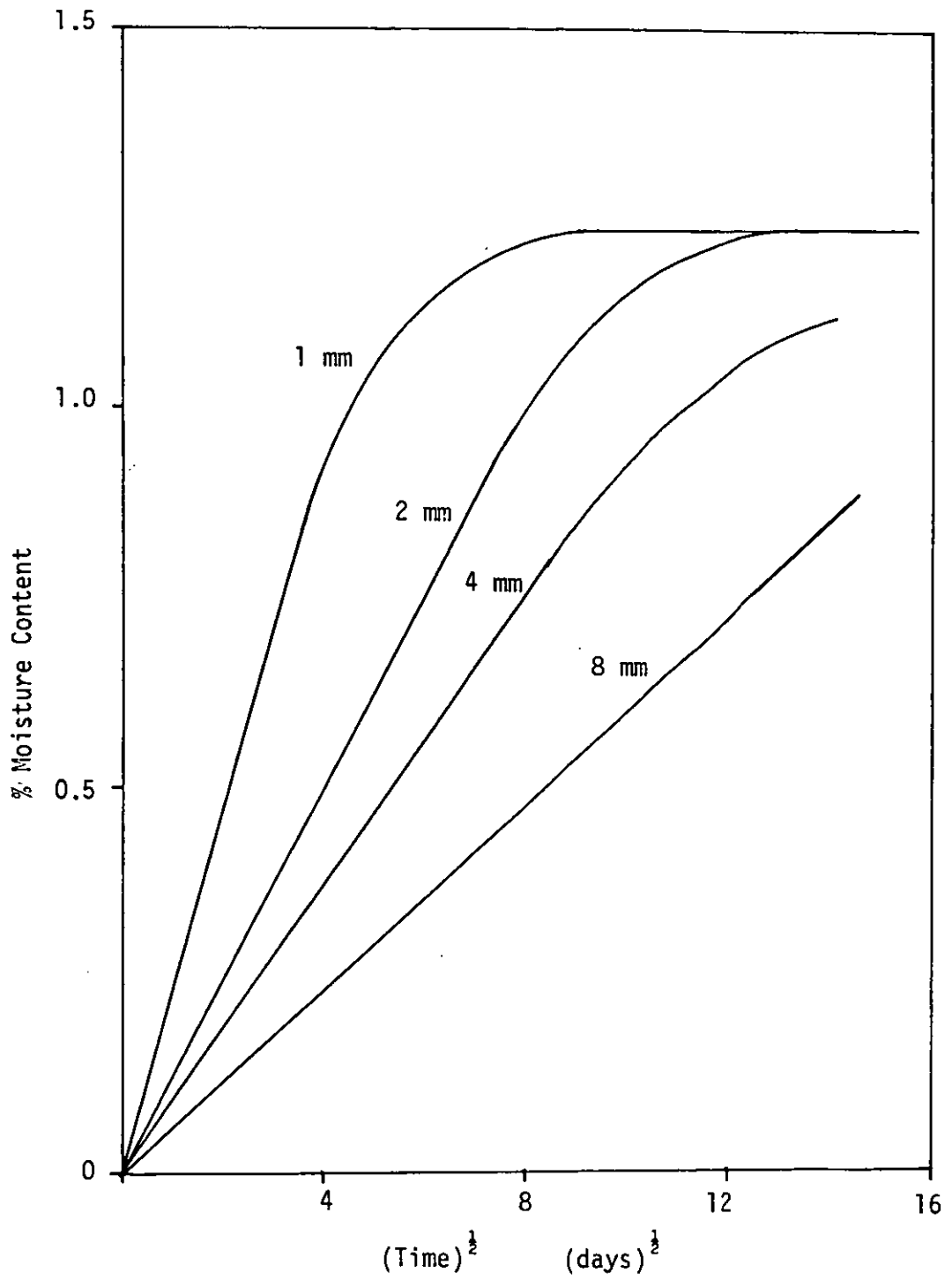


FIGURE 42: Moisture Uptake by CFRP Laminates of Different Thicknesses: 25°C: 100% RH³⁸

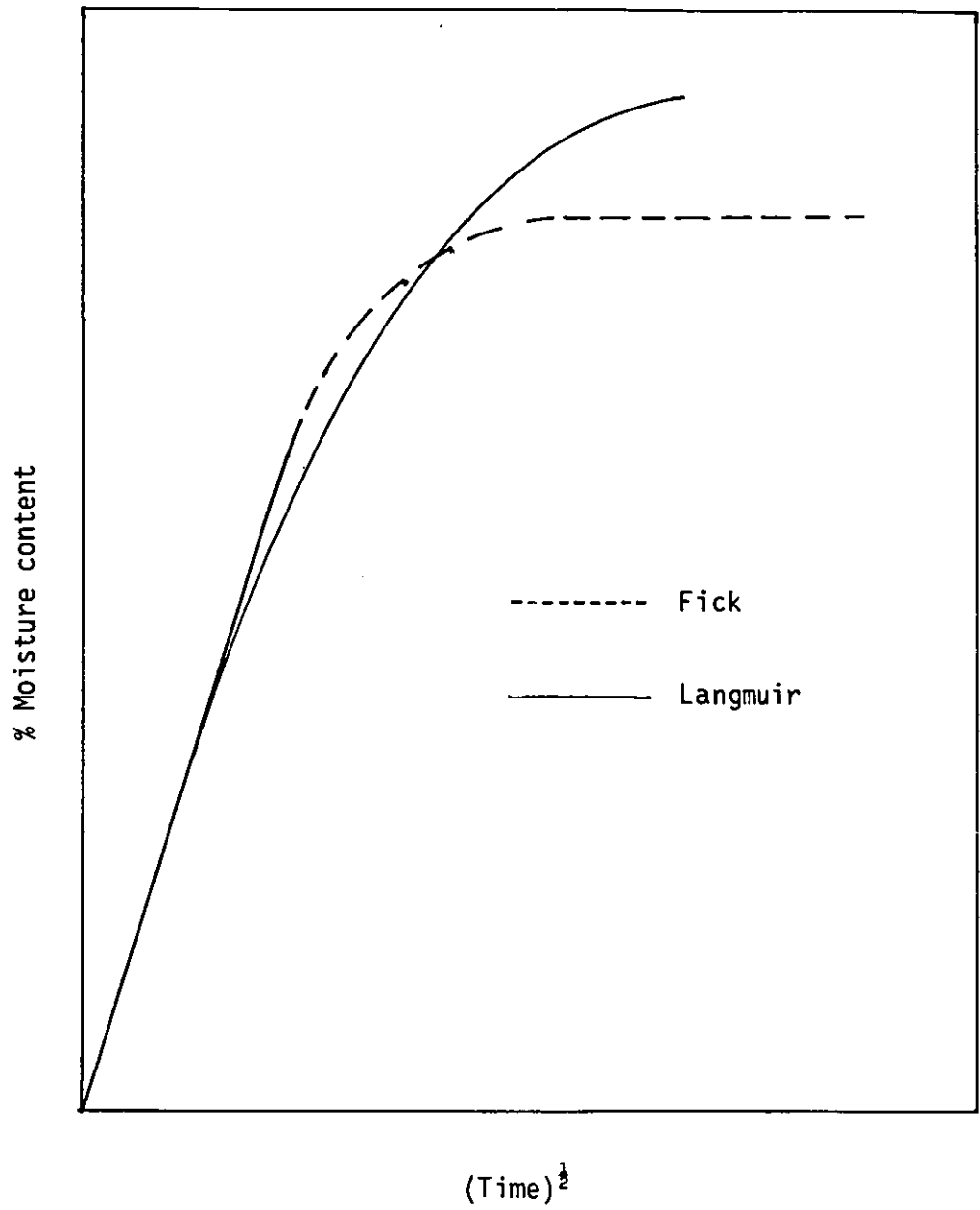


FIGURE 43: Comparison of Moisture Uptake for Classical Fickian Diffusion and Anomalous Langmuir Diffusion³⁸

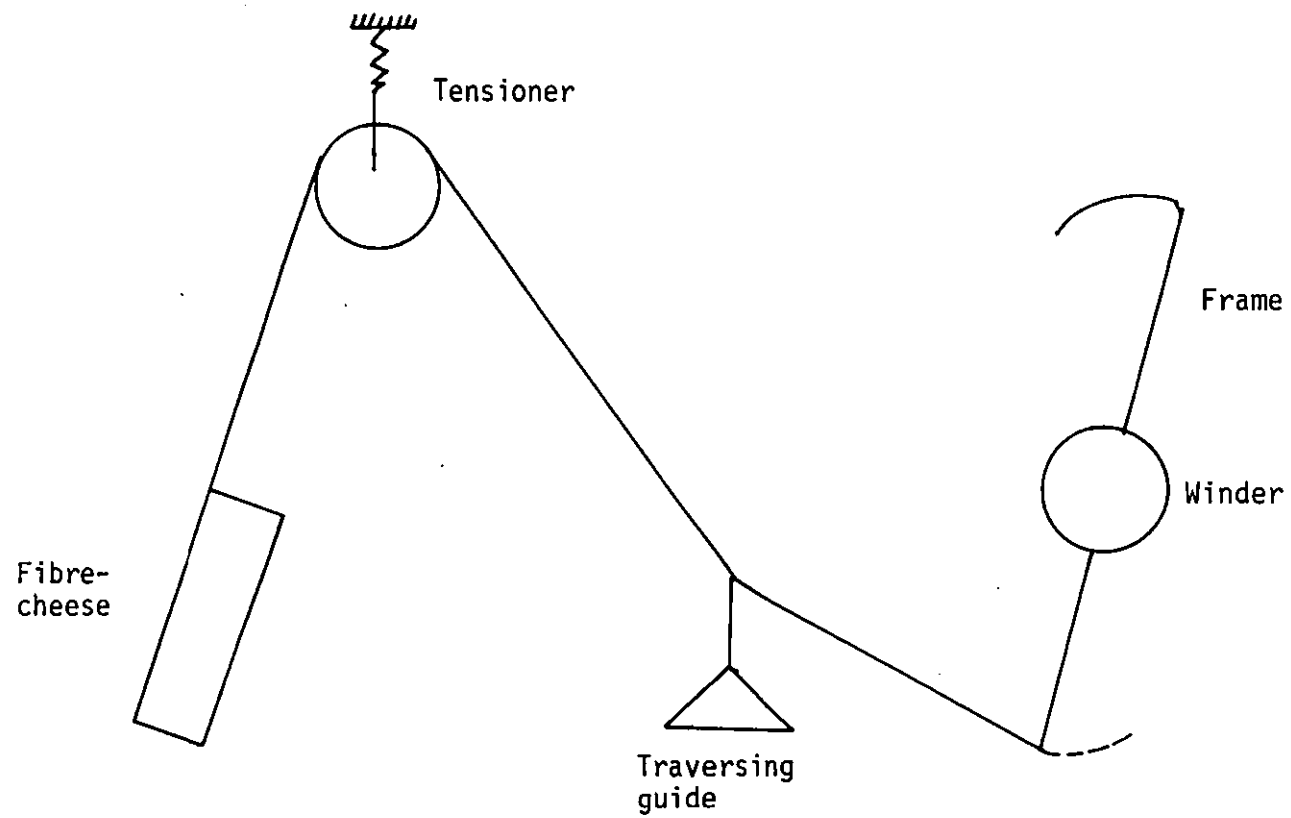


FIGURE 44a: Schematic Diagram of the Winding Machine

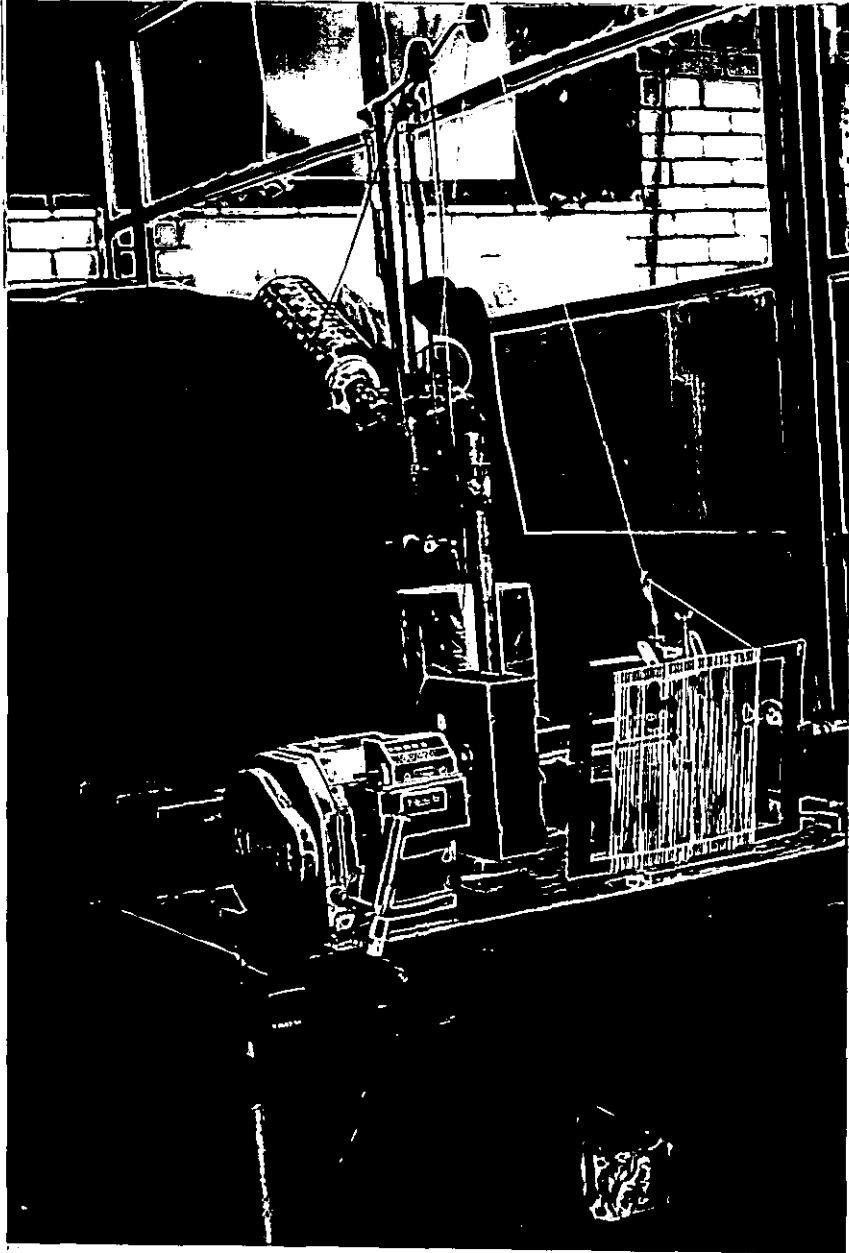


FIGURE 44b: Filament Winding Machine

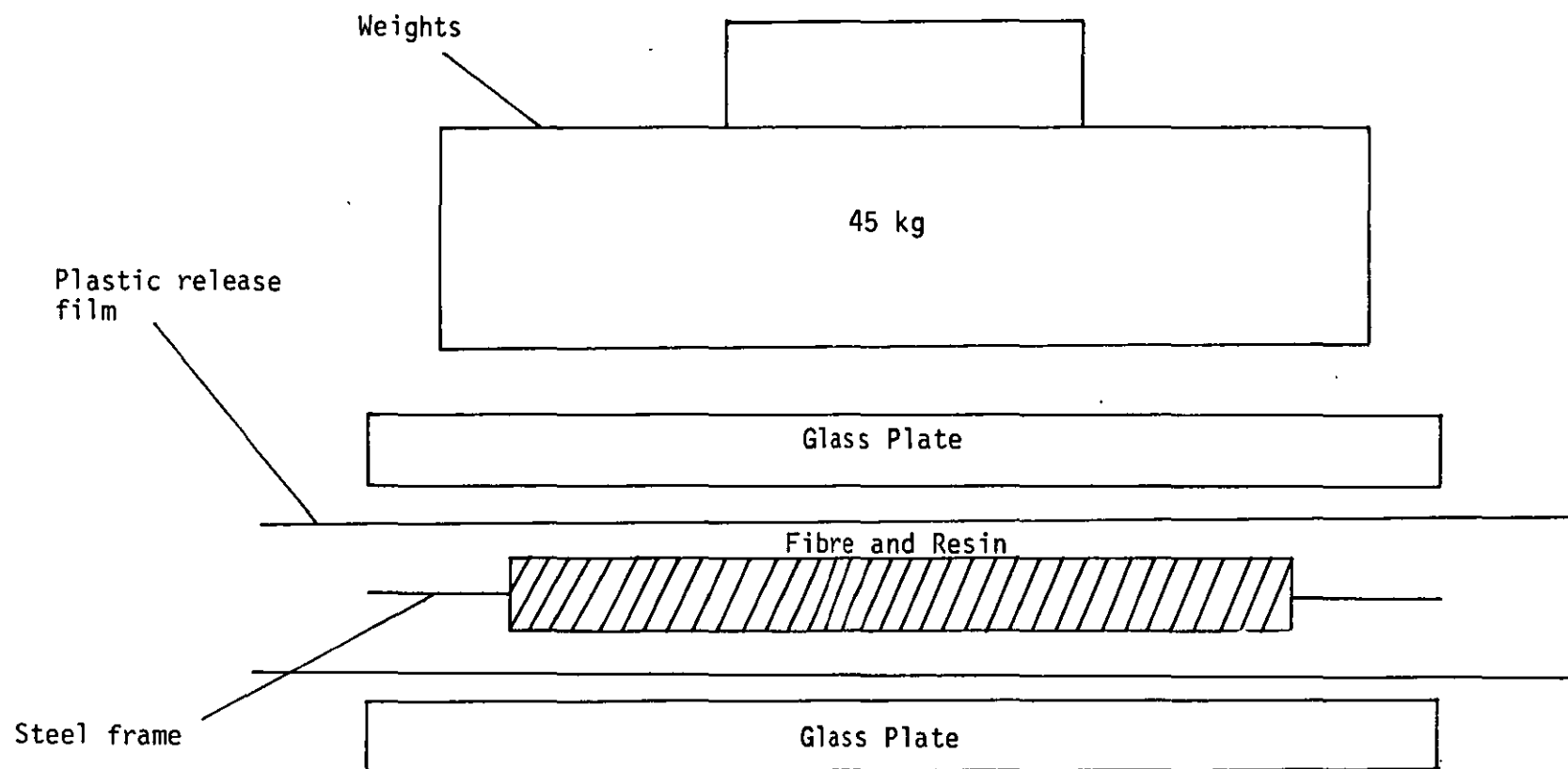
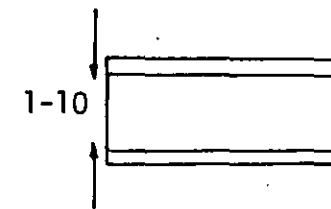
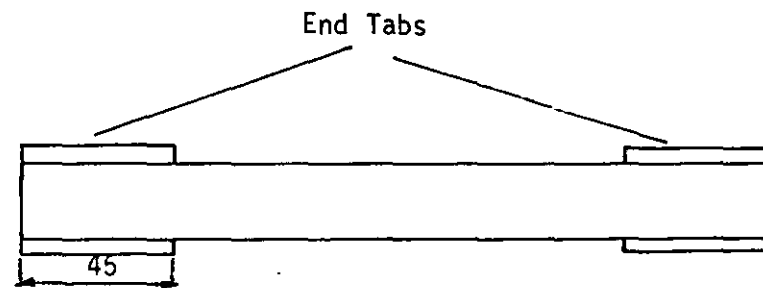
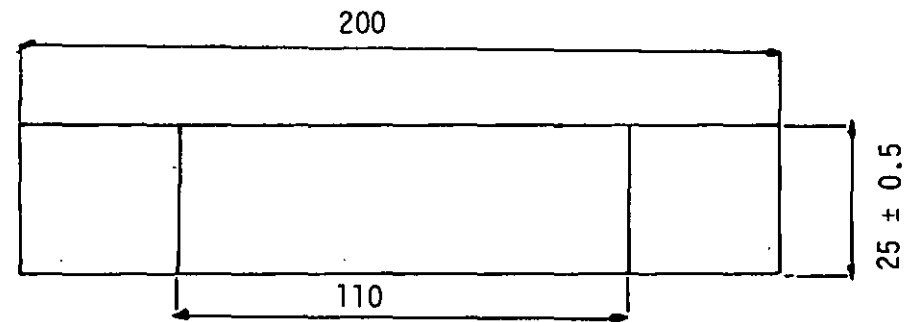


FIGURE 45: Arranging for Curing of Laminate



All dimensions in mm.

FIGURE 46: Tensile Test Piece. BS 2782 Part 3: Method 320E

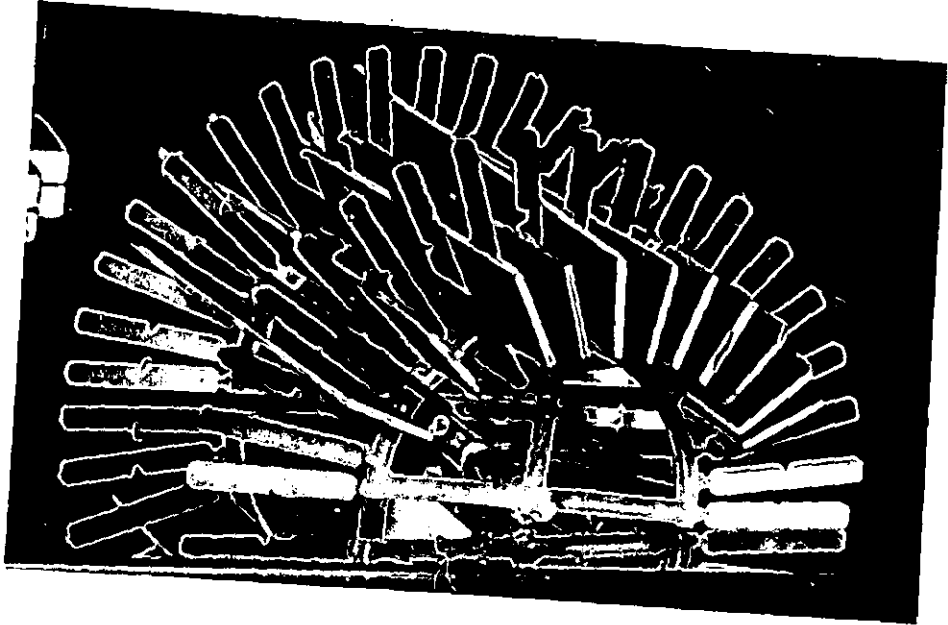


FIGURE 47: Specimen Holder

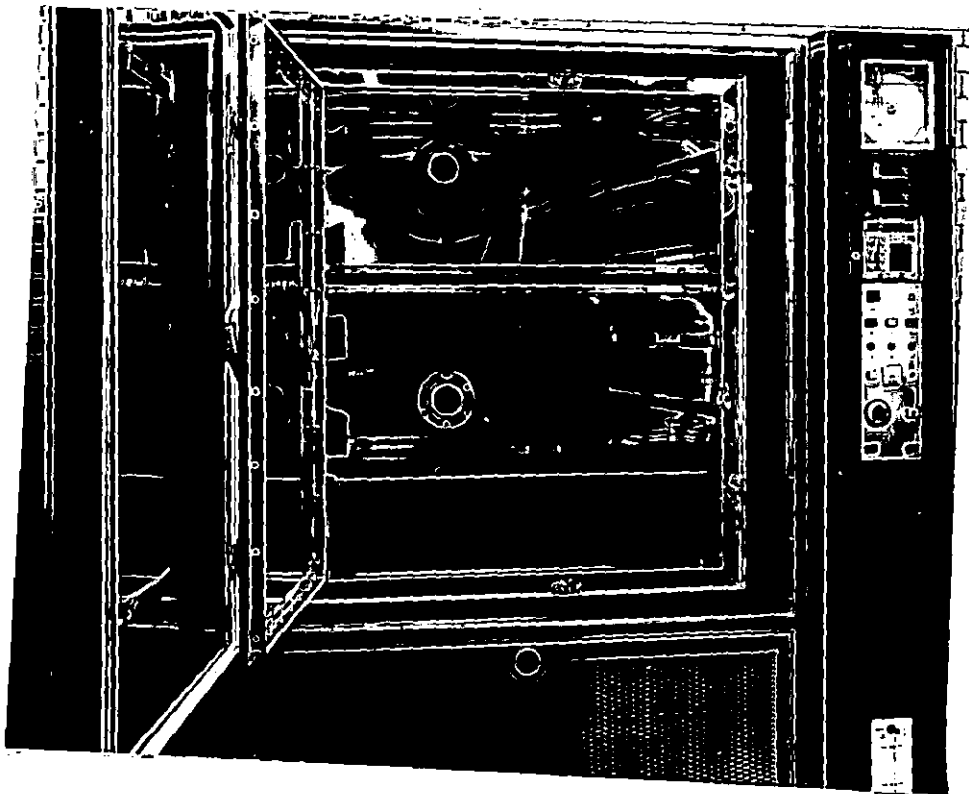


FIGURE 48: Environmental Cabinet

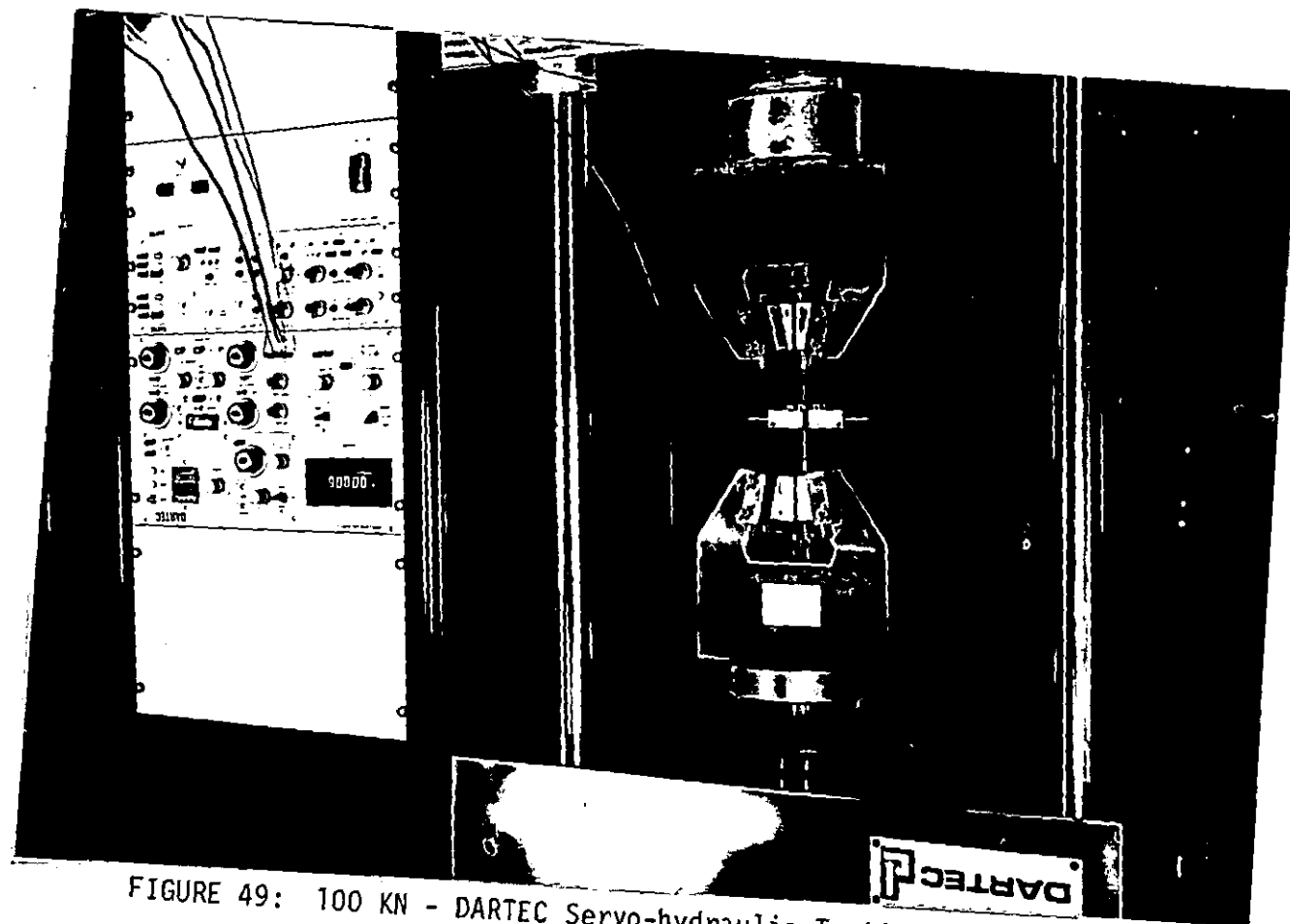


FIGURE 49: 100 KN - DARTEC Servo-hydraulic Testing Machine

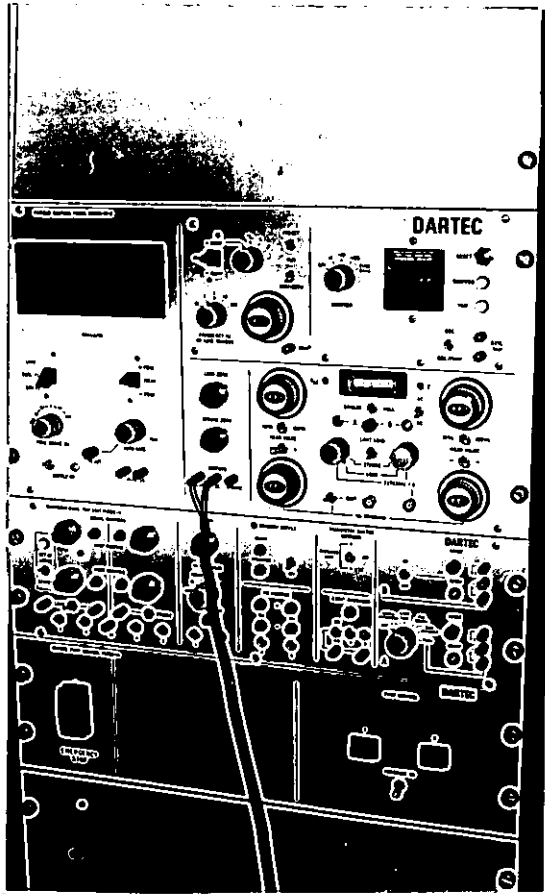


FIGURE 50: Control Panel of DARTEC Servo-hydraulic Testing Machine

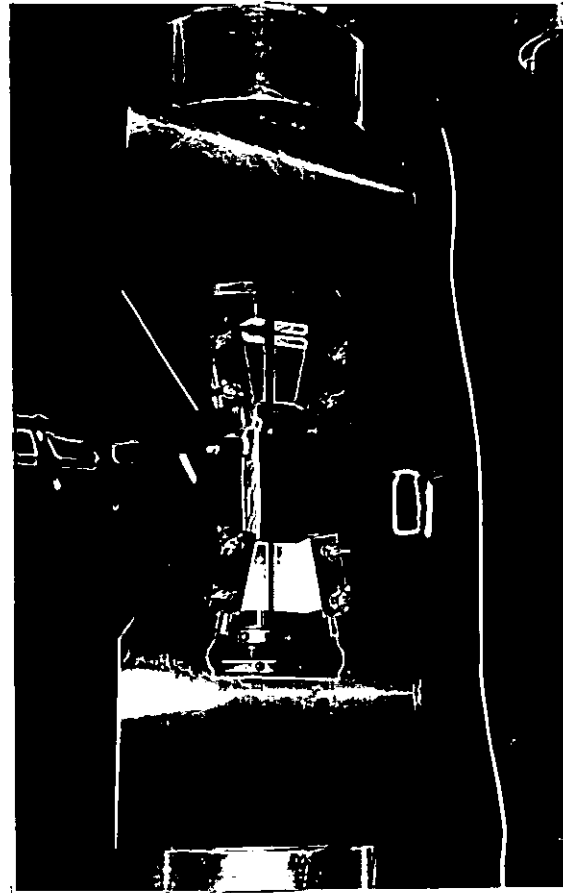


FIGURE 51: Grips of DARTEC Servo-hydraulic Testing Machine

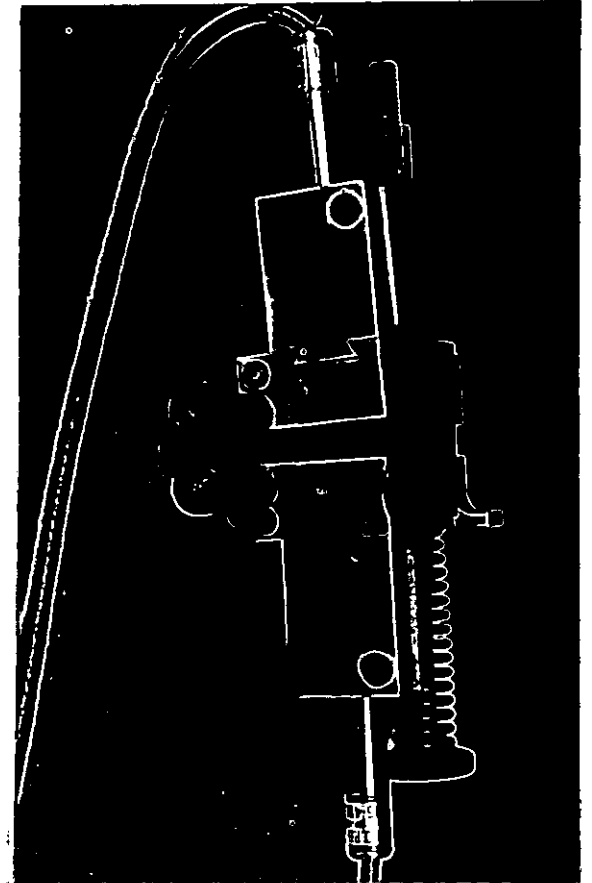


FIGURE 52: Extensometer

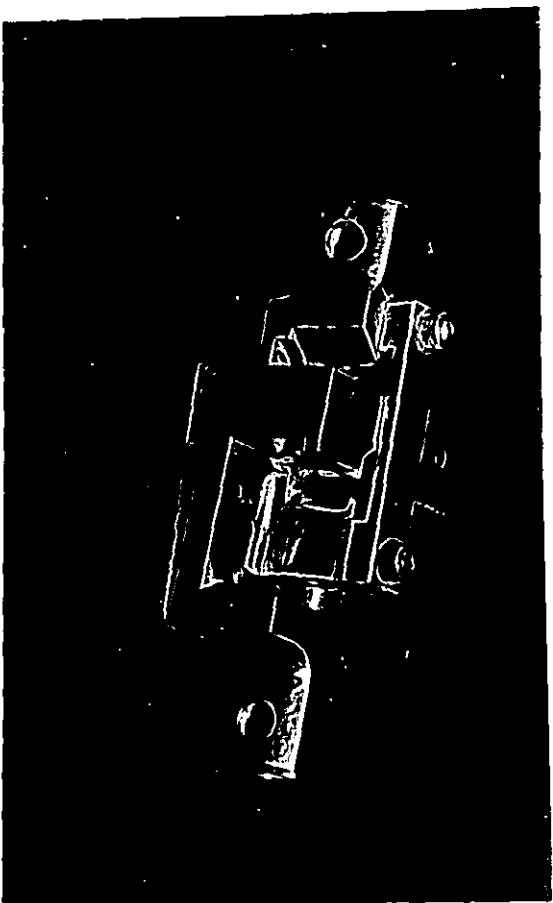


FIGURE 53: Three-Point Bending Rig

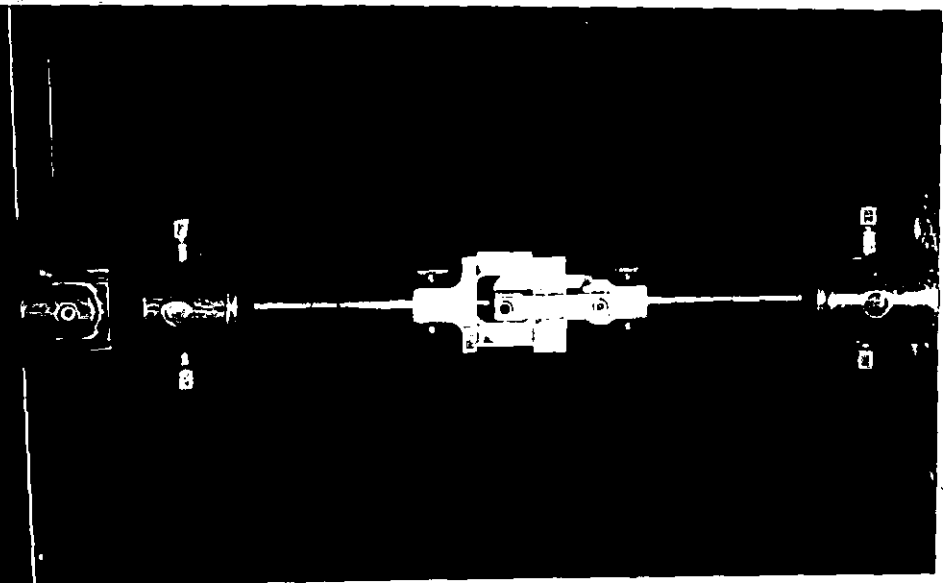


FIGURE 54: Experimental Set-Up for ILSS Testing

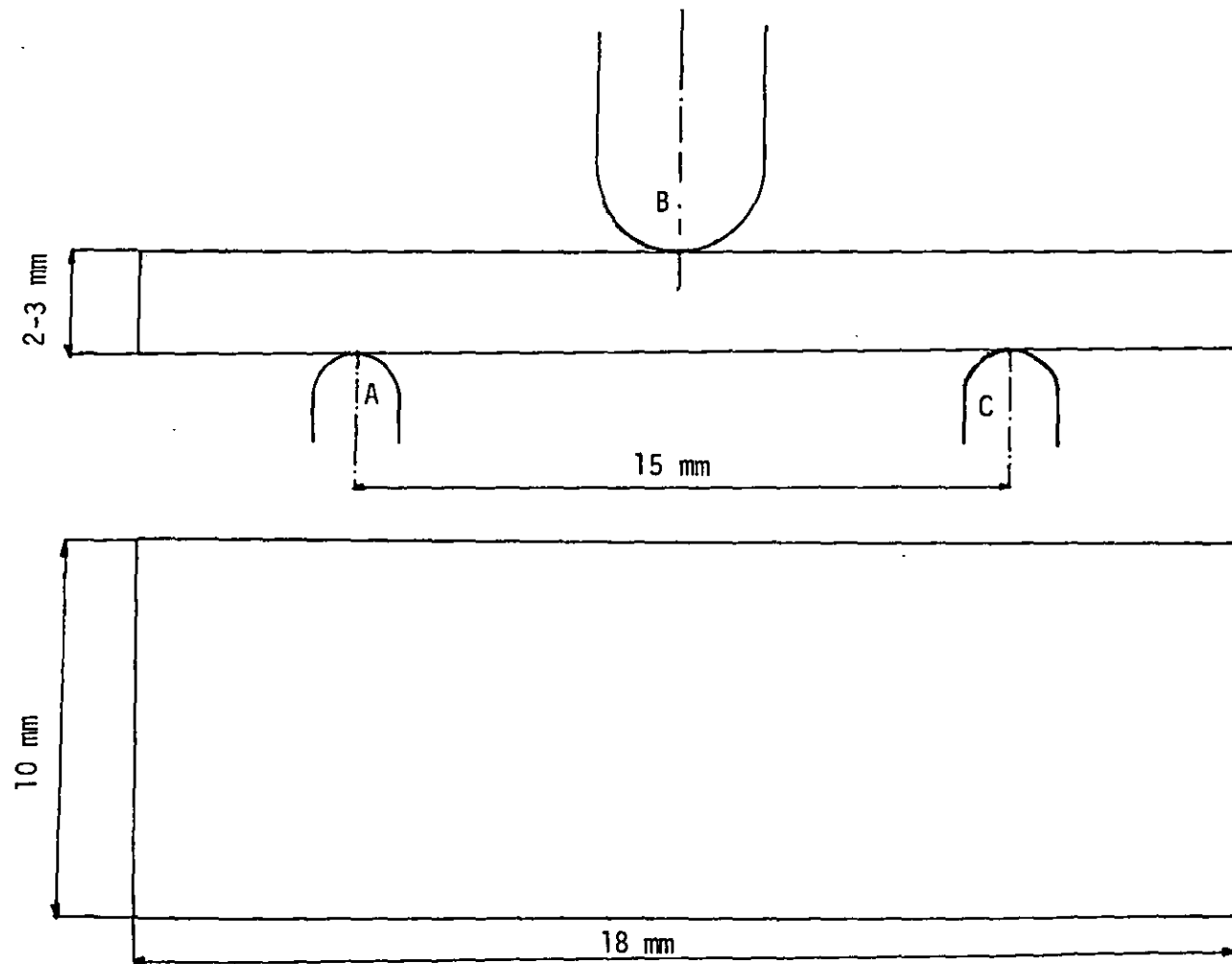


FIGURE 55: A Schematic Diagram of the Interlaminar Shear Test Rig

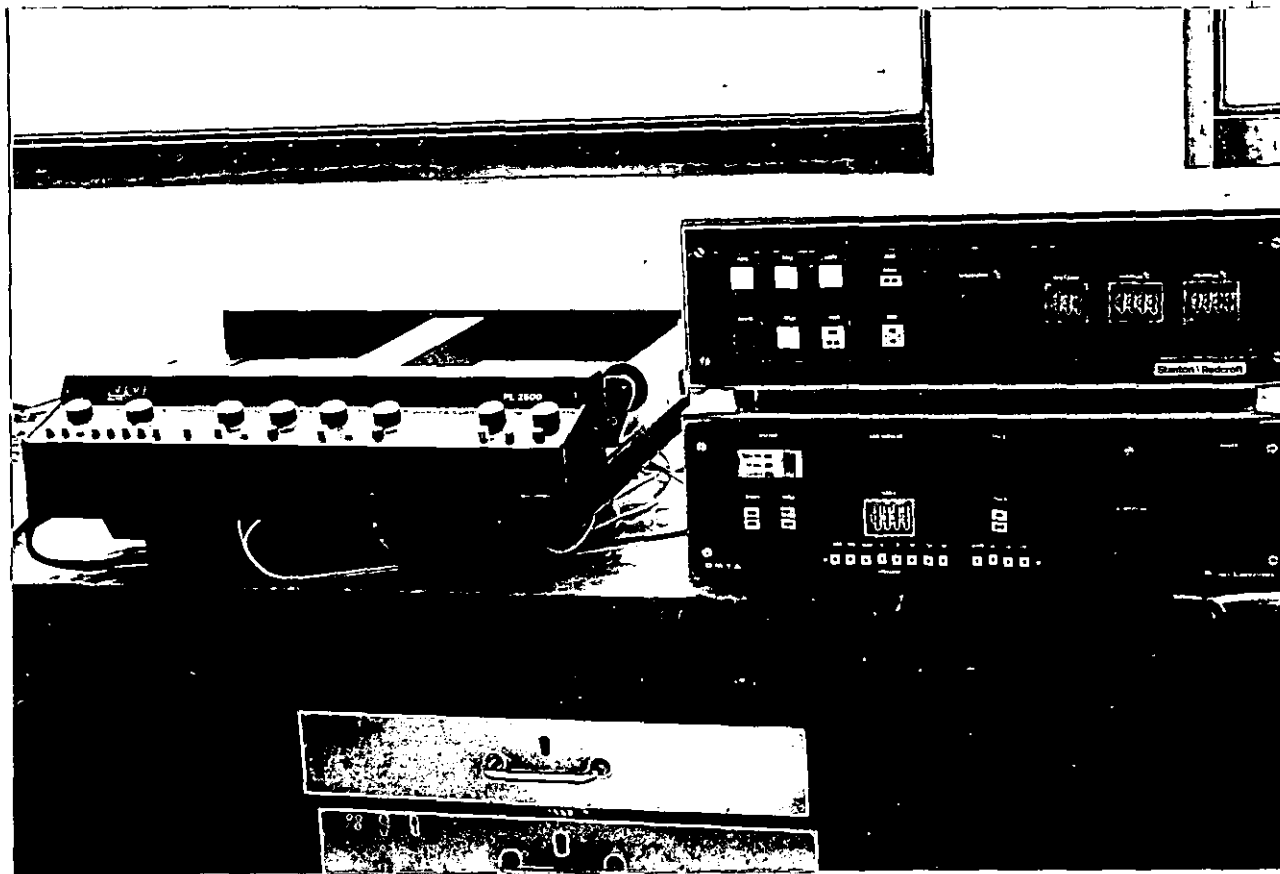


FIGURE 56: PL - Dynamic Mechanical Thermal Analyser

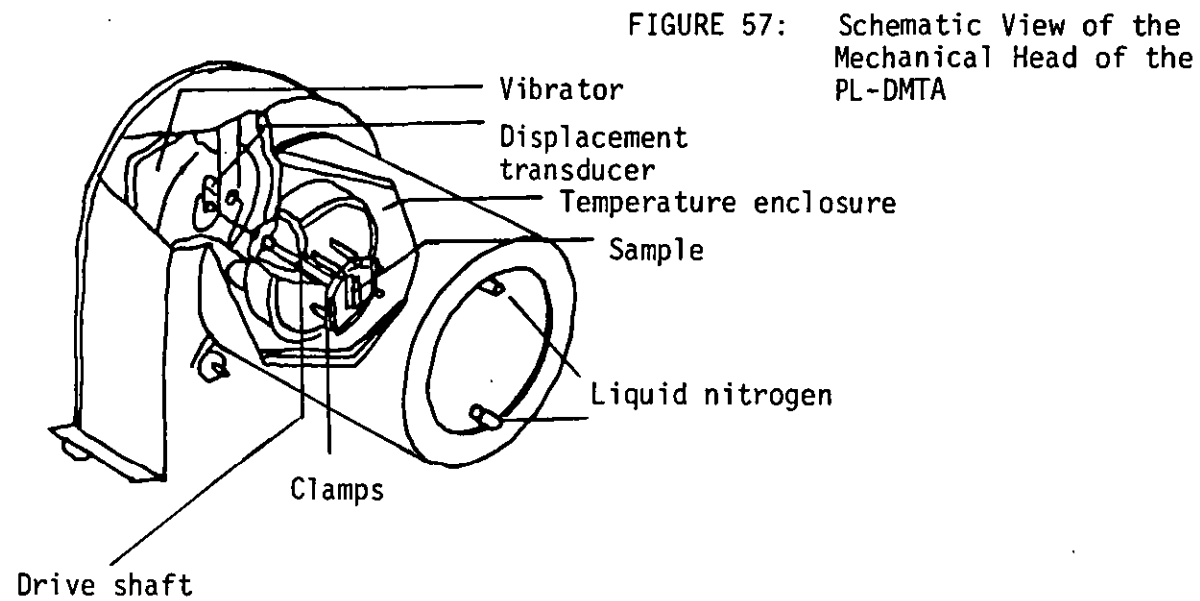
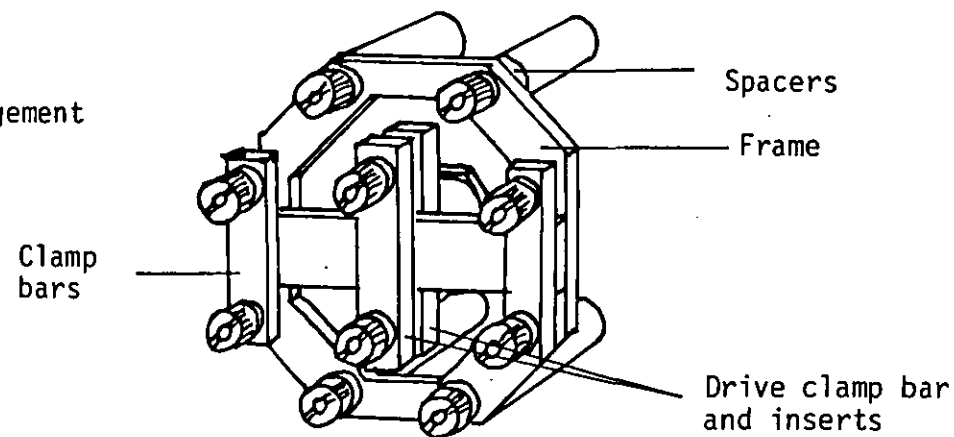


FIGURE 58: Clamping Arrangement



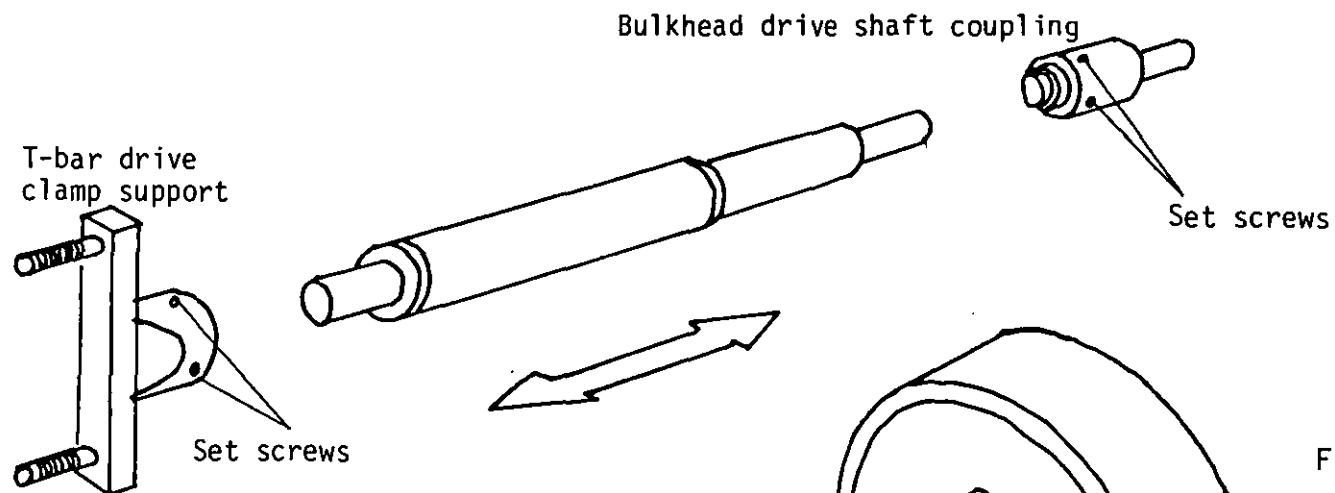


FIGURE 59: Drive Shaft Components

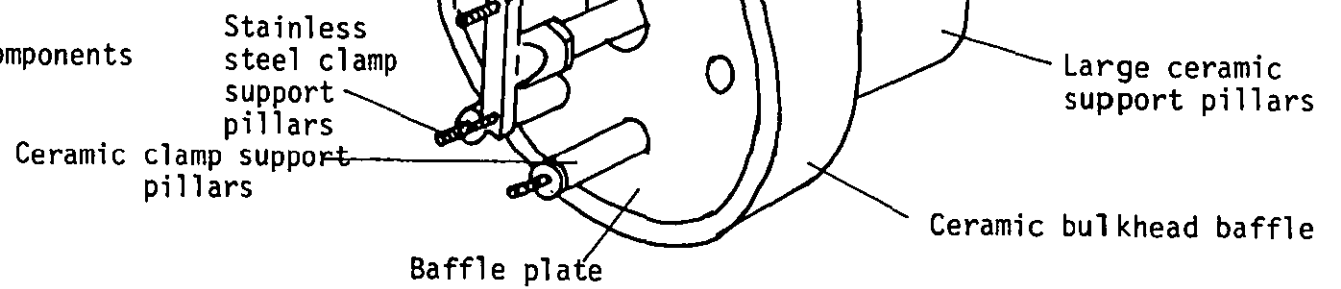


FIGURE 60: Clamping Frame Support

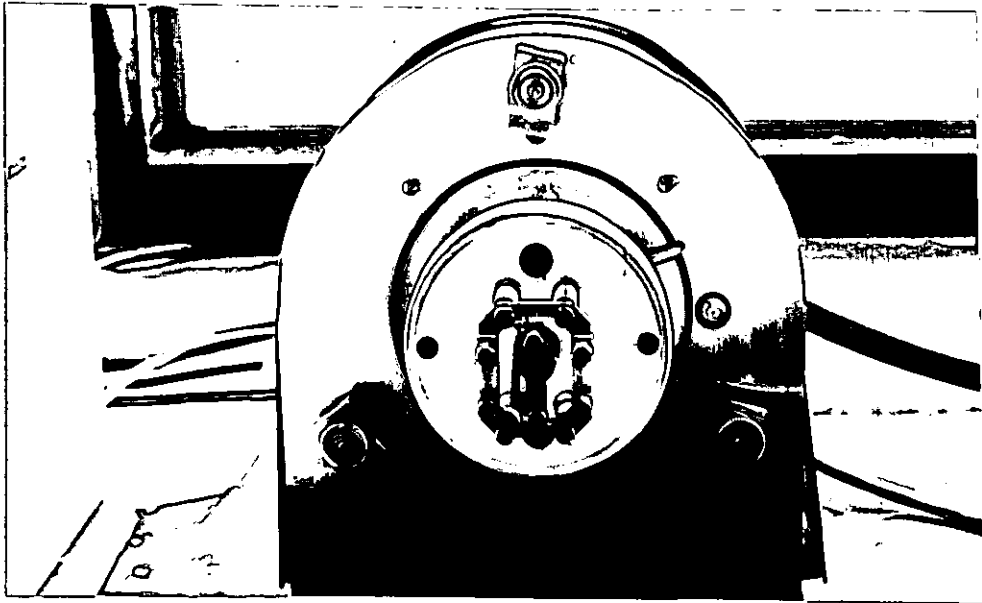


FIGURE 61: Mechanical Head

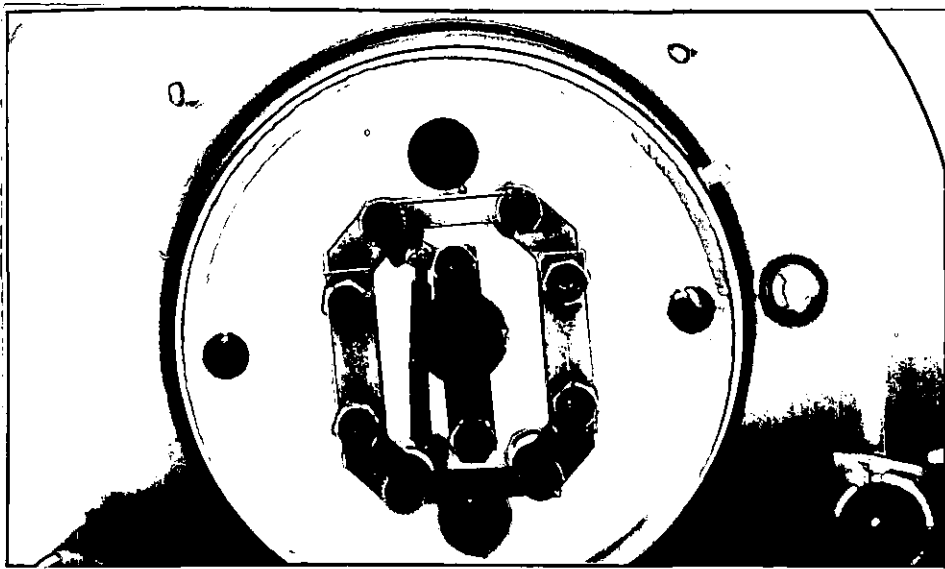


FIGURE 62: Specimen Holder

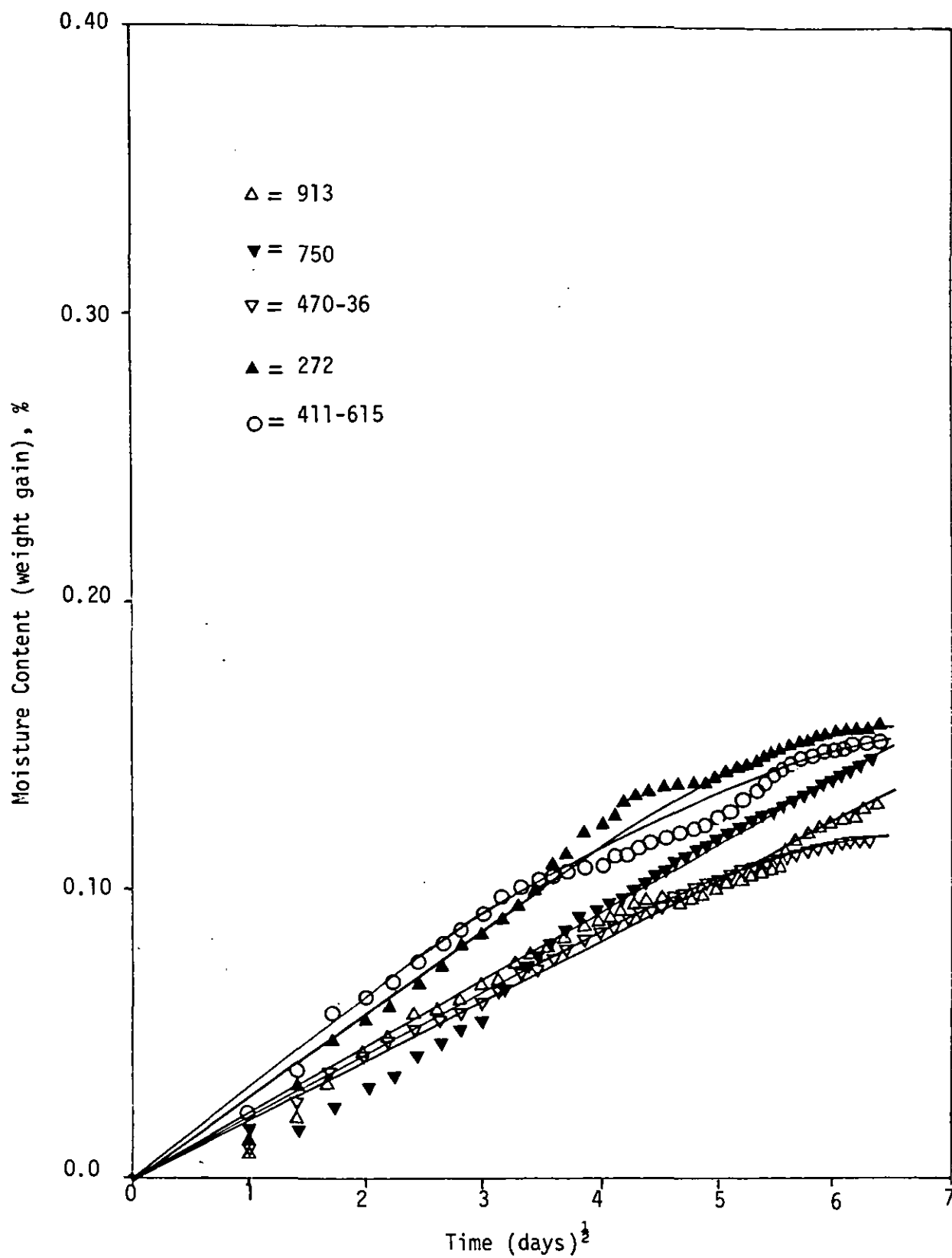


FIGURE 63: Weight change of specimens exposed to 60% RH at 25°C as a function of time (fibre orientation 0°)

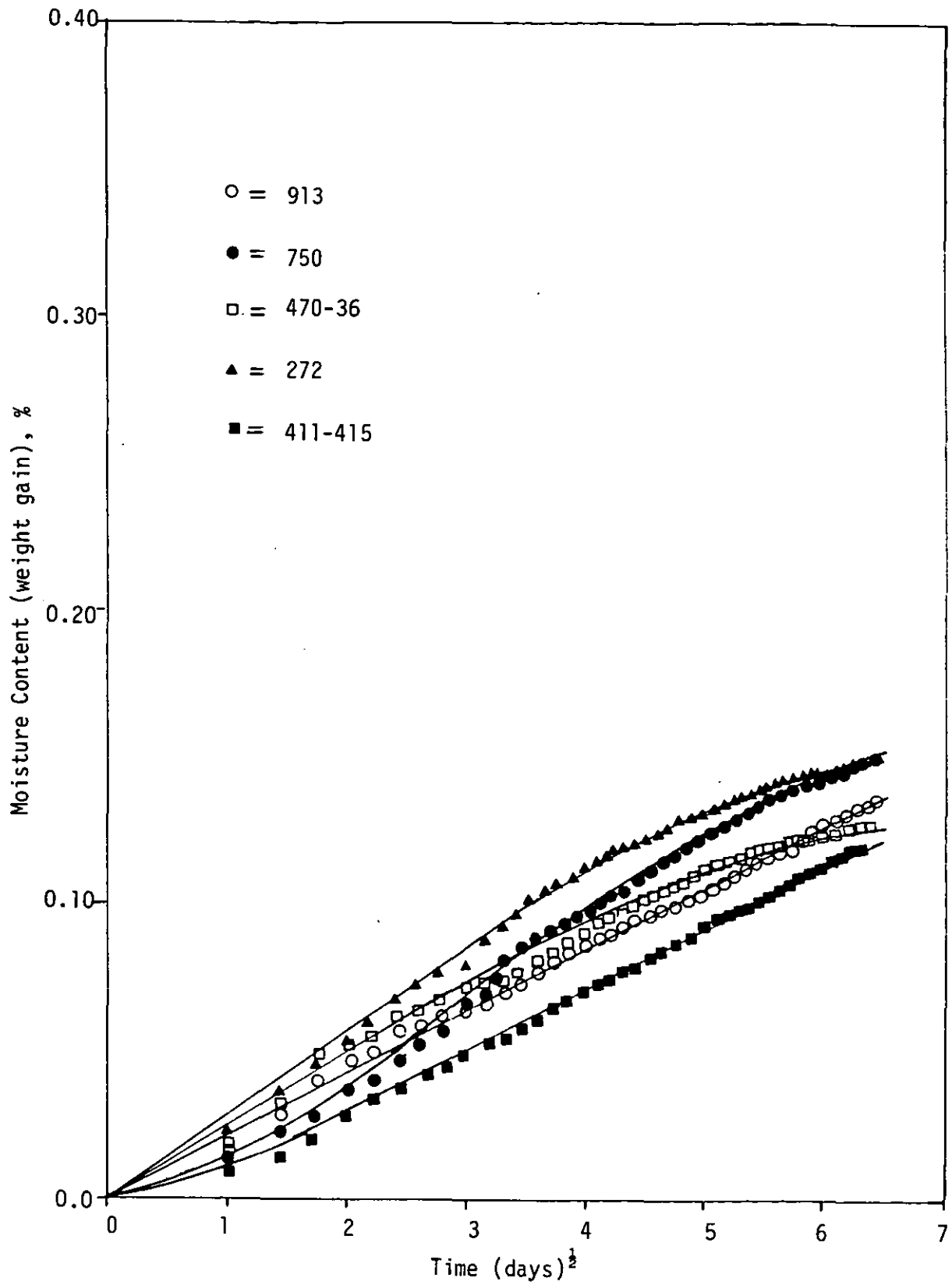


FIGURE 64: Weight change of specimens exposed to 60% RH at 25°C as a function of time (fibre orientation $\pm 45^\circ$)

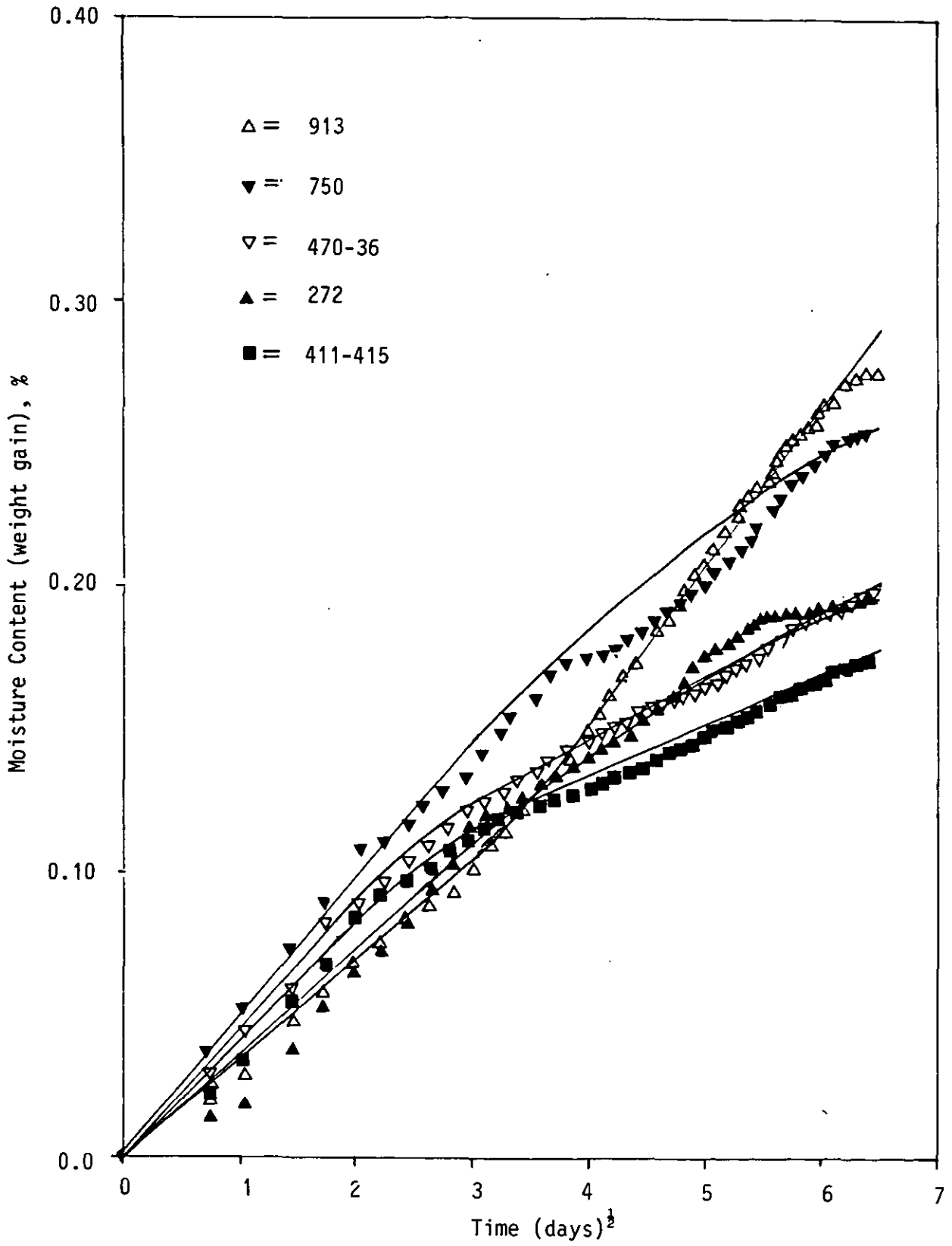


FIGURE 65: Weight change of specimens exposed to 60% RH at 40°C as a function of time (fibre orientation 0°)

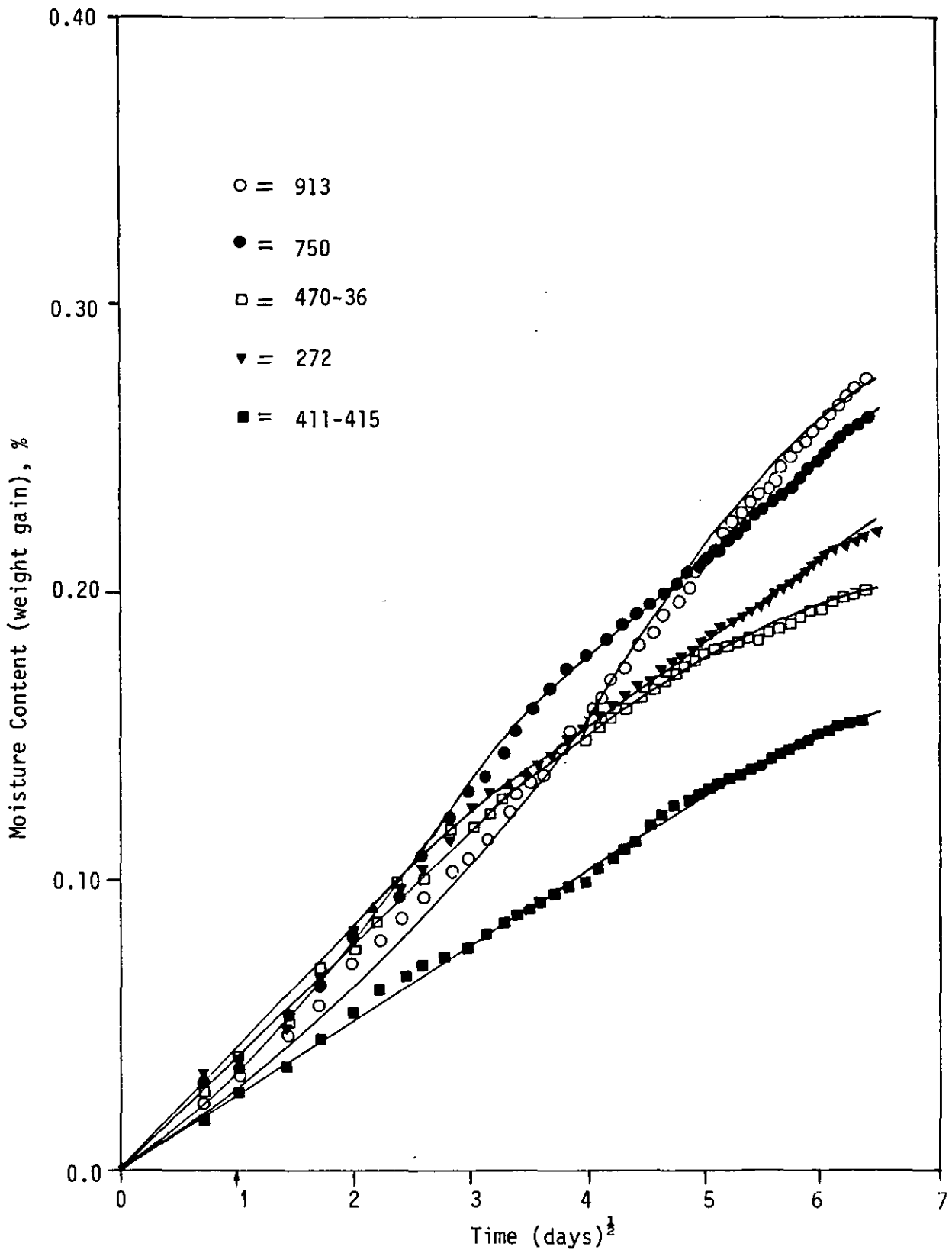


FIGURE 66: Weight change of specimens exposed to 60% RH at 40°C as a function of time (fibre orientation $\pm 45^\circ$)

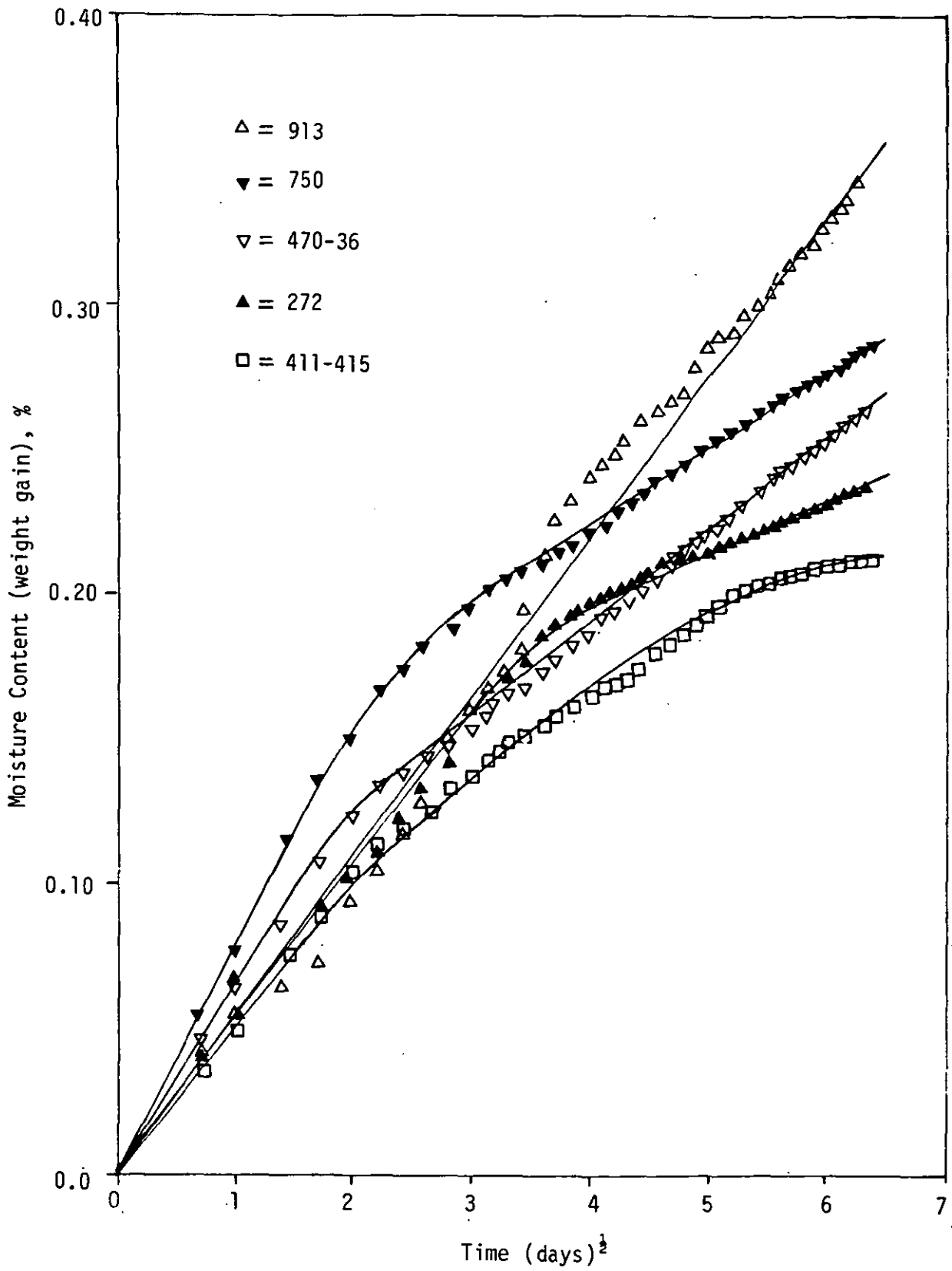


FIGURE 67: Weight change of specimens exposed to 60% RH at 50°C as a function of time (fibre orientation 0°)

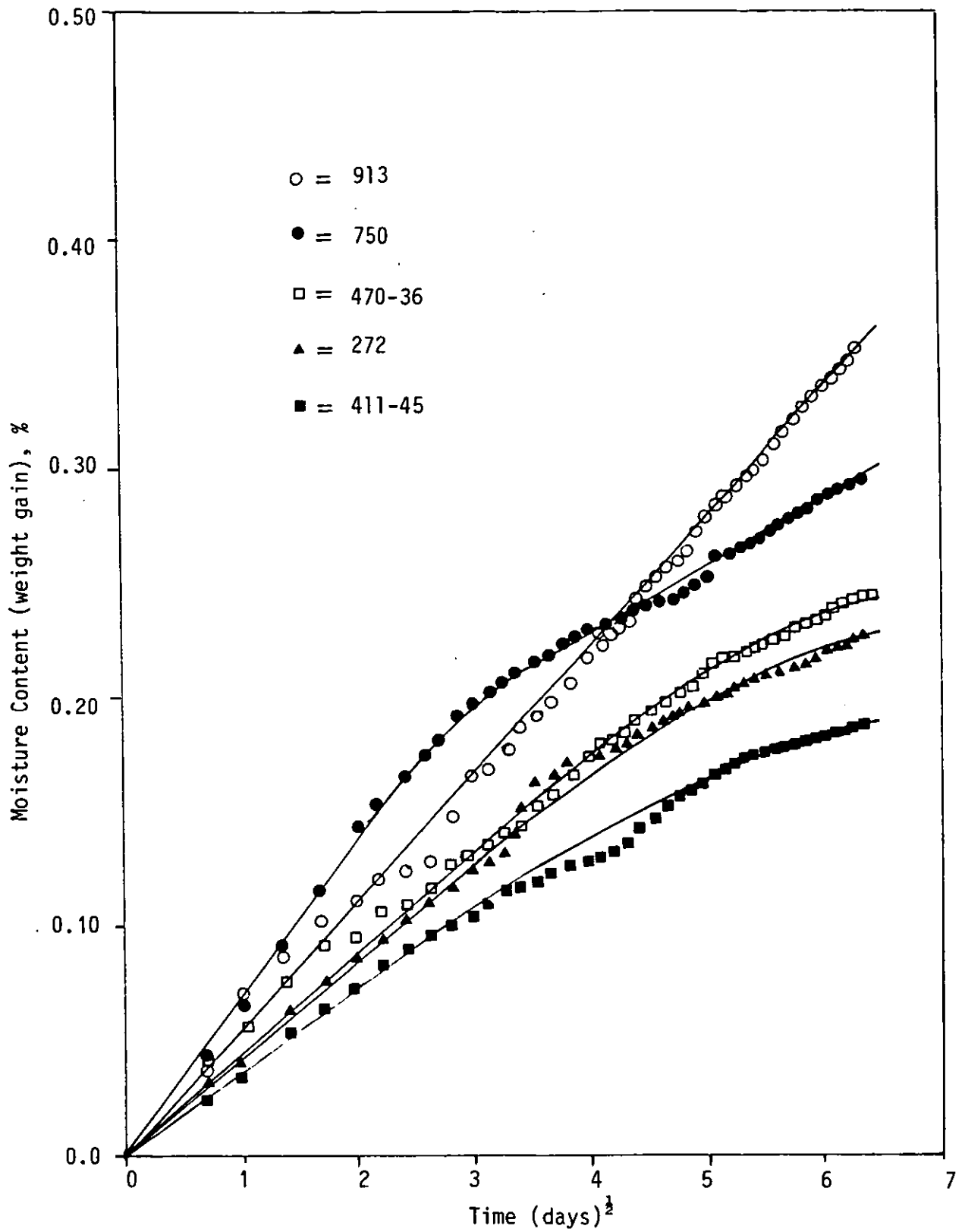


FIGURE 68: Weight change of specimens exposed to 60% RH at 50°C as a function of time (fibre orientation $\pm 45^\circ$)

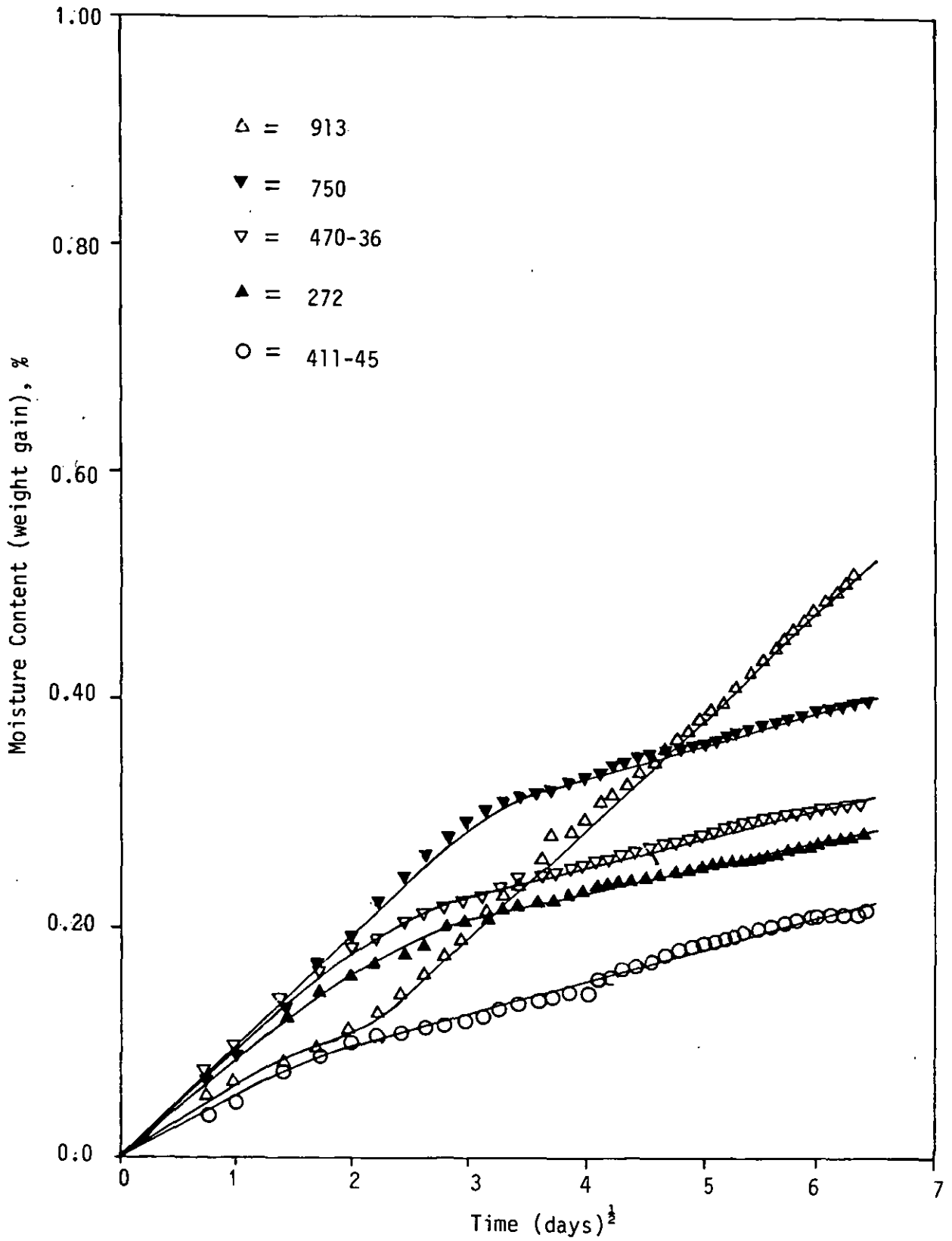


FIGURE 69: Weight change of specimens exposed to 60% RH at 60°C as a function of time (fibre orientation 0°)

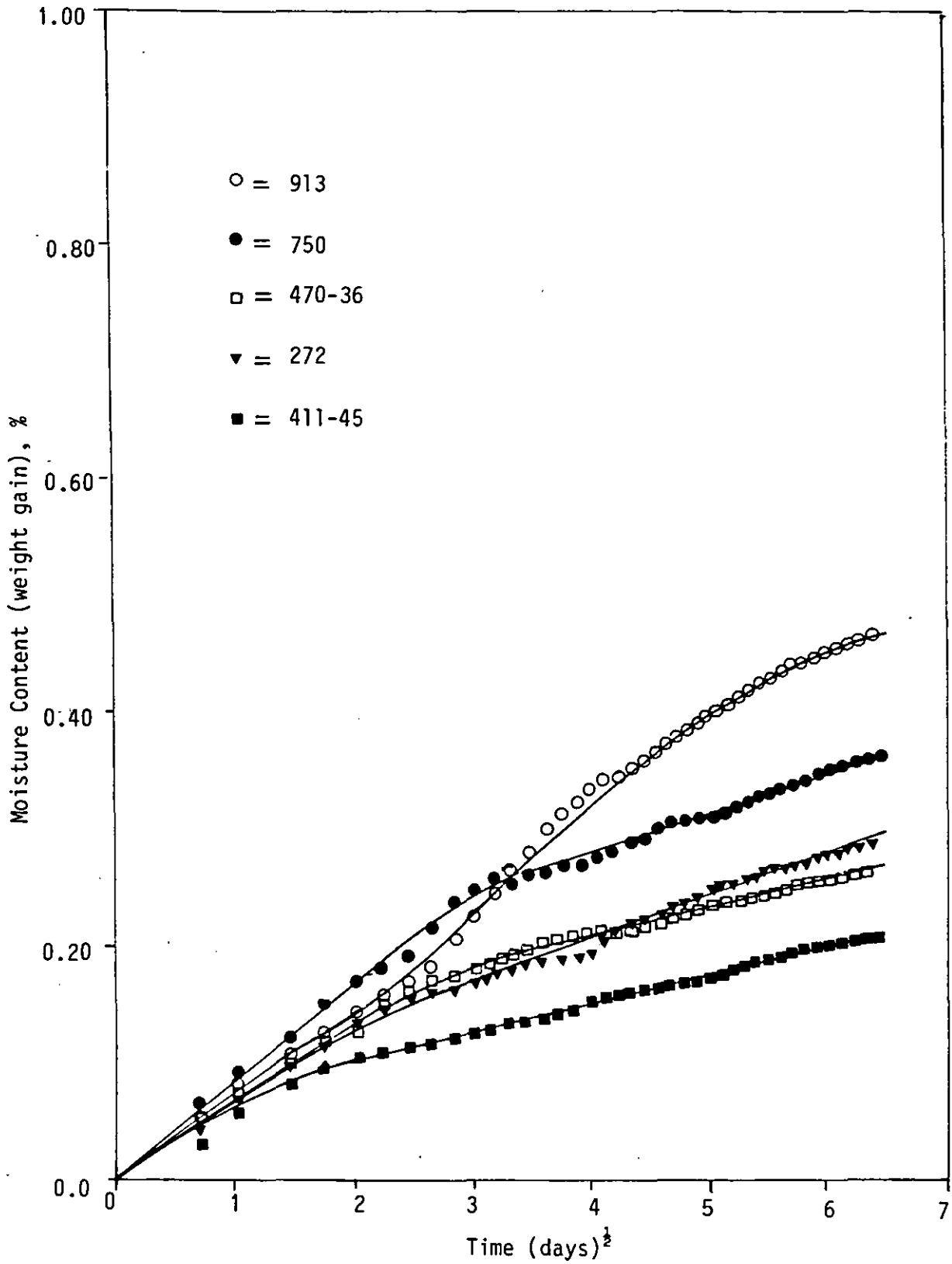


FIGURE 70: Weight change of specimens exposed to 60% RH at 60°C as a function of time (fibre orientation $\pm 45^\circ$)

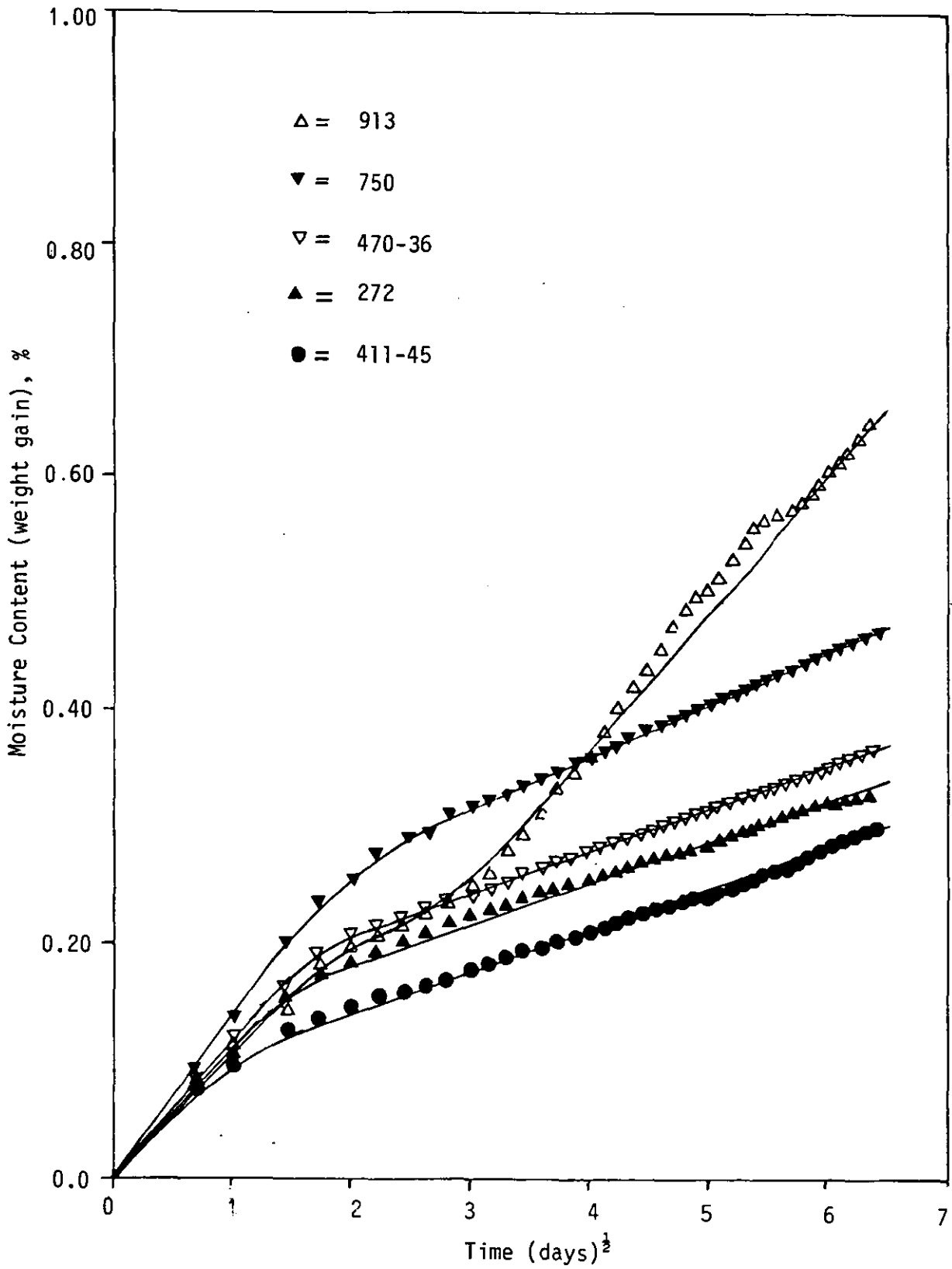


FIGURE 71: Weight change of specimens exposed to 60% RH at 70°C as a function of time (fibre orientation 0°)

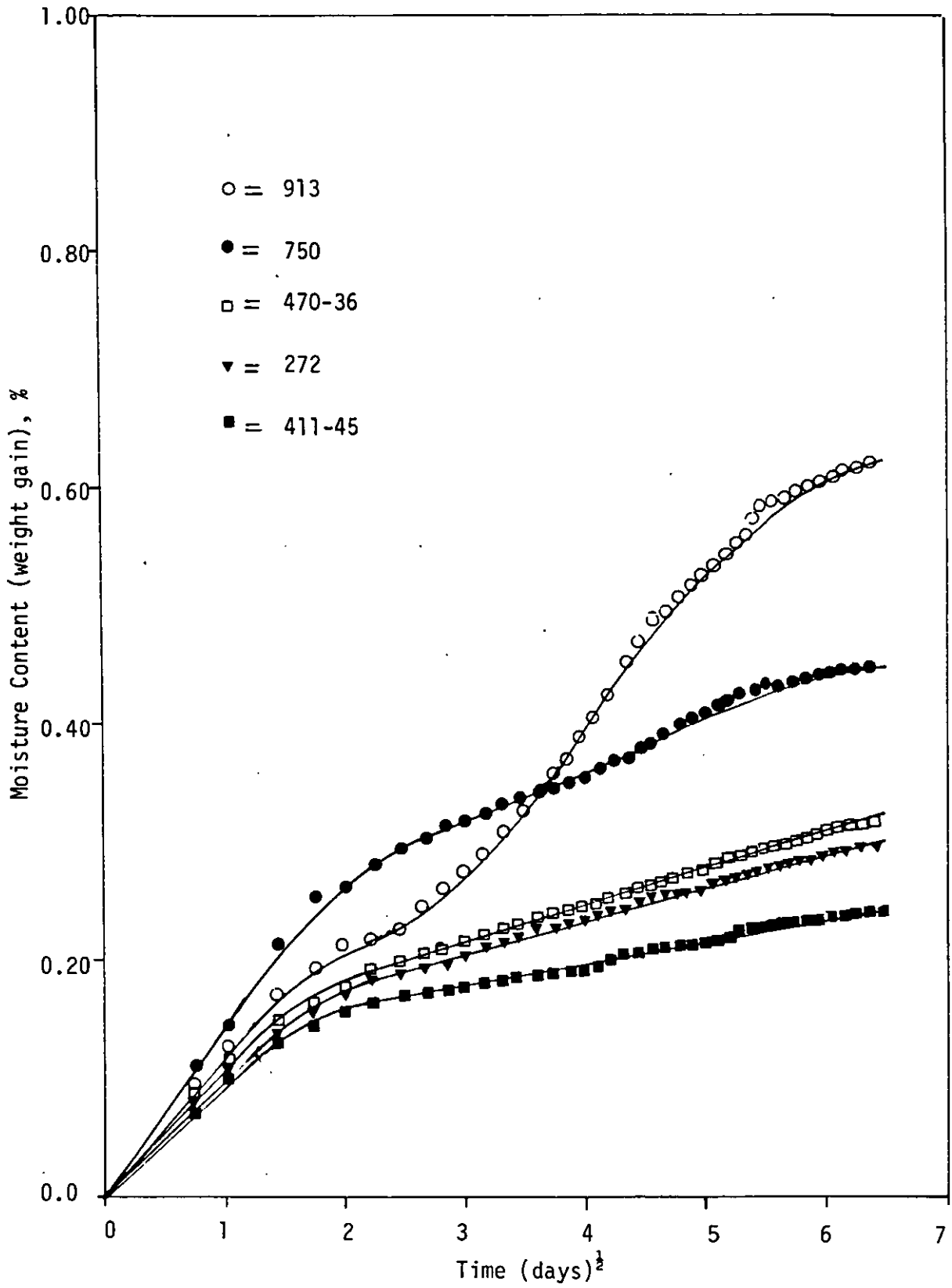


FIGURE 72: Weight change of specimens exposed to 60% RH at 70°C as a function of time (fibre orientation $\pm 45^\circ$)

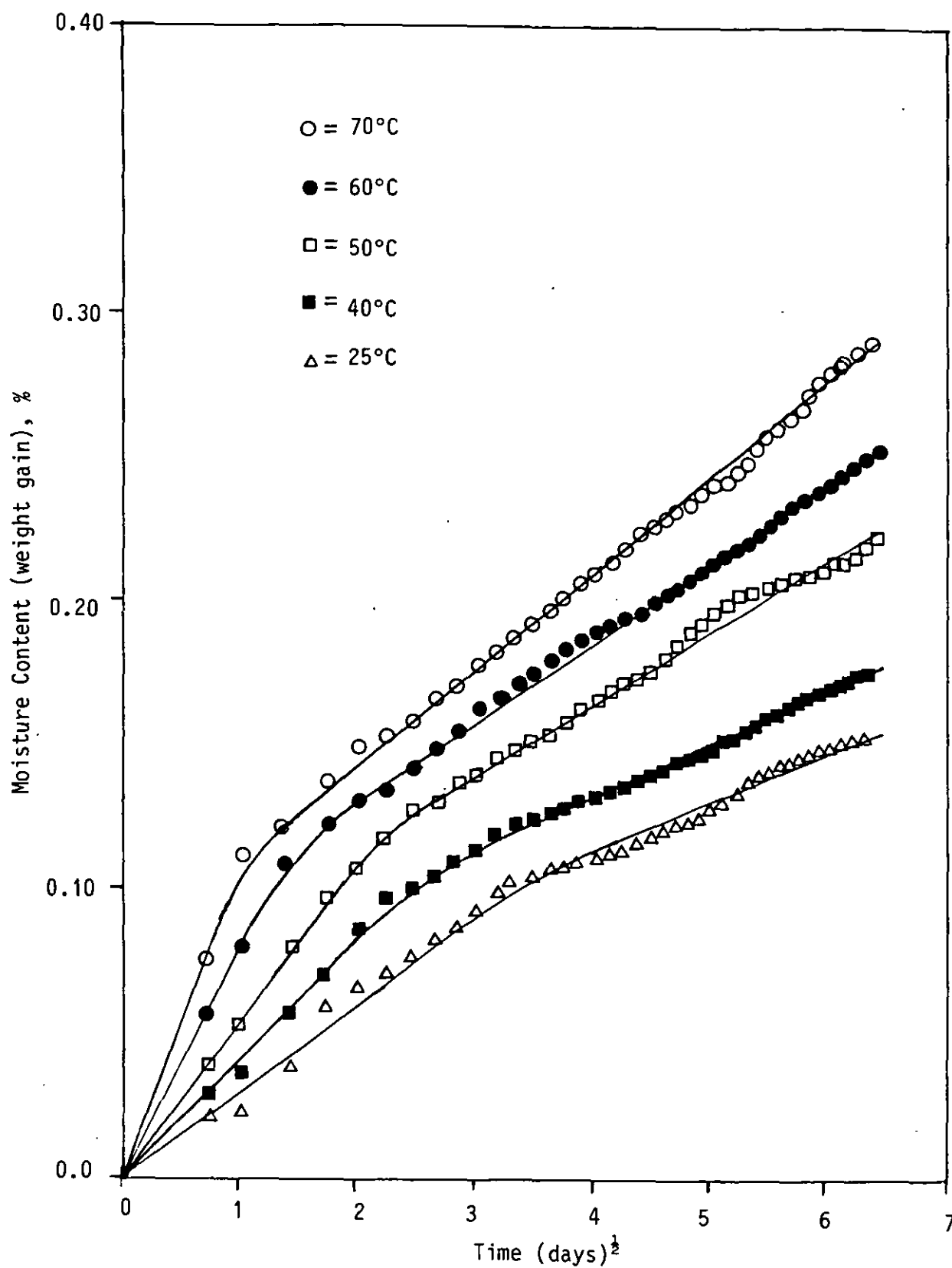


FIGURE 73: Weight change of 411-45 vinyl ester specimens exposed to 60% RH at different temperatures as a function of time (fibre orientation 0°)

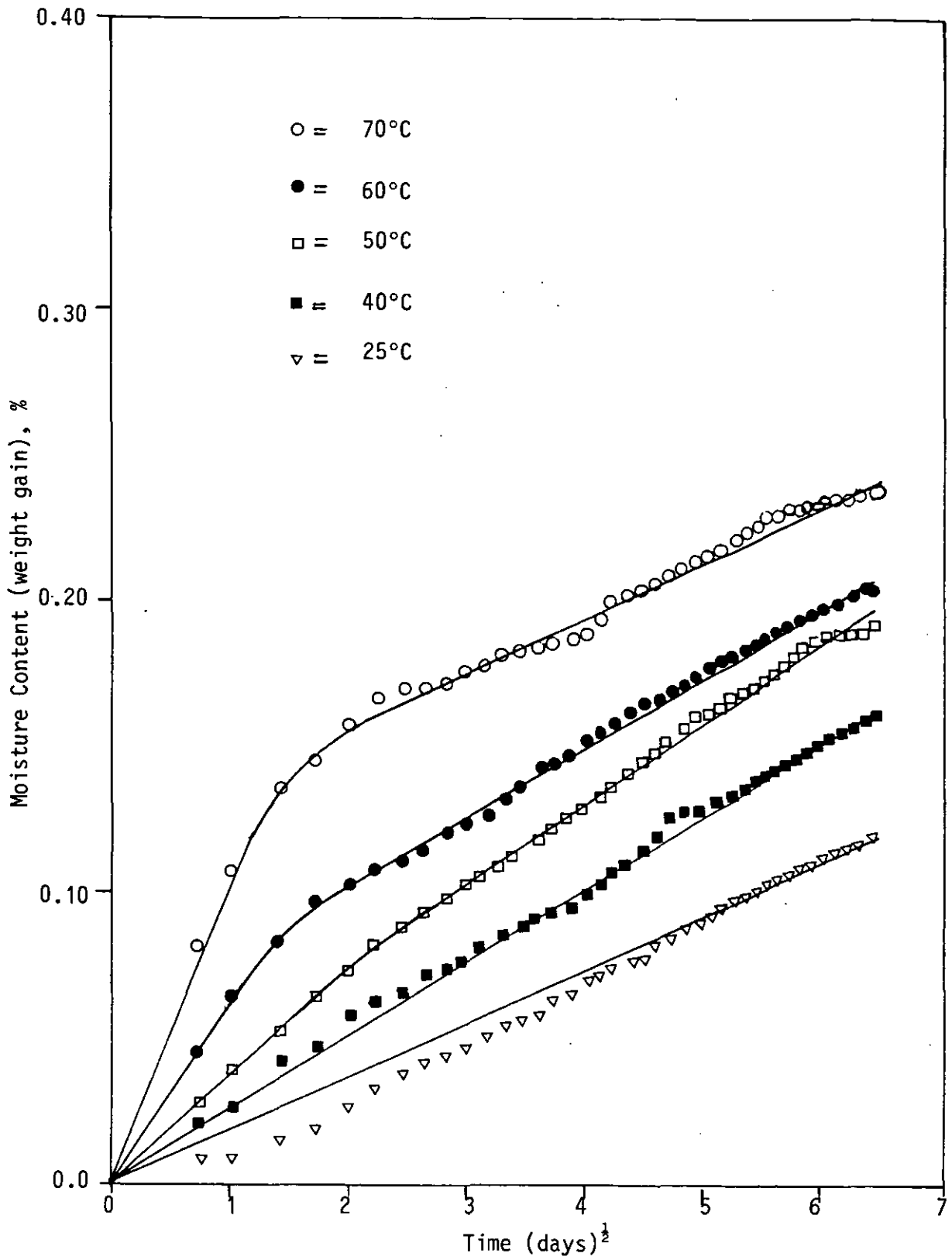


FIGURE 74: Weight change of 411-45 vinyl ester specimens exposed to 60% RH at different temperatures as a function of time (fibre orientation $\pm 45^\circ$)

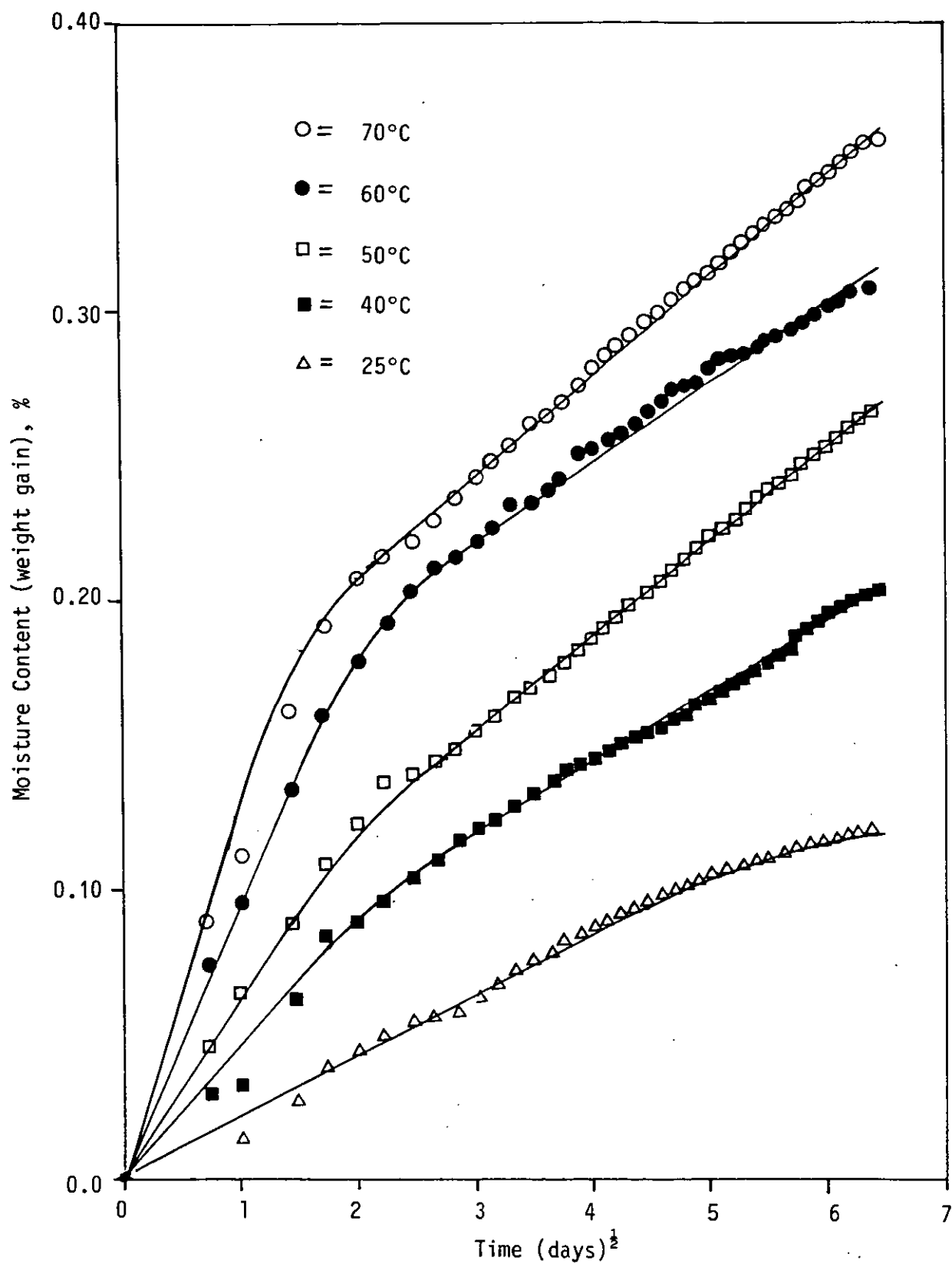


FIGURE 75: Weight change of 470-36 vinyl ester specimens exposed to 60% RH at different temperatures as a function of time (fibre orientation 0°)

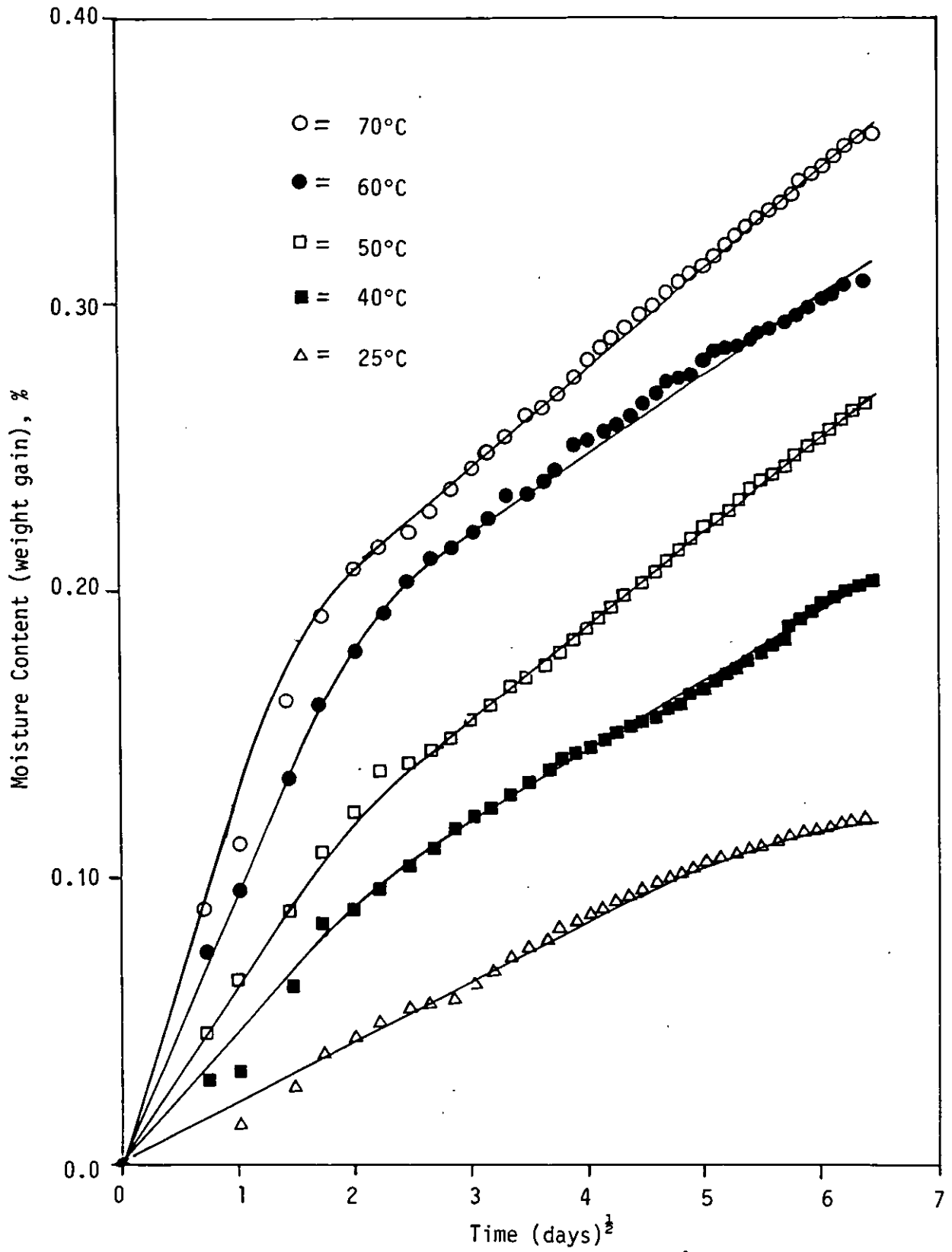


FIGURE 75: Weight change of 470-36 vinyl ester specimens exposed to 60% RH at different temperatures as a function of time (fibre orientation 0°)

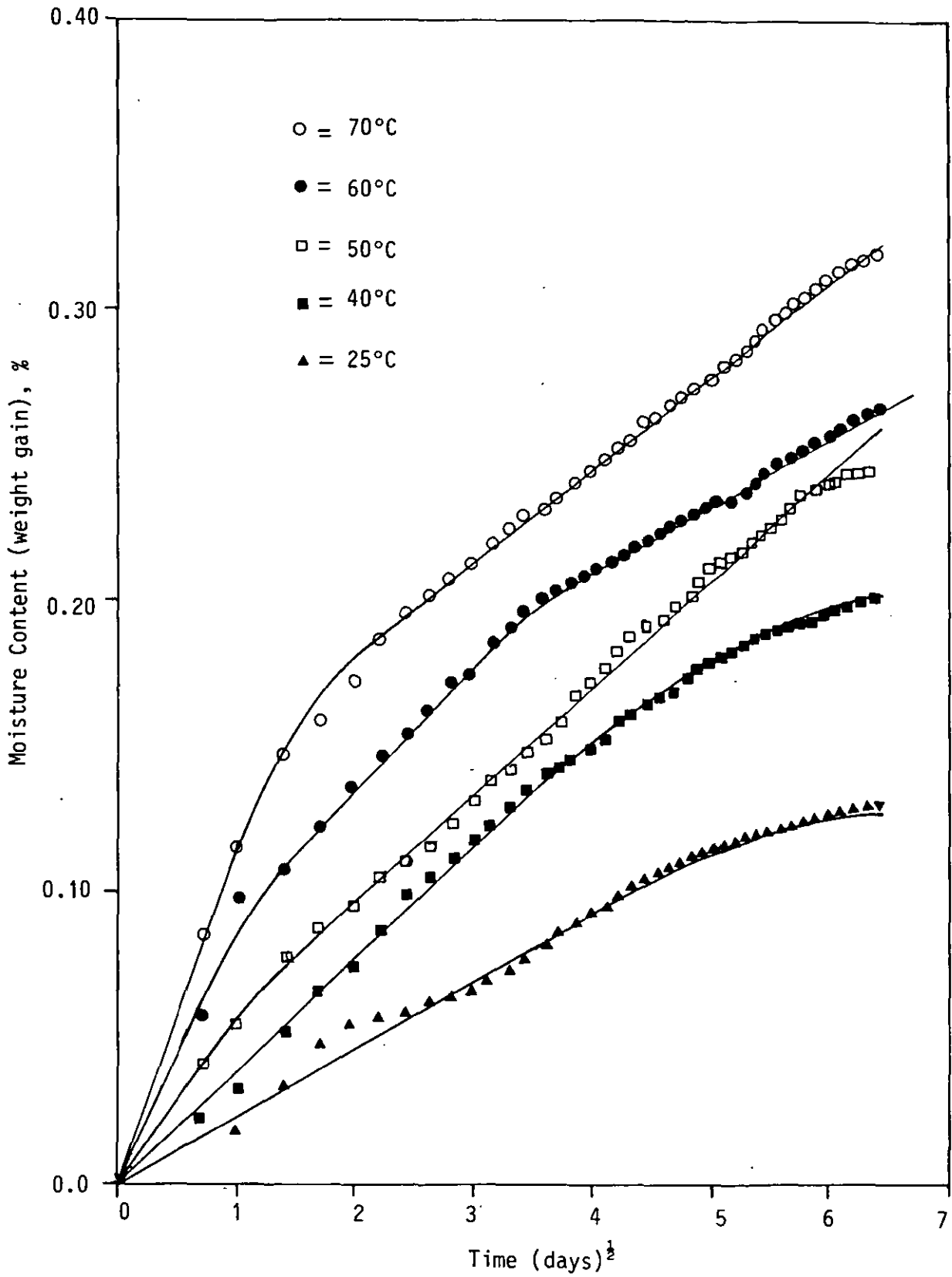


FIGURE 76: Weight change of 470-36 vinyl ester specimens exposed to 60% RH at different temperatures as a function of time (fibre orientation $\pm 45^\circ$)

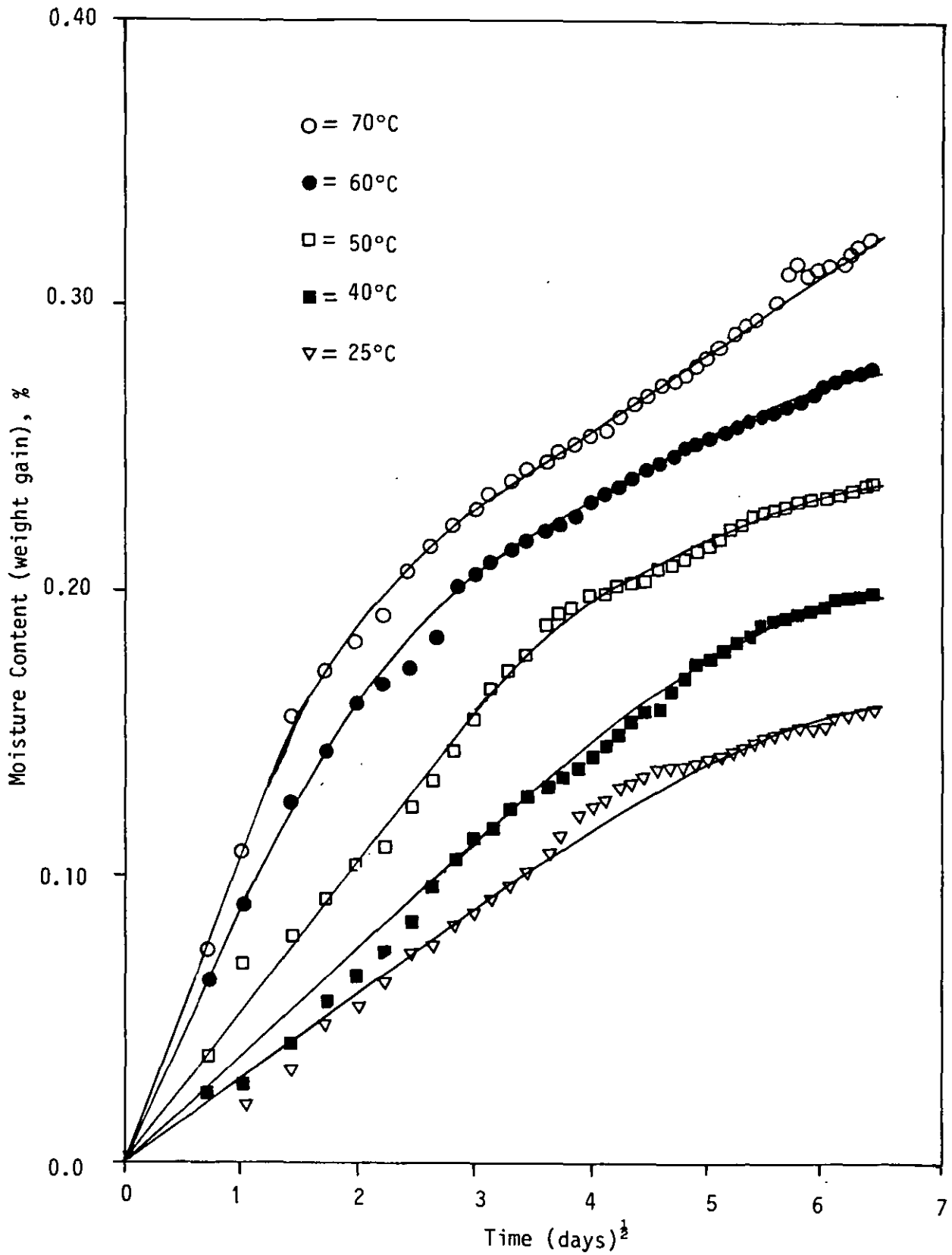


FIGURE 77: Weight change of Polyester 272 specimens exposed to 60% RH at different temperatures as a function of time (fibre orientation 0°)

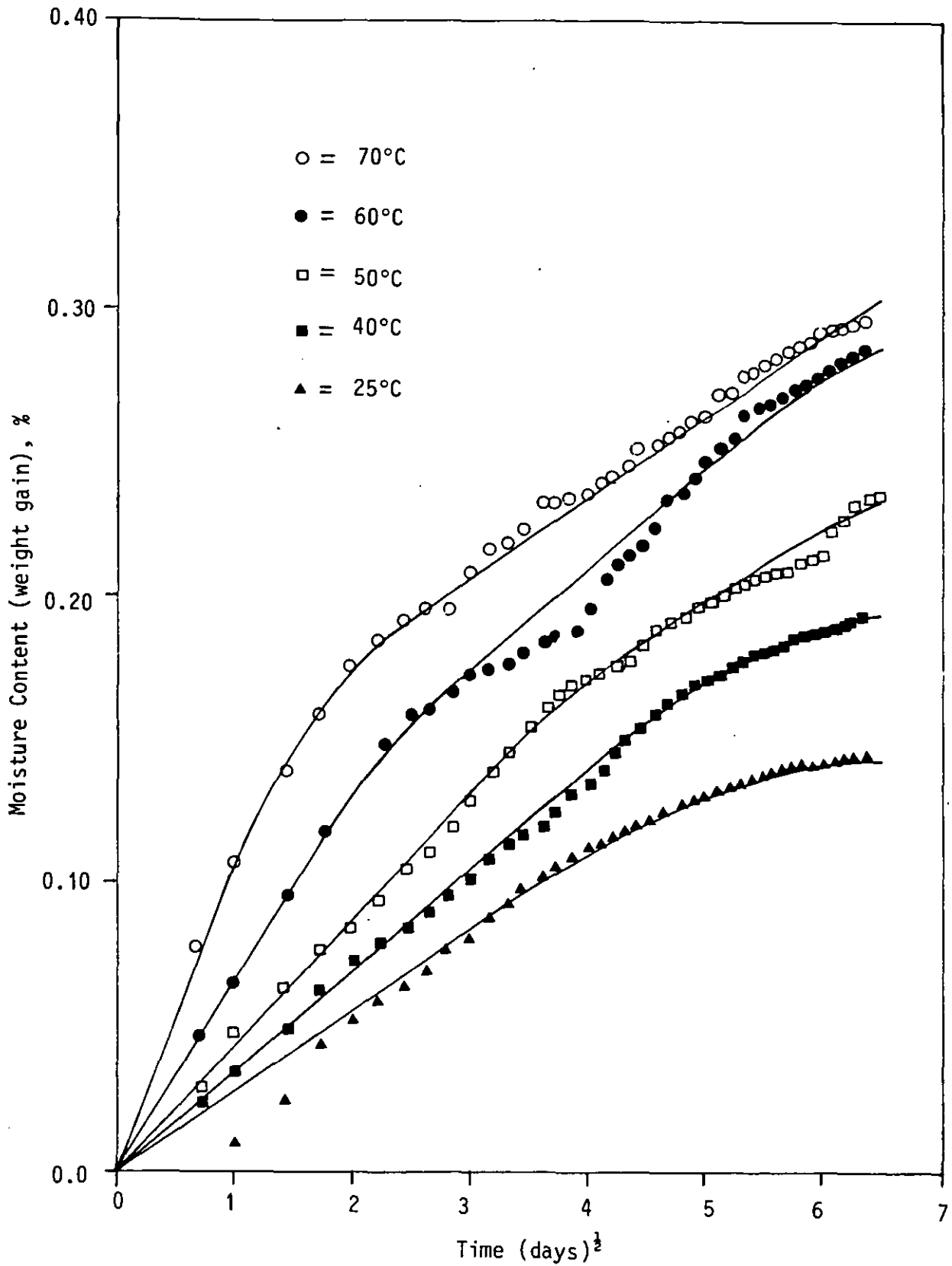


FIGURE 78: Weight change of Polyester 272 specimens exposed to 60% RH at different temperatures as a function of time (fibre orientation $\pm 45^\circ$)

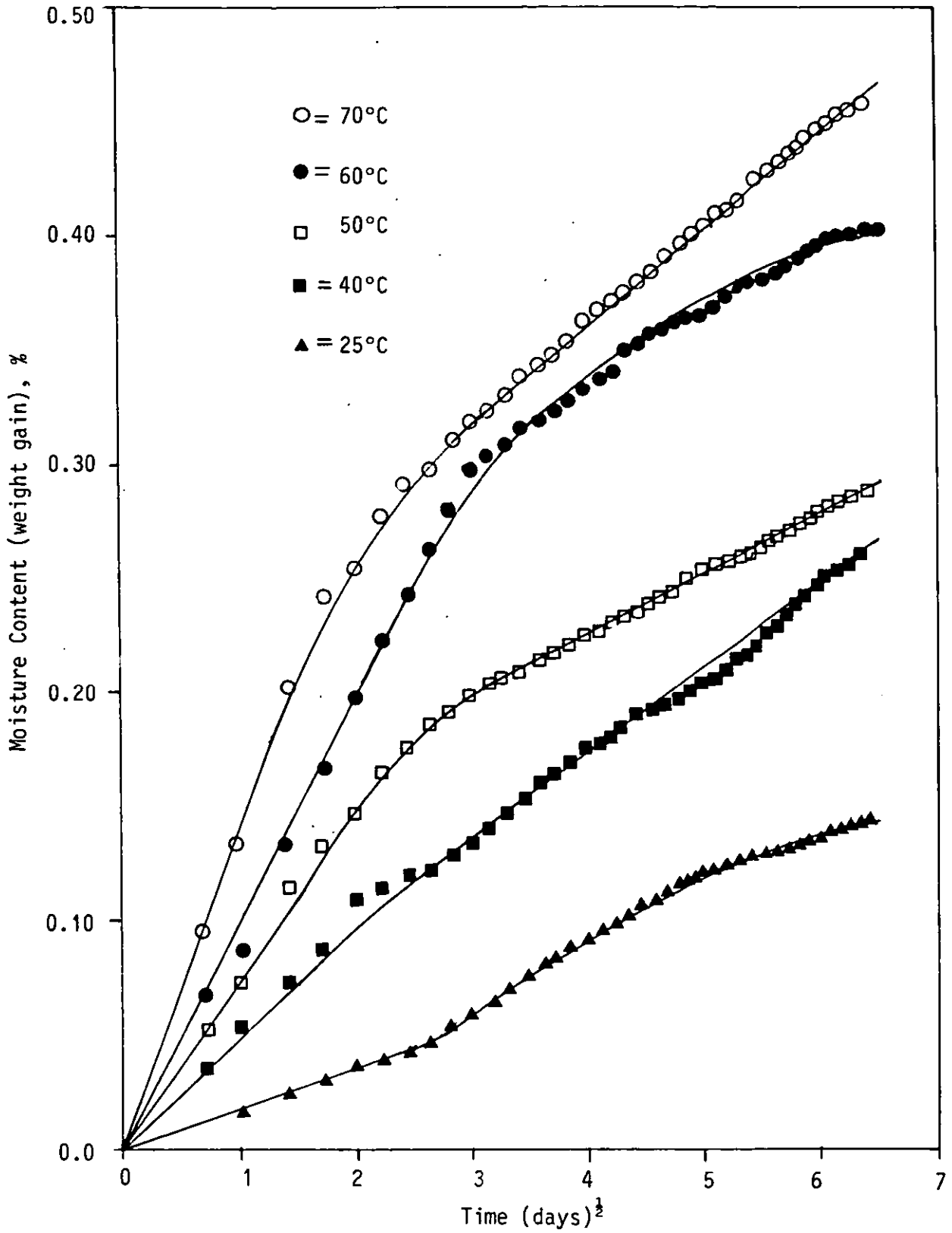


FIGURE 79: Weight change of Epoxy MY 750 specimens exposed to 60% RH at different temperatures as a function of time (fibre orientation 0°)

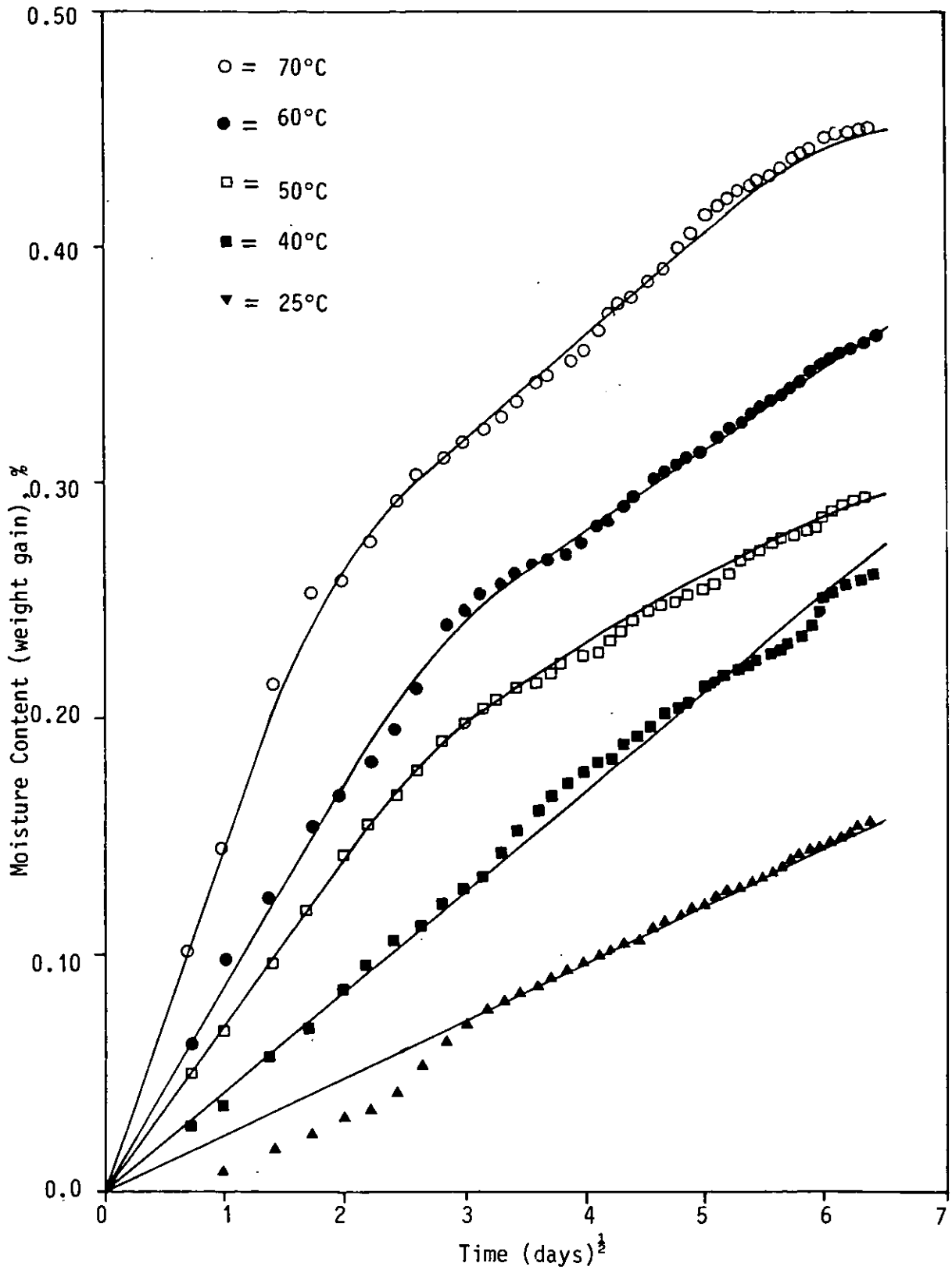


FIGURE 80: Weight change of Epoxy MY 750 specimens exposed to 60% RH at different temperatures as a function of time (fibre orientation $\pm 45^\circ$)

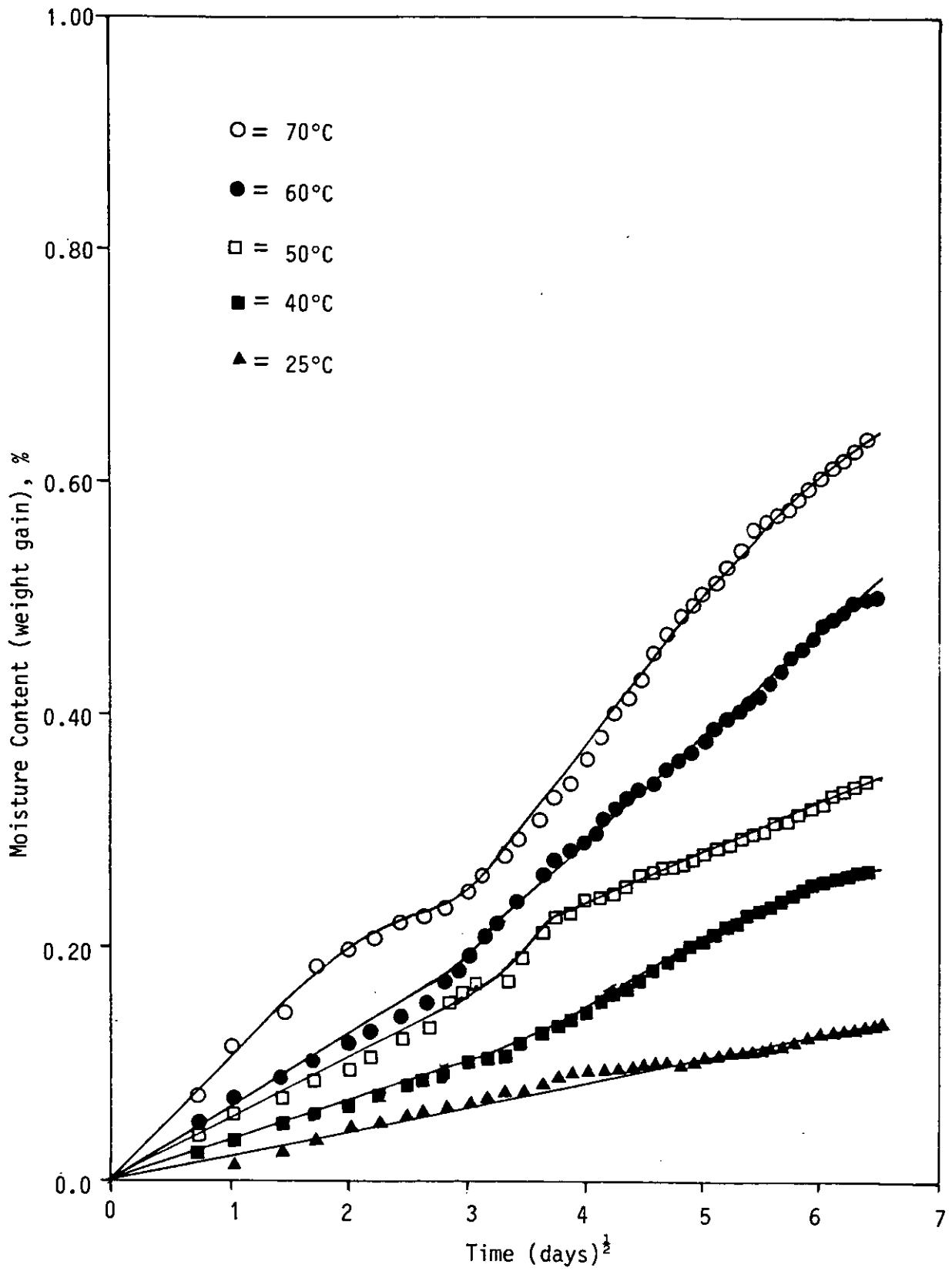


FIGURE 81: Weight change of 913 PrePreg specimens exposed to 60% RH at different temperatures as a function of time (fibre orientation 0°)

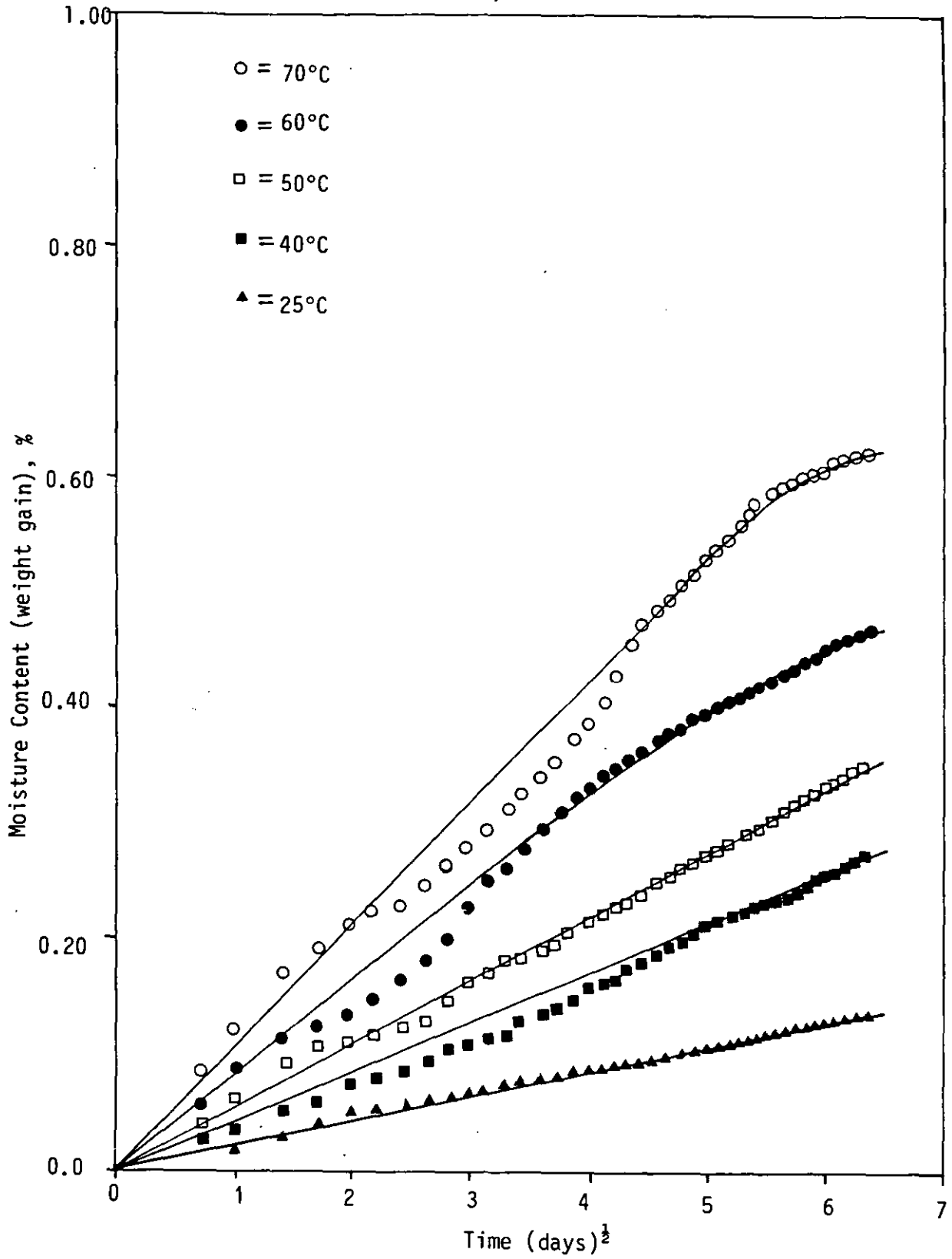


FIGURE 82: Weight change of 913 PrePreg specimens exposed to 60% RH at different temperatures as a function of time (fibre orientation $\pm 45^\circ$)

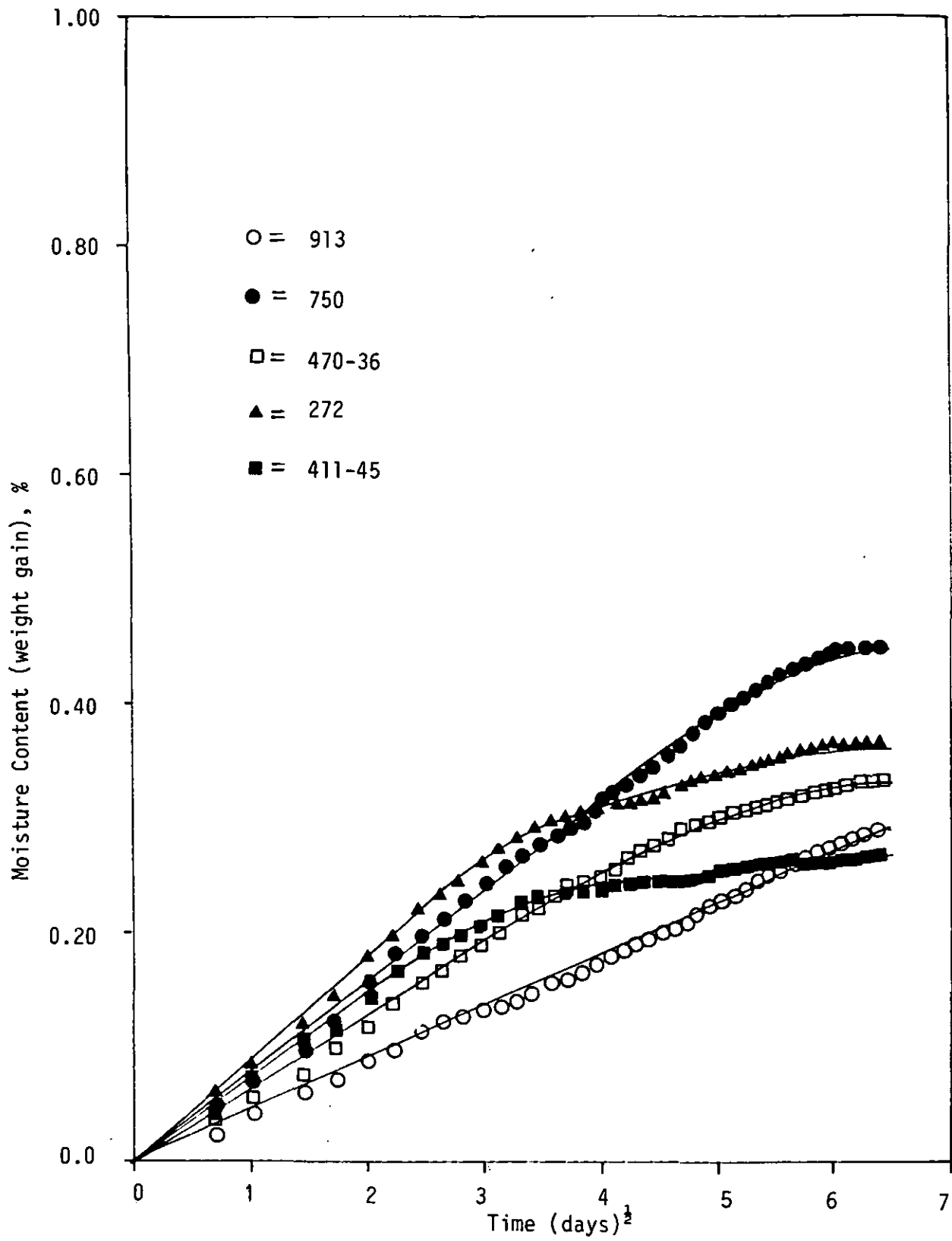


FIGURE 83: Weight change of specimens exposed to 95% RH at 25°C as a function of time (fibre orientation 0°)

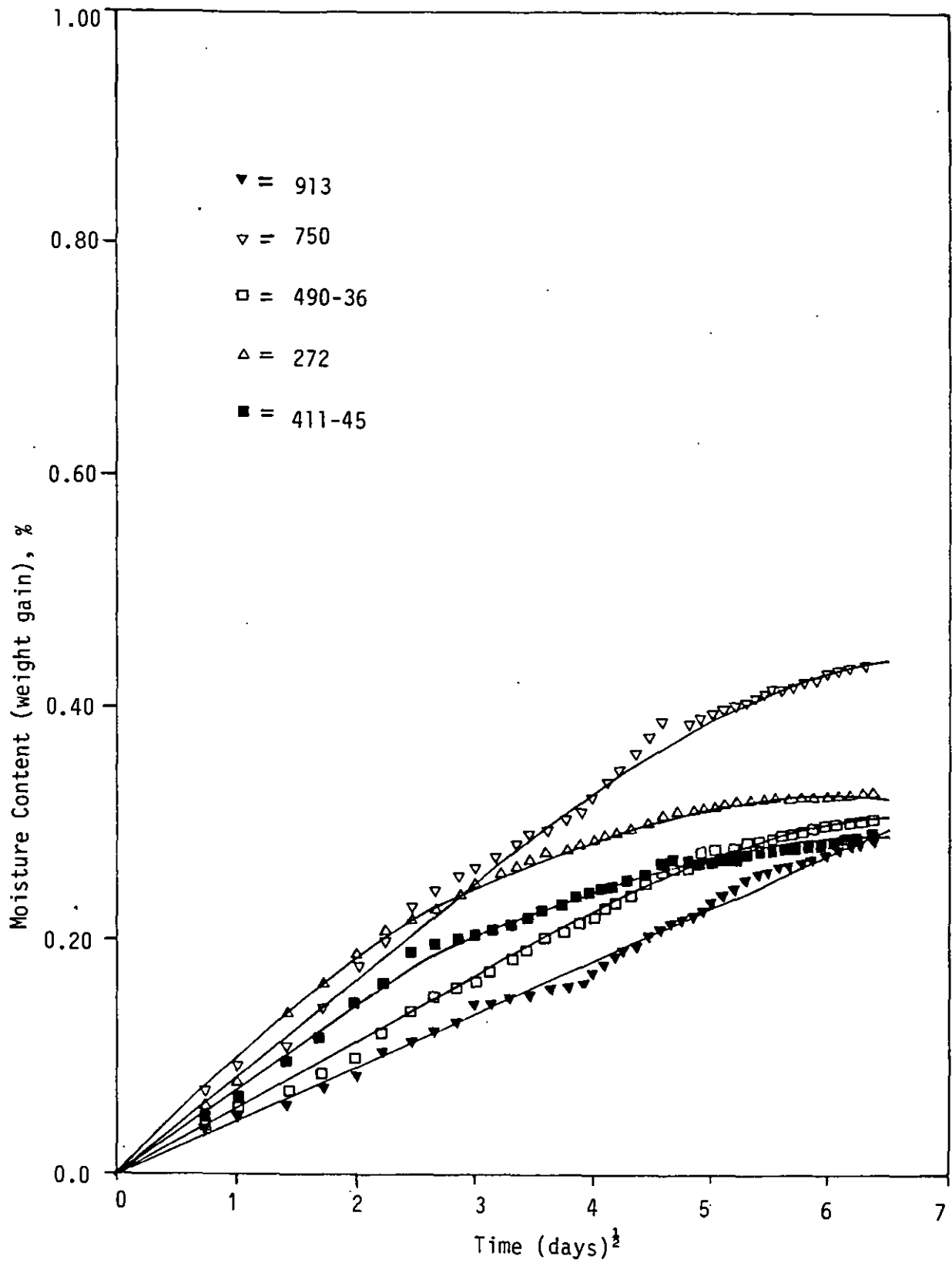


FIGURE 84: Weight change of specimens exposed to 95% RH at 25°C as a function of time (fibre orientation $\pm 45^\circ$)

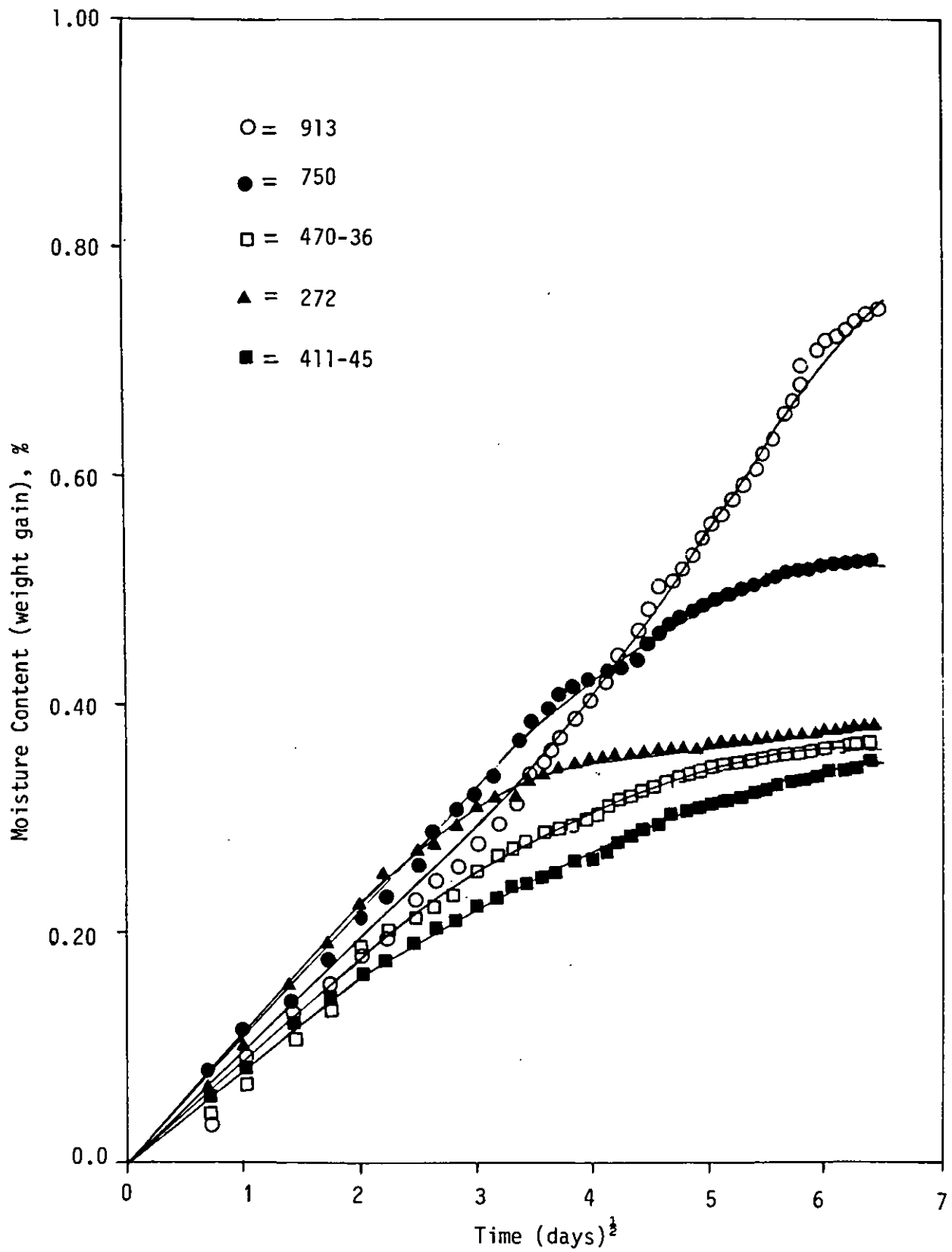


FIGURE 85: Weight change of specimens exposed to 95% RH at 40°C as a function of time (fibre orientation 0°)

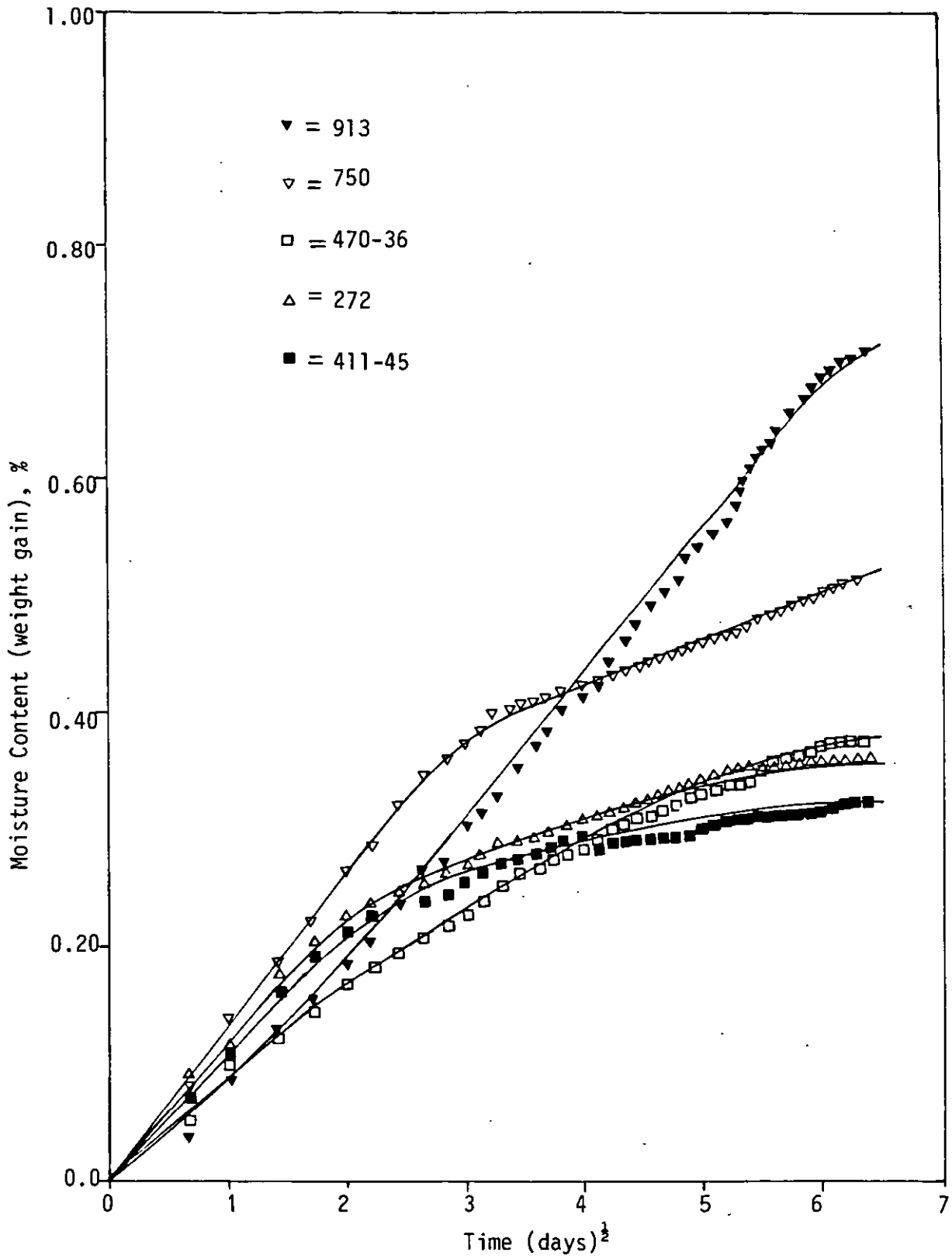


FIGURE 86: Weight change of specimens exposed to 95% RH at 40°C as a function of time (fibre orientation $\pm 45^\circ$)

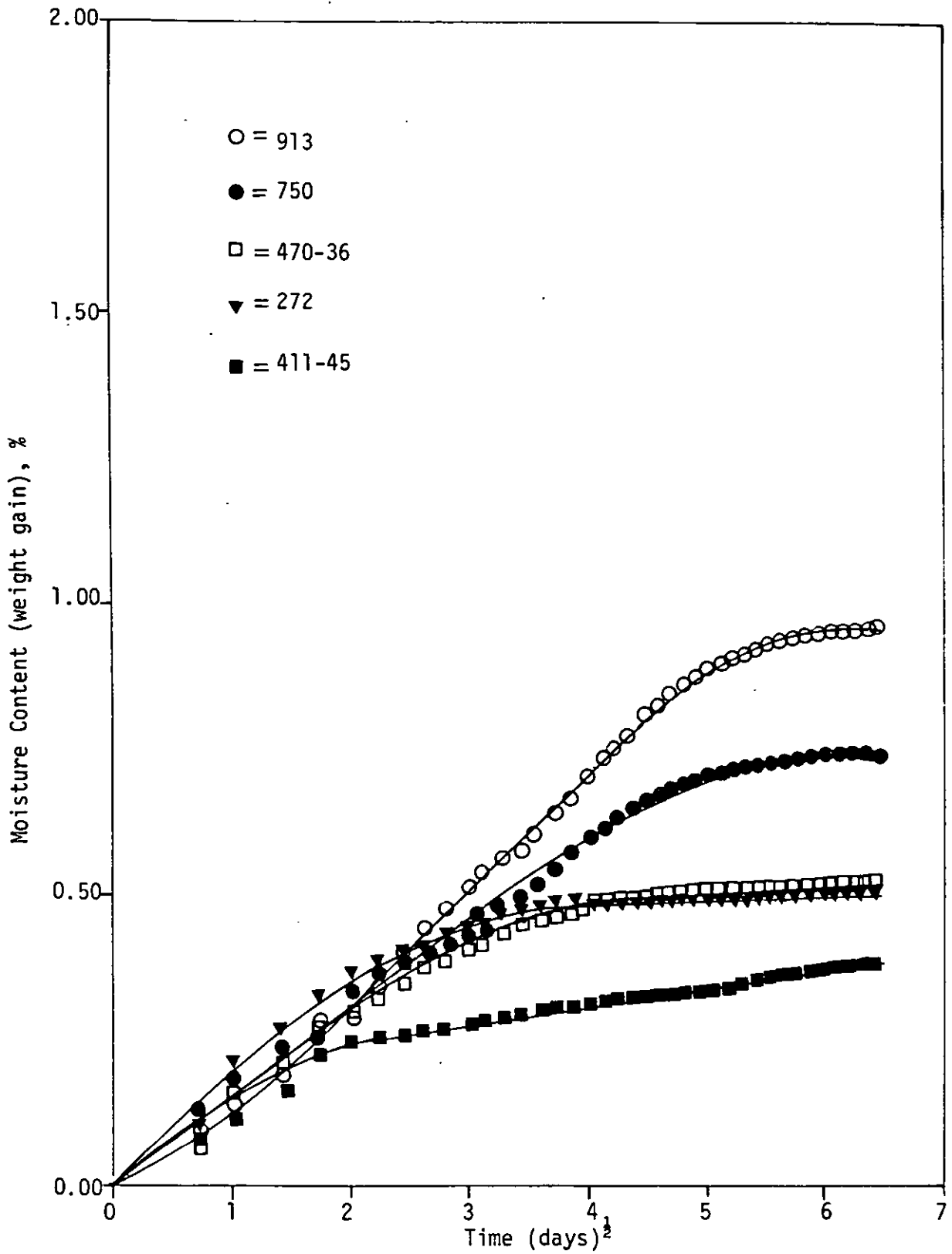


FIGURE 87: Weight change of specimens exposed to 95% RH at 50°C as a function of time (fibre orientation 0°)

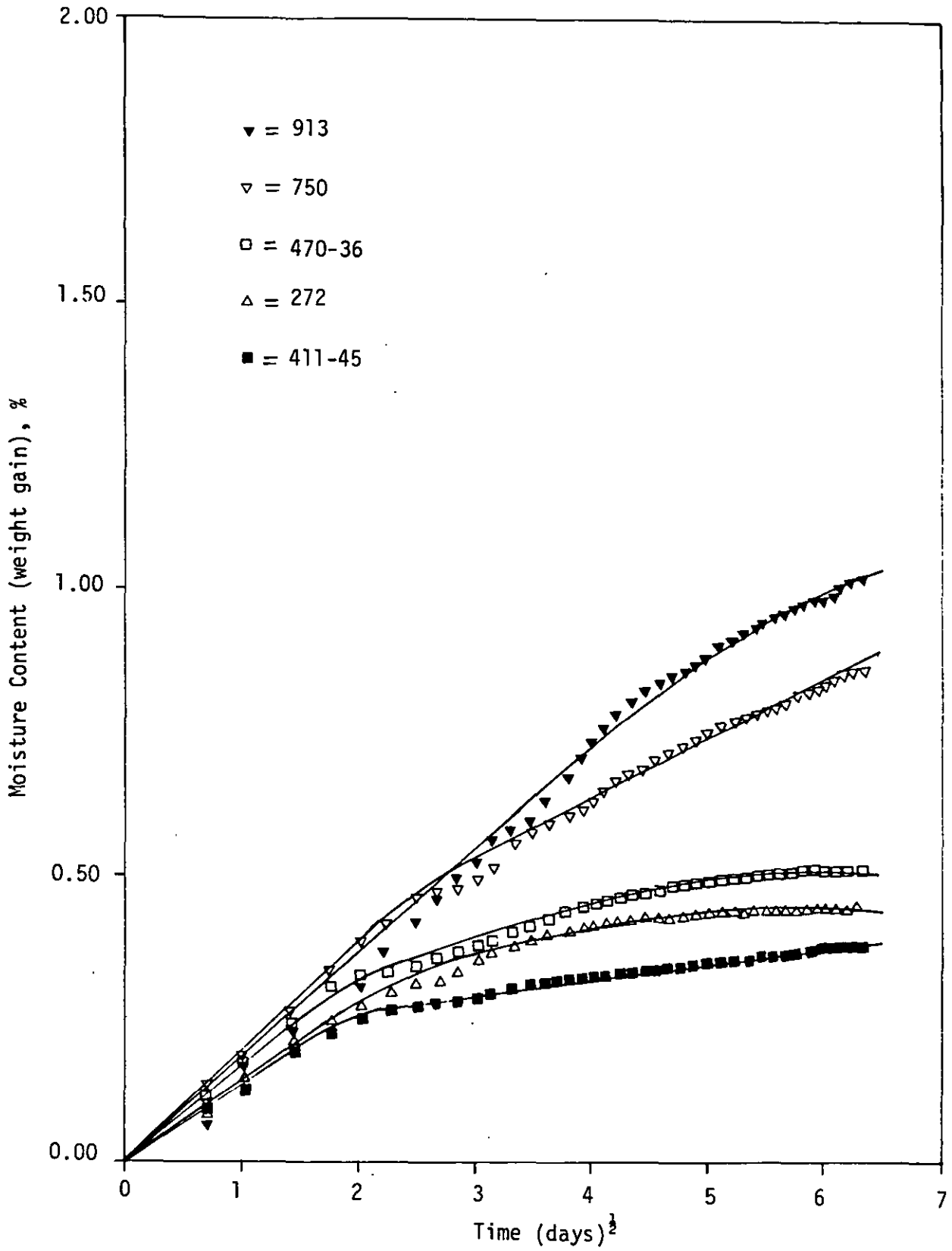


FIGURE 88: Weight change of specimens exposed to 95% RH at 50°C as a function of time (fibre orientation $\pm 45^\circ$)

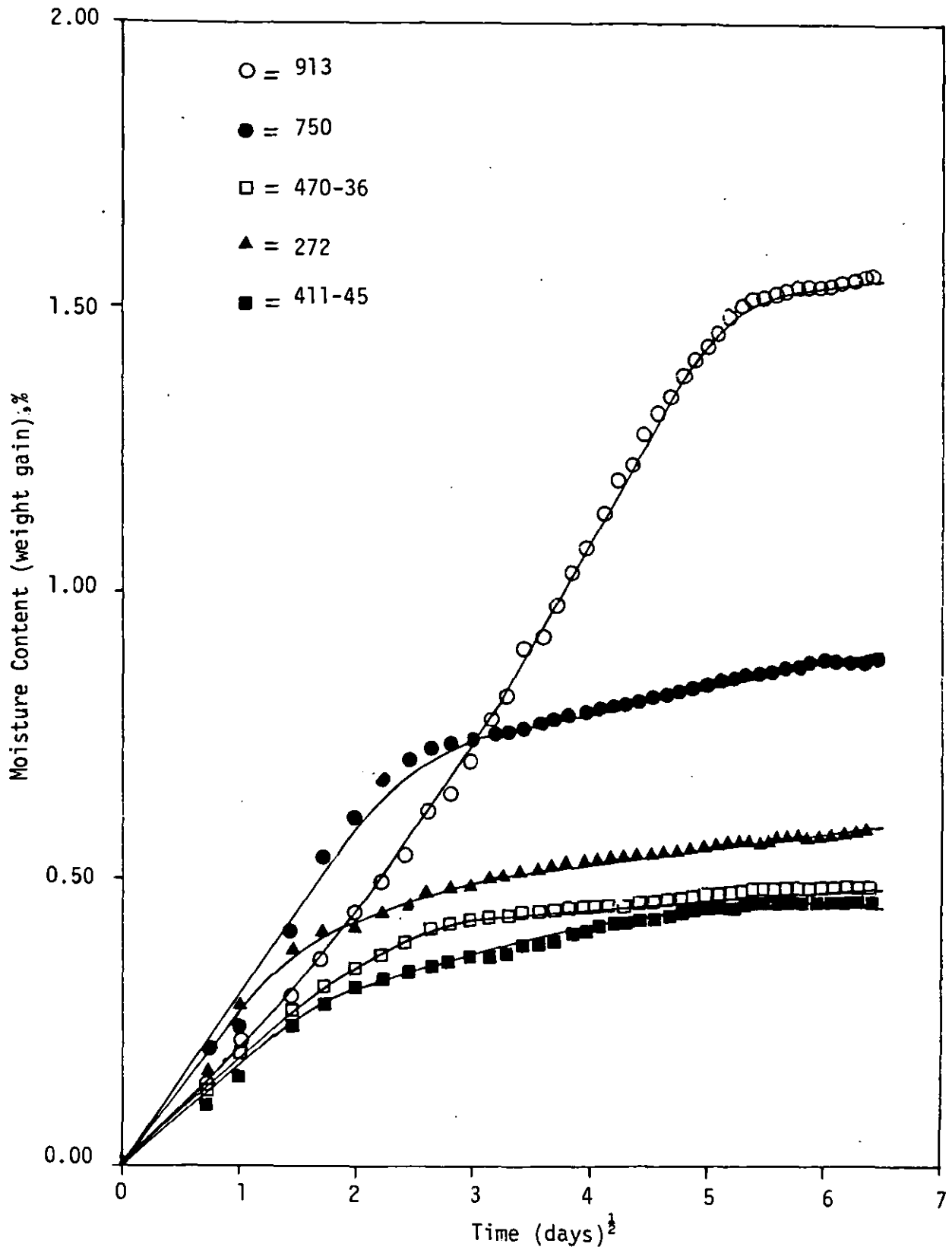


FIGURE 89: Weight change of specimens exposed to 95% RH at 60°C as a function of time (fibre orientation 0°)

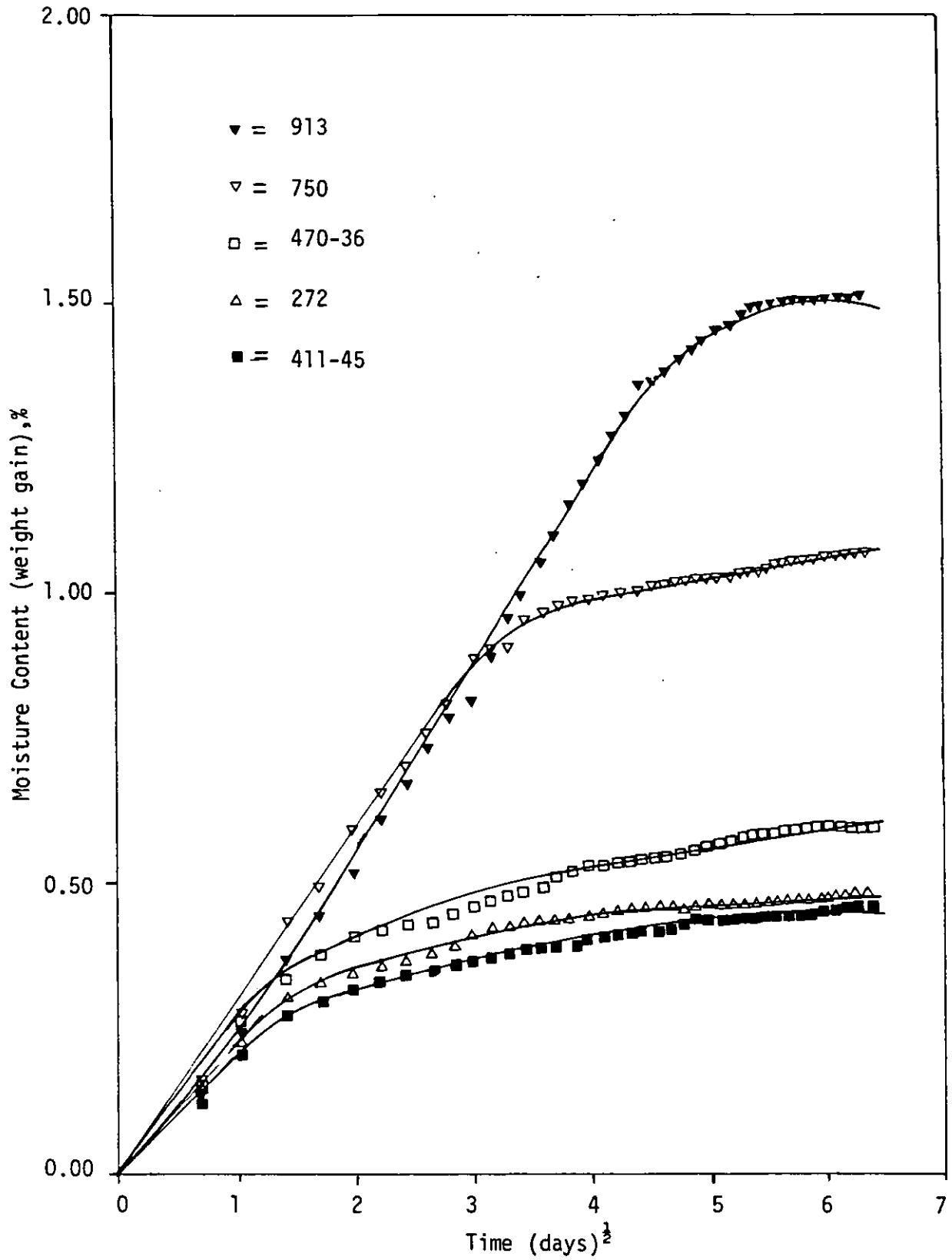


FIGURE 90: Weight change of specimens exposed to 95% RH at 60°C as a function of time (fibre orientation $\pm 45^\circ$)

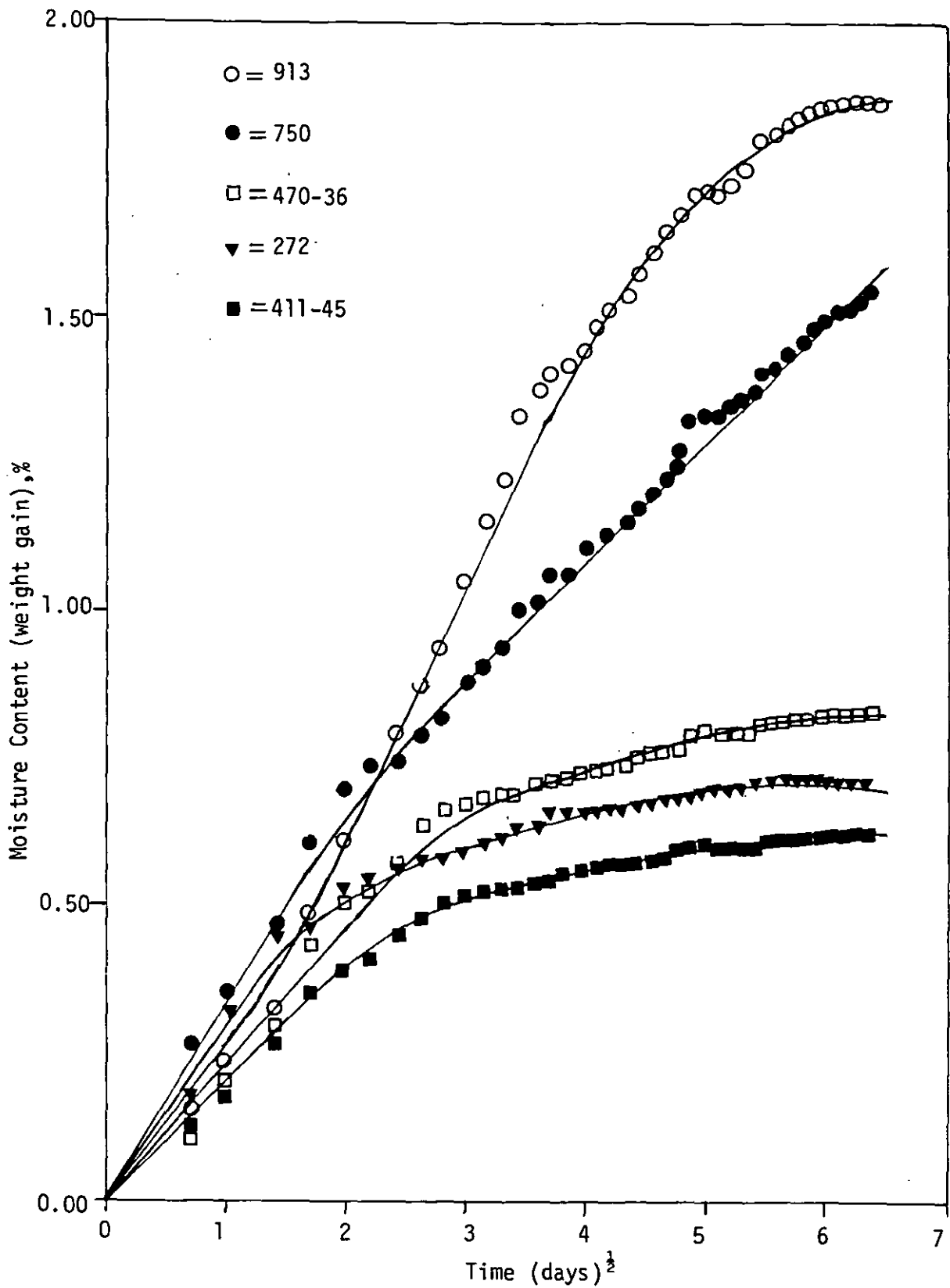


FIGURE 91: Weight change of specimens exposed to 95 % RH at 70°C as a function of time (fibre orientation 0°)

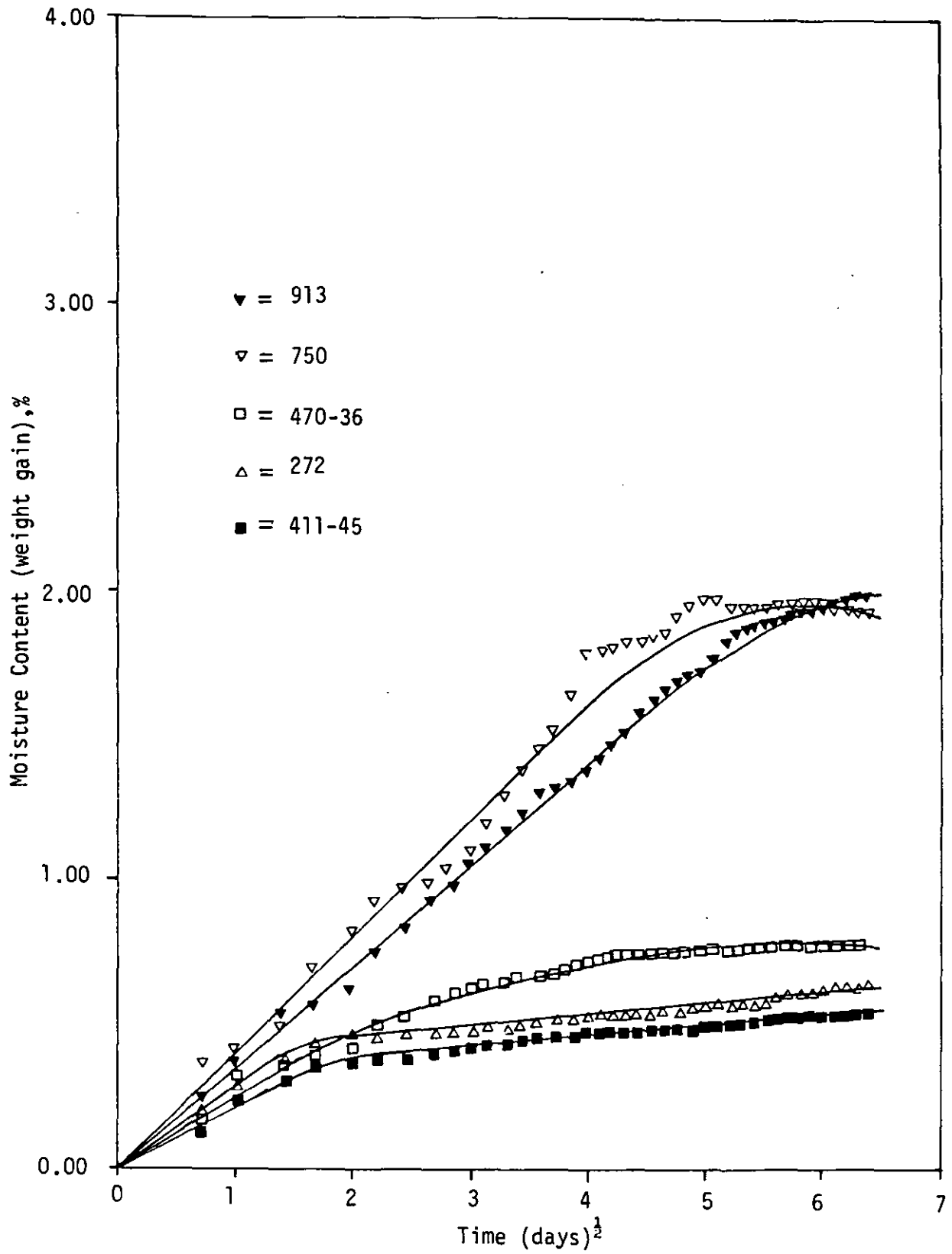


FIGURE 92: Weight change of specimens exposed to 95% RH at 70°C as a function of time (fibre orientation $\pm 45^\circ$)

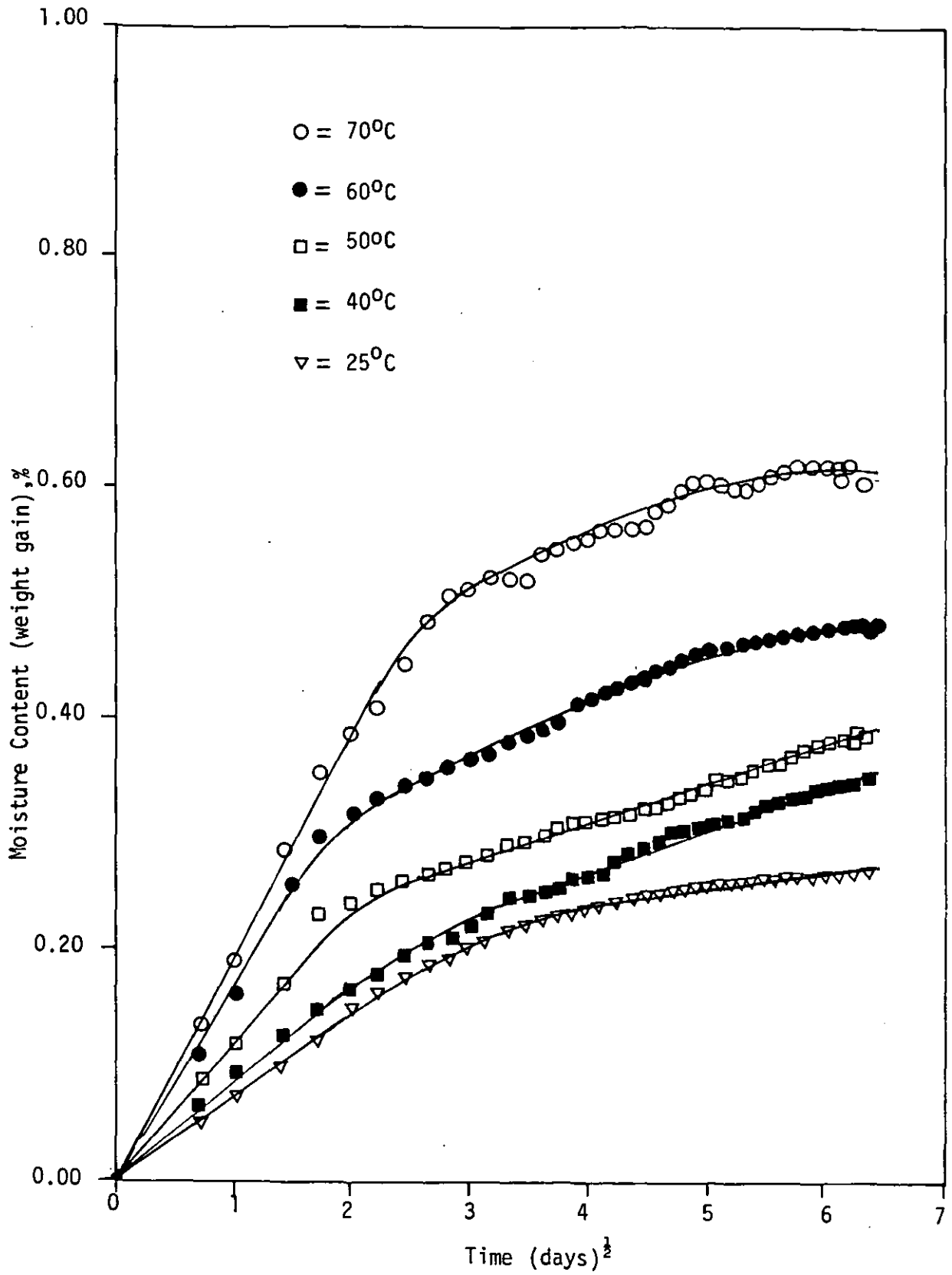


FIGURE 93: Weight change of 411-45 Vinylester specimens exposed to 95% RH at different temperatures as a function of time (fibre orientation 0°)

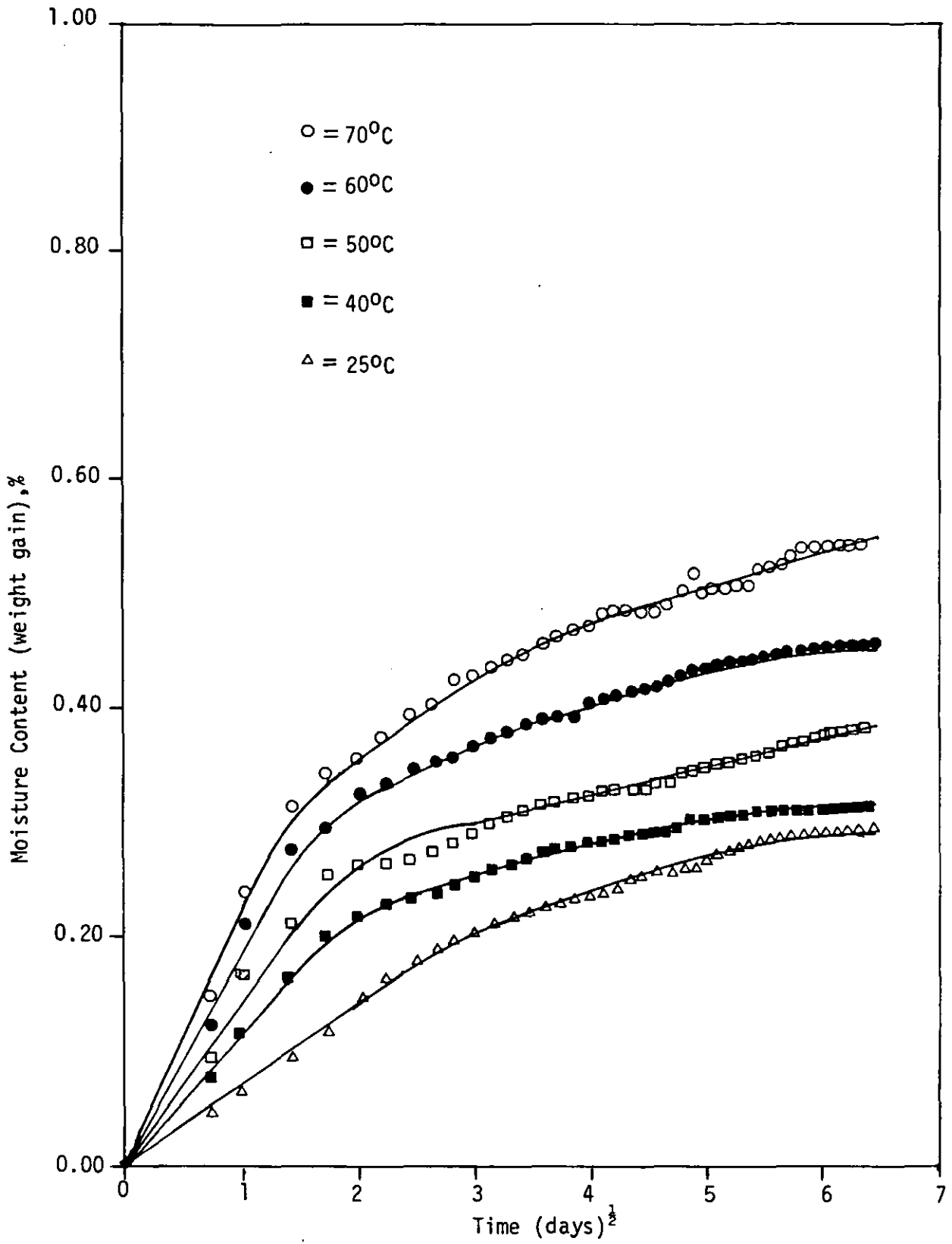


FIGURE 94: Weight change of 411-45 Vinylester specimens exposed to 95% RH at different temperatures as a function of time (fibre orientation $\pm 45^\circ$)

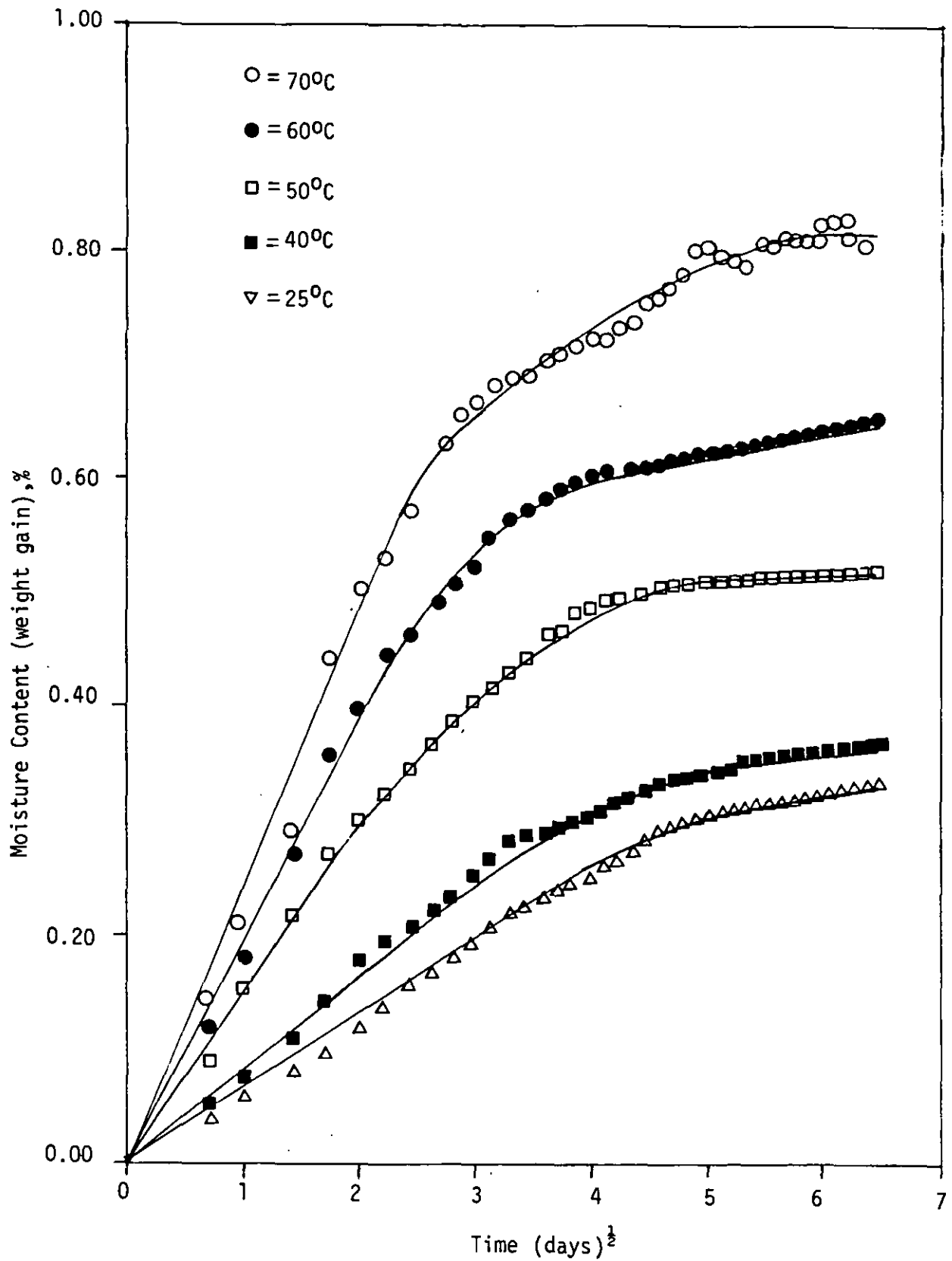


FIGURE 95: Weight change of 470-36 Vinylester specimens exposed to 95% RH at different temperatures as a function of time (fibre orientation 0°)

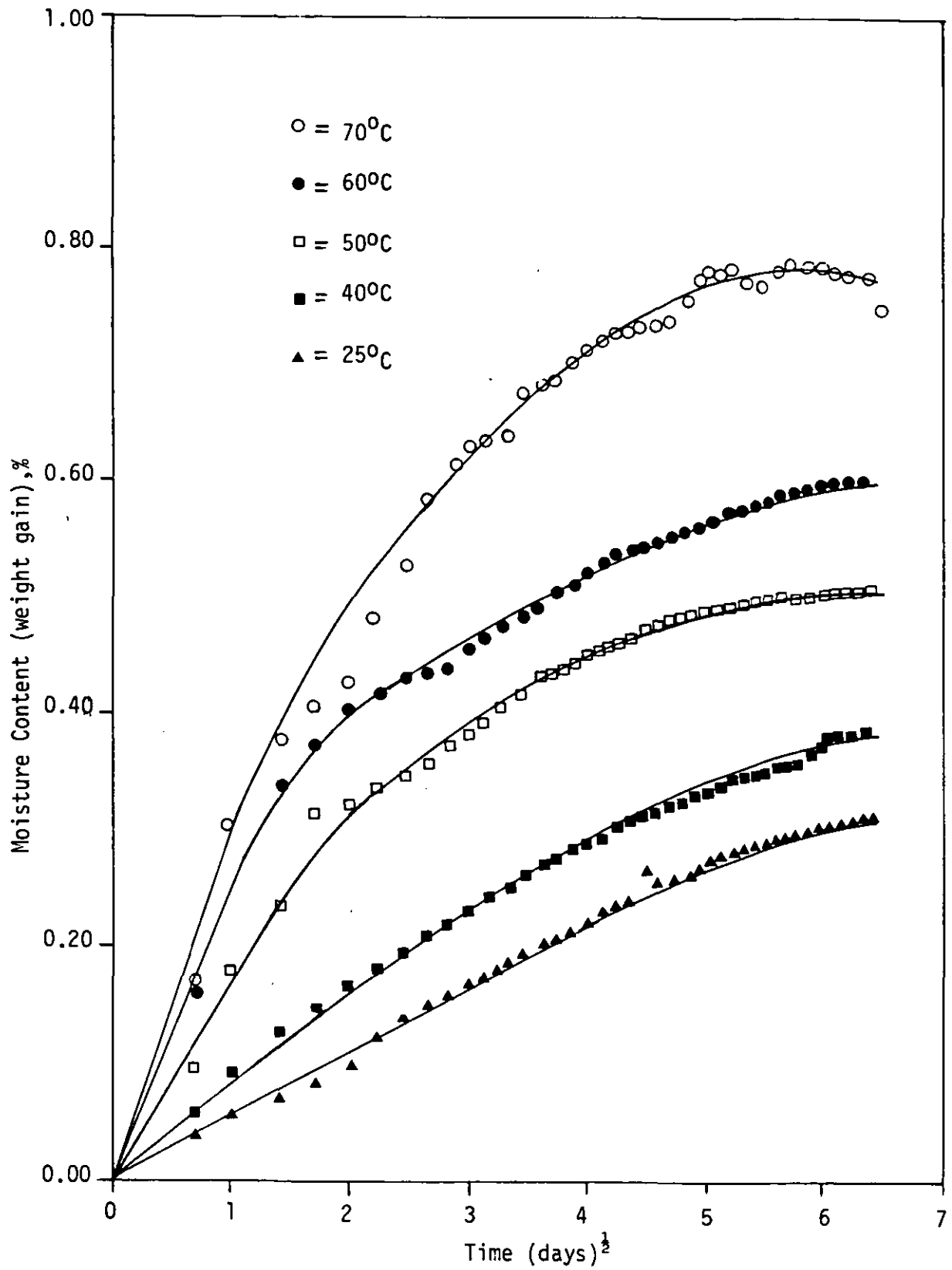


FIGURE 96: Weight change of 470-36 Vinylester specimens exposed to 95% RH at different temperatures as a function of time (fibre orientation $\pm 45^\circ$)

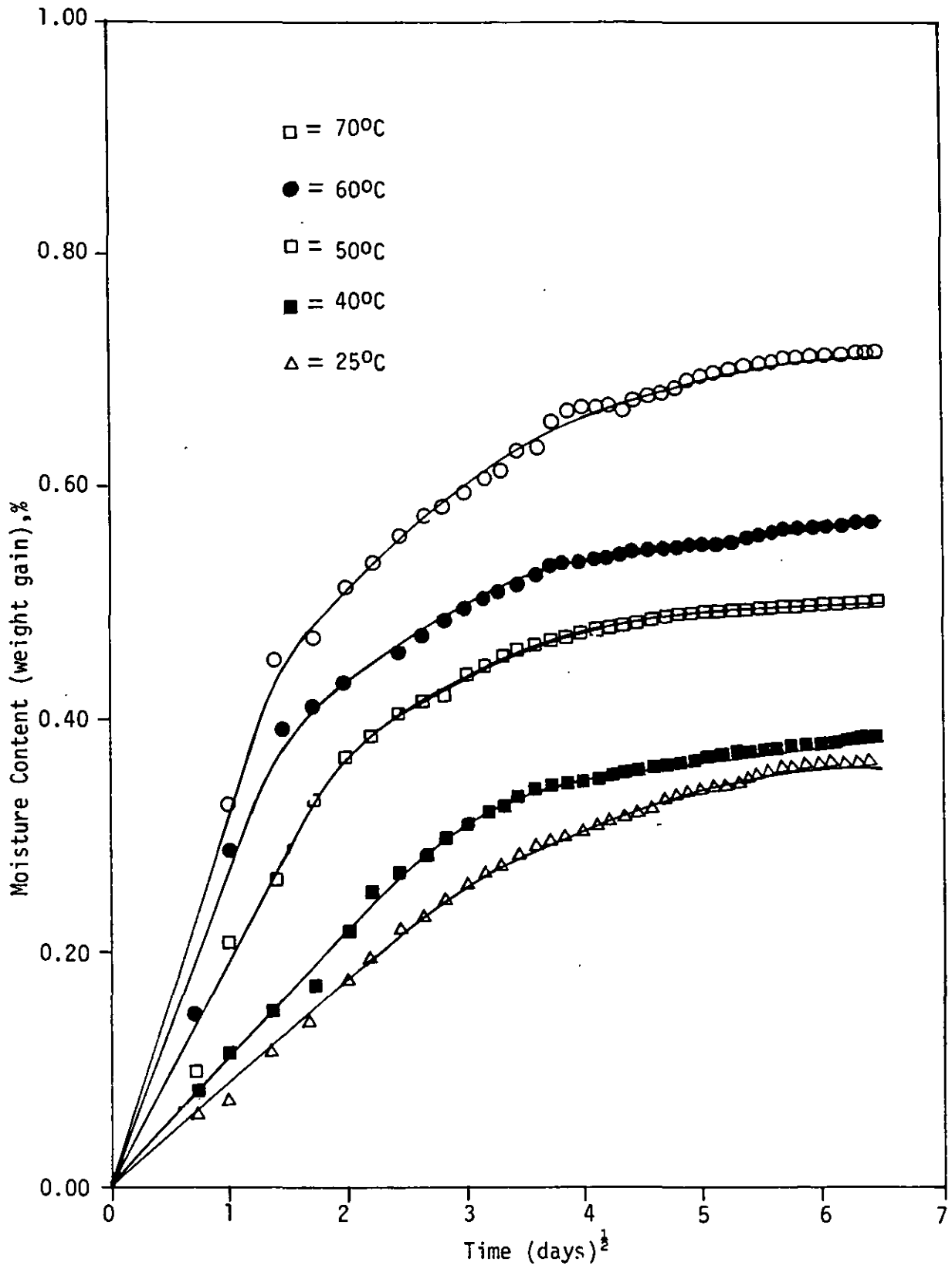


FIGURE 97: Weight change of Polyester 272 specimens exposed to 95% RH at different temperatures as a function of time (fibre orientation 0°)

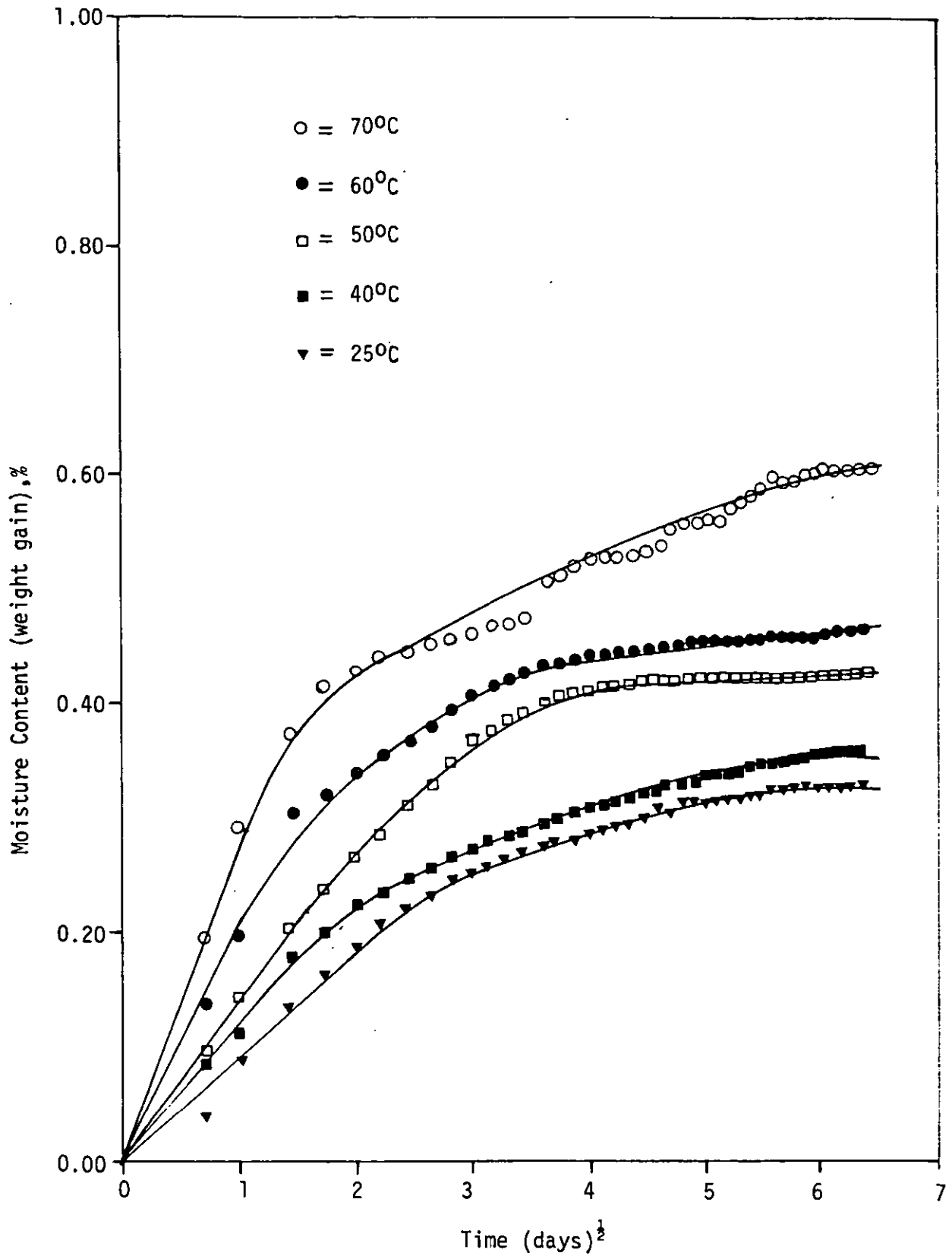


FIGURE 98: Weight change of Polyester 272 specimens exposed to 95% RH at different temperatures as a function of time (fibre orientation $\pm 45^\circ$)

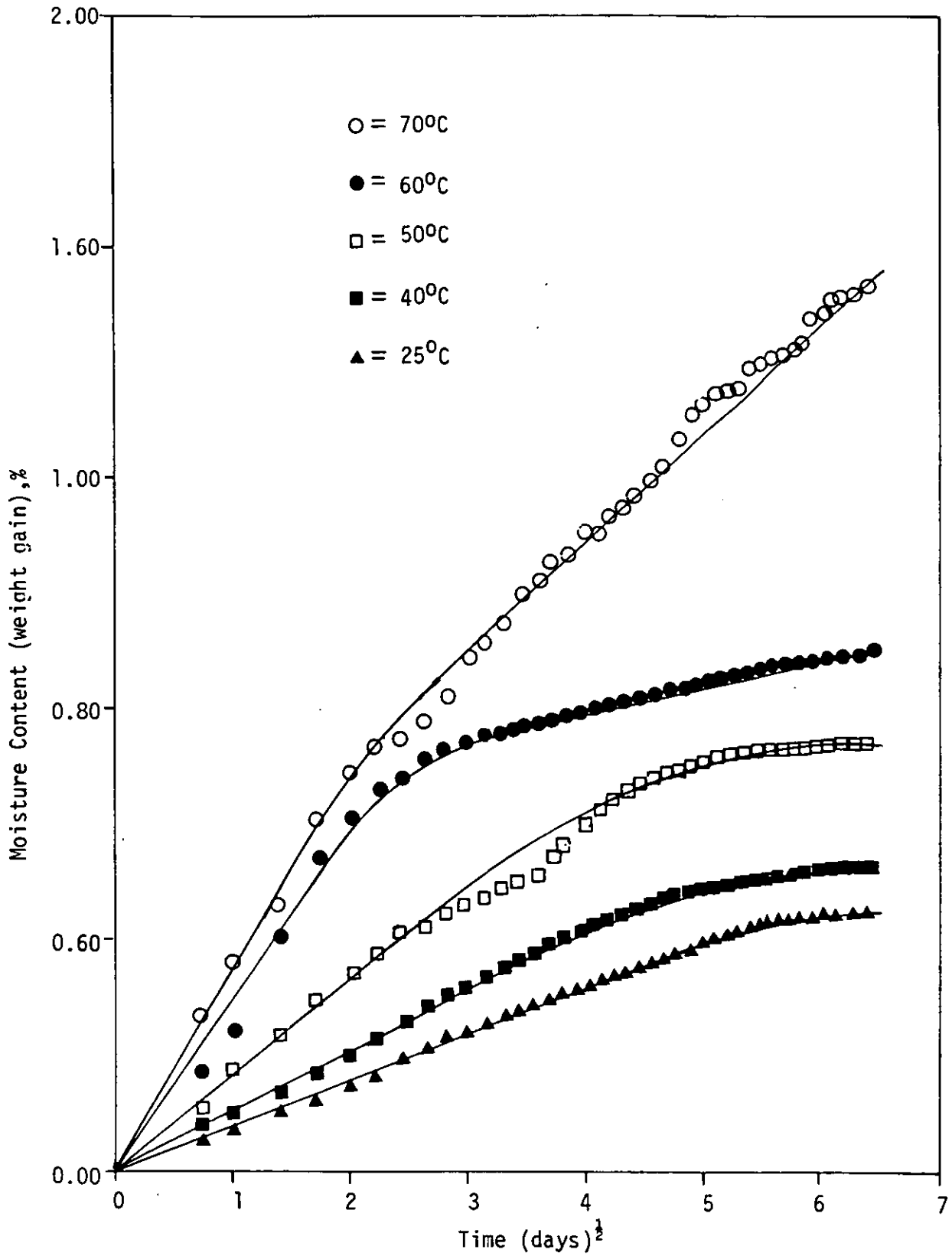


FIGURE 99: Weight change of Epoxy MY750 specimens exposed to 95% RH at different temperatures as a function of time (fibre orientation 0°)

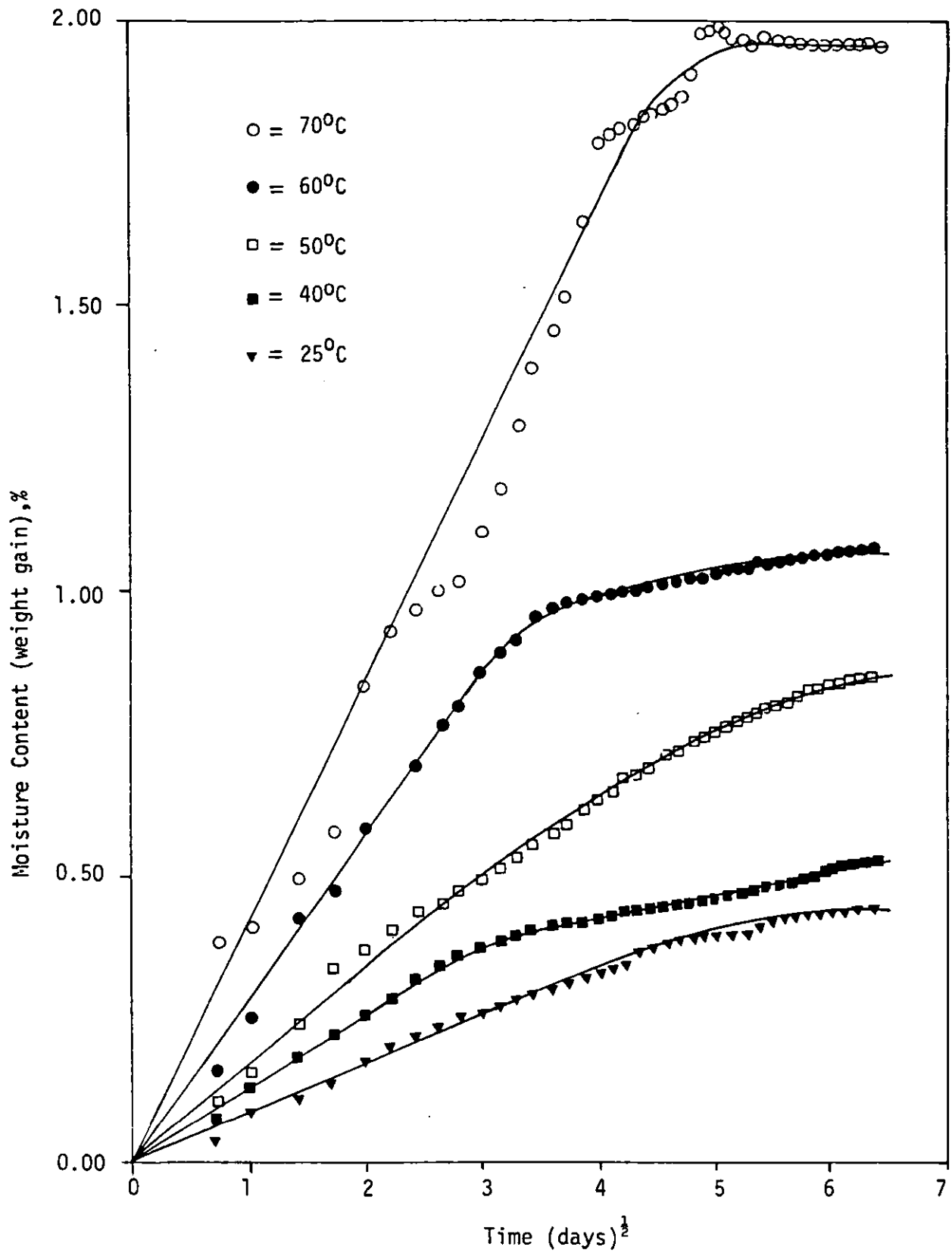


FIGURE 100: Weight change of Epoxy MY750 specimens exposed to 95% RH at different temperatures as a function of time (fibre orientation $\pm 45^\circ$)

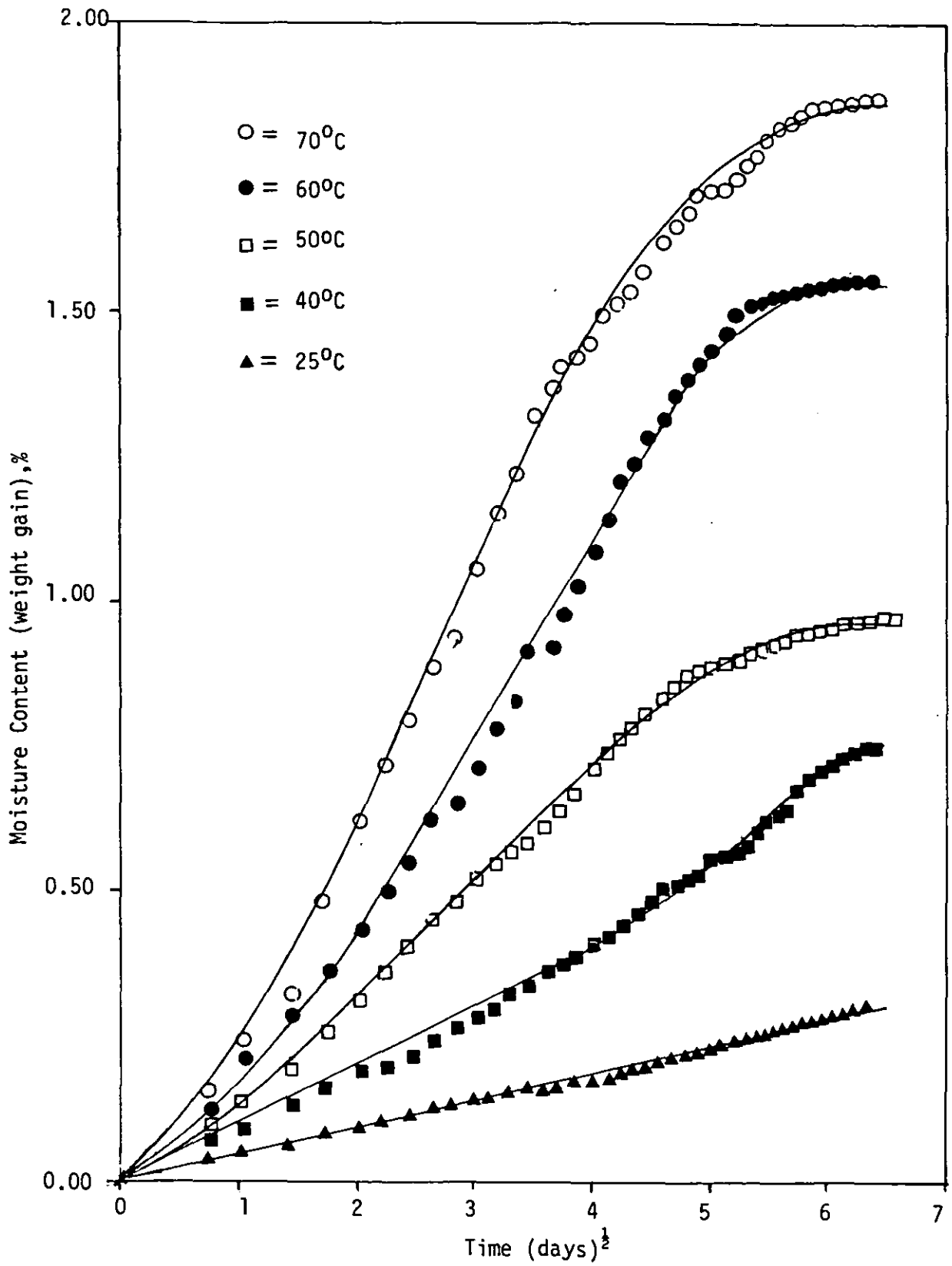


FIGURE 101: Weight change of 913 PrePreg specimens exposed to 95% RH at different temperatures as a function of time (fibre orientation 0°)

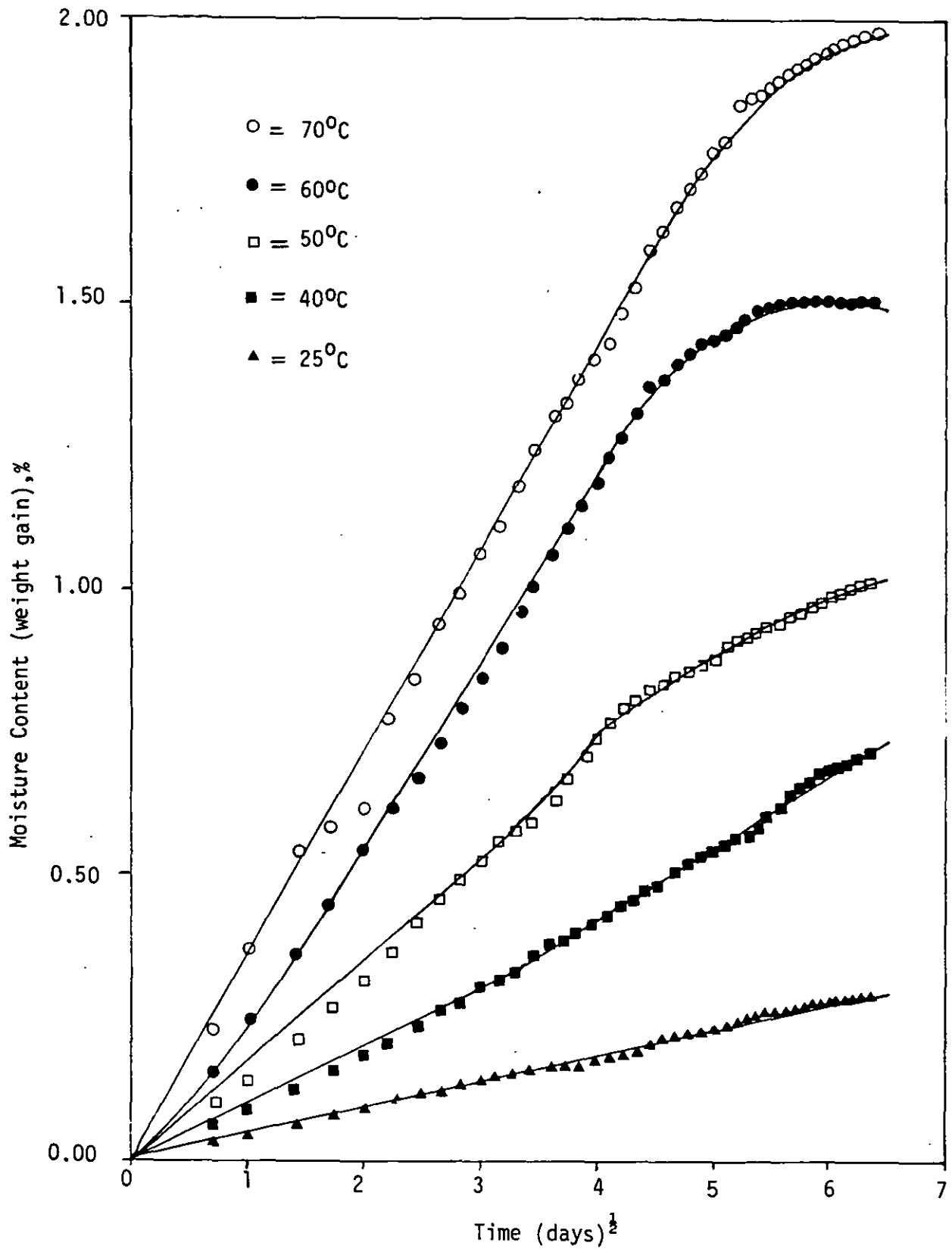


FIGURE 102: Weight change of 913 PrePreg specimens exposed to 95% RH at different temperatures as a function of time (fibre orientation $\pm 45^\circ$)

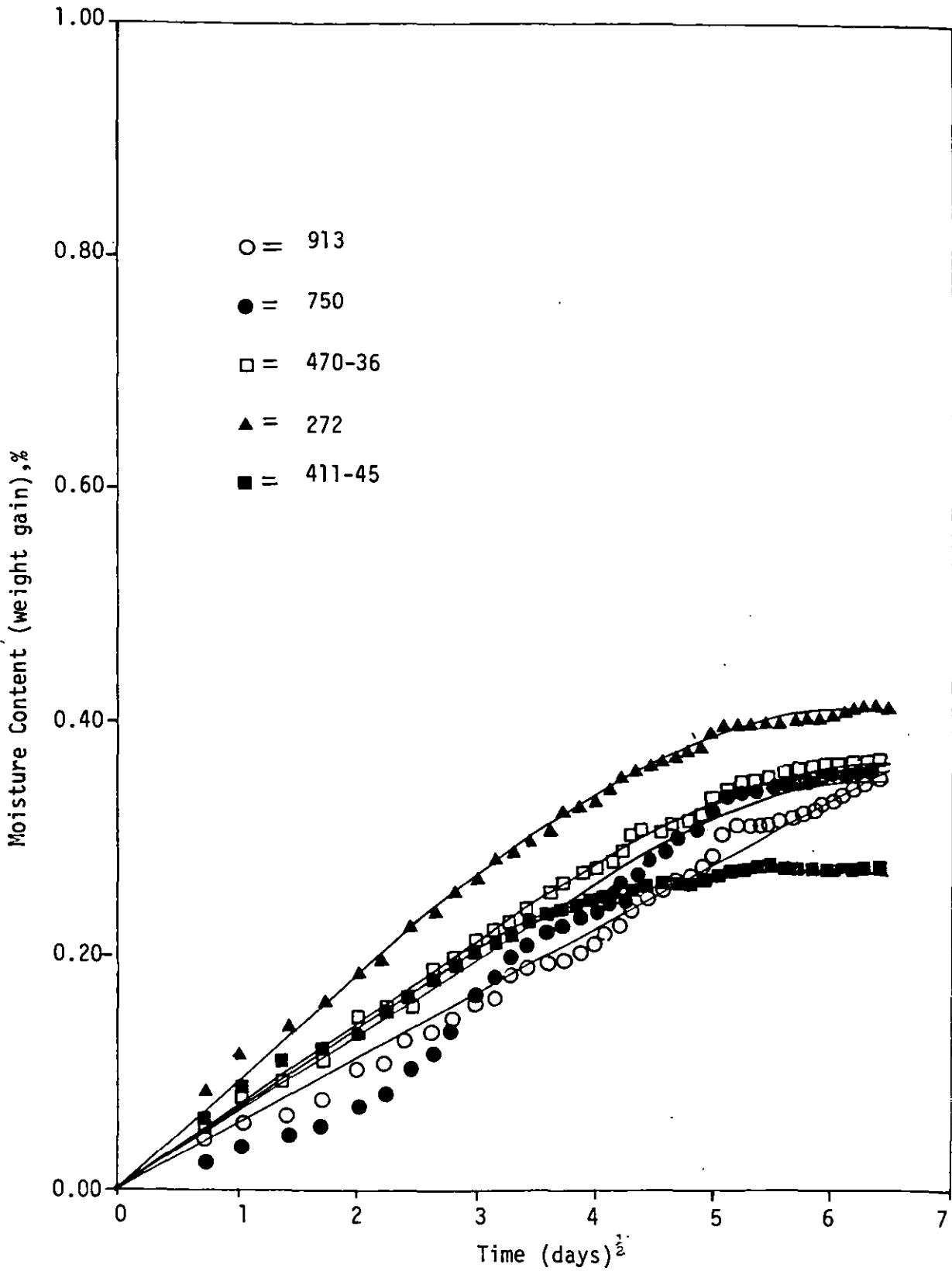


FIGURE 103: Weight change of specimens immersed in distilled water at 25°C as a function of time' (fibre orientation 0°)

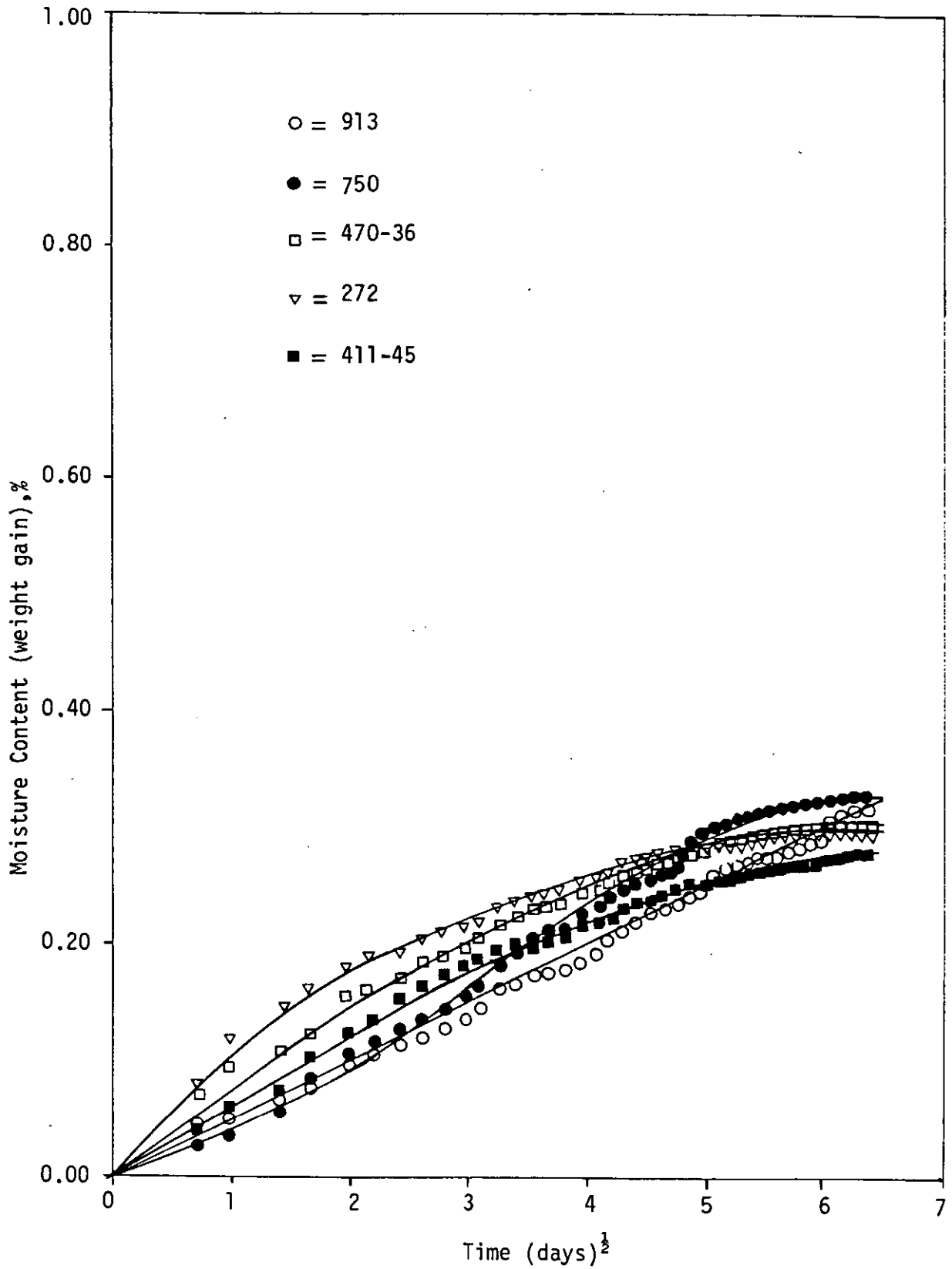


FIGURE 104: Weight change of specimens immersed in distilled water at 25°C as a function of time (fibre orientation $\pm 45^\circ$)

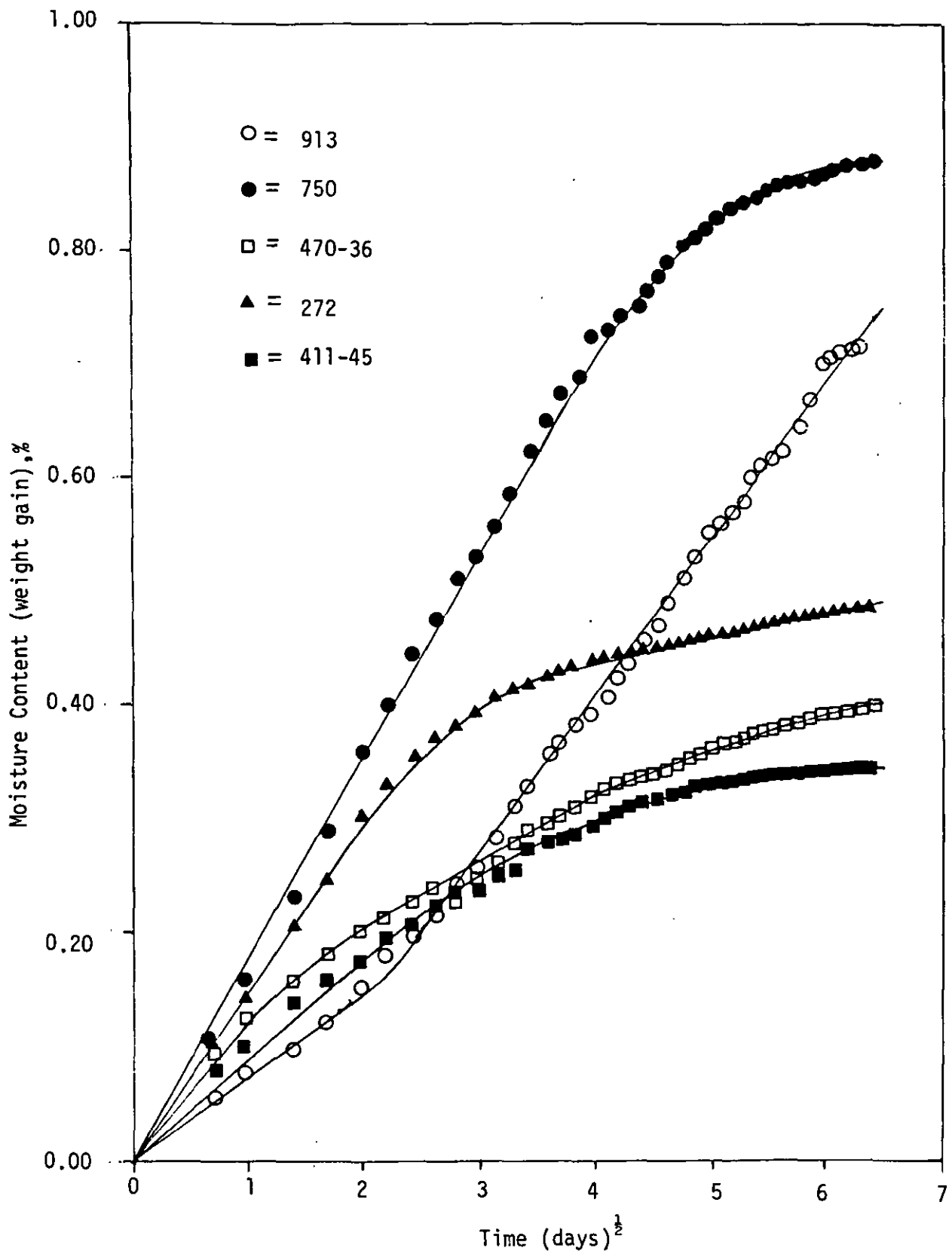


FIGURE 105: Weight change of specimens immersed in distilled water at 40°C as a function of time (fibre orientation 0°)

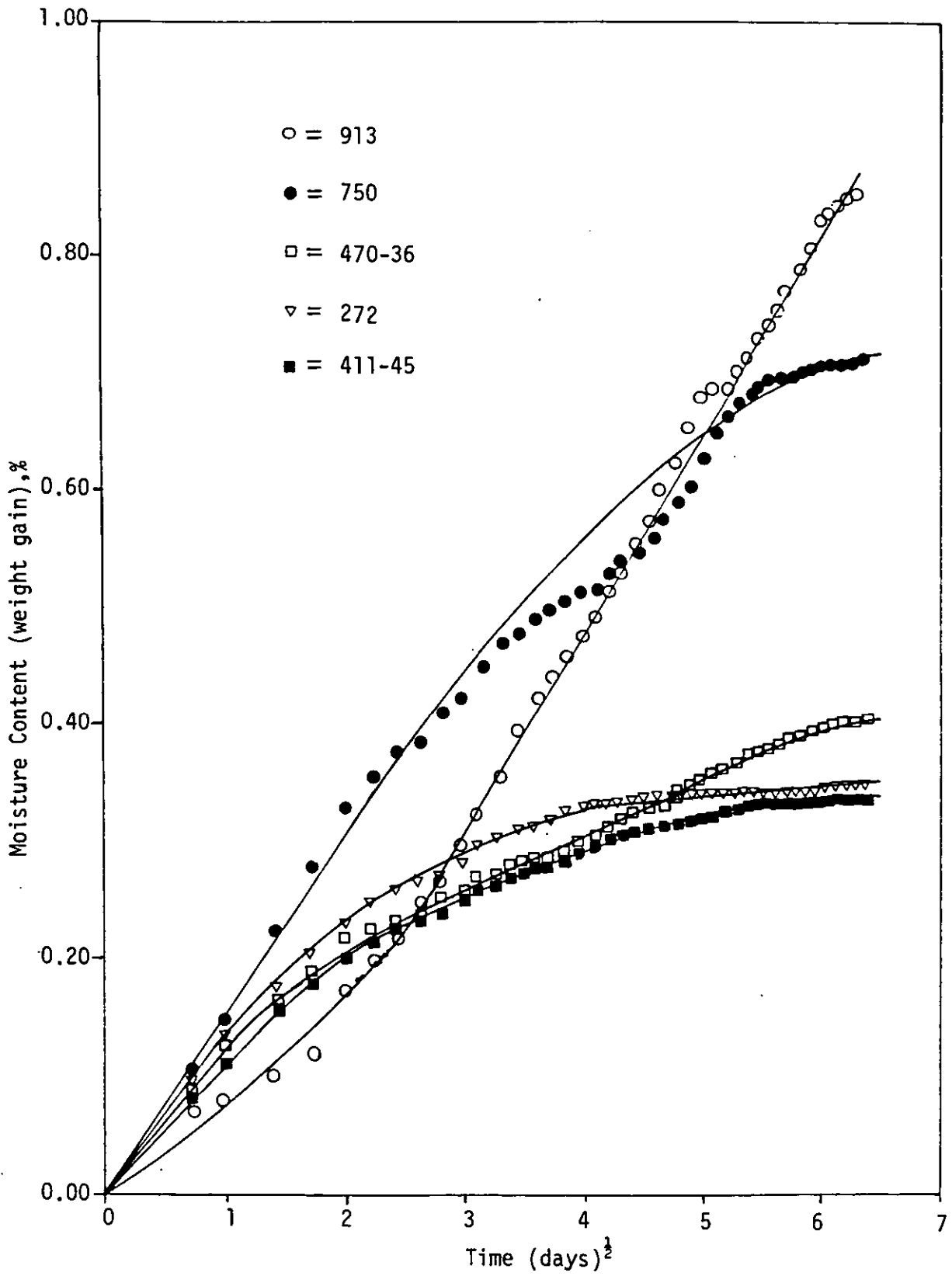


FIGURE 106: Weight change of specimens immersed in distilled water at 40°C as a function of time (fibre orientation $\pm 45^\circ$)

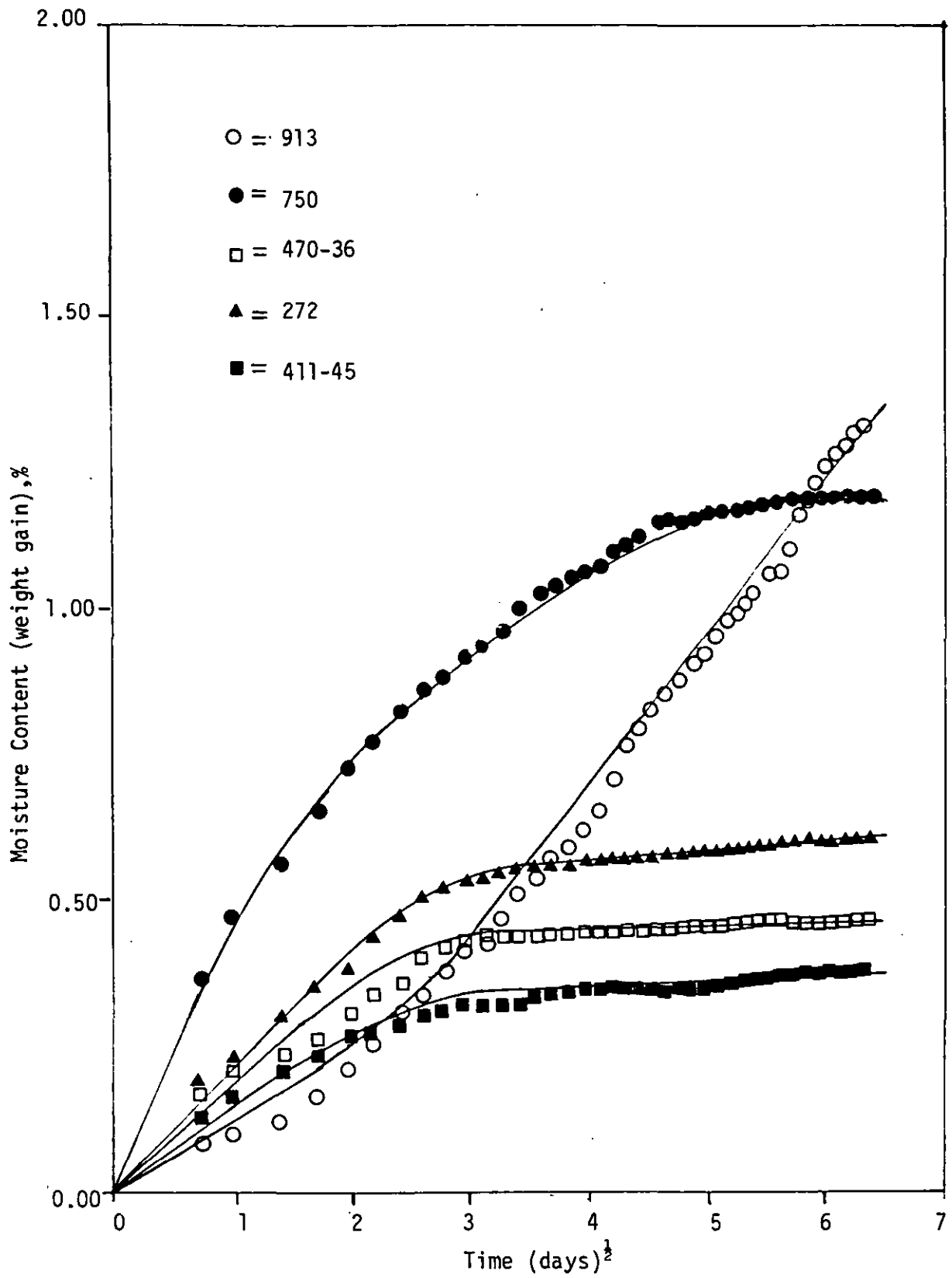


FIGURE 107: Weight change of specimens immersed in distilled water at 50°C as a function of time (fibre orientation 0°)

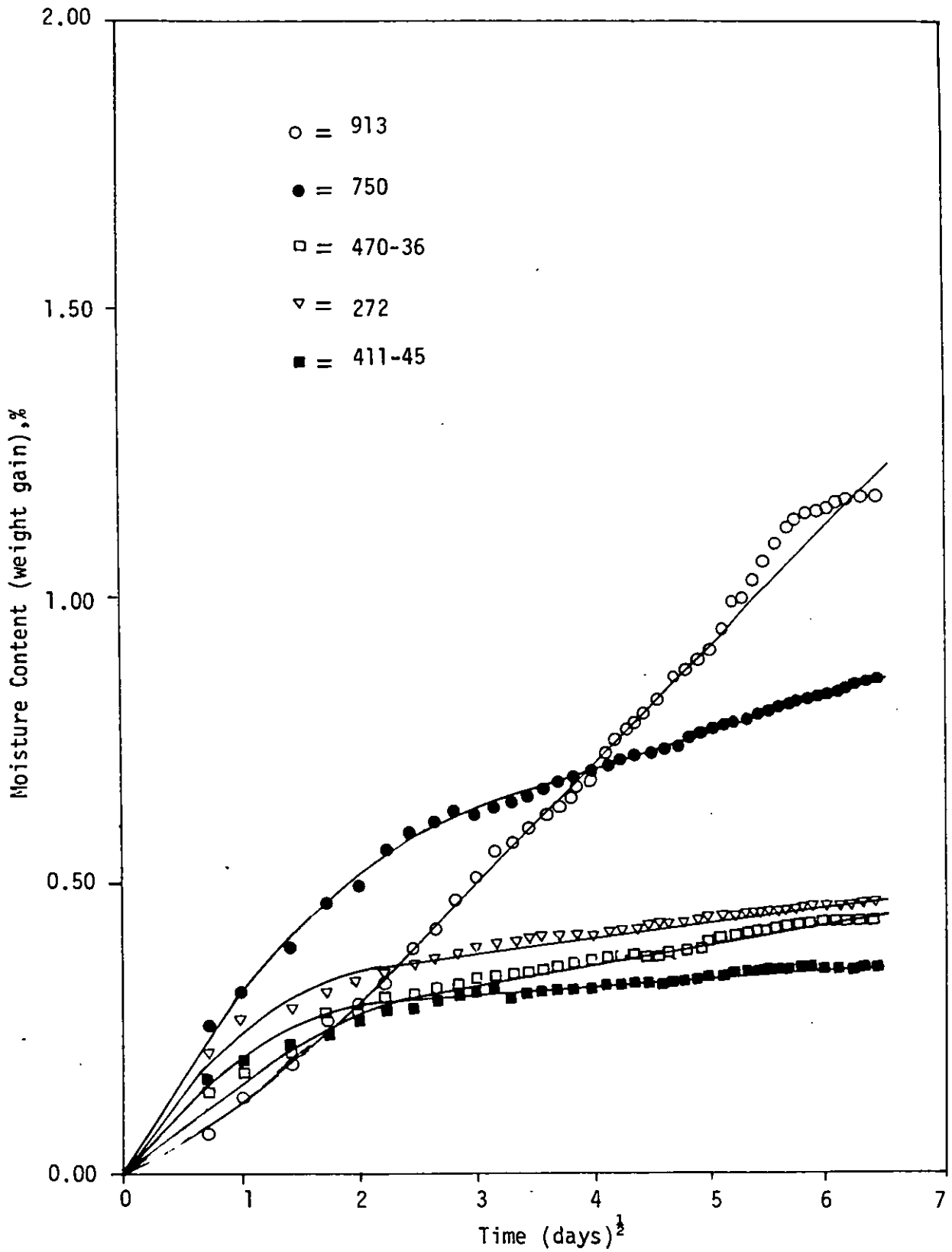


FIGURE 108: Weight change of specimens immersed in distilled water at 50°C as a function of time (fibre orientation $\pm 45^\circ$)

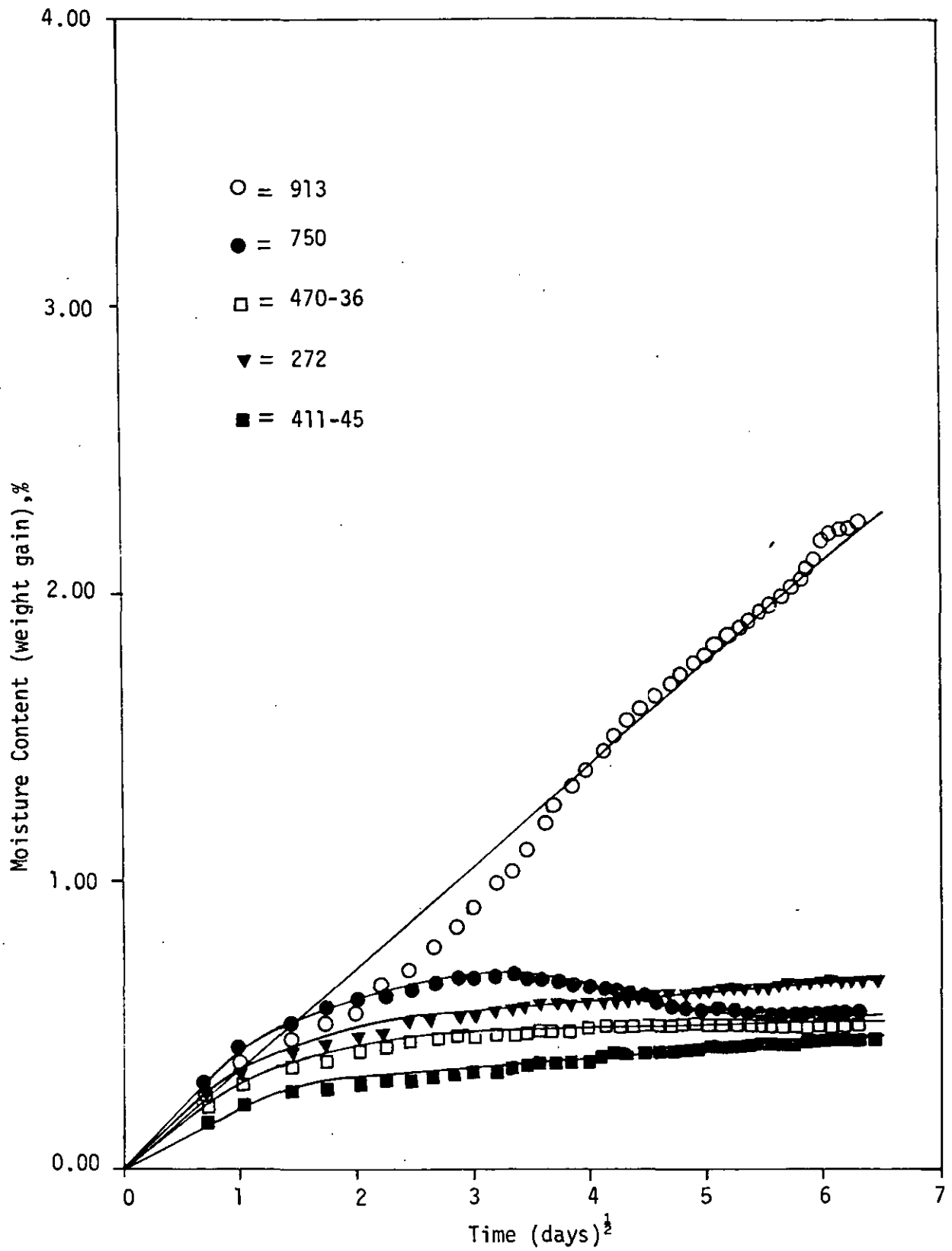


FIGURE 109: Weight change of specimens immersed in distilled water at 60°C as a function of time (fibre orientation 0°)

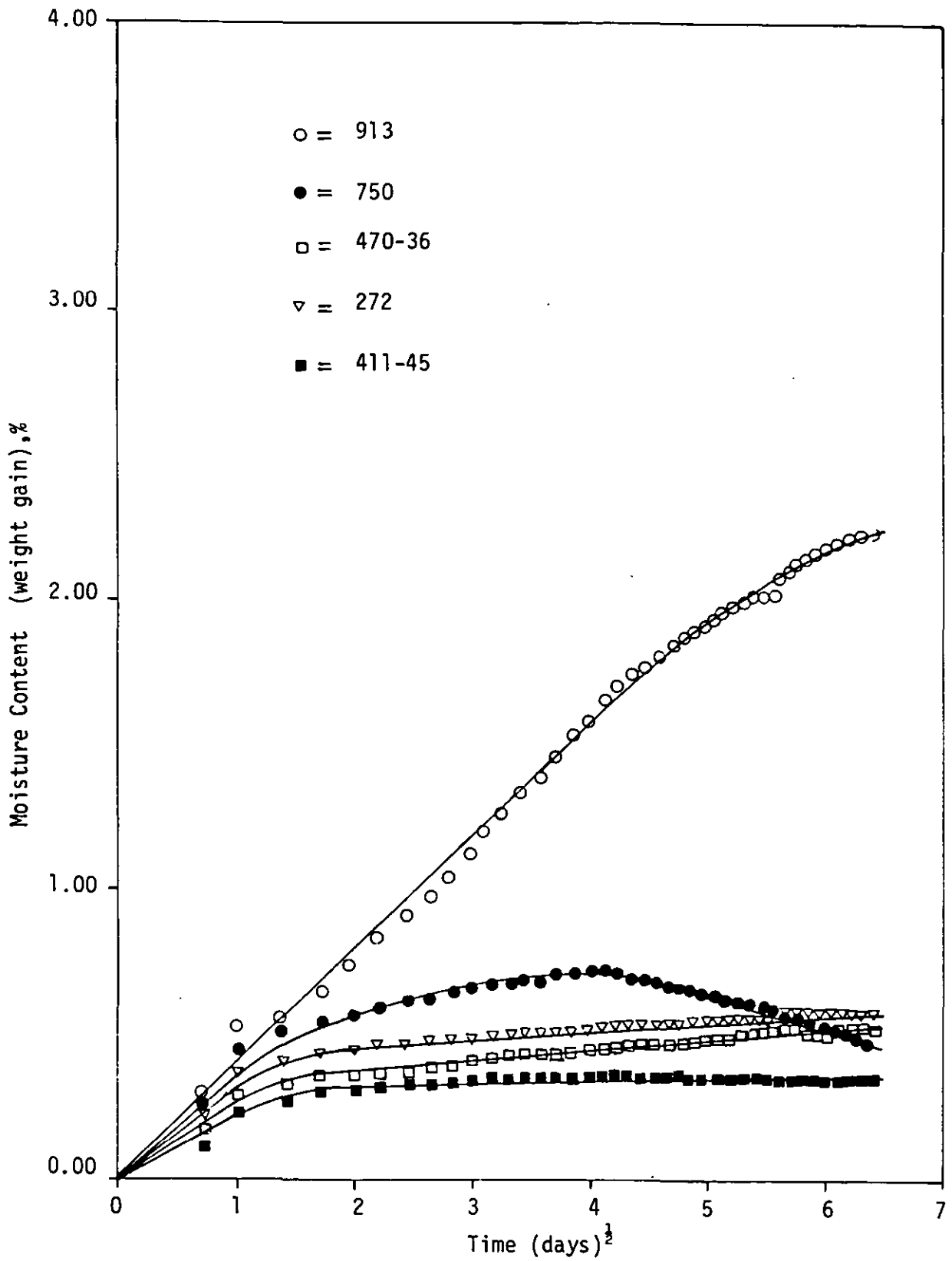


FIGURE 110: Weight change of specimens immersed in distilled water at 60°C as a function of time (fibre orientation $\pm 45^\circ$)

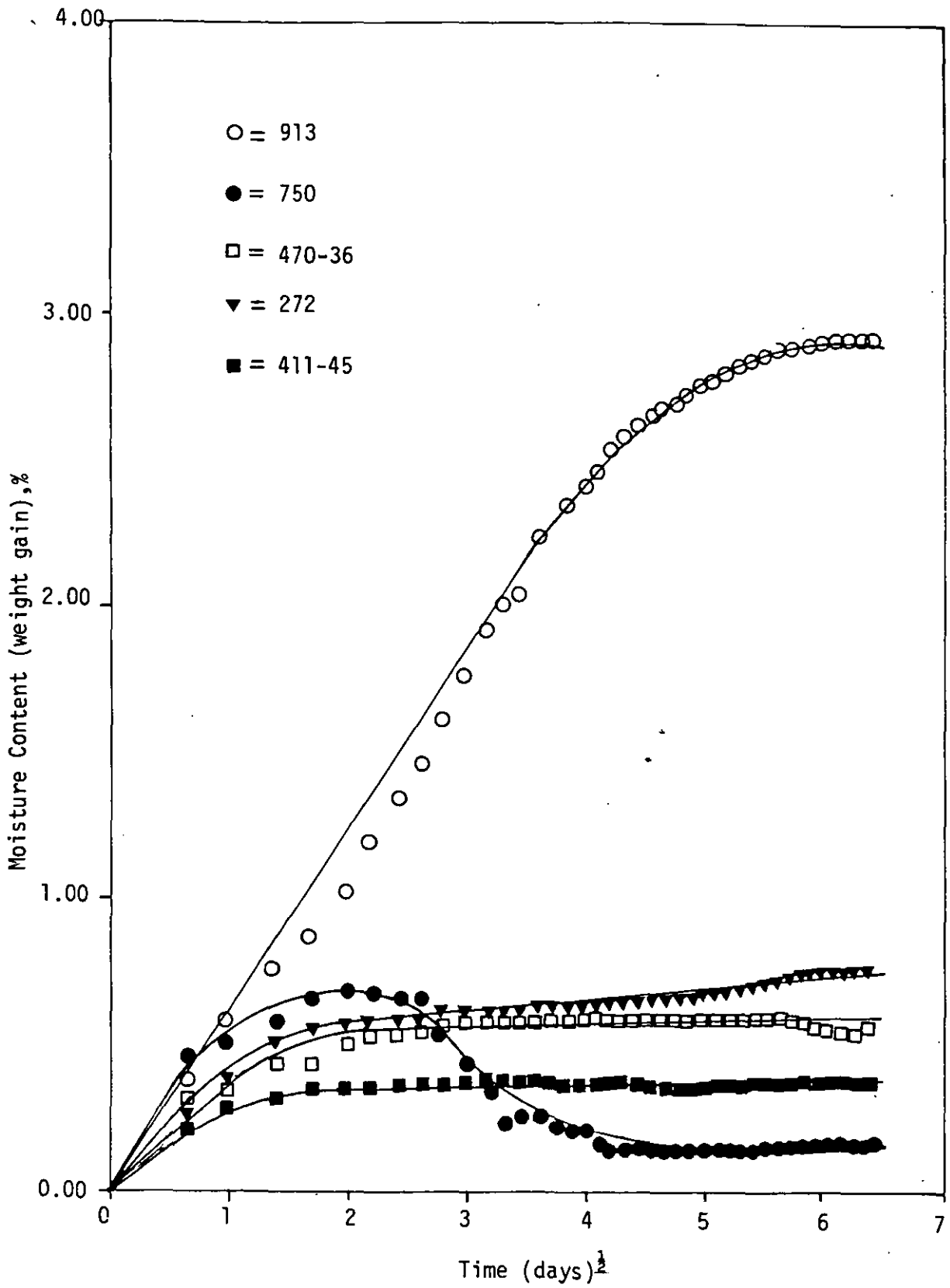


FIGURE 111: Weight change of specimens immersed in distilled water at 70°C as a function of time (fibre orientation 0°)

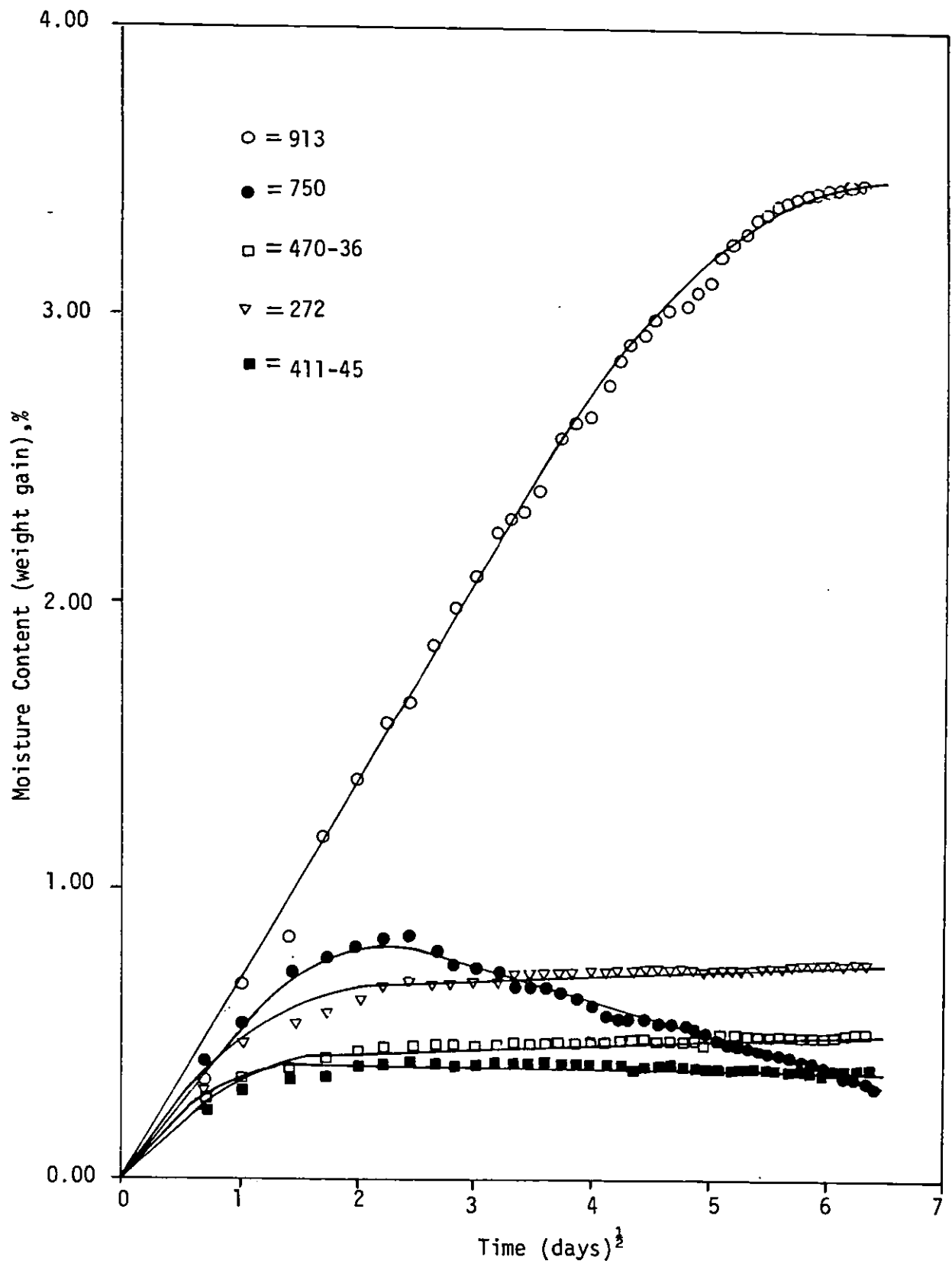


FIGURE 112: Weight change of specimens immersed in distilled water at 70°C as a function of time (fibre orientation $\pm 45^\circ$)

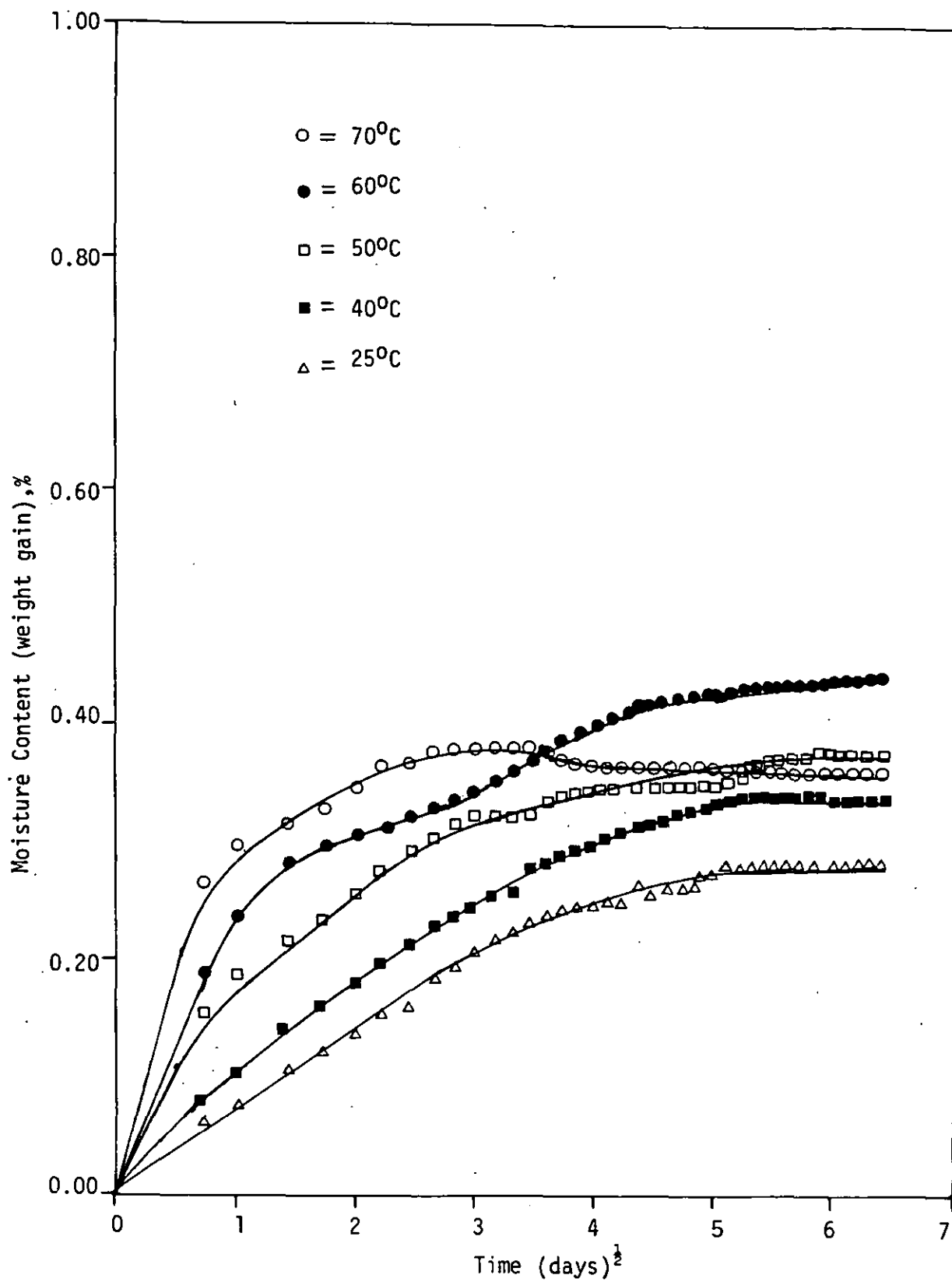


FIGURE 113: Weight change of 411-45 Vinylester specimens immersed in distilled water at different temperatures as a function of time (fibre orientation 0°)

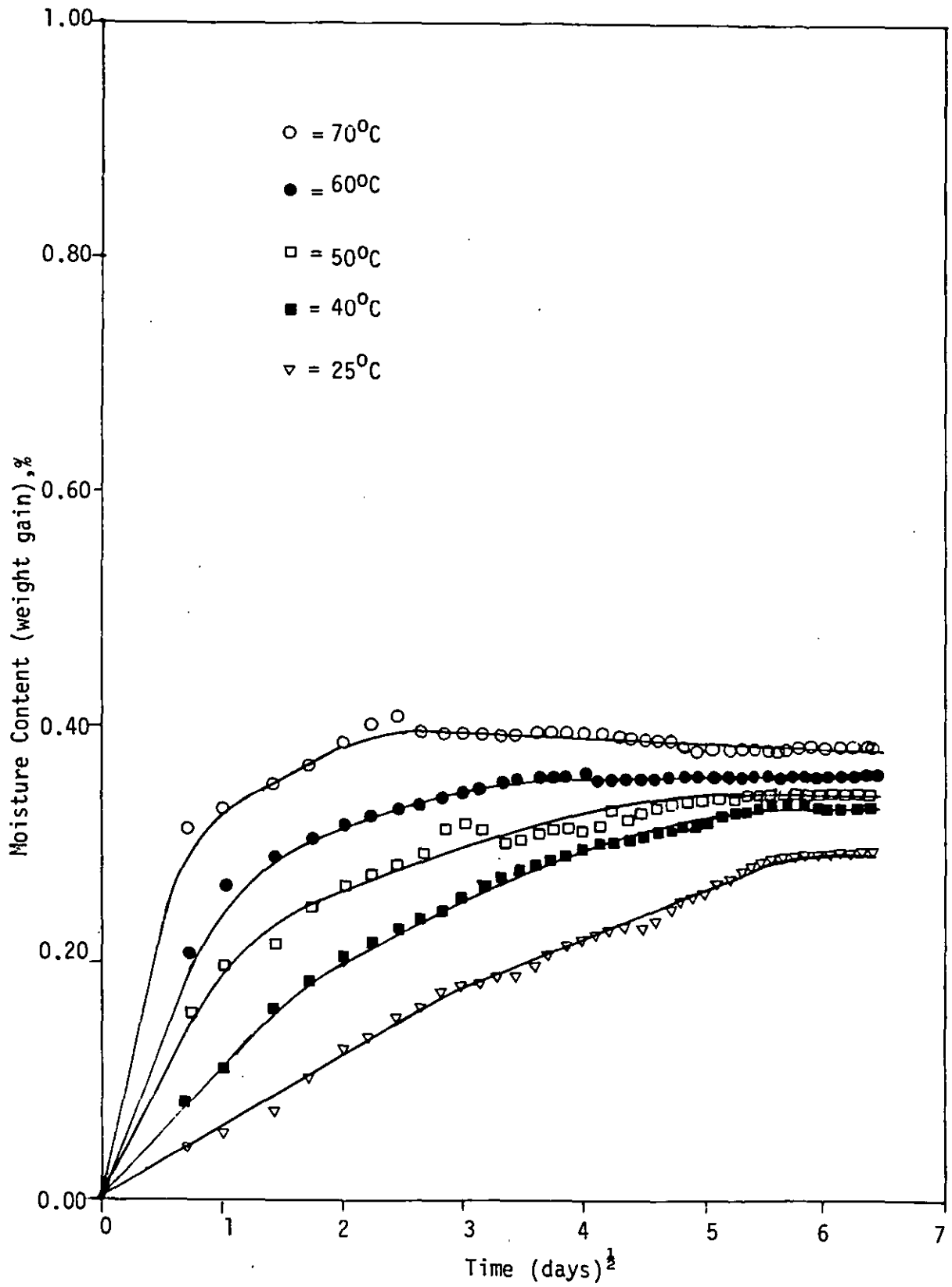


FIGURE 114: Weight change of 411-45 Vinylester specimens immersed in distilled water at different temperatures as a function of time (fibre orientation $\pm 45^\circ$)

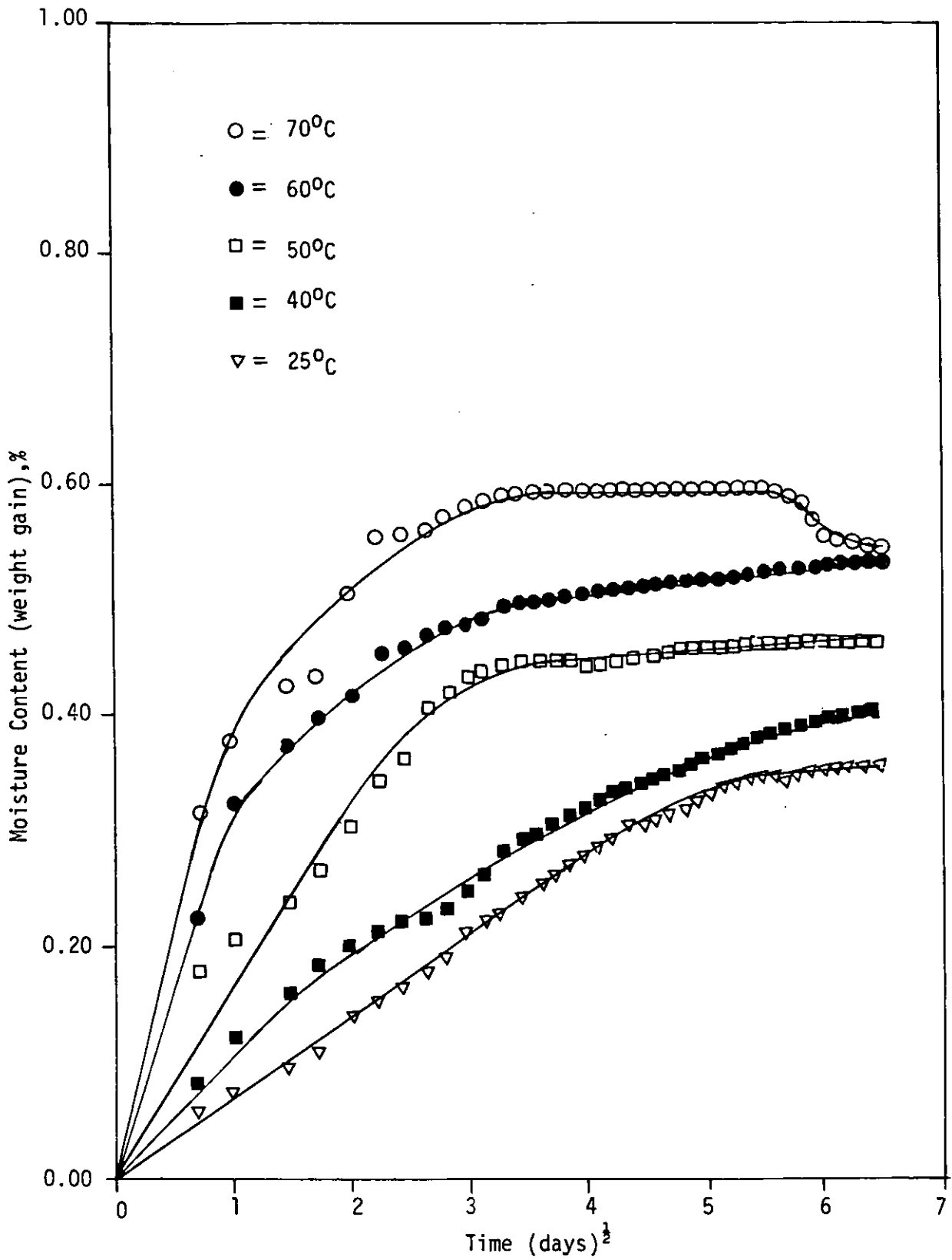


FIGURE 115: Weight change of 470-36 Vinylester specimens immersed in distilled water at different temperatures as a function of time (fibre orientation 0°)

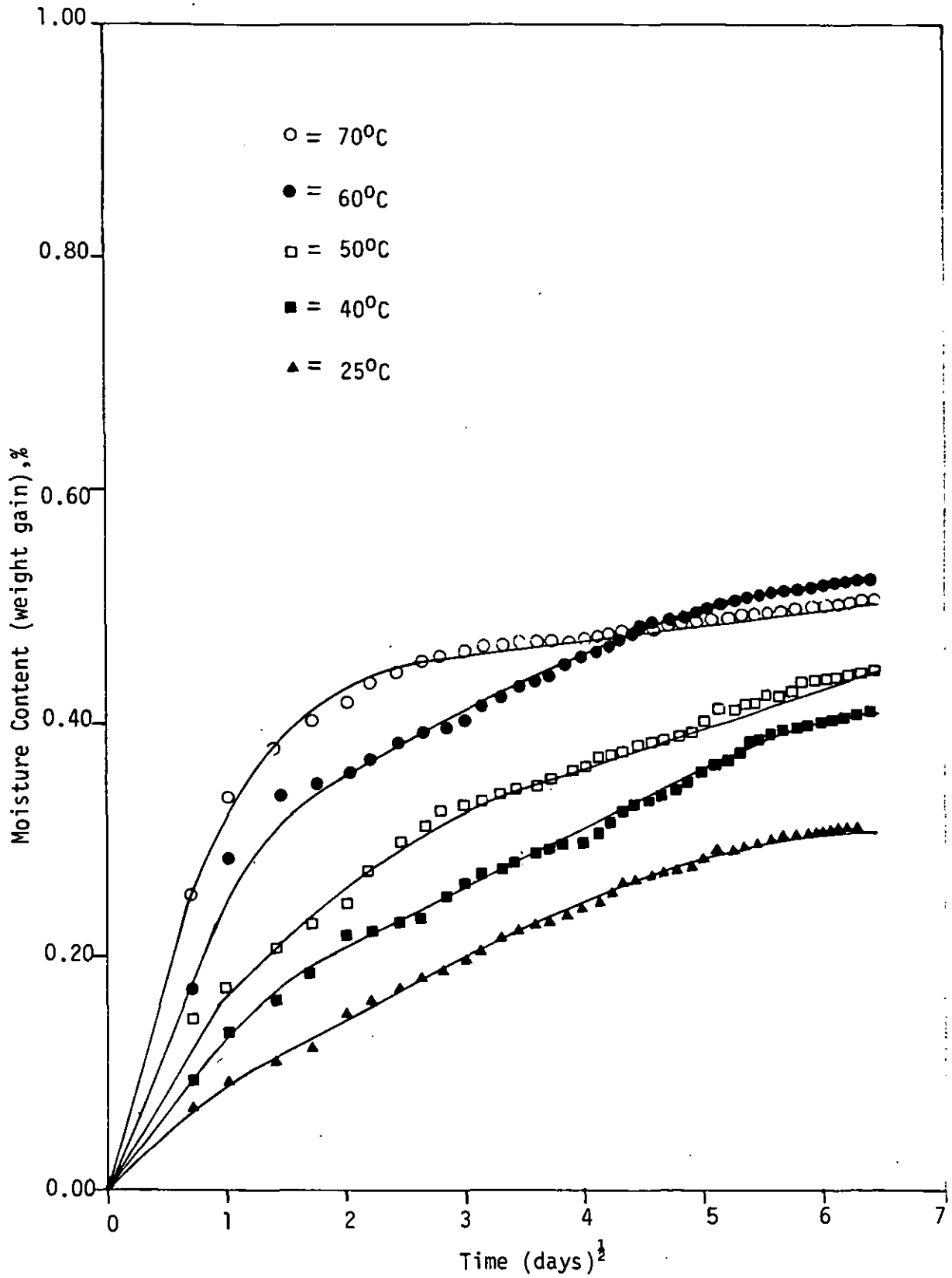


FIGURE 116: Weight change of 470-36 Vinylester specimens immersed in distilled water at different temperatures as a function of time (fibre orientation $\pm 45^\circ$)

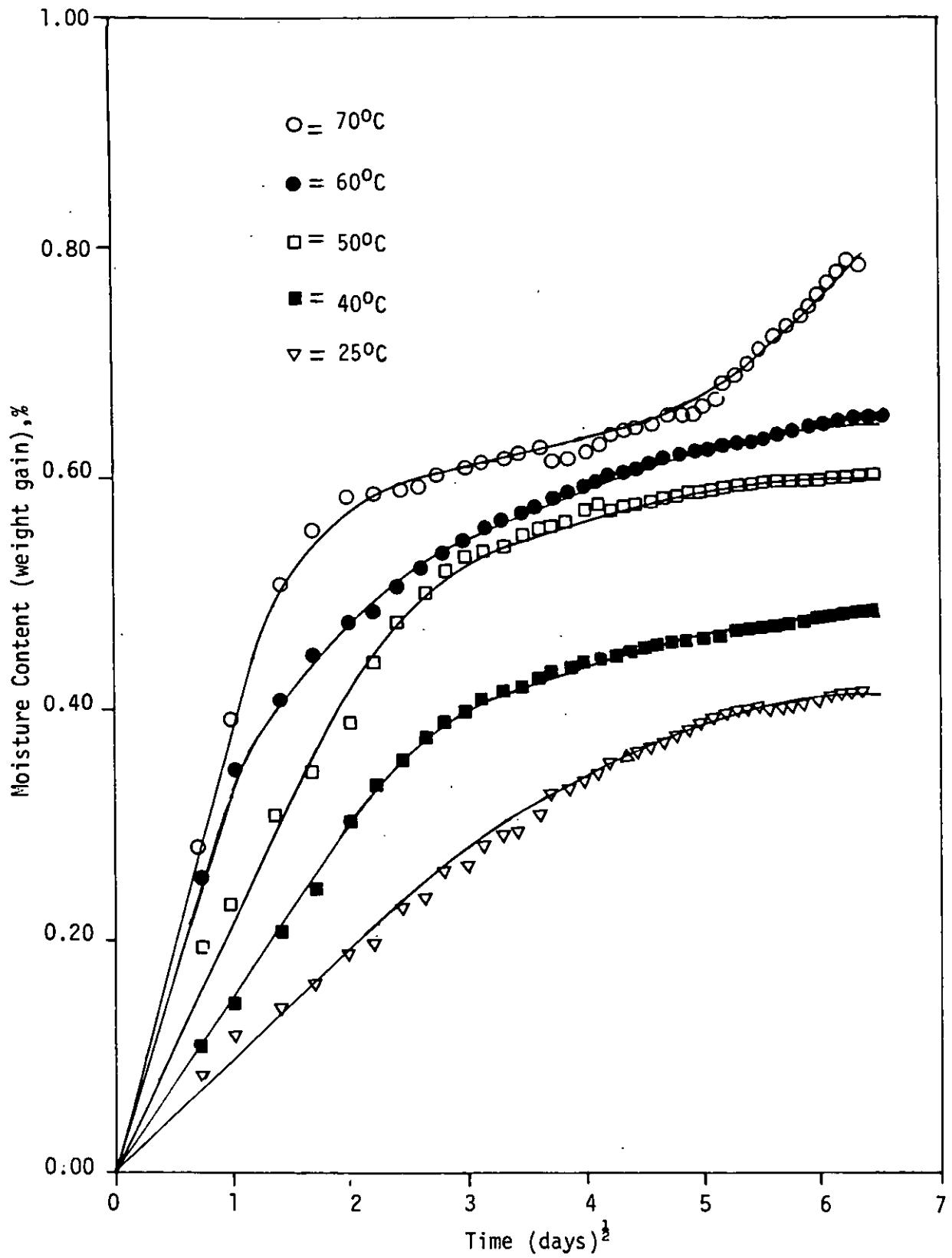


FIGURE 117: Weight change of Polyester 272 specimens immersed in distilled water at different temperatures as a function of time (fibre orientation 0°)

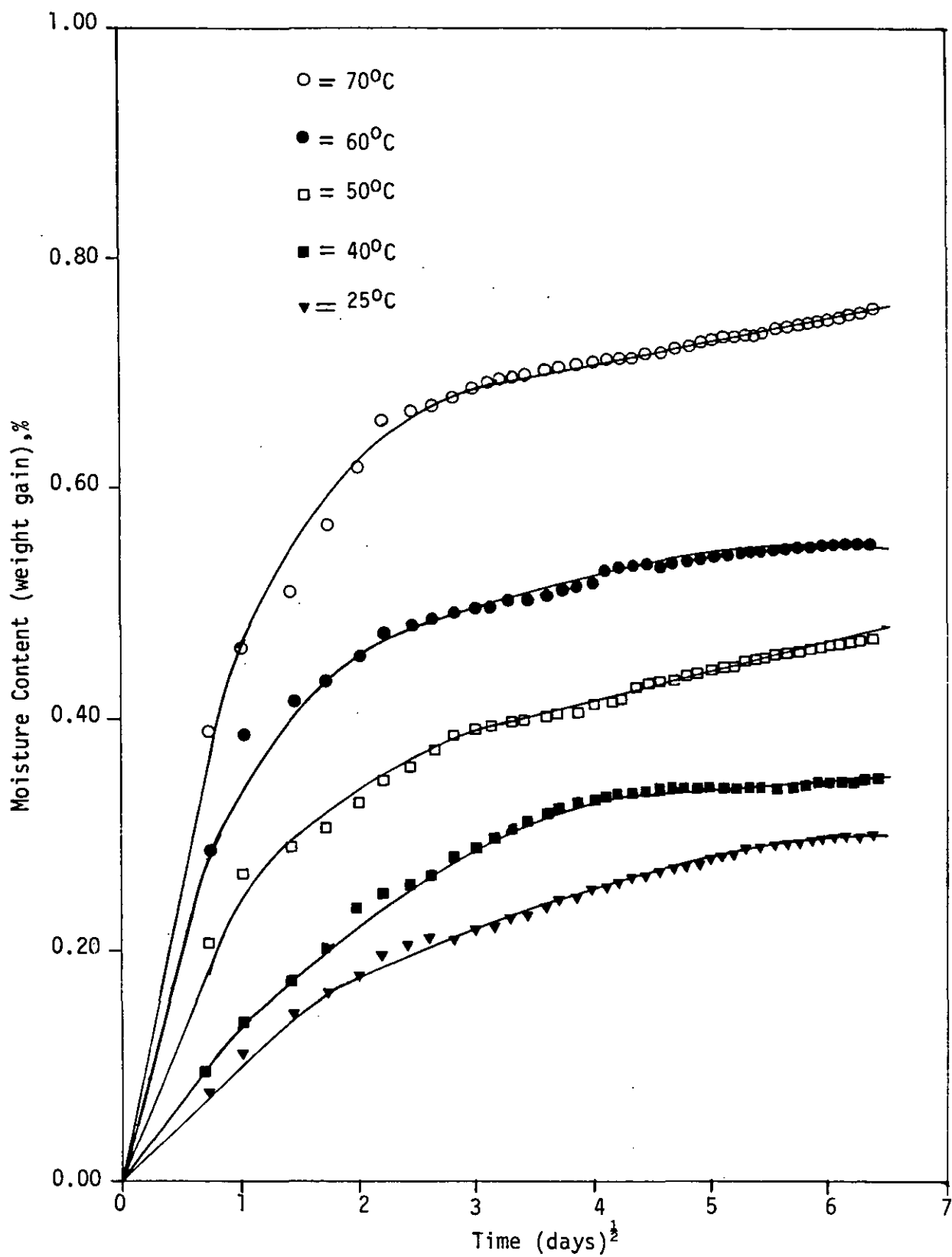


FIGURE 118: Weight change of Polyester 272 specimens immersed in distilled water at different temperatures as a function of time (fibre orientation $\pm 45^\circ$)

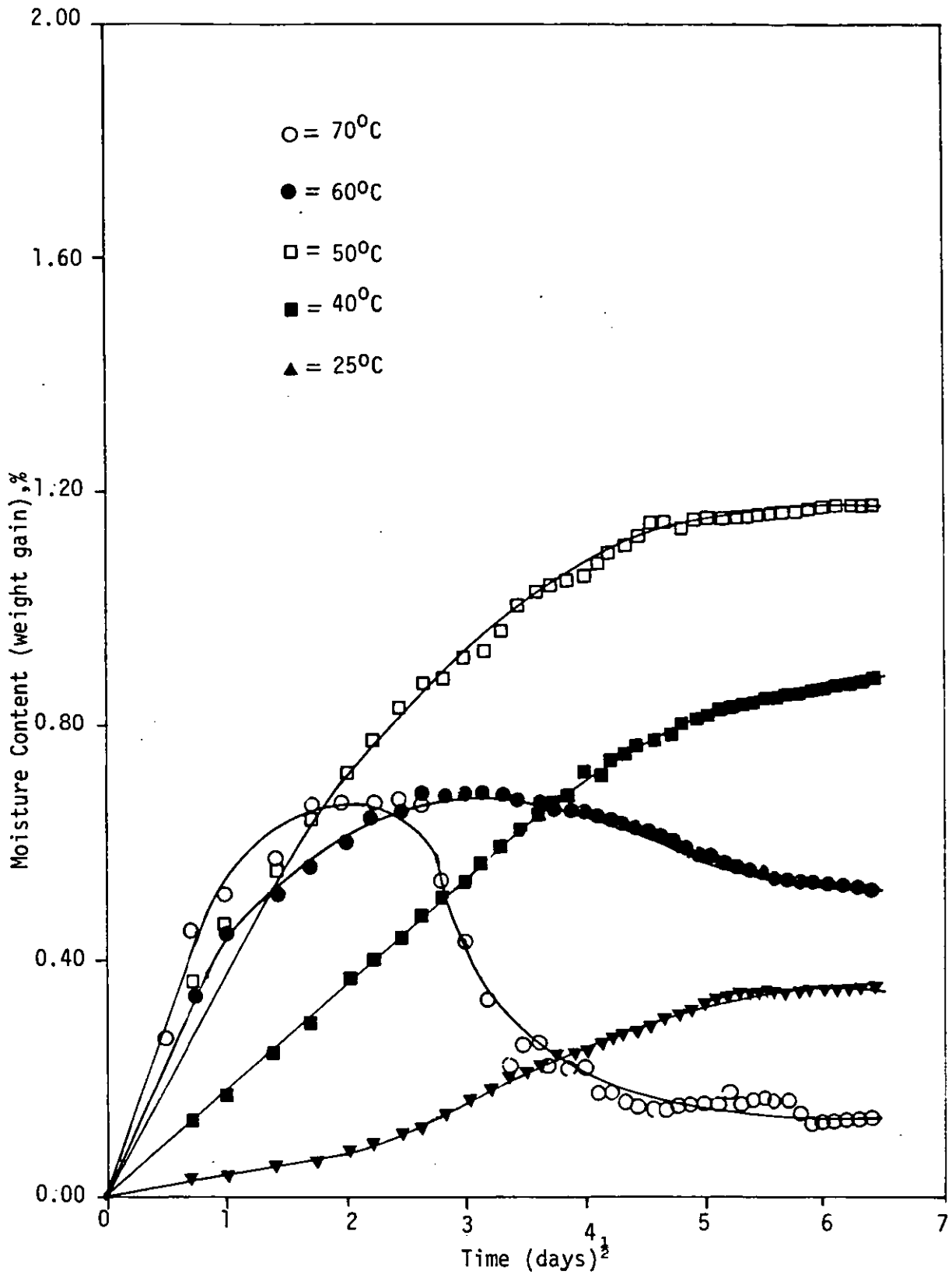


FIGURE 119: Weight change of Epoxy MY750 specimens immersed in distilled water at different temperatures as a function of time (fibre orientation 0°)

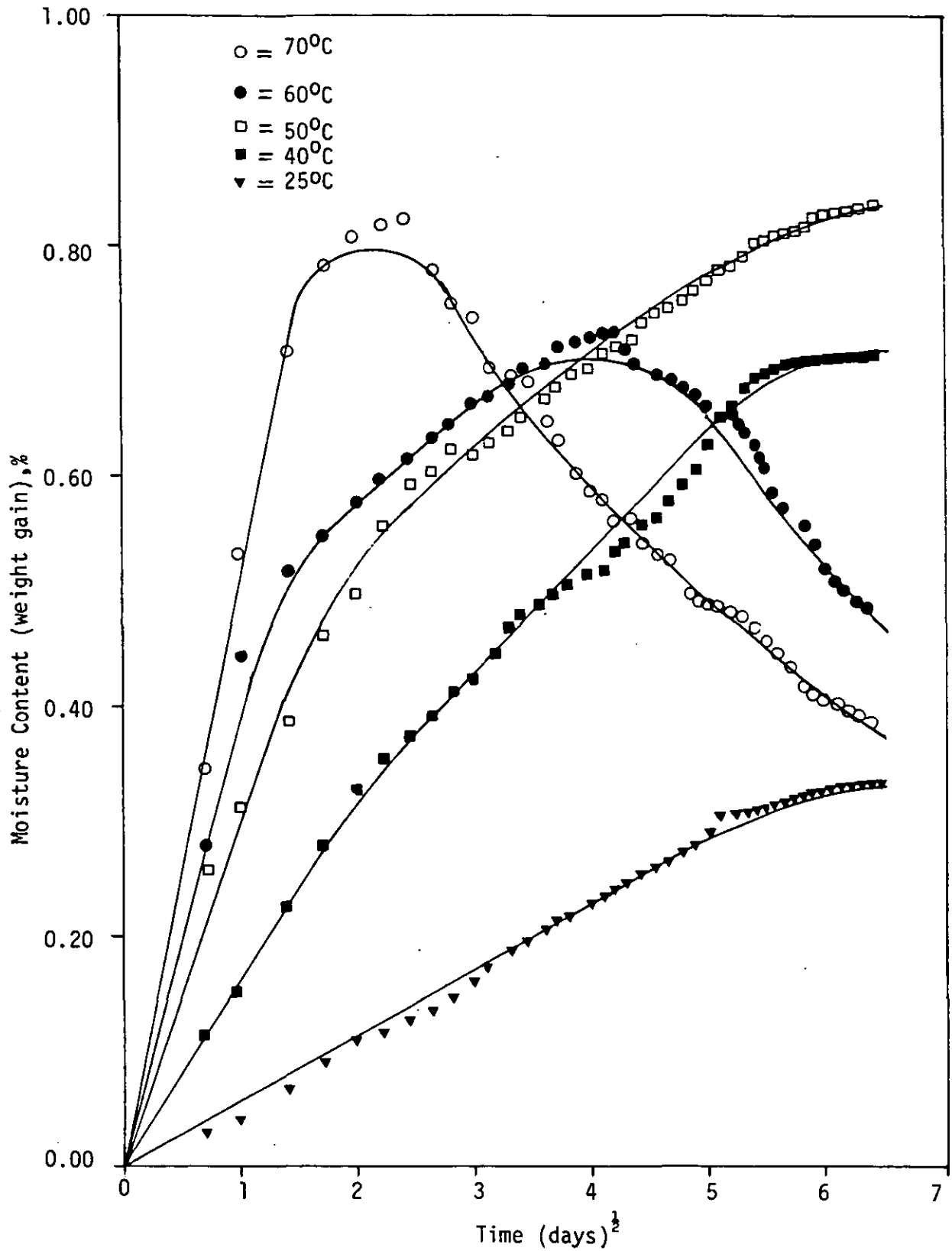


FIGURE 120: Weight change of Epoxy MY750 specimens immersed in distilled water at different temperatures as a function of time (fibre orientation $\pm 45^\circ$)

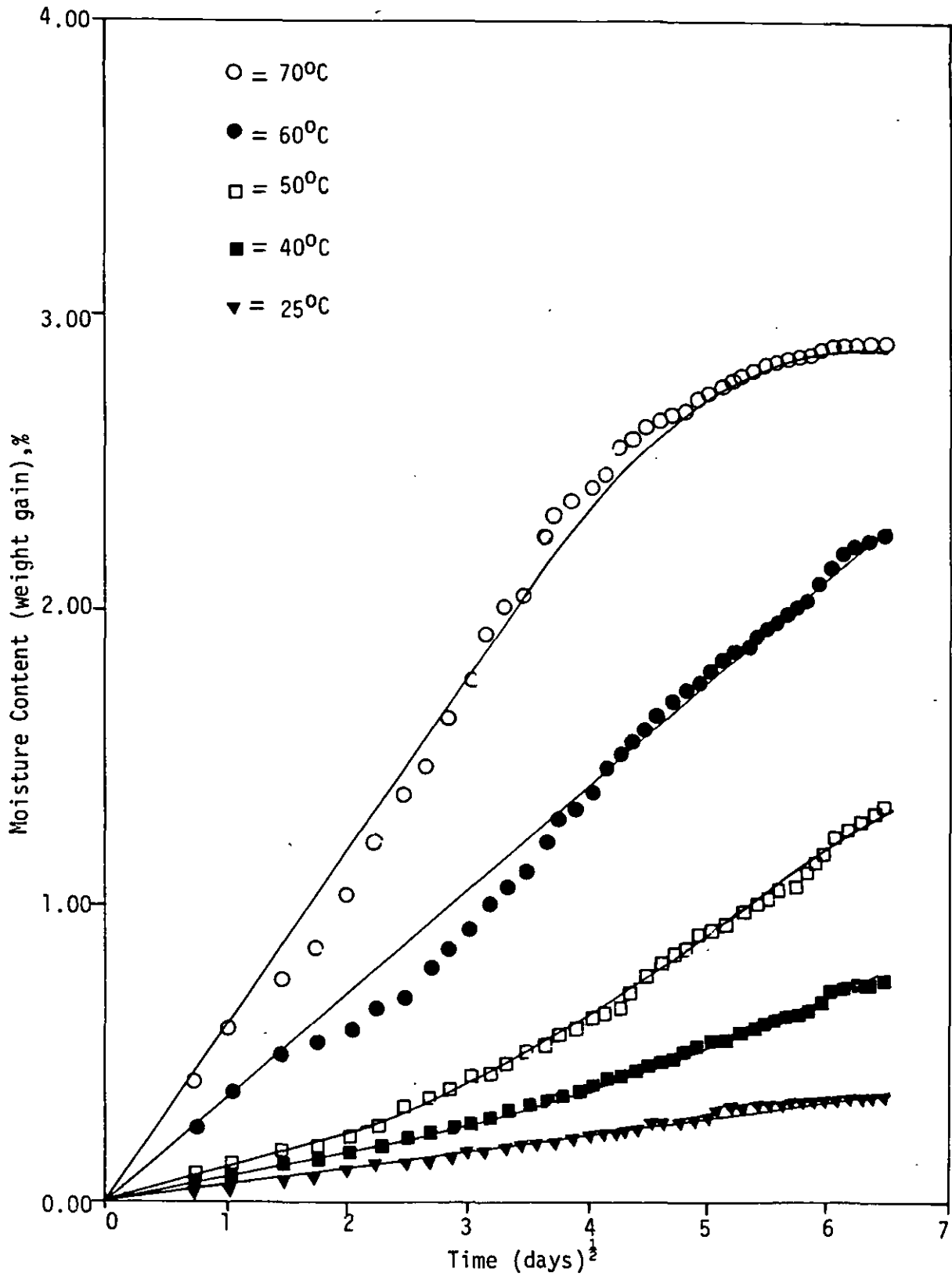


FIGURE 121: Weight change of 913 PrePreg specimens immersed in distilled water at different temperatures as a function of time (fibre orientation 0°)

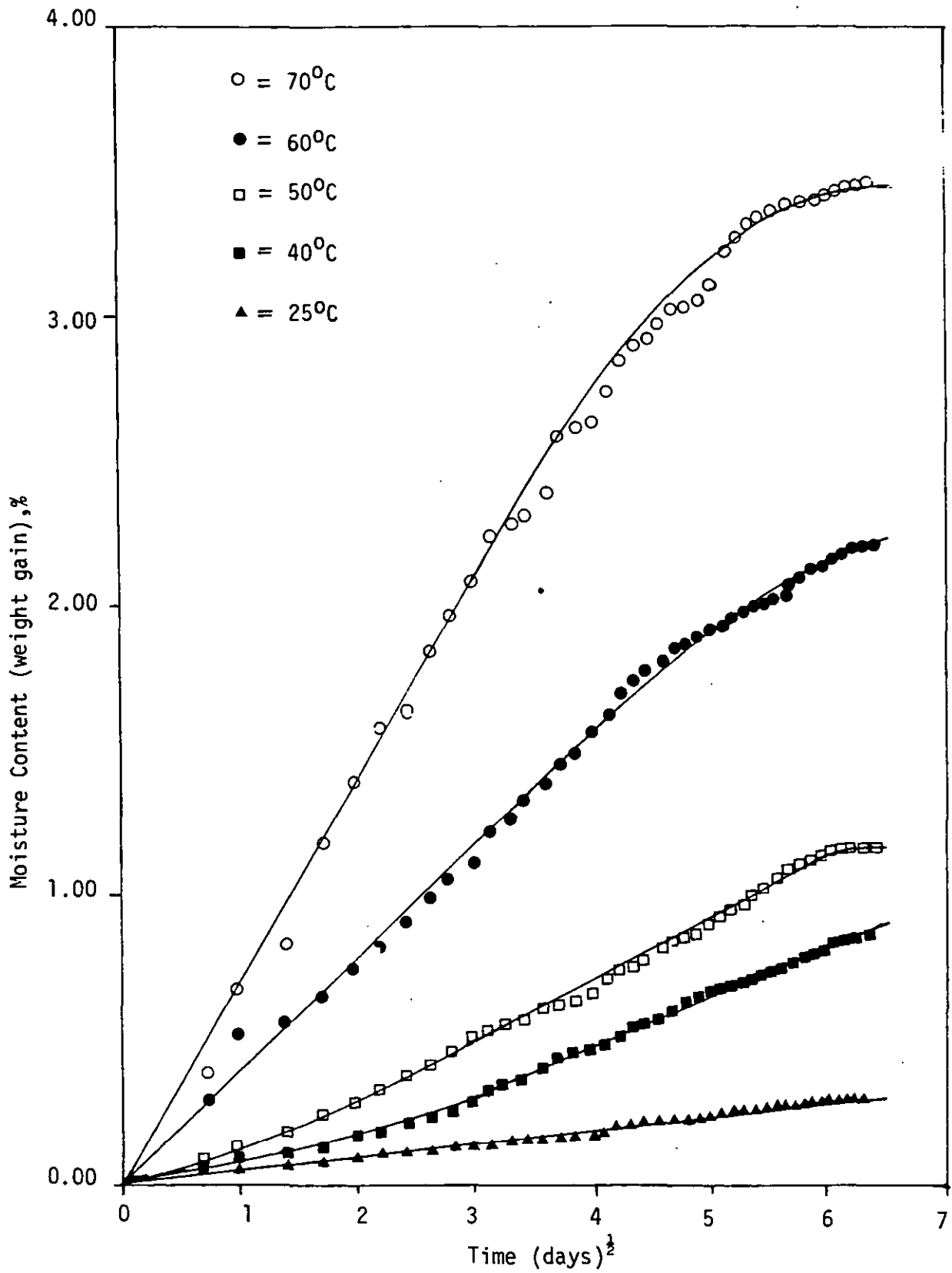


FIGURE 122: Weight change of 913 PrePreg specimens immersed in distilled water at different temperatures as a function of time (fibre orientation $\pm 45^\circ$)

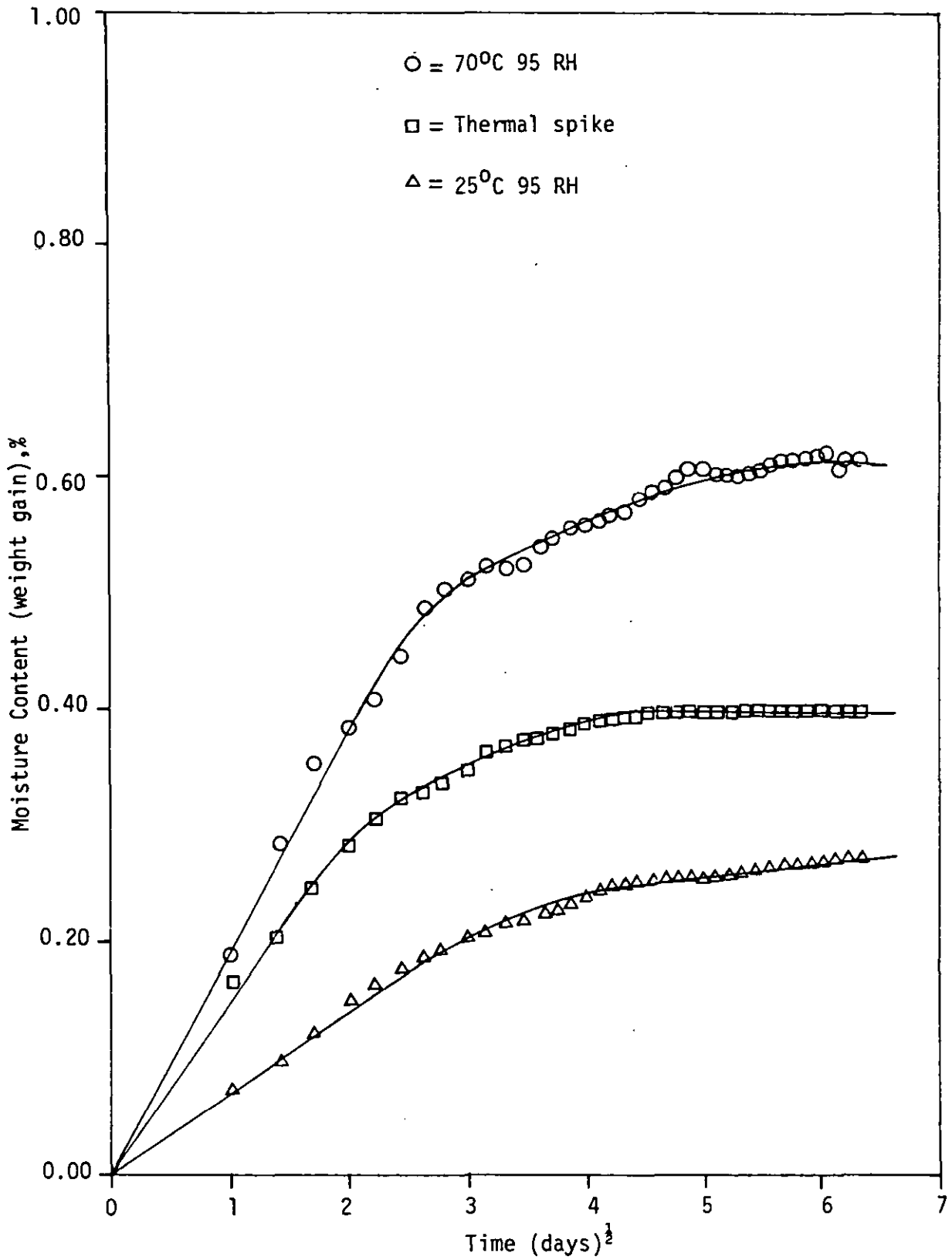


FIGURE 123: Effect of thermal spikes on 411-45 Vinylester moisture absorption. Specimens conditioned at 25°C, 95% RH and spiked daily for four hours to 70°C; 95% RH for 40 days (fibre orientation 0°)

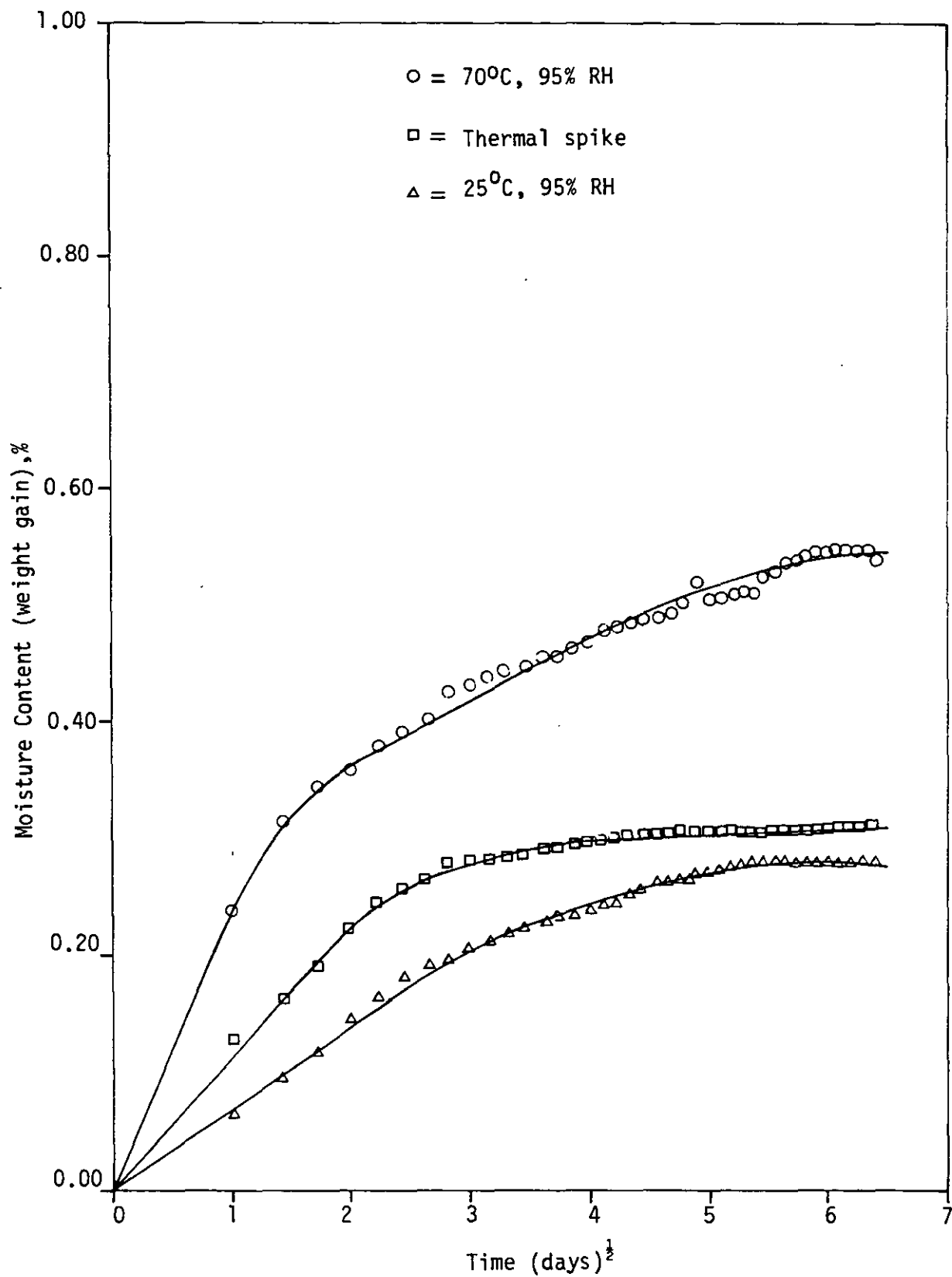


FIGURE 124: Effect of thermal spikes on 411-45 Vinylester moisture absorption. Specimens conditioned at 25°C; 95% RH and spiked daily for four hours to 70°C; 95% RH for 40 days (fibre orientation $\pm 45^\circ$)

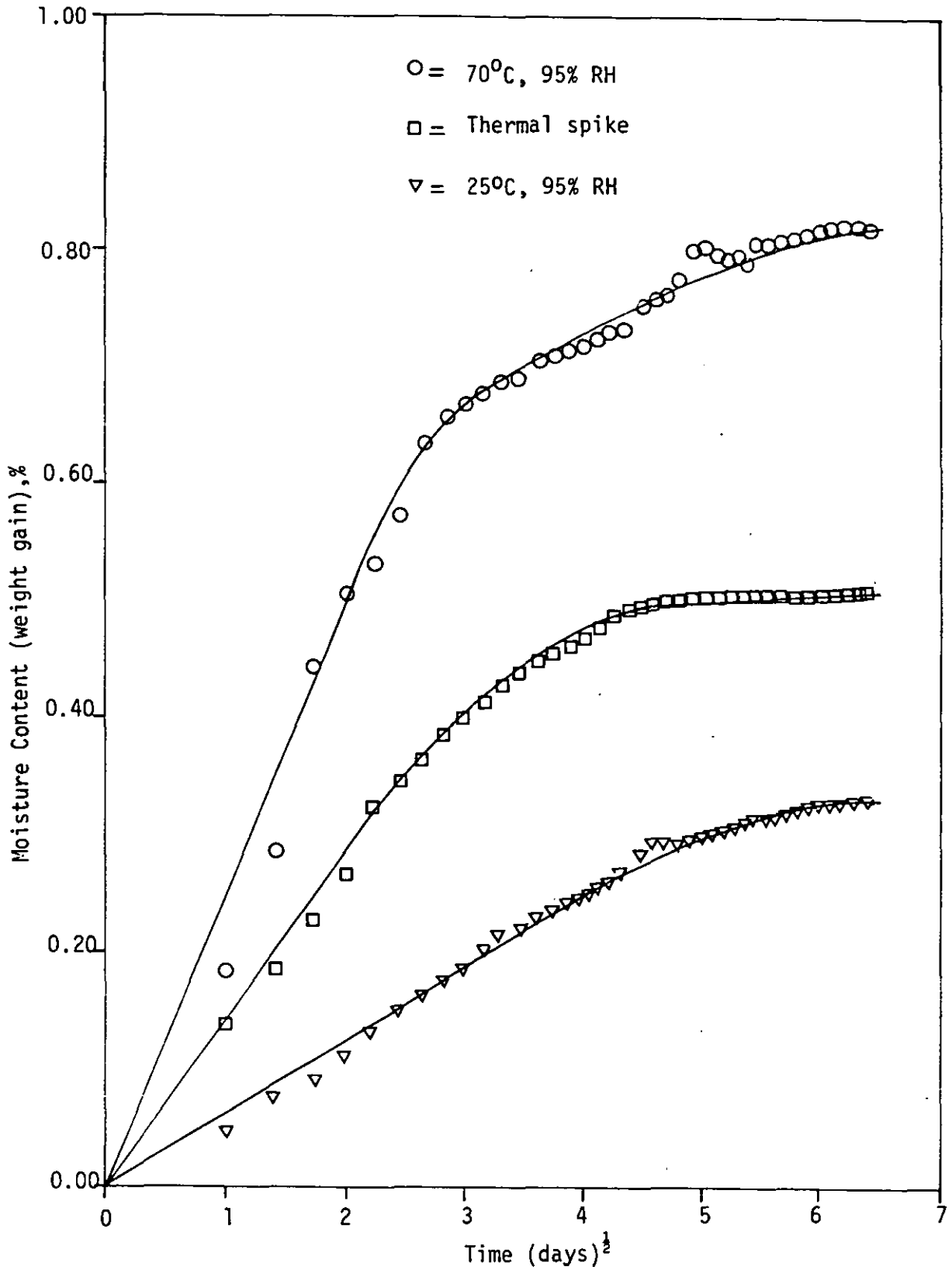


FIGURE 125: Effect of thermal spikes on 470-36 Vinylester moisture absorption. Specimens conditioned at 25°C; 95% RH and spiked daily for four hours to 70°C; 95% RH for 40 days (fibre orientation 0°)

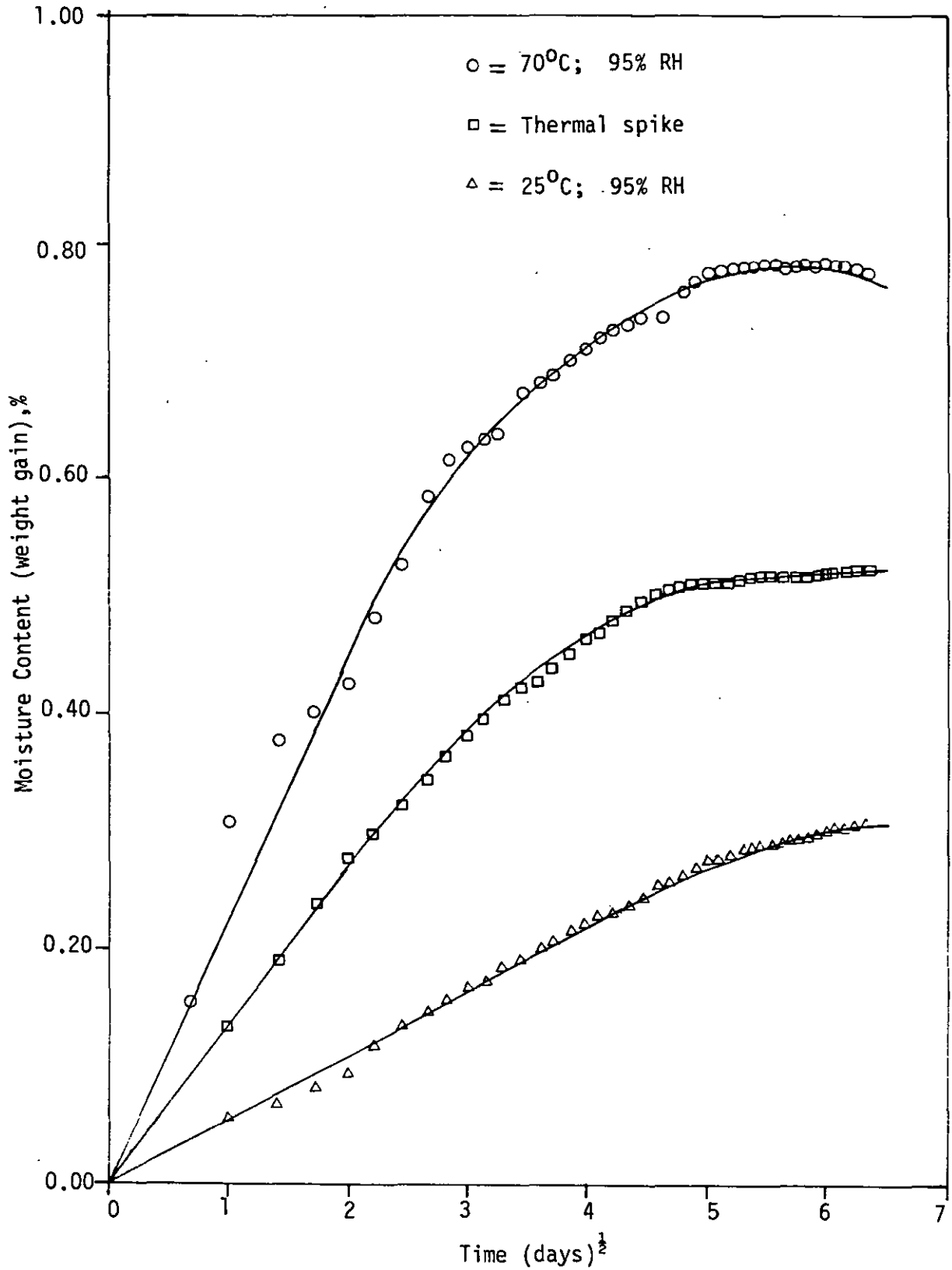


FIGURE 126: Effect of thermal spikes on 470-36 Vinylester moisture absorption. Specimens conditioned at 25°C; 95% RH and spiked daily for four hours to 70°C; 95% RH for 40 days (fibre orientation $\pm 45^\circ$)

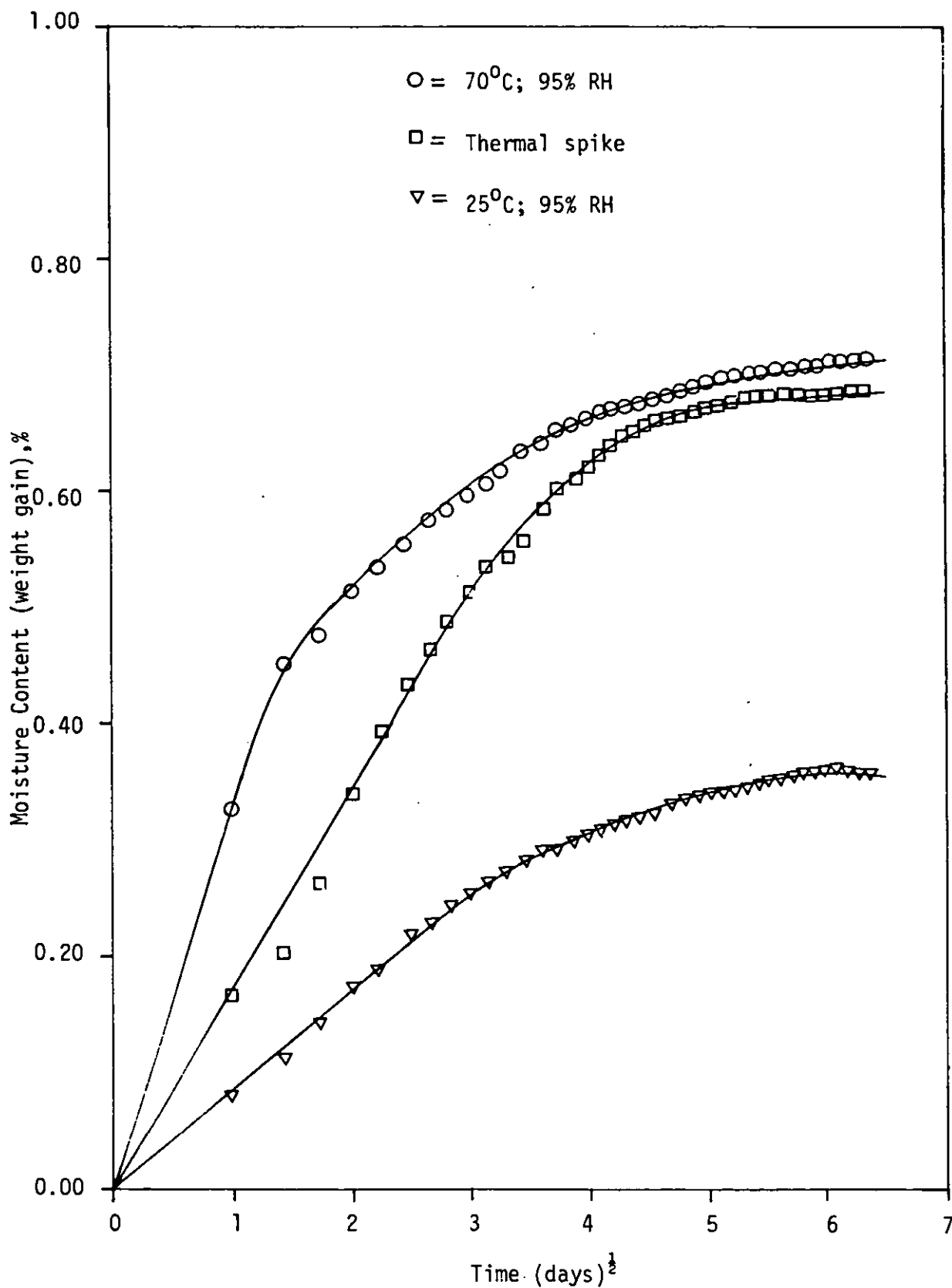


FIGURE 127: Effect of thermal spikes on Polyester 272 moisture absorption. Specimens conditioned at 25°C; 95% RH and spiked daily for four hours to 70°C; 95% RH for 40 days (fibre orientation 0°)

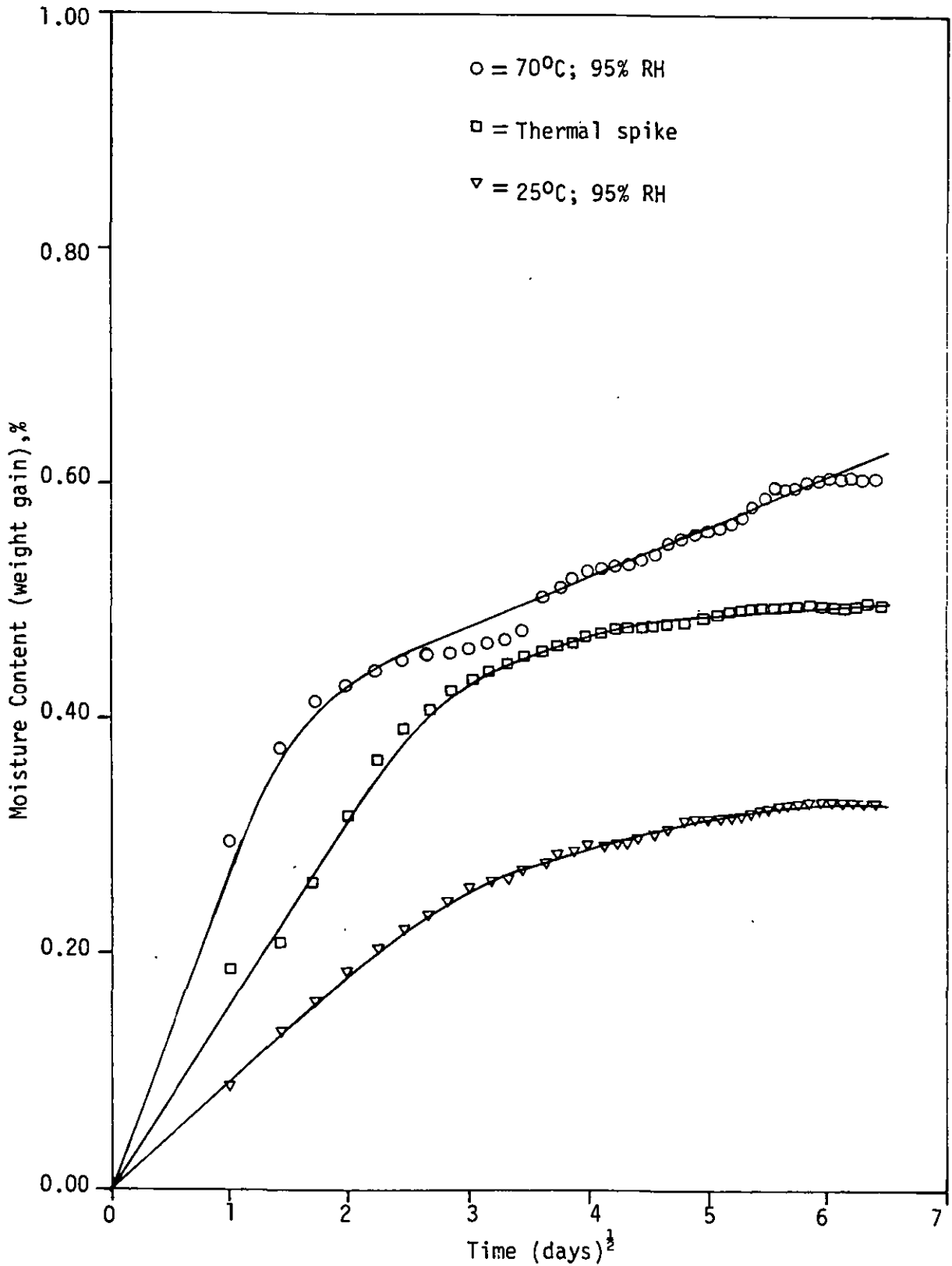


FIGURE 128: Effect of thermal spikes on Polyester 272 moisture absorption. Specimens conditioned at 25°C; 95% RH and spiked daily for four hours to 70°C; 95% RH for 40 days (fibre orientation $\pm 45^\circ$)

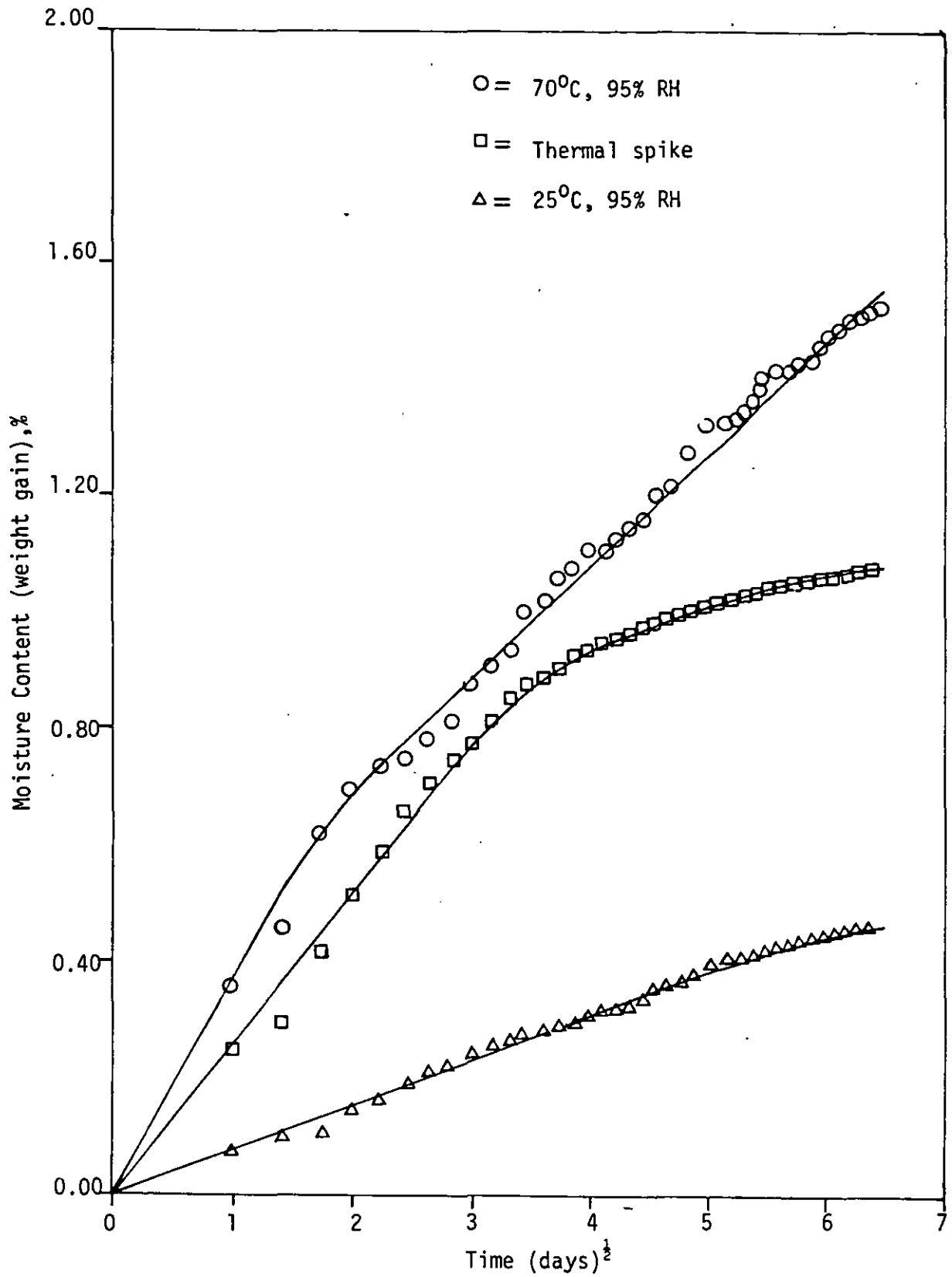


FIGURE 129: Effect of thermal spikes on Epoxy MY750 moisture absorption. Specimens conditioned at 25°C; 95% RH and spiked daily for four hours to 70°C; 95% RH for 40 days (fibre orientation 0°)

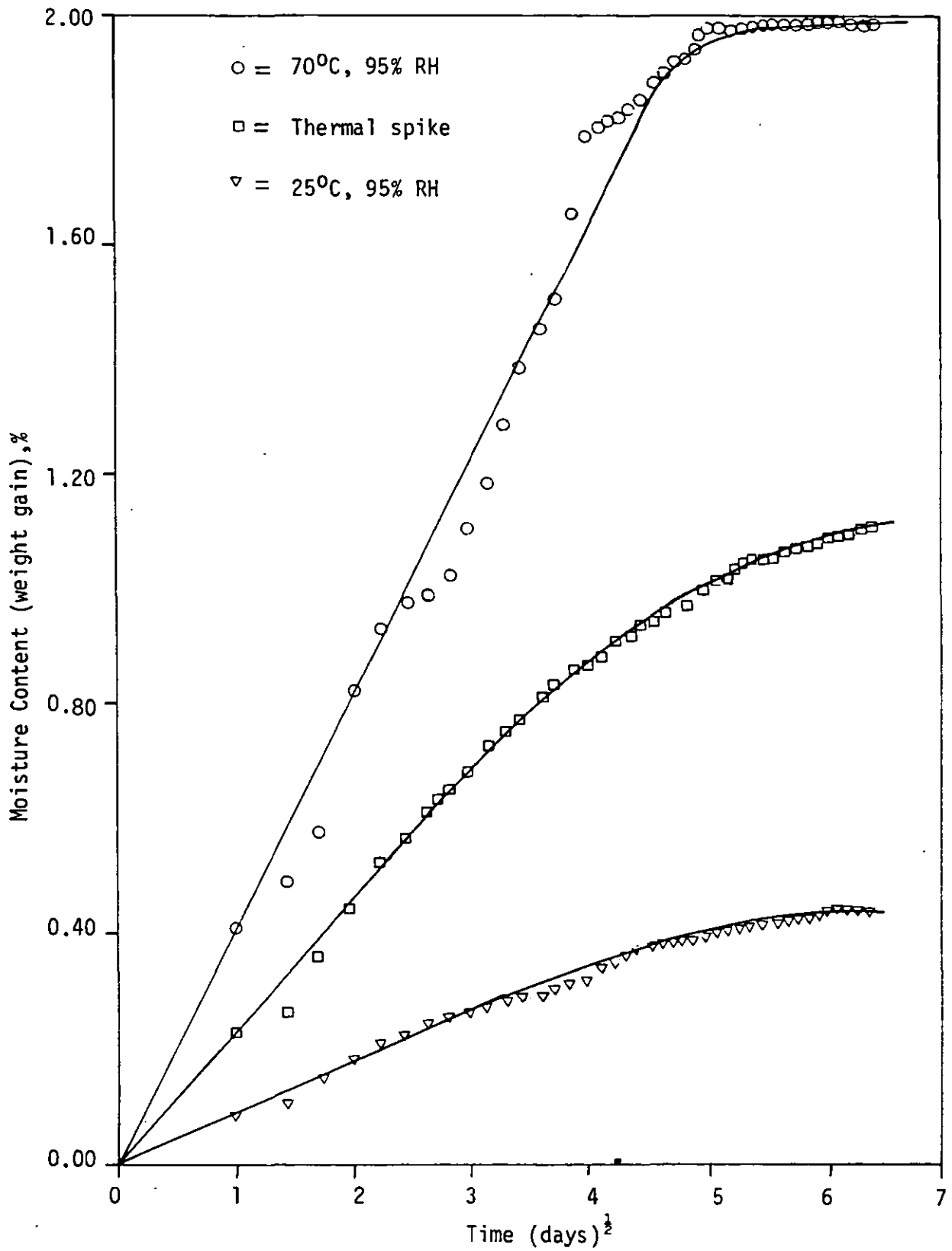


FIGURE 130: Effect of thermal spikes on Epoxy MY750 moisture absorption. Specimens conditioned at 25°C; 95% RH and spiked daily for four hours to 70°C; 95% RH for 40 days (fibre orientation $\pm 45^\circ$)

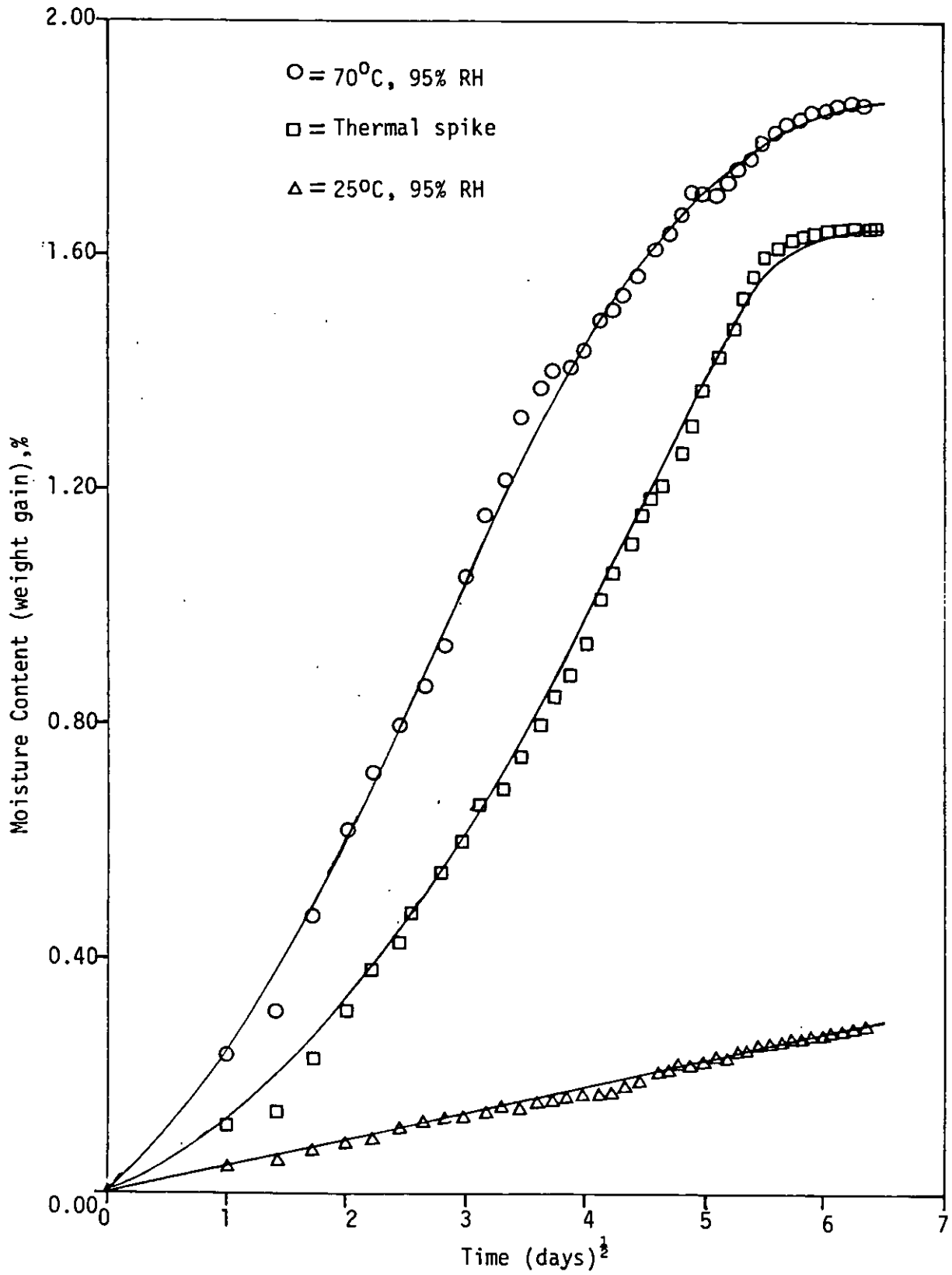


FIGURE 131: Effect of thermal spikes on 913 PrePreg moisture absorption. Specimens conditioned at 25°C; 95% RH and spiked daily for four hours to 70°C; 95% RH for 40 days (fibre orientation 0°)

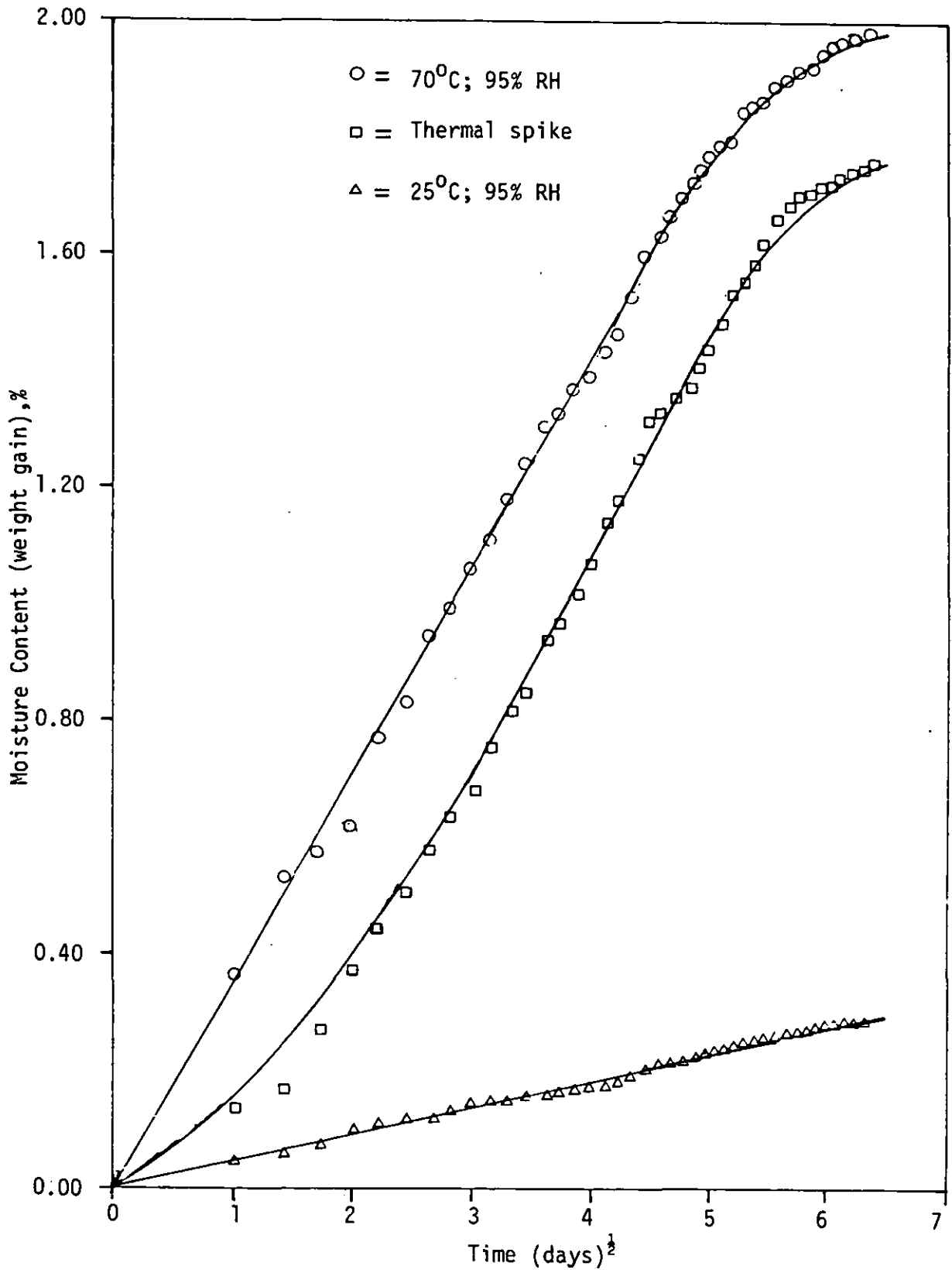


FIGURE 132: Effect of thermal spikes on 913 PrePreg moisture absorption. Specimens conditioned at 25°C; 95% RH and spiked daily for four hours to 70°C; 95% RH for 40 days (fibre orientation $\pm 45^\circ$)

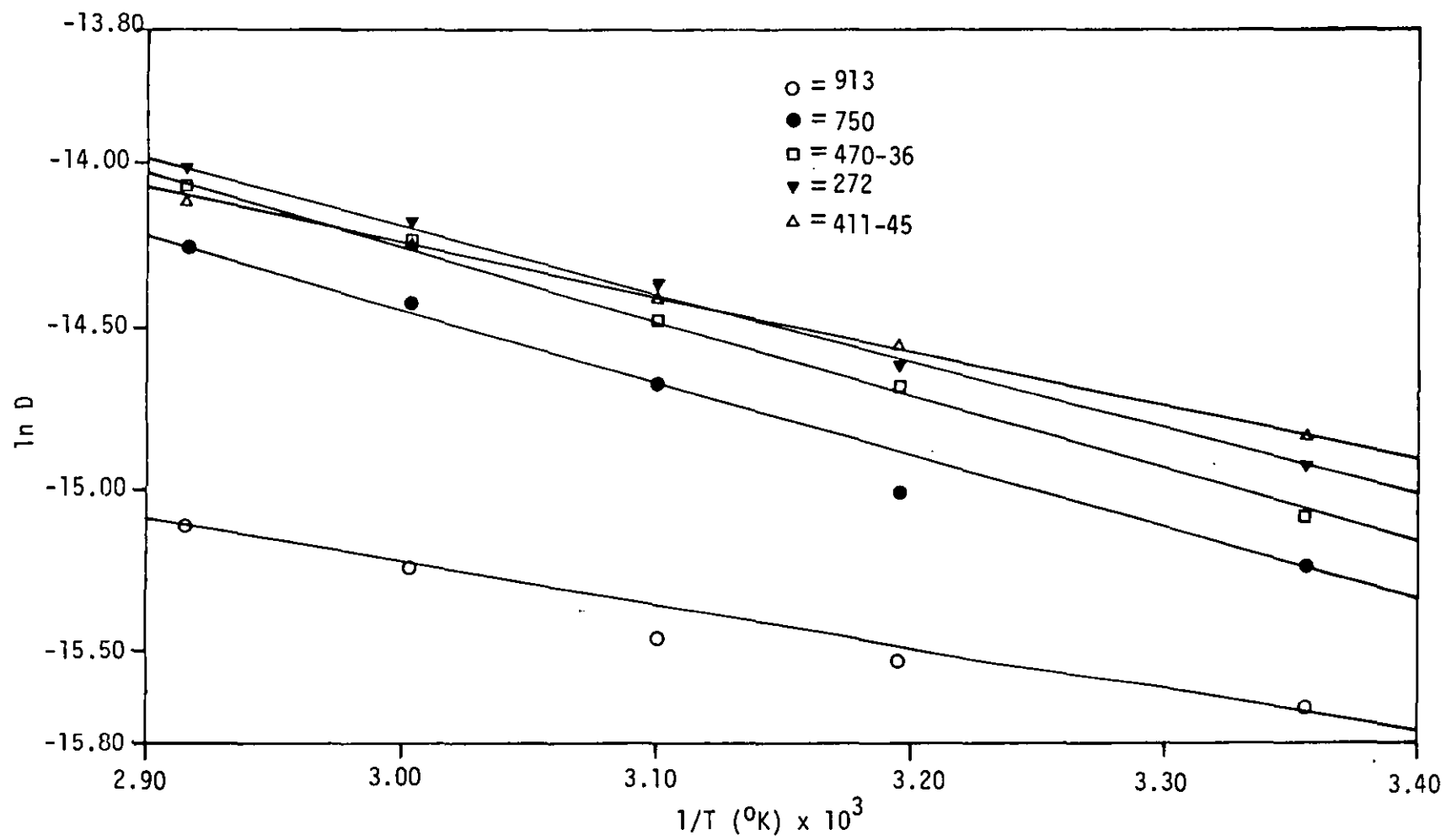


FIGURE 133: Arrhenius plot of specimens exposed to 60% RH (fibre orientation 0°)

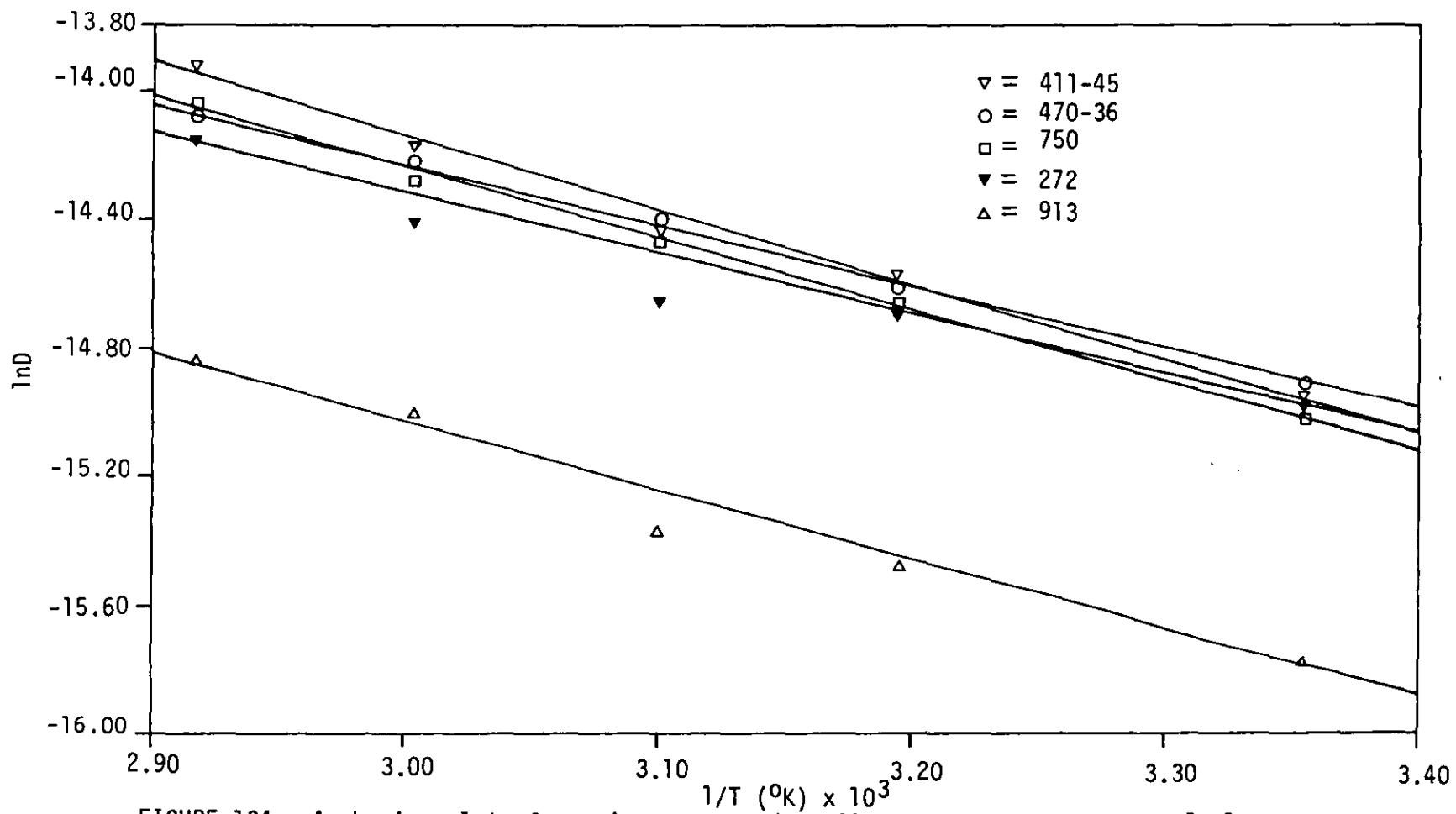


FIGURE 134: Arrhenius plot of specimens exposed to 60% RH (fibre orientation $\pm 45^{\circ}$)

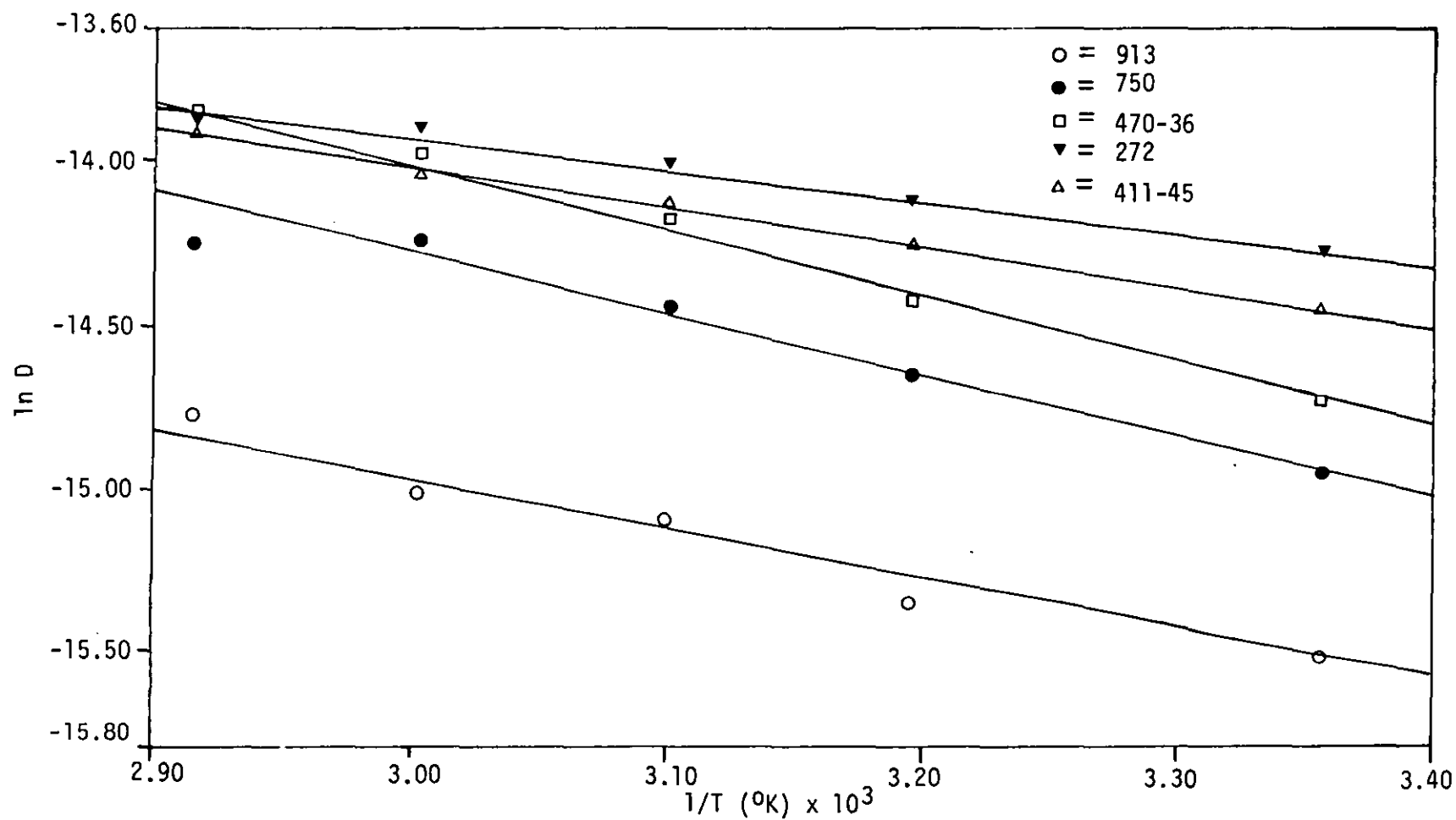


FIGURE 135: Arrhenius plot of specimens exposed to 95% RH (fibre orientation 0°)

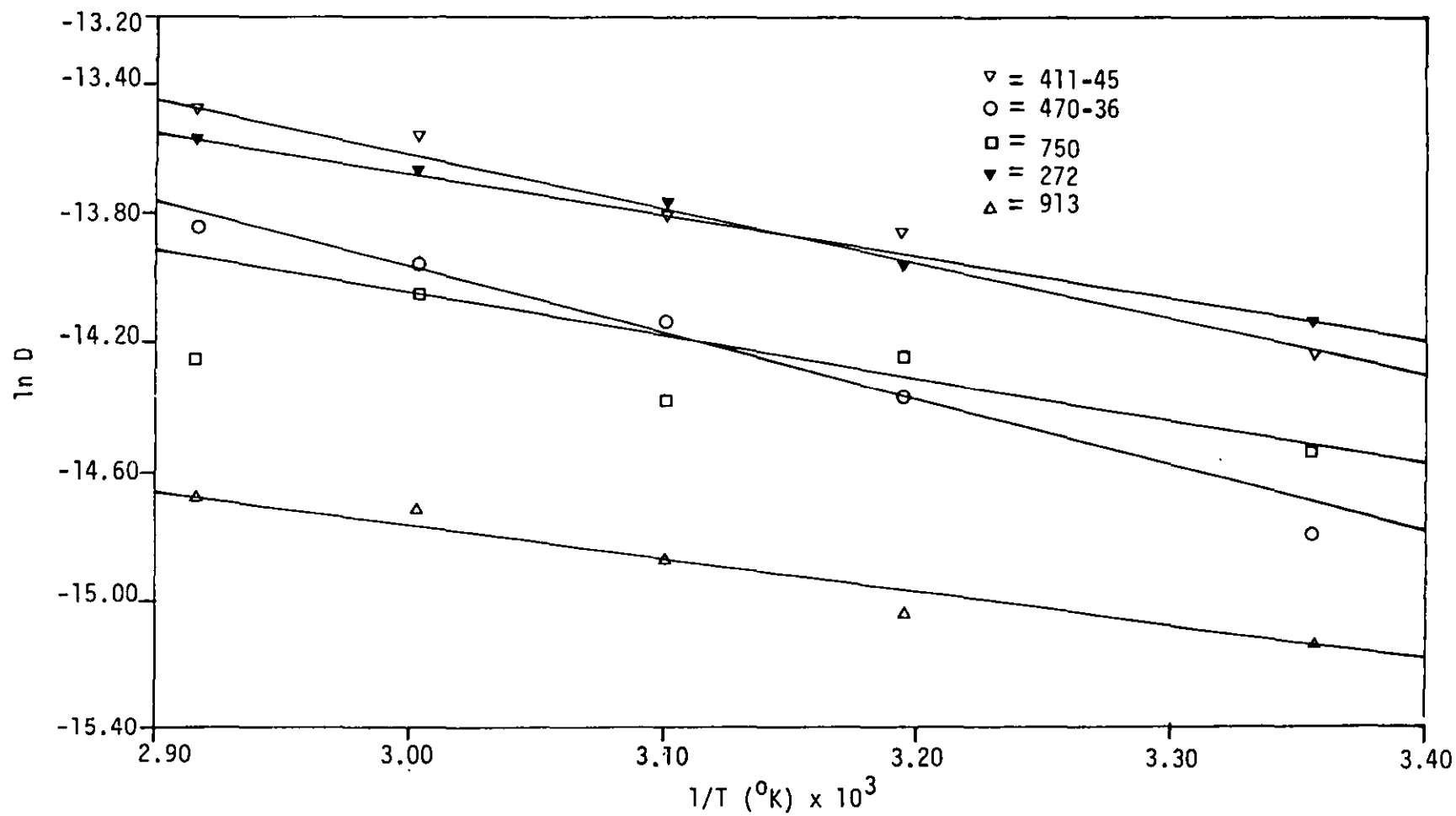


FIGURE 136: Arrhenius plot of specimens exposed to 95% RH (fibre orientation $\pm 45^{\circ}$)

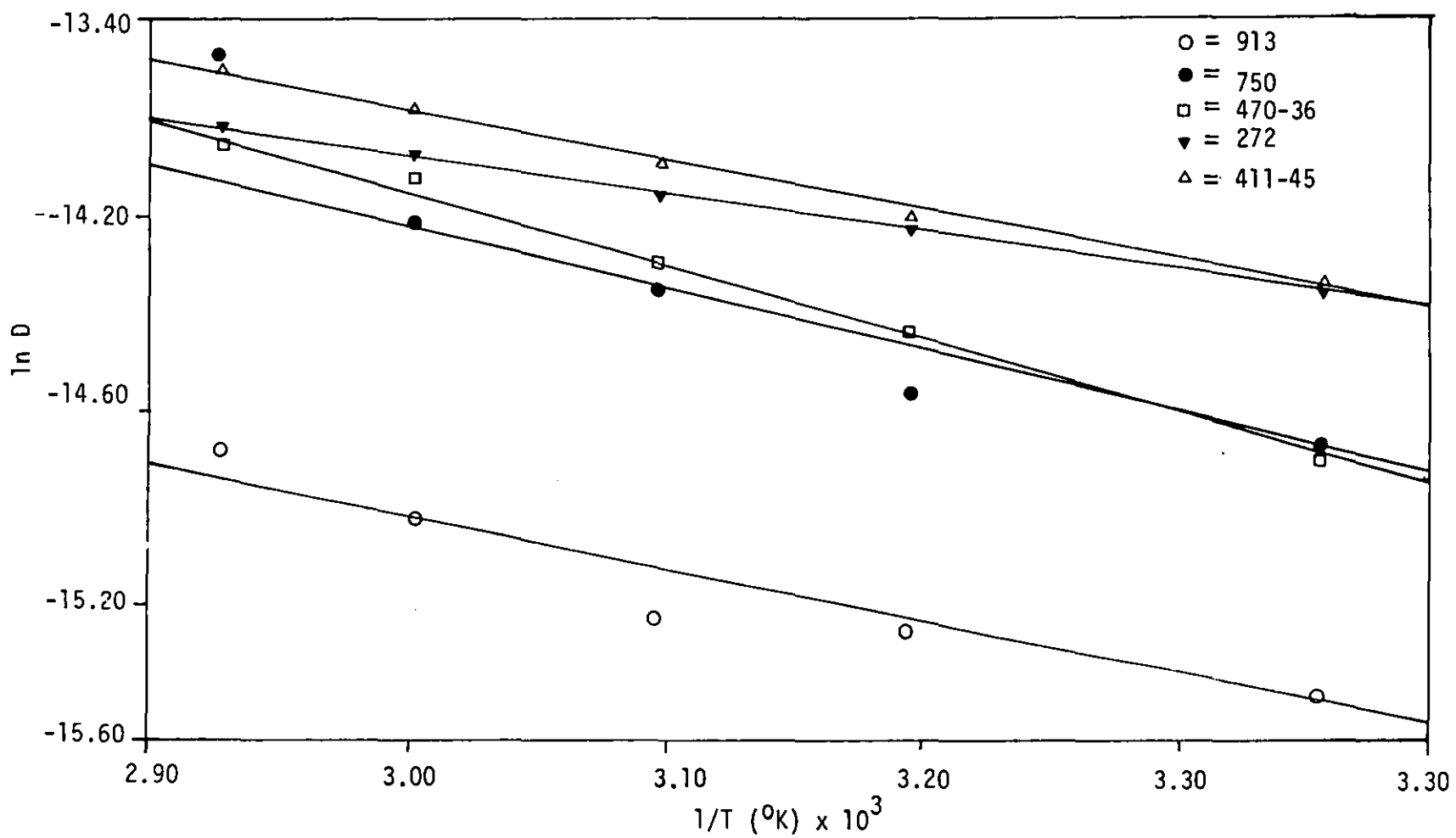


FIGURE 137: Arrhneius plot of specimens immersed in distilled water (fibre orientation 0°)

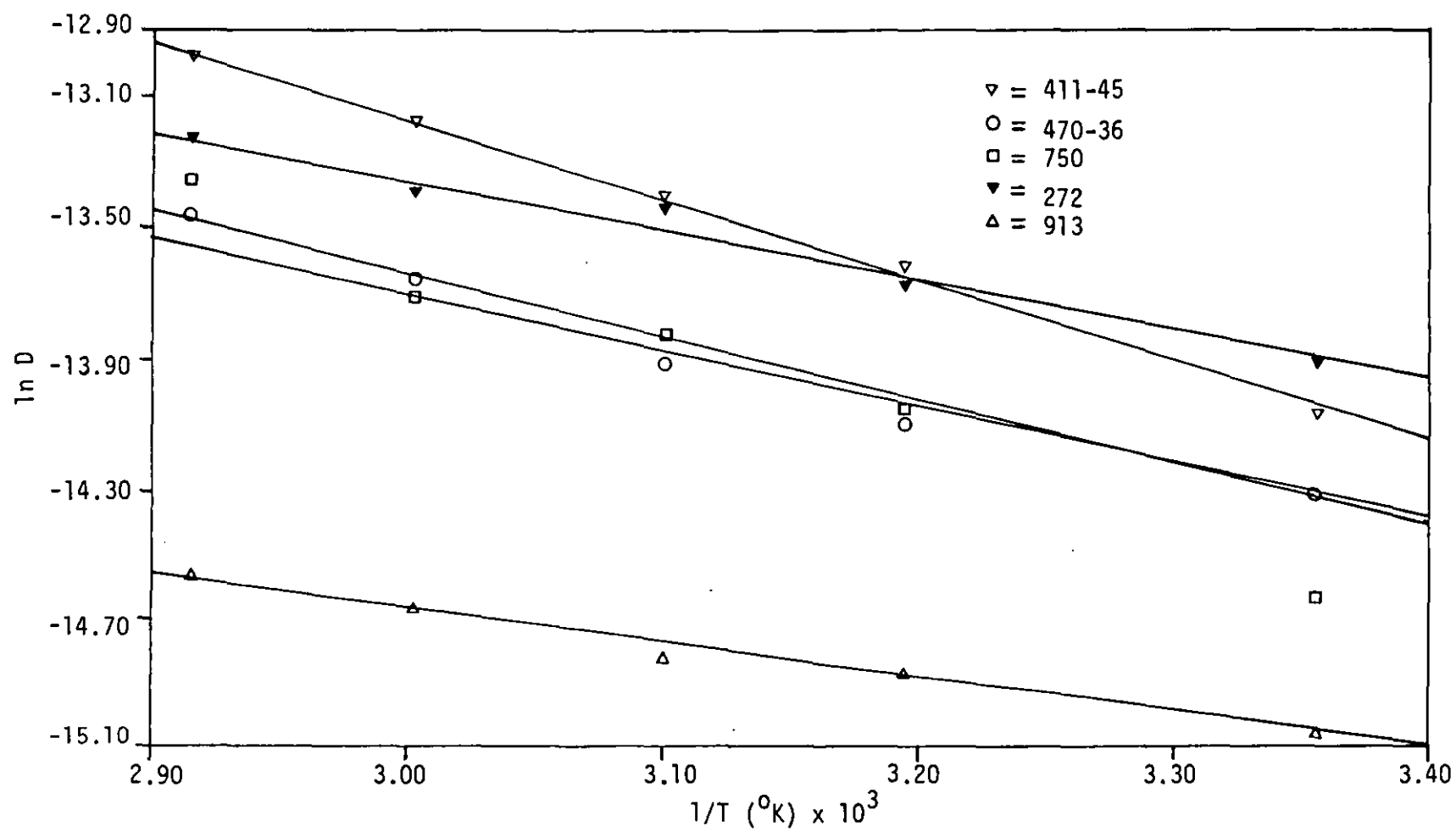


FIGURE 138: Arrhenius plot of specimens immersed in distilled water (fibre orientation $\pm 45^{\circ}$)

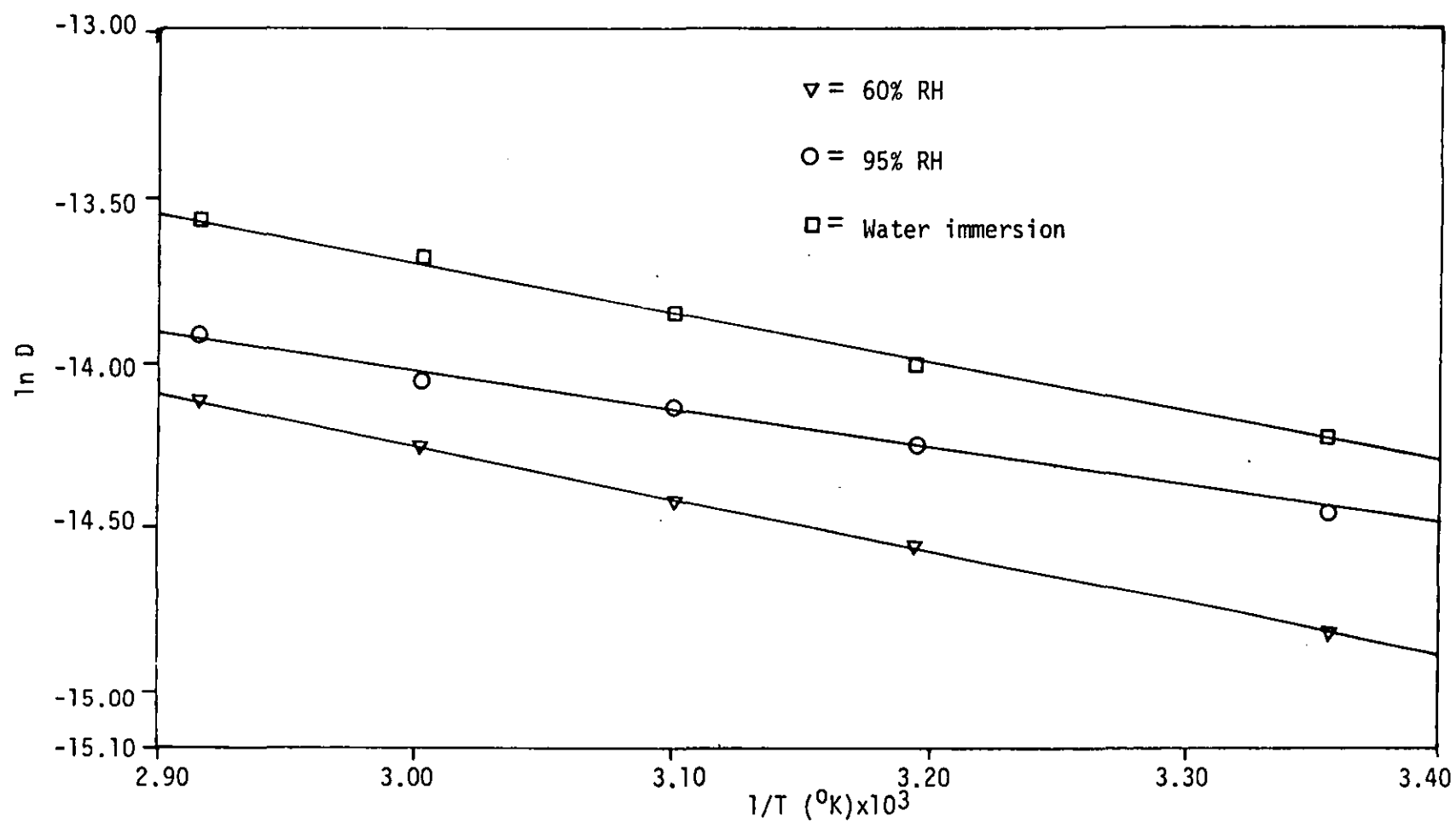


FIGURE 139: Arrhenius plot of 411-45 Vinylester specimens exposed to different environments (fibre orientation 0°)

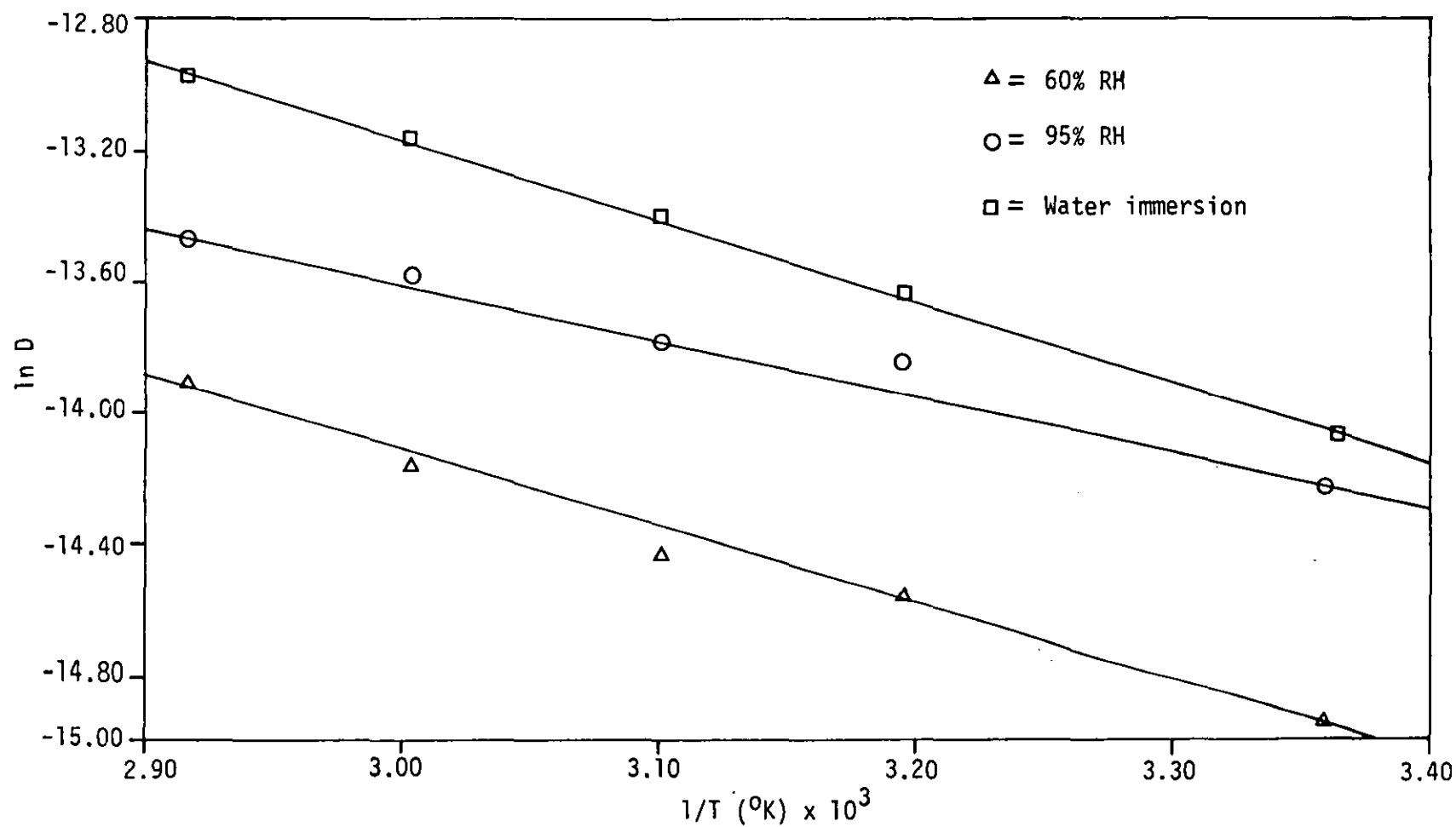


FIGURE 140: Arrhenius plot of 411-45 Vinylester specimens exposed to different environments (fibre orientation $\pm 45^{\circ}$)

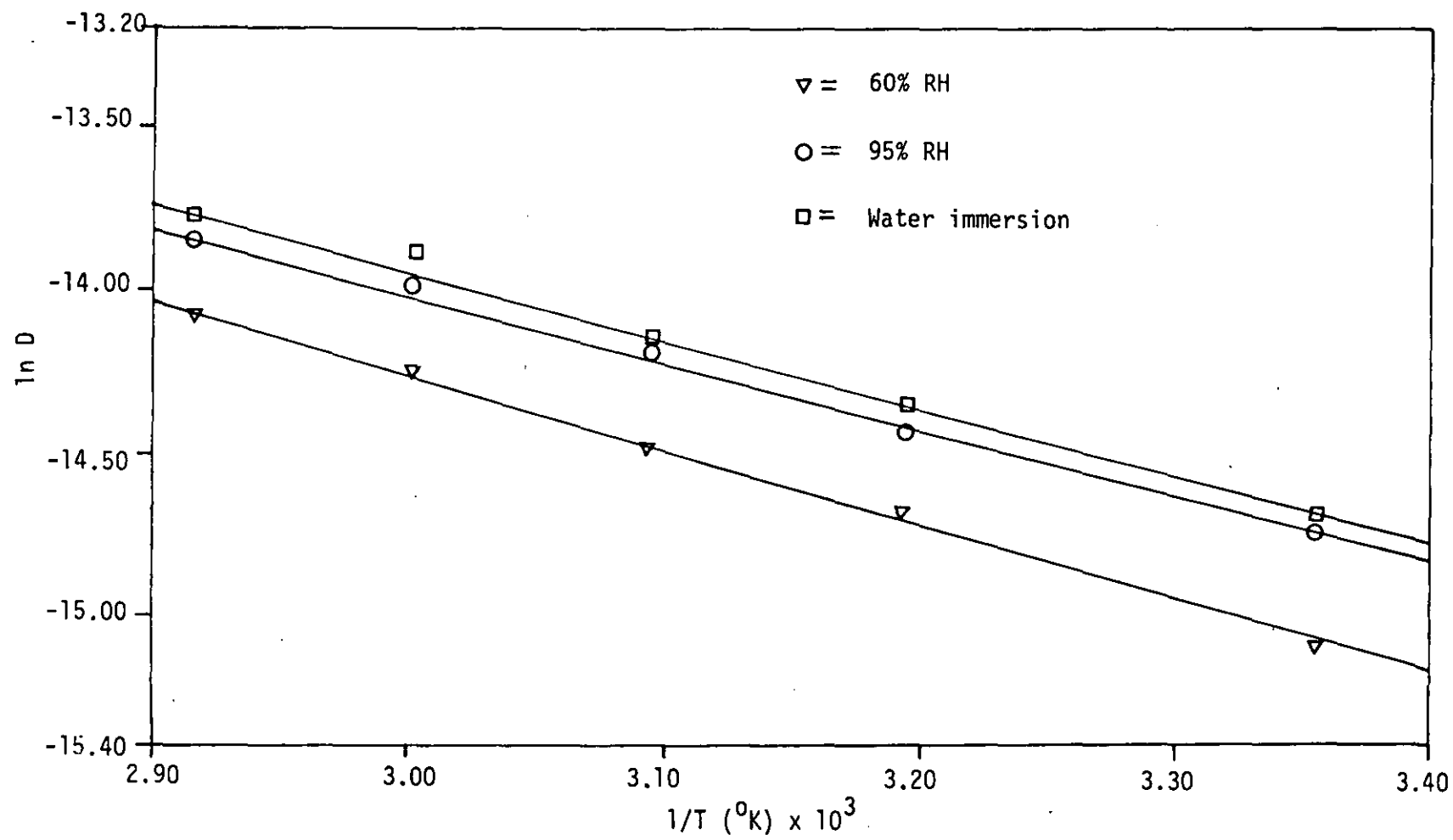


FIGURE 141: Arrhenius plot of 470-36 Vinylester specimens exposed to different environments (fibre orientation 0°)

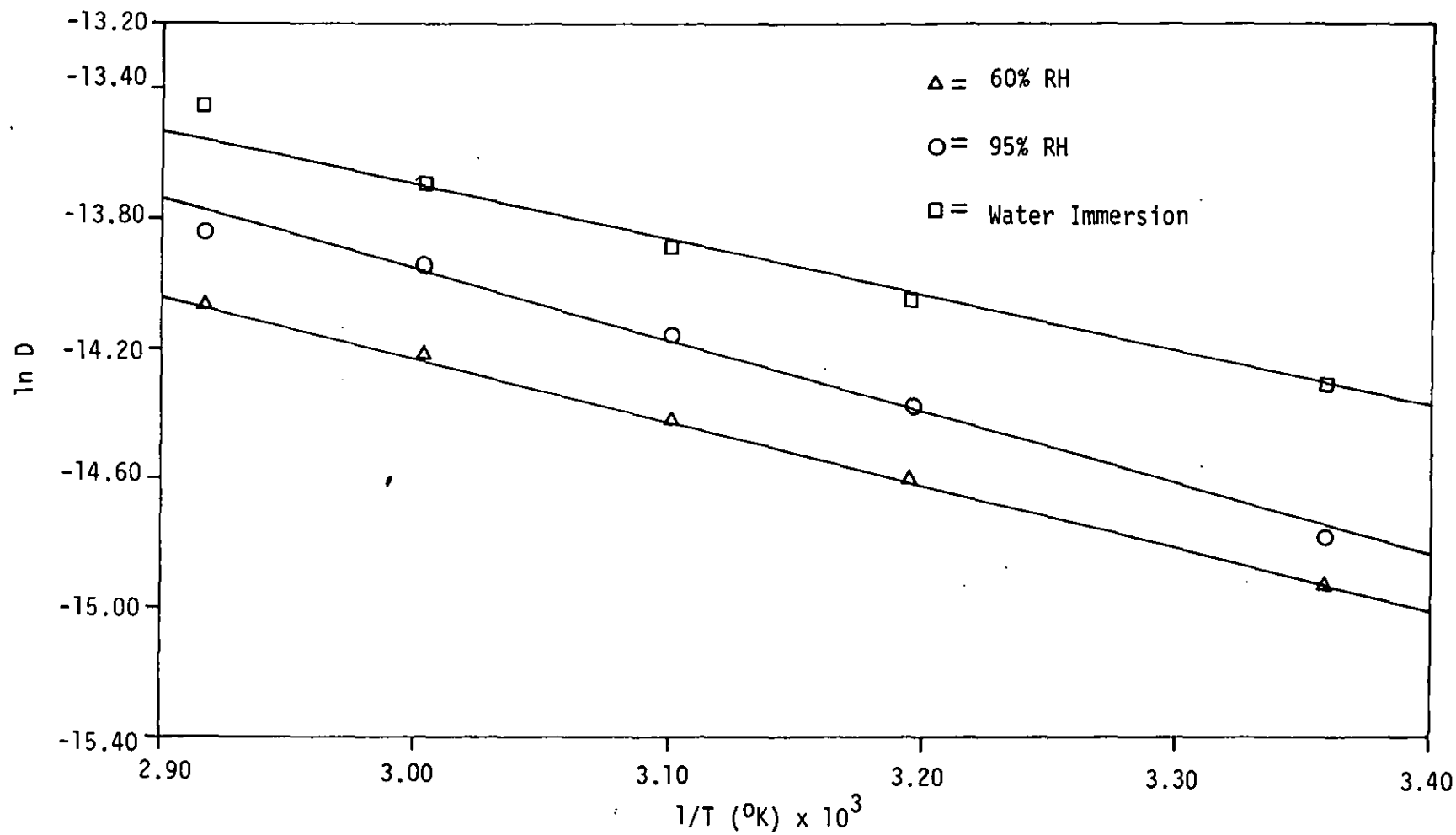


FIGURE 142: Arrhenius plot of 470-36 Viny Lester specimens exposed to different environments (fibre orientation $\pm 45^{\circ}$)

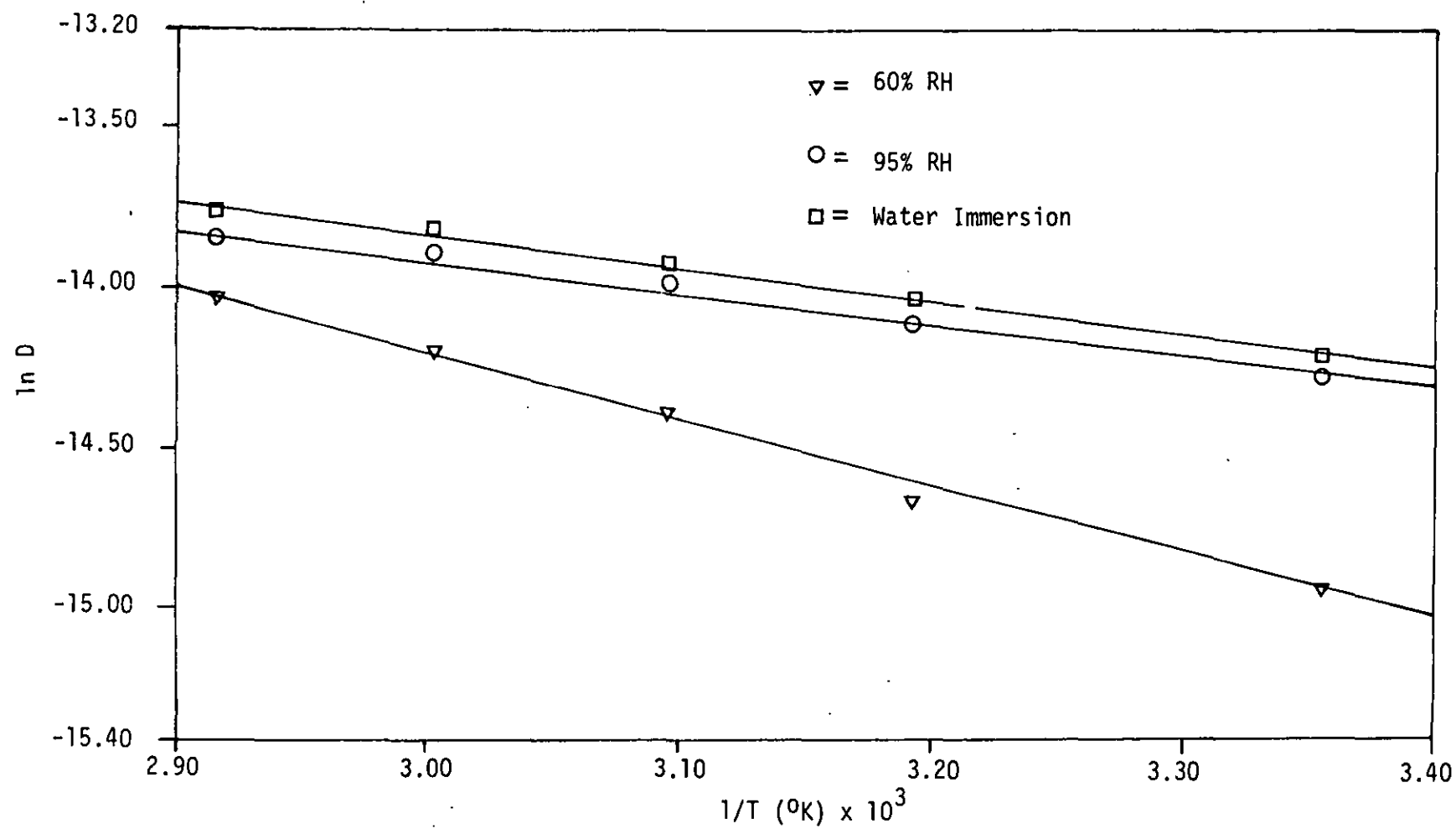


FIGURE 143: Arrhenius plot of Polyester 272 specimens exposed to different environments (fibre orientation 0°)

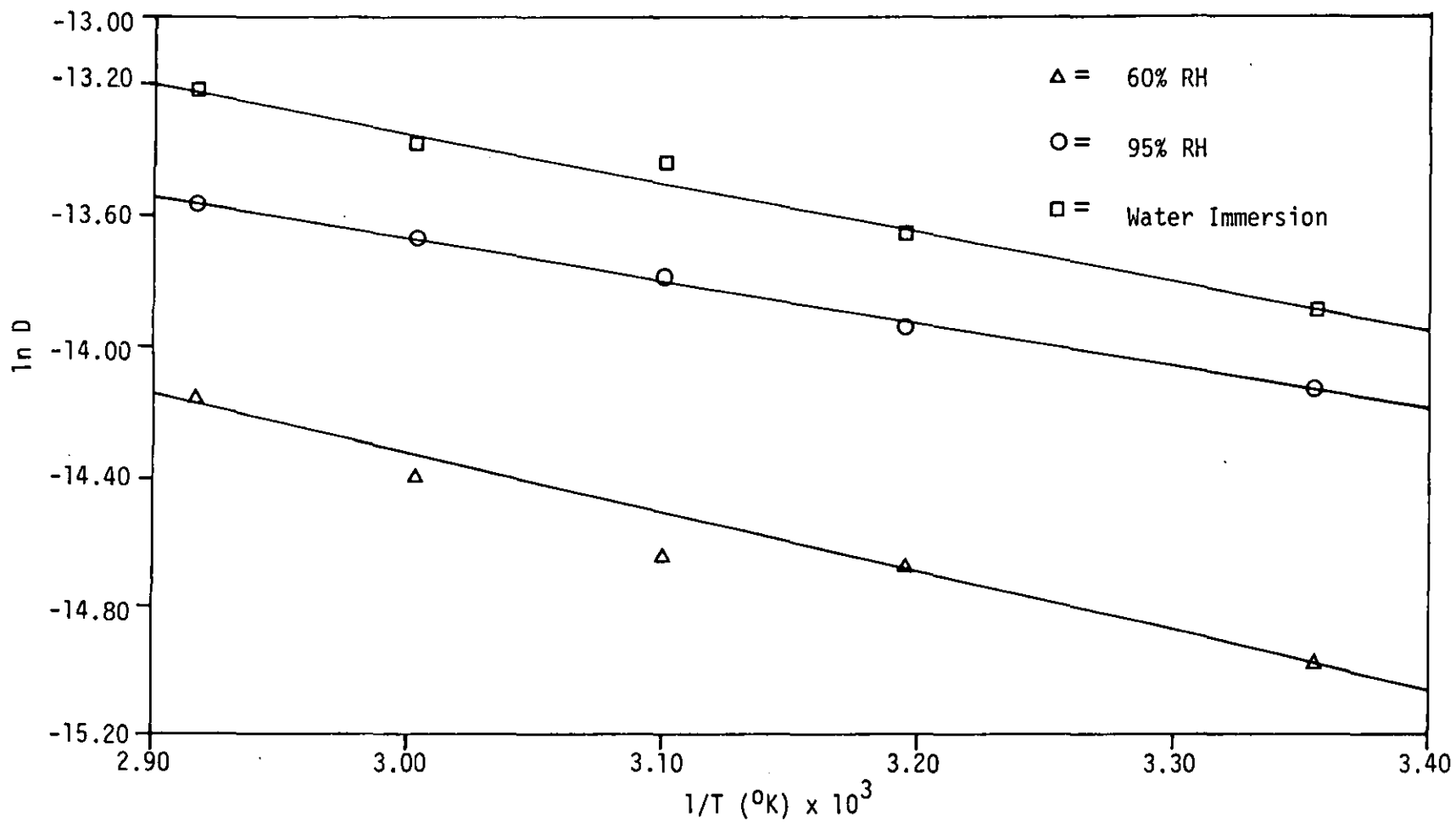


FIGURE 144: Arrhenius plot of Polyester 272 specimens exposed to different environments (fibre orientation $\pm 45^{\circ}$)

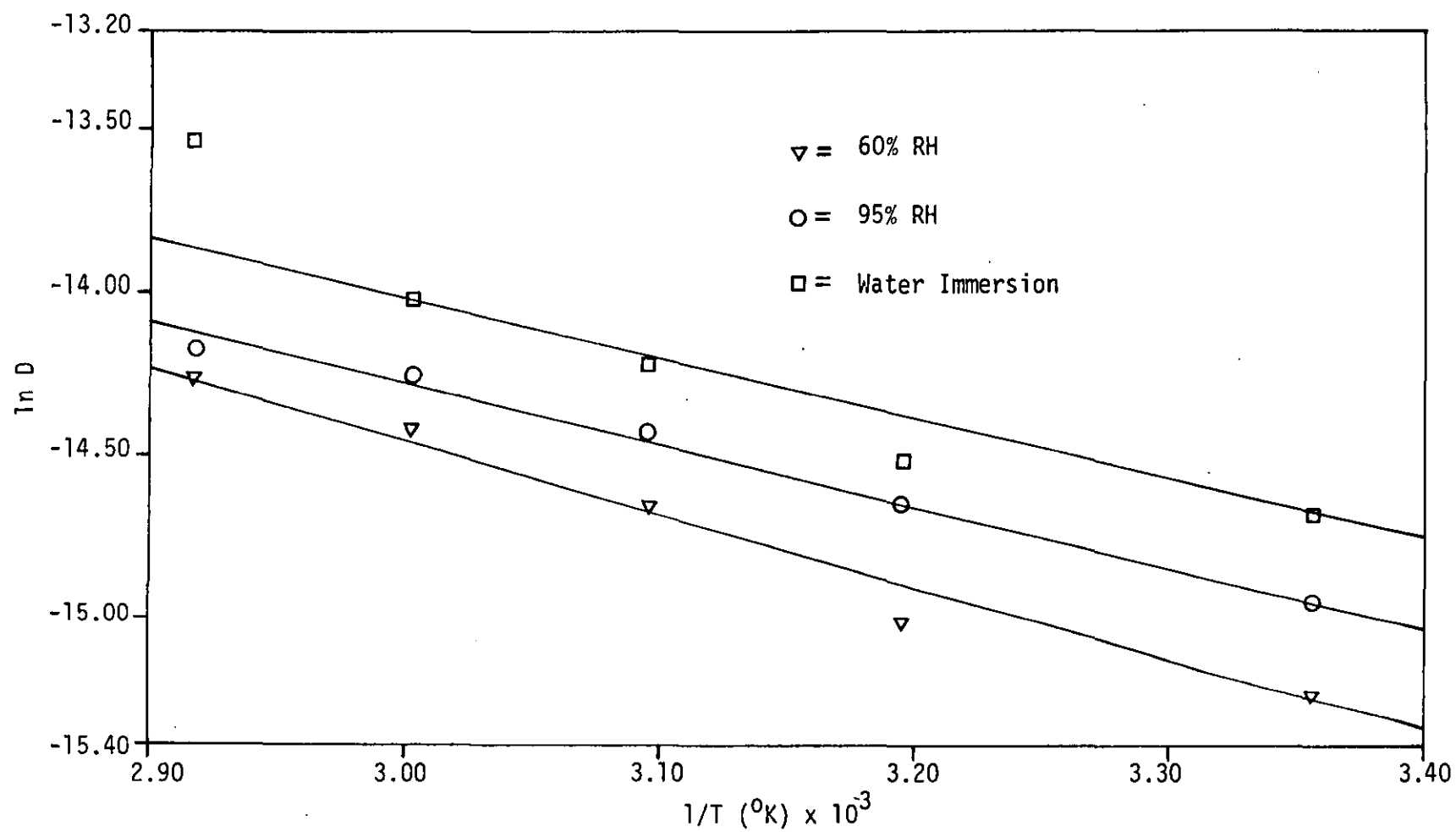


FIGURE 145: Arrhenius plot of Epoxy MY750 specimens exposed to different environments (fibre orientation 0°)

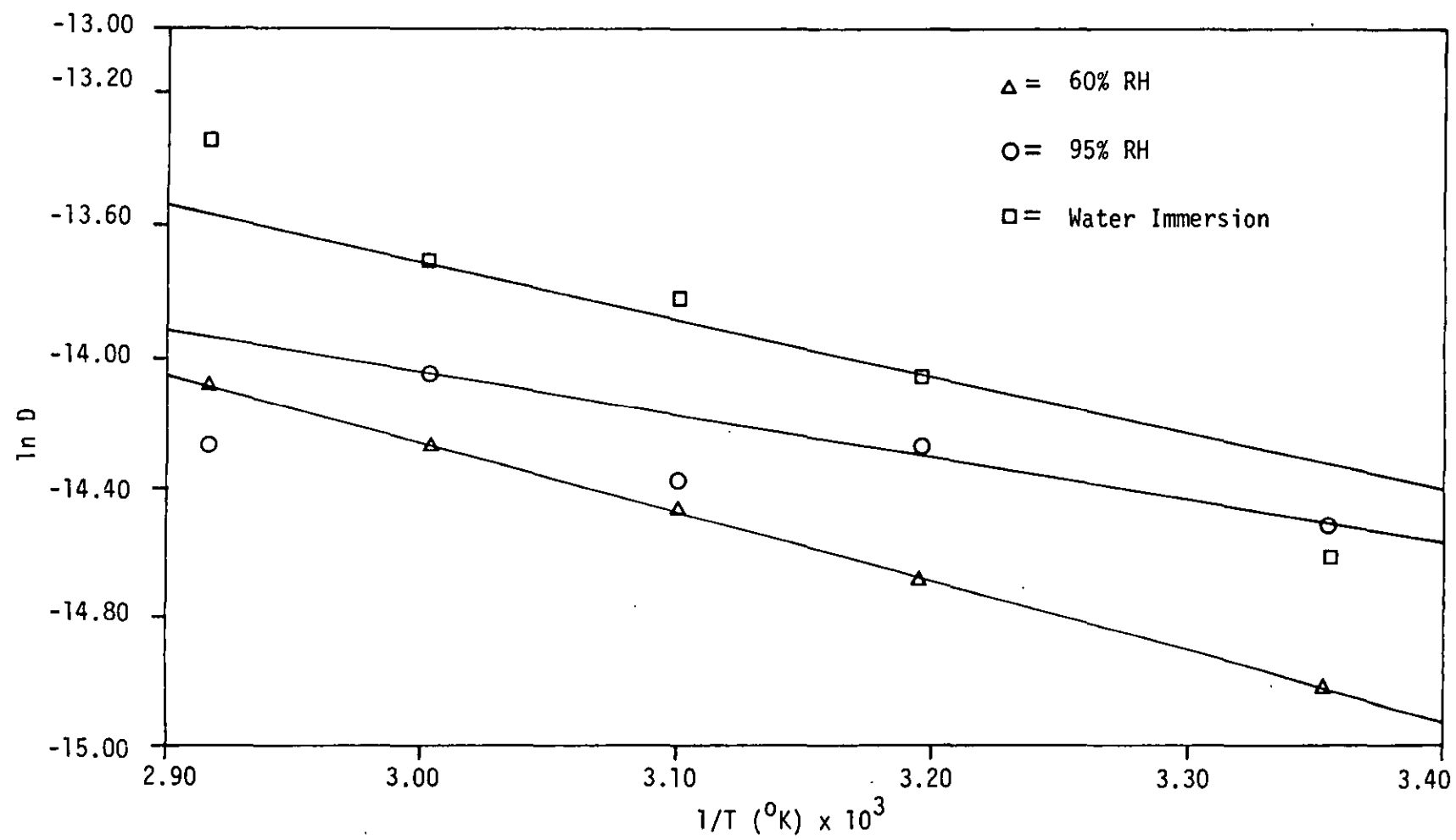


FIGURE 146: Arrhenius plot of Epoxy MY750 specimens exposed to different environments (fibre orientation $\pm 45^{\circ}$)

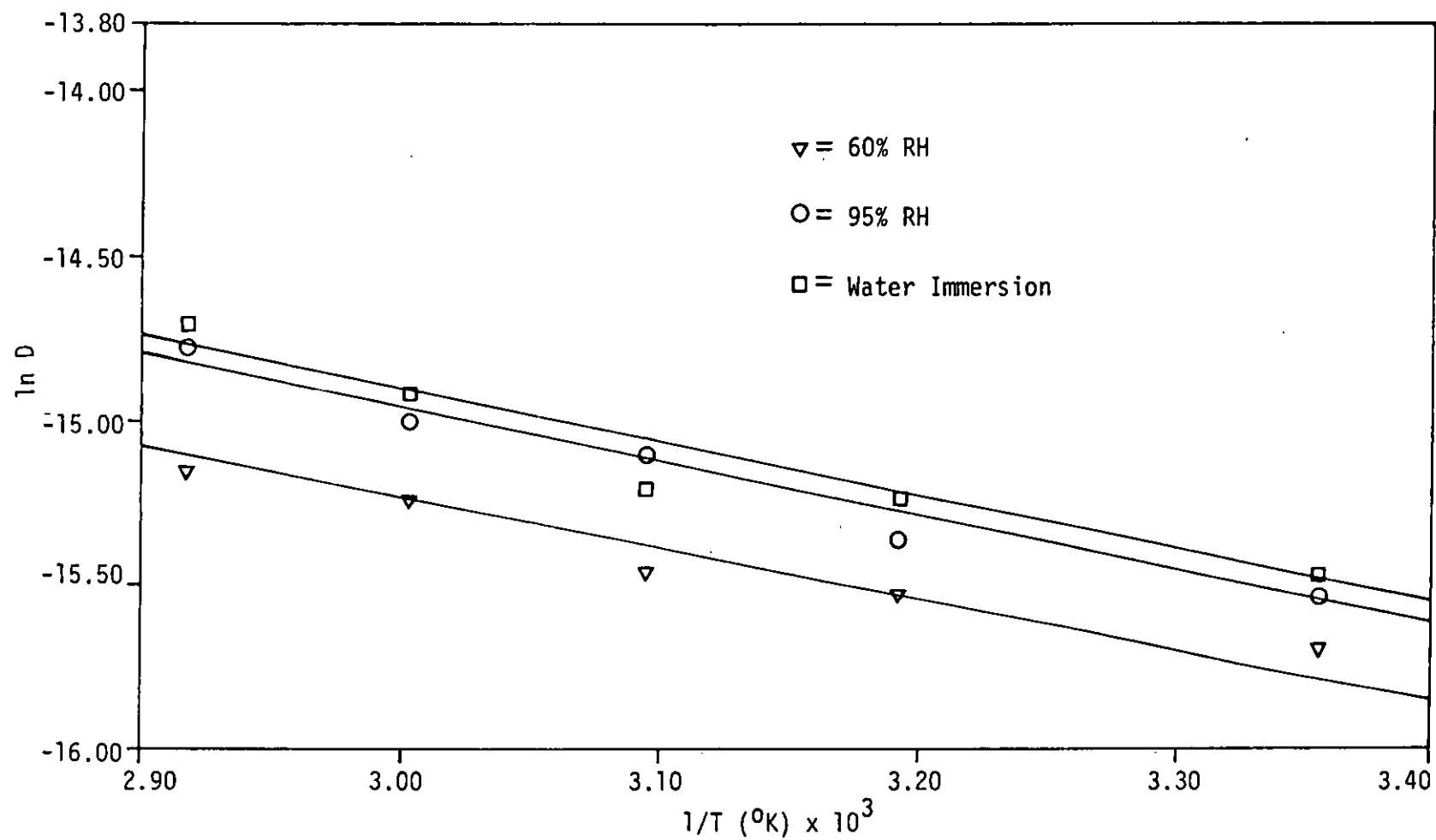


FIGURE 147: Arrhenius plot of 913 PrePreg specimens exposed to different environments (fibre orientation 0°)

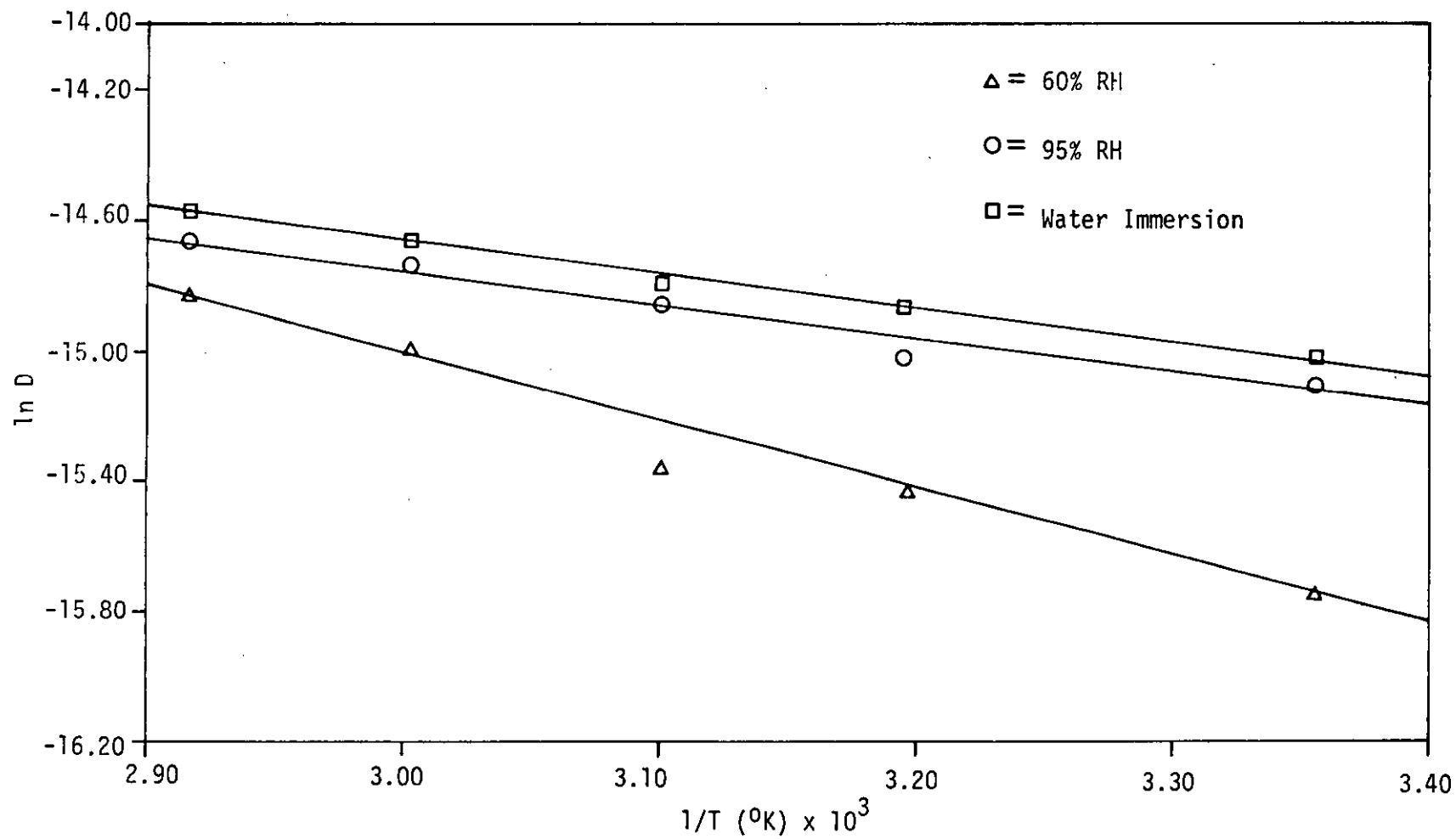


FIGURE 148: Arrhenius plot of 913 PrePreg specimens exposed to different environments (fibre orientation $\pm 45^{\circ}$)

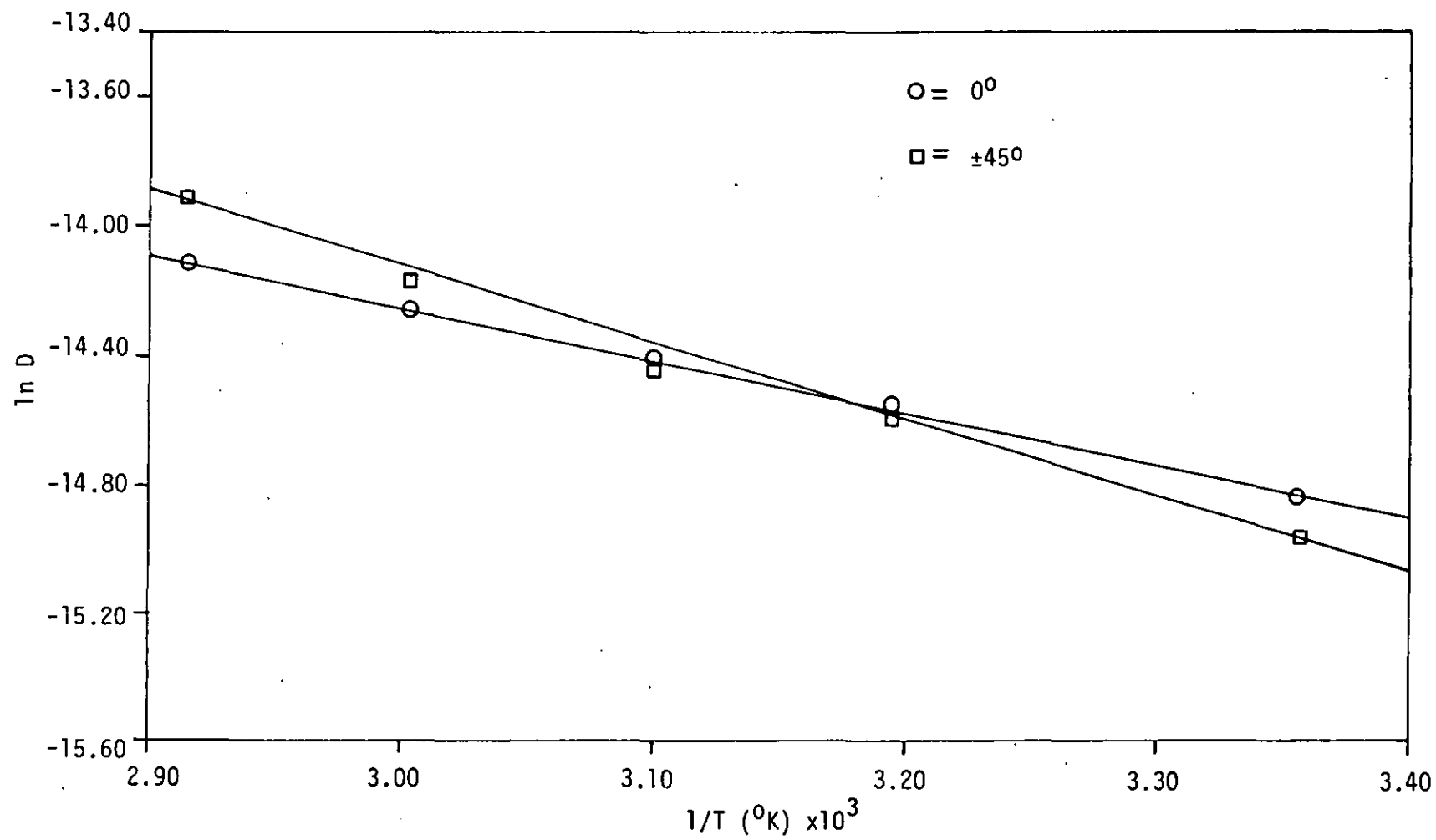


FIGURE 149: Arrhenius plot of 411-45 Vinylester 0° and $\pm 45^{\circ}$ specimens exposed to 60% RH

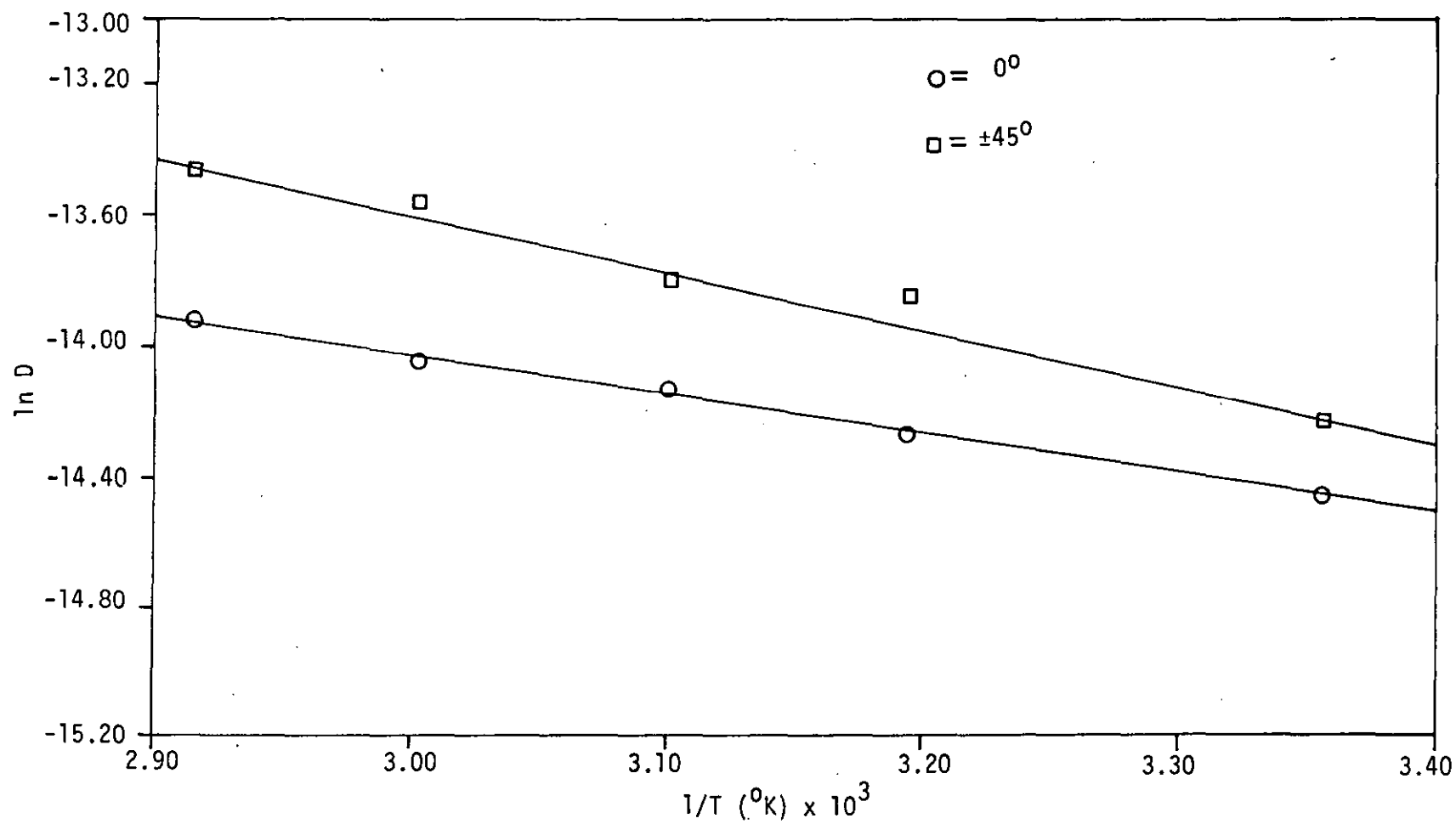


FIGURE 150: Arrhenius plot of 411-45 Vinylester 0° and $\pm 45^{\circ}$ specimens exposed to 95% RH

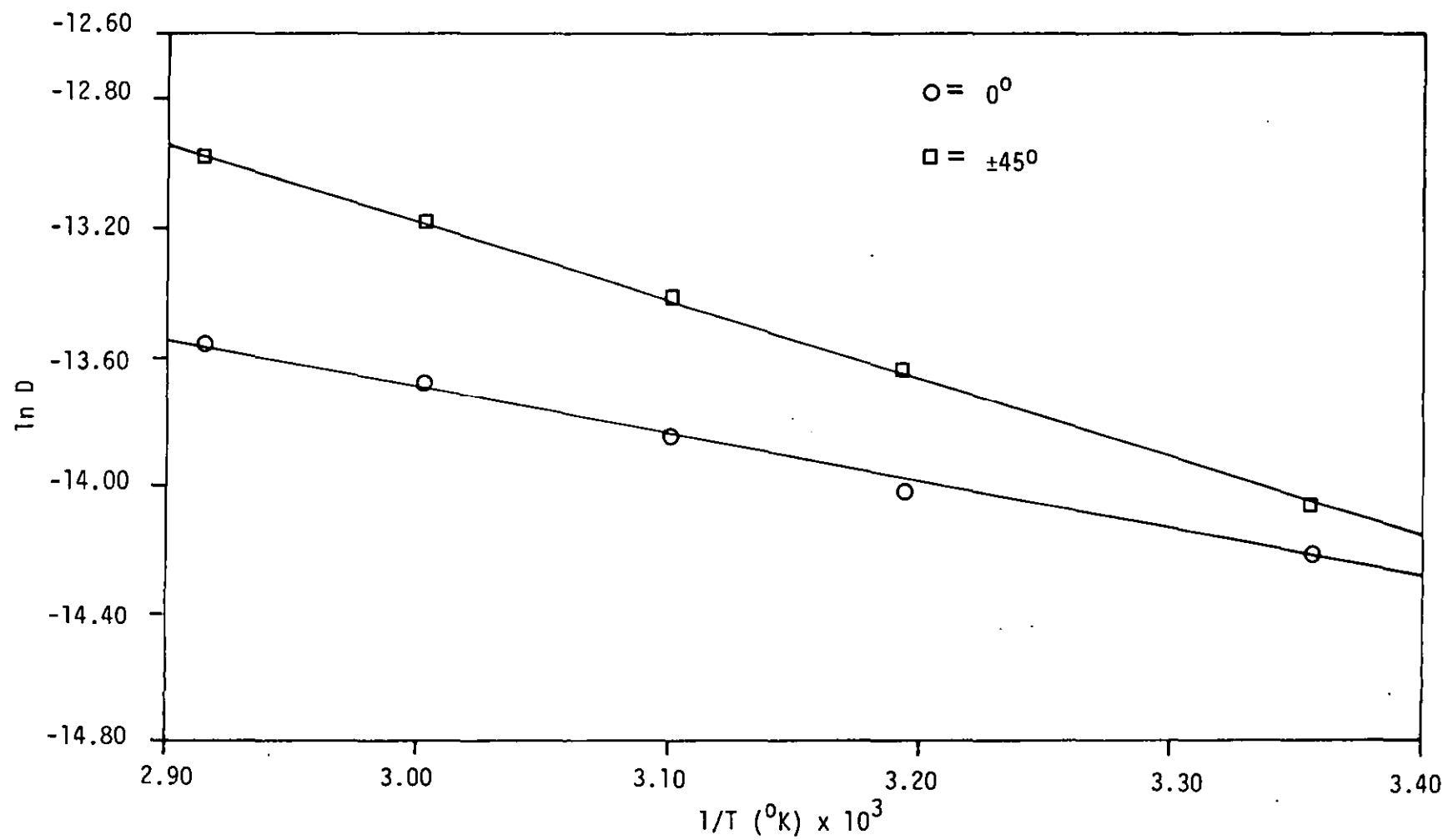


FIGURE 151: Arrhenius plot of 411-45 Vinylester 0° and $\pm 45^{\circ}$ specimens immersed in distilled water

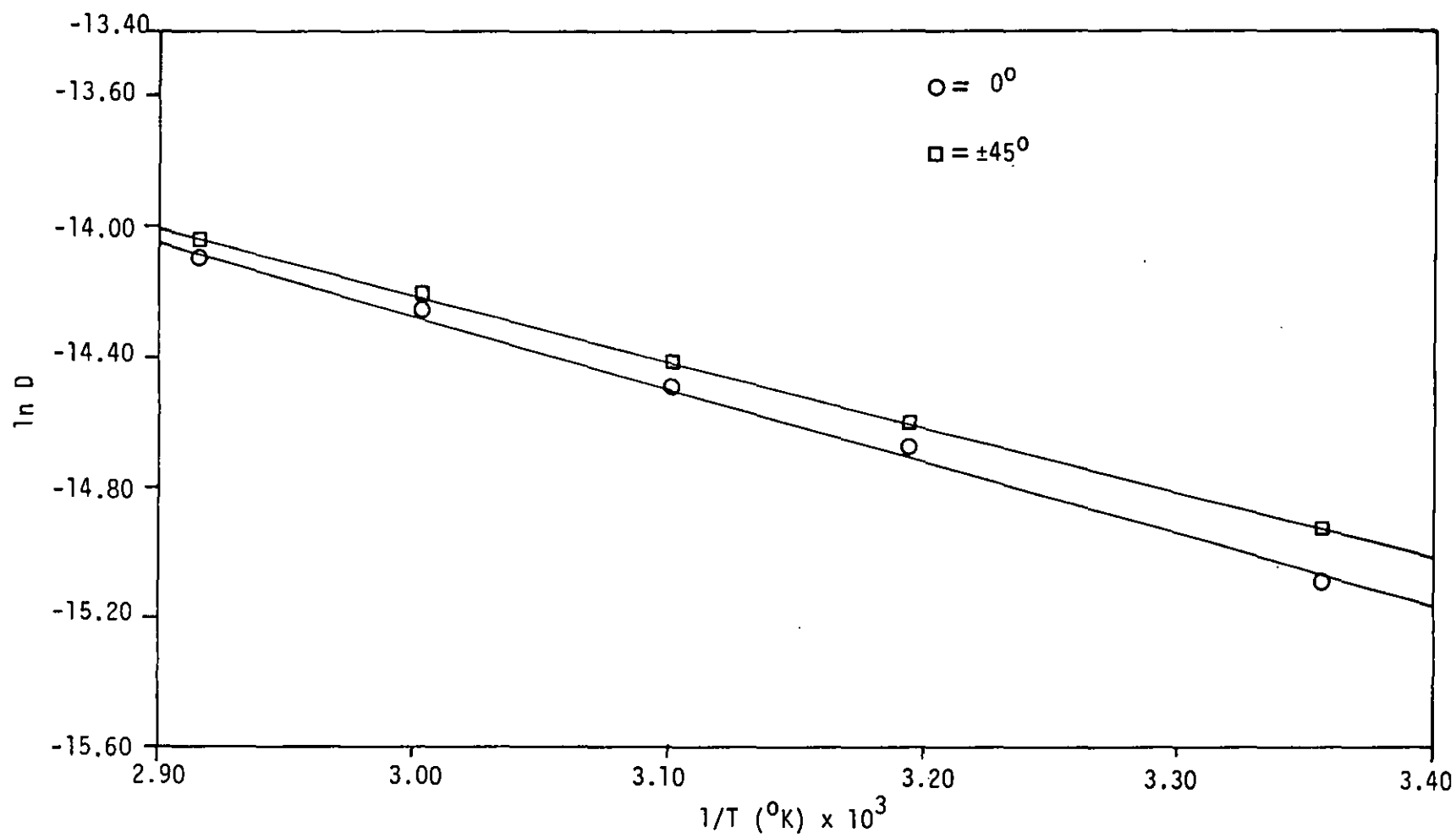


FIGURE 152: Arrhenius plot of 470-36 Vinylester 0° and $\pm 45^{\circ}$ specimens exposed to 60% RH

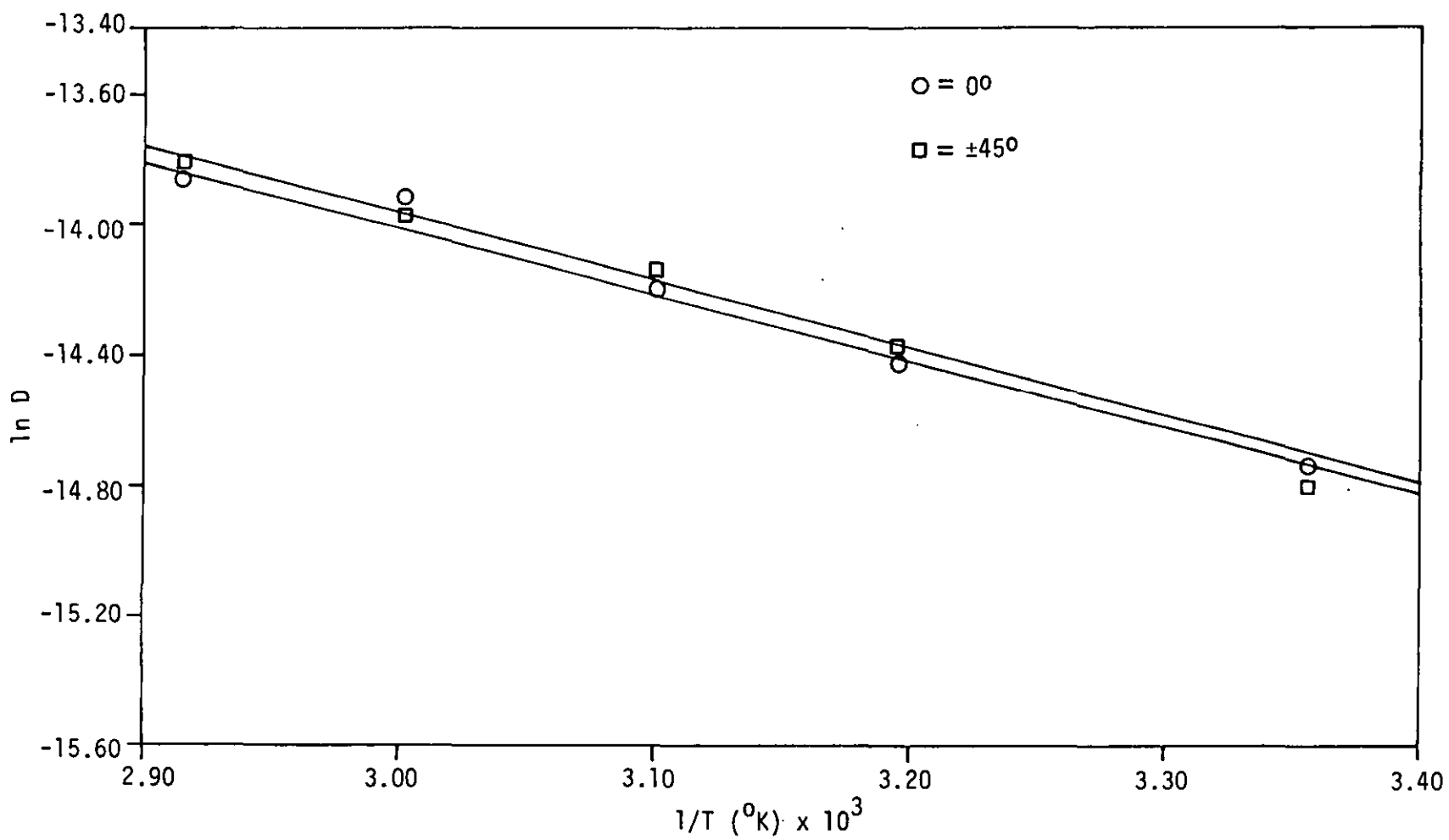


FIGURE 153: Arrhenius plot of 470-36 Vinylester 0° and $\pm 45^{\circ}$ specimens exposed to 95% RH

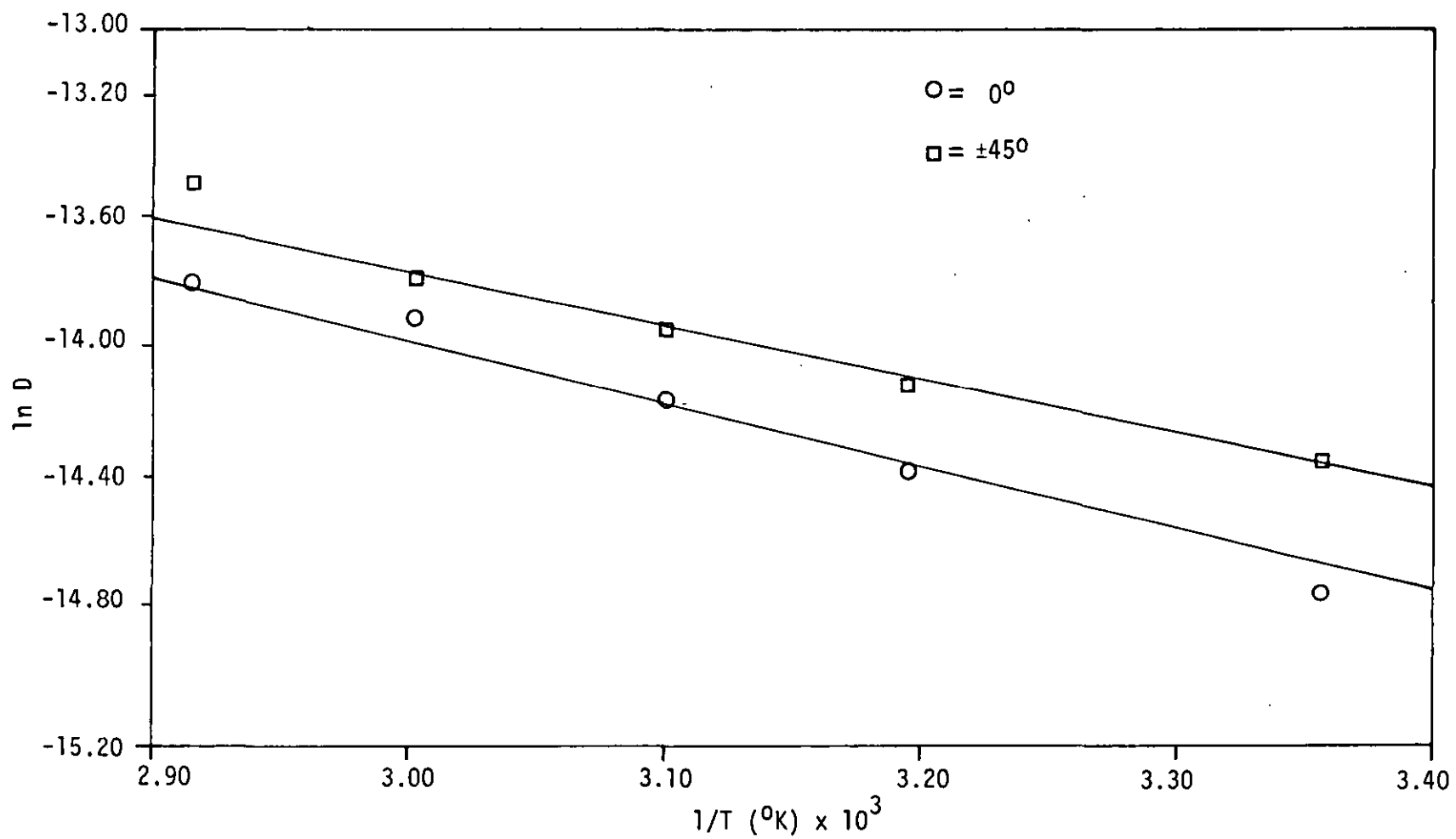


FIGURE 154: Arrhenius plot of 470-36 Vinylester 0° and $\pm 45^{\circ}$ specimens immersed in distilled water

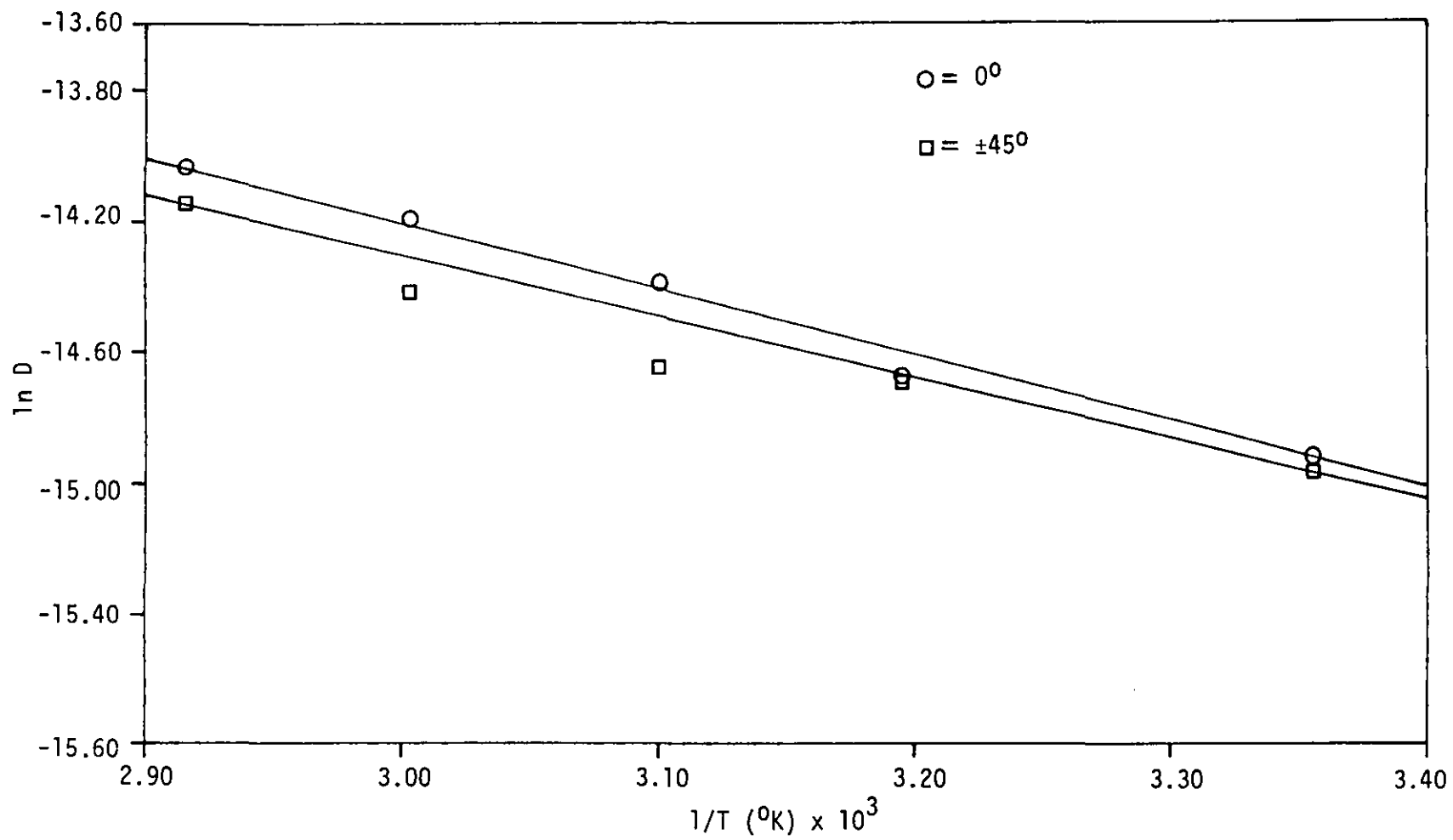


FIGURE 155: Arrhenius plot of Polyester 272 0° and $\pm 45^{\circ}$ specimens exposed to 60% RH

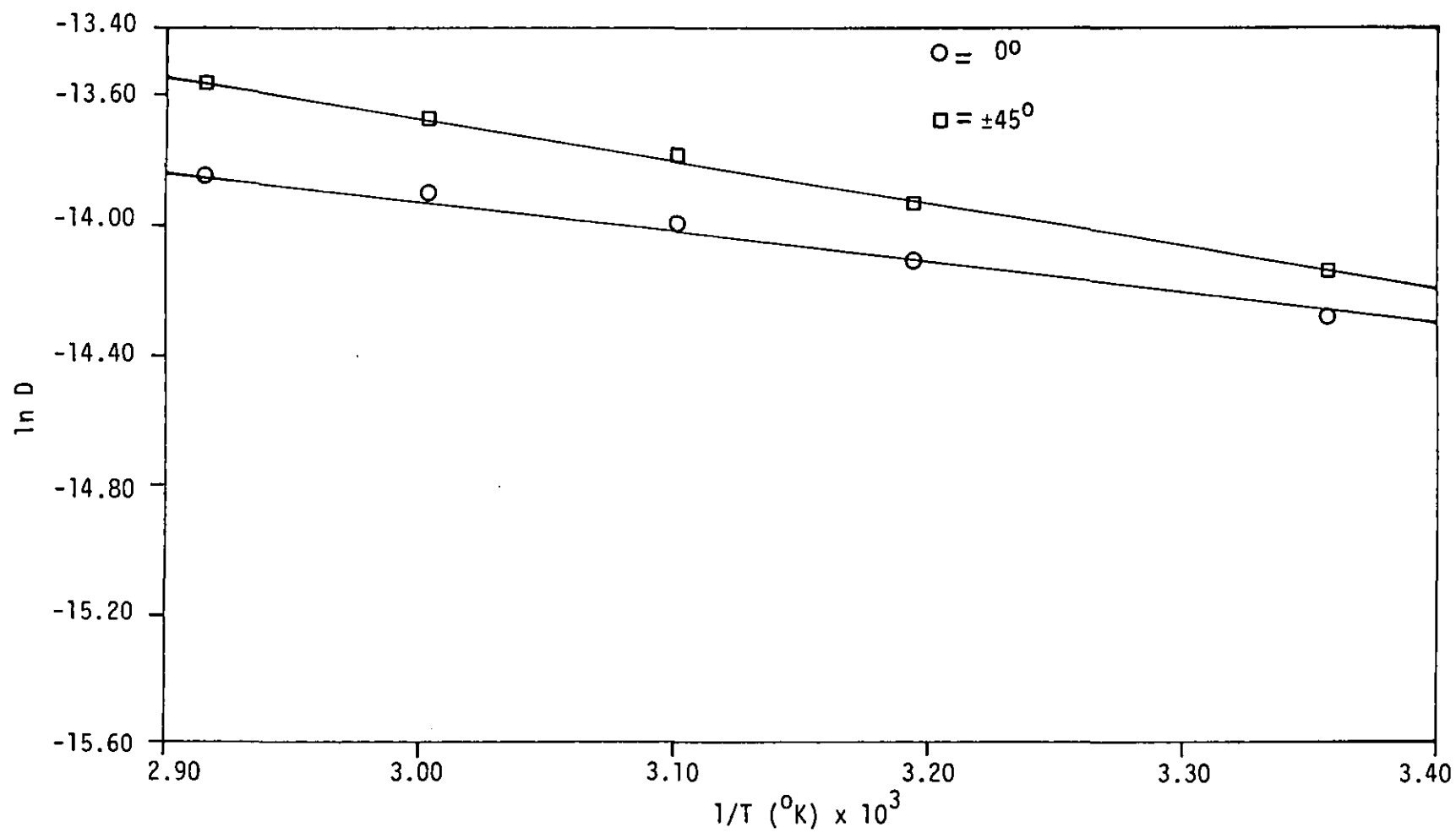


FIGURE 156: Arrhenius plot of Polyester 272 0° and $\pm 45^{\circ}$ specimens exposed to 95% RH

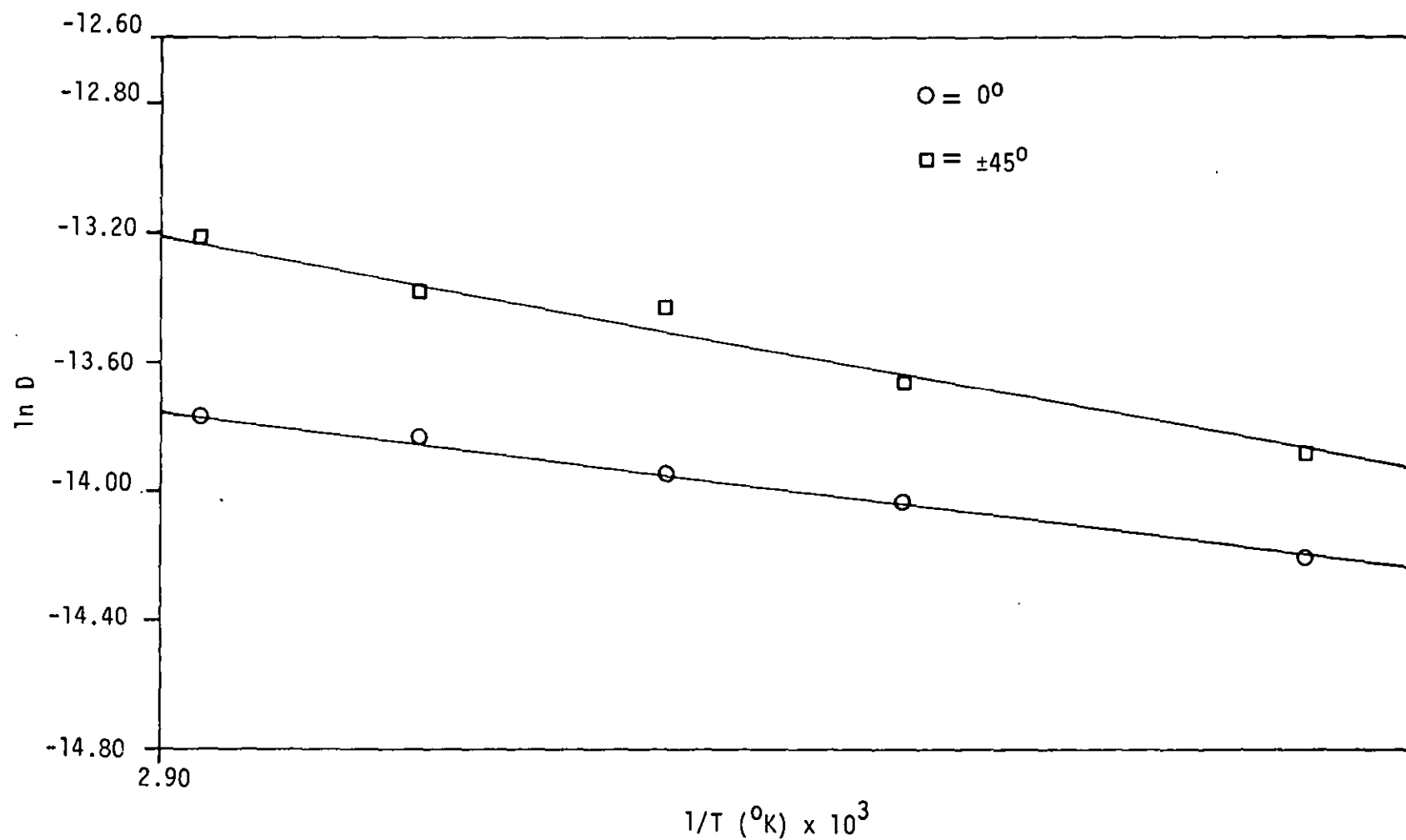


FIGURE 157: Arrhenius plot of Polyester 272 0° and $\pm 45^{\circ}$ specimens immersed in distilled water

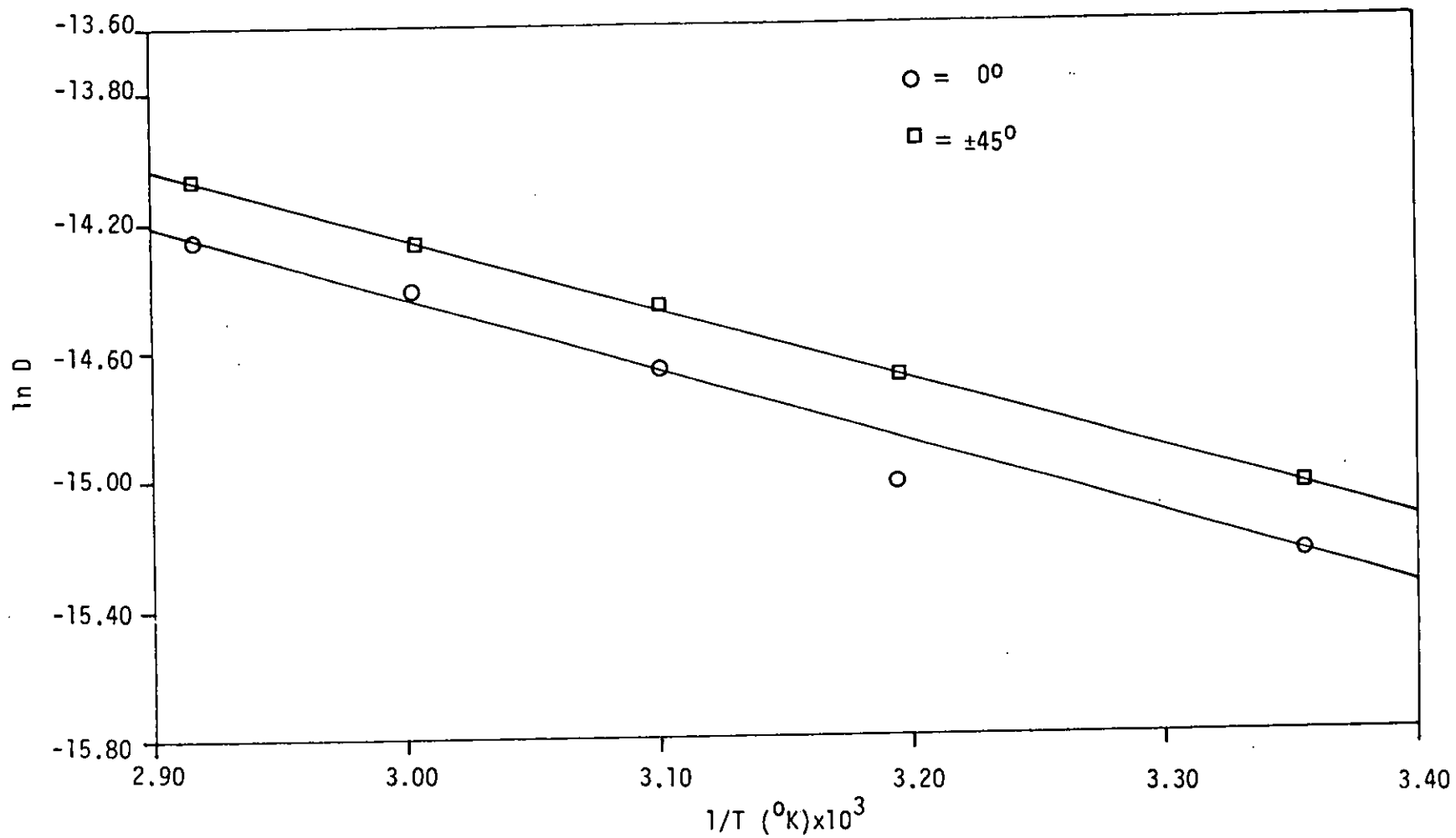


FIGURE 158: Arrhenius plot of Epoxy MY 750 0° and $\pm 45^\circ$ specimens exposed to 60% RH

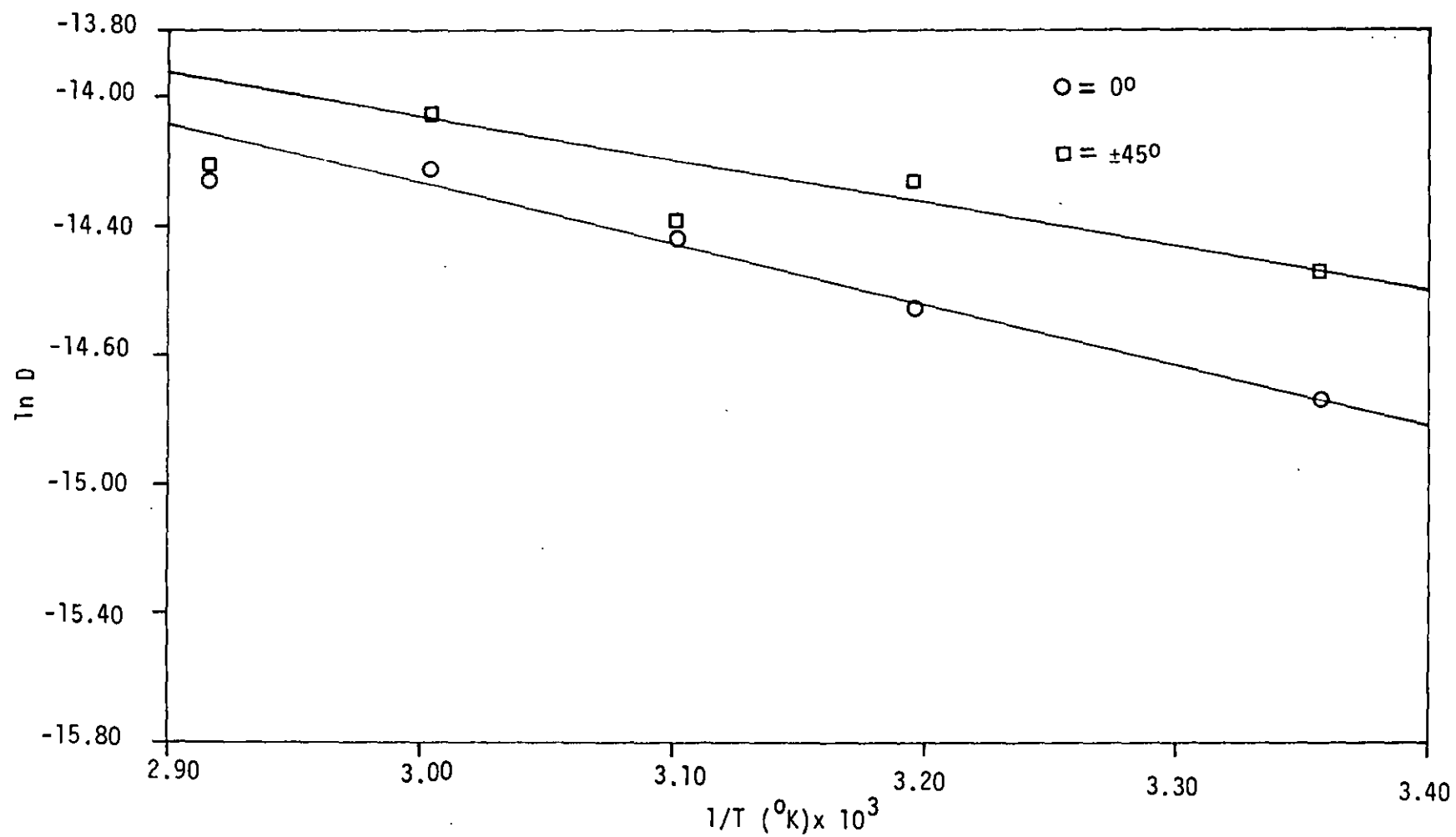


FIGURE 159: Arrhenius plot of Epoxy MY 750 0° and $\pm 45^{\circ}$ specimens exposed to 95% RH

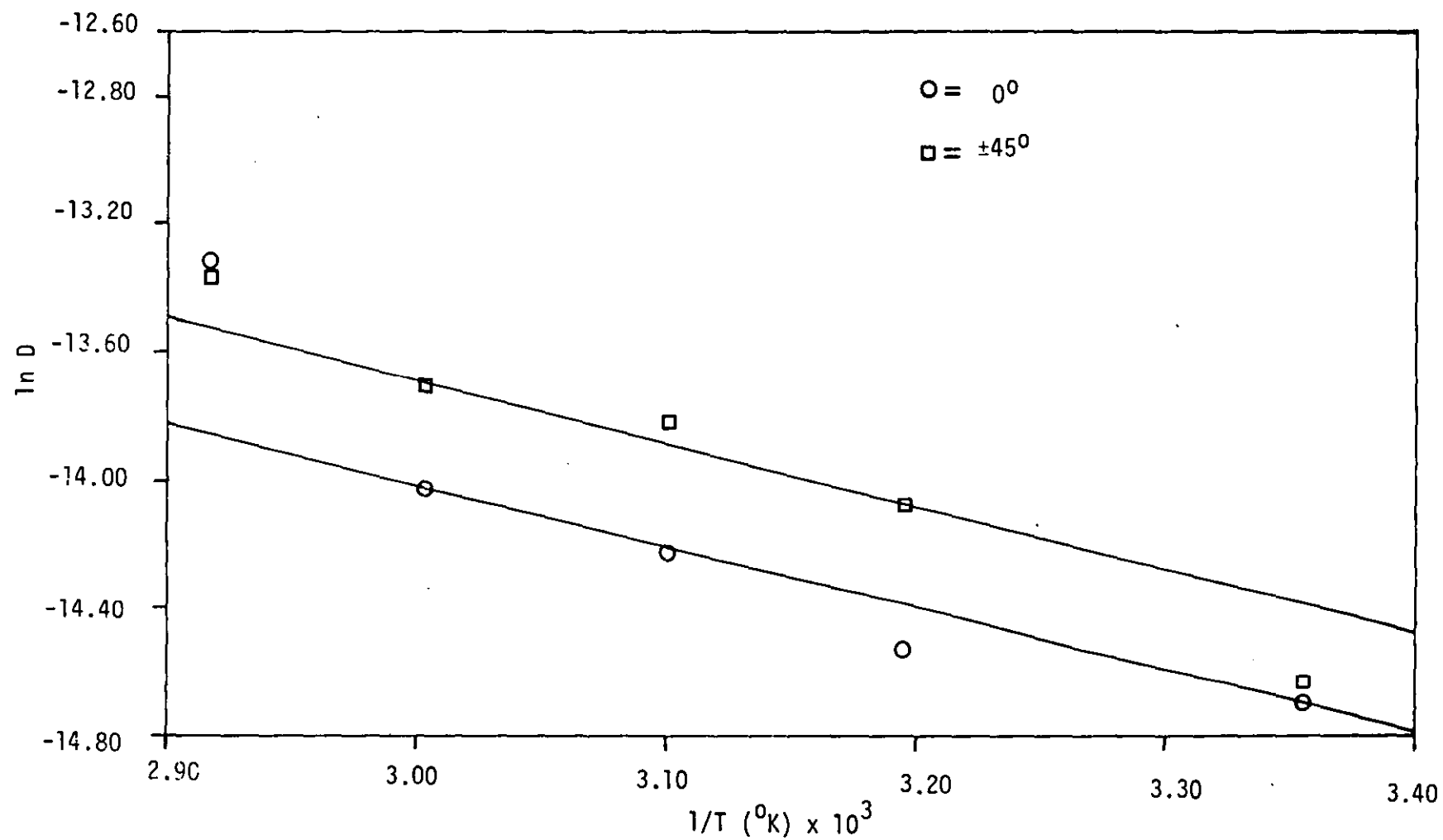


FIGURE 160: Arrhenius plot of Epoxy MY750 0° and $\pm 45^{\circ}$ specimens immersed in distilled water

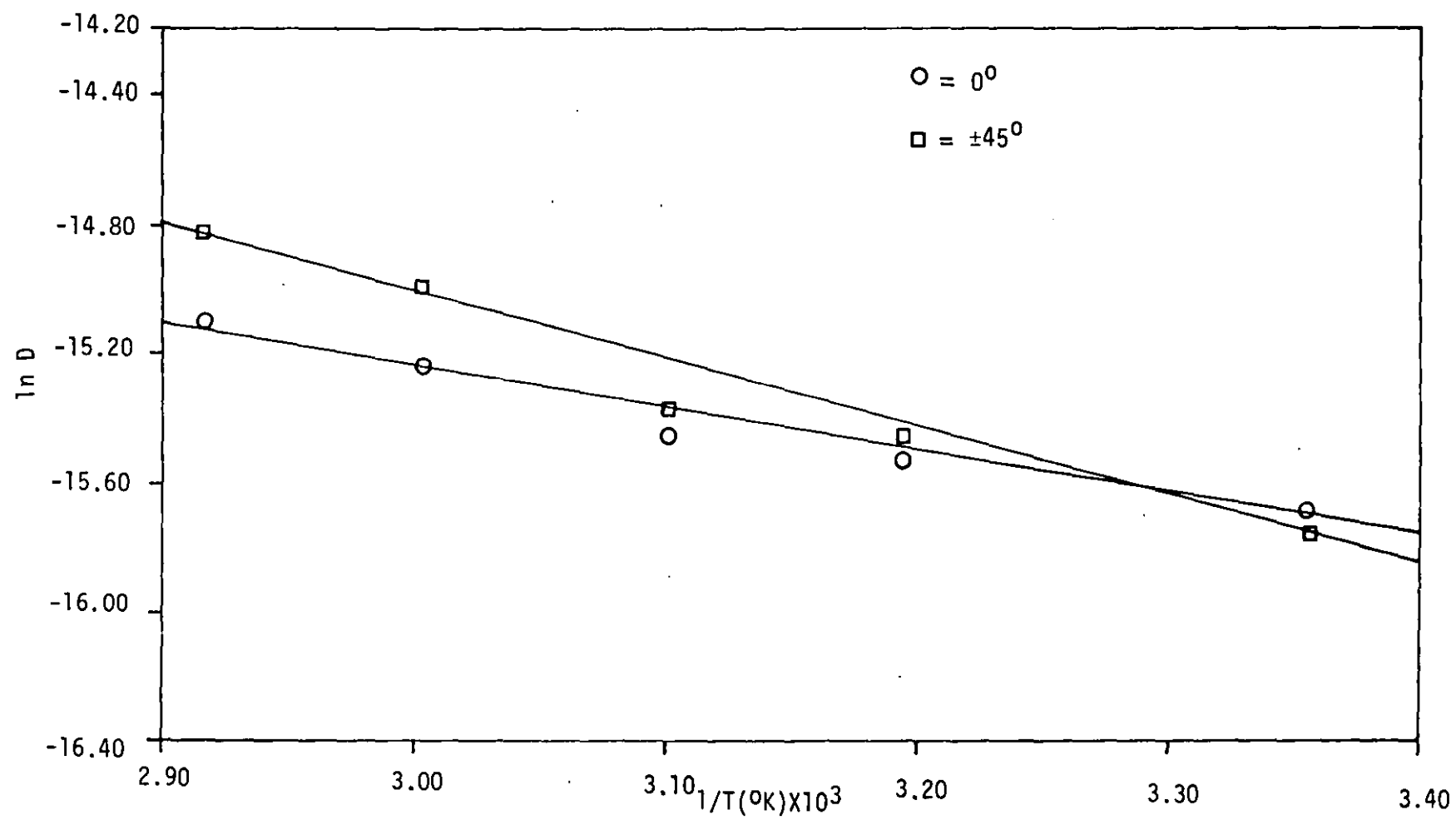


FIGURE 161: Arrhenius plot of 913 PrePreg 0 and $\pm 45^\circ$ specimens exposed to 60% RH

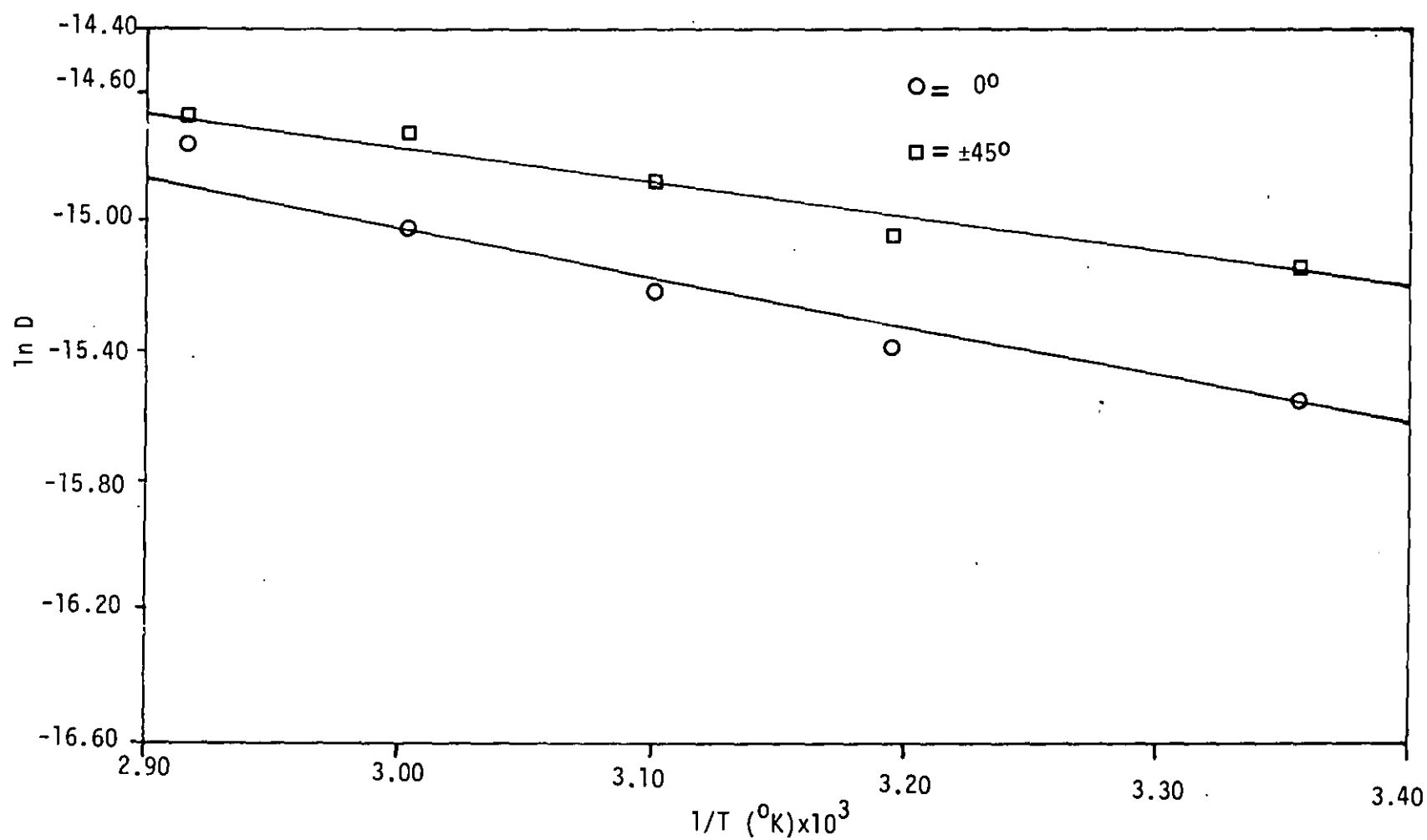


FIGURE 162: Arrhenius plot of 913 PrePreg 0° and $\pm 45^{\circ}$ specimens exposed to 95% RH

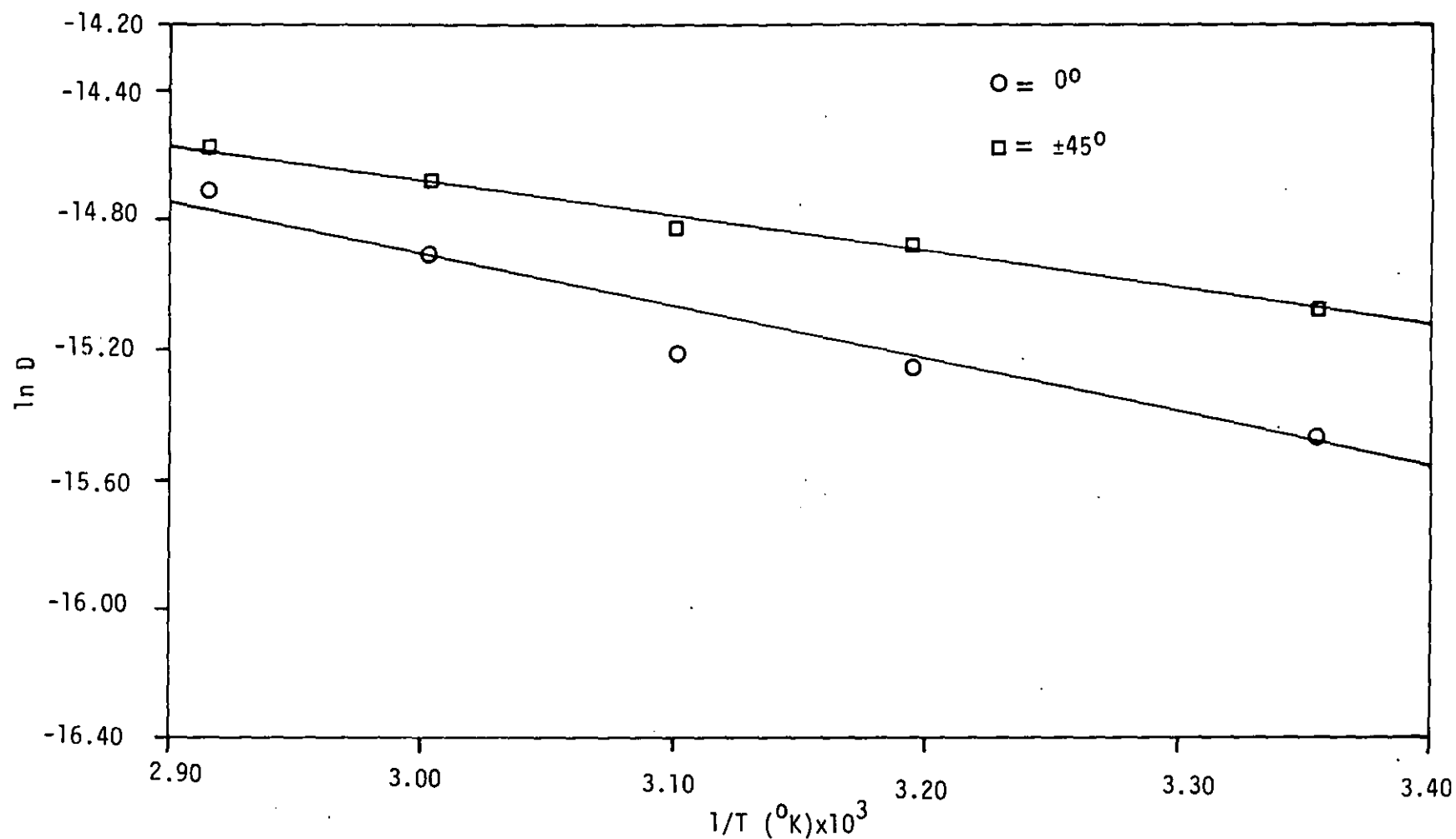


FIGURE 163: Arrhenius plot of 913 PrePreg 0° and $\pm 45^{\circ}$ specimens immersed in distilled water

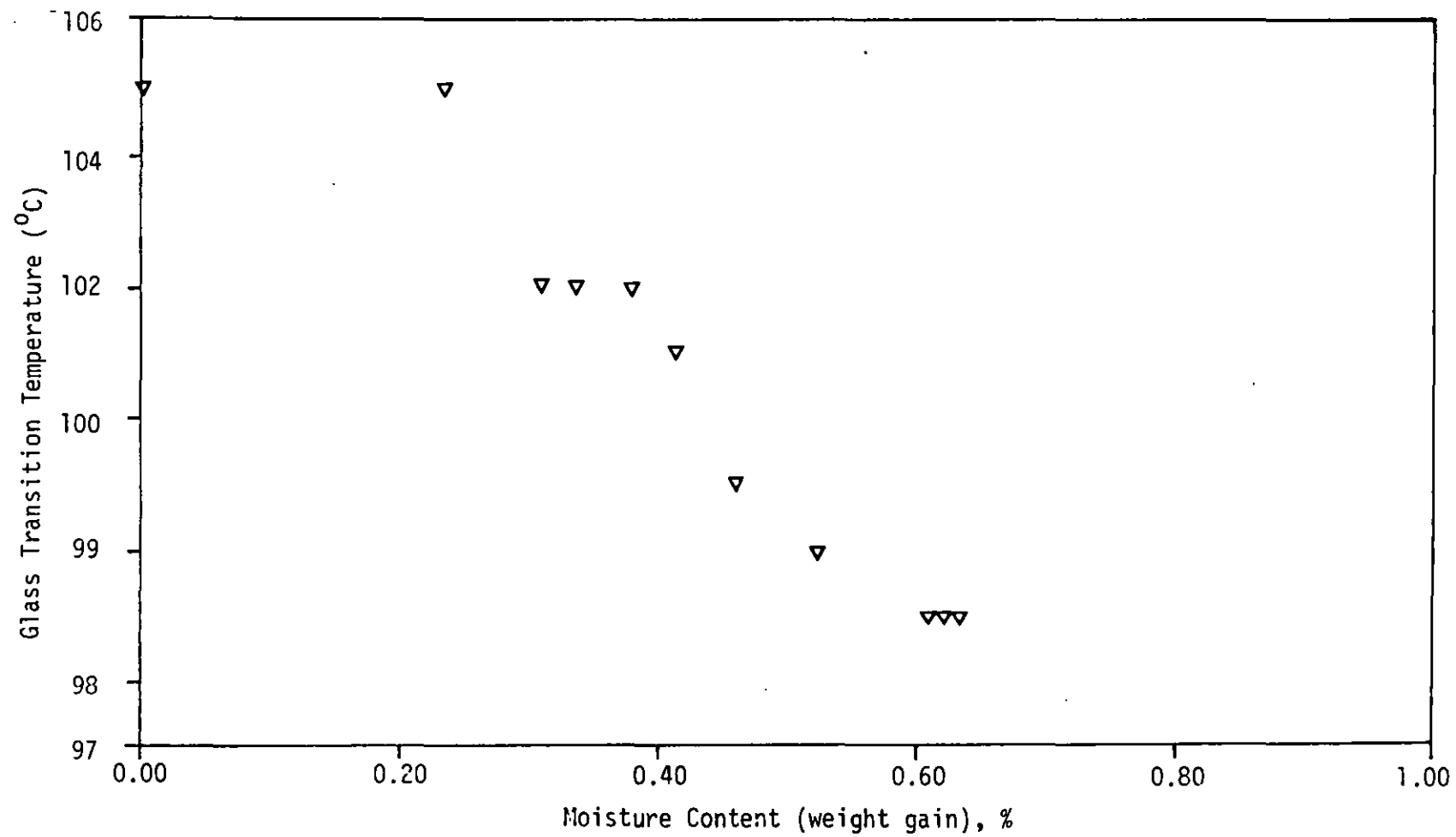


FIGURE 164: Effect of moisture content on glass transition temperature of 411-45 Vinylester specimens

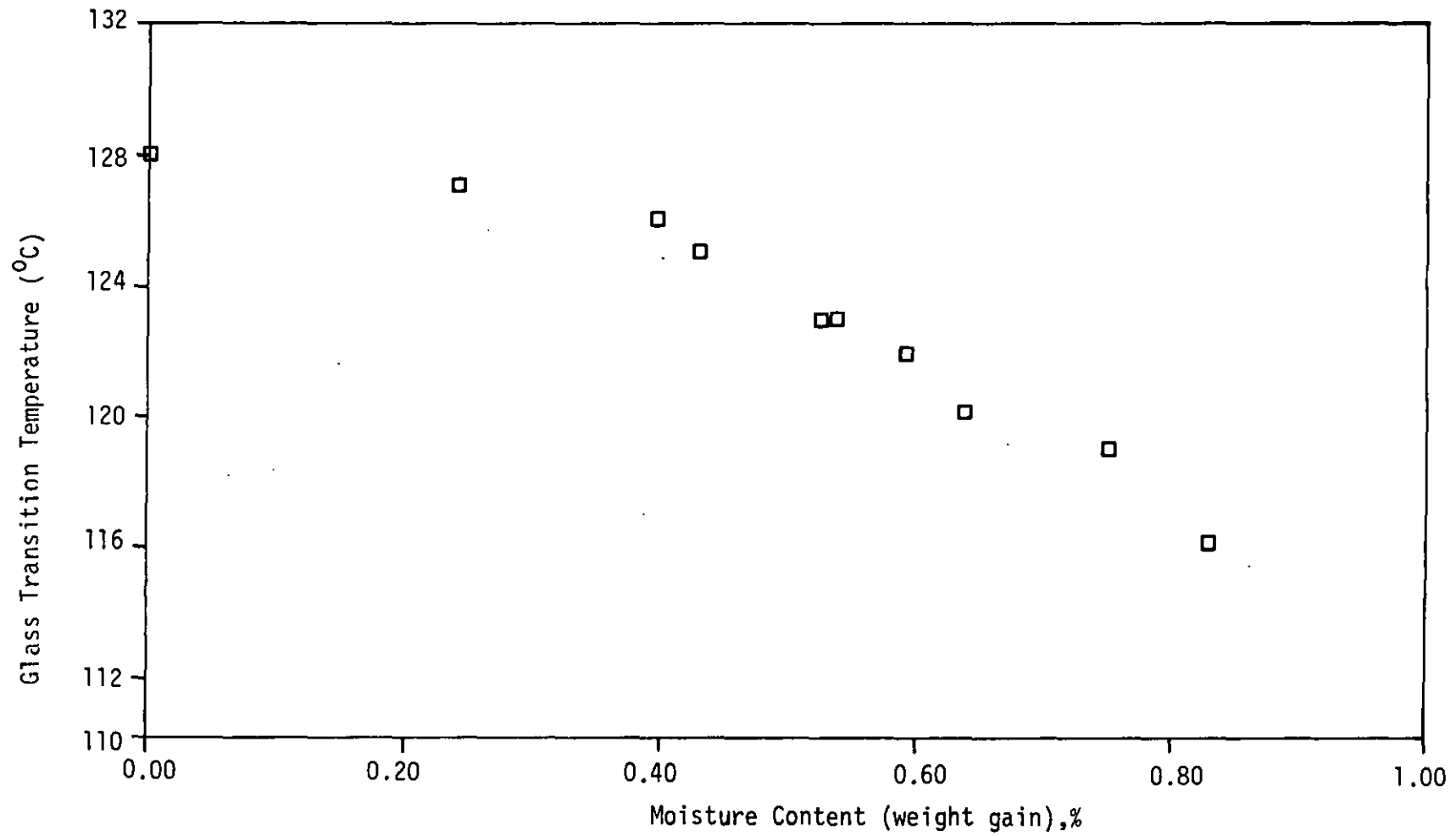


FIGURE 165: Effect of moisture content on glass transition temperature of 470-36 Vinylester specimens

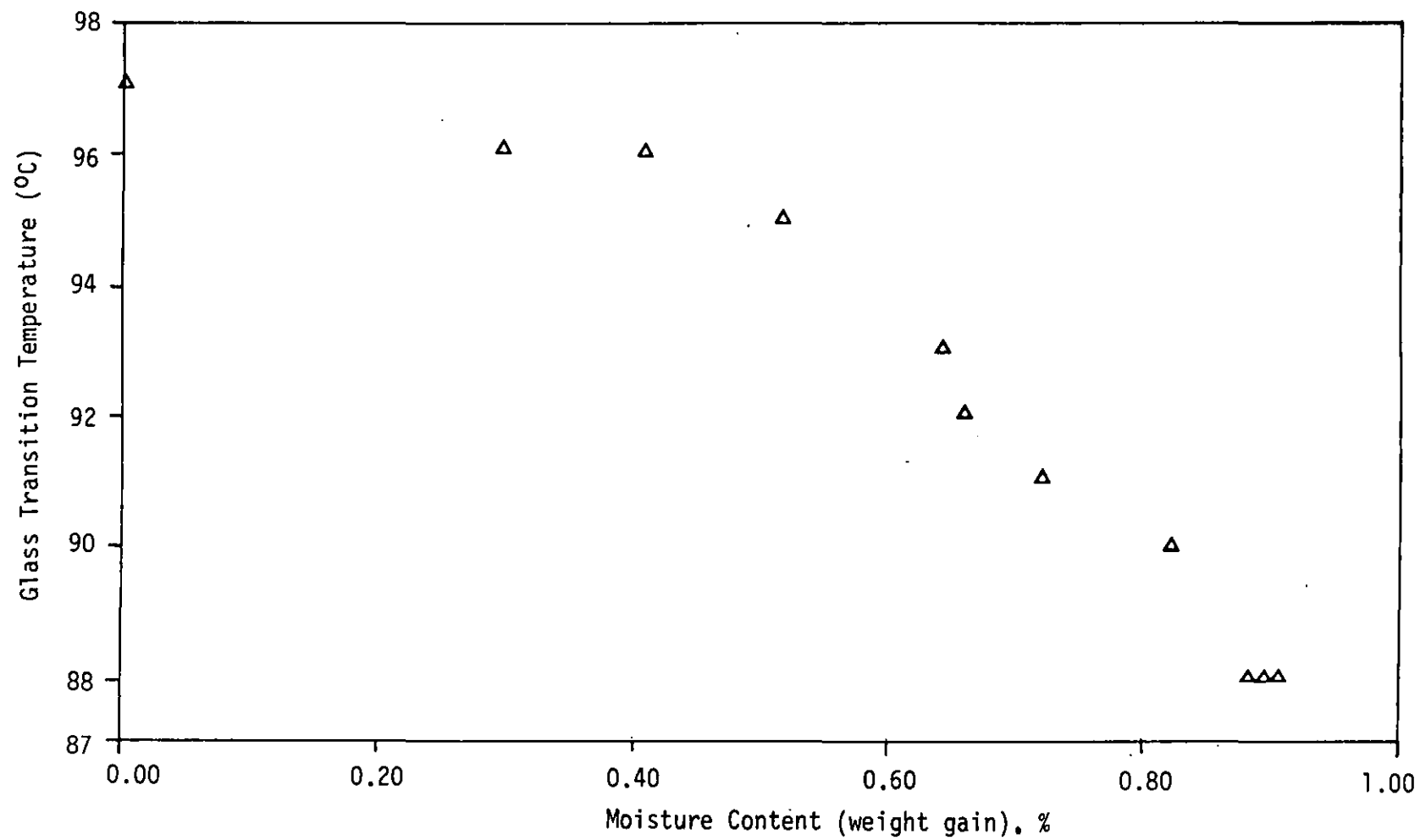


FIGURE 166: Effect of moisture content on glass transition temperature of Polyester 272 specimens

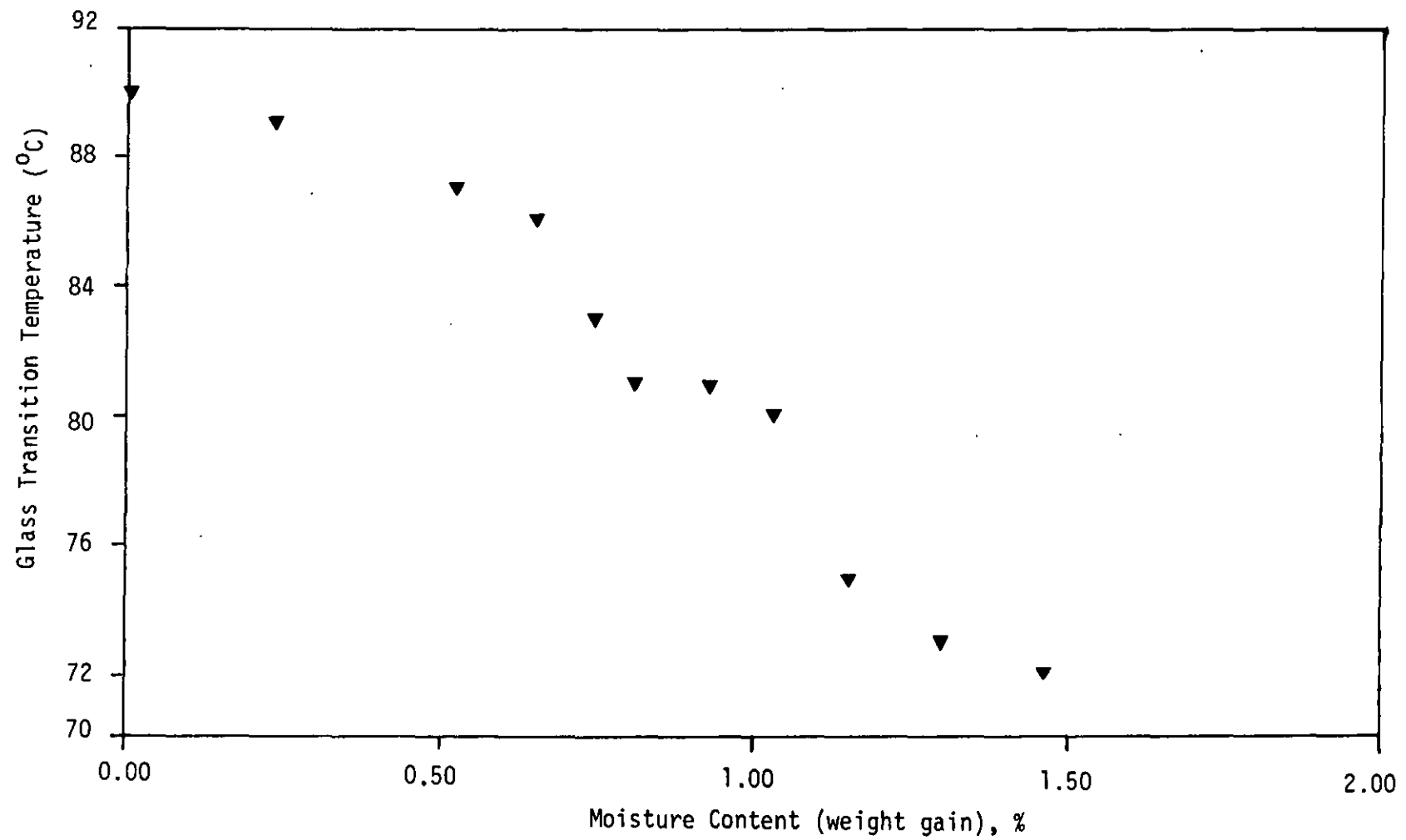


FIGURE 167: Effect of moisture content on glass transition temperature of Epoxy MY 750 specimens

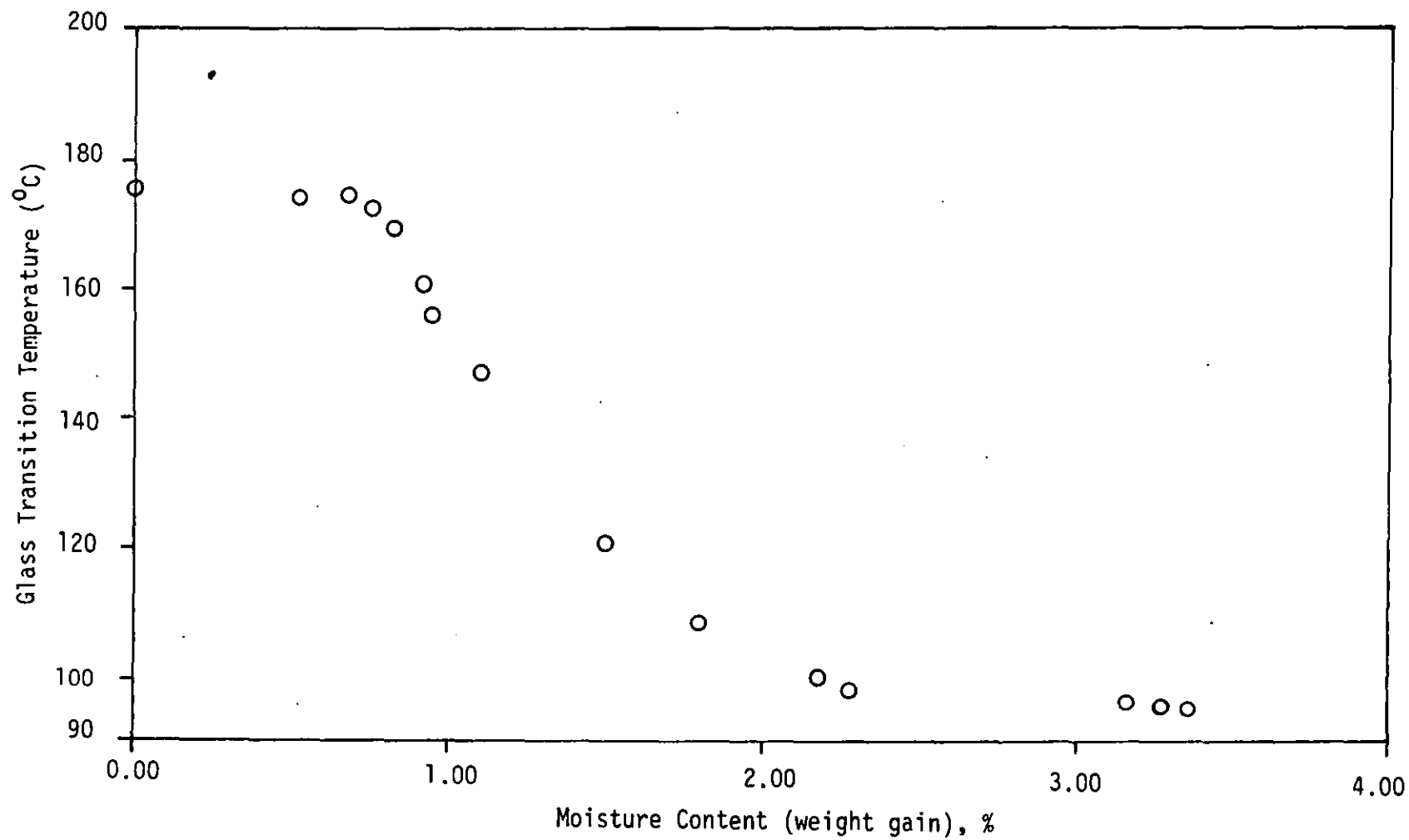


FIGURE 168: Effect of moisture content on glass transition temperature of 913 PrePreg specimens

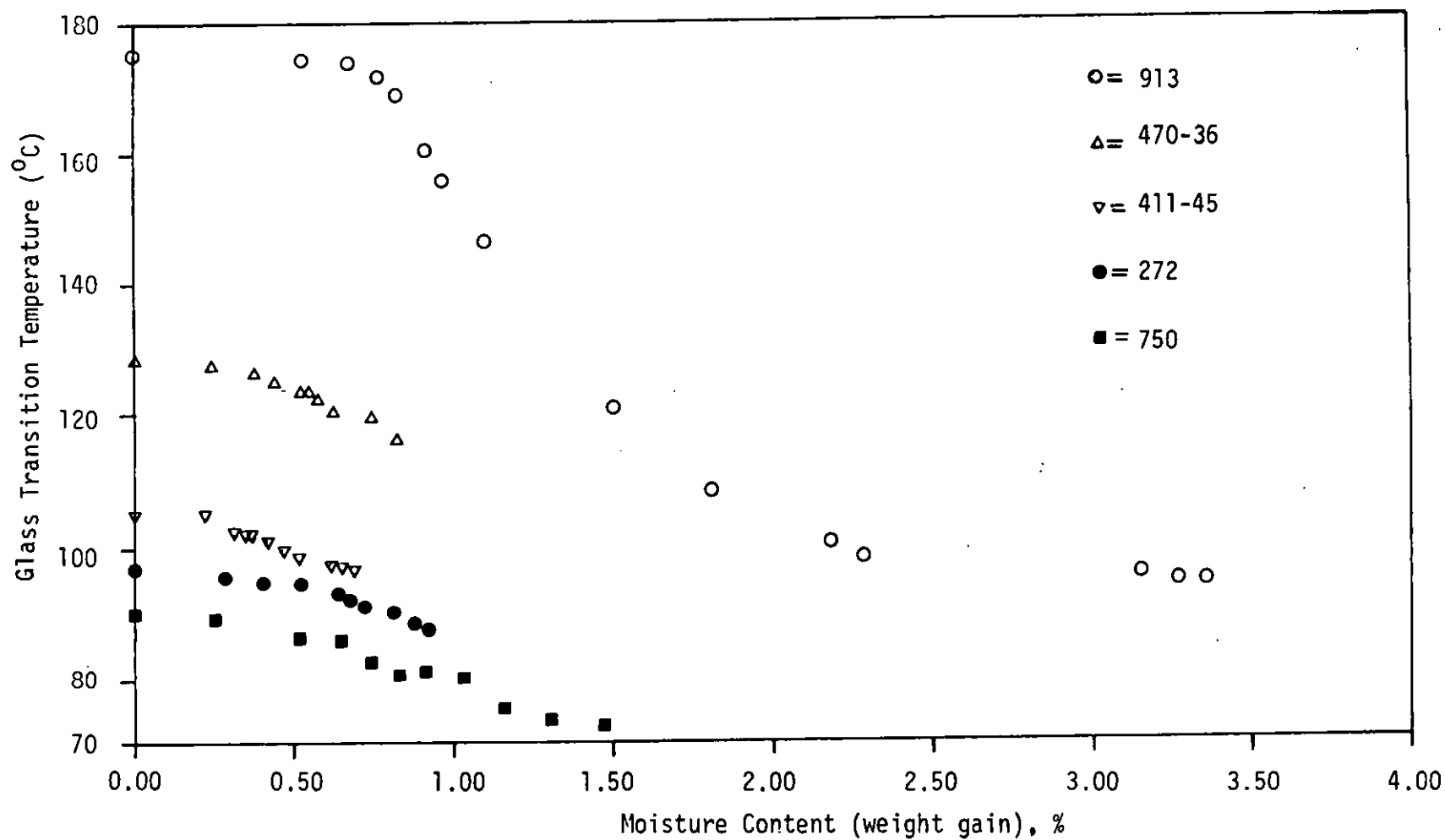


FIGURE 169: Relationship between moisture content and glass transition temperature of different specimens

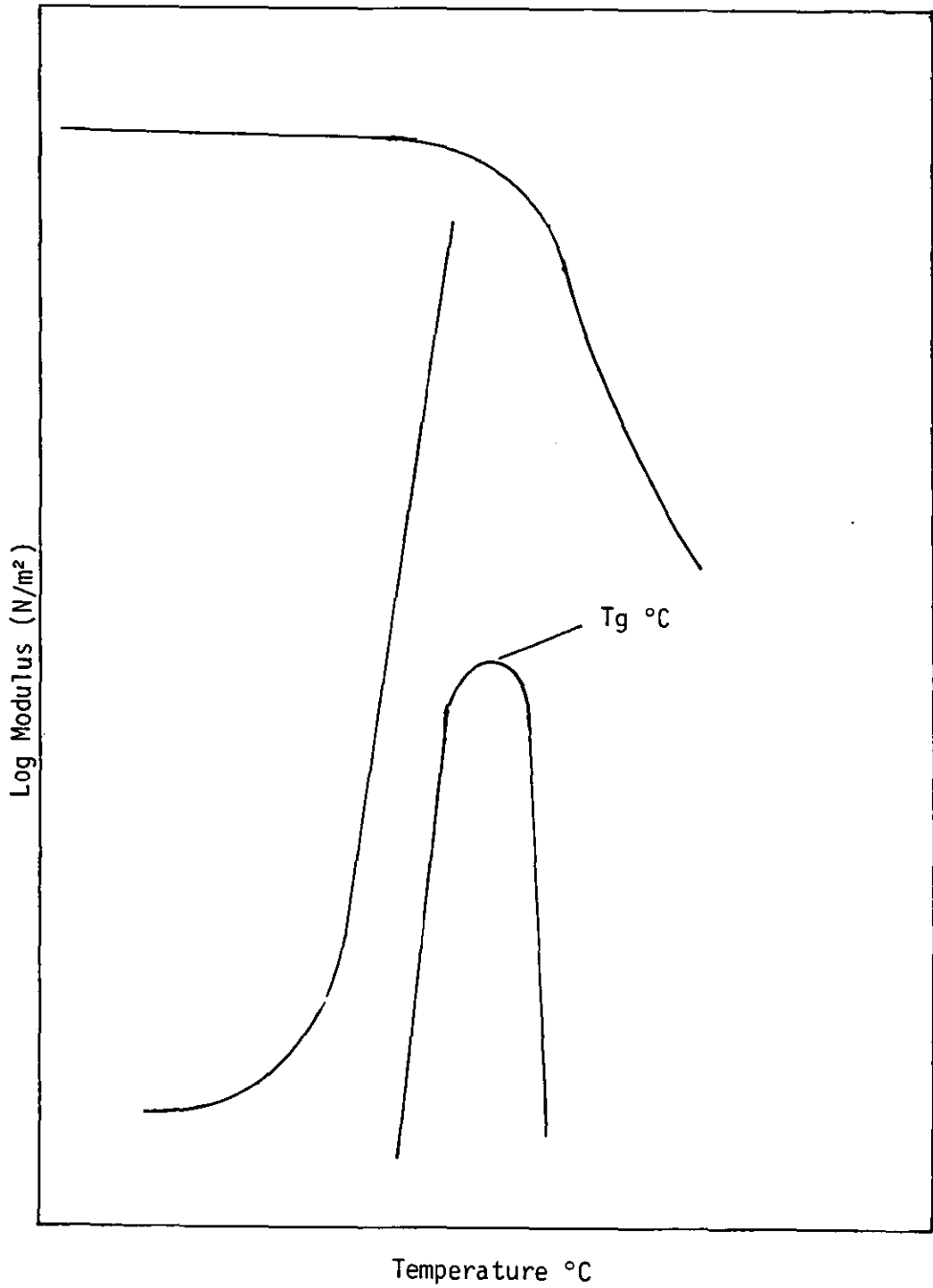


FIGURE 170: General form of graph obtained from PL-DMTA

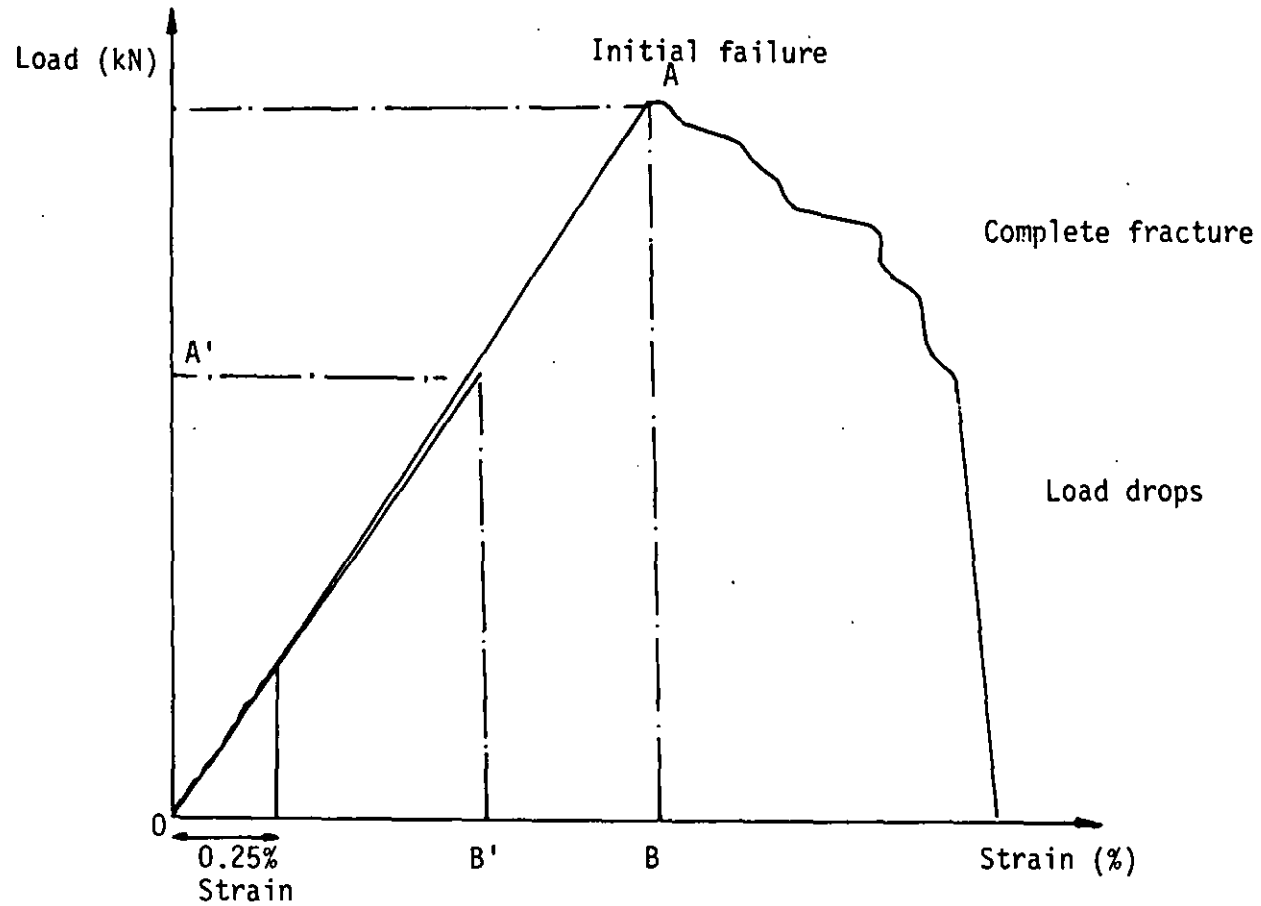


FIGURE 171(a): A typical load/strain curve for a longitudinal tensile test showing no "jumps"

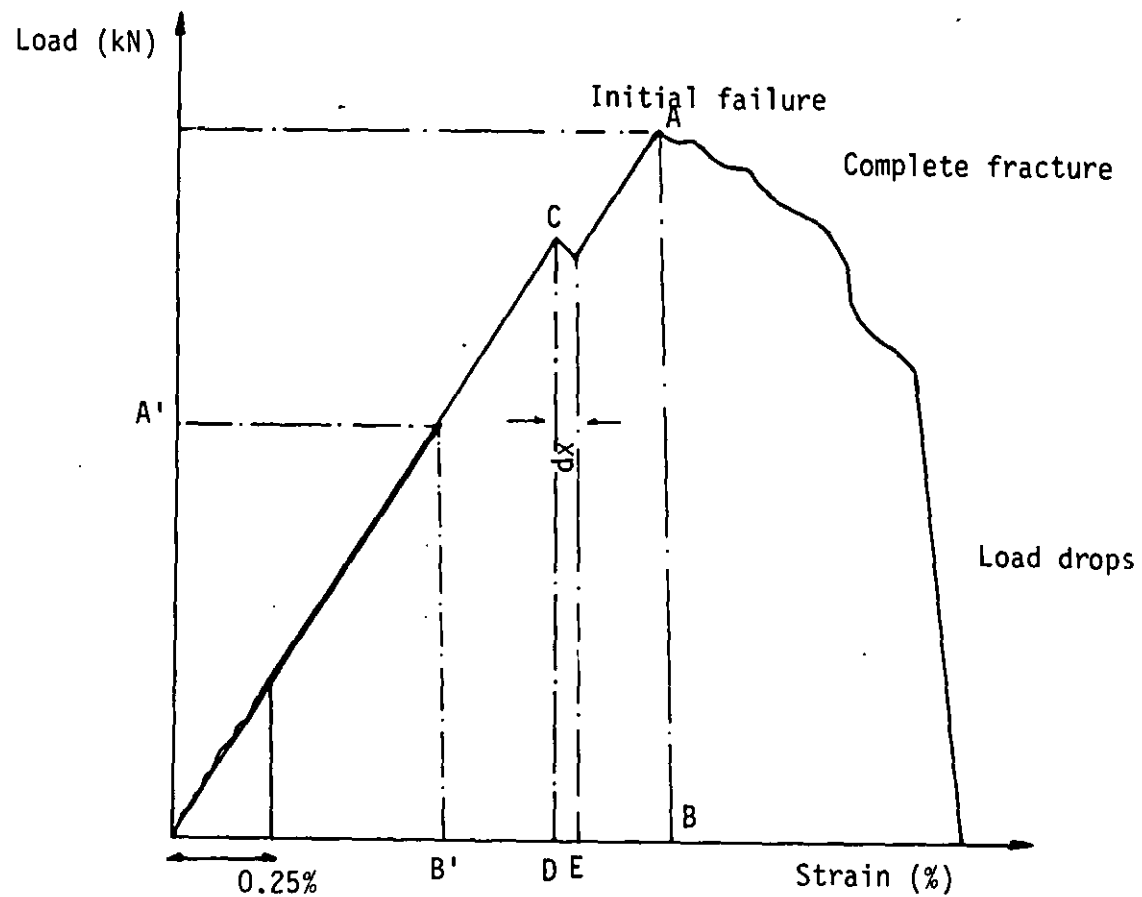


FIGURE 171(b): A typical load/strain curve for a longitudinal tensile test showing one of the "jumps" which often occurs.

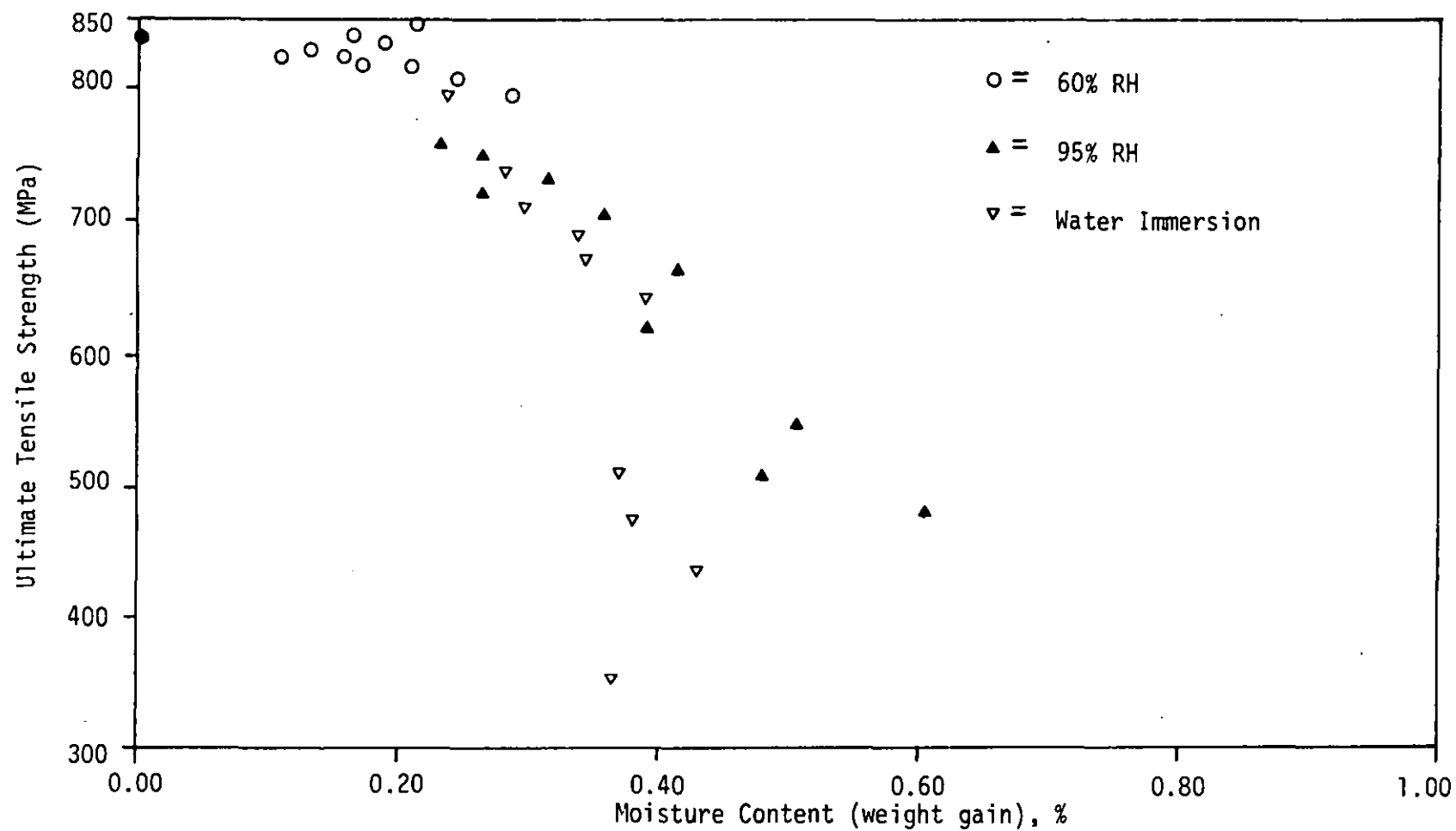


FIGURE 172: Effect of moisture on the ultimate tensile strength of 411-45 Vinylester specimens

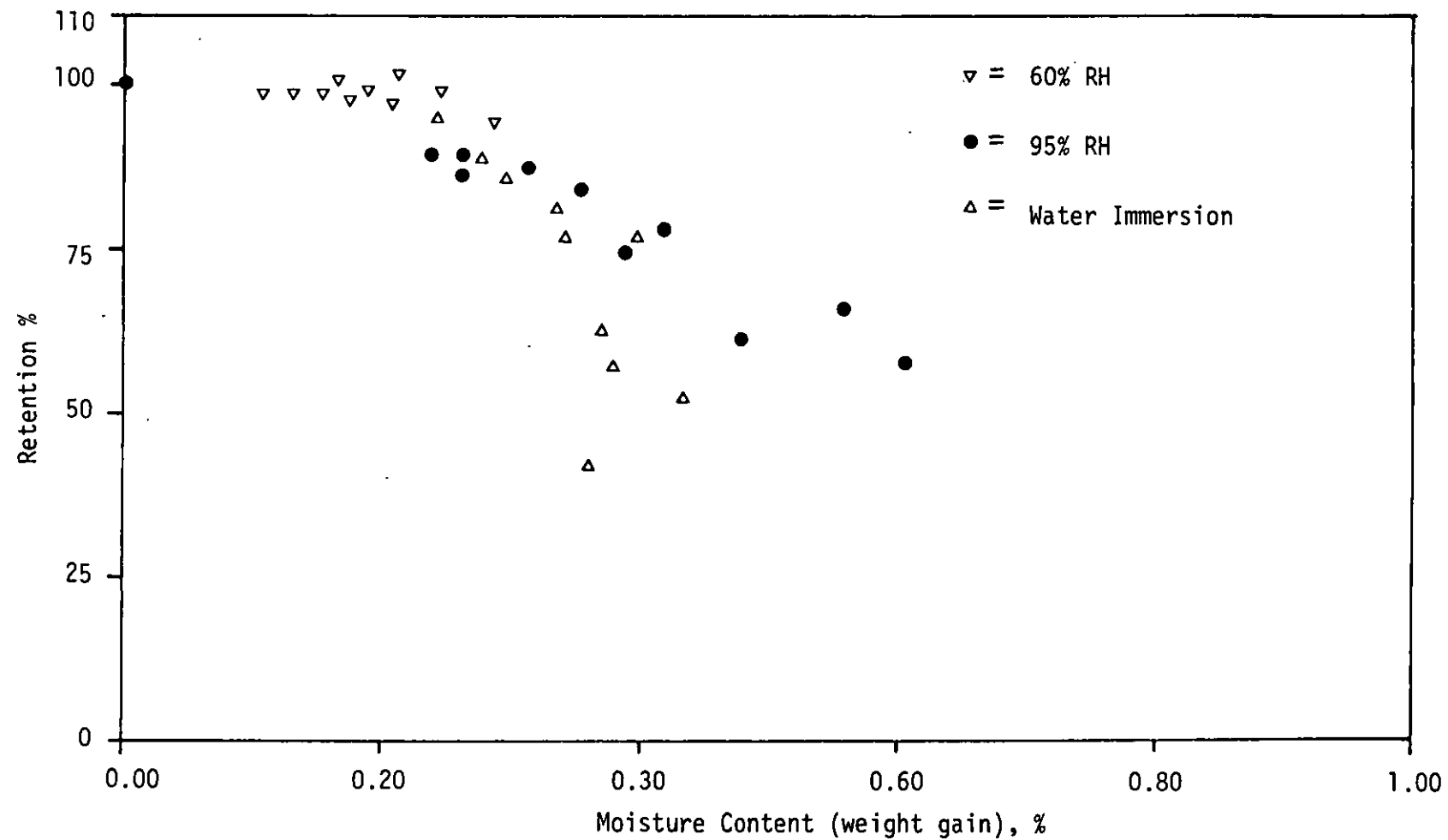


FIGURE 173: The effect of moisture on the % retention of ultimate tensile strength of 411-45 Vinylester specimens

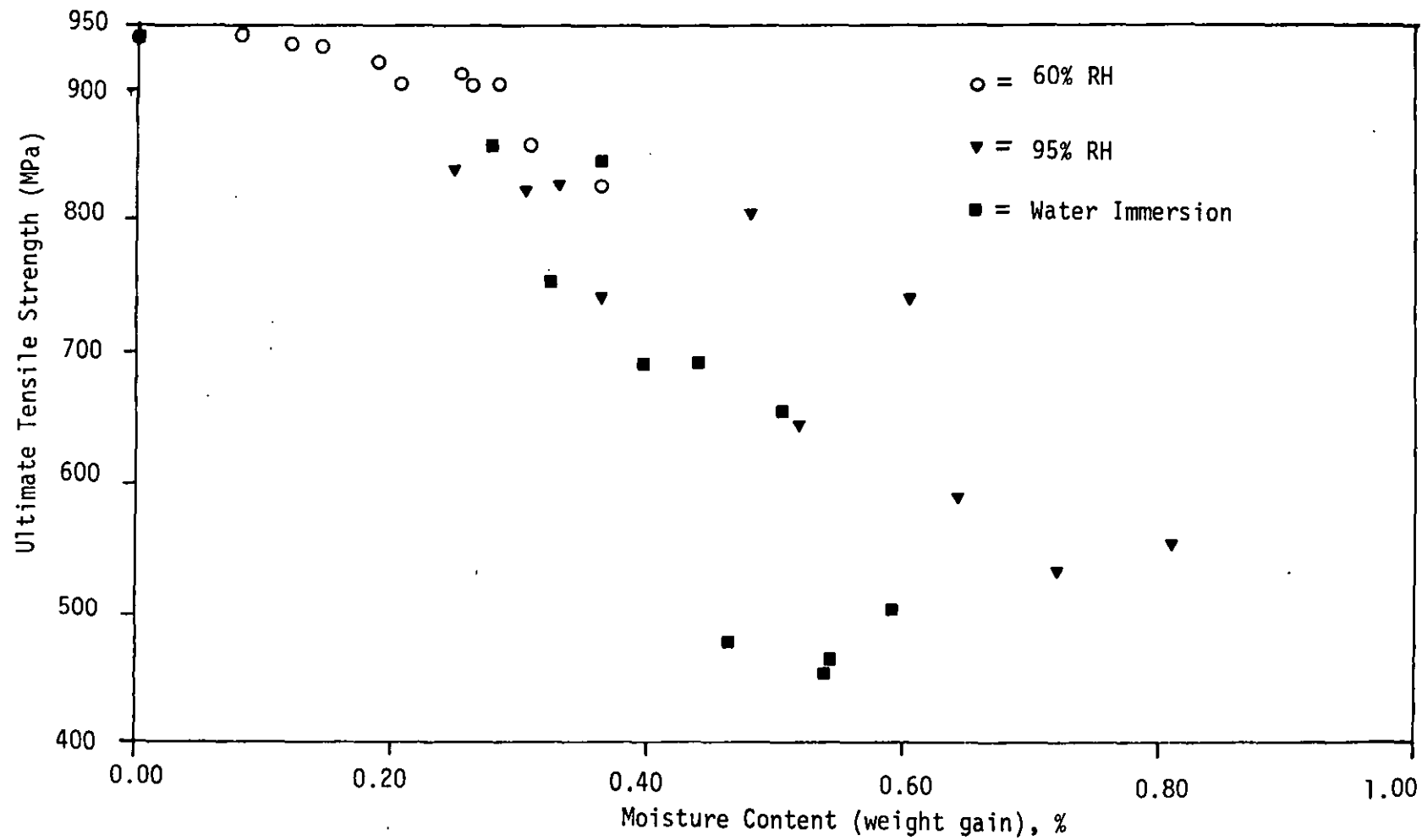


FIGURE 174: The effect of moisture on the ultimate tensile strength of 470-36 Vinylester specimens

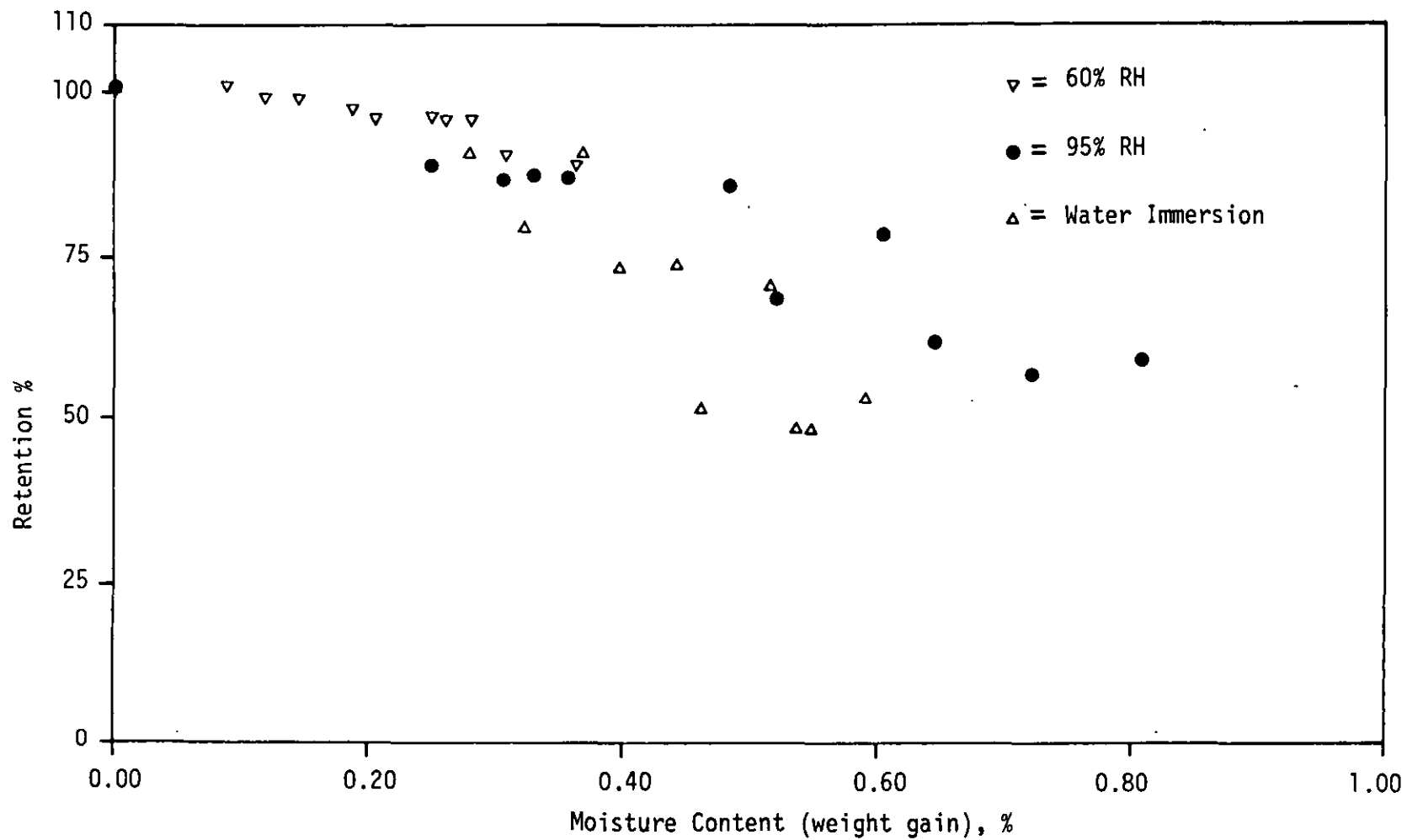


FIGURE 175: The effect of moisture on the % retention of ultimate tensile strength of 470-36 Vinylester specimens

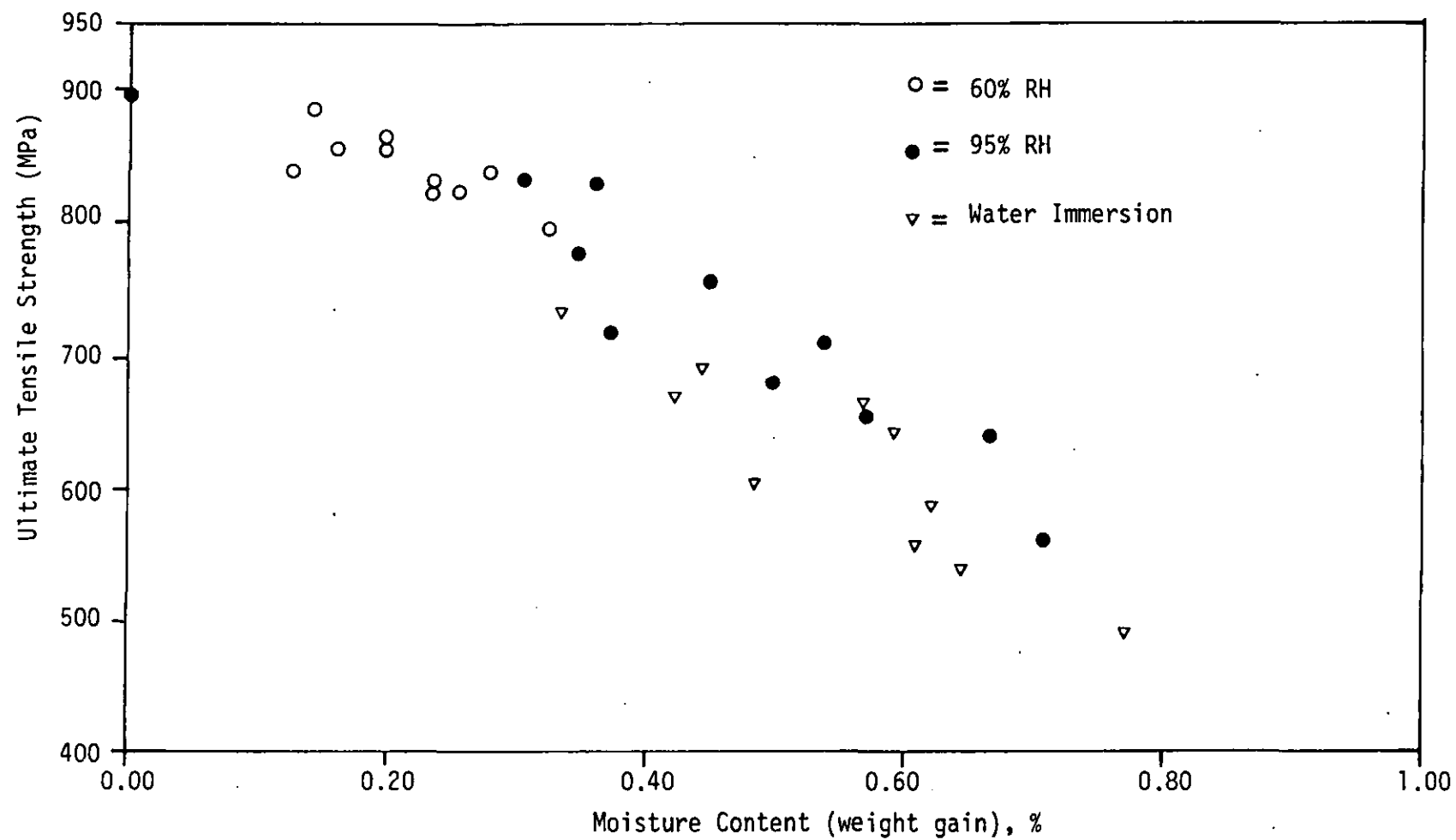


FIGURE 176: The effect of moisture on the ultimate tensile strength of Polyester 272 specimens

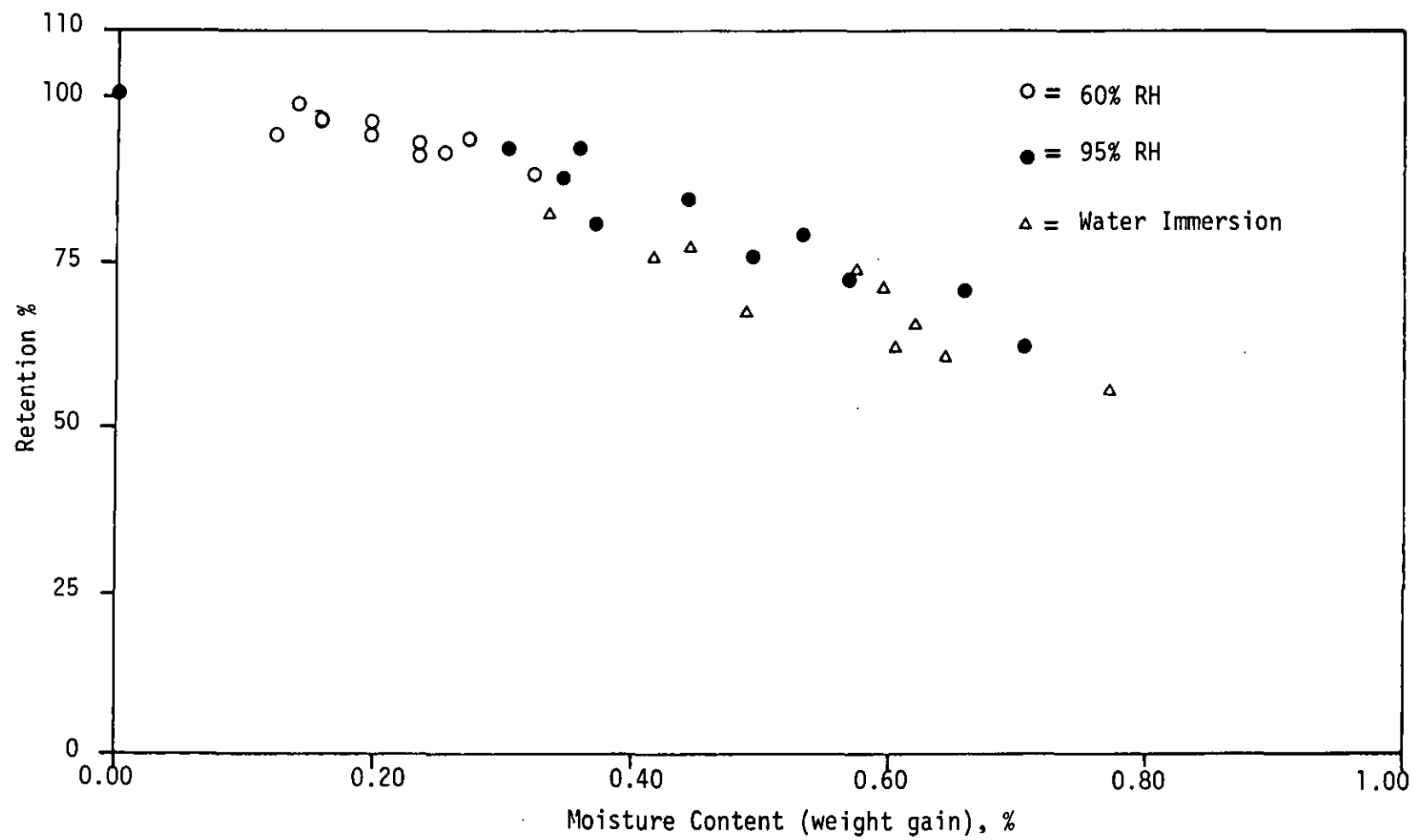


FIGURE 177: The effect of moisture on the % retention of ultimate tensile strength of Polyester 272 specimens

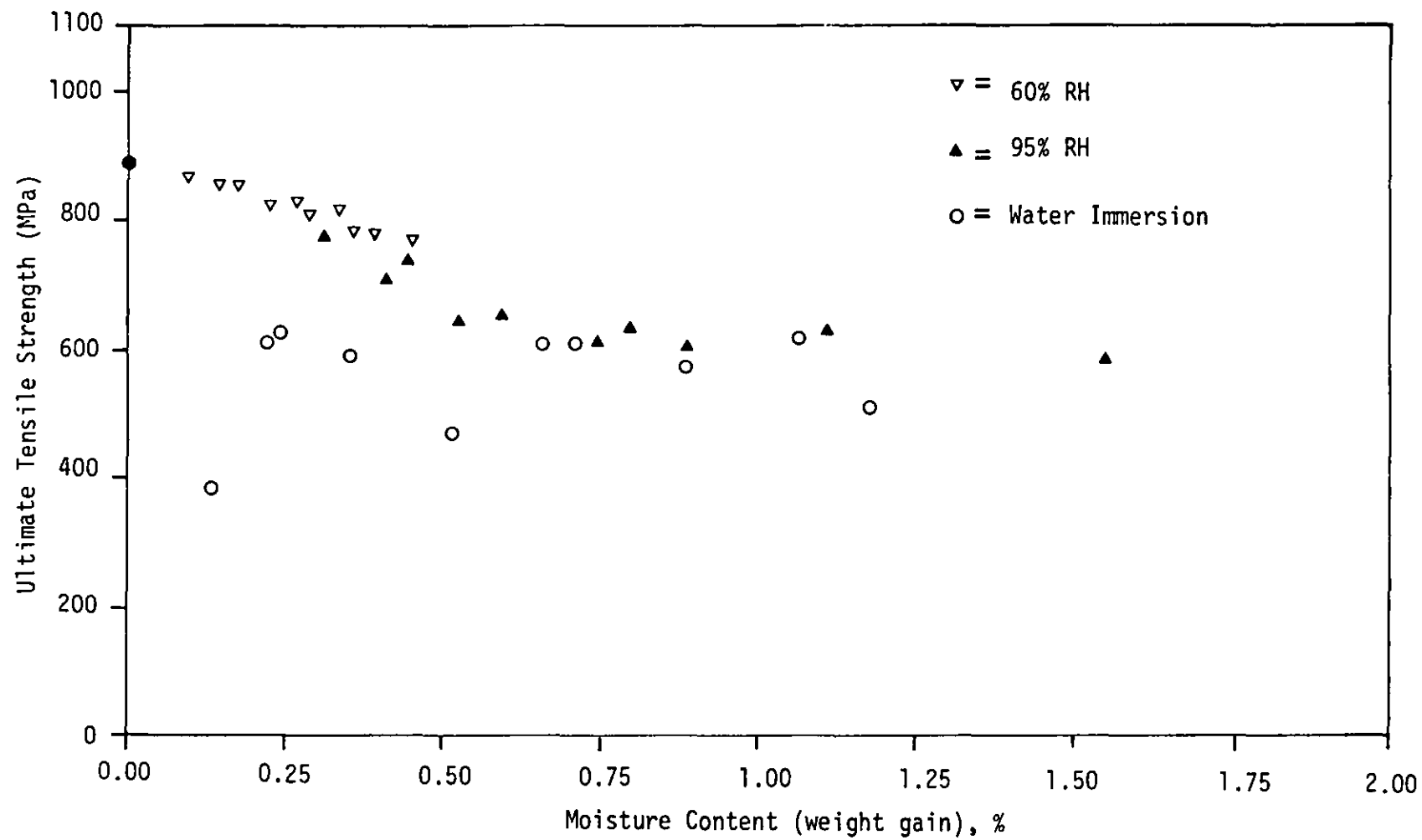


FIGURE 178: The effect of moisture on the ultimate tensile strength of Epoxy MY 750 specimens

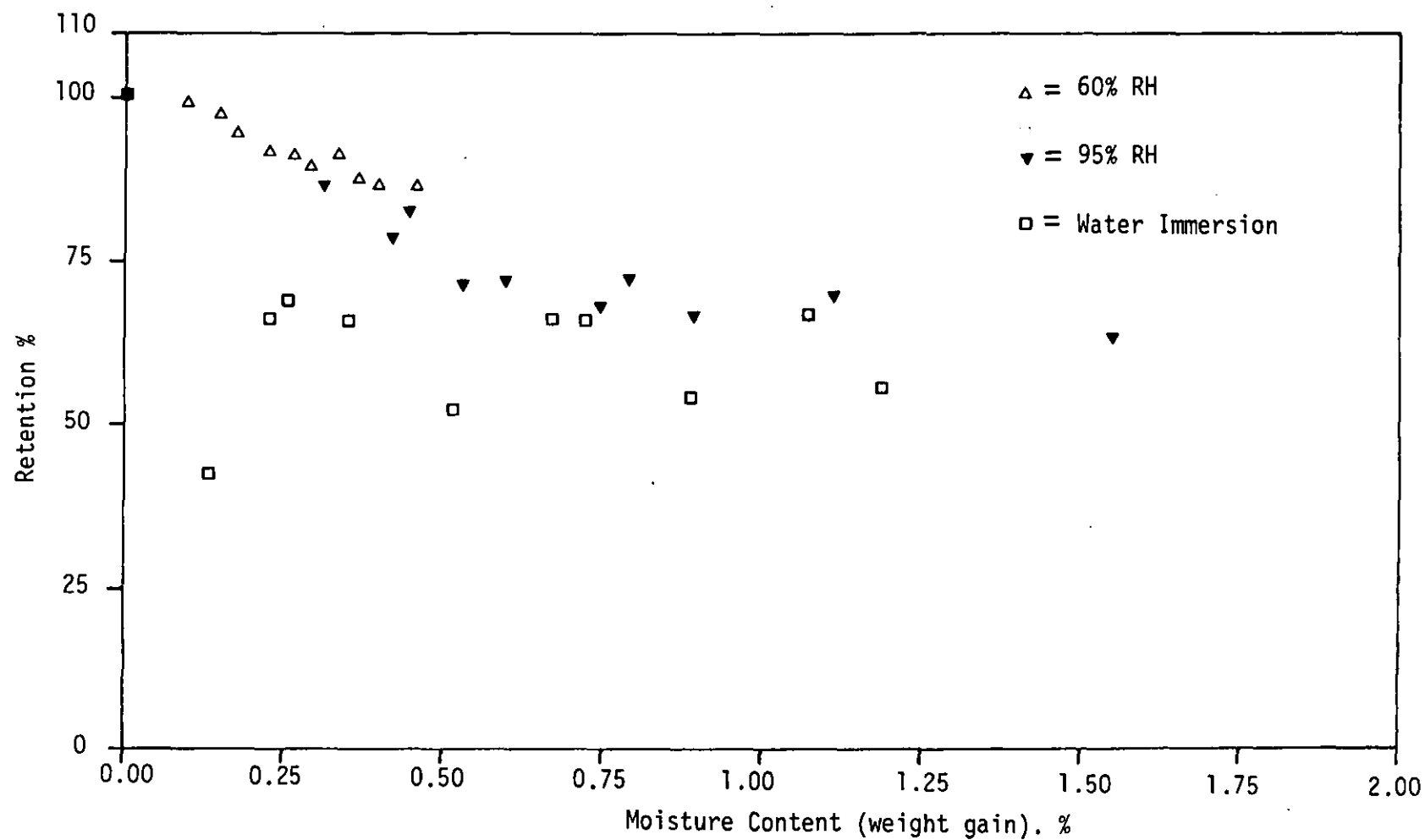


FIGURE 179: The effect of moisture on the % retention of ultimate tensile strength of Epoxy MY 750 specimens

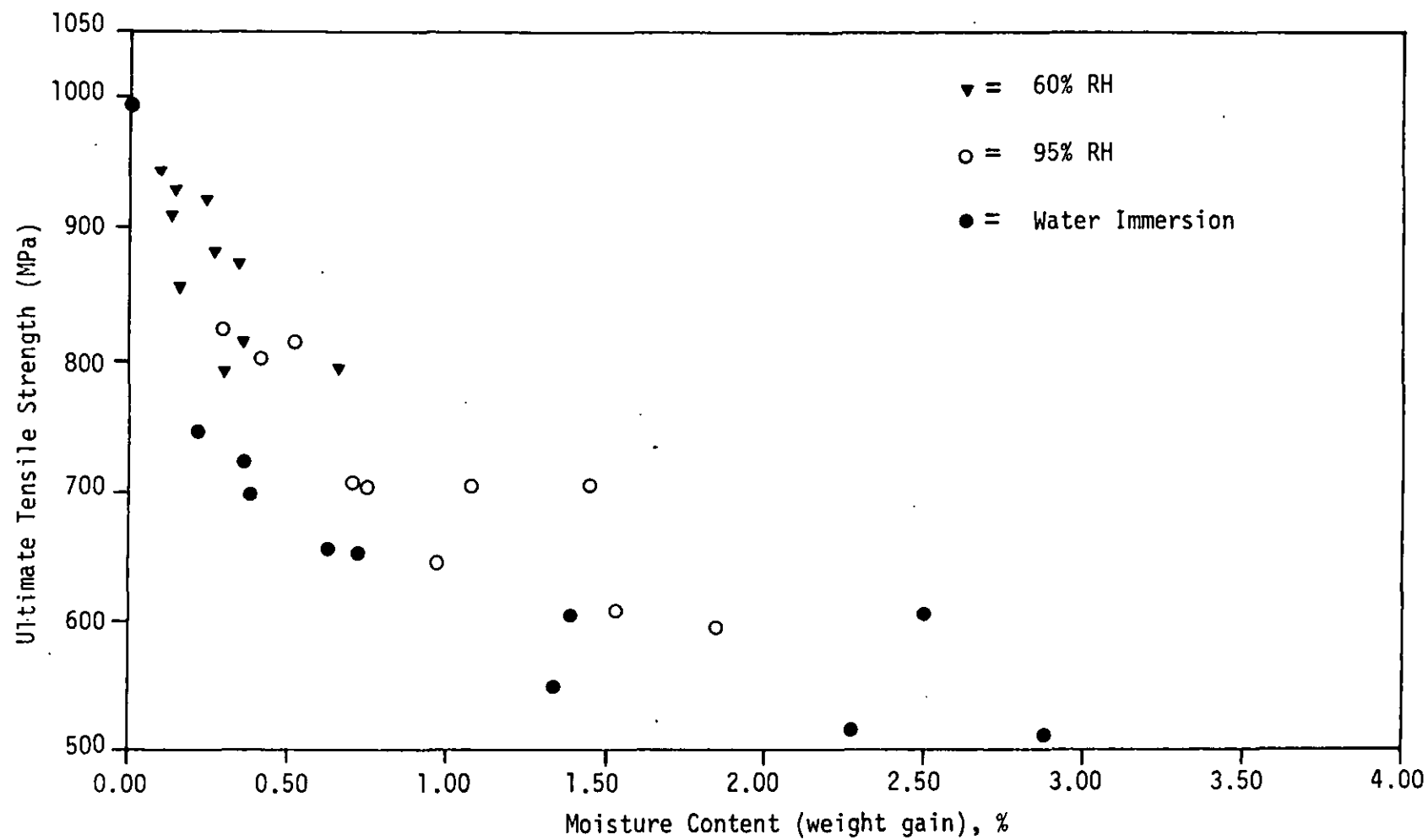


FIGURE 180: The effect of moisture on ultimate tensile strength of 913 PrePreg specimens

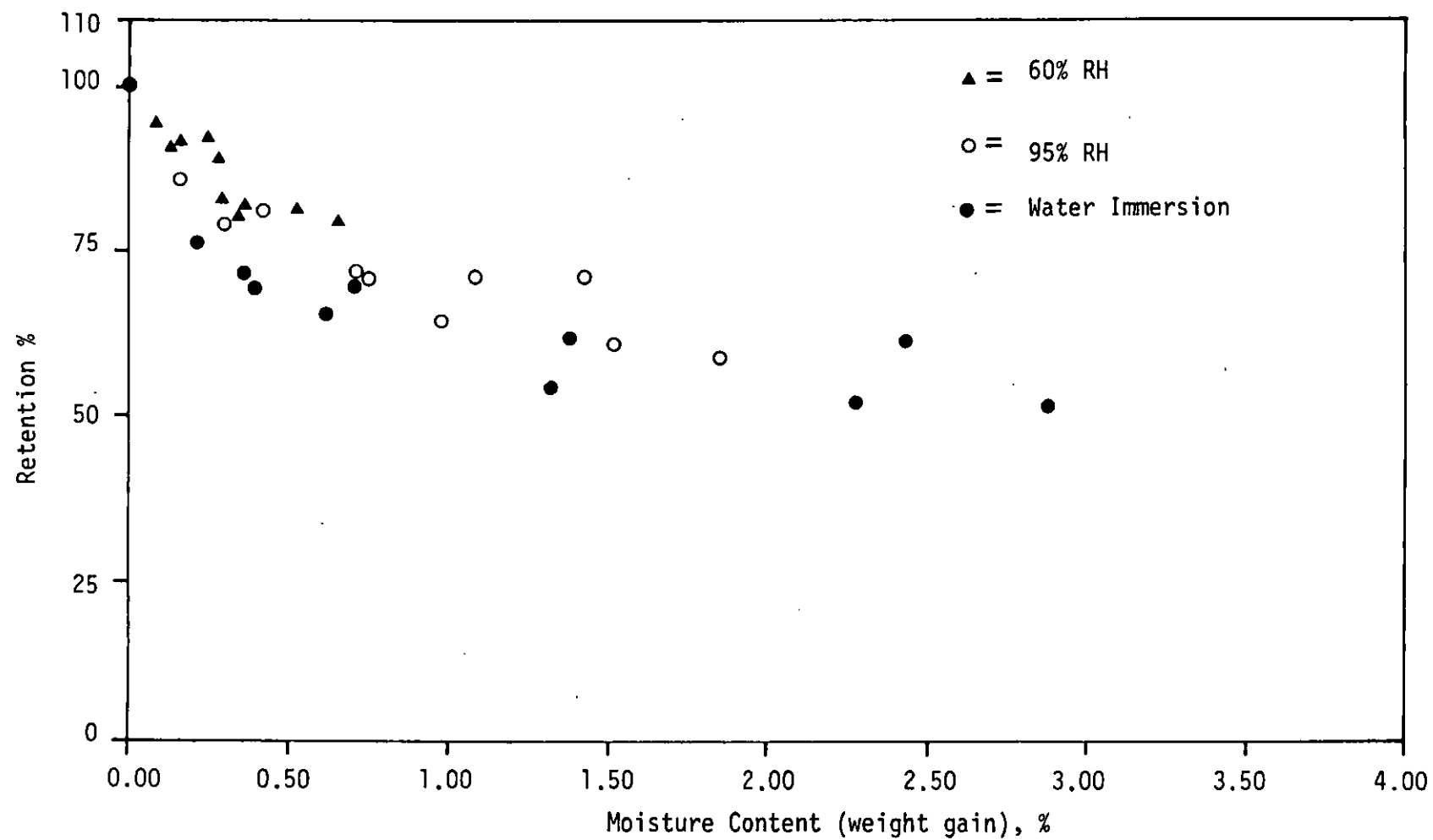


FIGURE 181: The effect of moisture on % retention of ultimate tensile strength of 913 PrePreg specimens

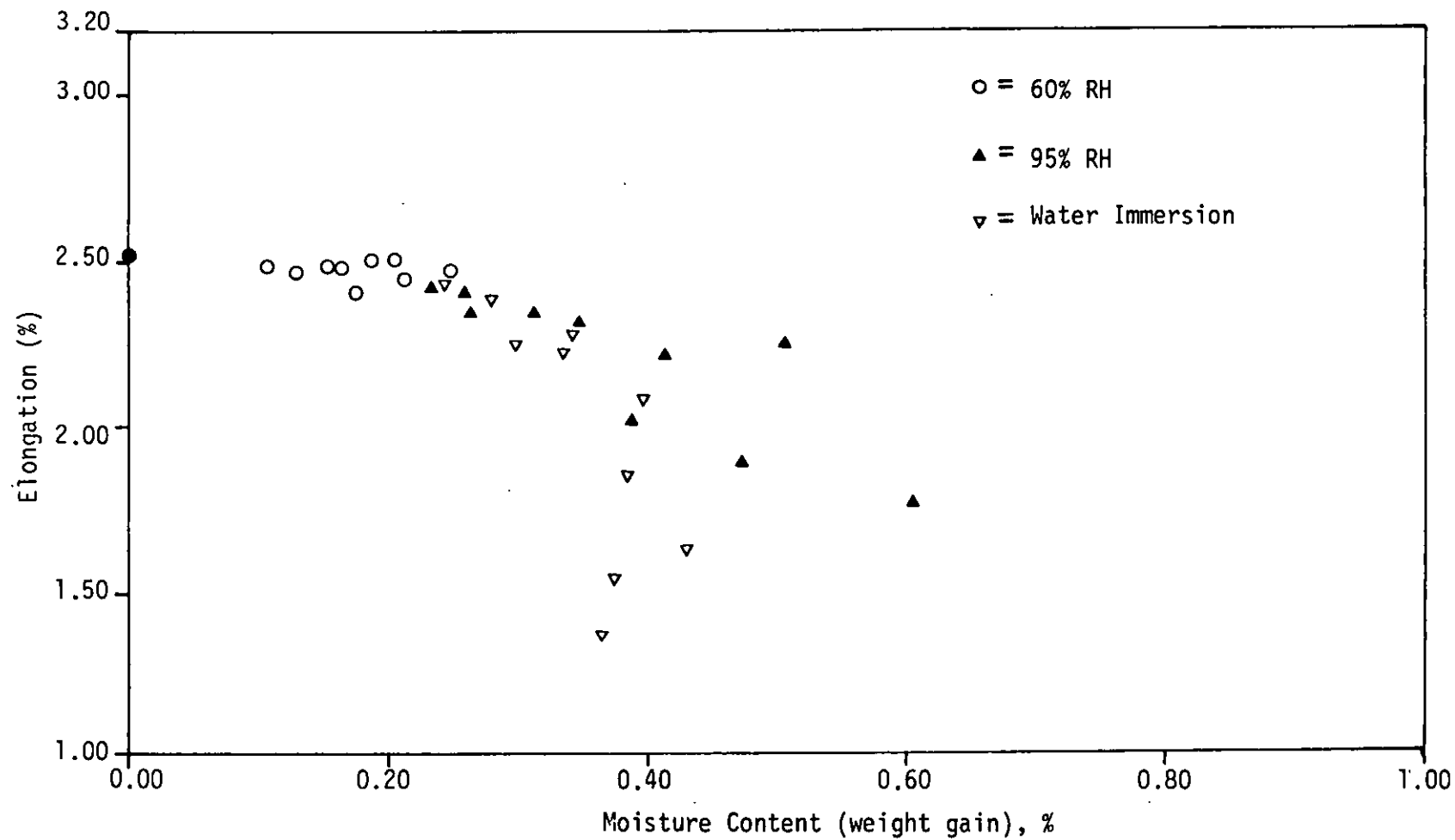


FIGURE 182: The effect of moisture on the % elongation of 411-45 Vinylester specimens

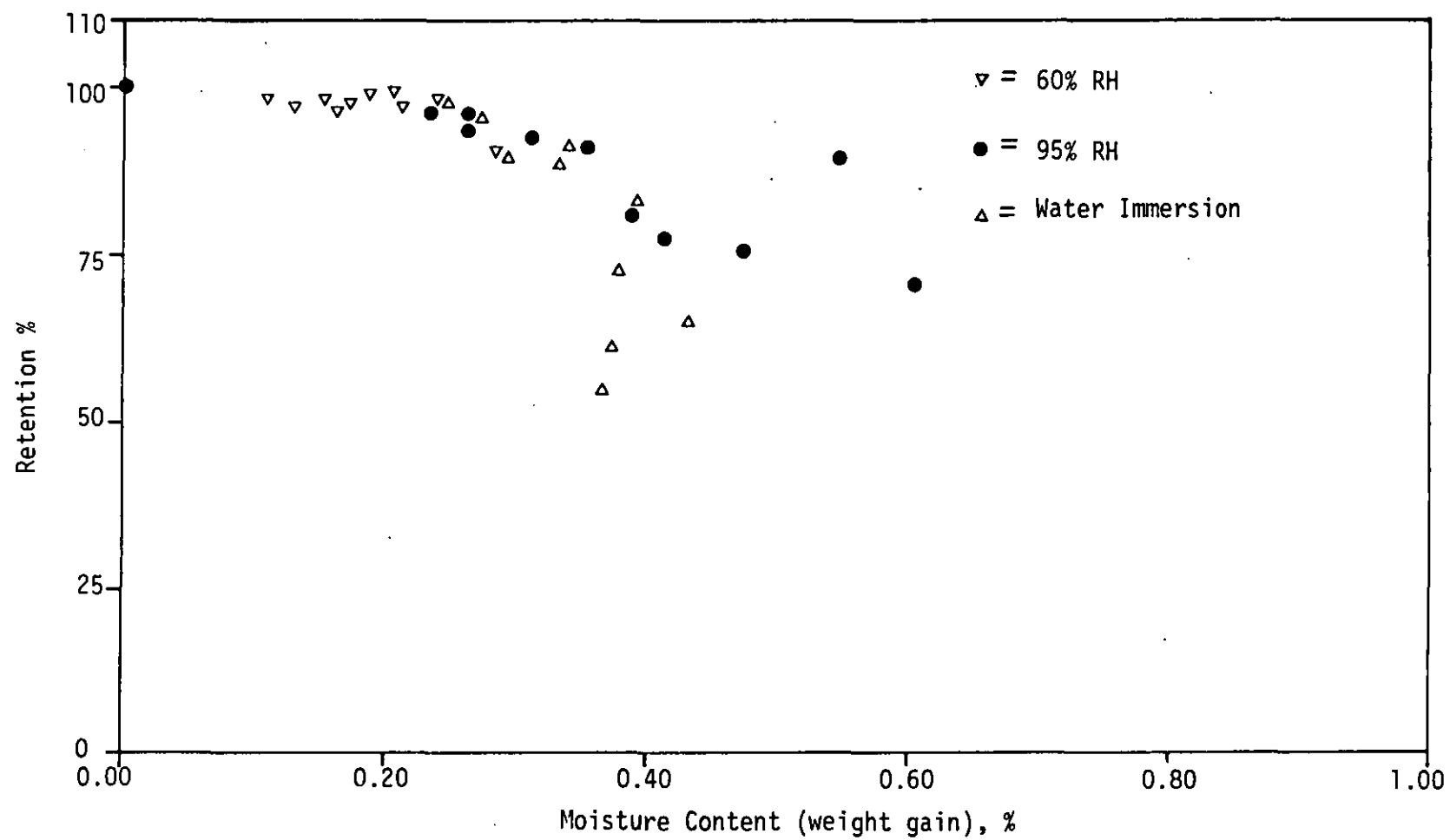


FIGURE 183: The effect of moisture on the % retention of % elongation of 411-45 Vinylester specimens

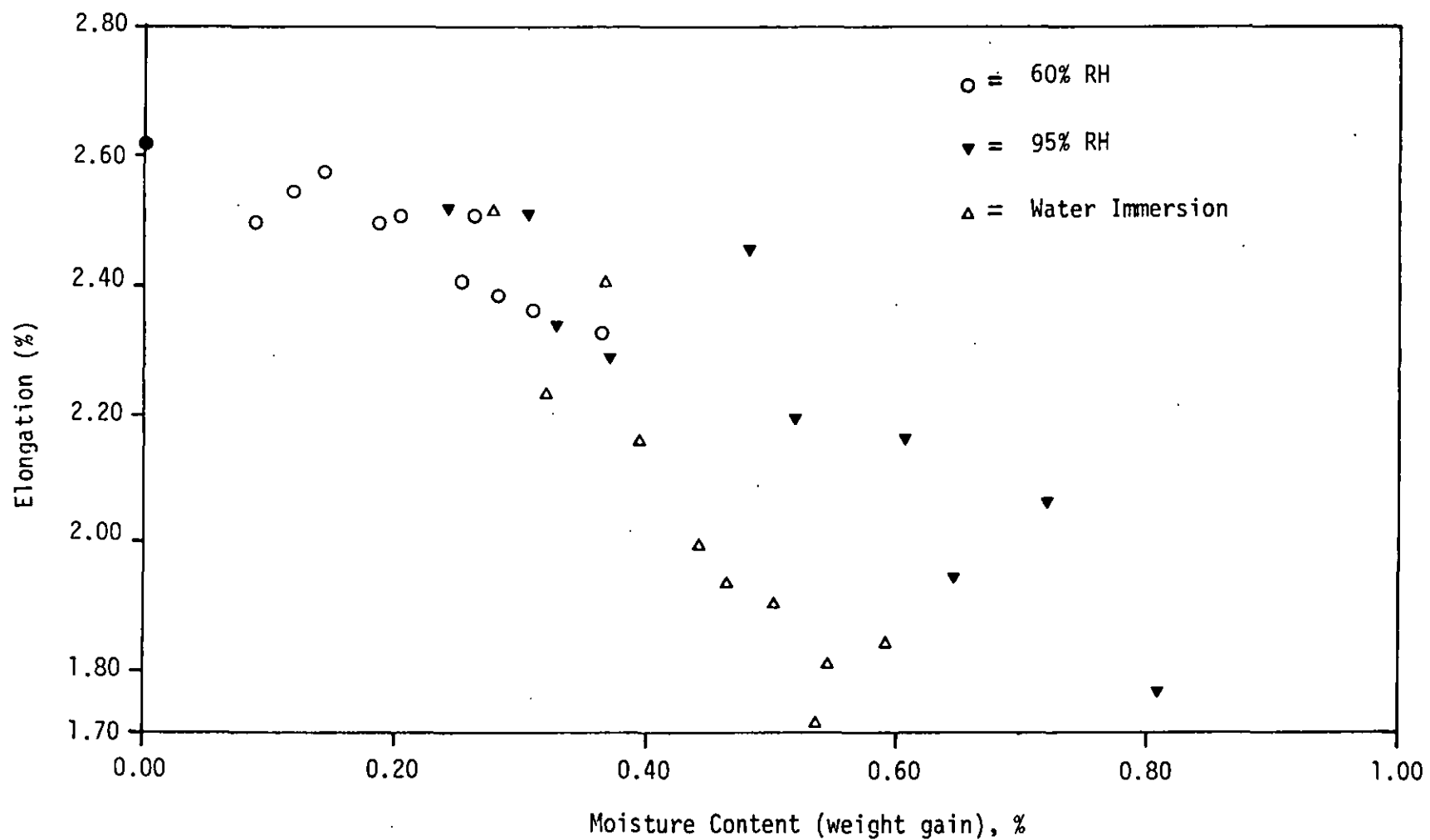


FIGURE 184: The effect of moisture on the % elongation of 470-36 vinyl ester specimens

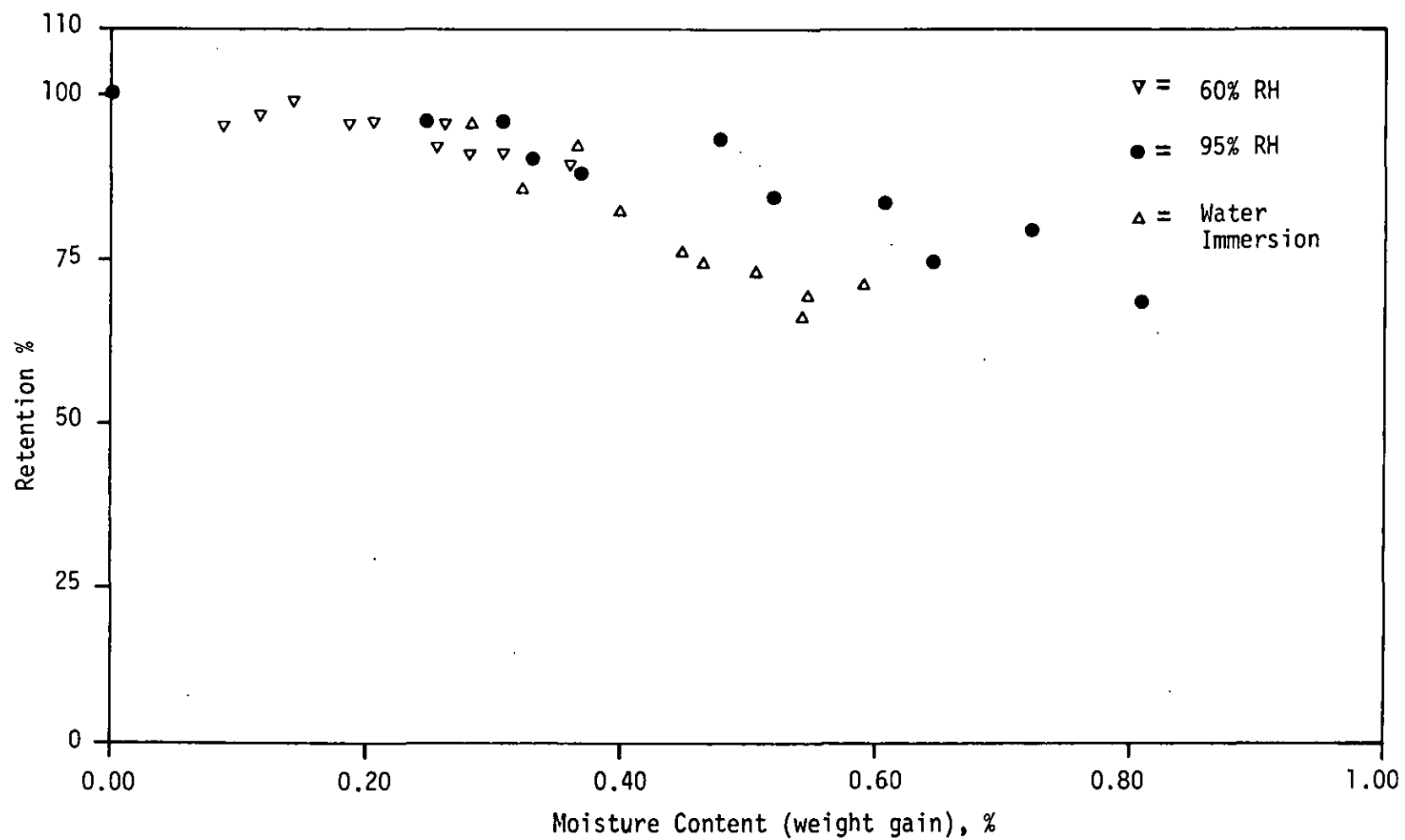


FIGURE 185: The effect of moisture on the % retention of % elongation of 470-36 vinyl ester specimens

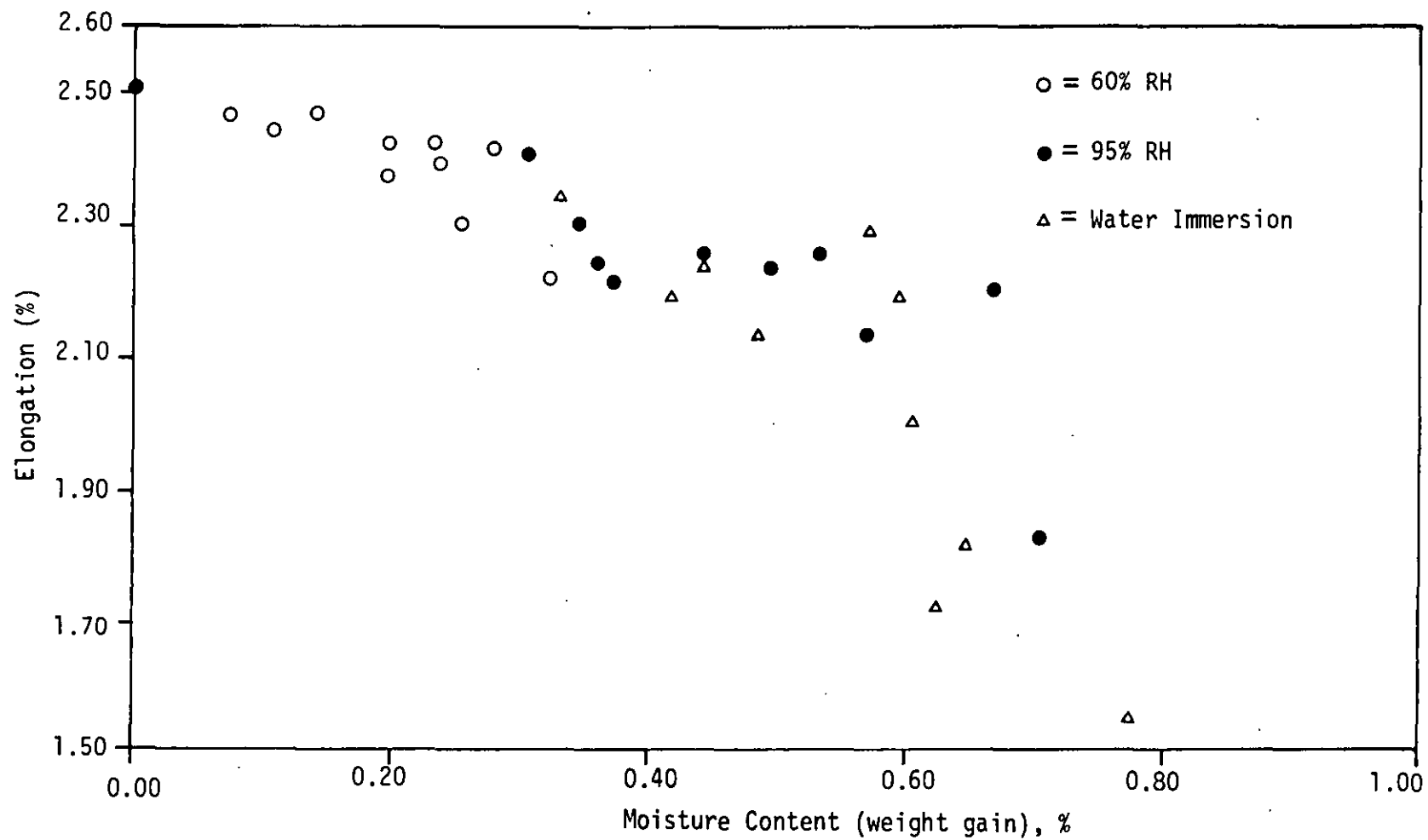


FIGURE 186: The effect of moisture on the % elongation of 272 polyester specimens

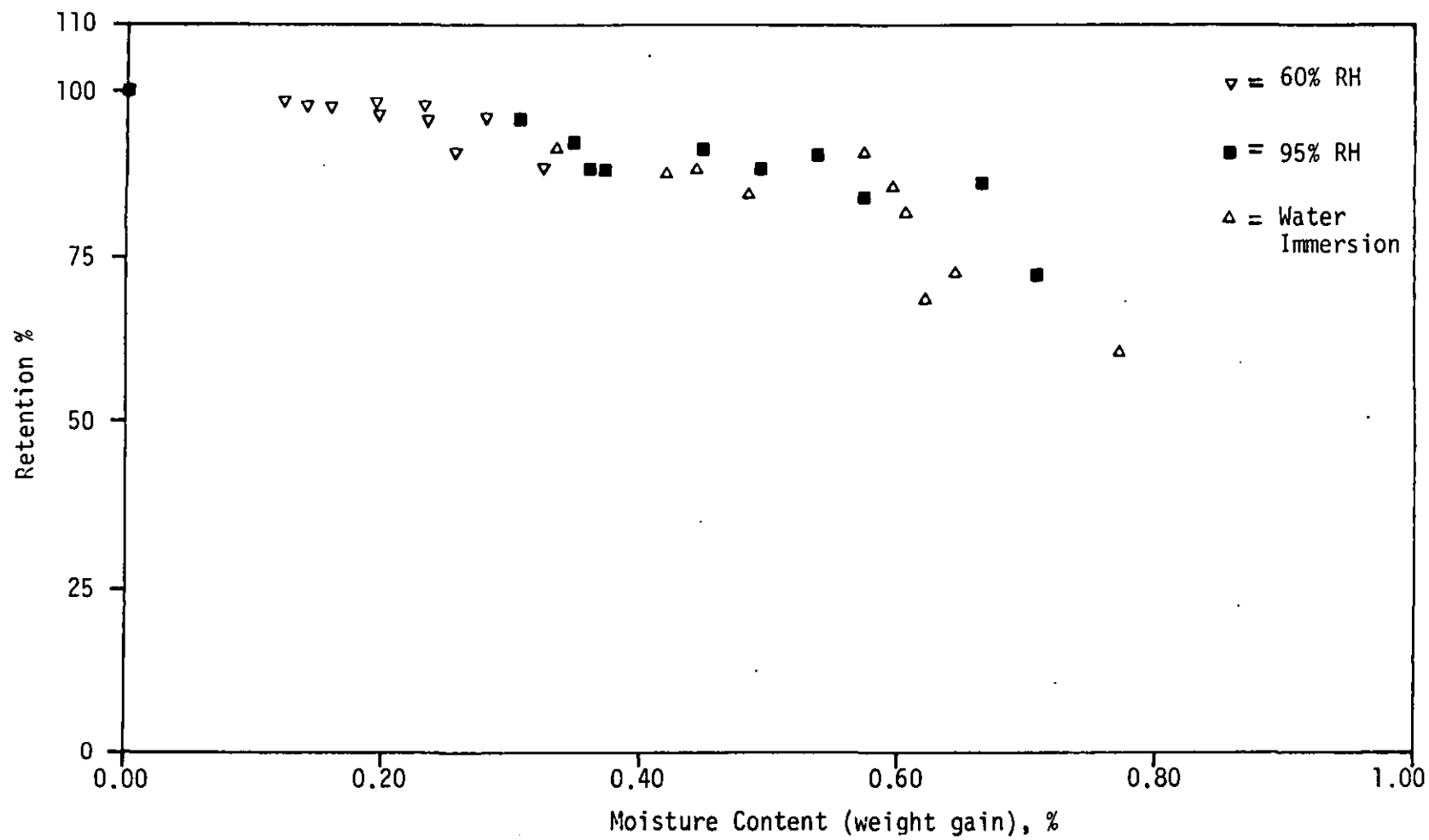


FIGURE 187: The effect of moisture on the % retention of % elongation of 272 polyester specimens

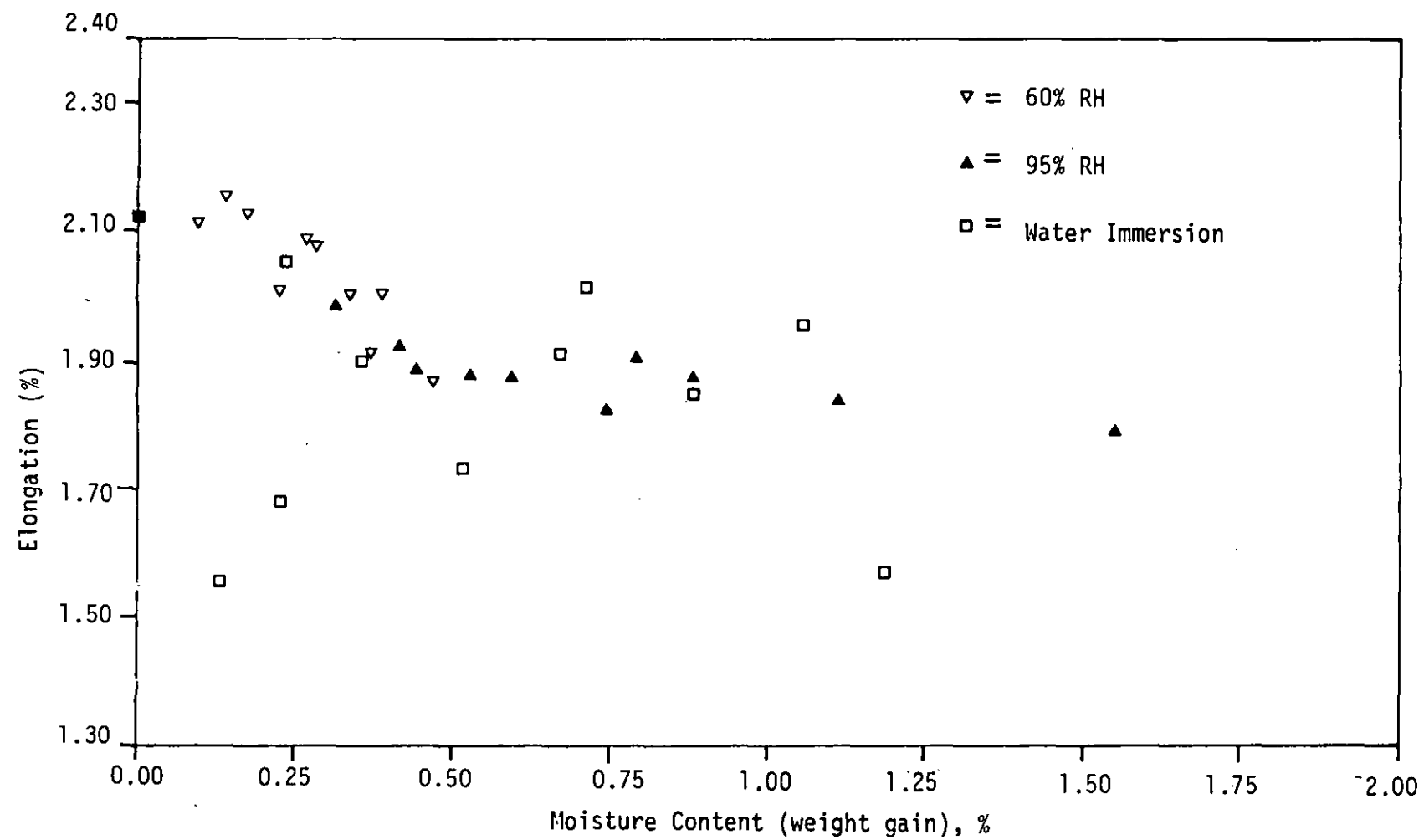


FIGURE 188: The effect of moisture on the % elongation of Epoxy HY 750 specimens

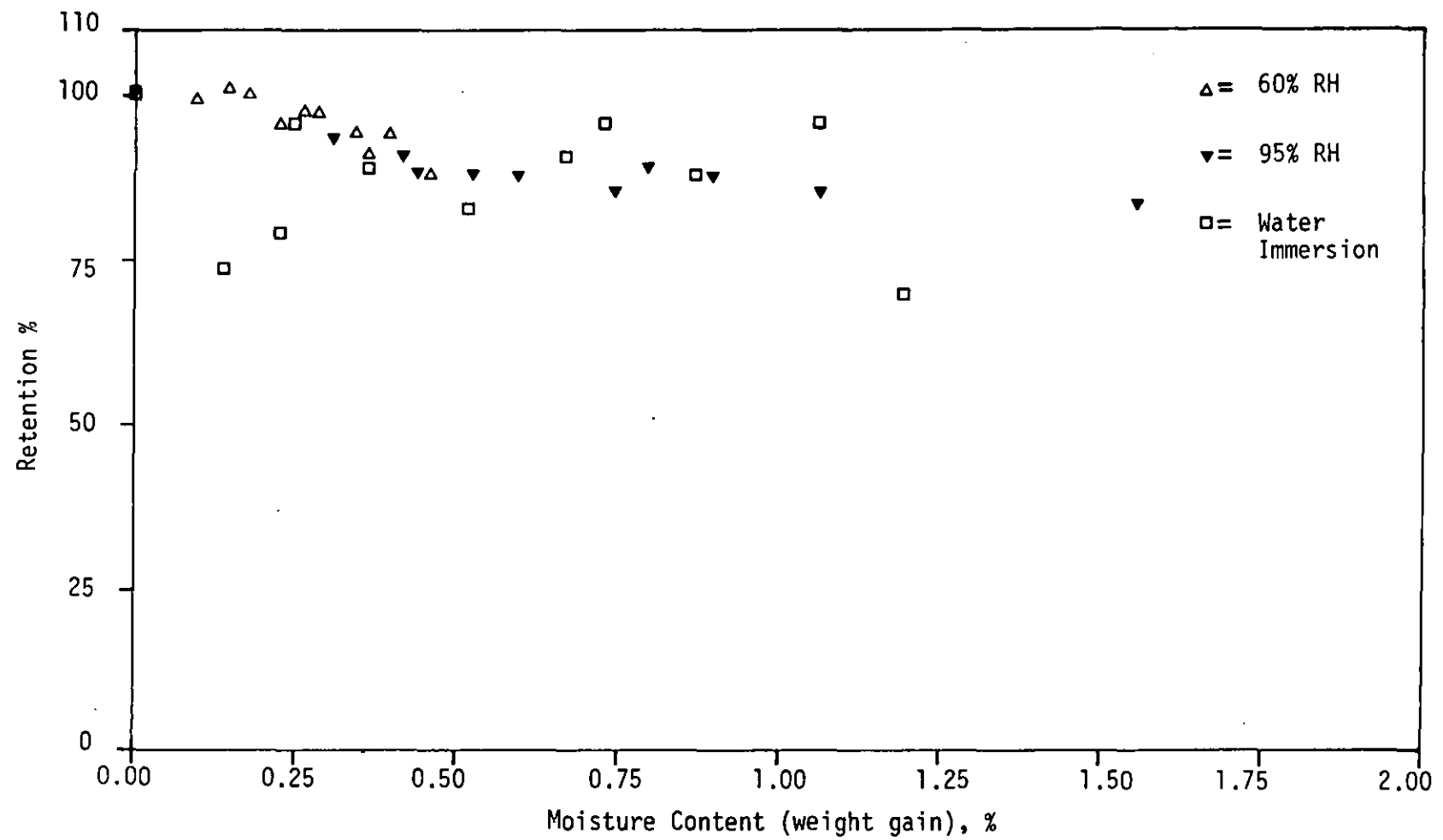


FIGURE 189: The effect of moisture on the % retention of Epoxy MY 750 specimens

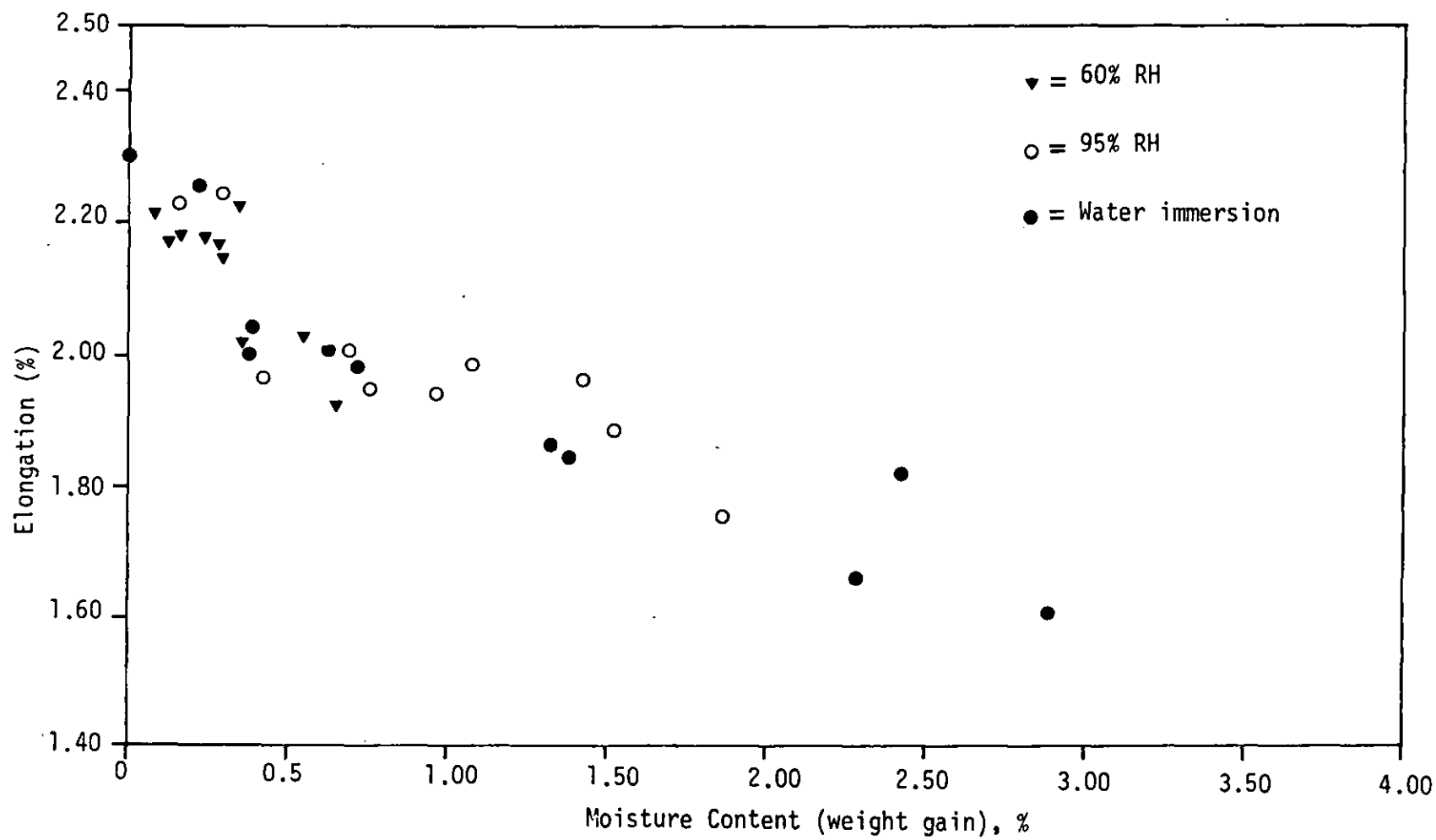


FIGURE 190: The effect of moisture on the % elongation of 913 PrePreg specimens

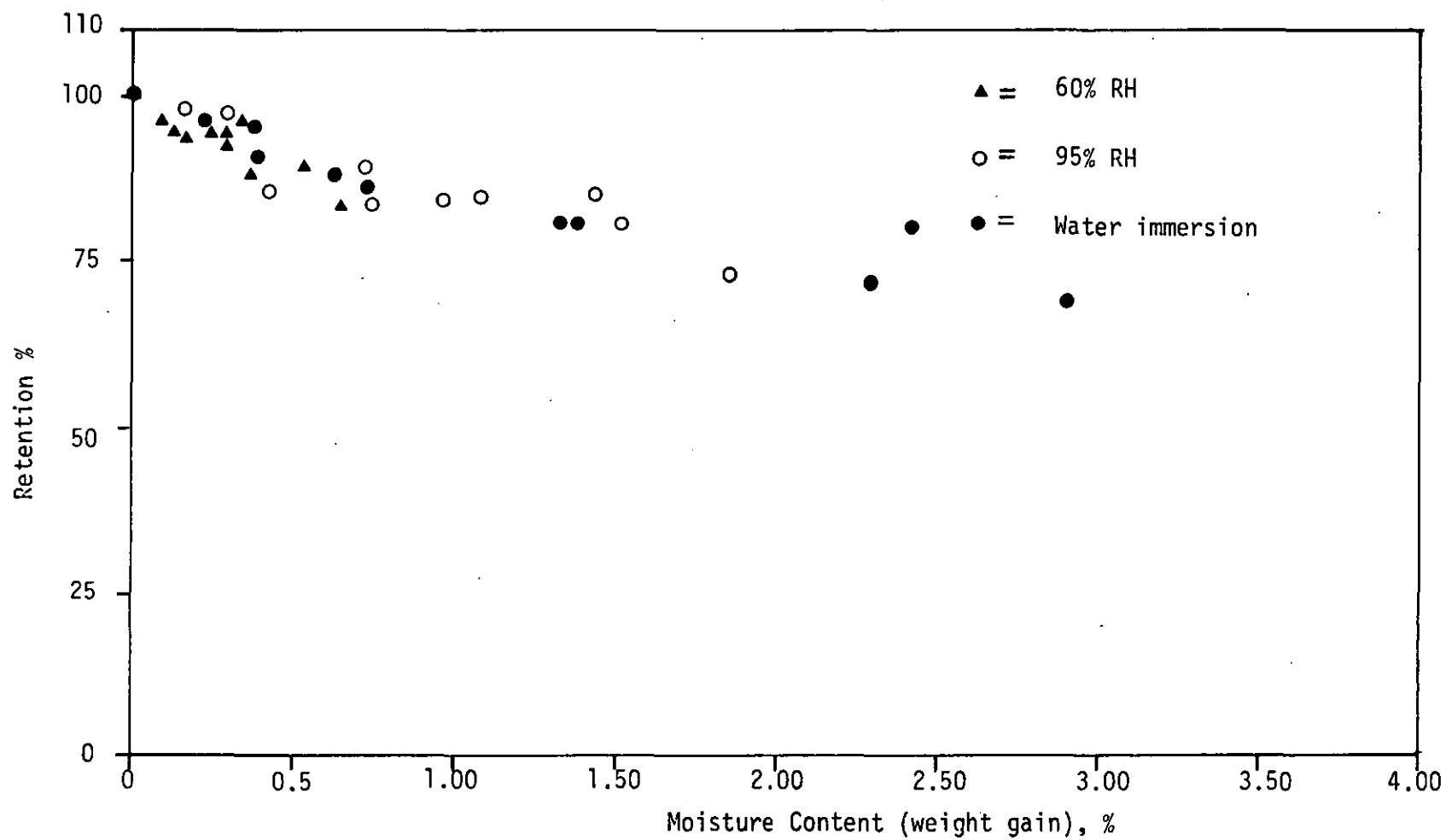


FIGURE 191: The effect of moisture on the % retention of % elongation of 913 PrePreg specimens

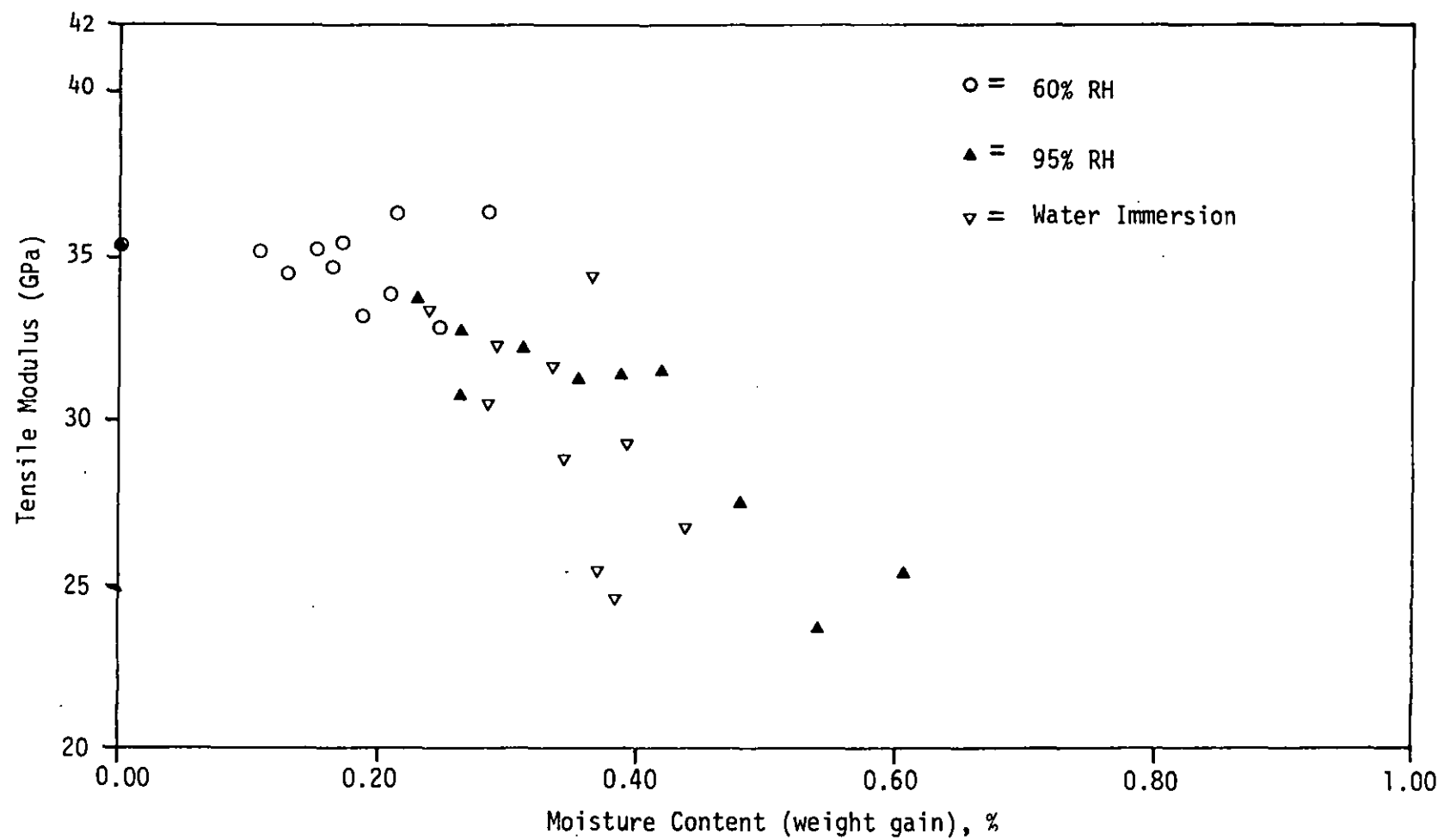


FIGURE 192: The effect of moisture on the tensile modulus of 411-45 Vinylester specimens

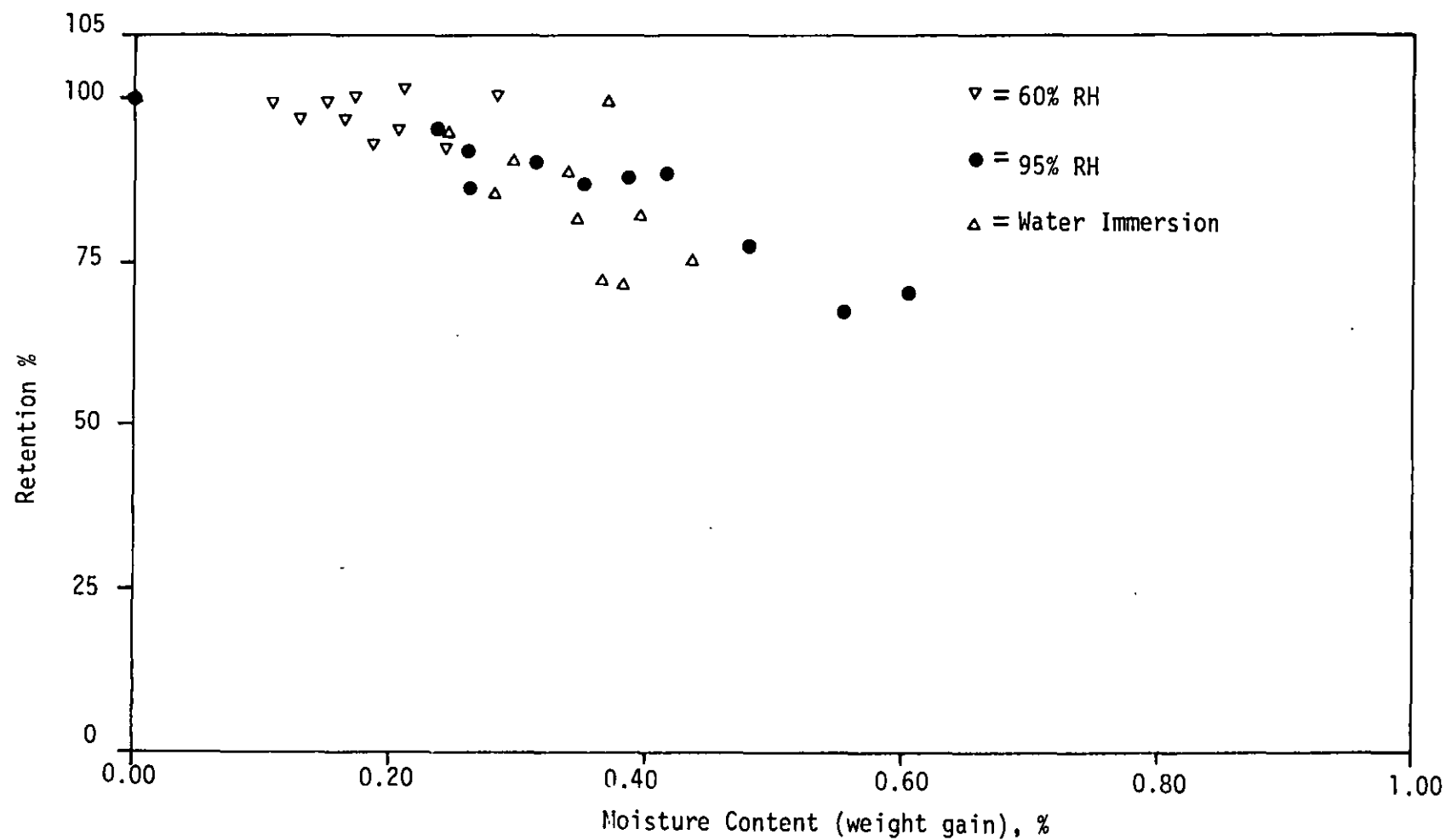


FIGURE 193: The effect of moisture on the % retention of tensile modulus of 411-45 Vinylester specimens

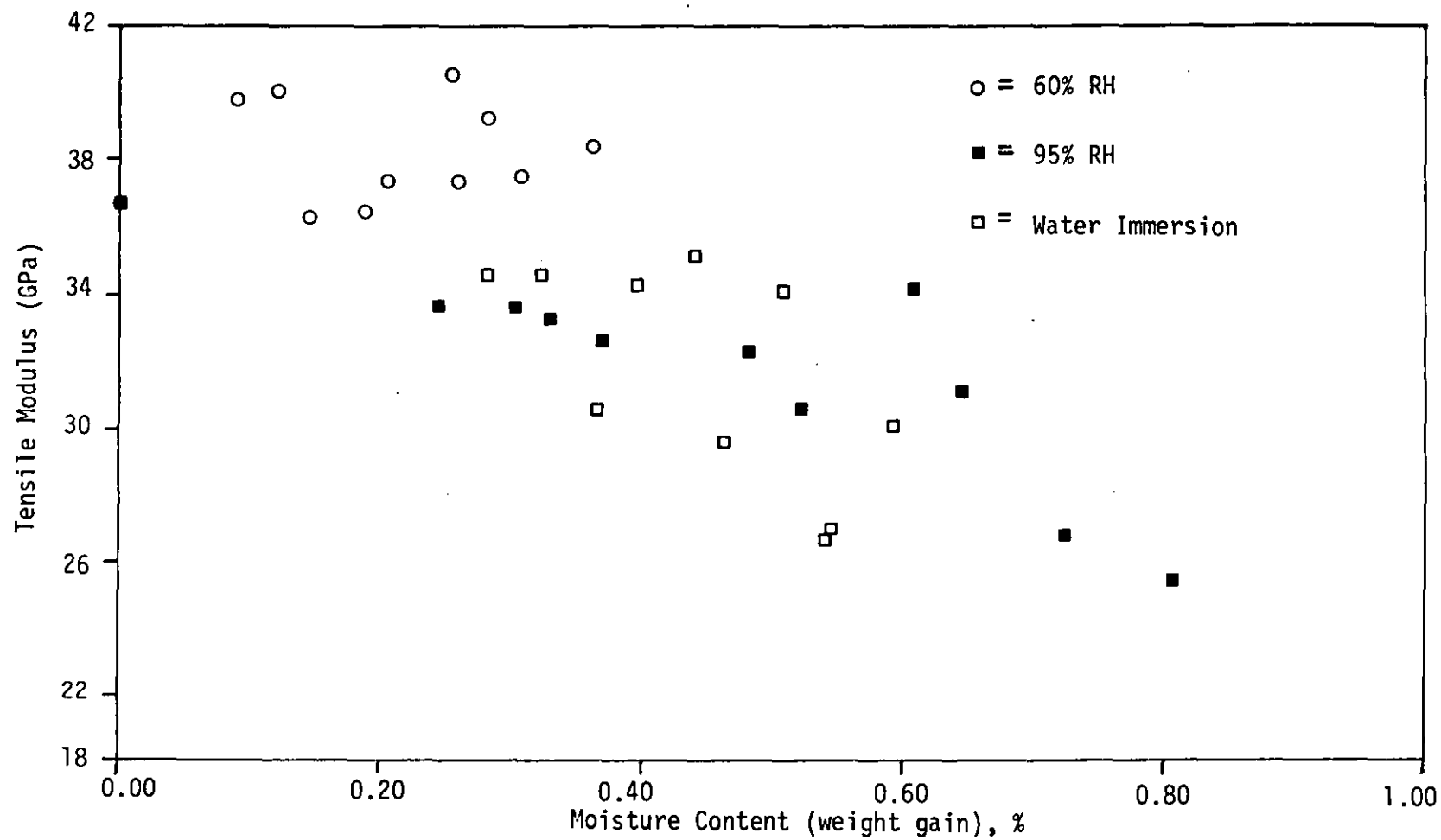


FIGURE 194: The effect of moisture on the tensile modulus of 470-36 Vinylester specimens

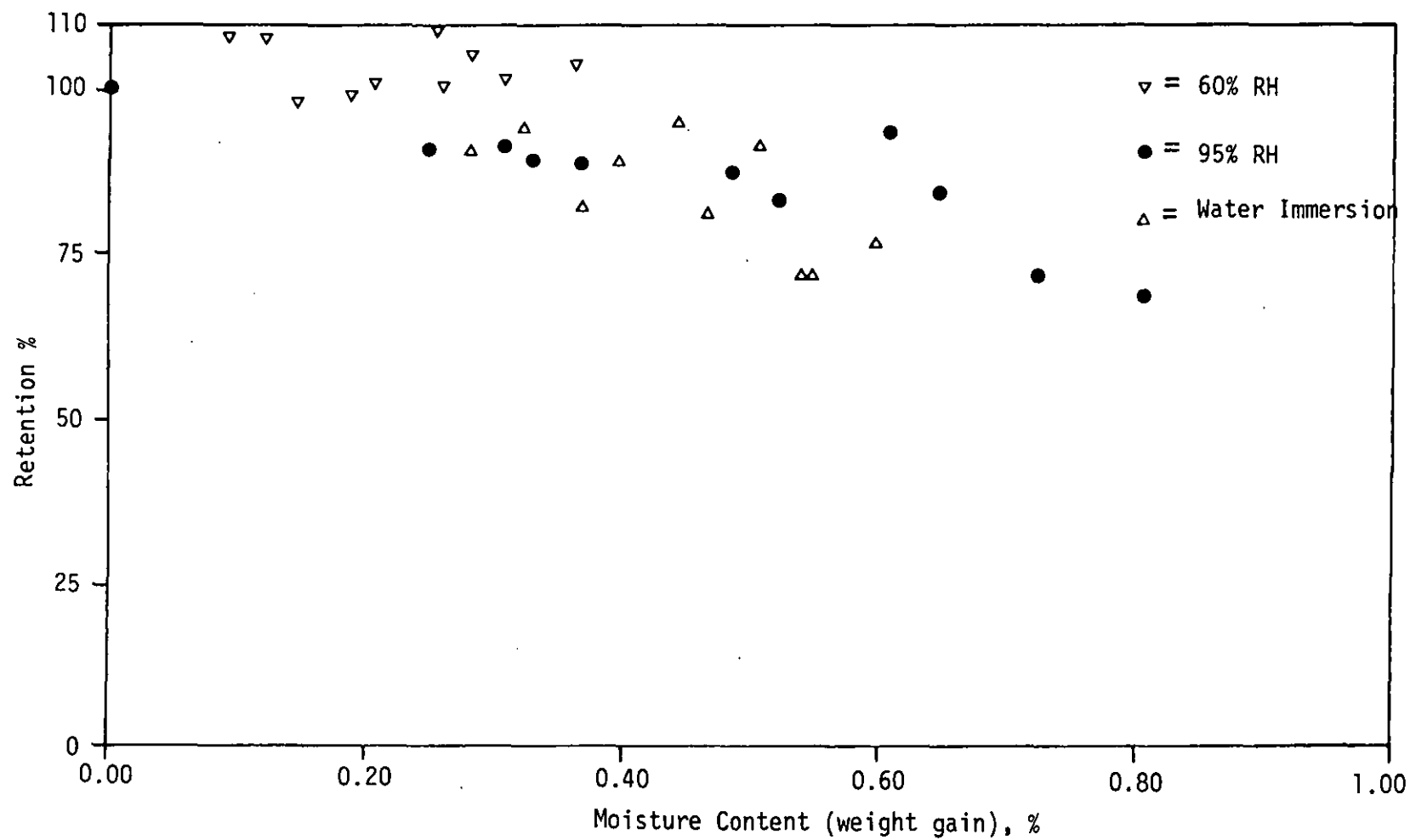


FIGURE 195: The effect of moisture on the % retention of tensile modulus of 470-36 Vinylester specimens

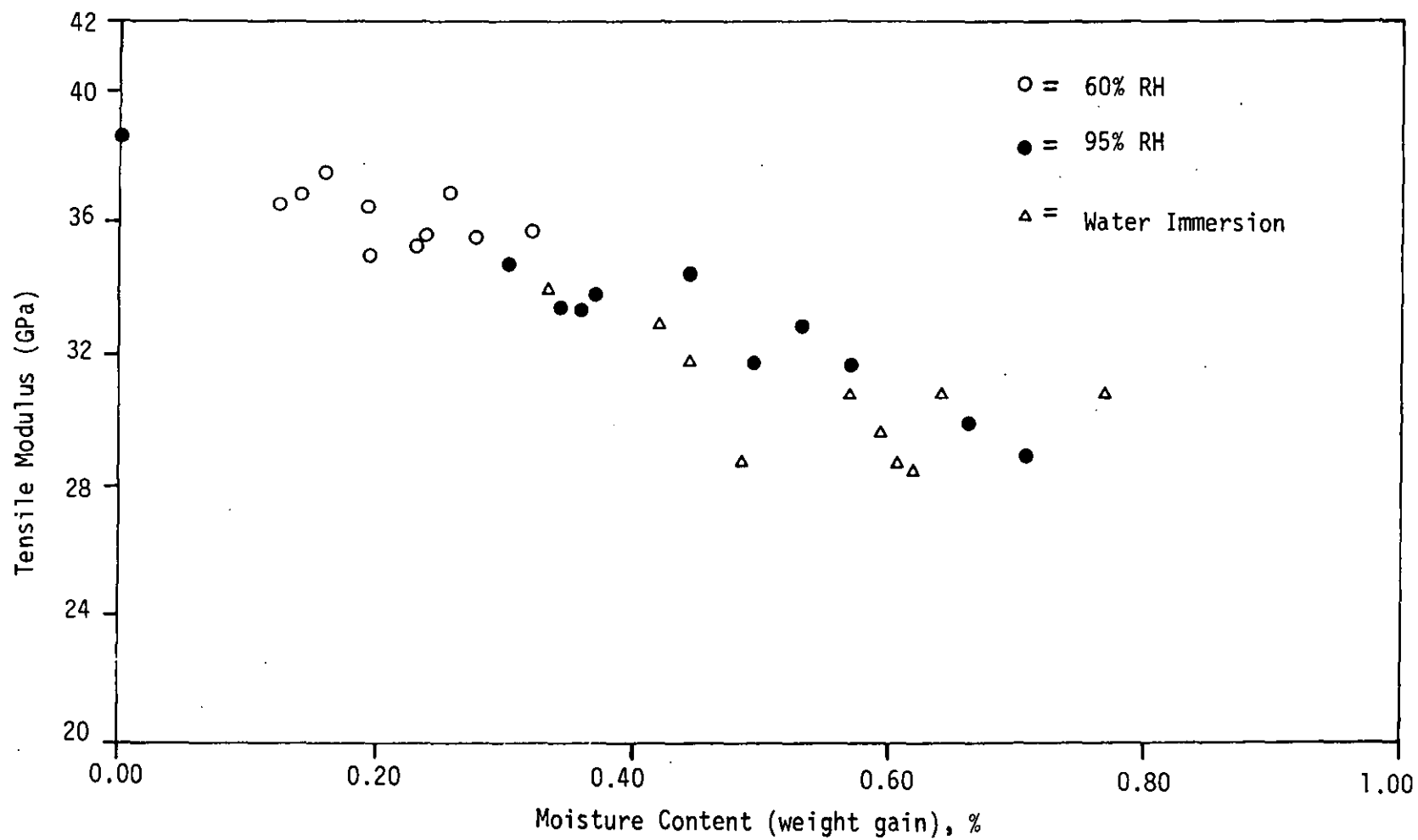


FIGURE 196: The effect of moisture on the tensile modulus of 272 Polyester specimens

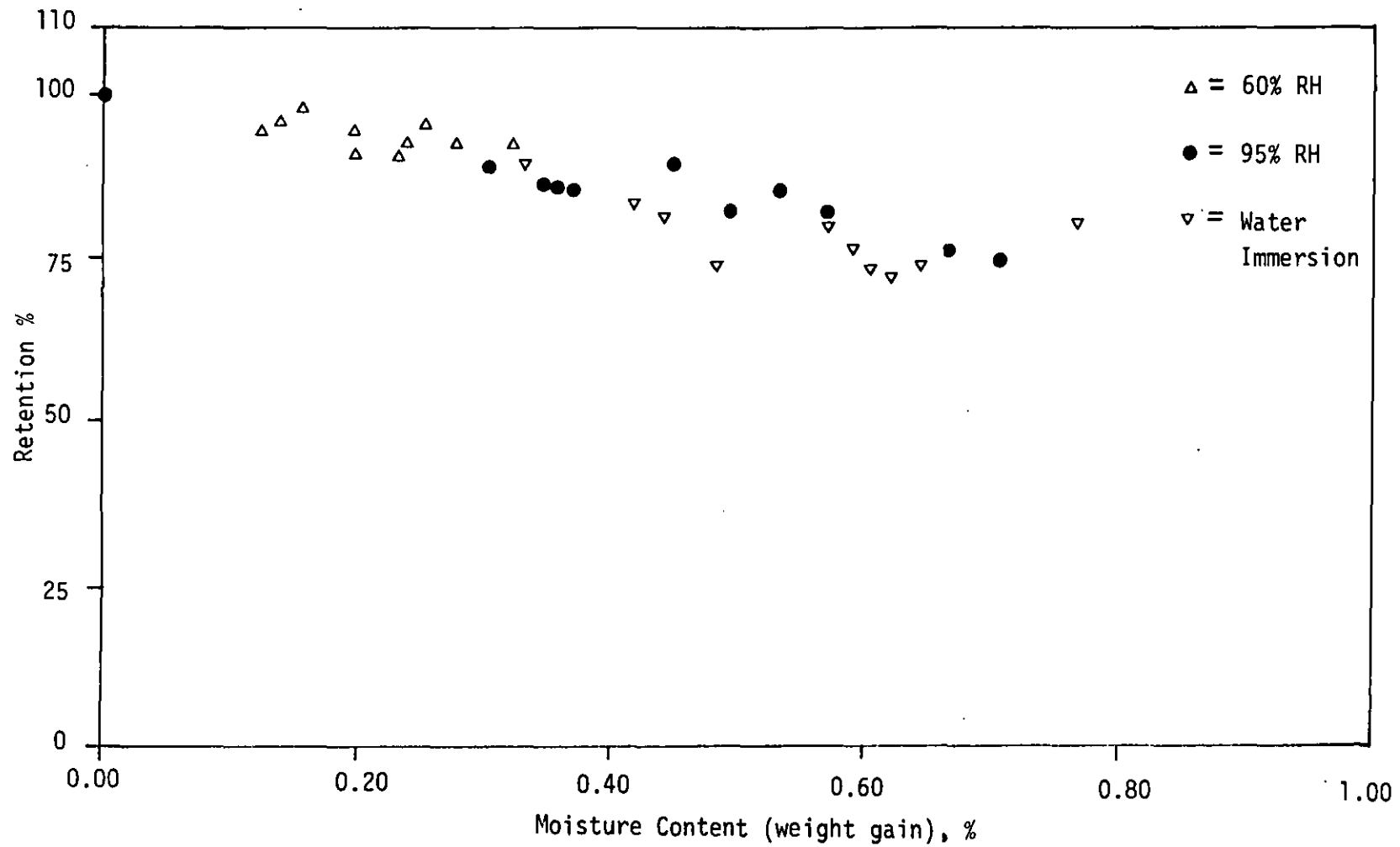


FIGURE 197: The effect of moisture on the % retention of tensile modulus of 272 Polyester specimens

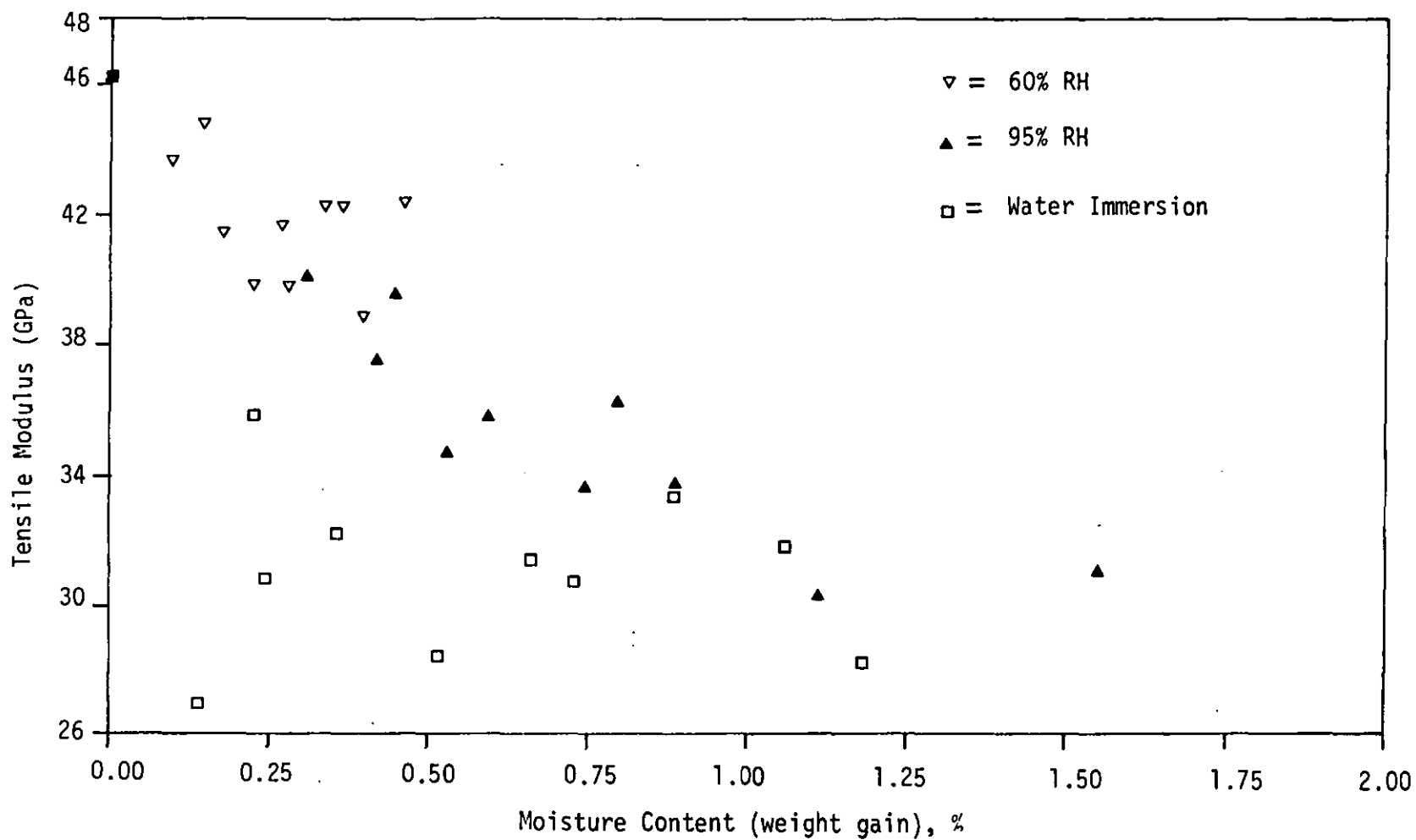


FIGURE 198: The effect of moisture on the tensile modulus of Epoxy HY 750 specimens

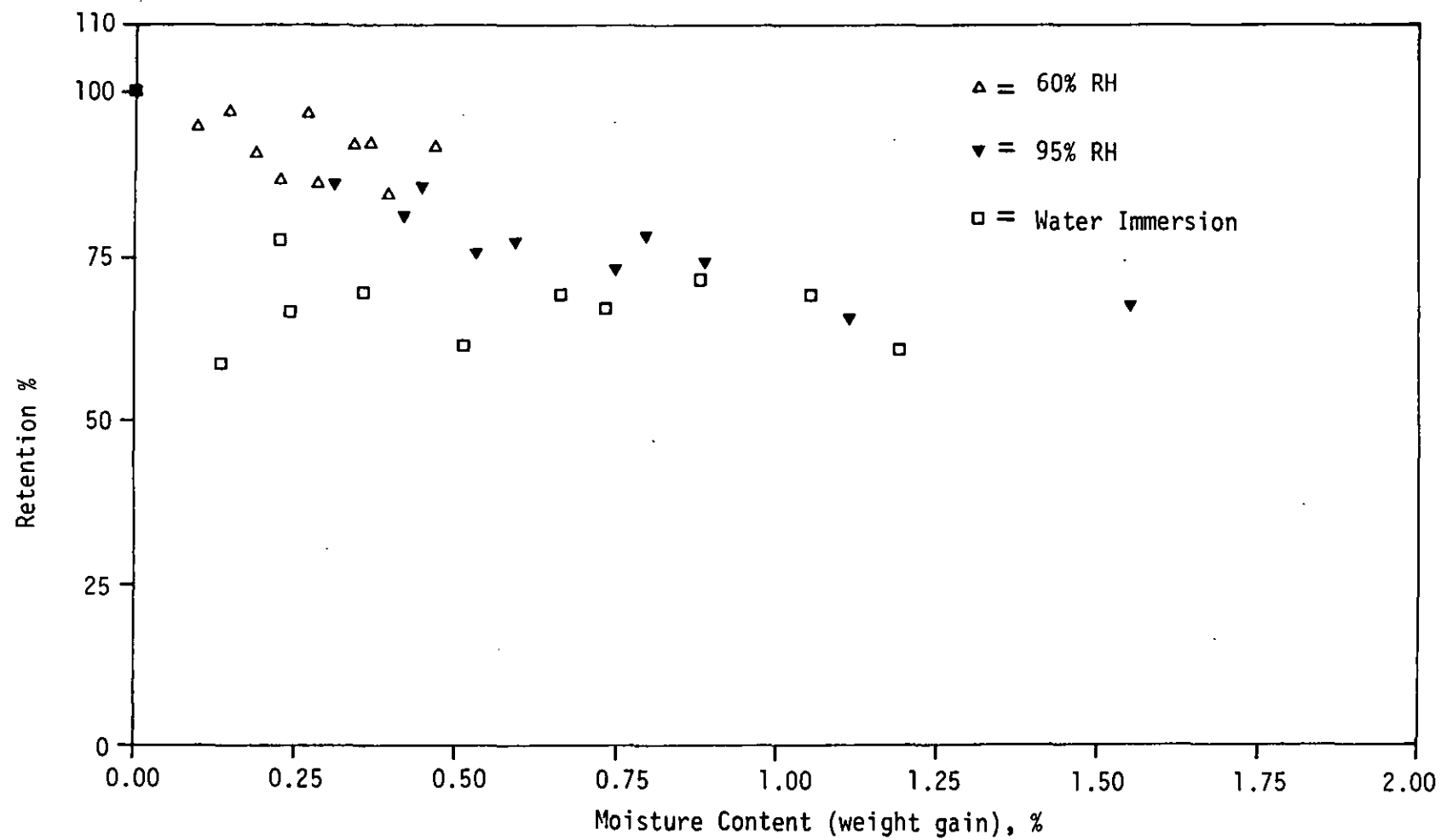


FIGURE 199: The effect of moisture on the % retention of tensile modulus of Epoxy MY 750 specimens

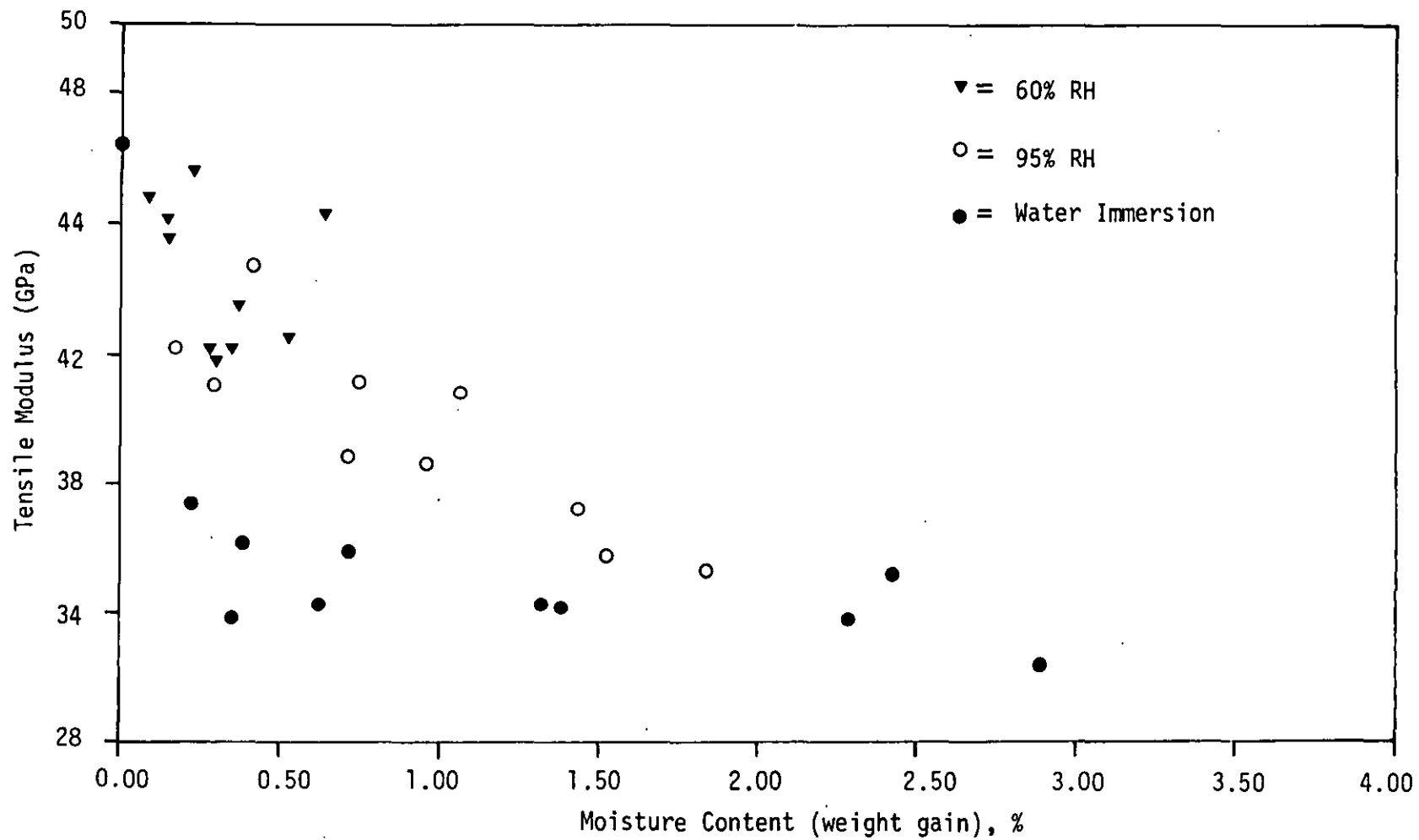


FIGURE 200: The effect of moisture on the tensile modulus of 913 PrePreg specimens

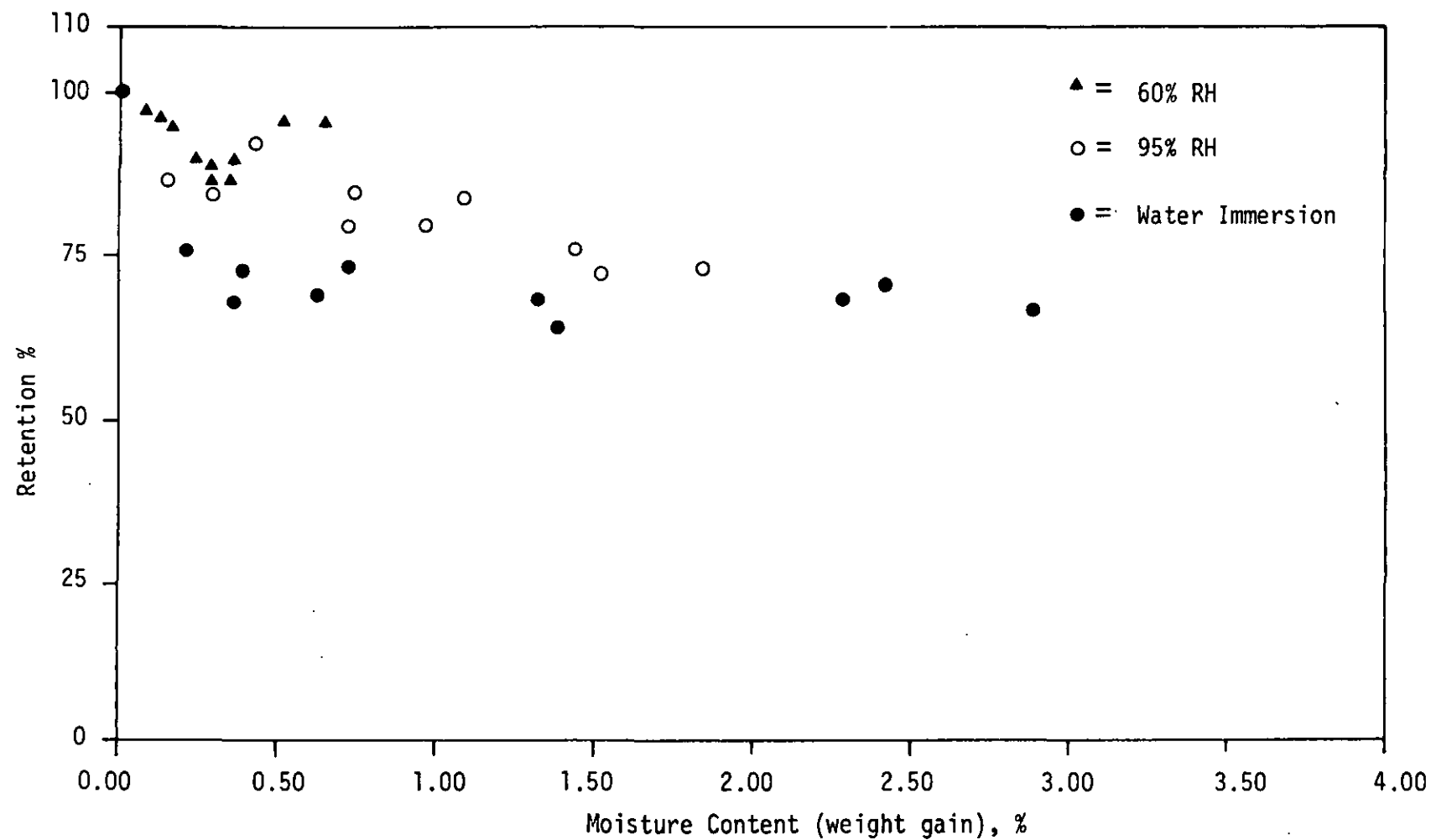


FIGURE 201: The effect of moisture on the % retention of tensile modulus of 913 PrePreg specimens

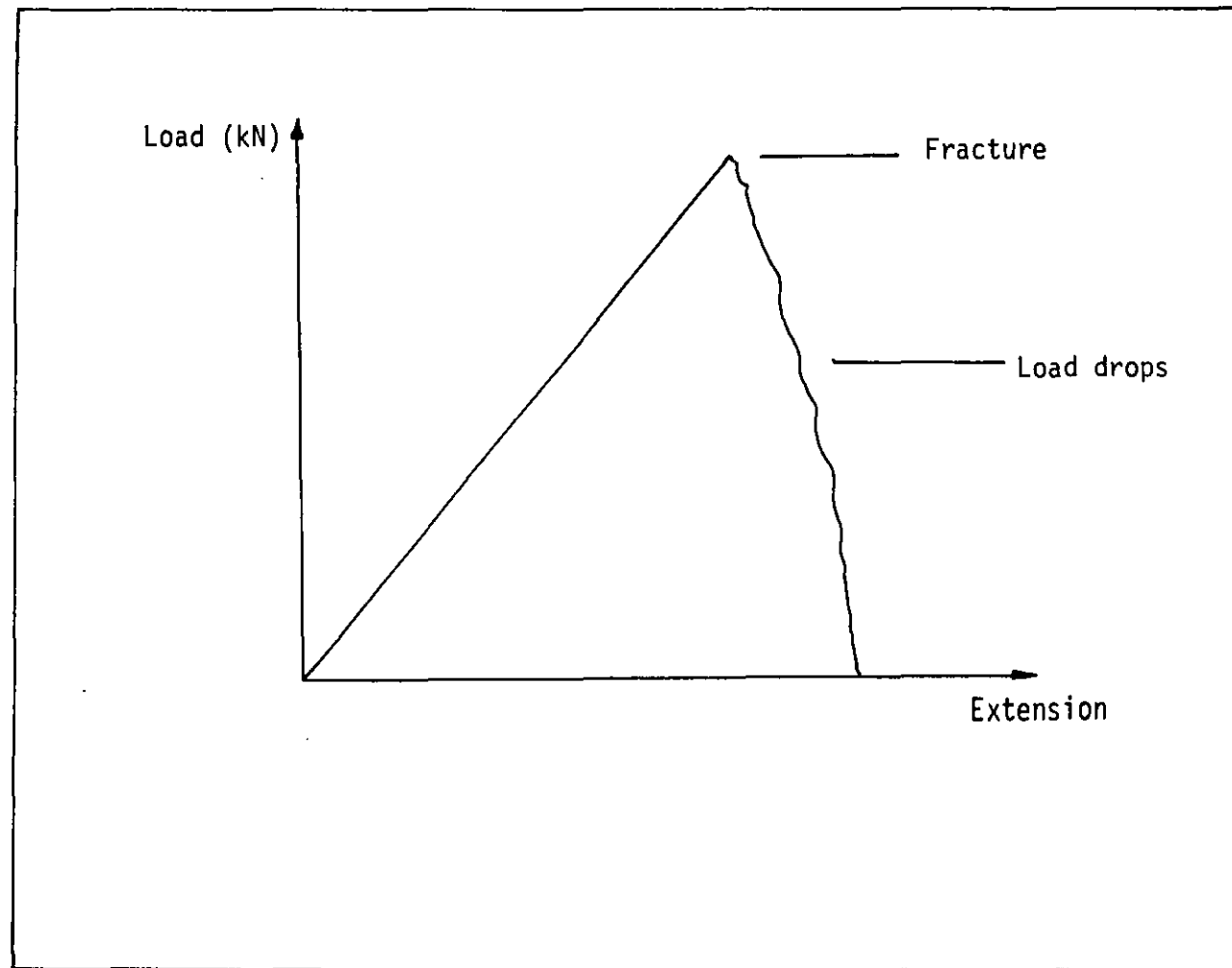


FIGURE 202: The General Form of the Graphs Obtained from the Interlaminar Shear Tests

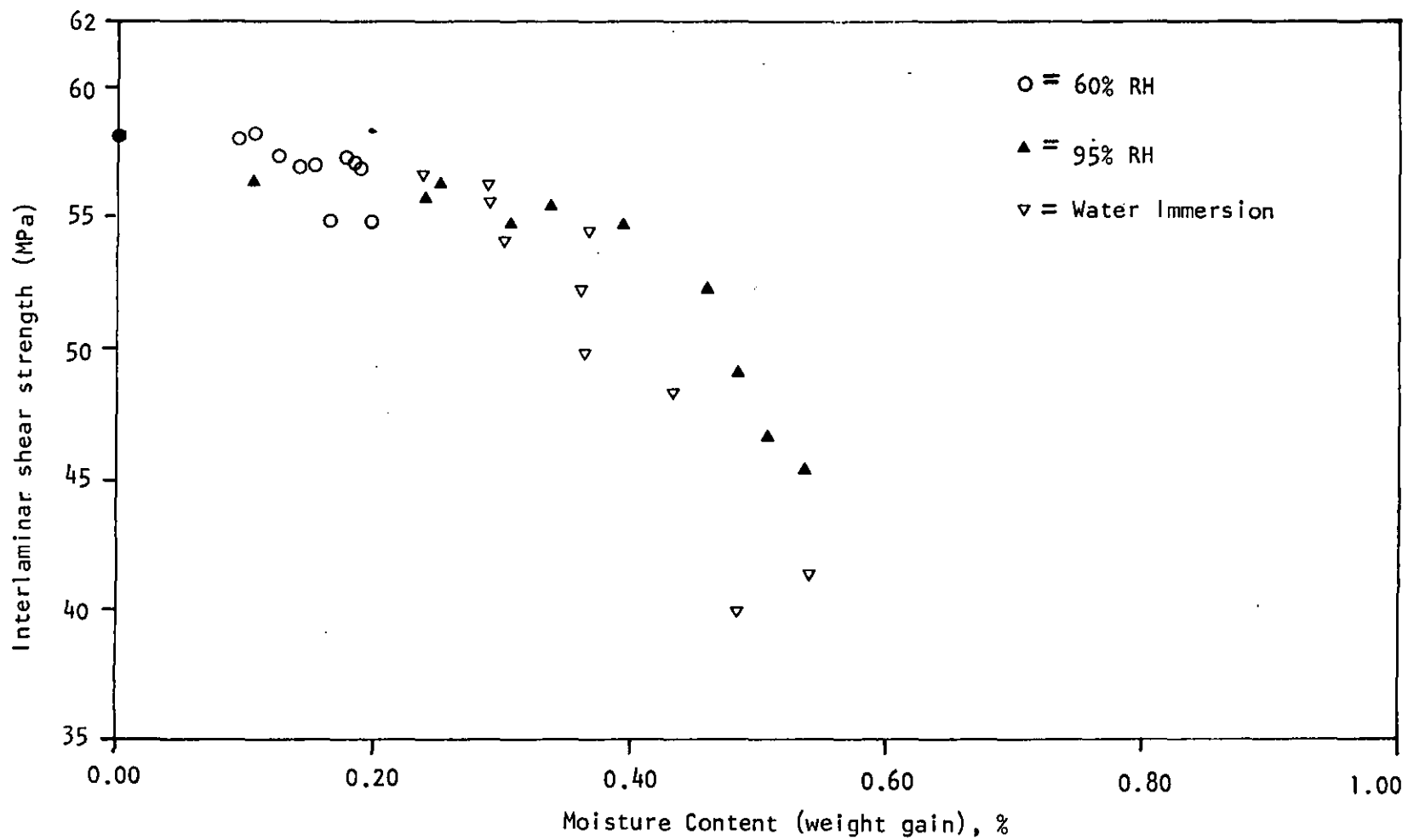


FIGURE 203: The effect of moisture on the interlaminar shear strength of 411-45 Vinylester specimens

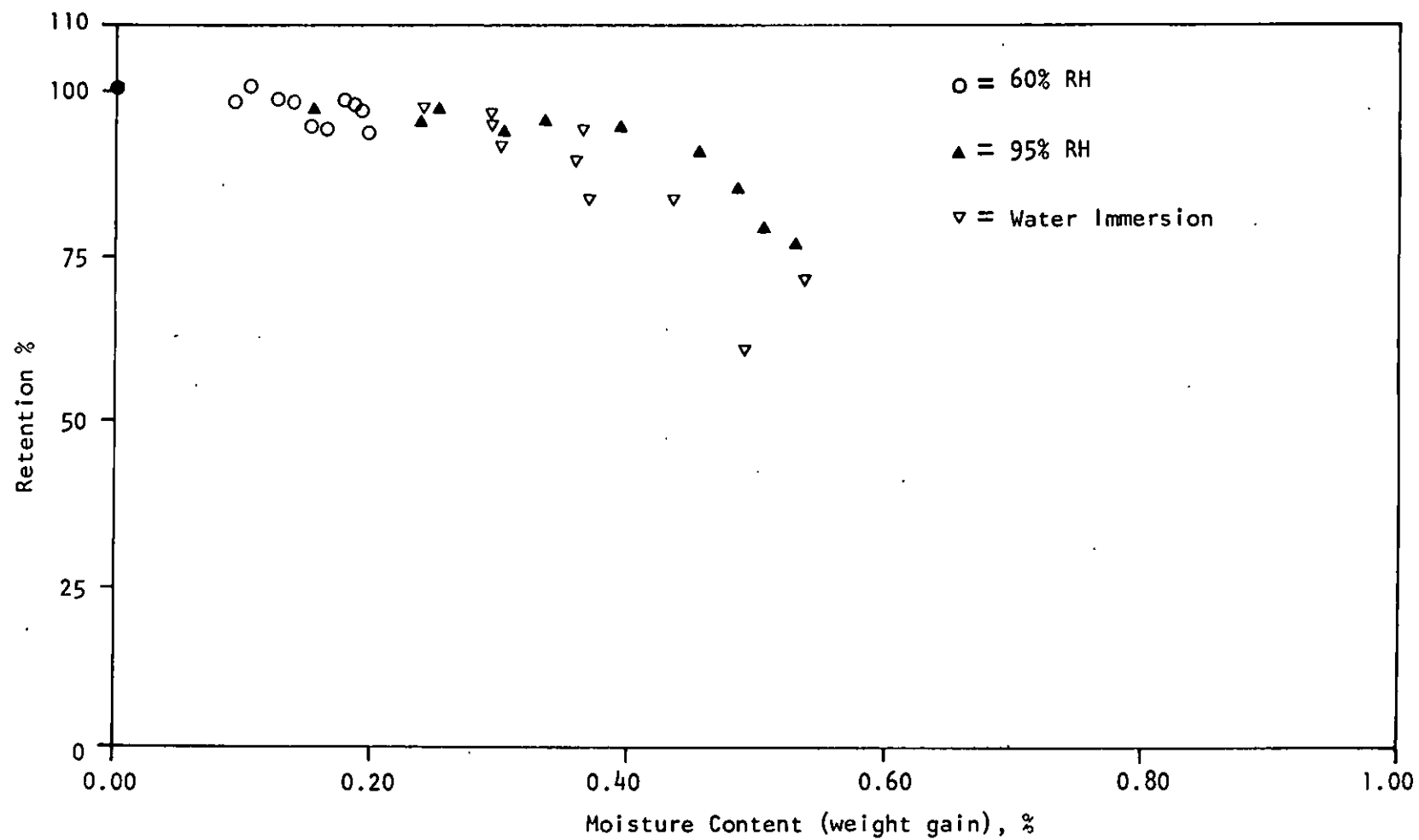


FIGURE 204: The effect of moisture on the % retention of interlaminar shear strength of 411-45 Vinylester specimens

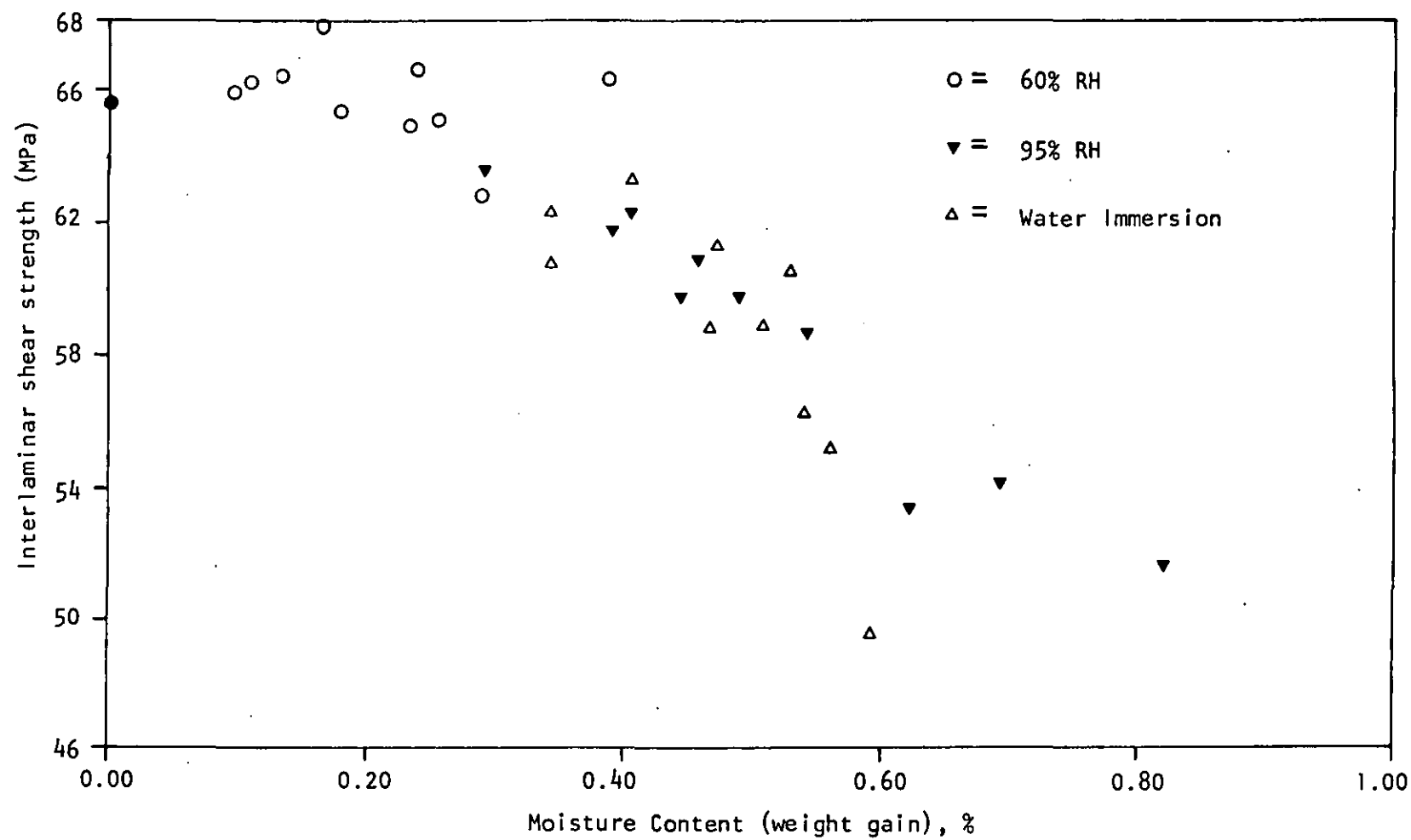


FIGURE 205: The effect of moisture on the interlaminar shear strength of 470-36 Vinylester specimens

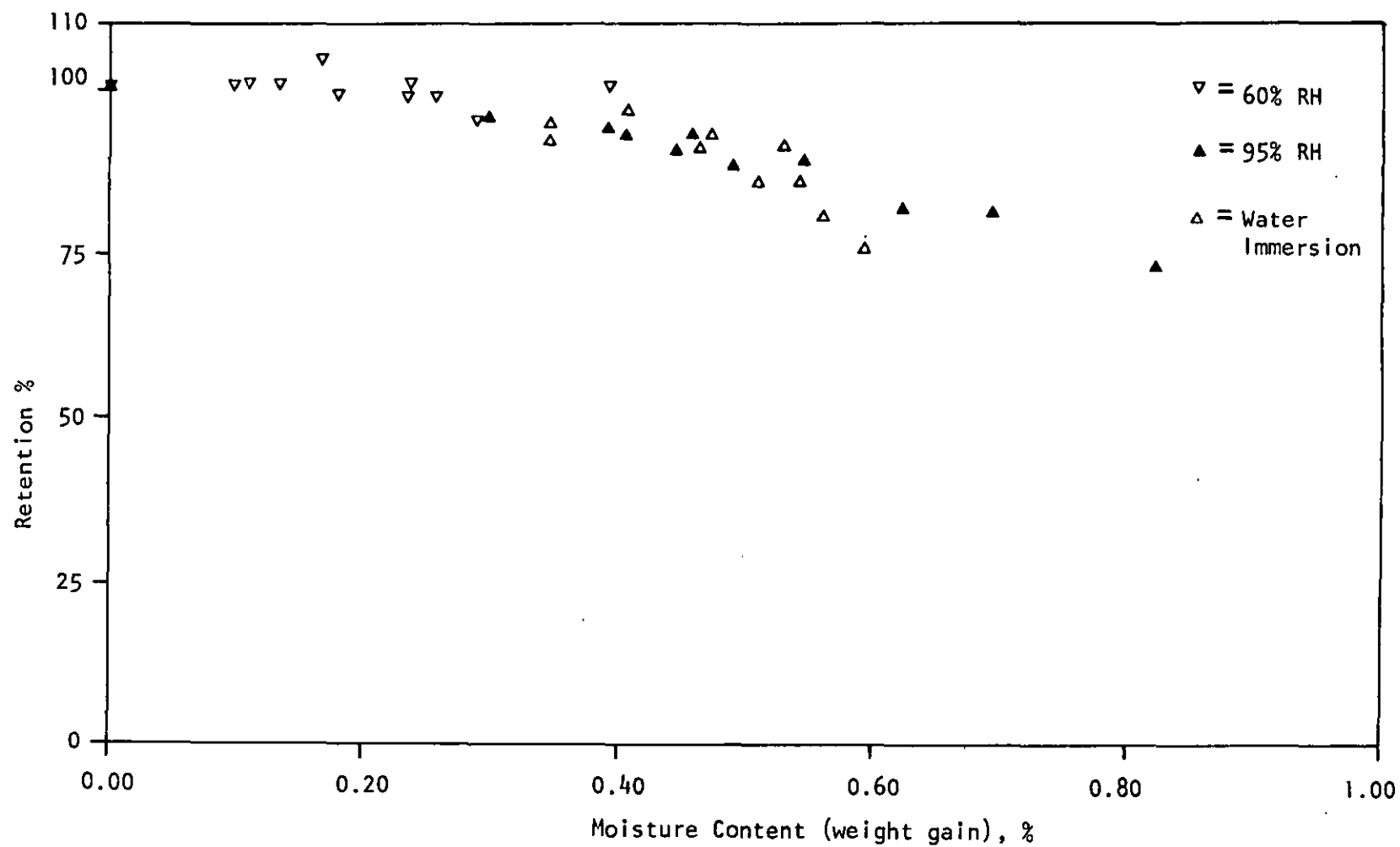


FIGURE 206: The effect of moisture on the % retention of interlaminar shear strength of 470-36 Vinylester specimens

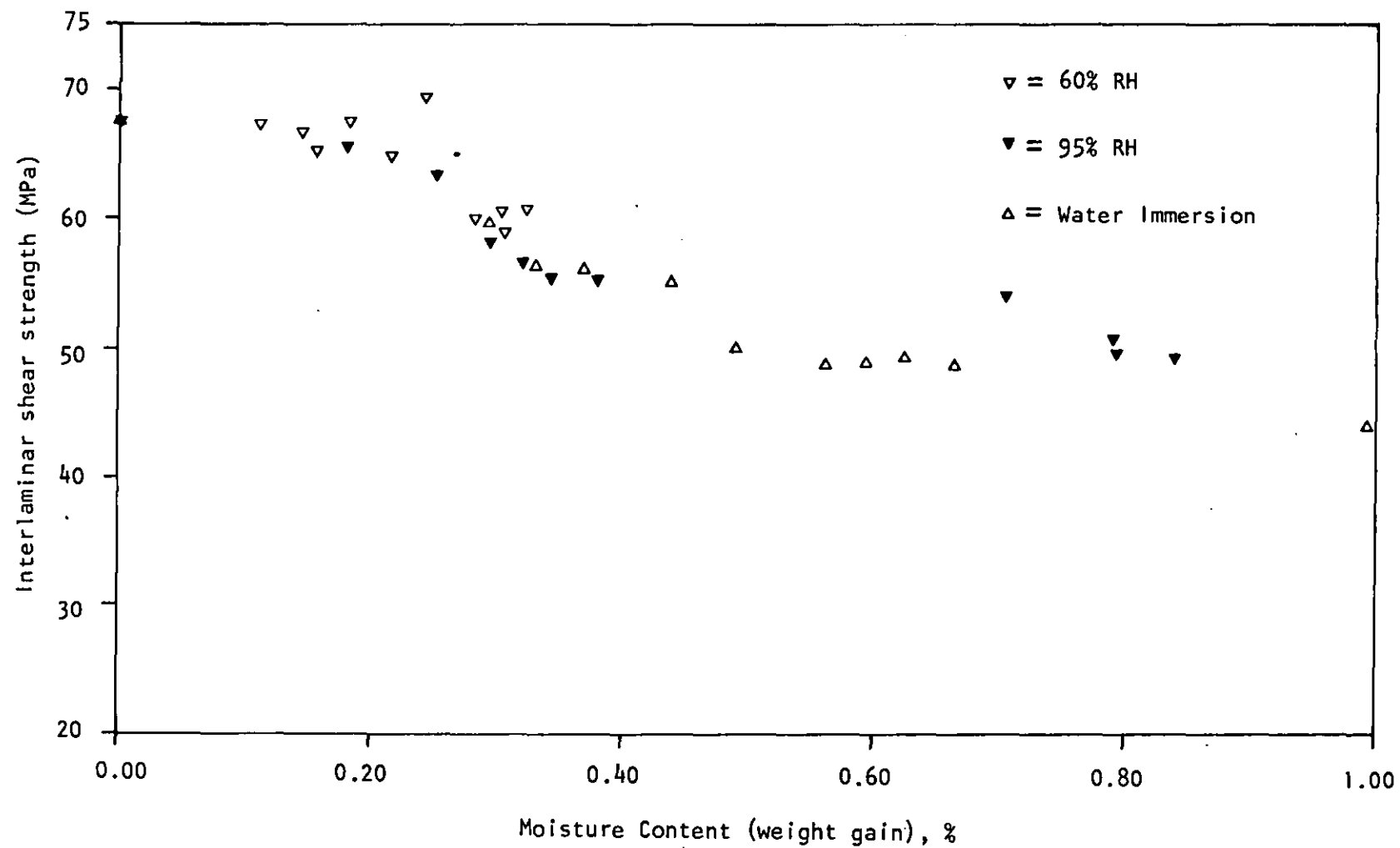


FIGURE 207: The effect of moisture on the interlaminar shear strength of 272 Polyester specimens

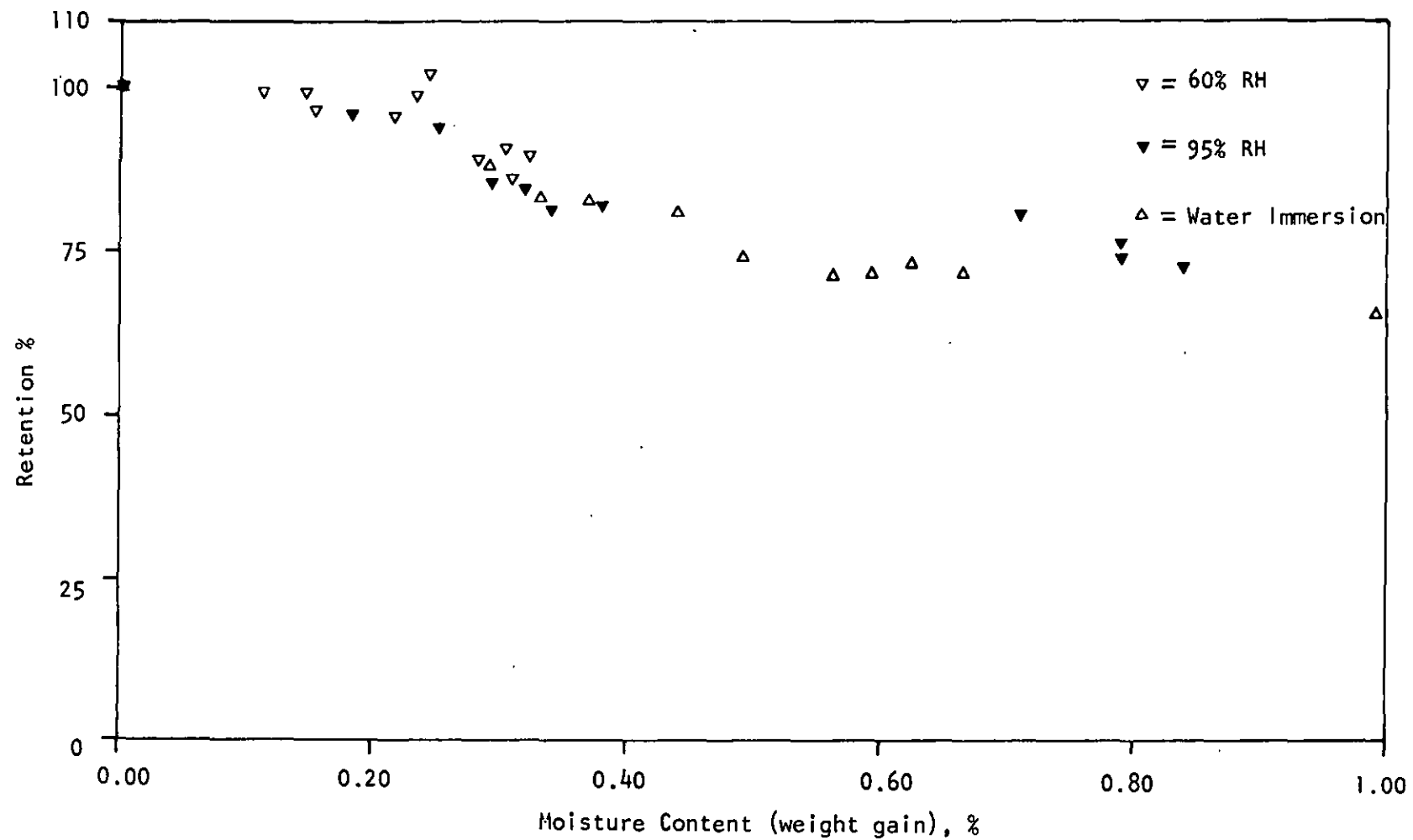


FIGURE 208: The effect of moisture on the % retention of interlaminar shear strength of 272 Polyester specimens

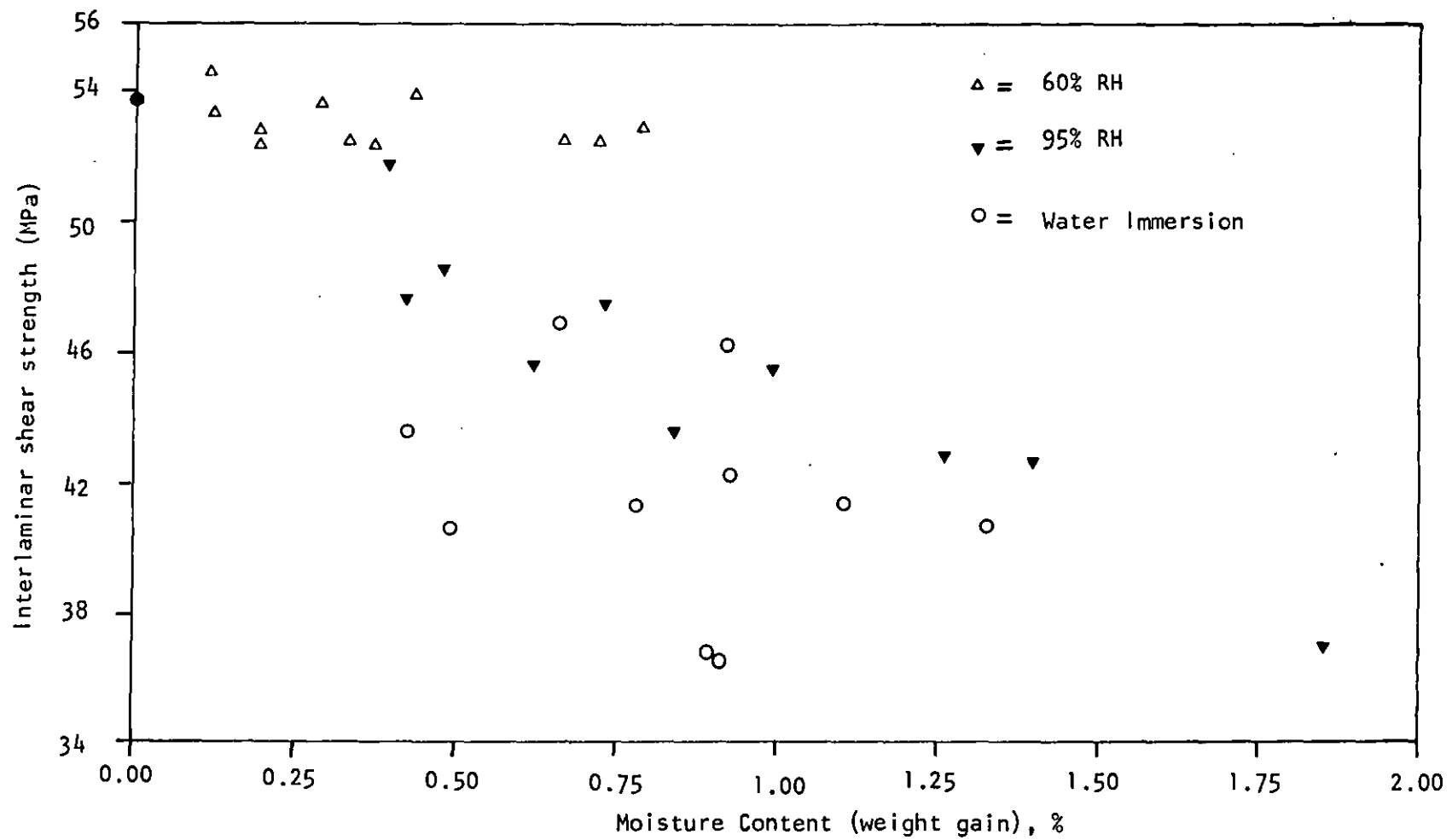


FIGURE 209: The effect of moisture on the interlaminar shear strength of Epoxy 750 Specimens

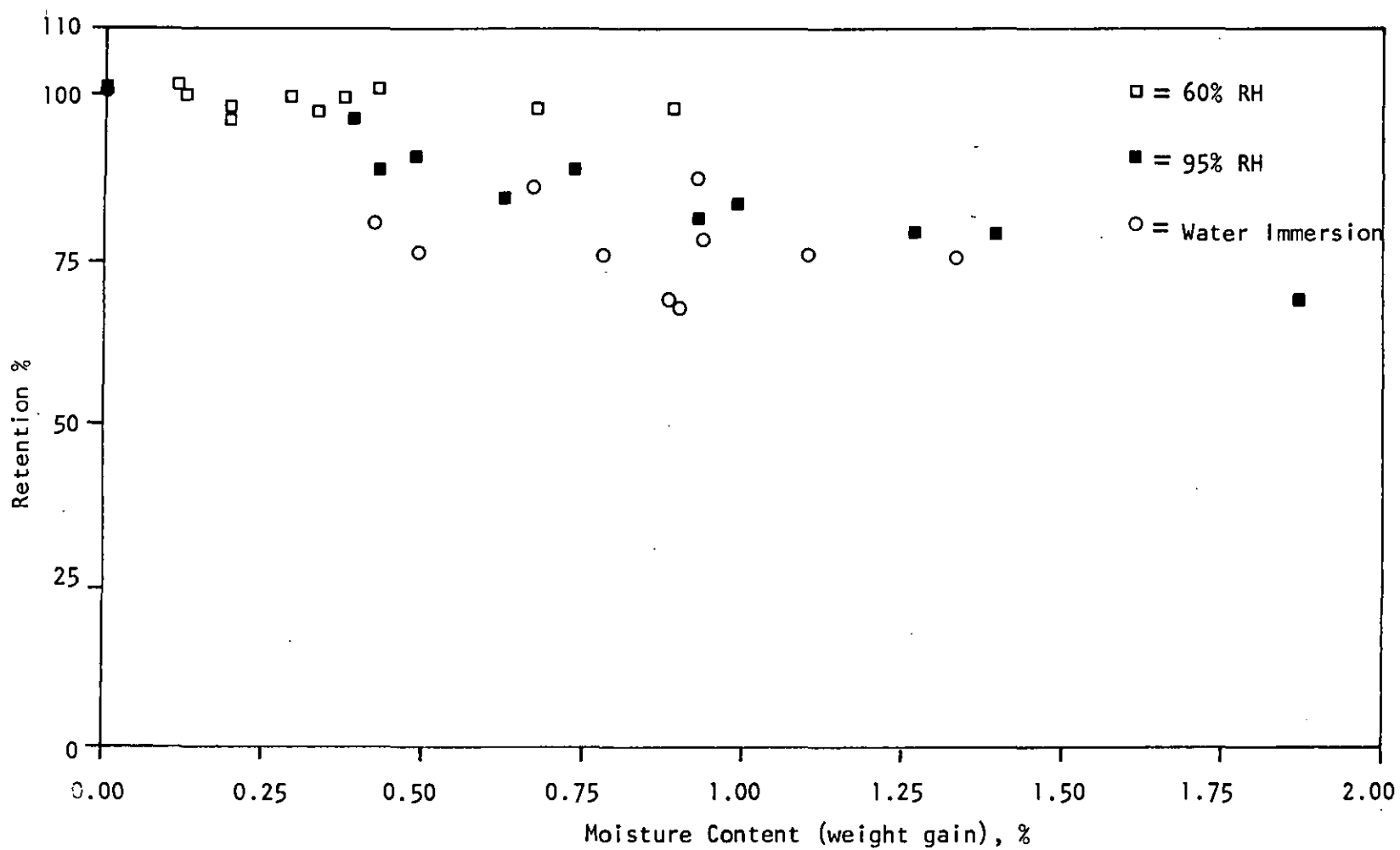


FIGURE 210: The effect of moisture on the % retention of interlaminar shear strength of Epoxy MY 750 specimens

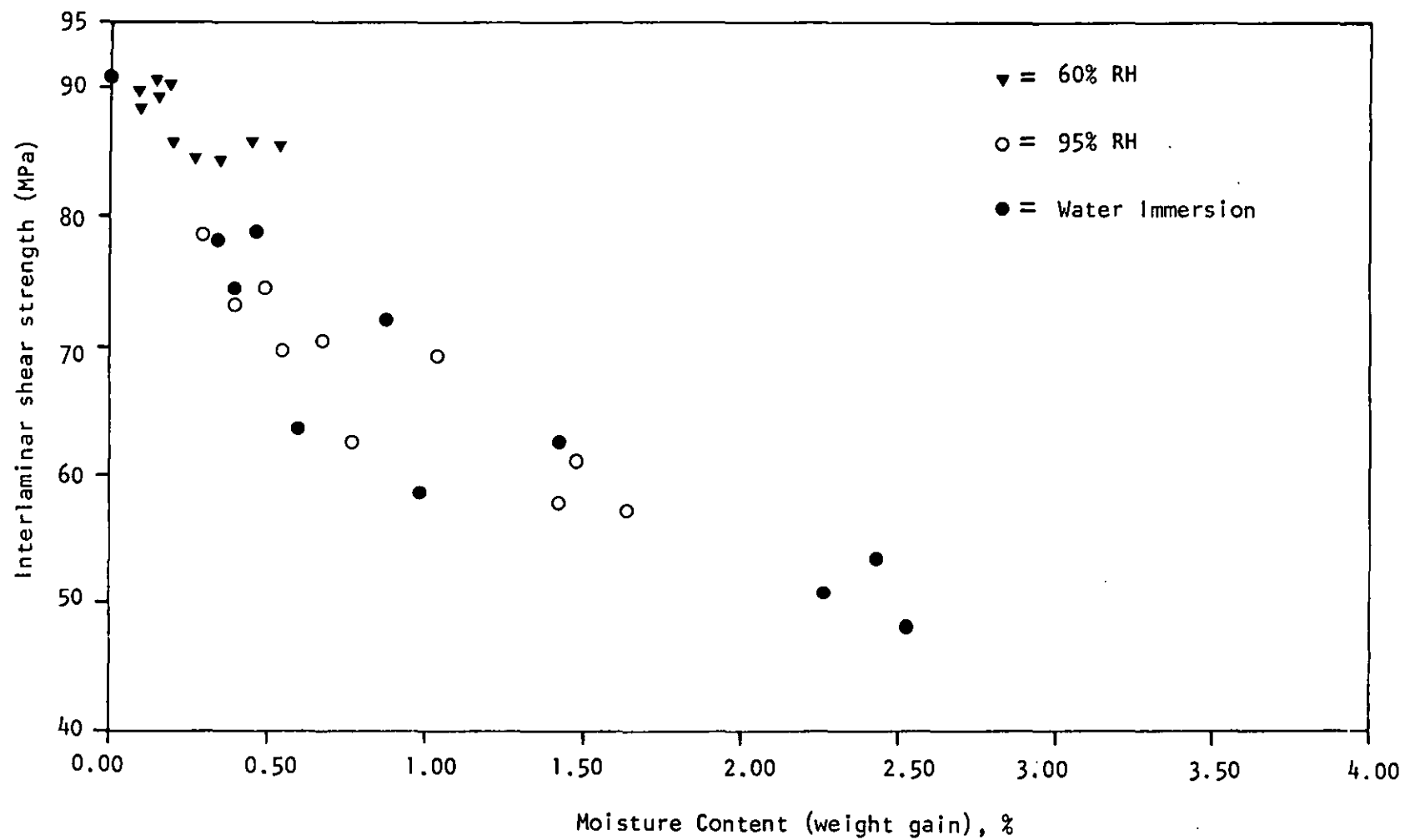


FIGURE 211: The effect of moisture on the interlaminar shear strength of 913 PrePreg specimens

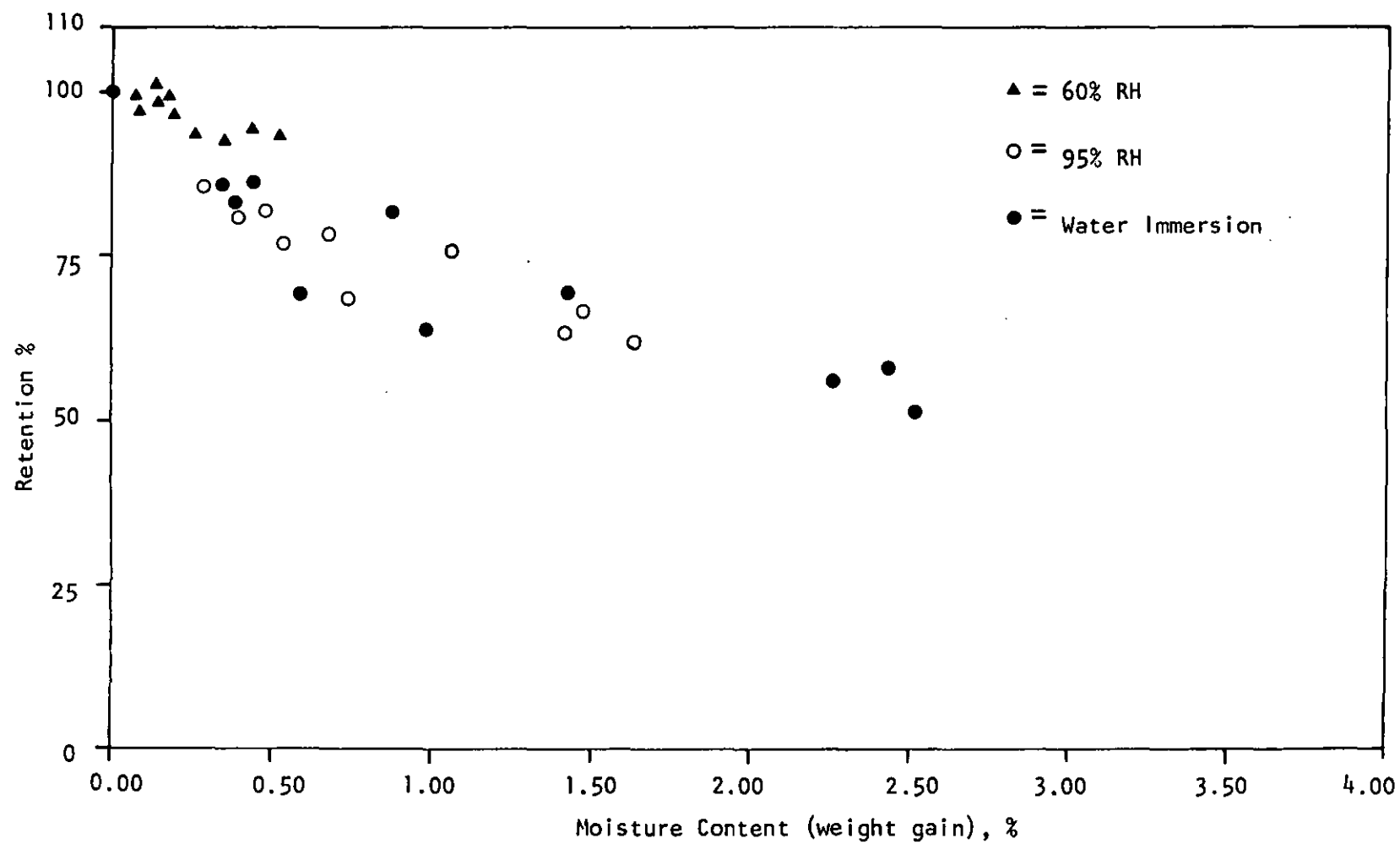
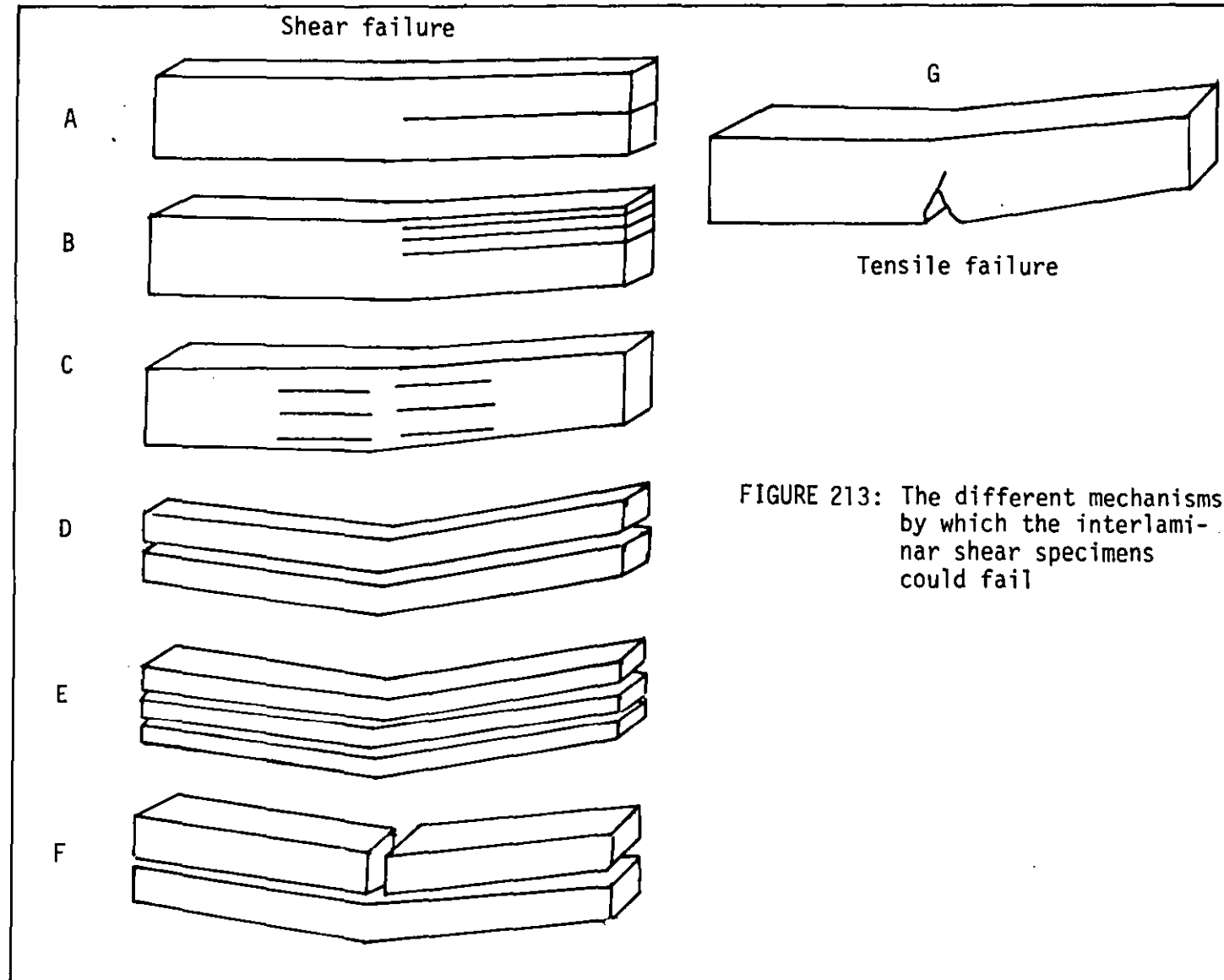


FIGURE 212: The effect of moisture on the % retention of interlaminar shear strength of 913 PrePreg specimens



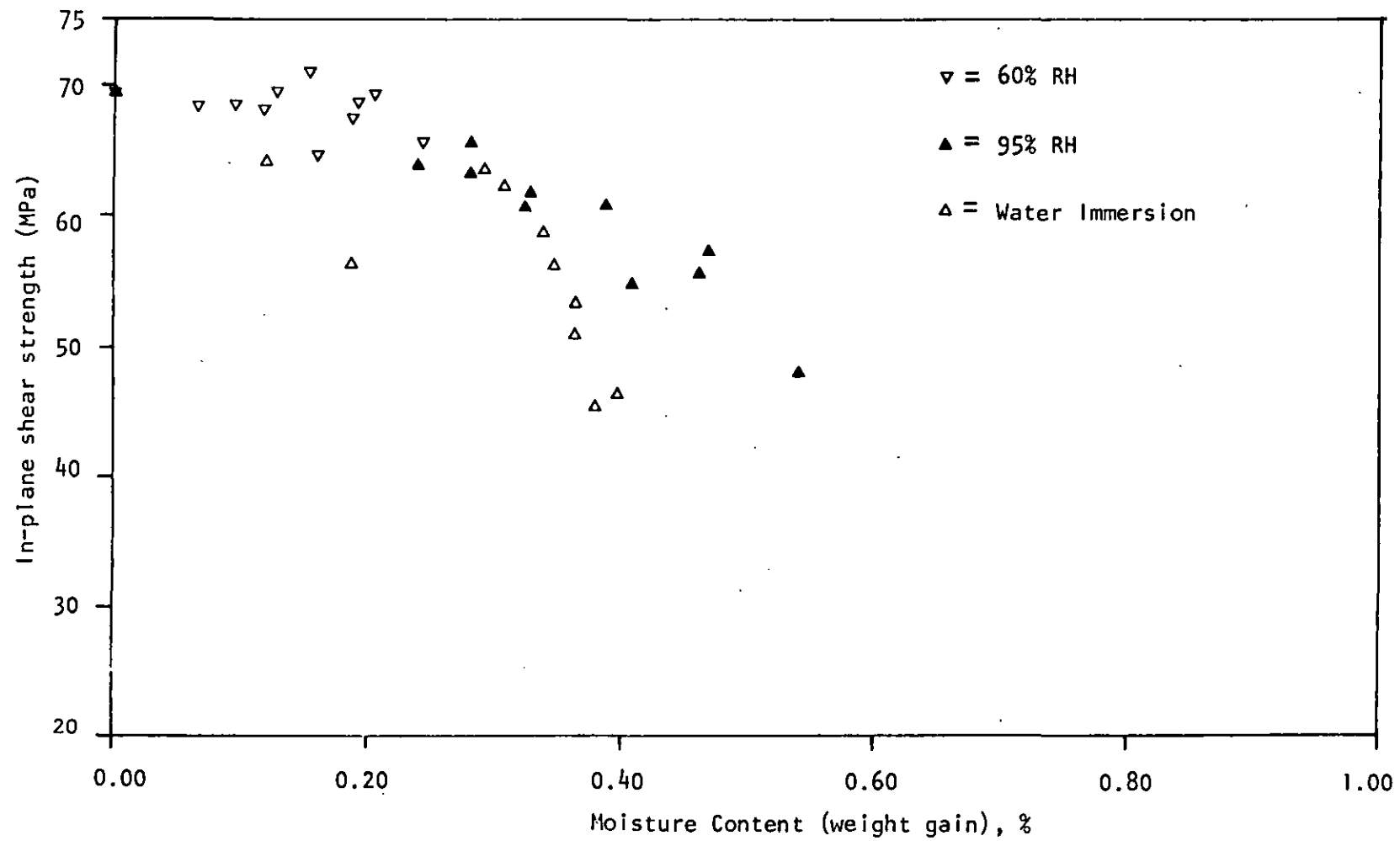


FIGURE 214: The effect of moisture on the in-plane shear strength of 411-45 vinylester specimens

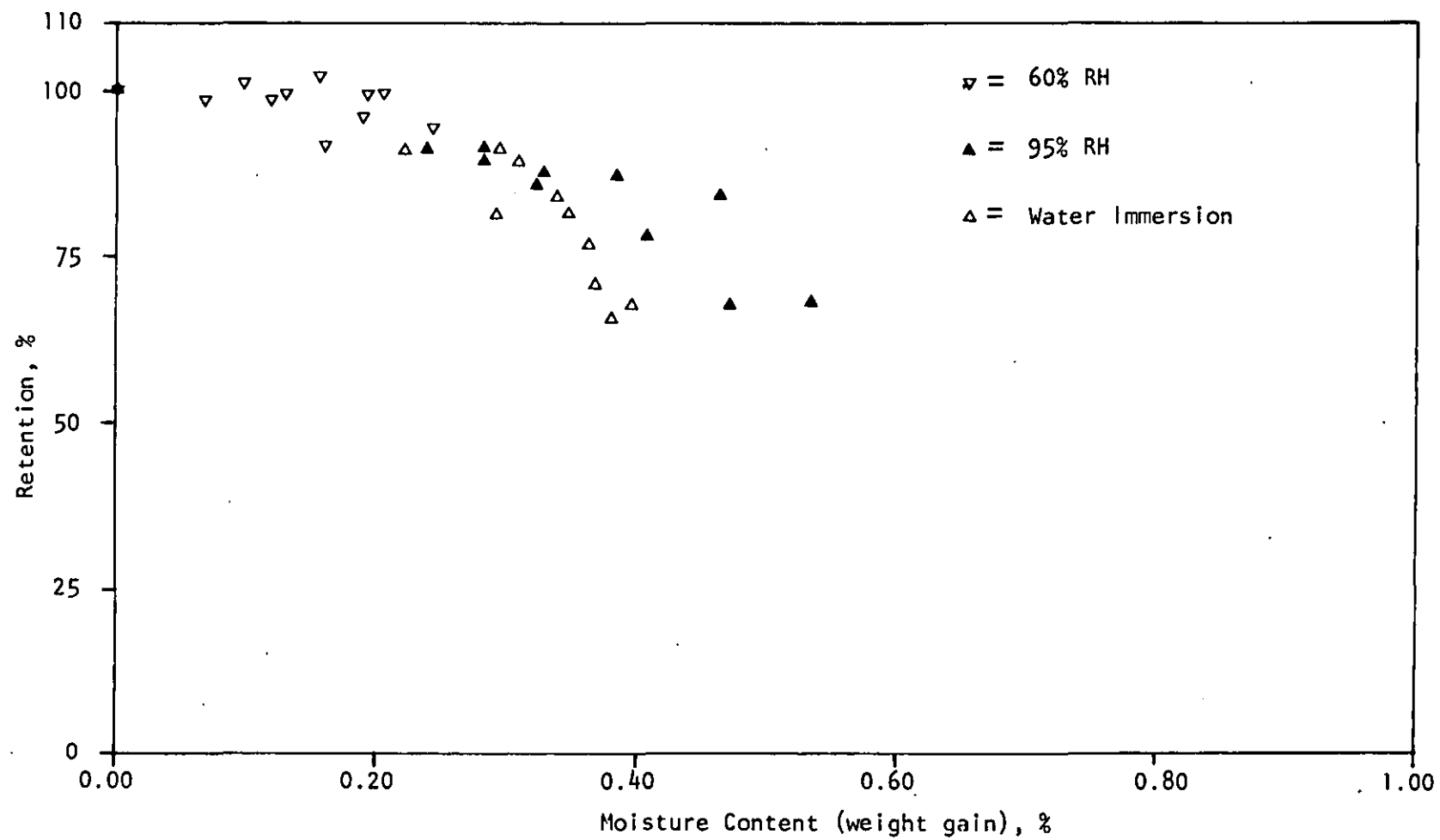


FIGURE 215: The effect of moisture on the % retention of in-plane shear strength of 411-45 Vinylester specimens

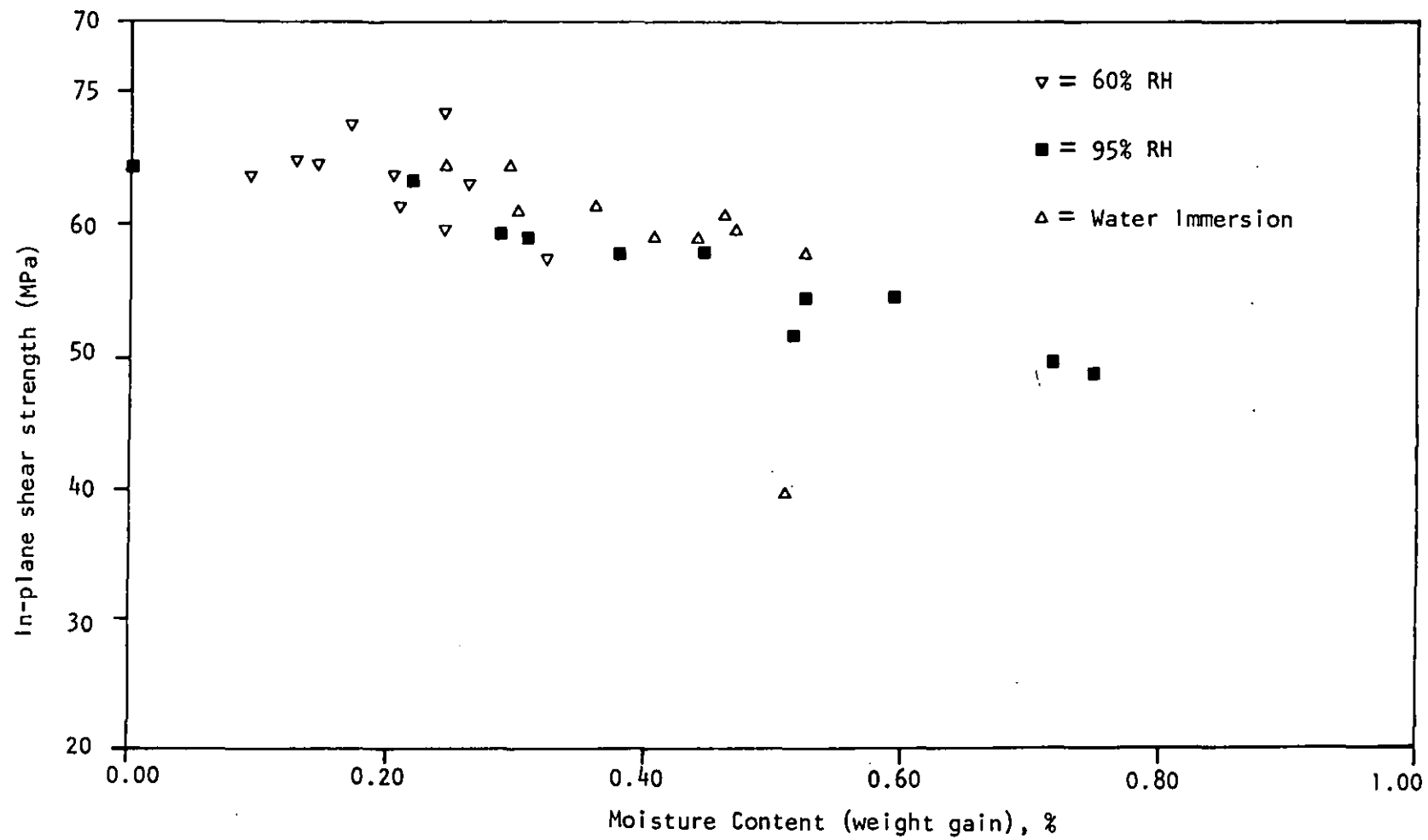


FIGURE 216: The effect of moisture on the in-plane shear strength of 470-36 Vinylester specimens

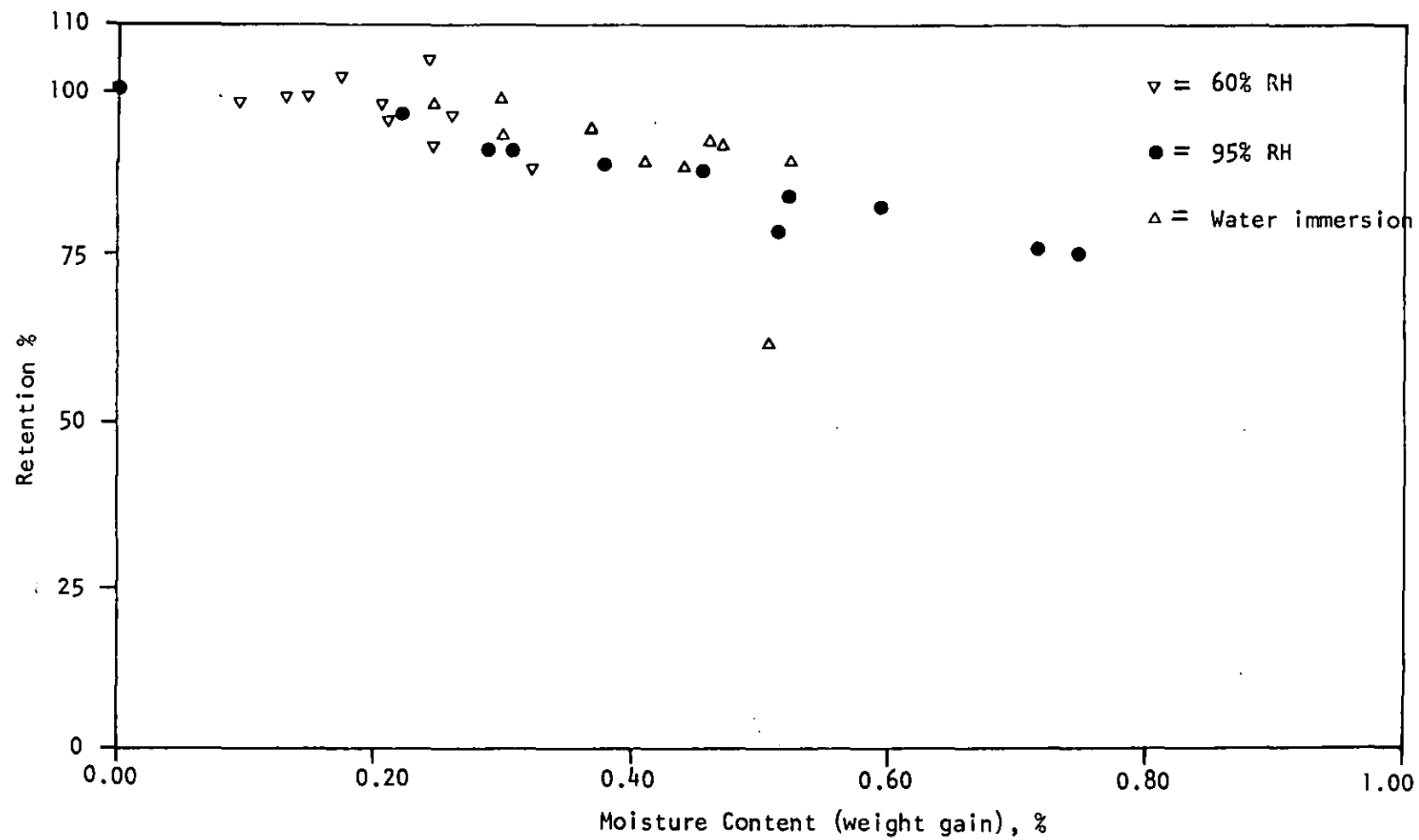


FIGURE 217: The effect of moisture on the % retention of in-plane shear strength of 470-36 Vinylester specimens

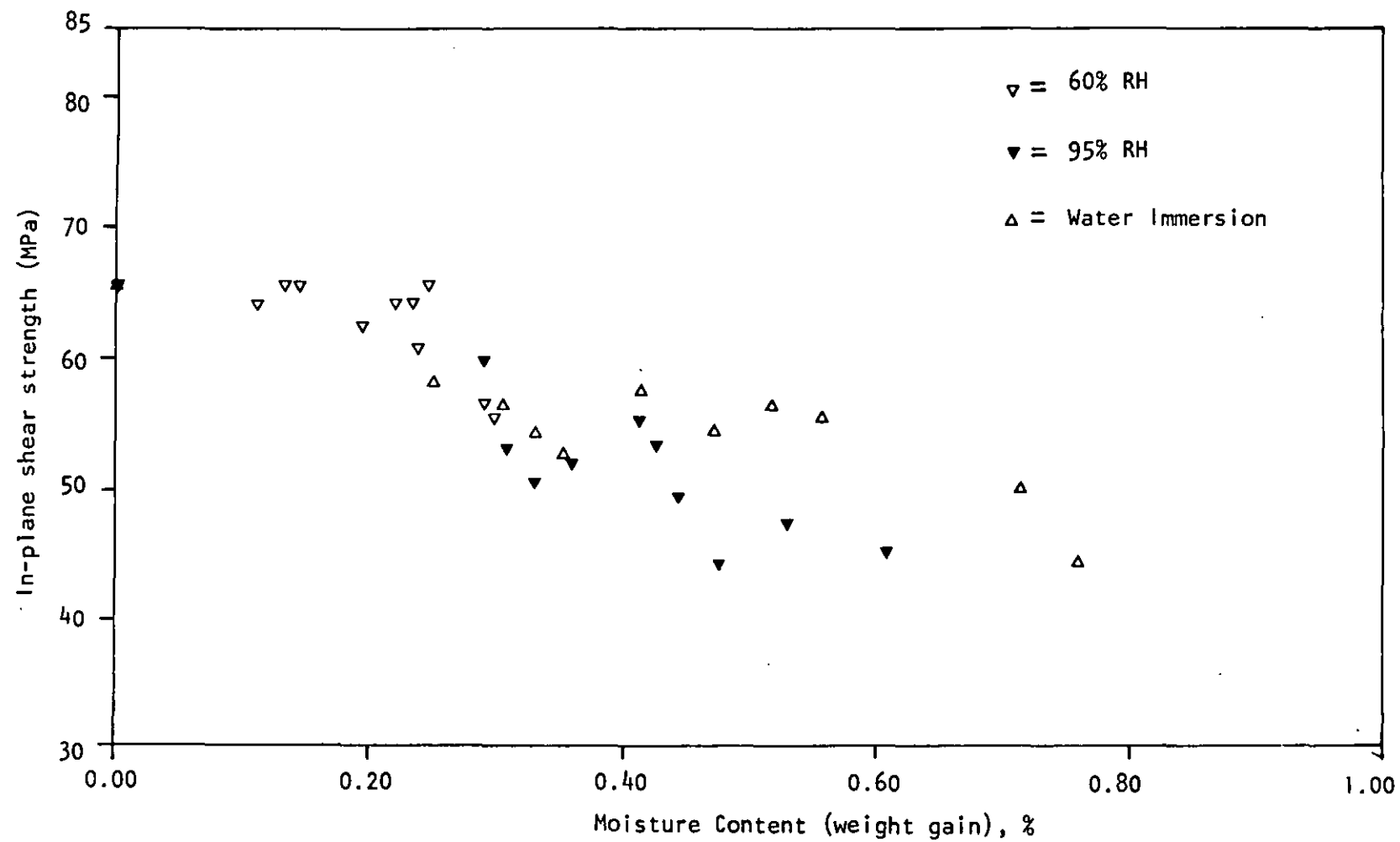


FIGURE 218: The effect of moisture on the in-plane shear strength of 272 Polyester specimens

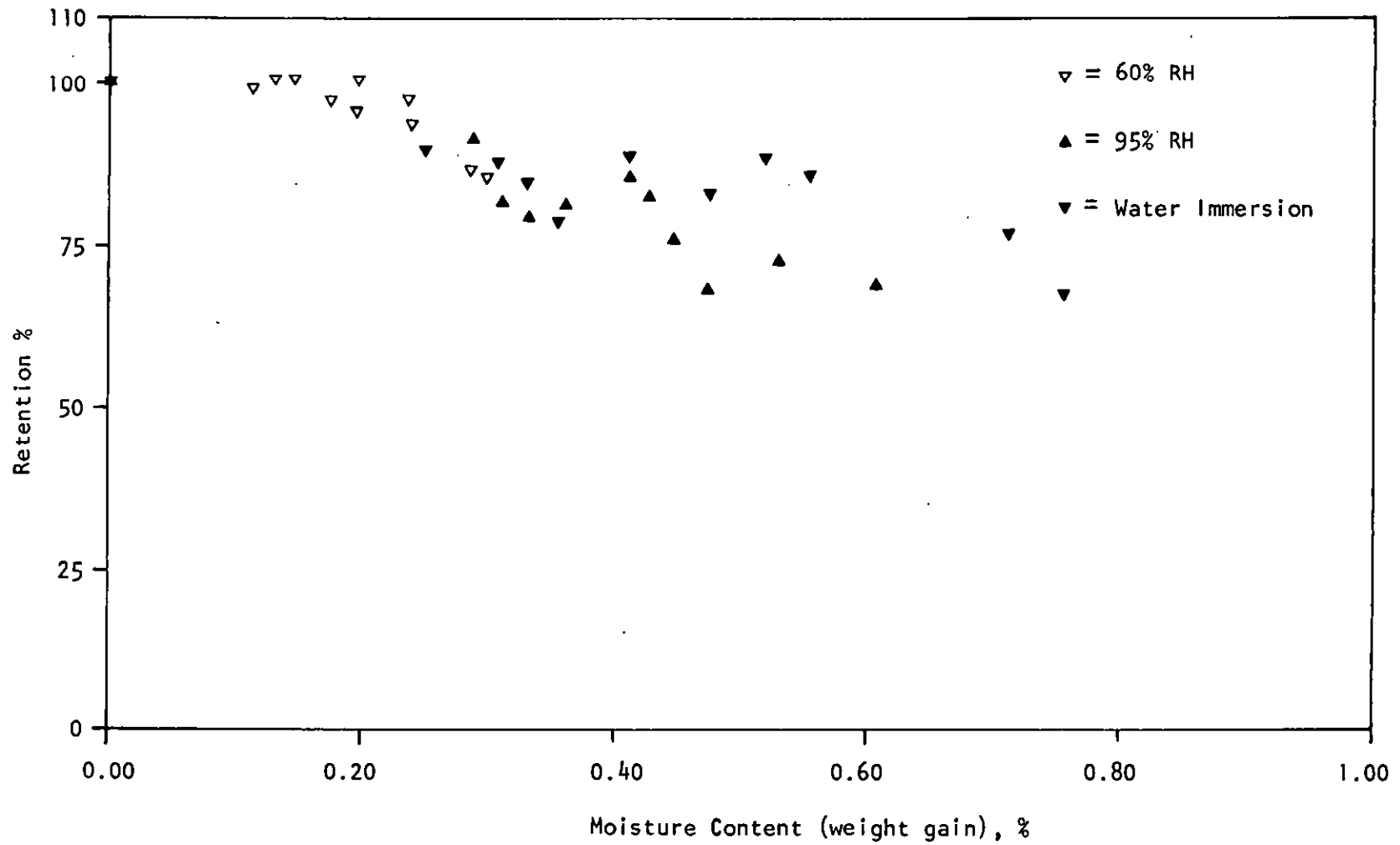


FIGURE 219: The effect of moisture on the % retention of in-plane shear strength of 272 Polyester specimens

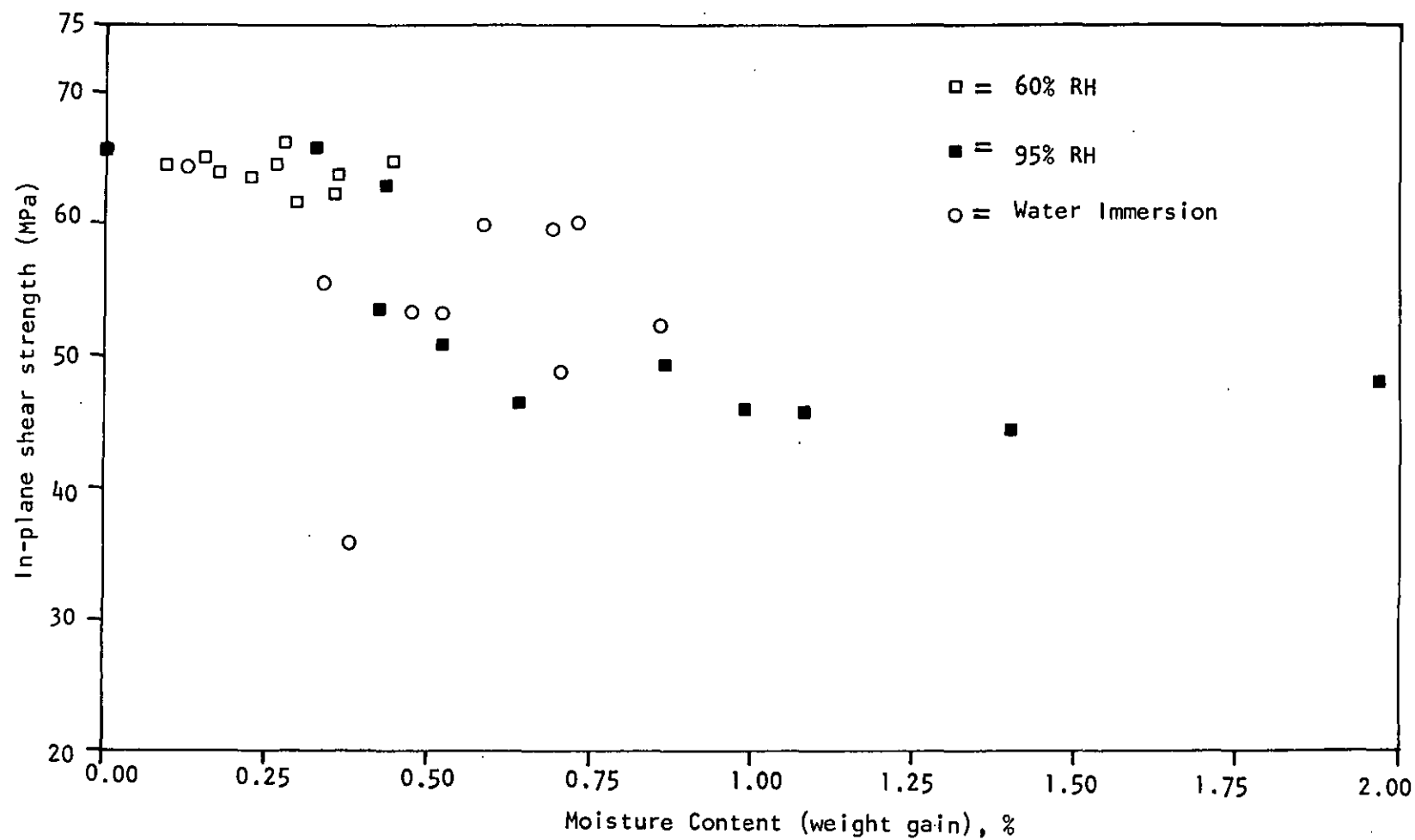


FIGURE 220: The effect of moisture on the in-plane shear strength of Epoxy MY 750 specimens

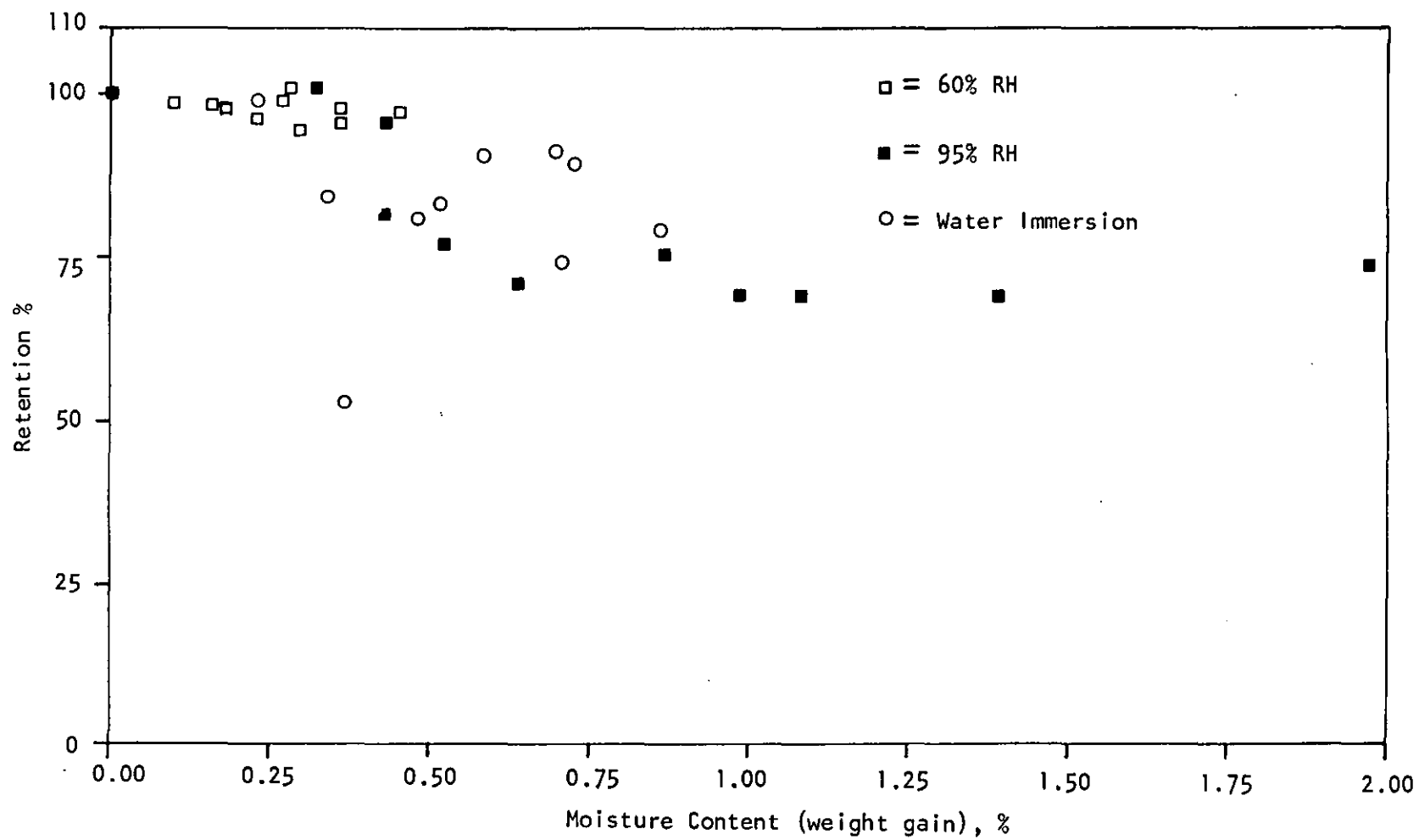


FIGURE 221: The effect of moisture on the % retention of in-plane shear strength of Epoxy MY 750

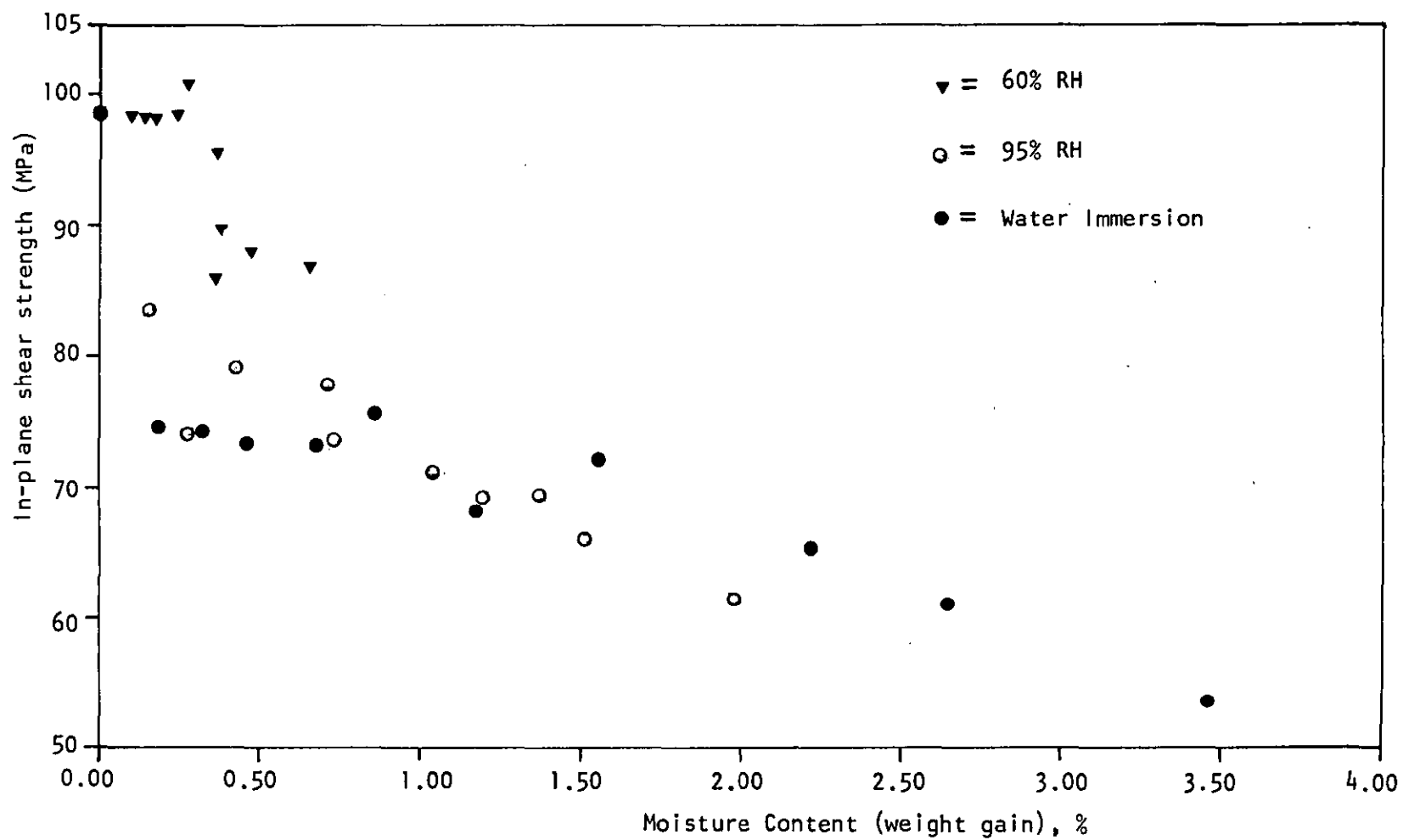


FIGURE 222: The effect of moisture on the in-plane shear strength of 913 PrePreg specimens

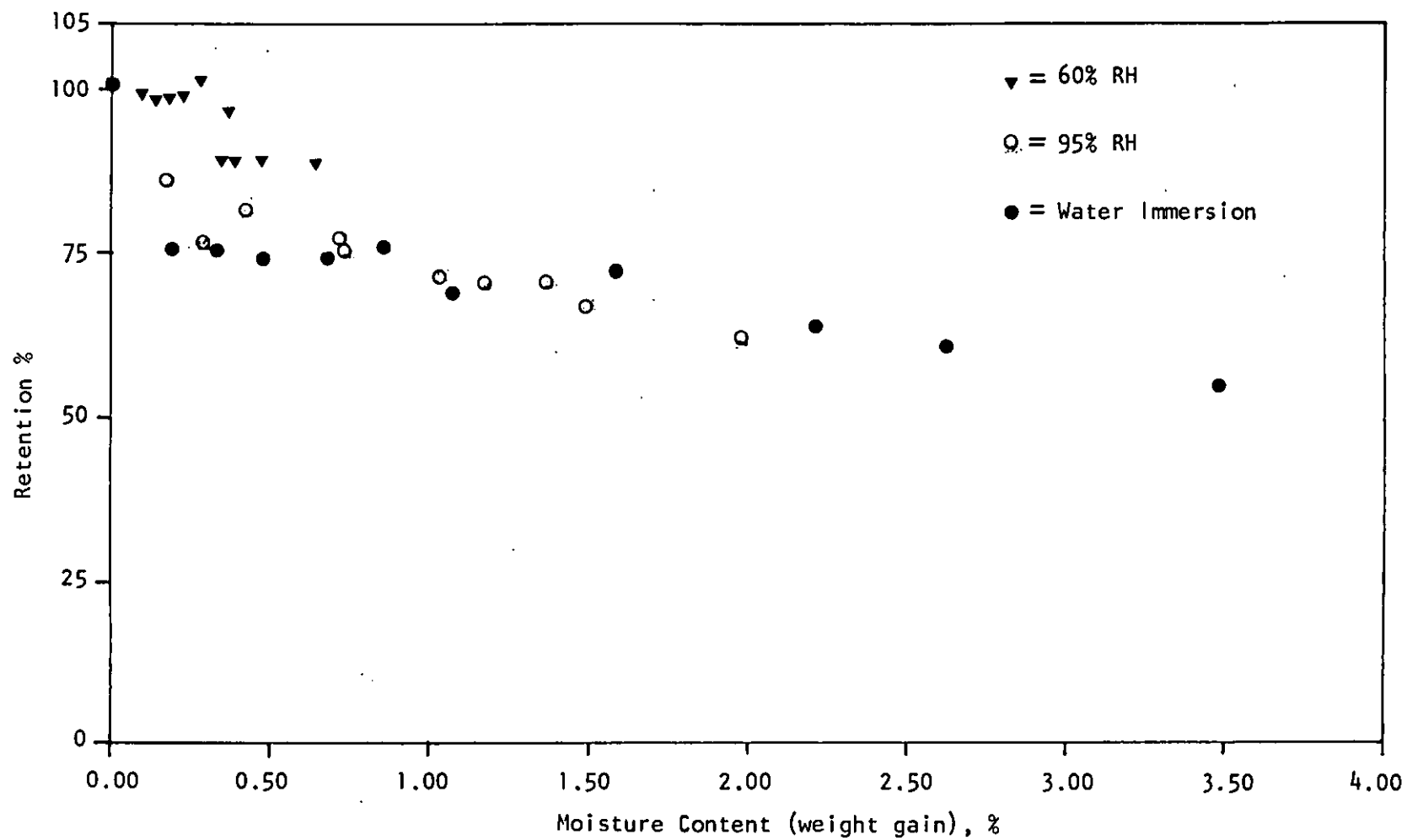


FIGURE 223: The effect of moisture on the % retention of in-plane shear strength of 913 PrePreg specimens

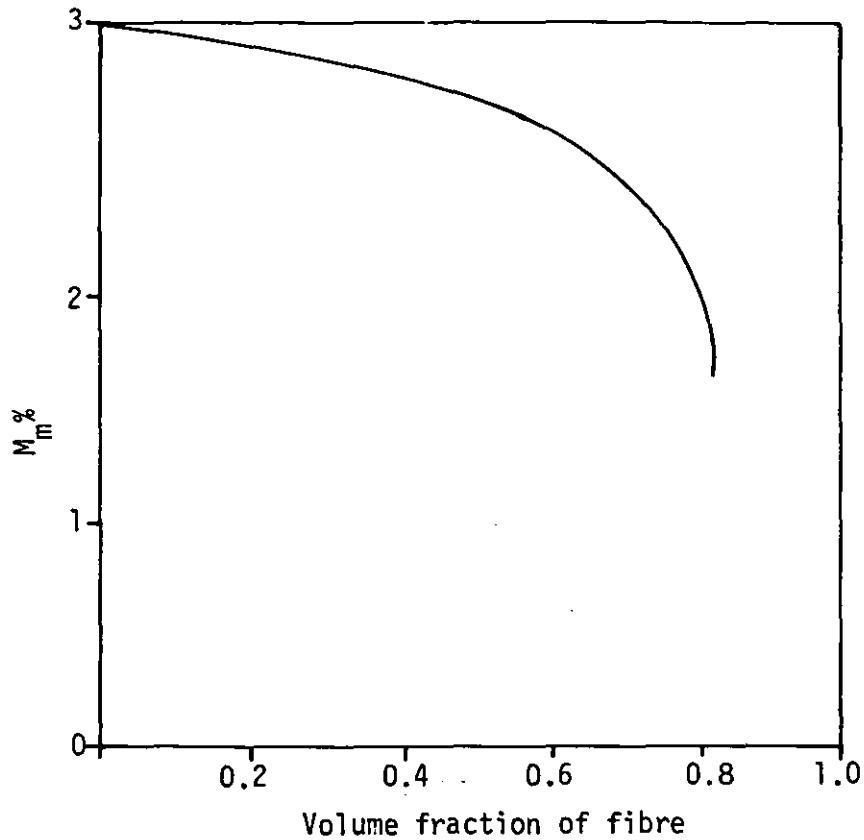


FIGURE 224: Variation of equilibrium moisture content (M_m) with fibre volume fraction to glass-epoxy composites (129)

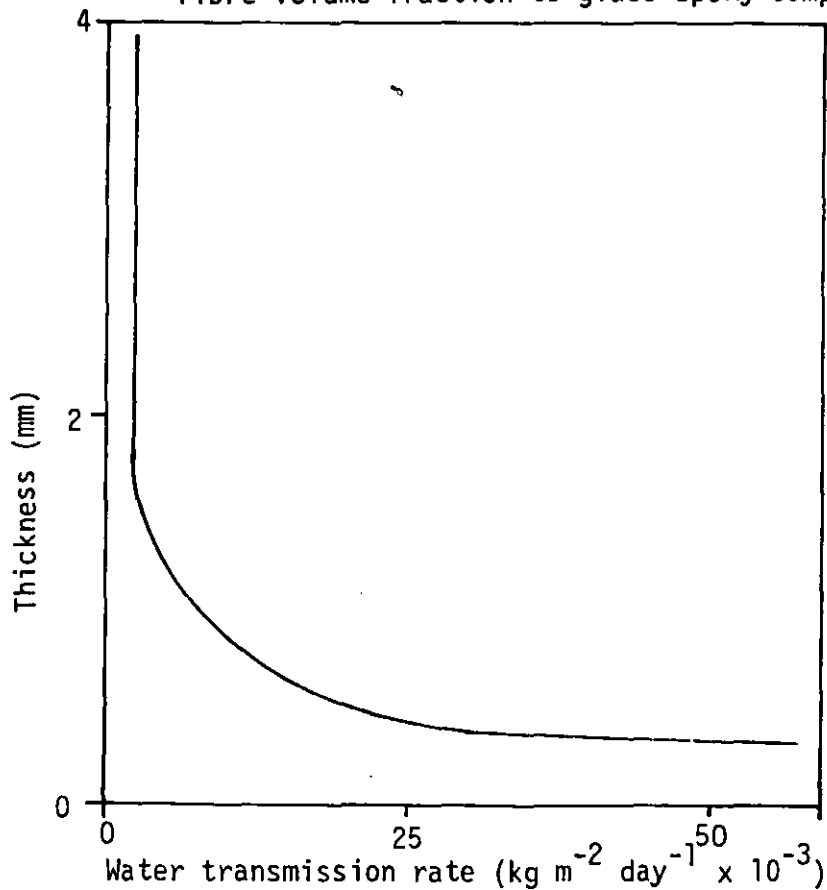
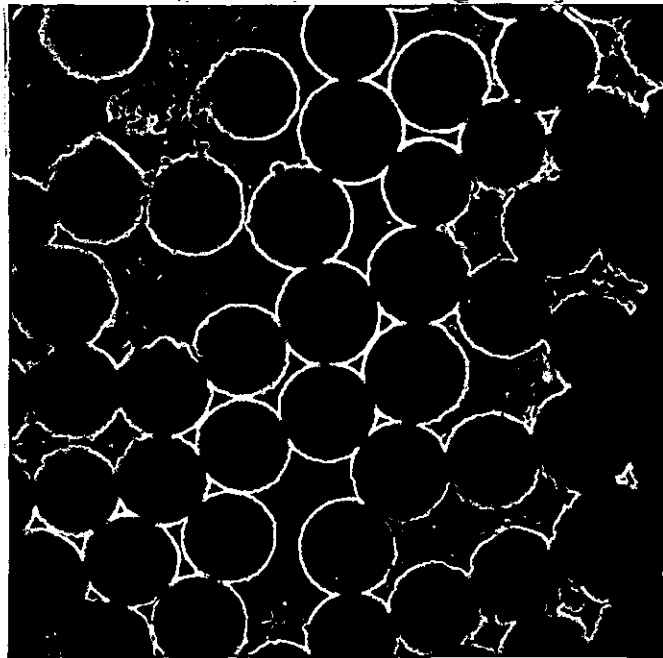
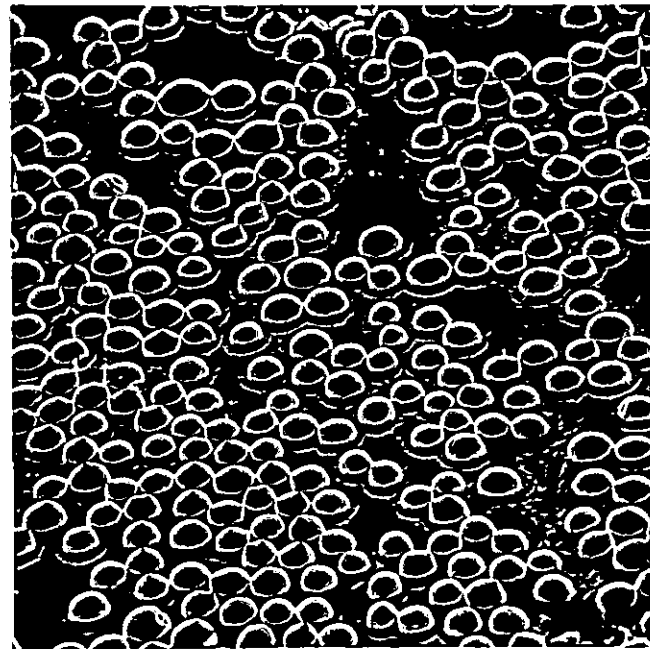


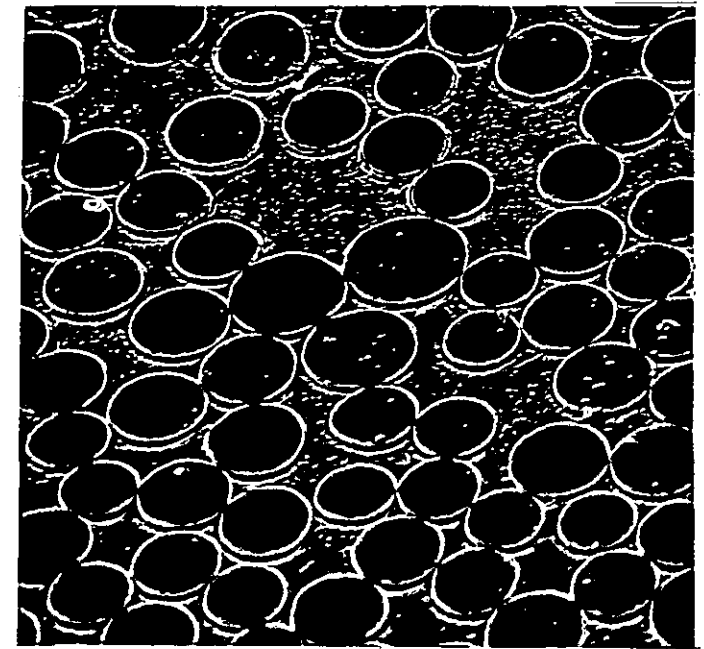
FIGURE 225: Relationship between thickness and water permeability for polyester resin cast films (96)



a) Optical micrograph x1000

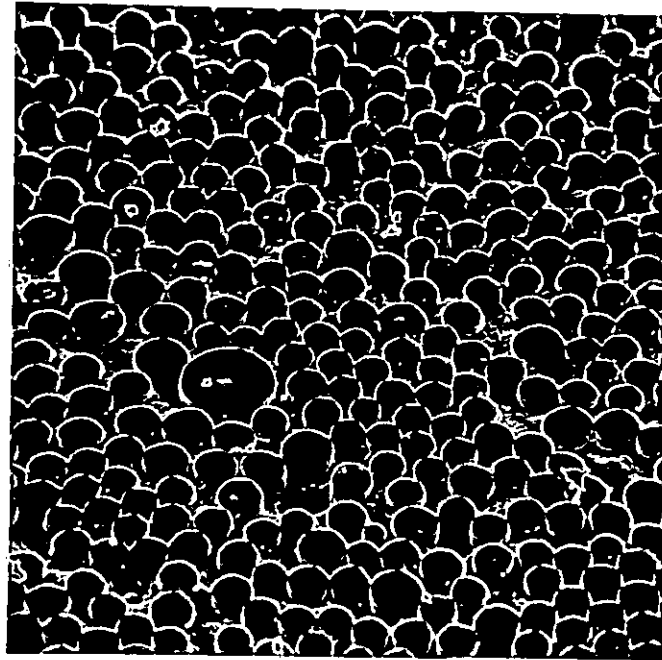


b) Scanning electron micrograph
x250

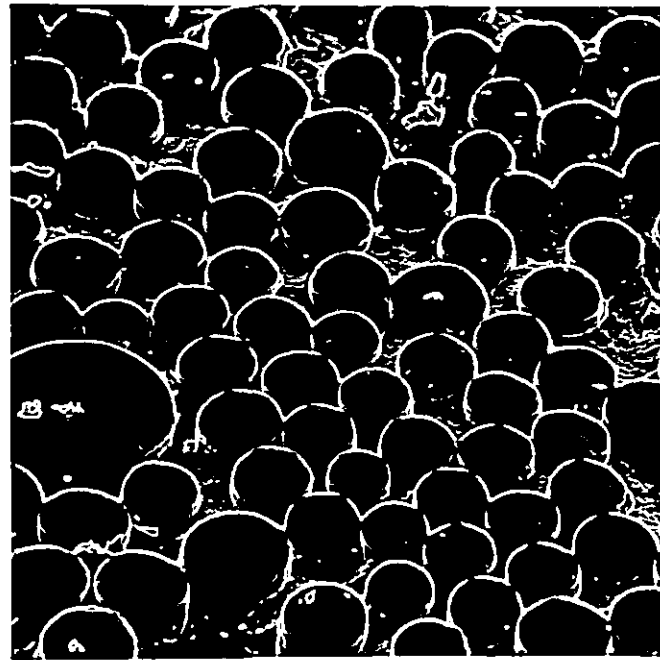


c) Scanning electron micrograph
x1000

FIGURE 226: Micrographs of a section cut at right angles to fibres in unidirectional laminate ($V_F = 0.42$)



a) x500



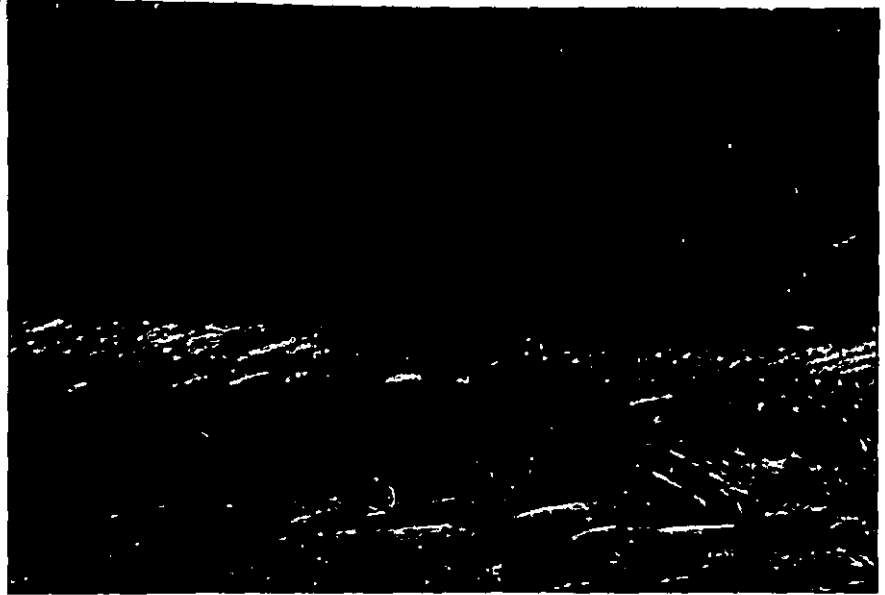
b) x1000



c) x2000

FIGURE 227: Scanning electron micrographs of a section cut at right angles to fibres in unidirectional laminate ($V_F = 0.60$)

Before
Immersion



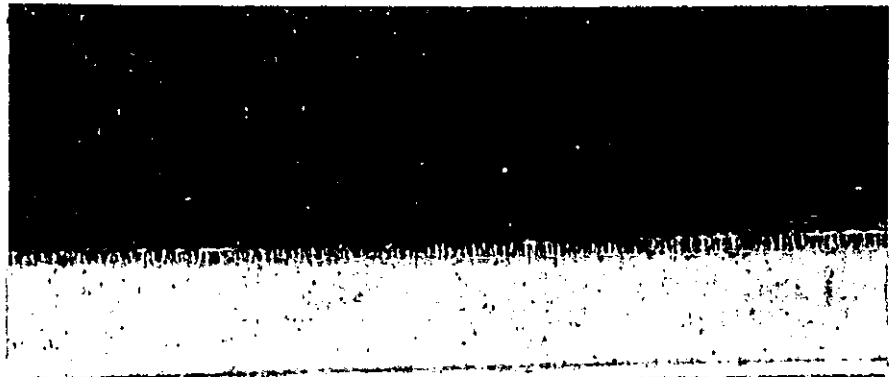
After
Immersion

FIGURE 228a: Photograph of Epoxy MY750 laminate's surface. The laminate was immersed in distilled water at 70°C for 40 days.

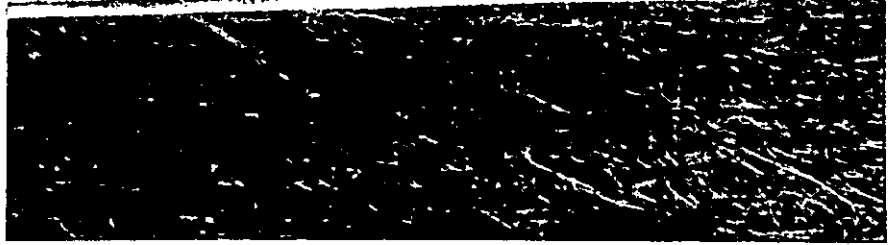


FIGURE 228b: Scanning electron micrograph of the surface. x500

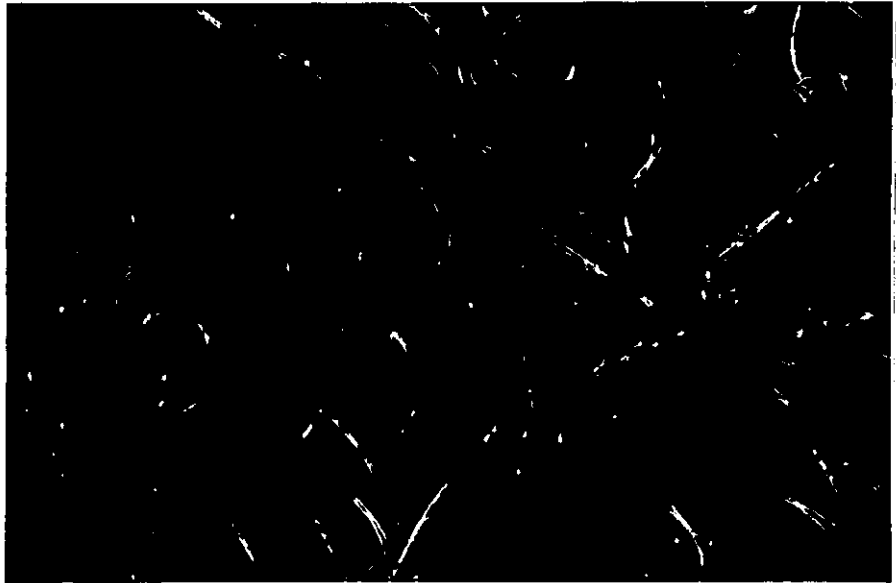
Before
Immersion



After
Immersion



a) Photograph of Polyester 272 laminate's surface.
The laminate was immersed in distilled water at
70°C for 40 days



b) After immersion



c) Scanning electron micrograph of the surface. x500

Before
Immersion



After
Immersion

FIGURE 230a: Photograph of 913 PrePreg laminate's surface. The laminate was immersed in distilled water at 70°C for 40 days

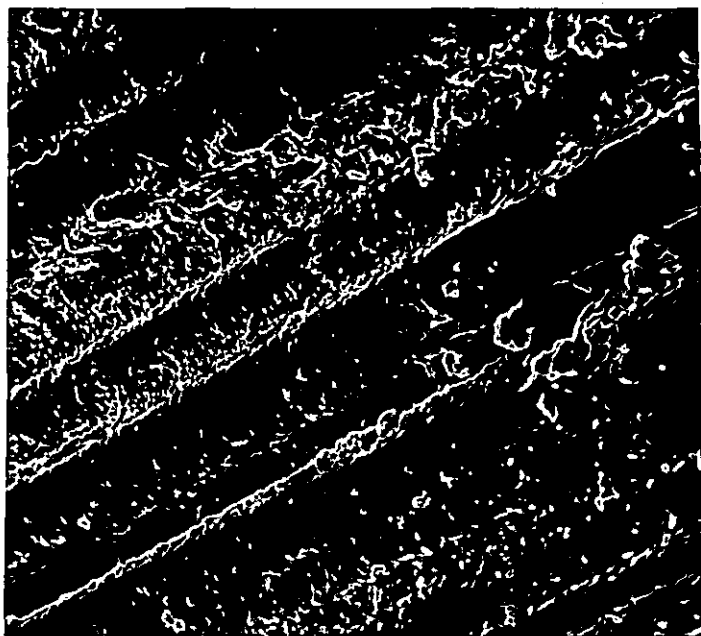


FIGURE 230b: Scanning electron micrograph of the surface. x1000

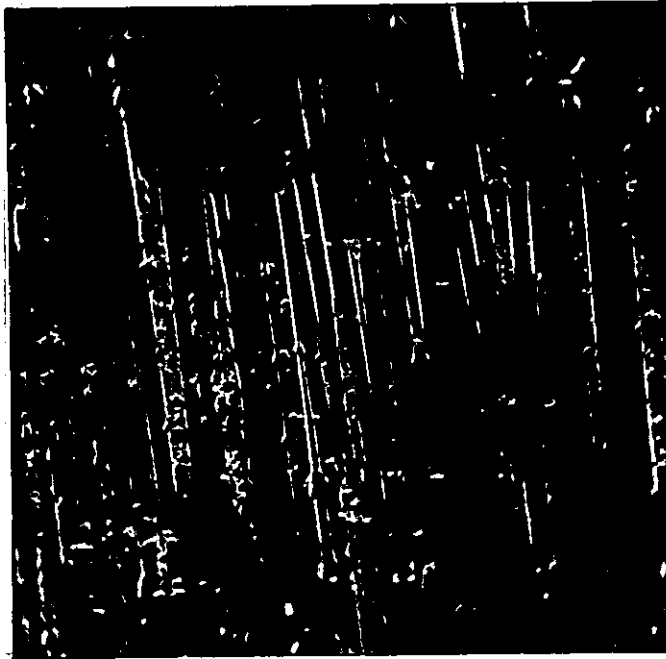


FIGURE 231: Scanning electron micrograph of 913 PrePreg showing substantial debonding. The sample was exposed to distilled water at 70°C for 40 days. x200

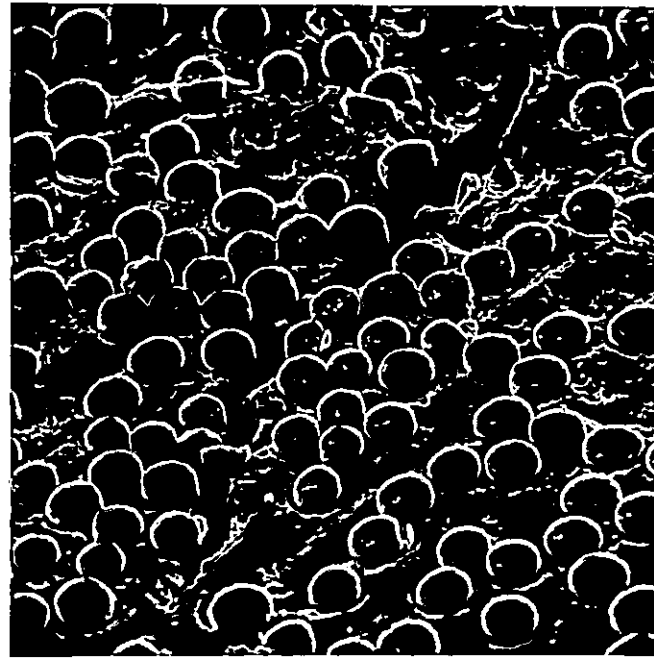


FIGURE 232: Scanning electron micrograph illustrating microcracking. These cracks were observed with Epoxy MY750 samples after being exposed to distilled water at 60°C and 70°C, respectively for 40 days. x500

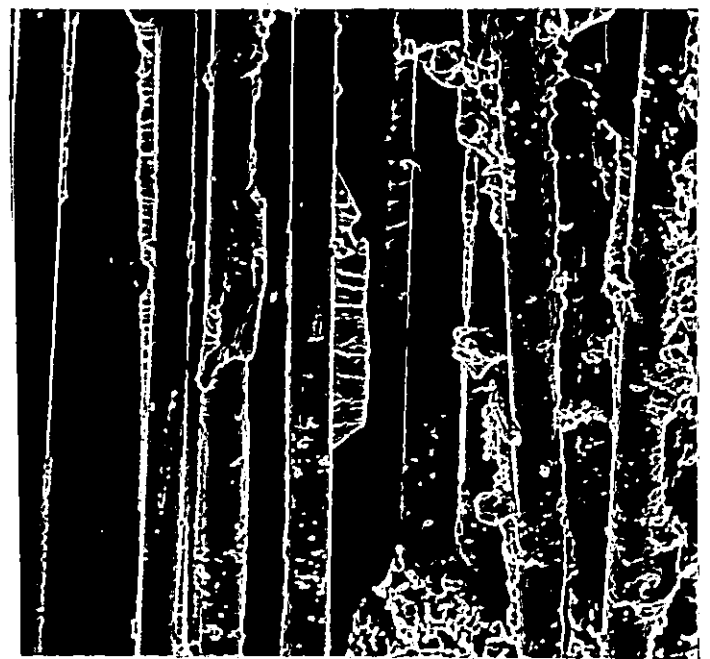


FIGURE 233: Scanning electron micrograph of Epoxy MY750 showing massive debonding. The samples were exposed to water at 60°C and 70°C respectively for 40 days. x500

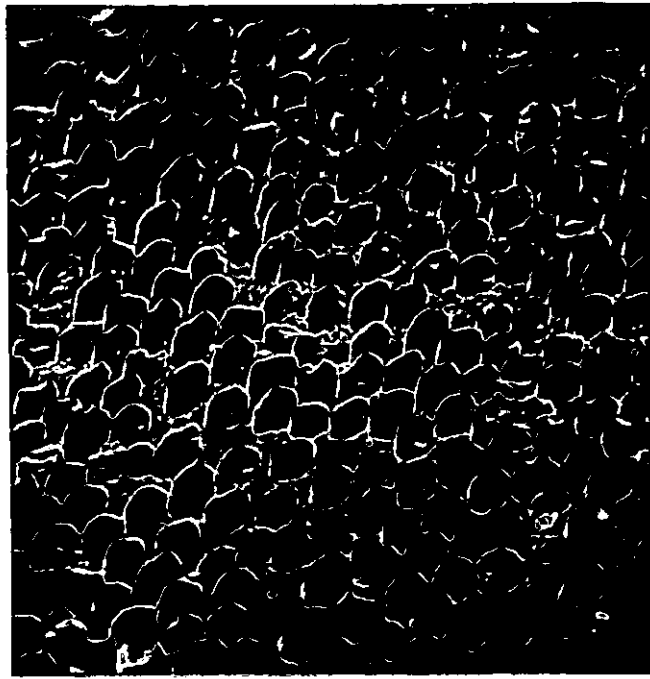


FIGURE 234a: - Scanning electron micrograph of cross-sectional area (perpendicular to fibre direction). Specimen exposed to water at 25°C for 40 days. x500

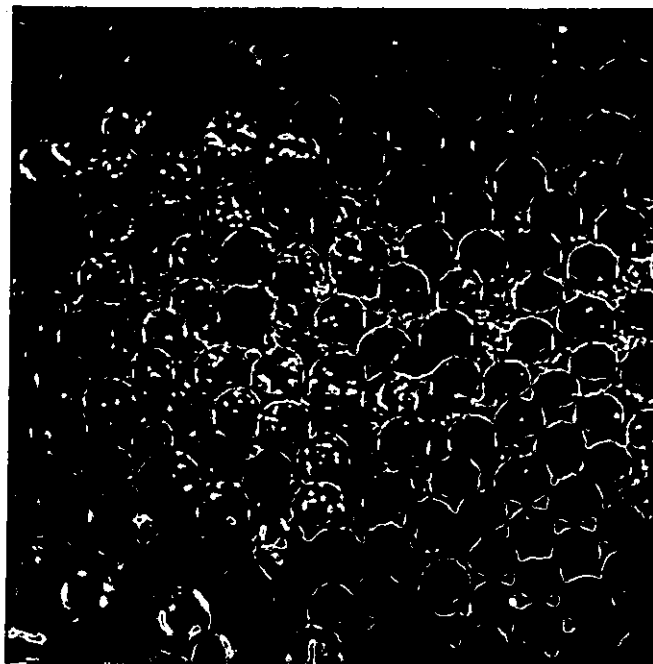


FIGURE 234b: Scanning electron micrograph of cross-sectional area (perpendicular to fibre direction). Specimen exposed to water at 70°C for 40 days. x500

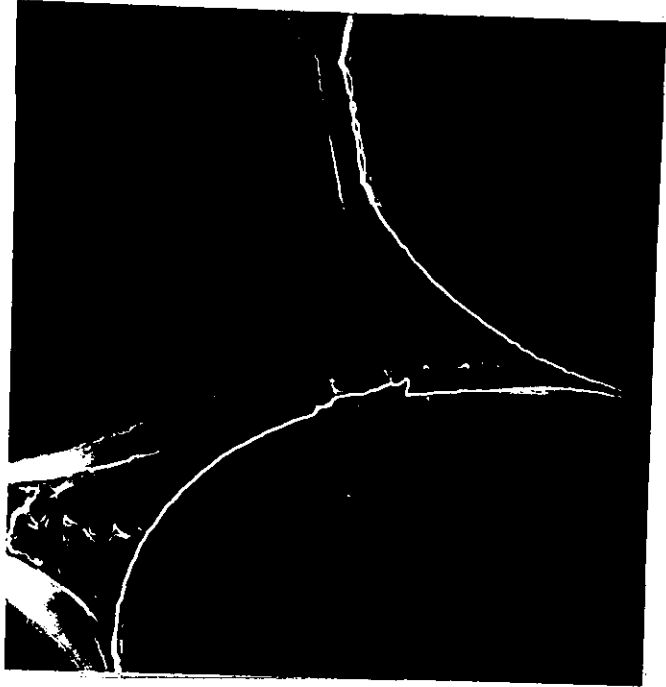


FIGURE 235a: Scanning electron micrograph illustrating good fibre wetting, after exposure to water at 25°C for 40 days x5500

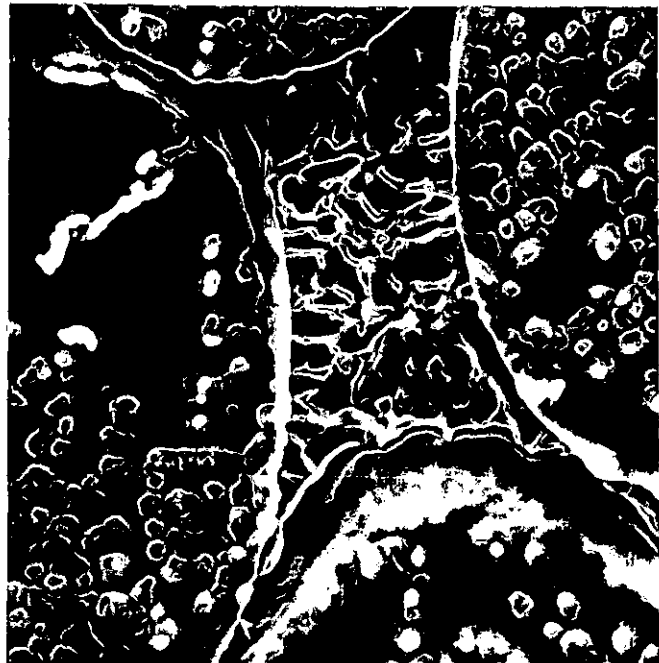


FIGURE 235b: Scanning electron micrograph illustrating poor fibre wetting, after exposure to water at 70°C for 40 days. x5500

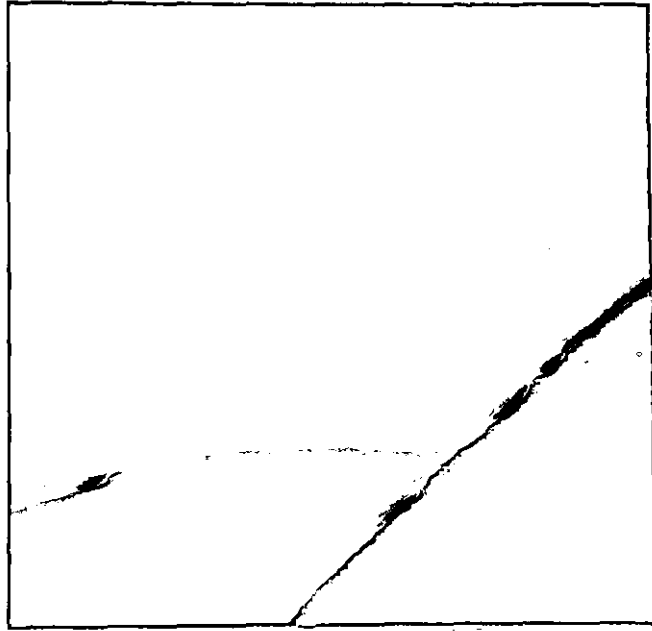


FIGURE 236a: Scanning electron micrograph of glass fibre surface, exposed to water at 25°C for 40 days, showing no damage of the surface
x22000

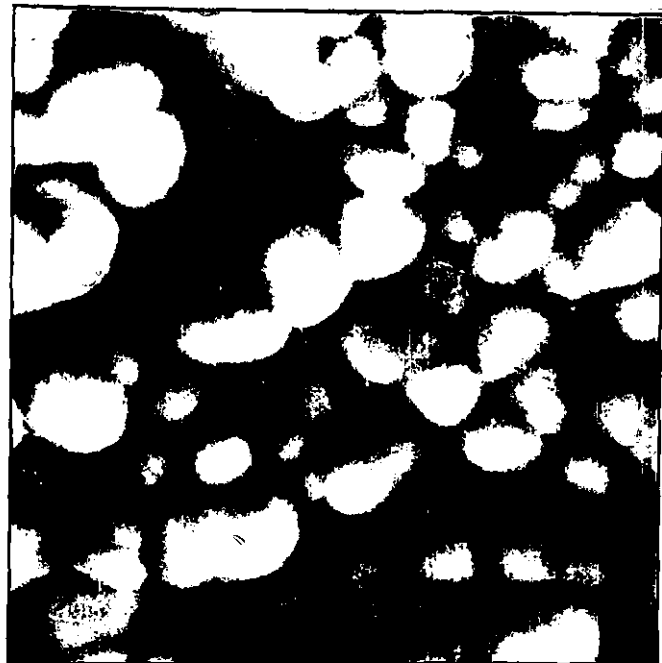
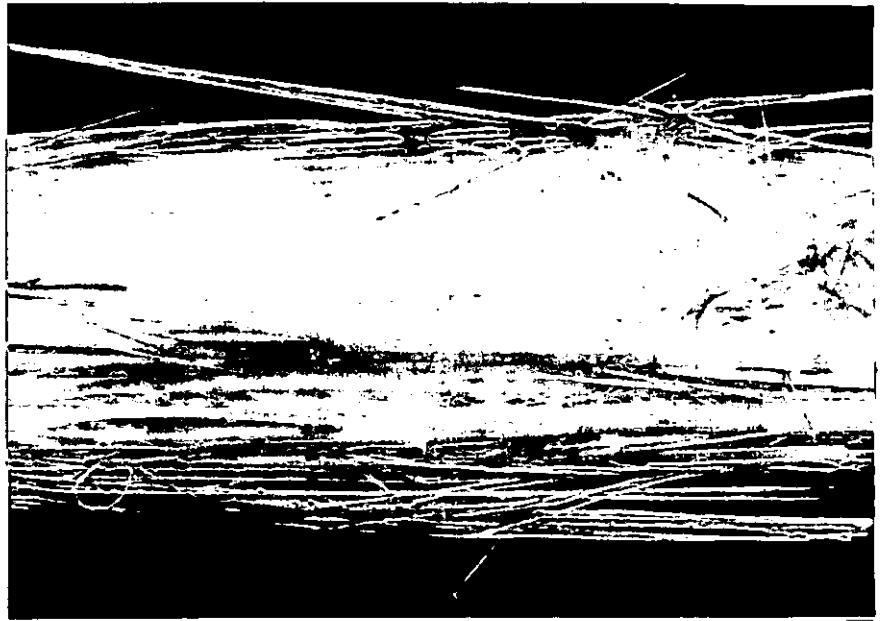
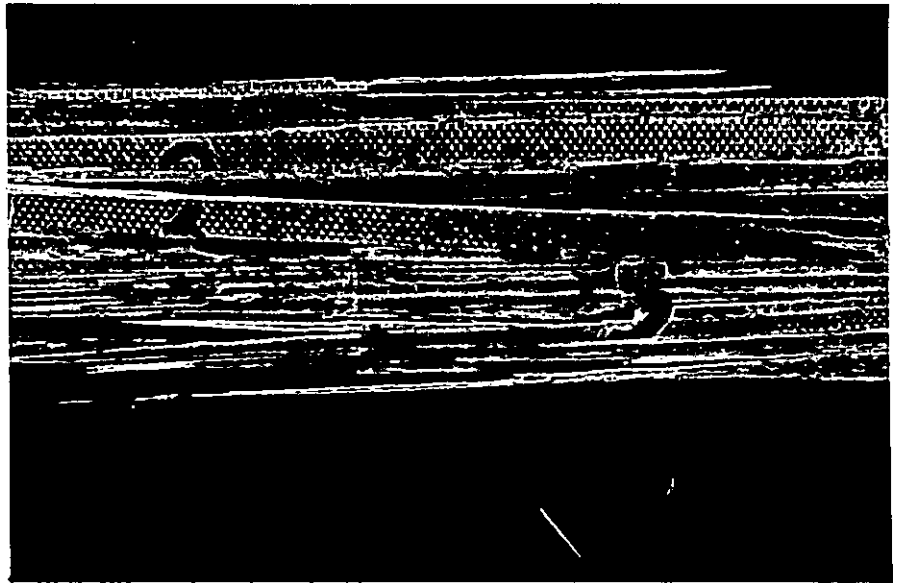


FIGURE 236b: Scanning electron micrograph of glass fibre surface, exposed to water at 70°C for 40 days, showing distorted and roughened surface
x2200

FIGURE 237: Typical photographs of the fracture surface tested in longitudinal tension after being conditioned at various environments



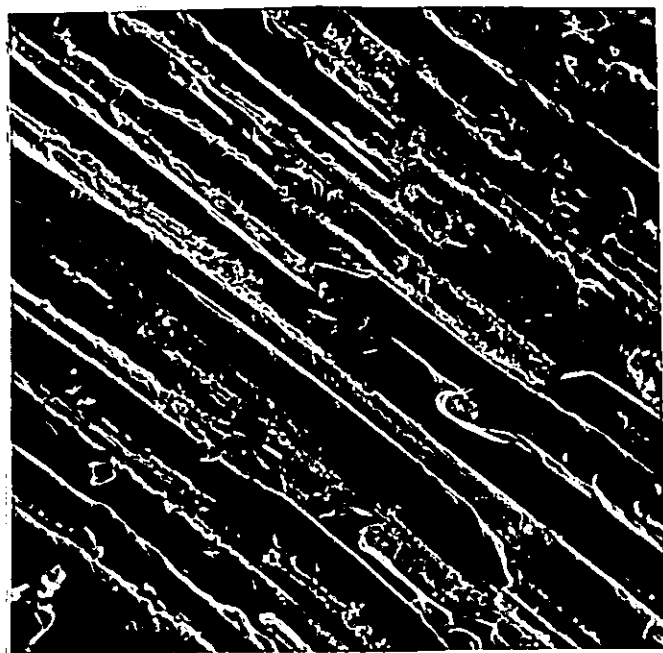
a) Dried and 60% RH



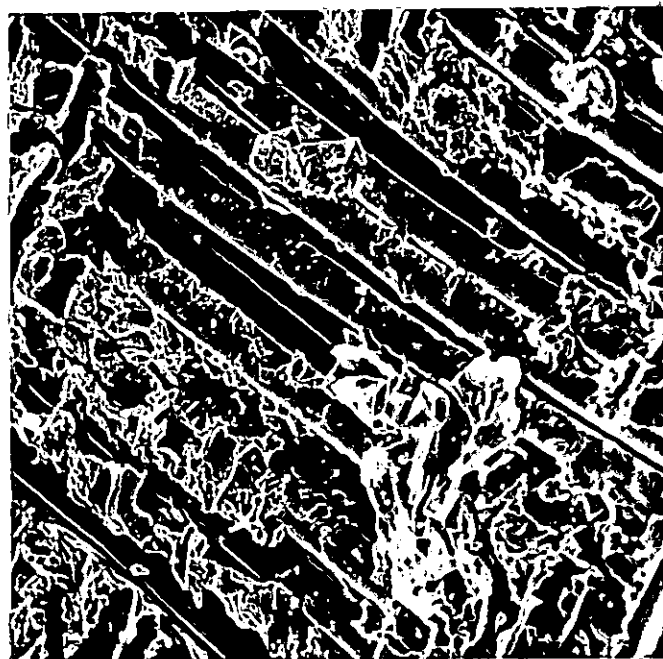
b) 95% RH and water bath



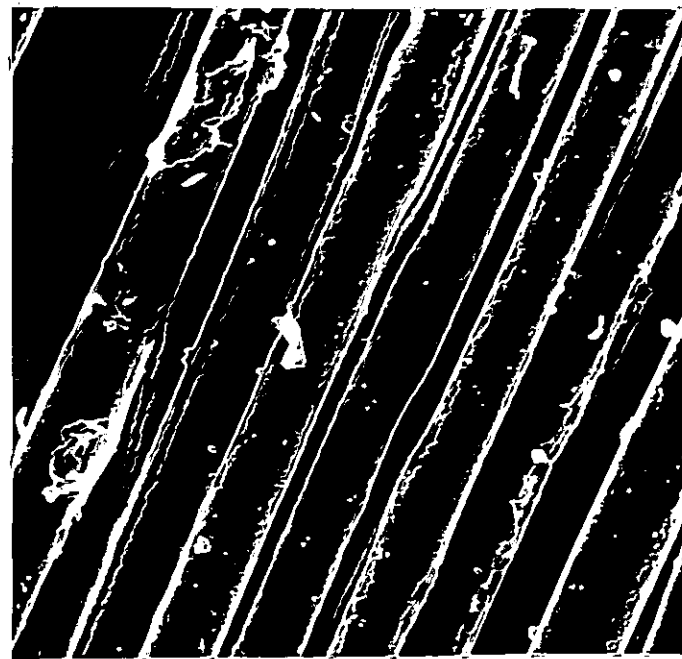
c) Fracture surface of 913 (conditioned at 95% and water bath)



a) 60% RH at 70°C, specimen 913 x 470



b) 95% RH at 70°C, specimen 913 x500



c) Water bath at 70°C, specimen 750 x500

FIGURE 238: Scanning electron micrographs of specimens exposed to different environments, illustrating fibre-resin adhesion

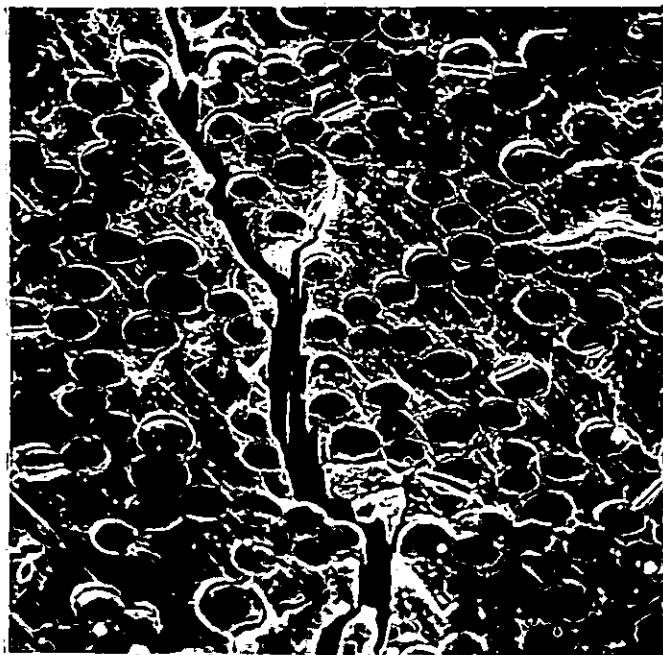


FIGURE 239: Scanning electron micrograph illustrating ILSS crack x500

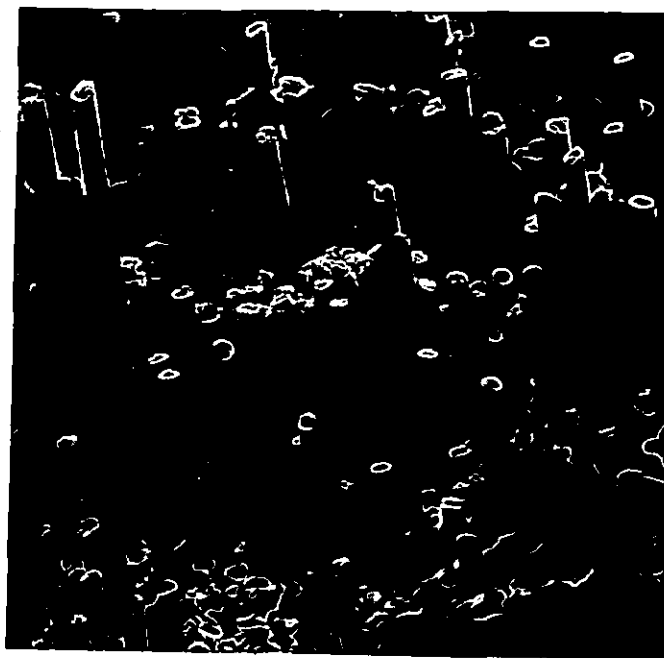


FIGURE 240a: Scanning electron micrograph of perpendicular failed area in ILSS fracture, showing good bond between the fibre/matrix, hence less fibre pullout, x200

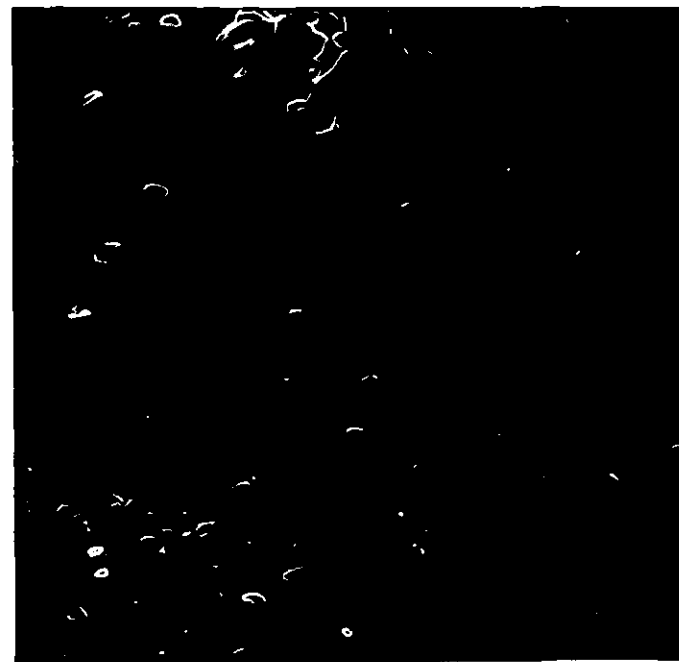
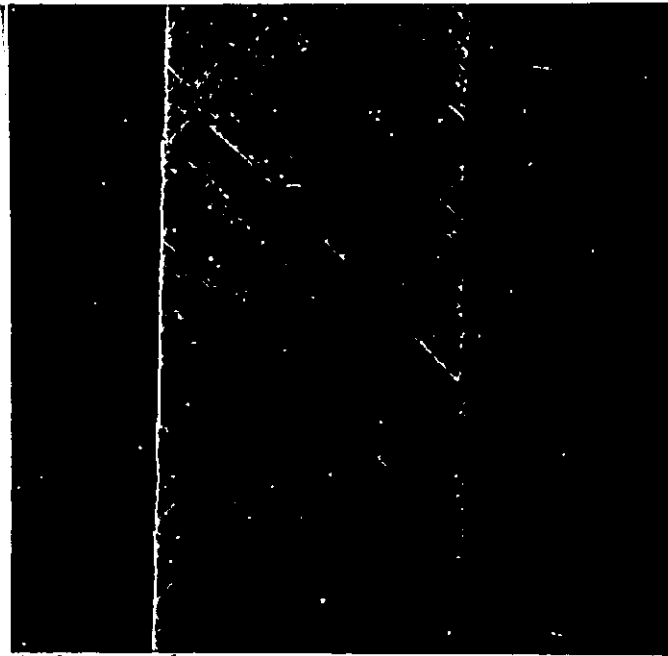
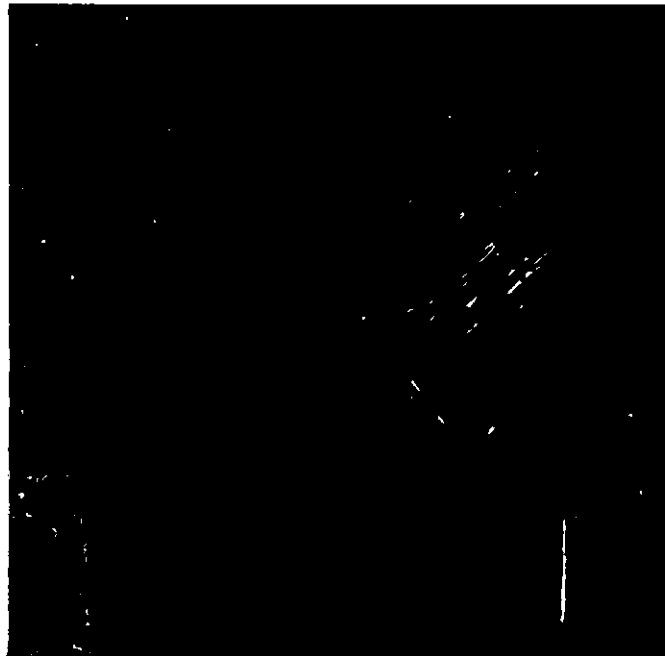


FIGURE 240b: Same as (a), but illustrating poor fibre/matrix bond, hence more fibre pullout



a) Photograph of failed ± 450 specimen, crazing area due to debonding of the interface



b) Typical photograph of the fracture surface of ± 450 specimen



c) Scanning electron micrograph of the fracture surface of ± 450 specimen x 250

FIGURE 241

